Werkzeuge zur Darstellung der subzellulären Lokalisation und funktionellen Charakterisierung von GABARAP und deren Anwendung

Inaugural-Dissertation

zur Erlangung des Doktorgrades

der Mathematisch-Naturwissenschaftlichen Fakultät

der Heinrich-Heine-Universität Düsseldorf

vorgelegt von

Indra Maria Simons

aus Aachen

Düsseldorf, Juli 2020

aus dem Institut für Physikalische Biologie
der Heinrich-Heine-Universität Düsseldorf

Gedruckt mit der Genehmigung der
Mathematisch-Naturwissenschaftlichen Fakultät der
Heinrich-Heine-Universität Düsseldorf

Berichterstatter:

1. Prof. Dr. Dieter Willbold

2. Prof. Dr. Björn Stork

Tag der mündlichen Prüfung: 18.08.2020

Eidesstattliche Erklärung

Ich versichere an Eides Statt, dass die Dissertation von mir selbstständig und ohne unzulässige fremde Hilfe unter Beachtung der „Grundsätze zur Sicherung guter wissenschaftlicher Praxis an der Heinrich-Heine-Universität Düsseldorf“ erstellt worden ist.

Ferner erkläre ich, dass ich in keinem anderen Dissertationsverfahren mit oder ohne Erfolg versucht habe, diese Dissertation einzureichen.

_____ _____

Düsseldorf, den Indra Maria Simons

“Das Leben ist ein Gleichgewichtszustand zwischen der Synthese und dem Abbau von Proteinen.“

- Yoshinori Ohsumi -

(eigene Übersetzung)

Für meine lieben Eltern

Inhaltsverzeichnis

Abbildungsverzeichnis

Tabellenverzeichnis

Abkürzungsverzeichnis

Acbp ..... *acyl coenzyme A-binding protein*
AIM ..... *ATG8-family interacting motif*
ALFY ..... *autophagy-linked FYVE protein*
AMBRA1 ..... *activating molecule in Beclin1-regulated autophagy protein 1*
AMP ..... Adenosinmonophosphat
AMPK ..... *AMP-activated protein kinase*
ARNO ..... *ADP ribosylation factor nucleotide-binding site opener*
AS ..... Aminosäure
ATG ..... *autophagy related*
ATP ..... Adenosintriphosphat
ATXN ..... *Ataxin*
BNIP3L ..... *BCL2/Adenovirus E1B 19 KDa protein-interacting protein 3-like*
BRUCE ..... *baculovirus IAP repeat (BIR)-containing ubiquitin-conjugating enzyme*
BSA ..... bovines Serumalbumin
C.elegans ..... *Caenorhabditis elegans*
CBL ..... *Casitas B-lineage Lymphoma*
CRISPR ..... *Clustered Regularly Interspaced Short Palindromic Repeats*
Cvt ..... *cytoplasm-to-vacuole targeting*
D. melanogaster ..... *Drosophila melanogaster*
DMEM ..... *Dulbecco's Modified Eagle's Medium*
DNA ..... *desoxyribonucleic acid*
EGFP ..... *enhanced green fluorescent protein*
EGFR ..... *epidermal growth factor receptor*
ELISA ..... *enzyme-linked immunosorbent assay*
EPF ..... *extracellular protein factor*
EPG5 ..... *ectopic P-granules autophagy protein 5 homolog*
EPN ..... *Epsin*
EPS15 ..... *epidermal growth factor receptor substrate 15*
ER ..... endoplasmatisches Retikulum
ErbB ..... *erythroblastosis oncogene B 2*
ERC ..... *endocytic recycling compartment*
ERK ..... *extracellular-signal regulated kinase*
ESCRT ..... *endosomal sorting complex required for transport*
EV ..... extrazelluläres Vesikel
EYFP ..... *enhanced yellow fluorescent protein*
Fab ..... *fragment antigen binding*
Fc ..... *fragment crystallizable*
FCS ..... *fetal calf serum*
FIP200 ..... *FAK family kinase interacting protein of 200 kDa*
FYCO1 ..... *FYVE and coiled-coil domain containing 1*
$GABA_A$ ..... *γ-aminobutyric acid A*
GABARAP ..... *$GABA_A$ receptor-associated protein*
GABARAPL1 ..... *GABARAP-like1*
GABARAPL2 ..... *GABARAP-like2*
GATE-16 ..... *Golgi-associated ATPase enhancer of 16 kDa*
GDP ..... Guanosindiphosphat
GEC1 ..... *Glandular epithelial cell protein*
GEF ..... *guanine-nucleotide exchange factor*
GFP ..... *green fluorescent protein*
GIM ..... *GABARAP-interacting motifs*

GRB2 ..... *growth factor receptor bound protein 2*
GTP ..... Guanosintriphosphat
HDR ..... *homology-directed repair*
HeLa ..... *Henrietta Lacks*
HER1 ..... *human EGFR related*
HOPS ..... *homotypic fusion and protein sorting*
Hsc70 ..... *heat shock cognate protein of 70 kDa*
IAP ..... *inhibitor of apoptosis*
IBI ..... Institut für Biologische Informationsprozesse
ICS ..... *Institute of Complex Systems*
IF ..... Immunfluoreszenz
ILVs ..... *intraluminal vesicles*
JACoP ..... *Just Another Colocalization Plugin*
JAK ..... Januskinase
JM ..... Juxtamembran
KI ..... *knock-in*
KO ..... *knockout*
LDL ..... *low density lipoprotein*
LIR ..... *LC3-interacting region*
LSM ..... *laser scanning microscopy*
mAb ..... monoklonaler Antikörper
MAP1A/1B LC3 ..... *microtubule-associated protein 1A/1B light chain 3*
MAPK ..... *mitogen-activated protein kinase*
MCC ..... *Mander`s Correlation Coefficient*
MEM NEAA ..... *Minimum Essential Medium with non-essential amino acids*
mTORC1 ..... *mammalian/mechanistic target of rapamycin complex 1*
MVBs ..... *multivesicular bodies*
NBR1 ..... *neighbor of BRCA1 gene 1 protein*
NHEJ ..... *non-homologous end joining*
NMD ..... *Nonsense-Mediated mRNA Decay*
NSF ..... *N-ethylmaleimidesensitive factor*
PAM ..... *protospacer adjacent motif*
PAS ..... *phagophore assembly site*
PBS ..... *phosphate-buffered salin*
PCC ..... *Pearson`s Correlation Coefficient*
PCM ..... *pericentriolar matrix*
PE ..... Phosphatidylethanolamin
PEG ..... Polyethylenglykol
PFA ..... Paraformaldehyd
PI(3)P Phosphatidylinositol-3-Phosphat
PI3KC3-C1 ..... *phosphatidylinositol-3-kinase complex I*
PI4K2A ..... *Phosphatidylinositol 4-kinase 2-alpha*
PINK1 ..... *PTEN-induced kinase 1*
PLEKHM1 ..... *homology domain containing protein family member 1*
PTB ..... *phosphotyrosine-binding*
pTyr ..... phosphorylierte Tyrosinreste
PX-RICS ..... *Rho GTPase-activating protein 32*
Rab ..... *ras-related in brain*, *ras related in brain*
Raptor ..... *regulatory associated protein of mTOR*
RBP ..... RNA-bindendes Protein
RBSN ..... *Rabenosyn*
RPN10 ..... *proteasome regulatory particle base subunit*
RT ..... Raumtemperatur
RTK ..... Rezeptor-Tyrosinkinasen
S. cerevisiae ..... *Saccharomyces cerevisiae*

SAR ..... *selective autophagy receptors*
SDM ..... *spinning disk microscopy*
SEM ..... *standard error of means*
SH2 ..... *Src homology region 2*
SMLM ..... *single-molecule localization microscopy*
SNAP ..... *synaptosome-associated protein*
SNAREs ..... *soluble N-ethylmaleimide-sensitive-factor attachment receptors*
SQSTM1 ..... *Sequestome 1*
STAT ..... *signal transducers and activators of transcription*
STED ..... *stimulated emission depletion*
STX ..... *Syntaxin*
TALEN ..... *transcription activator-like effector nucleases*
TGF ..... *transforming growth factor*
TGN ..... *trans*-Golgi-Netzwerk
TIDE ..... *Tracking of Indels by DEcomposition*
TKD ..... zytoplasmatische Tyrosinkinasen-Domäne
TM ..... Transmembran-Domäne
Trf ..... Transferrin
TrfR ..... Transferrin-Rezeptor
TRPV1 ..... *transient receptor potential vanilloid channel*
UBA5 ..... *ubiquitin like modifier activating enzyme 5*
UDS ..... *UIM docking site*
UIM ..... *ubiquitin-interacting motif*
ULK ..... *UNC51-like kinase*
UNC51 ..... *uncoordinated movement 51*
UPS ..... Ubiquitin-Proteasom-System
UVRAG ..... *UV irradiation resistance-associated gene*
VAMP ..... *vesicle-associated membrane protein*
VPS ..... *vacuolar protein sorting*
WIPI ..... *WD-repeat proteins interacting with phosphoinosites*
WT ..... Wildtyp
Y2H ..... *Yeast two-Hybrid*
ZNF ..... Zink-Finger-Nukleasen

Aminosäuren

A Alanin (Ala)	G Glycin (Gly)	M Methionin (Met)	S Serin (Ser)
C Cystein (Cys)	H Histidin (His)	N Asparagin (Asn)	T Threonin (Thr)
D Asparaginsäure (Asp)	I Isoleucin (Ile)	P Prolin (Pro)	V Valin (Val)
E Glutaminsäure (Glu)	K Lysin (Lys)	Q Glutamin (Gln)	W Tryptophan (Trp)
F Phenylalanin (Phe)	L Leucin (Leu)	R Arginin (Arg)	Y Tyrosin (Tyr)

Zusammenfassung

Spätestens seit Verleihung des Nobelpreises an Yoshinori Ohsumi im Jahr 2016 für die Entdeckung der *AuTophaGy related* (Atg) Proteine in Hefe steht die humane Proteinfamilie der ATG8s im Fokus der wissenschaftlichen Forschung. Die ATG8-Familie besteht aus der γ-*aminobutyric acid A (GABA$_A$) receptor-associated protein like-1/-2* (GABARAP/-L1/-L2) und der *microtubule-associated protein 1A/1B light chain 3* (MAP1A/1B LC3) A, -B, -B2, -C Unterfamilie. Die ATG8-Proteine sind sowohl für Autophagie-abhängige als auch Autophagie-unabhängige Prozesse in Zellen relevant. Neben den wichtigen Aufgaben während der Autophagie, einem dynamischen Prozess, der einen Abbau- und Recycling-Weg zelleigener und -fremder Bestandteile darstellt, wurde GABARAP zuerst als ein GABA$_A$-Rezeptor assoziiertes Protein, das den Transport des Rezeptors zur Plasmamembran vermittelt, beschrieben. Die ATG8-Proteinfamilie ist evolutionär hoch konserviert und weist eine hohe Sequenz- und Strukturhomologie vor allem innerhalb der jeweiligen Unterfamilie auf. Eine genaue Unterscheidung der ausgeübten Funktionen der einzelnen ATG8-Mitglieder auf endogenem Niveau ist bislang aufgrund mangelnder Methoden und Werkzeuge zur gezielten Untersuchung kaum möglich. Deshalb war es Ziel dieser Arbeit, Werkzeuge zur differenzierten Untersuchung der einzelnen ATG8-Mitglieder zu etablieren und anschließend zur Erforschung spezifischer Rollen und Funktionen, insbesondere der GABARAP-Proteinfamilie, einzusetzen.

Zunächst wurden innerhalb unserer Arbeitsgruppe *Clustered Regularly Interspaced Short Palindromic Repeats* (CRISPR/Cas9) *knockout* (KO) Plasmide kloniert und die KO-Zelllinien generiert.

Anschließend wurde ein in Kooperation mit der *Monoclonal Antibody Core Facility* des Helmholtz Zentrums München entwickelter anti-GABARAP Antikörper mit Hilfe diverser KO-Zelllinien getestet und validiert. Dabei zeigte sich in den Immunfluoreszenz (IF)-Färbungen eine hohe Spezifität für GABARAP, ohne mit LC3s und den nahe verwandten Proteinen GABARAPL1 und -L2 kreuzzureagieren.

Die GABARAP KO-Zelllinien waren zudem für die Untersuchung des Einflusses einer GABARAP-Defizienz bei der Endozytose des epidermalen Wachstums-Rezeptors (*epidermal growth factor receptor,* EGFR) grundlegend. Innerhalb unserer Arbeitsgruppe konnte gezeigt werden, dass in GABARAP KO-, aber nicht in GABARAPL1 KO- und

GABARAPL2 KO-Zellen, nach EGF-Stimulation eine zeitabhängige, schnellere Rezeptor-Degradation auf Proteinebene stattfindet und es zu Veränderungen hinsichtlich des *mitogen-activated protein kinase* (MAPK) Signalweges und der Ziel-Genexpression kommt. Ergänzend zu diesen Ergebnissen konnte innerhalb dieser Arbeit durch konfokale *laser scanning microscopy* (LSM) ebenfalls eine schnellere Internalisierung von fluoreszenzmarkierten EGF-gebundenem EGFR festgestellt werden. LSM Aufnahmen und deren Analyse ergaben eine hinsichtlich der Anzahl, Größe und Intensität zeitlich abhängige veränderte Vesikelzusammensetzung innerhalb der GABARAP-defizienten Zellen im Vergleich zu den Wildtyp (WT)-Zellen. Durch die durchgeführten IF-Färbungen der endosomalen Markerproteine *ras-related in brain* (Rab)5 (frühes Endosom), Rab7 (spätes Endosom) und Rab11 (Recycling-Endosom) und deren Analyse mittels diverser Kolokalisations-Auswertungsvarianten konnten insgesamt keine signifikanten Unterschiede zwischen den WT- und GABARAP KO-Zellen in Bezug auf die endosomalen Transportprozesse während des EGFR-Abbaus ausgemacht werden. Dies zeigt, dass der EGFR in den WT- und GABARAP KO-Zellen alle untersuchten Kompartimente durchlaufen kann.

Mittels *enhanced green fluorescent protein* (EGFP)-GABARAP *knock-in* (KI)-Zellen, die einen EGFP-KI hinter dem endogenen GABARAP-Promotor (EGFP-KI GABARAP HEK293-Zellen) besitzen, wurde der Einfluss von GABARAP in Bezug auf die EGFR-Internalisierung weitergehend untersucht. Durch konfokale Lebendzell-Mikroskopie mittels LSM und *spinning disk microscopy* (SDM) waren innerhalb dieser Arbeit partielle Komigrationen von GABARAP mit EGF(R) ersichtlich, was auf eine mögliche direkte oder auch indirekte Interaktion dieser beiden Proteine miteinander hindeutet. Co-Immunopräzipitationsdaten von GFP-GABARAP mit endogenem EGFR sowie ein *extended LC3-interacting region* (xLIR)-Motiv innerhalb des EGFRs deuten auf eine mögliche direkte Bindung von GABARAP und dem EGFR hin.

Zudem konnten durch Lebendzell-Mikroskopie ringförmige Vesikel mit membranständigem GABARAP, das teilweise mit fluoreszenzmarkiertem EGF und/oder Transferrin (Trf) kolokalisierte, beobachtet werden. Dies lässt vermuten, dass diese Strukturen an Recycling-Prozessen beteiligt sein könnten.

Parallel wurde in dieser Arbeit ein Beitrag zu einer auf *single-molecule localization microscopy* (SMLM) basierenden Studie geleistet. Durch Expression von *enhanced yellow fluorescent protein* (EYFP)-GABARAP und EYFP-LC3B wurden GABARAP- und LC3B-enthaltende Strukturen in Bezug auf ihre Größe und Form untersucht. Dabei konnte durch

SMLM im Vergleich zu konfokaler LSM eine weitaus höhere Auflösung erzielt werden. Die Klassifizierung nach Größe und Form zeigte, dass LC3 eher in einer U-Form und GABARAP vorwiegend in ringförmigen Strukturen vorliegt.

In Zukunft können nun unter anderem mit Hilfe der neu etablierten Werkzeuge GABARAP-abhängige Funktionen und weitere mögliche GABARAP-Interaktionspartner genauer untersucht werden.

Summary

Since the Nobel Prize was awarded in 2016 to Yoshinori Ohsumi for the discovery of AuTophaGy related (Atg) proteins in yeast, the human ATG8 protein family is in the focus of scientific research. The ATG8 family consists of the γ-aminobutyric acid A ($GABA_A$) receptor-associated protein like-1/2 (GABARAP/-L1/-L2) and the microtubule-associated protein 1A/1B light chain 3 (MAP1A/1B LC3) A, -B, -B2, -C subfamily,

The ATG8 proteins are relevant for both autophagy dependent and autophagy independent processes in cells. In addition to the important tasks during autophagy, a dynamic process that represents a degradation and recycling pathway of cellular and non-cellular components, GABARAP was first described as a $GABA_A$ receptor associated protein that mediates the transport of the receptor to the plasma membrane. The ATG8 protein family is evolutionarily highly conserved and shows a high sequence and structural homology, especially within the respective subfamily. An exact differentiation of the functions of the individual ATG8 members on an endogenous level has so far hardly been possible due to a lack of methods and utensils for a targeted investigation. Therefore, the aim of this work was to establish tools for the differentiated investigation of the individual ATG8 members and subsequently to use them for the investigation of specific roles and functions, especially of the GABARAP proteins.

First, Clustered Regularly Interspaced Short Palindromic Repeats (CRISPR/Cas9) knockout (KO) plasmids were cloned and the KO cell lines were generated within our working group.

Subsequently, an anti-GABARAP antibody was developed in cooperation with the Monoclonal Antibody Core Facility of the *Helmholtz Zentrum München*. Within this work, it was tested and validated using various KO cell lines. Immunofluorescence (IF) staining showed a high specificity for GABARAP without cross-reacting with LC3s and the closely related proteins GABARAPL1 and -L2.

The GABARAP KO cell lines were also pioneering in the investigation of the influence of GABARAP deficiency in epidermal growth factor receptor (EGFR) endocytosis. Within our working group, it was shown that in GABARAP KO, but not in GABARAPL1 KO and GABARAPL2 KO cells, a time-dependent, faster receptor degradation takes place at the protein level after EGF stimulation, leading to changes in the mitogen-activated protein kinase (MAPK) signalling pathway and target gene expression.

In addition to these results, confocal laser scanning microscopy (LSM) was also used in this study to detect a faster internalization of fluorescence-labelled EGF-bound EGF receptors. Moreover, analysis of the LSM images revealed an altered vesicle composition regarding vesicle number, size and intensity in GABARAP-deficient cells compared to the wild-type (WT) cells over time. IF-staining of the endosomal marker proteins ras-related in brain (Rab)5 (early endosome), Rab7 (late endosome), and Rab11 (recycling endosome), and subsequent analysis with various co-localization evaluation methods revealed no significant differences between WT and GABARAP KO cells with regard to endosomal transport processes during EGF receptor degradation. This shows that in WT and GABARAP KO cells, EGFR can pass through all compartments investigated.

Using enhanced green fluorescent protein (EGFP) knock-in (KI) cells, which possess an EGFP KI behind the endogenous GABARAP promoter, the influence of GABARAP on EGFR internalisation was further investigated.

Confocal live cell microscopy using LSM and spinning disk microscopy (SDM) revealed partial co-migrations of GABARAP with EGF(R), indicating a possible direct or indirect interaction of these two proteins with each other. Co-immunoprecipitation data of GFP-GABARAP with endogenous EGFR and an extended LC3-interacting region (xLIR) motif within EGFR indicate a direct binding of GABARAP and EGFR.

In addition, ring-like structures with membrane-bound GABARAP partially co-localizing with fluorescence-labelled EGF and/or transferrin (Trf) could be observed during live cell microscopy, suggesting that these structures might be associated with recycling.

In parallel, this work was a contribution to a study based on single molecule localization microscopy (SMLM). By expression of enhanced yellow fluorescent protein (EYFP)-GABARAP and EYFP-LC3B, GABARAP and LC3B-containing structures were investigated with respect to their size and shape. By SMLM, a much higher resolution could be achieved compared to confocal LSM. Classification by size and shape showed that LC3 tends to be present in U-shaped and GABARAP predominantly in ring-shaped structures.

In the future, the newly established tools will allow for a more detailed investigation of GABARAP-dependent functions and other possible GABARAP interaction partners.

1 Einleitung

1.1 Autophagie

Unter Autophagie versteht man einen in allen Eukaryoten evolutionär hoch konservierten, lysosomalen Abbau- und Recyclingprozess von beispielsweise ausgedienten Organellen oder Proteinaggregat-Anhäufungen in der Zelle, welcher vorrangig der Aufrechterhaltung der zellulären Homöostase dient [1-3]. Das Wort „Autophagie“ stammt aus dem Griechischen und bedeutet *αὐτος*- (autós-) „selbst“ und φαγεῖν (phagein) „fressen“ [4]. Russell Deter und Christian de Duve beschrieben in den 1960er Jahren eine durch Glucagon induzierte Autophagie, die zum Abbau von Mitochondrien und anderen zytosolischen Komponenten durch Lysosomen in der Rattenleber führt [5]. Nachfolgend wurde Autophagie von Yoshinori Ohsumi *et al.* als ein fundamentaler zellulärer Prozess, der für das Überleben von *Saccharomyces cerevisiae* (*S. cerevisiae*) nach Nährstoffmangel benötigt wird, beschrieben [6; 7].

In eukaryotischen Zellen wird zwischen Makroautophagie, Mikroautophagie (jeweils selektive und nicht selektive) und Chaperon-vermittelter Autophagie unterschieden [2; 8]. Als Makroautophagie (von nun an als Autophagie bezeichnet) versteht man den Abbau zellulärer Komponenten, beispielsweise von Proteinaggregaten, zytosolischen Proteinen oder alten, defekten Zellorganellen [9]. Dabei wird das abzubauende Material von einer neusynthetisierten doppelten Lipid-Doppelmembran umschlossen, die zunächst Phagophore genannt wird und dann zu einem sogenannten Autophagosom heranreift [10]. Anschließend verschmilzt das Autophagosom mit einem Lysosom und es kommt zu einem hydrolytischen Abbau des autophagosomalen Inhaltes, welcher anschließend ins Zytosol freigesetzt und wiederverwendet werden kann [11; 12].

Bei der Mikroautophagie wird das abzubauende zytosolische Material hingegen direkt über Invagination endosomaler oder lysosomaler Membranen aufgenommen und abgebaut [13].

Die Chaperon-vermittelte Autophagie basiert auf der Identifizierung eines ungefalteten oder fehlgefalteten Proteins, das ein Pentapeptid Konsensus (KFERQ-ähnliches)-Motiv beinhaltet, wodurch es von einem Hitzeschockprotein namens *heat shock cognate protein of 70 kDa* (Hsc70) erkannt wird. Von diesem sogenannten Chaperon wird das Ziel-Protein zur Lysosomenoberfläche transportiert und lysosomal abgebaut [14; 15].

Der Abbau ubiquitinylierter Proteine geschieht entweder über das Ubiquitin-Proteasom-System (UPS) oder aber auch selektiv durch das Autophagie-Lysosom-System [16]. Bei der selektiven Autophagie wird das Frachtgut zunächst durch membrangebundene oder lösliche Rezeptoren, auch selektive Autophagie-Rezeptoren (*selective autophagy receptors*, SAR) genannt, gebunden [17]. Dies führt zur Ausbildung eines Autophagosoms, welches anschließend mit einem Lysosom fusioniert [18]. Inzwischen gibt es mehrere speziell bezeichnete Formen der selektiven Autophagie, die zuerst durch den *cytoplasm-to-vacuole targeting* (Cvt) Weg in Hefe näher erörtert wurden [19; 20]. So spricht man bei einem gerichteten Abbau des endoplasmatischen Retikulums (ER) von ER-Phagie [21] und von Mitophagie beim Mitochondrien-Abbau [22-25]. Auch Xenophagie, was den Abbau pathogener Mikroben bezeichnet [26], Pexophagie (Peroxisomen-Abbau) [27-29], Aggrephagie (Proteinaggregat-Abbau) [30], Reticulophagie (Retikulozyten-Abbau) [31] und Ribophagie (Ribosomen-Abbau) [32] sind neben weiteren selektiven Abbauvarianten inzwischen ausgiebig untersuchte Autophagie-Prozesse [3; 18; 17].

Autophagie ist somit ein wichtiger Bestandteil zur Erhaltung der zellulären Homöostase und kann durch Nährstoffmangel oder anderen Stress induziert werden, was zu einem schnelleren Abbau von z.B. Proteinen und anschließender Freisetzung der gewonnenen Aminosäuren (AS) führt [33-35]. Eine fehlerhaft regulierte Autophagie hat teils schwere neurodegenerative (z.B. Morbus Parkinson), inflammatorische, kardiovaskuläre Erkrankungen oder auch Krebs zur Folge [36; 37].

1.1.1 Der Autophagie-Prozess unter Beteiligung von ATG-Proteinen

Der Autophagie-Prozess geschieht schrittweise und wird unter anderem durch sogenannte *AuTophaGy related* (ATG) Proteine reguliert. In Abbildung 1.1 ist der vereinfachte, schematische Ablauf der Autophagie dargestellt.

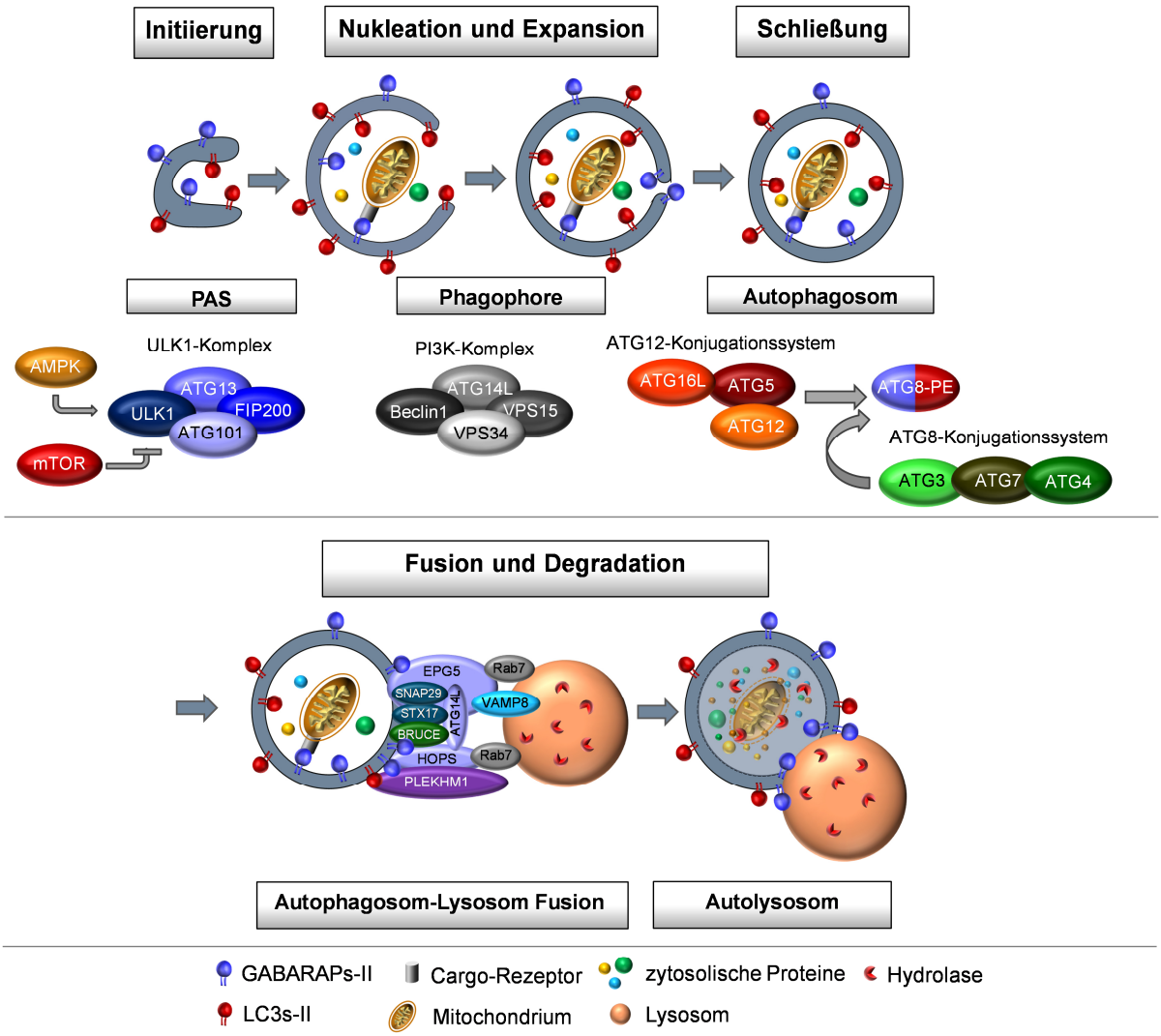

Abbildung 1.1: Schematischer Ablauf der Autophagie in Eukaryoten
Der Autophagie-Prozess wird zunächst über einen ULK-Komplex, bestehend aus ULK1/2, ATG13, FIP200 und ATG101 initiiert, was über AMPK und den mTORC1-Komplex reguliert wird. Unter nährstoffreichen Bedingungen fungiert AMPK als Aktivator und mTOR als Inhibitor. Unter nährstoffarmen Konditionen inhibiert mTOR nicht mehr den ULK-Komplex, sodass es zur Ausbildung einer Phagophore kommt, die in Hefezellen zunächst als *pre-autophagosomal structure* (PAS) bezeichnet wird. Anschließend kommt es zur Nukleation und Expansion der Phagophore, was durch den PI3KC3-C1-Komplex (Beclin1, ATG14L, VPS15, VPS34) vermittelt wird. Daran sind hauptsächlich LC3-Proteine aus der ATG8-Proteinfamilie in ihrer lipidierten Form (LC3-II) beteiligt. Die Schließung der Phagophore wird hingegen eher durch lipidierte ATG8-zugehörige GABARAPs (-II) vermittelt. Die Lipidierung der ATG8s mit PE wird durch das ATG8-Konjugationssystem (ATG3, ATG7, ATG4) und durch das ATG12-Konjugationssystem (ATG12, ATG5, ATG16L) vermittelt, wodurch die mit PE-lipidierten ATG8s als Membrananker dienen können. Die geschlossene Phagophore wird Autophagosom genannt und fusioniert letztendlich mit einem Lysosom. Für die Fusion mit dem Lysosom werden zunächst der HOPS-Komplex und PLEKHM1 rekrutiert, was durch Bindung über LIR-Motive gefördert wird. Des Weiteren sind die SNARE Proteine SNAP29, STX17 und VAMP8 sowie ATG14L, Rab7 und dessen Effektorprotein EPG5 maßgeblich für die Fusion. Die Fusion wird zudem durch das Protein BRUCE gefördert, das selektiv mit GABARAPs interagiert. Nach erfolgreicher Autophagosom-Lysosom Fusion wird das Frachtgut mittels saurer Hydrolasen abgebaut. (Modifiziert nach [38-42])

Autophagie kann über Faktoren wie z.B. Nährstoffmangel oder Hypoxie induziert werden [43]. Der erste Initiierungsschritt der Autophagie wird durch den *mammalian target of*

rapamycin complex 1 (mTORC1) und *adenosine monophosphate* (AMP*)-activated protein kinase* (AMPK) reguliert. Unter nährstoffreichen Bedingungen wird der ULK1-Komplex durch mTORC1 inhibiert, indem mTOR an ULK1/2 bindet und sowohl ULK1/ULK2 als auch ATG13 phosphoryliert [44]. Kommt es jedoch zum Hungern (*starving*) der Zelle, wird beispielsweise als einer der vielen Signalwege das Protein *regulatory associated protein of mTOR* (Raptor), ein Bestandteil des mTORC1, durch AMPK phosphoryliert und mTORC1 dadurch inhibiert. Dies führt wiederum dazu, dass der mTORC1-Komplex den ULK1/2-Komplex nicht mehr phosphoryliert und ihn dadurch folglich nicht mehr inhibiert, wodurch es letztlich zur Initiierung der Autophagie kommt. [44-46]

Nach Autophagie-Initiierung vermittelt zunächst der *uncoordinated movement 51* (UNC51)-*like kinase* (ULK)-Komplex, der aus ULK1 oder ULK2 [47], ATG13, *FAK family kinase interacting protein of 200 kDa* (FIP200) und ATG101 besteht, die Ausbildung einer in Hefe sogenannten *pre-autophagosomal structure*/*phagophore assembly site* (PAS) [48-51]. Dabei dienen ATG8-Proteine (nachfolgend „ATG8s“) als Bindeglied zwischen dem ULK1/2-Komplex und dem neu entstehenden Autophagosom, da ATG8s direkt mit Komponenten des ULK1/2-Komplexes interagieren [52; 53]. Die ATG8-Proteinfamilie wird in zwei Unterfamilien, die *microtubule-associated protein 1A/1B light chain 3* (MAP1A/1B LC3) (nachfolgend „LC3s“) und die γ-*aminobutyric acid receptor-associated A (GABA$_A$) protein* (GABARAP)-Familie (nachfolgend „GABARAPs“), unterteilt [54]. Auf diese Proteinfamilie wird in Kapitel 1.1.2 detaillierter eingegangen.

Nachfolgend wird der Klasse III *phosphatidylinositol-3-kinase complex I* (PI3KC3-C1)-Komplex gebildet. Der PI3KC3-C1-Komplex besteht aus dem *vacuolar protein sorting* (VPS) 34, ATG14L, VPS15, *activating molecule in Beclin1-regulated autophagy protein 1* (AMBRA1) und Beclin 1. Dieser Komplex sowie ATG2, das Transmembranprotein ATG9 und *WD-repeat proteins interacting with phosphoinosites* (WIPI)1-4 sind nach aktuellem Wissensstand an der weiteren Ausbildung der Phagophore beteiligt. [55-57] Die genaue Herkunft der Lipide zur Ausbildung der Phagophore ist noch nicht gänzlich geklärt, neueren Erkenntnissen zufolge wird jedoch das im ER lokalisierte Phosphatidylinositol-3-Phosphat (PI(3)P) (Omegasom) als Ausgangsbasis favorisiert [58-60]. Anschließend kommt es zur Expansion der Phagophore, wobei ATG8s beteiligt sind, die sowohl auf der konkaven als auch der konvexen Membranseite zu finden sind und die vollständige Ausbildung der Phagophore zum sogenannten Autophagosom unterstützen [61-63]. Durch ein Ubiquitin-artiges Konjugationssystem, das zuerst einen außenseitig auf der Membran agierenden ATG5-ATG12-Komplex bildet [61], welcher dann an ATG16L bindet, kommt es zur C-terminalen

Konjugation der ATG8-Proteine mit z.B. Phosphatidylethanolamin (PE) [64; 65]. ATG8 wird zuvor durch die ATG4-Protease C-terminal geschnitten und zu ATG8-I prozessiert. Dann wird es über das E1-ähnliche Enzym ATG7 aktiviert und schließlich durch das E2-ähnliche Enzym ATG3 reversibel mit PE am freien C-terminalen Glycin 116 konjugiert [65-67] (Abbildung 1.1). Dabei dienen WIPI-Proteine als Andockstelle [68]. Die lipidierte Form der ATG8s, im Weiteren ATG8(s)-II bzw. LC3(s)-II oder GABARAP(s)-II genannt, kann mit Membranen und bei der selektiven Autophagie mit Cargo-Rezeptoren wie beispielsweise p62/Sequestome 1 (SQSTM1) oder *neighbor of BRCA1 gene 1 protein* (NBR1) interagieren und somit als Adapter bzw. Andockstelle fungieren [39; 69; 18]. Das abzubauende Frachtgut wird beispielsweise bei der Mitophagie gezielt durch einen Autophagie-Rezeptor wie *BCL2/Adenovirus E1B 19 KDa protein-interacting protein 3-like* (BNIP3L/Nix), welcher an GABARAP(s) bindet und als Adapterprotein dient, in das Autophagosom geleitet [70; 71].

Während die Nukleation und Expansion der Phagophore eher durch LC3s-II vermittelt werden [72], werden die Autophagie-Initiierung [73; 47], die Schließung der Phagophore sowie die Fusion des Autophagosoms mit einem Lysosom, auch Auto(phago)lysosom genannt, vor allem durch GABARAPs vermittelt [74; 48]. Zudem konnten Bozic *et al.* kürzlich zeigen, dass es eine ATG2-GABARAP/GABARAPL1 Interaktion gibt, die für die Phagophorenausbildung maßgeblich ist [75]. Die Autophagosomen-Reifung und die Fusion eines Autophagosoms mit einem Lysosom sind außerdem von anderen Proteinen, wie z.B. von der kleinen Guanosintriphosphat (GTP)ase *ras related in brain* (Rab) 7 [35] und dem *homotypic fusion and protein sorting* (HOPS)-Anbindungskomplex, abhängig. Durch *UV irradiation resistance-associated gene* (UVRAG) kommt es zur Aktivierung des PI3KC3-C1- und C-VPS/HOPS-Komplexes [76], wodurch Guanosindiphosphat (GDP) gegen GTP ausgetauscht wird [77], was zu einer Rab7-Aktivierung führt. Dabei fungiert Rubicon, eine Komponente des PI3KC3-Komplexes, als Rab7 Effektor [78] und Mon1-Ccz1 als GTP-Austauschfaktor (*guanine-nucleotide exchange factor*, GEF), was eine Inaktivierung von Rab7 bewirkt [79], wodurch die endosomale Reifung und Fusion kontrolliert wird [80].

Der HOPS-Komplex interagiert direkt mit *Pleckstrin homology domain containing protein family member 1* (PLEKHM1) [81]. Über sogenannte *LC3-interacting region* (LIR)-Motive [82] können insbesondere GABARAPs mit PLEKHM1 interagieren und dessen Rekrutierung fördern, wodurch die Autophagosom-Lysosom Fusion mitgesteuert wird [74; 81]. Weitere Regulatoren der Autophagom-Lysosom Fusion sind die zu den *soluble N-ethylmaleimide-sensitive-factor attachment receptors* (SNAREs) gehörenden Anbindungsfaktoren (*tethering factors*). Dazu zählen unter anderem *synaptosome-associated*

protein 29 (SNAP29), *Syntaxin 17* (STX17) [83] und *vesicle-associated membrane protein* 8 (VAMP8) [77]. Zusätzlich sind Rab7 und der Rab7-Effektor *ectopic P-granules autophagy protein 5 homolog* (EPG5) [84] sowie ATG14L [85] an der Fusion beteiligt. Das *inhibitor of apoptosis* (IAP)-Protein *baculovirus IAP repeat (BIR)-containing ubiquitin-conjugating enzyme* (BRUCE) interagiert selektiv mit GABARAP und GABARAPL1 und fördert dadurch die Autophagosom-Lysosom Fusion [41]. Schließlich wird der autophagosomale Inhalt nach Fusion mit dem Lysosom über lysosomale, pH-abhängige, saure Hydrolasen abgebaut [86; 11; 87]. Durch Zugabe von z.B. Bafilomycin A1, einem Makrolidantibiotikum, das die vakuoläre H^+-Adenosintriphosphat (ATP)ase hemmt, wird die Fusion des Autophagosoms mit dem Lysosom blockiert und somit der autophagische Flux inhibiert [88; 89]. Dies macht man sich bei experimentellen Versuchen zu nutzen, da es dadurch vorrangig nach Hunger-induzierter Autophagie zu einer Akkumulation von Autophagosomen in der Zelle kommt, die man als sogenannte „*puncta*“ in IF-Färbungen detektieren und quantifizieren kann.

Trotz der abundanten Beteiligung der ATG8-Proteine an der Autophagie konnten Nguyen *et al.* (2016) in HeLa (Henrietta Lacks)-Zellen mit vollständigen KOs aller ATG8-Proteine (ATG8-Hexa-KO) zeigen, dass es bei der *PTEN-induced kinase 1* (PINK1)/Parkin vermittelten Mitophagie und unter hungernden Bedingungen auch ohne ATG8s noch zur Ausbildung von insgesamt kleineren Autophagosomen in geringerer Rate kommt. Auch wenn ATG8s somit nicht zwingend unter diesen Bedingungen für die Autophagosomen-Biogenese notwendig sind, sind vermutlich vor allem GABARAPs für die Autophagosom-Lysosom Fusion essenziell, da nur in GABARAPs KO- und nicht in LC3s KO-Zellen eine signifikante Blockierung der autophagischen Aktivität gezeigt werden konnte [90]. Durch das Fehlen der GABARAPs kann das Adapterprotein PLEKHM1 nicht mehr zur Autophagosomen-Oberfläche rekrutiert werden. Dies führt wiederum dazu, dass der HOPS-Komplex nicht rekrutiert wird und die Fusion eines Autophagosoms mit einem Lysosom nicht stattfinden kann [74; 91].

Joachim *et al.* konnten zeigen, dass unlipidiertes GABARAP-I unter nährstoffreichen Bedingungen am Golgi-Apparat und der perizentriolaren Matrix *(pericentriolar matrix*, PCM) akkumuliert, um bei Nährstoffmangel direkt verfügbar zu sein [92; 93]. Bei Bedarf kann GABARAP somit schnell aus dem PCM-*pool* freigesetzt werden und an der Autophagosomen-Generierung partizipieren [92; 93]. Eine ähnliche Akkumulation konnte ebenfalls für LC3 beobachtet werden [94]. Unter nährstoffreichen Bedingungen liegen die nukleären und zytoplasmatischen unlipidierten LC3-I Formen acetyliert vor. Bei Nährstoffmangel wird nukleäres LC3-I deacetyliert und ins Zytoplasma transportiert. Dort

wird LC3 mit PE konjugiert, wodurch die an der Autophagosomenausbildung beteiligte lipidierte LC3-II Form entsteht [94].

1.1.2 Die hochkonservierte ATG8-Proteinfamilie mit Fokus auf GABARAP

Mit der Verleihung des Nobelpreises in Physiologie oder Medizin an Yoshinori Ohsumi im Jahr 2016 für die Entdeckung der Atg-Proteine in Hefe und den maßgeblichen Beitrag zur Erforschung der Autophagie [4], stieg die Anzahl an Veröffentlichungen, die sich mit ATG8 und GABARAP befassen rapide an.

Das in Eukaryoten hochkonservierte Atg8-Protein wurde zuerst in *S. cerevisiae* entdeckt, wo es nur ein Atg8-Gen sowie -Protein gibt [7]. Atg8 und seine Homologe sind ubiquitär verbreitet. So findet man in *Caenorhabditis elegans* (*C. elegans*) zwei Atg8-ähnliche Proteine, nämlich LGG-1 und LGG-2 [95], welche in *Drosophila melanogaster* (*D. melanogaster*) Atg8a und Atg8b genannt werden (siehe Abbildung 1.2). In Menschen existieren hingegen sieben Ubiquitin-artige ATG8-Paraloge mit einer Größe von ca. 15 kDa [96]. Diese werden wie bereits erwähnt (siehe Kapitel 1.1.1) in die MAP1LC3-, bestehend aus LC3A, LC3B, LC3B2 und LC3C und die GABARAP-Familie, bestehend aus GABARAP [97], GABARAPL1/GEC1 (GABARAP-*like1/Glandular epithelial cell protein*) [98] und GABARAPL2/GATE-16 (GABARAP-*like2/Golgi-associated ATPase enhancer of 16 kDa*) [99], unterteilt [54].

Die ATG8-Proteinfamilie weist eine sehr hohe Sequenzähnlichkeit insbesondere innerhalb der jeweiligen Unterfamilie auf (siehe Abbildung 1.2). Dabei hat GABARAP zu GABARAPL1 eine Sequenzidentität von 87 % [98] und GABARAP zu GABARAPL2 57 % Sequenzidentität [100].

Neben der bereits in Kapitel 1.1.1 beschriebenen Beteiligung an der Autophagie sind ATG8s ebenfalls an einer Reihe nicht-autophagischer Sekretions- und Transportprozesse beteiligt. Der Fokus dieser Arbeit wird auf die GABARAP-Subfamilie gelegt, weshalb nachfolgend detaillierter auf diese Proteinfamilie eingegangen wird.

Die GABARAPs wurden zuerst als γ-Aminobuttersäure A ($GABA_A$)-Rezeptor-assoziierte Proteine, die am Transport des Neurotransmitters GABA in Neuronen beteiligt sind, entdeckt [97; 101]. Analog zu GABARAP assoziiert auch GABARAPL1 mit dem $GABA_A$- und dem κ-Opioid Rezeptor [102; 103].

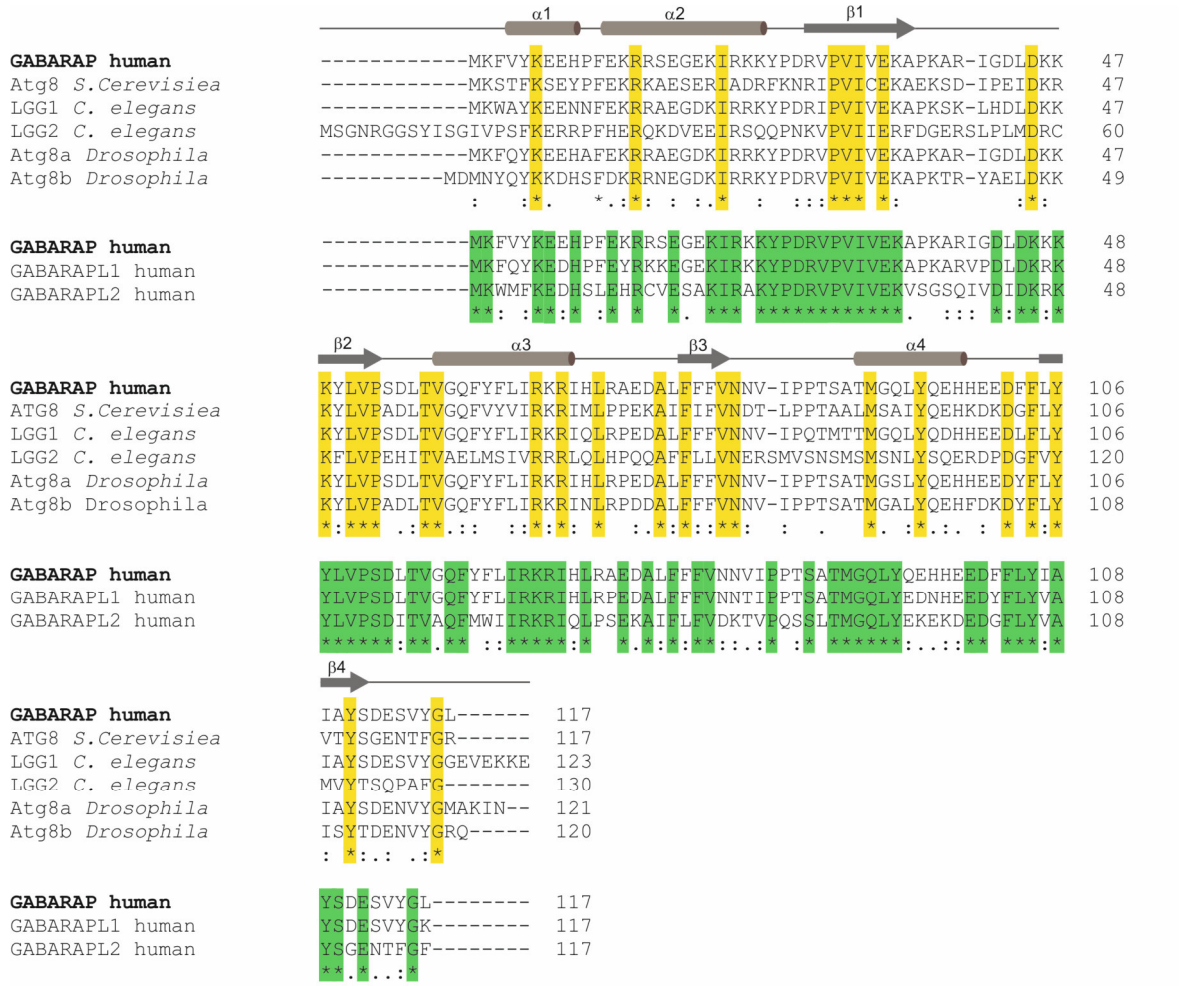

Abbildung 1.2: Sequenzalignment der Atg8- und Atg8-artigen Proteine
Das Sequenzalignment (Clustal Ω [104]) zeigt die Sequenzhomologie der hochkonservierten Atg8-Proteine aus *S. cerevisiae*, LGG1/LGG2 aus *C. elegans* sowie Atg8a/b aus *D. melanogaster* mit humanen GABARAP sowie einen Homologie-Vergleich innerhalb der GABARAP Unterfamilie mit GABARAPL1 und GABARAPL2 (gelb bzw. grün markierte Sterne (*) kennzeichnen vollständig konservierte AS, (:) AS mit stark ähnlichen Eigenschaften, (.) AS mit schwach ähnlichen Eigenschaften).

GABARAPL2/GATE-16 wurde zuerst in Zusammenhang mit dem intra-Golgi Transport entdeckt, wo es die Verbindung von *N-ethylmaleimidesensitive factor* (NSF) mit einem SNARE-Protein an Golgi-Membranen fördert [100; 105; 106].

ATG8s sind ebenfalls beim unkonventionellen Transport von Proteinen, die keine Signalsequenz besitzen, wie z.B. *acyl coenzyme A-binding protein* (Acbp) aus Hefe beteiligt [107; 108]. Außerdem wurden Assoziationen viraler Proteine, wie z.B. Proteine des Epstein-Barr Virus, Varizella Zoster Virus [109] oder Bornavirus [110], mit ATG8s beschrieben.

ATG8-Proteine können auf verschiedene Arten mit Proteinen interagieren. So sind nicht nur, wie der Name bereits sagt, Mikrotubuli-assoziierte MAP1LC3-Proteine, sondern auch GABARAPs über ihren positiv geladenen Amino (N)-Terminus über ein sogenanntes *tubulin-binding motif* in der Lage, an Mikrotubuli und Tubulin zu binden [101; 111]. Dadurch können sie sich an antero- und retrograden Transport-Prozessen zwischen Golgi-Apparat und

Plasmamembran über das *trans*-Golgi-Netzwerk (TGN) von z.B. Transmembran-Rezeptoren [112] und vesikulären Sekretionsprozessen [113; 114] beteiligen. Auch Autophagosomen können mit Hilfe von GABARAP, das als Adaptermolekül dient, indem es über den N-Terminus Mikrotubuli und über den lipidierten C-Terminus die Autophagosomen-Membran bindet [115], zu den perinukleär gelegenen Lysosomen transportiert werden [116; 117; 42].

Neben der Interaktion mit der γ_2-Unterheit des $GABA_A$-Rezeptors [97], ist für GABARAP auch eine Assoziation mit dem Transferrin-Rezeptor (TrfR) [112], dem *transient receptor potential vanilloid channel* (TRPV1) [118], dem Angiotensin AT_1-Rezeptor [119] und dem κ-Opioid Rezeptor [120] beschrieben. Rezeptoren, wie z.B. der $GABA_A$-Rezeptor [121] oder der EGFR [122], können über Clathrin-vermittelte Endozytose in Zellen aufgenommen werden. Innerhalb unseres Institutes wurde durch Mohrlüder *et al.* eine Interaktion von GABARAP mit den schweren Ketten von Clathrin beschrieben [123].

GABARAP besitzt zudem eine Carboxy (C)-terminale Ubiquitin-artige Domäne (Aminosäuren 27-117). Wie bereits in Kapitel 1.1.1 beschrieben, sind ATG8s nach C-terminaler Lipidierung mit z.B. PE in der Lage, mit Membranstrukturen, wie z.B. mit Vesikelmembranen autophagischen und nicht-autophagischen Ursprungs, zu interagieren, da PE als Membrananker dient. Somit können GABARAPs als Adaptermoleküle fungieren, indem sie beispielsweise Autophagie-Rezeptoren binden, die bei der selektiven Autophagie das Frachtgut in das Autophagosom transportieren (siehe Abbildung 1.3).

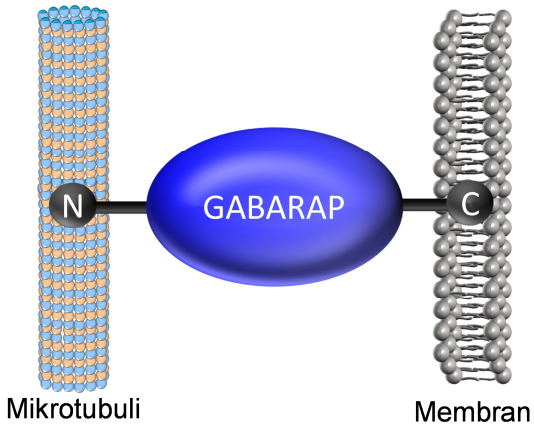

Abbildung 1.3: GABARAP interagiert N-terminal mit dem Zytoskelett und C-terminal mit Membranstrukturen
GABARAP kann zum einen über den N-Terminus mit Mikrotubuli und zum anderen über den lipidierten C-Terminus mit Membranen interagieren. Dadurch kann GABARAP als Transportvehikel fungieren und z.B. Vesikel entlang des Zytoskeletts zu Lysosomen transportieren.

Zudem kann GABARAP entsprechenden Cargo in Transportvesikel, die vom Golgi-Apparat stammen, rekrutieren und den Transport zur Plasmamembran vermitteln. So spielt

die Interaktion von *Phosphatidylinositol 4-kinase 2-alpha* (PI4K2A) mit GABARAP unter autophagischen und nicht-autophagischen Bedingungen, bei der keine C-terminale Lipidierung notwendig ist [124], eine Rolle beim Membrantransport [125]. Beim Proteintransport vom ER zum Golgi-Apparat ist GABARAP ebenfalls beteiligt, indem es mit dem β-Catenin-interagierenden GTPase-aktivierenden Protein für *cell division control protein 42 homolog* (Cdc42), *Rho GTPase-activating protein 32* (PX-RICS) genannt, interagiert und so den Transport des N-cadherin/β-Catenin Komplexes vermittelt [126].

Über zwei hydrophobe Taschen [127; 128] können ATG8s an kanonische *ATG8-family interacting motifs* (AIMs)/*LC3-interacting regions* (LIRs) [W/F/Y]-X_1-X_2-[I/L/V] bzw. *GABARAP-interacting motifs* (GIMs) ([W/F]-[V/I]-X_2-V)-Motive, die in Zielproteinen [129], beispielsweise selektiven Autophagie-Rezeptoren (SAR) vorkommen, binden und so ebenfalls als Adapterproteine fungieren [18]. Das Protein p62/SQMST1 [130] ist einer der ersten beschriebenen SAR und besitzt eine LIR [131]. Bei der selektiven Autophagie kann p62 als Autophagie-Rezeptor agieren, indem es ubiquitinylierte Substrate erkennt [131; 132]. Das Protein kann aber auch als Autophagie-Adapter durch Bindung von ATG8s dienen oder aber auch selbst Substrat sein, da p62 autophagisch abgebaut wird [133; 134].

Interaktionen mit Autophagie-Rezeptoren werden meist über ein LIR-Motiv vermittelt [82]. Neben N-terminalen LIR-Motiven sind auch C-terminale LIR-Motive, die z.B. bei den Proteinen FAM134B [135; 136], AnkyrinG/B [137], *autophagy-linked FYVE protein* (ALFY) und dem Rab7-Effektorprotein *FYVE and coiled-coil domain containing 1* (FYCO1) [138; 139] vorkommen, beschrieben.

Mit einem atypischen LIR-Motiv innerhalb von *ubiquitin like modifier activating enzyme 5* (UBA5) kann GABARAP über zwei kanonische hydrophobe Taschen (HP1 und HP2) sowie über eine neu entdeckte hydrophobe Tasche (HP0), die ein N-terminales Tryptophan innerhalb des UBA5-LIRs bindet, interagieren [140].

Da GABARAP ein Ubiquitin-artiges Protein (*ubiquitin-like protein*, UBL) ist und eine Ubiquitin-artige Faltung (*ubiquitin-like fold*) besitzt, kann GABARAP auch auf diese Weise mit anderen Proteinen wechselwirken. Über sogenannte Ubiquitin-interagierende Motive (*ubiquitin-interacting motif*, UIM) [141; 142], die sich z.B. in Autophagie-Adaptern und Rezeptoren befinden, kann es zu einer Interaktion mit GABARAP kommen. So konnte für GABARAP in einem Hefe-Zwei-Hybrid (*Yeast two-Hybrid*, Y2H) Screen eine Interaktion über ein N-terminales UIM mit den Deubiquitinylierungsenzymen Ataxin (ATXN)-3 bzw. ATXN-3 (*like*) L, Epsin 1-3 (EPN1-3) und Rabenosyn (RBSN) detektiert werden [143; 144]. Für ATG8 aus *Arabidopsis thaliana* konnte gezeigt werden, dass es zwei Adaptoren und/oder

Rezeptoren gleichzeitig binden kann. Dabei bindet die *proteasome regulatory particle base subunit* RPN10 an die UIM-Bindungsstelle (*UIM docking site*, UDS) und das Ubiquitin-Familien Protein *ubiquitin domain-containing protein* DSK2 an die LIR-Bindungsstelle (*LIR/AIM docking site* – LDS) des ATG8s [143].

GABARAP kann somit auf verschiedenste Arten mit Liganden wechselwirken und es sind inzwischen eine Vielzahl von Proteinen, die über ein LIR-Motiv oder auch auf oben beschriebene andere Weisen mit ATG8s interagieren, bekannt.

Innerhalb unserer Arbeitsgruppe konnte bereits gezeigt werden, dass es einen Autophagie-unabhängigen Zusammenhang von ATG8-Proteinen, insbesondere von GABARAP und dem epidermalen Wachstumsfaktor-Rezeptor (*epidermal growth factor receptor*, EGFR), unter anderem in Bezug auf den Rezeptortransport und -abbau gibt [145]. Ferner konnten für den EGFR bereits LIR-Motive in der extrazellulären und zytoplasmatischen Domäne mit Hilfe der iLIR Datenbank [146] ausfindig gemacht werden.

In der Literatur gibt es zudem Hinweise auf einen potentiellen *cross-talk* zwischen Autophagie und den EGFR-vermittelten Signalwegen [147-151], wobei eine mögliche Interaktion von GABARAP und dem EGFR von Relevanz sein könnte.

1.1.3 Der epidermale Wachstumsfaktor-Rezeptor

Der epidermale Wachstumsfaktor-Rezeptor (EGFR/ErbB1) wurde erstmals im Jahre 1979 isoliert [152] und wird ubiquitär im Gewebe des Körpers exprimiert [153; 154]. Er gehört zur *erythroblastosis oncogene B 2* (ErbB)-Proteinfamilie, die aus den vier Rezeptor-Tyrosinkinasen (RTK) HER1 (*human EGFR related*, EGFR/ErbB-1), HER2 (Neu/ErbB-2), HER3 (ErbB-3) und HER4 (ErbB-4) besteht [155; 156]. Der EGFR besteht aus einer 1210 AS-großen Vorläufer-Form, welche N-terminal in die mature 1186 AS-Form des transmembranen EGFR prozessiert wird [157; 158]. Ein schematischer Aufbau des EGFR ist in Abbildung 1.4 gezeigt, auch wenn der gesamte detaillierte strukturelle Aufbau, insbesondere der C-terminalen Domäne, bis dato noch nicht vollständig geklärt ist [159-161]. Extrazellulär befindet sich eine Cystein-reiche Liganden-Bindungsstelle, die aus vier Subdomänen (I-IV) aufgebaut ist. Dabei findet die Ligandenbindung durch die Domänen I und III statt. Danach folgt eine einzelne Transmembran-Domäne (TM), ein Juxtamembran (JM)-Segment, eine zytoplasmatische Tyrosinkinasen-Domäne (TKD) und eine C-terminale regulatorische Signal-Domäne (C-terminaler Schwanz) [162-164].

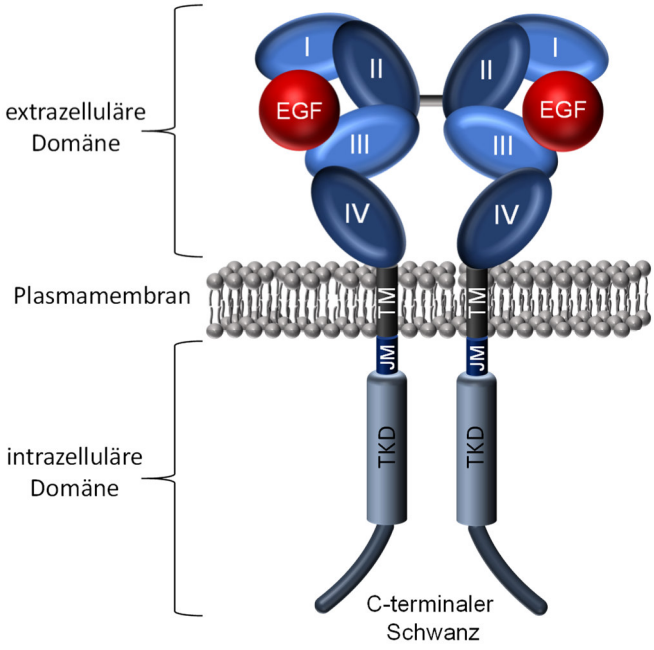

Abbildung 1.4: Schematische Darstellung des strukturellen Aufbaus eines EGF-Rezeptor-Dimers
Jeder EGFR besteht aus einer extrazellulären Domäne, die aus vier Sub-Domänen (I-IV) aufgebaut ist. An der Liganden-Bindung (hier EGF) sind die Domänen I und III beteiligt. Über eine Transmembran-Domäne (TM), die durch die Plasmamembran verläuft, ist die extrazelluläre Domäne mit der intrazellulären Domäne verbunden. Diese besteht aus dem sich an die Transmembran-Domäne anschließenden Juxtamembran (JM)-Segment, der Tyrosinkinase-Domäne und dem regulatorischen C-terminalen Schwanz. (Modifiziert nach [162])

Inaktive EGFR-Monomere stehen im Gleichgewicht mit inaktiven oder aktiven EGFR-Dimeren. Nach Liganden-Bindung kommt es zur Stabilisierung der aktiven EGFR-Dimere und dadurch zur Aktivierung der RTK [165; 166]. Neben der Homodimerisierung [167] kann es auch zur Ausbildung von Heterodimeren mit anderen ErbB-Familienmitgliedern kommen [168]. Zu den ausschließlich an EGFR bindenden Liganden zählen verschiedene Wachstumsfaktoren wie *transforming growth factor* (TGF)α [169], Amphiregulin [170], *extracellular protein factor* (EPF) [162] und der namensgebende epidermale Wachstumsfaktor EGF [171]. Durch Liganden-induzierte Aktivierung der Tyrosinkinase kommt es zu einer *trans*-Autophosphorylierung zahlreicher Tyrosinreste, die sich auf dem C-terminalen Schwanz befinden [172; 173]. Die phosphorylierten Tyrosinreste (pTyr) dienen als Andockstellen einer Vielzahl von intrazellulären Proteinen, welche beispielsweise *Src homology region 2* (SH2)- oder andere *phosphotyrosine-binding* (PTB)-Domänen besitzen [174-176]. Dadurch kommt es zur Aktivierung von Signalkaskaden wie dem PI3K/Akt/mTOR- [177; 178], *mitogen activated protein kinase / extracellular-signal regulated kinase* (MAPK/ERK)- [179] und Januskinase (JAK)/*signal transducers and activators of transcription* (STAT)-Signalweg [180-182; 165]. Die EGFR-Aktivität kann nicht nur durch extrazelluläre Liganden-Bindung, sondern auch durch intrazelluläre

Modulatoren reguliert werden, indem z.B. zytoplasmatische Faktoren mit der JM-Domäne interagieren [183]. Neben den C-terminalen Phosphorylierungen kann beispielsweise auch das im JM-Segment befindliche Threonin (T669) durch ERK phosphoryliert werden, was zu einer Herabregulierung des EGFRs führt [184]. Über die JM-Domäne kann der EGFR z.B. auch mit *ADP ribosylation factor nucleotide-binding site opener* (ARNO-Sec7), Calmodulin und Lipiddoppelschichten, die aus anionischen Lipiden bestehen, *in vitro* interagieren, was zu einer Autoinhibition führt [183; 185; 186].

Je nach aktiviertem Signalweg hat der EGFR einen Einfluss auf Proliferation, Differenzierung, Migration, Adhäsion und Apoptose [176]. Eine Fehlregulation der EGFR-Signalkaskaden führt somit zu diversen Erkrankungen wie beispielsweise Entzündungen [187], neurodegenerativen Erkrankungen [155] und zahlreichen Krebserkrankungen [158]. Umso wichtiger erscheinen eine permanente Kontrolle und Steuerung der EGFR-Signalrate zur Aufrechterhaltung der EGFR-Homöostase, die unter anderem durch Autoinhibition und Rezeptor-Internalisierung reguliert wird.

1.1.3.1 Rezeptor-Internalisierung

Die Regulation der Rezeptor-Homöostase geschieht durch Dephosphorylierung und/oder Internalisierung mit anschließendem Abbau oder Recycling des Rezeptors [188; 189]. In Abbildung 1.5 ist die EGF-Rezeptor-Internalisierung nach EGF-Bindung schematisch dargestellt. Diese kann entweder Clathrin-abhängig [122] oder Clathrin-unabhängig [190] sein, was von der EGF-Konzentration abhängig ist. Bei niedrigen EGF-Konzentrationen wird der Rezeptor vornehmlich über den Clathrin-abhängigen Weg internalisiert und eher nicht degradiert, sondern zur Zelloberfläche recycelt [191]. Demgegenüber wird der EGFR bei hohen EGF-Konzentrationen monoubiquitinyliert und Clathrin-unabhängig internalisiert, wobei es dann eher zu einer Degradation kommt [191]. Die Ubiquitinylierung von aktivierten Rezeptoren wird über *Casitas B-lineage Lymphoma* (CBL) [192], einer E3-Ubiquitin-Ligase, direkt oder indirekt über Adapterproteine, wie z.B. *growth factor receptor bound protein 2* (GRB2) vermittelt [193-196]. An der Ubiquitin-vermittelten endosomalen Sortierung des EGFRs sind zudem Proteine der endozytischen Maschinerie wie *epidermal growth factor receptor substrate 15* (EPS15) [197], Epsine [198] und diverse *endosomal sorting complex required for transport* (ESCRT)-Komponenten beteiligt [199-202]. Der EGFR kann über *intraluminal vesicles* (ILVs), die sich in *multivesicular bodies* (MVBs)/späten Endosomen befinden direkt dem lysosomalen Abbau zugeführt werden [203; 204]. Eventuell kann der

EGFR auch über Autophagosomen, die schlussendlich mit Lysosomen fusionieren, abgebaut werden [205]. Über Recycling-Endosomen kann der EGFR zurück zur Plasmamembran transportiert werden, wobei nicht ubiquitinylierte EGFRs eine höhere Recyclingrate aufweisen [206; 207; 202].

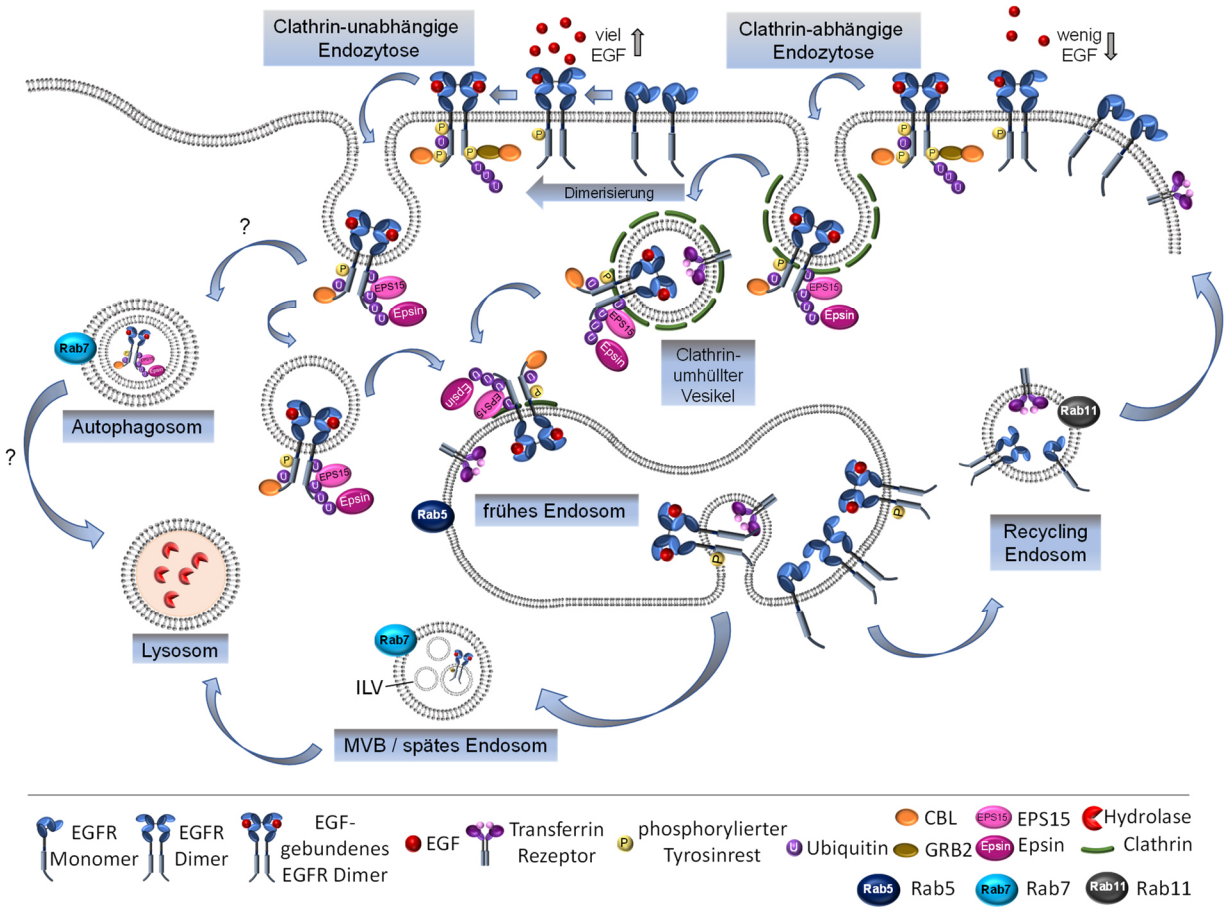

Abbildung 1.5: Epidermaler Wachstumsfaktor-Rezeptor (EGFR) Internalisierung
Nach Bindung des Liganden (EGF) kommt es vermehrt zu einer Dimerisierung der EGF-Rezeptoren, welche anschließend phosphoryliert werden. Die EGFR-Internalisierung ist EGF-konzentrationsabhängig. So kommt es bei hohen EGF-Konzentrationen eher zur Clathrin-unabhängigen und bei niedrigen EGF-Konzentrationen zur Clathrin-abhängigen Endozytose. Die Rezeptor-Ubiquitinylierung wird entweder direkt über CBL oder indirekt über das Adapterprotein Grb2, das an CBL bindet, vermittelt. Nach erfolgter (Mono)ubiquitinylierung wird der Rezeptor durch die Ubiquitin-bindenden Proteine EPS15 und Epsin über das frühe Endosom in *intraluminal vesicles* (ILVs) von *multivesicular bodies* (MVBs)/späten Endosomen transportiert und anschließend lysosomal abgebaut. Der Rezeptorabbau kann eventuell auch direkt über Autophagosomen, welche mit dem Lysosom fusionieren, geschehen. Rezeptoren, die nicht ubiquitinyliert sind, werden über Recycling-Endosomen zurück zur Plasmamembran transportiert. Der Transferrin-Rezeptor ist ein Paradebeispiel und kann neben Rab11 als Recycling-Marker dienen. Das Protein Rab5 dient als Marker für frühe Endosomen und Rab7 als Marker für späte Endosomen. (Modifiziert nach [202])

Ein oft genutzter Marker für den Recycling-Weg zurück zur Plasmamembran ist der Transferrin-Rezeptor (TrfR) (Abbildung 1.5). Der TrfR ist für den Transport von Eisen-gebundenem Trf (zwei Eisenmoleküle pro Transferrin) in das endosomale Kompartiment verantwortlich [208-210]. Der mit Eisen beladene TrfR wird internalisiert und das Eisen aufgrund des niedrigen pH-Wertes im Lysosom freigesetzt. Das nun nicht mehr eisengebundene, jetzt als Apotransferrin bezeichnete Molekül, welches noch am TrfR gebunden ist, entgeht dem lysosomalen Abbau und wird anschließend über das Recycling-Endosom zurück zur Plasmamembran transportiert. Beim Kontakt mit neutralem pH-Wert im extrazellulären Raum dissoziiert Apotransferrin vom Rezeptor und der Zyklus kann von neuem beginnen. [211-213]

1.1.3.2 *Ras-related in brain* (Rab)-Proteine

Bei der Rezeptor-Internalisierung durch endozytotische Vesikel sind unter anderem sogenannte Rab-Proteine [214], die zur Familie der kleinen GTP-bindende Proteine (GTPasen) gehören, beteiligt. Die Rolle der Rab-Proteine beim vesikulären Transport wurde zuerst in Hefe entdeckt [215]. Rab-Proteine sind evolutionär hochkonserviert und es sind bislang beinahe 70 verschiedene Rab-Proteine im Menschen entdeckt worden [216; 217]. Rab-Proteine sind essenzielle Regulatoren des intrazellulären Transports [218], der dadurch reguliert wird, dass Rab-Proteine Effektormoleküle wie Motorproteine, Hüllproteine, *tethering*-Faktoren, Kinasen und Phosphatasen rekrutieren [219; 220; 217].

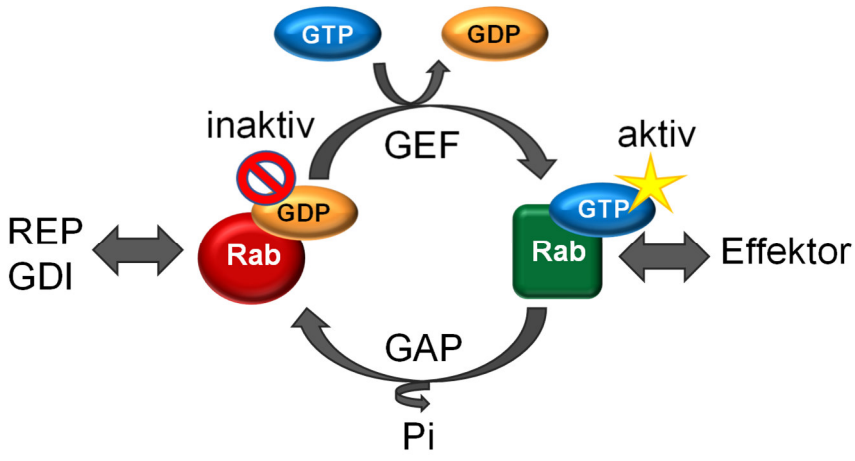

Abbildung 1.6: Funktionsweise kleiner Rab-GTPasen
Das Rab-Protein liegt, wenn Guanosindiphosphat (GDP) gebunden ist, inaktiv vor. Das *Rab escort protein* (REP) bindet an Rab, wodurch es zu einer Geranylgeranyl-Transferase vermittelten Prenylierung kommt, was eine Membranbindung des Rab-Proteins ermöglicht. Die Bindung eines *GDP dissociation inhibitors* (GDI) führt dazu, dass Rab im Zytosol gelöst vorliegt. Durch den *guanosin exchange factor* (GEF) wird der Austausch von GDP durch GTP vermittelt und Rab dadurch aktiviert. Folglich kommt es zur Rekrutierung von Effektorproteinen zur Membran. Die Inaktivierung der Rab-Proteine geschieht durch intrinsische GTPasen, die durch Rab *GTPase activating proteins* (GAPs) aktiviert werden. (Modifiziert nach [221])

In Abbildung 1.6 ist die Funktionsweise kleiner Rab-GTPasen schematisch dargestellt. Die Aktivierung der Rab-Proteine wird über den Austausch von Guanosindiphosphat (GDP) gegen GTP gesteuert, was durch den *guanosine exchange factor* (GEF) vermittelt wird [222]. Das unprenylierte Rab-Protein wird durch Bindung an ein *Rab escort protein* (REP) der Geranylgeranyl-Transferase präsentiert und durch sie prenyliert [219; 223] . Mit Hilfe ihrer C-terminalen Prenylierung können Rab-Proteine an Membranen binden und dadurch mit ihnen interagieren [224]. Nach Bindung eines GDP *dissociation inhibitor* (GDI) liegt Rab gelöst im Zytosol vor [225; 226]. In der GTP-gebundenen, aktivierten Form werden durch die Rab-GTPase diverse Effektorproteine zur Membran rekrutiert [221]. Das Ausschalten der Rab-Proteine geschieht durch intrinsische Rab-GTPasen, die durch Rab-GAPs (*GTPase activating proteins*) aktiviert werden [216].
Popovic *et al.* (2012) haben gezeigt, dass ATG8-Proteine direkt mit TBC (Tre2, Bub2, and Cdc16)-Domänen der Rab-GAPs interagieren und dadurch endosomale Transportwege mitsteuern können [227].

Einige Rab-Proteine wurden in dieser Arbeit als Endosomen-Marker eingesetzt (Abbildung 1.5). So findet man Rab5 auf der zytoplasmatischen Plasmamembranoberfläche sowie frühen Endosomen und Rab7 auf späten Endosomen [228]. Rab11 kontrolliert den Transport durch Recycling-Endosomen und kann neben Transferrin als ein Markerprotein für Recycling verwendet werden [229-231]. Unter Autophagie-induzierten Bedingungen wird der Transferrin-Rezeptor selbst als Autophagie-Substrat zu Autophagosomen transportiert und abgebaut, wobei Rab11a-positive Membranen als direkte Plattform für die kanonische Autophagosomen-Ausbildung dienen können [232].

Wie bereits in Kapitel 1.1.1 beschrieben, spielen Rab-Proteine nicht nur bei der Endozytose, sondern auch bei Autophagie eine Rolle, indem z.B. Rab7 an der Autophagosom-Lysosom Fusion beteiligt ist [35]. Neuere Veröffentlichungen weisen auf einen Zusammenhang von Autophagie und dem EGFR-Transport hin [147; 149]. So bindet der EGFR an Beclin1, das an der Phagophoren-Ausbildung beteiligt ist. Dadurch kommt es zur Tyrosin-Phosphorylierung an mehreren Stellen, was die Bindung von Inhibitoren begünstigt, die zu einer verminderten Beclin1-assoziierten VPS34 Kinaseaktivität führt [233]. Zudem haben Fraser *et al.* (2019) gezeigt, dass es bei Verlust Autophagie-essentieller Proteine zu einer Störung des EGF-induzierten endozytotischen EGFR-Transports kommt [149].

Zusammenfassend kann gesagt werden, dass Rezeptor-Tyrosinkinasen, zu denen der EGFR zählt, direkt und indirekt an der Regulation des Autophagie-Prozesses beteiligt sein können und in der Literatur bereits ein komplexer *cross-talk* zwischen Autophagie-beteiligten Komponenten und RTKs beschrieben werden konnte, da beide gemeinsame Signal- und Vesikel-Transportwege miteinander teilen [147; 151].

1.2 Methoden und Werkzeuge zur differenziellen Untersuchung humaner Atg8-Paraloge

Um einzigartige Funktionen der einzelnen Atg8-Paraloge sicher feststellen zu können, bedarf es eindeutiger Paralog-spezifischer Ergebnisse. Solche können beispielsweise unter Verwendung entsprechender KO-Zelllinien erbracht werden. Ein weiterer Ansatz ein bestimmtes Atg8-Paralog unter endogenen Bedingungen und zudem im Lebendzellmodus zu untersuchen, ist der Einsatz entsprechender KI-Zelllinien. Bei den sonst oftmals verwendeten Überexpressionslinien können durch zu hohe Proteinkonzentrationen Artefakte entstehen [234; 9]. So kann eine erhöhte ATG8-Proteinmenge in der Zelle zu Proteinaggregationen führen, wodurch es zum Abbau der ATG8s durch Aggrephagie, also dem selektiven Abbau der Proteinaggregate, kommen kann [235]. Um diesem Problem entgegen zu wirken, können *Clustered Regularly Interspaced Short Palindromic Repeats* (CRISPR)/Cas9-generierte KI-Zellen verwendet werden, in denen man z.B. ein Fluoreszenzmarkerprotein unter dem endogenen Promotor des zu untersuchenden Gens bzw. Proteins exprimieren lässt. Dadurch sind Untersuchungen wie z.B. Lebendzellmikroskopie von Proteinen auf endogenem Proteinniveau ohne Protein-Akkumulation möglich. Sterische Hinderungen aufgrund des relativ großen angehängten Fluoreszenzproteins (z.B. *green fluorescent protein* (GFP), 26,9 kDa) sind jedoch auch bei den KI-Zelllinien zu bedenken [236].

Alternativ können einzelne Paraloge im wildtypischen Kontext untersucht werden, wenn ein spezifischer Antikörper gegen dieses Paralog vorliegt. Dabei ist die Antikörperspezifität für jede verwendete Technik bzw. Methode erneut zu erörtern.

Aufgrund der hohen sequentiellen und strukturellen Homologie der ATG8s [96] und der bislang mangelnd vorhandenen und validierten, spezifischen Antikörper, ist eine genaue Untersuchung der endogenen GABARAP-spezifischen Rollen mittels IF-Färbung als schwierig erachtet worden [9]. Viele kommerziell erhältliche Antikörper sind, insbesondere für IF-Anwendungen, nicht ausreichend validiert und binden neben dem Zielprotein oft auch nahe verwandte Proteine, wodurch es zur sogenannten Kreuzreaktion kommt [237]. So kann

es sein, dass eine strukturell ähnliche Antigenbindungsstelle, auch Paratop genannt, fälschlicherweise vom Antikörper-Epitop, also der Proteinsequenz, die sich als Gegenstück zum Paratop auf dem Antikörper befindet, gebunden wird [238; 239]. Dies kann bei IF-Färbungen zu Fehlinterpretationen führen, da nicht nur das Zielprotein (z.B. GABARAP), sondern auch ein nahe verwandtes Protein (z.B. GABARAPL1) irrtümlich vom Antikörper detektiert werden kann [240]. Außerdem ist es bei der Auswahl des Antikörpers wichtig, dass der Antikörper für die jeweilige Anwendung validiert wurde, denn ein Antikörper, der im *Western Blot* spezifisch bindet, kann bei IF- oder Immunhistochemie-Färbungen, wo die Proben anders aufbereitet werden und das Protein gegebenenfalls in einem nativen Zustand vorliegt, unspezifisch binden [241; 242]. Die Validierung von Antikörpern kann unter anderem mit Hilfe von Zellen geschehen, in denen das zu untersuchende Protein herunterreguliert (*knockdown*, KD) oder bestenfalls vollständig ausgeschaltet (*knockout*, KO) wurde.

Da alle oben beschriebenen Möglichkeiten in dieser Arbeit Anwendung fanden, werden die zugrundeliegenden Techniken im Folgenden im Detail behandelt.

1.2.1 CRISPR/Cas9-basierte Genomeditierung zur Erzeugung von KO- und KI-Zelllinien

Ein mittlerweile weit verbreitetes Verfahren zur gezielten vollständigen Ausschaltung einzelner Gene und Funktionen (*loss of function*) oder auch zum gezielten Einbringen von Genen (KI) ist das CRISPR/Cas9-System, welches als Teil des adaptiven Immunsystems von Bakterien entdeckt wurde [243]. Im Vergleich zu den bis dato verwendeten transkriptionsaktivator-ähnlichen Effektornukleasen (*transcription activator-like effector nucleases*, TALEN) und den Zink-Finger-Nukleasen (ZNF) ist das CRISPR/Cas9-Verfahren hochspezifisch, effizienter, einfacher zu designen und insgesamt schneller in seiner Handhabung [243; 244], weshalb es inzwischen in der klinischen Forschung und Grundlagenforschung weit verbreitet ist [245]. Alle Genomeditierungsverfahren beruhen auf einer spezifischen *desoxyribonucleic acid* (DNA)-bindenden Region und einer unspezifischen Nuklease [245], die anschließend in der zuvor definierten DNA-Region gezielte Doppelstrangbrüche einbringt [246]. Diese werden anschließend durch natürliche DNA-Reparaturmechanismen wie der nichthomologen Endverknüpfung (*non-homologous end joining*, NHEJ) oder Homologie-vermittelten Reparatur (*homology-directed repair*, HDR) repariert [246; 247]. Die fehleranfällige NHEJ führt oft zu Insertionen oder Deletionen

(InDel), was eine Geninaktivierung zur Folge haben kann, wohingegen die HDR als eher fehlerfreier Reparaturmechanismus beschrieben wird und zur Einbringung von Gen-KIs verwendet werden kann [247].

Das CRIPSR/Cas9-System ist im Vergleich zu TALEN und ZFN weniger komplex. Der CRISPR/Cas9-Komplex ist lediglich aus der Cas9-Nuklease und einer 20 bp-langen *guide* (g)RNA aufgebaut, die entweder aus einer separaten CRISPR (cr)RNA-Sequenz und *trans-activating* crRNA (tracrRNA) oder einer chimären *single-guide* RNA (sgRNA)-Komponente besteht [248]. Die gRNA Sequenz ist komplementär zu der DNA-Erkennungsregion, wodurch die Schnittregion der Cas9-Endonuklease definiert werden kann. Zur Generierung eines Doppelstrangbruches durch Cas9 wird ein sogenanntes *protospacer adjacent motif* (PAM) in der Nähe der DNA-Erkennungssequenz benötigt [249; 243; 248]. Im Gegensatz dazu beruhen TALEN und ZFN alleinig auf Fusionsproteinen [245]. Die ZFN bestehen beispielsweise aus einer unspezifischen DNA-Spaltungsdomäne des *Fok*I-Restriktionsenzyms, die an eine Zinkfinger-DNA-Bindungsdomäne fusioniert ist [250].

1.2.1.1 Exemplarische Darstellung einer KO- und KI-Zelllinien Generierung mittels CRISPR/Cas9

Zur Erzeugung von Einzel-(*single*, S) KO- bzw. KI-Zelllinien mit Hilfe des CRISPR/Cas9-Systems werden die entsprechenden CRISPR/Cas9 KO- oder KI-Plasmide (z.B. basierend auf dem PX458-2A-GFP Plasmid, siehe unter 8.4) durch z.B. Elektroporation (Nukleofektion) in die gewünschten Zelllinien eingebracht (siehe Abbildung 1.7).

Bei der KI-Generierung kann das Gen mit Hilfe eines HDR-Plasmids, das zum PAM-Motiv flankierende Homologie-Arme beinhaltet und als Vorlage (*template*) für die Reparaturmaschinerie dient, gezielt in die favorisierte Insertionsstelle eingebracht werden. Nach 2-3 Tagen können die Zellen durch FACS entsprechend ihrer in diesem Beispiel gezeigten grünen Fluoreszenz nach erfolgreicher Transfektion einzeln in jeweils ein *well* einer *Multiwell*-Platte sortiert werden.

Durch die grüne GFP-Fluoreszenz wird lediglich eine positive Einbringung des KO/KI-Plasmids in die Zelle bestätigt. Es wird daraus nicht ersichtlich, ob und wie effizient die CRISPR/Cas9-vermittelte Genomeditierung erfolgt ist.

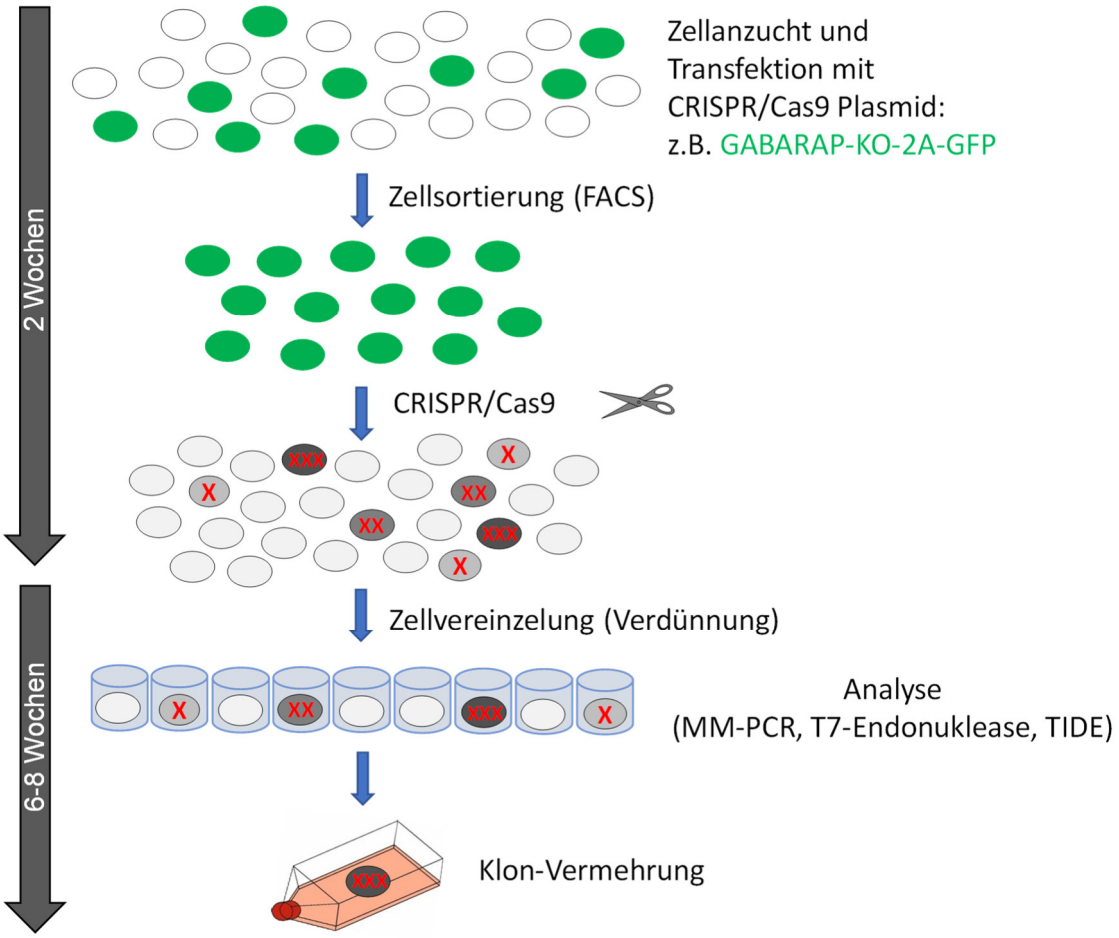

Abbildung 1.7: Erzeugung von KO-Zelllinien mit Hilfe des CRISPR/Cas9-Systems
Die erfolgreich transfizierten Zellen können durch die Expression des Fluoreszenzmarkerproteins GFP mittels FACS erkannt, sortiert und vereinzelt werden. Nach Regeneration und Vermehrung der vereinzelten Zellen werden diese hinsichtlich einer erfolgen Genomeditierung mittels *mismatch* PCR bzw. T7-Endonuklease Spaltungs-*Assay* analysiert und die Anzahl eingebrachter Insertionen und Deletionen (InDels) nach erfolgter Sequenzierung durch eine Software namens *Tracking of Indels by DEcomposition* (TIDE) ermittelt.

Da viele humane Zelllinien polyploid sind, also nicht zwei, sondern drei oder mehr Chromosomensätze besitzen können [251], ist das Generieren eines vollständigen homozygoten KOs bzw. KIs in vielen gängigen Zelllinien, wie z.B. in hypotriploiden HEK293-Zellen, eine Herausforderung. HAP1-Zellen, die einen nahezu haploiden Chromosomensatz besitzen [252] bieten hier Erleichterung, da für nahezu jedes Zielgen nur ein Editierungsevent notwendig ist. Unter den GFP-positiven Zellen können bei polyploiden Zellen solche mit KO/KI eines, zweier oder aller vorhandenen Genkopien sein. Um herauszufinden, ob es sich um homo- oder heterozygote KOs/KIs handelt, müssen die Zellen nachfolgend analysiert werden. Dies kann durch Mutationsanalysen, wie eine *mismatch* PCR bzw. einen T7-Endonuklease-*Assay* erfolgen. Die T7-Endonuklease erkennt DNA-Fehlpaarungen, *nicked* DNA, kreuzförmige DNA, *Holliday*-Strukturen und heteroduplexe DNA und schneidet diese, was durch eine Agarose-Gelelektrophorese sichtbar gemacht

werden kann [253-256]. Die DNA kann anschließend aus dem Gel ausgeschnitten, aufgereinigt und zur Sequenzierung geschickt werden. Die Sequenzierungsergebnisse können anschließend durch ein online verfügbares Programm namens *Tracking of Indels by DEcomposition* (TIDE) [257] gegen eine unveränderte Referenz-DNA abgeglichen und analysiert werden. Dadurch kann die Art, Anzahl und Position von InDels innerhalb der DNA-Sequenz ermittelt werden [257]. Zeigt die TIDE-Analyse Insertionen und/oder Deletionen, ist die Wahrscheinlichkeit hoch, dass es zu einem *frame shift* gekommen ist. Daraus resultierende verfrühte Stopp-Codons bedingen eine unvollständige Proteinbiosynthese des editierten Zielgens, meist sogar einen kompletten Stopp der jeweiligen Proteinsynthese aufgrund von *Nonsense-Mediated mRNA Decay* (NMD)-basierten Prozessen [258]. Eine weitere Analyse mittels *Western Blot* sollte anschließend als Nachweis eines vollständigen, auch auf Proteinebene vorhandenen KOs/KIs, durchgeführt werden. Die Zelllinie mit erfolgreichem KO/KI sollte ausreichend vermehrt und kryokonserviert werden, um für Versuche verfügbar zu sein.

Insgesamt wurde durch das CRISPR/Cas9-System eine einfachere und praktikablere Möglichkeit zur Erzeugung von KO-Zellen geschaffen [243]. Zu Beginn dieser Arbeit lagen PX458 (GFP)-KO-Plasmide mit jeweils bis zu drei verschiedenen sgRNAs zur Induzierung von Doppelstrangbrüchen in Exon 1, 2 oder 3 für die Editierung der humanen GABARAP-, GABARAPL1- und GABARAPL2-Genloci vor [259].

1.2.2 Herstellung monoklonaler Antikörper und des anti-GABARAP (8H5) Antikörpers aus Ratte

Bei Antikörpern wird zwischen polyklonalen und monoklonalen Antikörpern (mAb) unterschieden. Polyklonale Antikörper sind eine heterogene Misch-Population von Antikörpern, die an verschiedene Regionen auf dem Zielmolekül binden [260]. Bei den mAbs handelt es sich hingegen um eine einzige, aus einem Klon stammende Antikörperspezies, die nur ein spezifisches Epitop bindet [260]. Diese mAbs können mit Hilfe der Hybridom-Technik gewonnen werden.

1.2.2.1 Hybridom-Technik zur Herstellung monoklonaler Antikörper

Zur unbegrenzten Herstellung eines spezifischen monoklonalen anti-GABARAP Antikörpers wird die sogenannte Hybridom-Technik verwendet. Dieses Verfahren zur Herstellung von

mAbs wurde im Jahr 1975 von Georges Köhler und César Milstein entwickelt [261] und ist schematisch in Abbildung 1.8 dargestellt.

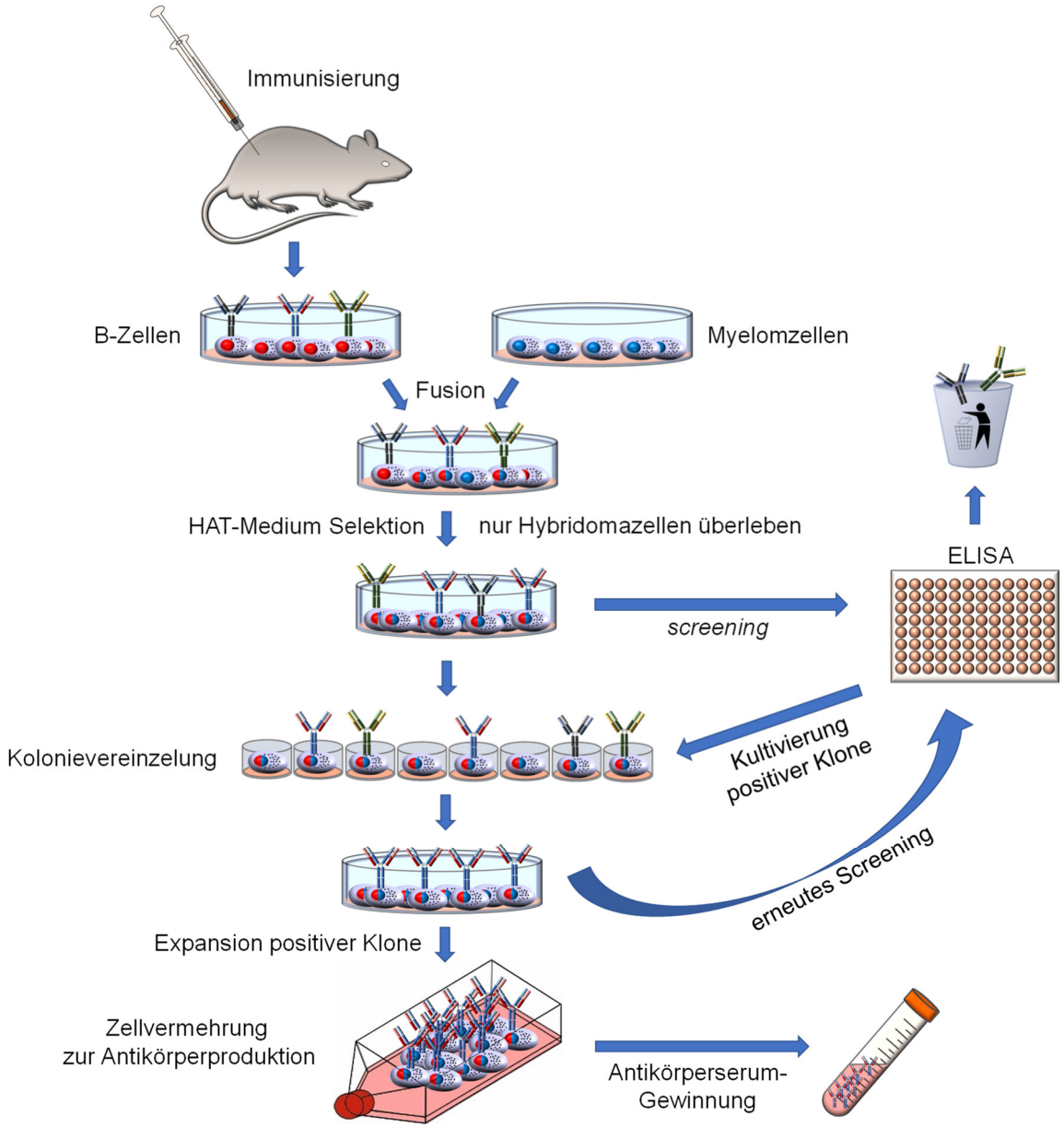

Abbildung 1.8: Monoklonale Antikörpergenerierung mit Hilfe der Hybridom-Technik
Zunächst wird z.B. eine Ratte immunisiert, welche daraufhin B-Zellen, welche teilweise den gewünschten Antikörper enthalten, produziert. Mittels Polyethylenglykol werden die B-Zellen mit immortalisierten Myelomzellen fusioniert und in einem Hypoxanthin, Aminopterin, Thymidin (HAT)-Selektionsmedium in einer *Multiwell*-Platte selektiert. Dabei sterben alle nicht erfolgreich fusionierten Zellen. Die überlebenden Hybridomazellen werden mittels ELISA auf den gewünschten Antikörper untersucht. Anschließend werden die positiven Zellklone vereinzelt und weiter kultiviert. Danach werden sie nochmals getestet und positive Zellklone expandiert, sodass ausreichend Antikörper-Serum gewonnen werden kann. (Modifiziert nach [239])

Zur Gewinnung großer Mengen eines homogenen Antikörpers wird bei dieser Technik ein Zellklon vermehrt, der aus einem B-Lymphozyt entstanden ist, der nur diesen einzelnen Antikörper produziert. Zur Gewinnung der entsprechenden Antikörper-produzierenden B-

Zellen werden zur Herstellung zunächst Nagetiere (z.B. Mäuse, Kaninchen oder Ratten) mit dem gewünschten Antigen, z.B. rekombinanten Proteinen oder kurzen Peptidfragmenten, immunisiert und die Antikörper-produzierenden B-Zellen aus der Milz (Splenozyten) entnommen. Da B-Zellen in Kultur nur eine begrenzte Überlebensdauer haben, wird eine Hybrid-Zelllinie (Hybridomazellen) generiert, indem die gewonnenen B-Zellen mit immortalisierten (unsterblichen) Myelomzellen (z.B. P3X63-Ag8.653), beispielsweise durch Polyethylenglykol (PEG), fusioniert werden [262]. Mit Hilfe eines Hypoxanthin, Aminopterin, Thymidin (HAT)-Selektionsmediums, in dem nur fusionierte Zellen mit Heterokaryon (also erfolgreich fusionierte Zellen) längere Zeit überleben können, werden die fusionierten Zellen in einer *Multiwell*-Platte selektiert. [263; 239; 238; 264; 265] Die aus den Hybridomazellen gewonnenen Zellkultur-Überstände werden zunächst mittels *enzyme-linked immunosorbent assay* (ELISA) auf den gewünschten Antikörper getestet. Nach erfolgreicher Identifikation von primären Überständen, die den gewünschten spezifischen Antikörper enthalten, werden die positiven Klone jeweils zweifach durch serielle Verdünnung vereinzelt (Subklonierung) und gegebenenfalls erneut mittels ELISA auf den gewünschten Antikörper getestet. Dadurch werden die Antigen-spezifischen Zellen von anderen Zellen separiert und eine chromosomal stabile IgG-produzierende Hybridomazelllinie selektiert. Positive Zellklone können nun im großen Maßstab kultiviert werden und als stetige Quelle für neue mAbs dienen. [266; 264; 239]

Der in dieser Arbeit zu validierende monoklonale anti-GABARAP (8H5) Antikörper beruht auf einer Kooperation unseres Institutes (Institut für Biologische Informationsprozesse (IBI) Strukturbiochemie (IBI-7), ehemals *Institute of Complex Systems* 6 (ICS-6)) mit der *Monoclonal Antibody (MAB) Core Facility* des Helmholtz Zentrums München.

Die aus den Hybridomazellen gewonnenen Zellkultur-Überstände wurden durch die MAB *Facility* mittels ELISA auf die gewünschten Antikörper getestet und positive Oligoklone kryokonserviert. Der anti-GABARAP (8H5) Antikörper ist einer von insgesamt 38 getesteten anti-GABARAP Antikörperseren.

Die Hybridoma-Überstände der anti-GABARAP positiven Zellen wurden anschließend zur weiteren Validierung in unser Institut geschickt, wo die Bindungsspezifität der anti-GABARAP Antikörper enthaltenen Hybridomaüberstände mittels ELISA getestet wurde [267]. Die Zellklone, bei denen im ELISA eine hohe Bindungsaffinität und GABARAP Spezifität ermittelt werden konnte, können nun auf Wunsch im großen Maßstab kultiviert werden. Die daraus gewonnenen Hybridoma-Überstände dienen fortan als stetige Quelle für neue mAbs. [266; 264; 239]

Insgesamt gingen aus der Selektion und den weiteren Analysen auf Spezifität und Bindungsstärke drei Ratte-anti-GABARAP (8H5, 23G3, 19G10) Antikörper-Klone, ein Ratte-anti-GABARAPL1 (1C2) und ein Maus-anti-GABARAPL2 (1E5) Antikörper-Klon erfolgreich hervor. Davon wurden neben dem anti-GABARAP (8H5) Antikörper, der von den drei untersuchten anti-GABARAP Antikörper Hybridoma-Überständen die höchste Spezifität für GABARAP aufwies, ebenfalls die Hybridoma-Überstände aus Immunisierungen mit von GABARAPL1 und GABARAPL2 abgeleiteten Peptidantigenen untersucht (siehe Kapitel 4.2).

1.2.2.2 Aufbau eines IgG-Antikörpers

In der Wissenschaft werden z.B. bei IF-Färbungen sehr oft Antikörper der Isotypklasse IgG als Primärantikörper eingesetzt, weshalb nachfolgend diese Subklasse näher erläutert wird. Der IgG-Subtyp trägt mit 75 % den Hauptimmunglobulin-Anteil im Serum mit einer Halbwertszeit von ca. 21 Tagen [238]. Es gibt beim Menschen vier IgG-Subklassen, die IgG_1-, IgG_2-, IgG_3- und IgG_4-Unterklasse, deren schwere Ketten entsprechend γ_1, γ_2, γ_3 und γ_4 heißen [239]. Bei IgG handelt es sich um ein Monomer, das aus drei konstanten (C) Domänen, einer variablen (V) Domäne und einer Gelenk-Region besteht. Die IgG-Klassen unterscheiden sich hinsichtlich der Anzahl und Lage der Disulfidbrücken (S-S), die die Ketten untereinander verbinden [238; 268]. In Abbildung 1.9 ist der schematische, vereinfachte Aufbau eines IgG_2-Immunglobulins, entsprechend des in dieser Arbeit validierten IgG_{2a}-anti-GABARAP (8H5) Antikörpers, dargestellt.

Die leichten Ketten bestehen jeweils aus einer variablen Domäne (V_L) und einer konstanten Domäne (C_L). Dabei werden in Säugetieren zwei Arten von leichten Ketten unterschieden, die κ- und λ-Kette. Die schweren Ketten sind jeweils aus drei konstanten Domänen ($C_{\gamma 2}1$, $C_{\gamma 2}2$, $C_{\gamma 2}3$) und einer variablen Domäne (V_H) aufgebaut. [269] Im Gegensatz zum IgG_1, wo zwei Disulfidbrückenbindungen die jeweiligen Gelenkregionen miteinander verbinden, sind beim IgG_2-Antikörper an dieser Stelle vier Disulfidbrückenbindungen vorhanden. Beim IgG_1-Isotyp verbindet die Disulfidbrückenbindung die leichte Kette C_L mit der schweren Kette $C_{\gamma 1}1$, während beim IgG_2-Isotyp die leichte Kette C_L mit der schweren Kette V_H über eine Disulfidbrücke verbunden ist. [238; 239] Zudem sind innerhalb der jeweiligen Domänen der leichten und schweren Ketten Disulfidbrücken vorhanden, welche in der vereinfachten Abbildung 1.9 nicht alle eingezeichnet sind.

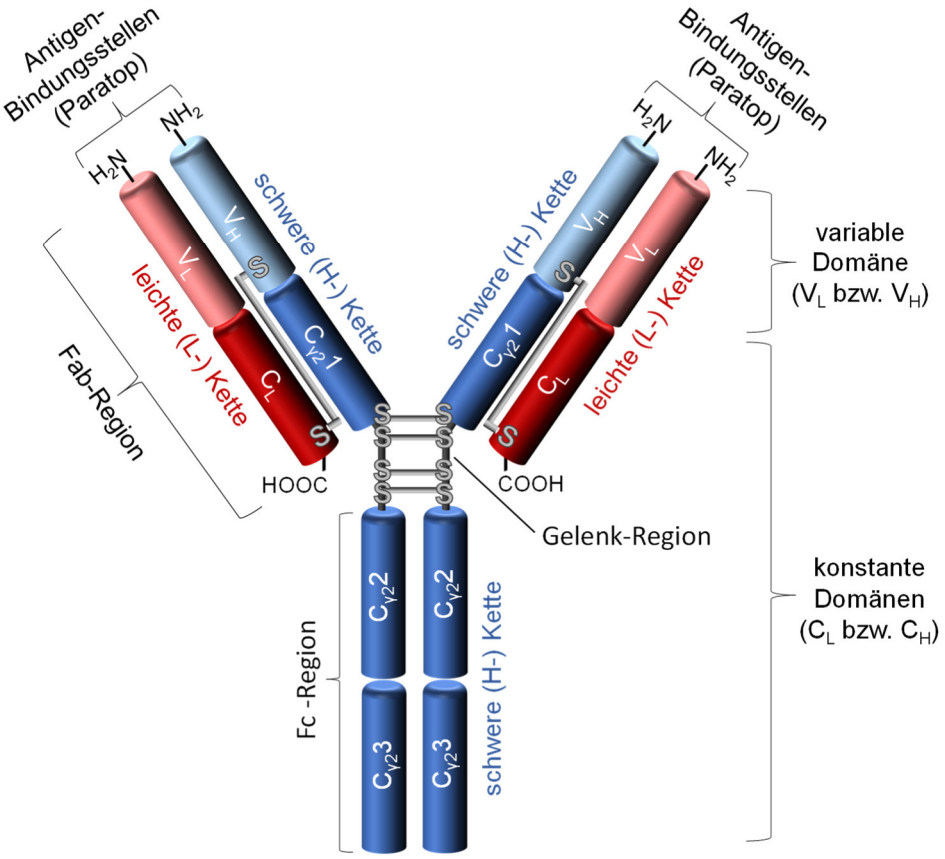

Abbildung 1.9: Schema einer IgG_2-Antikörperstruktur
Der IgG_2-Antikörper besteht aus zwei schweren (H-) Ketten, die jeweils aus 3 konstanten Domänen ($C_{\gamma2}1$-3) und einer variablen Domäne (V_H) aufgebaut sind und zwei leichten (L-) Ketten, die sich aus je einer konstanten (C_L) und einer variablen Domäne (V_L) zusammensetzen. Die Ketten werden über Disulfidbrückenbindungen (S-S) und eine Gelenkregion verbunden. Der untere Teil des Antikörpers wird *fragment crystallizable* (Fc)-Region und der obere Teil *fragment antigen binding* (Fab)-Region genannt. In der Fab-Region befindet sich die Antigen-Bindungsstelle (Paratop). (Modifiziert nach [238] [239])

Bei der enzymatischen Spaltung eines IgG-Antikörpers mit z.B. der Protease Papain entstehen drei Spaltungsfragmente, der Fc (*fragment crystallizable*)-Teil und zwei Fab (*fragment antigen binding*)-Fragmente. Unter der Fab-Region versteht man die Region, wo die Antigen-Bindungsstelle, das sogenannte Antikörper-Paratop, liegt. [270; 271] Das Gegenstück zum Paratop ist das Epitop, was einer Aminosäurensequenz im Zielprotein (z.B. GABARAP) entspricht. Die Fc-Region beinhaltet die konstanten Regionen unterhalb der Gelenkregion. [238; 239; 272; 269] Bei dem in dieser Arbeit validierten monoklonalen anti-GABARAP (8H5) Antikörper handelt es sich um einen aus mit Volllängen-GST-GABARAP immunisierten Ratten gewonnenen Antikörper der IgG_{2A}-Subklasse. Viele kommerziell erhältliche monoklonale Antikörper stammen aus Mäusen oder Kaninchen und eher selten aus Ratten. Da die Primärantikörper für eine gleichzeitige IF-Färbung aus jeweils einer anderen

Spezies stammen sollten, ist es aufgrund gleicher Abstammung der Primärantikörper oftmals nicht möglich IF-Färbungen mehrerer Proteine gleichzeitig durchzuführen. Mit Hilfe des aus Ratte stammenden anti-GABARAP Antikörpers ist eine Mehrfachfärbung leichter möglich, da z.B. eine Kombination von aus Maus, Ratte und Kaninchen abstammenden Antikörpern gewählt werden kann.

2 Ziele der Doktorarbeit

In den letzten Jahren wurden enorme Fortschritte im Bereich der Autophagie und der ATG-Proteine, zu denen auch die Familie der ATG8-Proteine gehört, erzielt. Bei der humanen ATG8 Familie, die aus der LC3- und GABARAP-Unterfamilie besteht, gibt es dennoch Wissensdefizite hinsichtlich spezifischer und redundanter Funktionen, insbesondere bei GABARAP und dessen Paralogen GABARAPL1 und GABARAPL2. Neben Autophagie liegt ein weiterer Fokus unserer Arbeitsgruppe (AG) auf der Untersuchung nicht-autophagischer Funktionen von GABARAP während Rezeptor-Transportprozessen, die anhand des EGFRs, der als Modell-Rezeptor-Tyrosinkinase dient, erforscht werden sollen.

Die ATG8-Familie und vor allem die jeweiligen Unterfamilien sind evolutiv hochkonserviert und weisen eine sehr hohe Sequenz- und Strukturhomologie auf, weshalb eine klare Unterscheidung der jeweiligen Funktionen nach wie vor als schwierig erachtet wird. Um funktionelle Redundanzen bzw. Einzigartigkeiten zweifelsfrei unter den GABARAPs ermitteln zu können, sind entsprechende Methoden und Werkzeuge zur Analyse notwendig. Dazu sollten zum einen diverse genomeditierte Zellen mit Defizienz einzelner oder einer Kombination verschiedener GABARAP-Paraloge und zum anderen ein entsprechend applikationsabhängig validierter Paralog-spezifischer Antiköper generiert und etabliert werden.

2.1 *Multi-color* FACS-fähige KO-Plasmide zur effizienten Erzeugung von Einzel-, Doppel- und Dreifach-KO-Zelllinien für GABARAP, GABARAPL1 und GABARAPL2

Zu Beginn dieser Arbeit waren außer den haploiden HAP1 Zelllinien mit (*single*, S) KOs für GABARAP, GABARAPL1 und GABARAPL2 (Horizon Discovery, Cambridge, UK) keine anderen Zelllinien mit SKOs dieser Proteine verfügbar. Ebenfalls waren keine Zelllinien mit einem Doppel- (*double*, D)- oder Dreifach- (*triple*, T)-KO, wie z.B. GABARAP/GABARAPL1^{DKO} oder GABARAP/GABARAPL1/GABARAPL2^{TKO} vorhanden oder in der Literatur beschrieben.

Aufgrund dessen sollte innerhalb dieser Arbeit ein System zur effizienten, möglichst simultanen Editierung der GABARAP, -L1, -L2 Genloci etabliert werden. Theoretisch sollte die Verwendung von drei Fluoreszenzproteinen mit entsprechend unterschiedlichen

Extinktions- und Emissionseigenschaften wie *enhanced green fluorescent protein* (EGFP, $488_{ex}/507_{em}$) [273; 274], *enhanced cyan fluorescent protein* (ECFP, $434_{ex}/477_{em}$) [275-277] und mCherry ($587_{ex}/610_{em}$) [278] eine Fluoreszenz-basierte Sortierung (FACS) erfolgreich transfizierter Zellen ermöglichen.

Als Basis dienten die bereits in der AG vorhandenen KO-Plasmide [259], die auf dem CRISPR/Cas9 PX458-2A-GFP Plasmid des Feng Zhang Labors (siehe 8.4) beruhen.

2.2 Validierung eines monoklonalen anti-GABARAP Antikörpers aus Ratte für die Immunfluoreszenz

Immunfluoreszenz (IF)-basierte Mikroskopietechniken gehören heute zu den Standardtechniken, um unter anderem Proteinlokalisationen innerhalb der Zelle oder Kolokalisationen eines Zielproteins und seiner möglichen Bindungspartner zu beobachten. Allerdings hängen die erhaltenen Ergebnisse von der Güte der verwendeten Antikörper ab. Nur wenn diese eine ausgeprägte Spezifität zum Zielprotein in dieser Anwendung zeigen, können letztlich brauchbare Ergebnisse erzielt werden.

Zu Beginn dieser Arbeit war weder ein kommerziell erhältlicher noch ein in der wissenschaftlichen Gemeinschaft gebräuchlicher anti-GABARAP Antikörper bekannt, der Spezifität für GABARAP in IF-Färbungen zeigte, also nicht mit GABARAPL1 oder GABARAPL2 kreuzreagierte. Deshalb sollte innerhalb dieser Arbeit ein zuvor an unserem Institut in Kooperation mit der monoklonalen Antikörper (MAB)-*Facility* des Helmholtz-Institutes in München entwickelter monoklonaler anti-GABARAP Antikörper aus Ratte hinsichtlich seiner Spezifität für die IF-Anwendung u.a. unter Zuhilfenahme entsprechender KO-Zelllinien validiert werden.

2.3 Mikroskopische Betrachtung möglicher GABARAP-abhängiger Transportprozesse des humanen EGF-Rezeptors

Im weiteren Verlauf dieser Arbeit sollten u.a. mit Hilfe der geplanten KO- und KI-Linien sowie durch Einsatz Paralog-spezifischer Antikörper Teilaspekte des erst kürzlich beobachteten GABARAP-vermittelten EGFR-*traffickings* untersucht werden. Hierbei sollten vornehmlich die konfokale *laser scanning microscopy* (LSM) sowohl im Lebendzellmodus als auch nach Fixierung sowie *spinning disk microscopy* (SDM) lebender Zellen Verwendung finden.

Unabhängig von obigen Projekten sollten besonders der zu validierende Paralog-spezifische anti-GABARAP Antikörper, nach Feststellung seiner Funktionalität in der IF, auf seine Tauglichkeit für die *single molecule localization microscopy* (SMLM) geprüft werden. Solange diese Überprüfung ausstand, sollten SMLM-basierte Studien zur Analyse von der Lokalisation und Größe GABARAP- bzw. LC3B-haltiger Strukturen im IBI-1 (Iman Abdollahzadeh und Thomas Gensch) durch die Bereitstellung entsprechender EYFP-GABARAP oder EYFP-LC3 (über)exprimierender Zelllinien unterstützt werden.

2.3.1 Komigrationsstudien von GABARAP und EGFR

Durch eine endogene Fluoreszenzprotein (FP)-basierte Markierungsstrategie, hier einem EGFP-KI am GABARAP-Genlokus, ist eine regulierte Expression entsprechender FP-GABARAP-Proteinfusionen unter dem eigenen Promotor möglich. Entsprechende homo- und heterozygote EGFP-KI GABARAP HEK293-Zelllinien sollten in dieser Arbeit in der Lebendzellmikroskopie eingesetzt werden, um die subzellulären Lokalisationen von GABARAP, EGFR und dem TrfR zu bestimmen. So sollten eventuelle Komigrationen von GABARAP mit den entsprechenden Rezeptormolekülen sichtbar gemacht und erste Erkenntnisse über beteiligte Zellkompartimente gewonnen werden.

2.3.2 Analyse der intrazellulären Transportprozesse von EGFR und GABARAP anhand der endosomalen Markerproteine Rab5, Rab7 und Rab11

Die endosomalen Transportprozesse von GABARAP und EGFR galt es in dieser Arbeit anhand von Färbungen zusammen mit den endosomalen Markerproteinen Rab5 (frühes Endosom), Rab 7 (spätes Endosom) oder Rab11 (Recycling-Endosom) in fixierten Zellen zu untersuchen. Mit Hilfe von Kolokalisationsauswertungen sollten putative Unterschiede des Protein-*traffickings* zwischen Wildtyp- und GABARAPs KO-Zellen analysiert werden.

3 Manuskripte

3.1 The highly GABARAP specific rat monoclonal antibody 8H5 visualizes GABARAP in immunofluorescence imaging at endogenous levels

Autoren:	Simons, I. M., Mohrlüder, J., Feederle, R., Kremmer, E., Zobel, T., Dobner, J., Bleffert, N., Hoffmann, S., Willbold, D.
Journal:	*Scientific Reports* **2019**, 9, 526 veröffentlicht am 24.01.2019
DOI:	10.1038/s41598-018-36717-1
Impact Factor:	4,011 (2018/2019), 5 Jahre: 4,525
Beitrag:	Klonierung, DNA-Präparation, Zellkultivierung Methodenetablierung und Versuchsdurchführung Mikroskopie (LSM710), Auswertung und Darstellung aller Immunfluoreszenz-Daten Anfertigung der meisten Abbildungen, statistische Auswertung Hauptverfasserin des Manuskriptes (gemeinsam mit S. Hoffmann)
Druckgenehmigung:	Dieser Abschnitt enthält eine vollständige Druckversion der Publikation publiziert in www.nature.com/scientificreports/

www.nature.com/scientificreports

SCIENTIFIC REPORTS
nature research

OPEN

Published online: 11 December 2019

Author Correction: The highly GABARAP specific rat monoclonal antibody 8H5 visualizes GABARAP in immunofluorescence imaging at endogenous levels

Indra M. Simons, Jeannine Mohrlüder, Regina Feederle, Elisabeth Kremmer, Thomas Zobel, Jochen Dobner, Nicole Bleffert, Silke Hoffmann & Dieter Willbold

Correction to: *Scientific Report* https://doi.org/10.1038/s41598-018-36717-1, published online 24 January 2019

This Article contains typographical errors in the Acknowledgements section.

"This study was funded by the Deutsche Forschungsgemeinschaft (DFG, German Research Foundation) – Projektnummer 190586431 – SFB 974, project B02 (D.W., I.M.S.), and project WE5343/1–1 (T.Z.), and by a grant from the Jürgen Manchot Foundation, Molecules of Infection Graduate School (MOI III) (D.W. and J.D.)."

should read:

"This study was funded by the Deutsche Forschungsgemeinschaft (DFG, German Research Foundation) – Projektnummer 267205415 – SFB 1208, project B02 (D.W., I.M.S.), and project WE5343/1–1 (T.Z.), and by a grant from the Jürgen Manchot Foundation, Molecules of Infection Graduate School (MOI III) (D.W. and J.D.)."

www.nature.com/scientificreports

SCIENTIFIC REPORTS

Corrected: Author Correction

OPEN

The highly GABARAP specific rat monoclonal antibody 8H5 visualizes GABARAP in immunofluorescence imaging at endogenous levels

Received: 8 March 2018
Accepted: 25 November 2018
Published online: 24 January 2019

Indra M. Simons[1], Jeannine Mohrlüder[2], Regina Feederle[3], Elisabeth Kremmer[4], Thomas Zobel[5], Jochen Dobner[1], Nicole Bleffert[1], Silke Hoffmann[2] & Dieter Willbold[1,2]

The determination of unique functions of GABARAP (gamma-aminobutyric acid type A receptor-associated protein), a member of the highly conserved protein family of mammalian autophagy-related 8 protein (mATG8), within diverse cellular processes remains challenging. Because available anti-GABARAP antibodies perform inadequate, especially within various microscopy-based applications, we aimed to develop an antibody that targets GABARAP but not its close orthologs. Following the latest recommendations for antibody validation including fluorescence protein tagging, genetic and orthogonal strategies, we characterized the resulting anti-GABARAP (8H5) antibody during confocal immunofluorescence imaging in-depth. We compared the antibody staining pattern with that obtained for fluorescence protein tagged GABARAP, GABARAPL1 or GABARAPL2 each ectopically expressed in GABARAP knockout cells. Furthermore, we imaged cells expressing all mATG8 family members at endogenous levels and checked GABARAP knockout cells for unspecific staining under fed or macroautophagy-inducing conditions. Finally, we simultaneously stained cells for endogenous GABARAP and the common autophagosomal marker LC3B. Summarized, the presented antibody shows high specificity for GABARAP without cross-reactivity to other mATG8 family members in immunofluorescence imaging making it a valuable tool for the identification of unique GABARAP functions.

Autophagy-related 8 (ATG8) proteins form a highly conserved eukaryotic protein family, which generate small-sized products of approximately 15 kDa with high overall structural similarities[1]. Contrary to the situation in yeast which has one single *Atg8* gene, mammalian genomes code for several ATG8 paralogs. The respective proteins are divided in two subfamilies: the microtubule-associated protein 1 light chain 3 (MAP1LC3) subfamily (referred to as LC3s) including LC3A, LC3B, LC3B2, LC3C, and the GABARAP (γ-amino-butyric acid receptor-associated protein) subfamily (referred to as GABARAPs) with GABARAP, GABARAPL1/GEC1 (GABARAP-like 1/Glandular epithelial cell protein) and GABARAPL2/GATE-16 (GABARAP-like 2/Golgi-associated ATPase enhancer of 16 kDa) in humans. Mammalian (m)ATG8s show ubiquitous expression patterns, although for some family members increased expression levels are documented in certain tissues and their expression underlies regulation through various mechanisms[2].

The broad action spectrum of these adaptor-like proteins with partially overlapping features is far from being completely understood[3]. First described to participate in the trafficking of type-A receptors for the neurotransmitter gamma-aminobutyric acid (GABA) in neurons[4], GABARAP, the prototype of the GABARAP subfamily, is implicated in a variety of intracellular transport processes including the shipping and correct organization of further receptors[5–7] as well as in autophagy, an evolutionarily highly conserved process essential for cellular

[1]Institut für Physikalische Biologie, Heinrich-Heine-Universität, 40225, Düsseldorf, Germany. [2]Institute of Complex Systems, Structural Biochemistry (ICS-6), Forschungszentrum Jülich, 52425, Jülich, Germany. [3]Institute for Diabetes and Obesity, Monoclonal Antibody Core Facility, 85764, Neuherberg, Germany. [4]Institute for Molecular Immunology, Helmholtz Center Munich, German Research Center for Environmental Health, 85764, Neuherberg, Germany. [5]Department of Biology, Center for Advanced Imaging (CAi), Heinrich-Heine-Universität, 40225, Düsseldorf, Germany. Correspondence and requests for materials should be addressed to S.H. (email: si.hoffmann@fz-juelich.de) or D.W. (email: dieter.willbold@uni-duesseldorf.de)

homeostasis[8]. Like all ATG8s, GABARAP can undergo lipidation by an ubiquitin-like conjugation system[9,10] promoting its association to autophagosomal membranes[11,12] but likely also to (tubule)vesicular structures in GABARAP-mediated protein trafficking[13]. Meanwhile, functional divergences between the divers ATG8s became obvious, like their action at different stages of autophagosome biogenesis as well as during autophagosomal cargo recruitment, where specific interactions with divers scaffolding proteins or autophagic receptors are formed in selective autophagy[3,14]. Within the mATG8s, LC3B is considered as an established and widely accepted marker for autophagosomes[15]. In this context, recent studies point towards a crucial role of the GABARAP subfamily members especially in autophagosome and lysosome fusion[16]. Under nutrient rich conditions, GABARAP was shown to accumulate in the pericentriolar material from which it can be translocated to forming autophagosomes during starvation[17,18].

Despite this apparent progress, elucidation of unique roles for individual ATG8 members within a specific process remains to be a challenging task. Although fluorescent protein (FP)-tagged ATG8 reporters, which are widely used to study autophagy as well as ATG8s' functions, delivered multiple new insights, their application might be accompanied by artifacts resulting from overexpression or steric hindrance due to the bulky FP-tag. In parallel, available antibodies against diverse ATG8 family members often show cross-reactivity, and are frequently not sufficiently validated in a transparent manner for the user, especially regarding their performance within diverse applications. As long as such information is lacking, every ATG8-targeted antibody result has to be interpreted with caution unless specificity of the antibody in use has clearly been demonstrated for the application and the ATG8 member chosen[15].

In this study, we performed an in-depth characterization of an in-house generated rat monoclonal antibody (mAb) against human (h)GABARAP (anti-GABARAP (8H5) antibody) by taking the latest recommendations for antibody validation into account[19]. Thereby, we focused on immunofluorescence (IF) staining, and included genetic (knockout (KO) cell-based), orthogonal (autophagosome counting under growth factor depleted conditions), tagged-target protein expression and independent antibody-based (commercial anti-GABARAP and anti-LC3B) strategies as validation pillars. Our analysis revealed that the anti-GABARAP (8H5) antibody shows high specificity for GABARAP without cross-reactivity for GABARAPL1, -L2 or LC3 subfamily members in our set-up. With the help of this antibody we investigated the colocalization of GABARAP and LC3B under endogenous conditions. To our knowledge, anti-GABARAP (8H5) antibody outperforms so far available antibody resources during localization studies in fixed cells, and thus reasonably enlarges our current tool box that is needed to identify unique GABARAP activities with high quality and consistency in an unambiguous manner.

Results

Anti-GABARAP (8H5) antibody discriminates between purified recombinant GABARAP, -L1, and -L2. In order to generate a monoclonal GABARAP antibody that is able to discriminate GABARAP from its various related ATG8 family members, rats were immunized with full-length hGABARAP fused to GST (glutathione S-transferase) (GST-GABARAP). After fusion of their immune spleen cells with the myeloma cell line P3X63-Ag8.653, the resulting hybridoma supernatants were collected and confirmed to react with immobilized GST-GABARAP by ELISA (enzyme-linked immunosorbent assay) (data not shown). Next, selectivity of in total 38 reacting supernatants was assessed using the dot blot technique. To this end, recombinant purified GABARAP, -L1, -L2 as well as the LC3s A, B, and C were spotted as target. Approximately 80% of the tested GABARAP-reactive supernatants failed this quality check, because, besides GABARAP, they also bound to its closest relative, GABARAPL1, as exemplarily shown for the supernatant corresponding to clonal line 8E5 (Fig. 1A, top panel). A few, among them anti-GABARAP (8H5) and anti-GABARAP (15A11) mAb containing supernatants, showed selective binding to GABARAP demonstrating their high specificity in this application (Fig. 1A, mid and bottom panels). Finally, binding specificity of anti-GABARAP (8H5) and (15A11) antibodies was confirmed by ELISA (Fig. 1B) and western blot analysis (Fig. 1C), respectively. Again, immunoreactivity could exclusively be detected for GABARAP but not the other family members in both applications. Besides its good selectivity, particularly anti-GABARAP (8H5) antibody revealed a very good signal-to-noise ratio of the GABARAP-related ELISA signal, assuming a considerably high affinity of anti-GABARAP (8H5) antibody to its given antigen, a promising feature for immunostaining applications with fixed cells.

Anti-GABARAP (8H5) antibody recognizes the GABARAP amino-terminal region. To identify the binding epitope of anti-GABARAP (8H5) antibody which was raised against full-length GABARAP, an array-based oligo-peptide scanning was performed. In total 54 dodecapeptides (12mers) with a peptide-peptide overlap of 10 amino acids, which represent the complete sequence of hGABARAP, were spotted on a cellulose membrane. Anti-GABARAP (8H5) antibody showed a strong signal with the fourth 12mer and weak signals with the adjacent 12mers three and five, suggesting that the epitope recognized by anti-GABARAP (8H5) antibody is formed by the GABARAP residues ranging from position 7 to 18 (Fig. 2A). The alignment of GABARAP, -L1, and -L2 shows that the epitope forming region is highly similar between GABARAP and GABARAPL1, with 10 out of 12 positions being conserved (GABARAPL2: 7/12). In contrast, this region is much more variable when GABARAP is compared with the LC3s (Fig. 2B). Structurally, the identified epitope overlaps with the second half of helix α1 and first half of helix α2 (Fig. 2C), which N-terminally extend the ubiquitin-like fold that is highly conserved between all hATG8s. With K13 and S16 both non-conserved epitope residues between GABARAP and GABARAPL1 (and also -L2) expose their sidechains for antibody binding (Fig. 2D), suggesting that K13 and S16 define binding specificity of anti-GABARAP (8H5) antibody.

Anti-GABARAP (8H5) antibody specifically stains YFP-GABARAP but not YFP-GABARAPL1 and CFP-GABARAPL2 in HAP1 GABARAP-KO cells by IF staining. In order to study if anti-GABARAP (8H5) antibody successfully stains GABARAP in IF application in fixed cells, YFP (yellow fluorescent

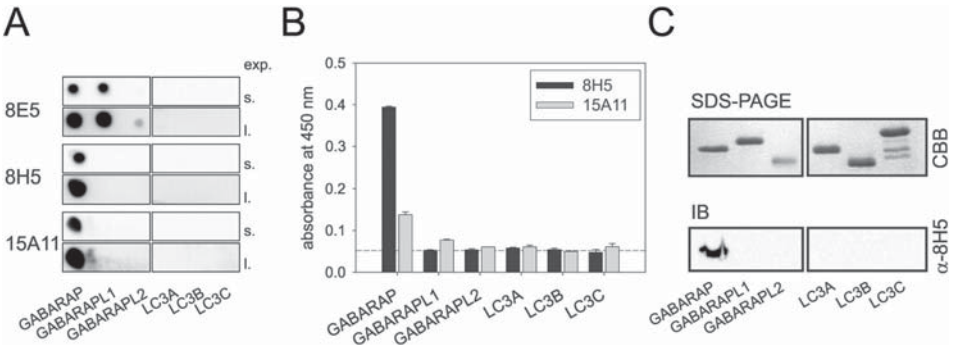

Figure 1. Anti-GABARAP (8H5) antibody does not react with LC3s and discriminates between GABARAP, GABARAPL1 and GABARAPL2. (**A**) Dot blots analysis using three different hybridoma supernatants to detect GABARAP binding and putative cross-reactivity to the other ATG8 family members. Purified recombinant proteins (10 µM each) were transferred to a cellulose nitrate membrane. Short (s.) and long (l.) exposure times of one representative blot each (n = 2) are given. (**B**) ELISA using anti-GABARAP (8H5) and anti-GABARAP (15A11) antibodies to confirm binding specificity and to assess the signal-to-noise ratio as a measure for mAb binding strength. Purified recombinant proteins (700 ng each) were coated on a 96-well plate and were incubated for 1 h at room temperature (RT) before antibody detection. Primary antibody containing hybridoma supernatants anti-GABARAP (8E5) and anti-GABARAP (15A11) and secondary goat anti-rat IgG-HRP antibody were incubated for 1 h at RT, respectively (n = 2). (**C**) Purified recombinant proteins (1 µg each) were subjected to SDS-PAGE in duplicate and were stained with Coomassie brilliant blue (CBB) to visualize the input or were used for immunoblotting with anti-GABARAP (8H5) mAb followed by HRP-coupled mouse anti-rat IgG2a antibody detection. Uncropped versions of (**A**) and (**C**) are given in Supplementary Fig. S3A,B.

protein)-GABARAP or YFP alone were transiently overexpressed in HAP1 GABARAP knockout (KO) cells. To do so, cells were incubated in growth factor-depleted medium in the presence of Bafilomycin A1 (BafA1). This macrolide antibiotic drug inhibits the vacuolar type H^+-ATPase (adenosine triphosphatase) and thereby blocks the autophagic flux by preventing the fusion between autophagosomes and lysosomes[20,21]. Under these conditions, the lipidated form of YFP-GABARAP is well known to be associated to the inner and outer lipid bilayer of mature autophagosomes, which under BafA1 treatment accumulates within the cytoplasm, and can be visualized easily as bright puncta in confocal imaging applications[2,12]. As expected, in the channel used for YFP detection, punctate YFP-GABARAP accumulations and a faint cytoplasmic stain were observed within the transfected HAP1 GABARAP KO cells (Fig. 3A, top, red). Likewise, immunostaining of these cells with anti-GABARAP (8H5) antibody and a secondary antibody conjugated with Cy5 produced many puncta (green) that showed a near to perfect colocalization with the YFP-GABARAP signals obtained (merge). In contrast, transfection with the YFP control vector produced fluorescence signals in the nuclear and cytoplasmic region solely in the channel for YFP detection (Fig. 3A, bottom, red), confirming that anti-GABARAP (8H5) antibody was reacting with the GABARAP part of the YFP-GABARAP fusion protein.

To further analyze the specificity of anti-GABARAP (8H5) antibody, plasmids encoding YFP-GABARAPL1 and CFP (cyan fluorescent protein)-GABARAPL2 were transfected in HAP1 GABARAP KO cells, respectively. Transfected cells showed fluorescence exclusively in the channels for YFP or CFP detection, but not after staining with anti-GABARAP (8H5) antibody (Fig. 3B), indicating that the antibody does not cross-react with its closest relatives, GABARAPL1 and GABARAPL2, even under overexpressing conditions.

Anti-GABARAP (8H5) antibody detects endogenous GABARAP, but not its close relatives -L1 and -L2 in IF. To further investigate if anti-GABARAP (8H5) antibody specifically stains endogenous GABARAP, HAP1 parental control cells expressing all ATG8s at endogenous levels, and HAP1 GABARAP KO cells, lacking GABARAP but expressing GABARAPL1 and -L2 were stained. Before fixation and immunostaining with anti-GABARAP (8H5) antibody, HAP1 cells were cultured in complete growth medium (IMDM + 10% FCS) without BafA1 or under growth factor deprivation (IMDM w/o FCS) with BafA1 to accumulate autophagosomes in the cells. As expected, we obtained a prominent cytoplasmic stain accompanied with some punctate structures when staining parental HAP1 cells with anti-GABARAP (8H5) antibody under basal autophagic conditions (Fig. 4A, top. left). After growth factor depletion and BafA1 treatment, anti-GABARAP (8H5) antibody staining revealed an accumulation of many bright GABARAP-positive puncta (Fig. 4A, top, right). Only a weak background stain was obtained with anti-GABARAP (8H5) antibody when cells lacking GABARAP but expressing all the other ATG8s at endogenous levels were used (immunoblot (IB) results of GABARAPL1, -L2 in HAP1 KO cells: please refer to Supplementary Fig. S1). A quantitative analysis of in total 513 parental cells and 460 GABARAP KO cells from 5 separate stains imaged under growth factor depletion and BafA1 treatment is given in Fig. 4B, confirming the selectivity of anti-GABARAP (8H5) antibody for GABARAP at high significance ($p < 0.0001$).

In parallel, we also tested three commercially available anti-GABARAP antibodies. Each of them selectively detects GABARAP in immunoblotting upon SDS-PAGE (see Supplementary Fig. S1B). Interestingly,

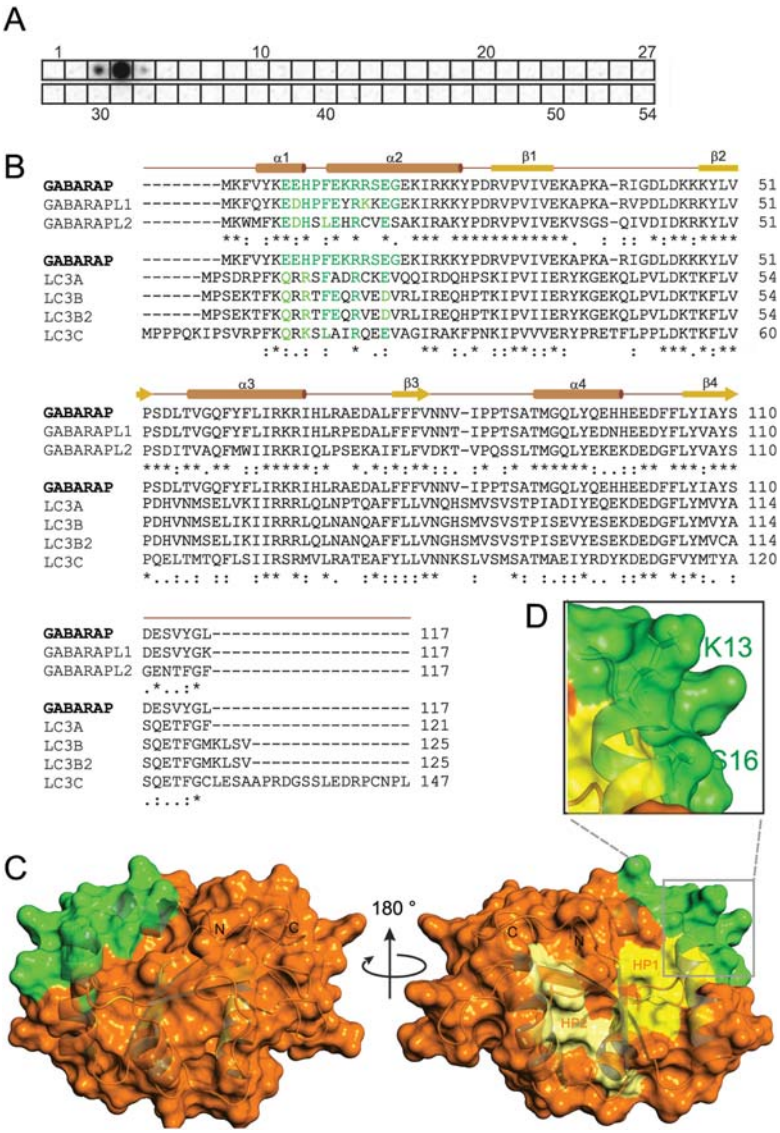

Figure 2. Anti-GABARAP (8H5) antibody binds an amino-terminally located epitope within GABARAP. (**A**) Peptide scanning was performed using a cellulose membrane loaded with 12mer peptides representing the complete sequence of human GABARAP and overlapping by 10 amino acids, respectively. Bound anti-GABARAP (8H5) antibody was detected using HRP-coupled mouse anti-rat IgG2a secondary antibody. Shown is one representative result. For reason of clarity peptide spot positions are boxed. Figure S3C includes source blots and membranes. (**B**) Sequence alignment of the GABARAPs (top) and of GABARAP with the LC3 family members (bottom) using Clustal Ω[42]. Regular secondary structure elements are depicted above the GABARAP sequence. The identified anti-GABARAP (8H5) antibody epitope is colored green within the GABARAP sequence. Identical residues in the sequences of the homologs listed are depicted in green, while highly similar residues are highlighted in light green. (**C**) Illustration of the anti-GABARAP (8H5) antibody epitope on the GABARAP structure (PDB ID: 1KOT) shown as combined ribbon and surface diagram using PyMOL (v1.860). Residues forming the epitope are shown in green, those forming the hydrophobic pockets HP1 and HP2 are colored dark and light yellow, respectively. In (**D**) the side chains of K13 and S16 are highlighted to illustrate their surface exposure and availability for anti-GABARAP (8H5) antibody binding.

the same antibodies showed pronounced unspecific staining in GABARAP KO cells during IF in our hands (see Supplementary Fig. S2), justifying the need for an in-depth application-based antibody characterization, and impressively illustrating that specificity features of antibodies should not be transferred between

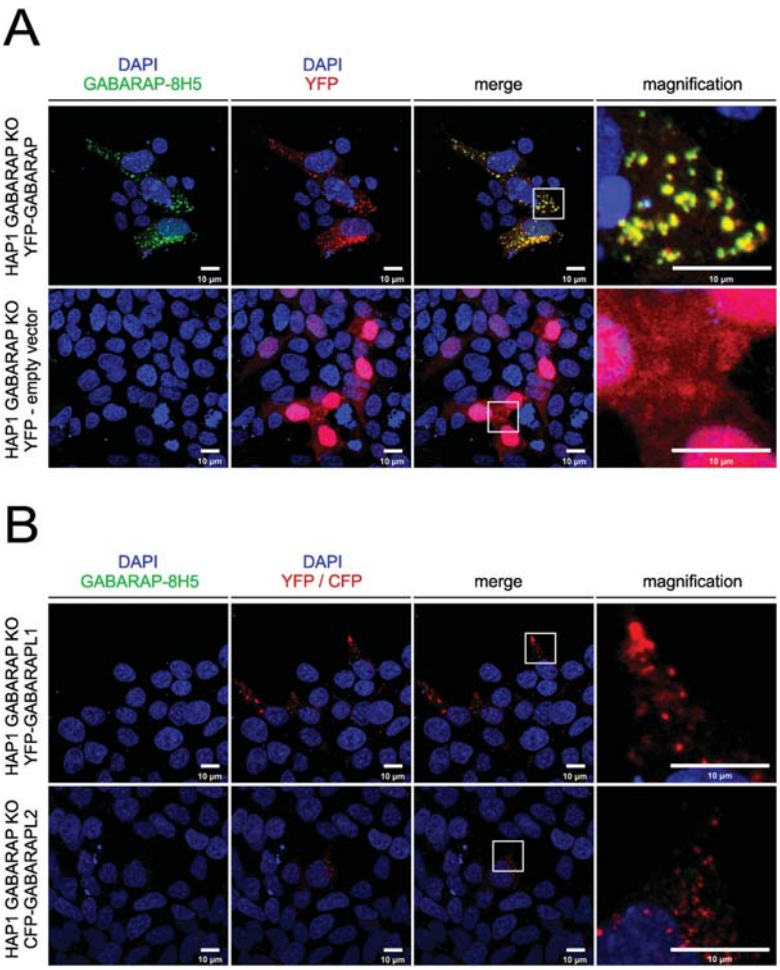

Figure 3. Anti-GABARAP (8H5) antibody detects YFP-GABARAP, but not YFP-GABARAPL1 and CFP-GABARAPL2 in immunofluorescence. HAP1 GABARAP KO cells were transfected with YFP-GABARAP and YFP-empty vector (**A**) or YFP-GABARAPL1 and CFP-GABARAPL2, respectively (**B**). After 48 h cells were incubated for 3 h with 100 nM Bafilomycin A1 (BafA1) in growth factor depleted medium (w/o FCS). Fixed cells (4% PFA) were immunolabeled with anti-GABARAP (8H5) antibody. Colocalization of GABARAP (green) and YFP (red) is indicated by yellow puncta. Nuclei were counterstained with DAPI.

different applications without separate experimental proof. In addition, we examined the performance of the anti-GABARAP (8H5) antibody in tissue sections in a preliminary manner. Therefore, two brain regions (motor-cortex, hippocampus) derived from mice with a GABARAP$^{+/+}$ background were applied to IF. In contrast to the negative control clear intracellular staining of different intensities could be obtained only in presence of anti-GABARAP (8H5) antibody (Supplementary Fig. S4). Thus, this anti-GABARAP antibody might also be applicable for IF-labelling of tissue sections.

Anti-GABARAP (8H5) antibody distinguishes LC3B^{+}/GABARAP^{+} from LC3B^{+}/GABARAP^{-} vesicular structures in two-color IF. Finally, we tested anti-GABARAP (8H5) antibody performance in two-color IF applications and chose LC3B as the second hATG8 to be targeted (to our knowledge, GABARAPL1 and -L2 trustworthy antibody-based analysis tools for IF are yet still lacking). We used anti-LC3B mAb clone 5F10 (anti-LC3B (5F10)), because this antibody reliably detects LC3B only and not the other LC3 family members[22]. LC3B is a common marker for autophagosomal structures[23], and consequently, anti-LC3B (5F10) antibody (Fig. 5A in red) stained a multitude of autophagosomes coated with endogenous LC3B under growth factor depletion and BafA1 treatment, regardless whether HAP1 parental or HAP1 GABARAP KO cells were imaged. Overall, anti-GABARAP (8H5) antibody (green) stained a smaller number of punctate structures compared to anti-LC3B (5F10) antibody in the parental cell line. Clearly, magnification and intensity plot (Fig. 5B) revealed that several of the imaged bright puncta are positive for LC3B but are negative for GABARAP under the conditions used. A comparable staining pattern, but with less GABARAP positive puncta after starvation, could also be observed in

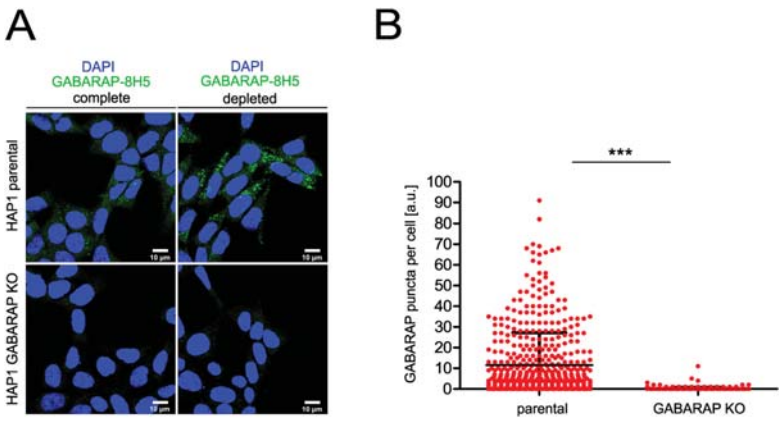

Figure 4. Anti-GABARAP (8H5) antibody specifically detects endogenous GABARAP in immunofluorescence. (**A**) HAP1 parental and GABARAP KO cells were incubated for 4 h in complete growth medium (IMDM + 10% FCS) and growth factor depleted medium (IMDM w/o FCS) with 100 nM Bafilomycin A1 (BafA1), respectively. Fixed cells were immunolabeled with anti-GABARAP (8H5) antibody. Nuclei were counterstained with DAPI. (**B**) Counted GABARAP puncta per cell in HAP1 cells. HAP1 cells grown under growth factor deprivation and BafA1 incubation (**A**) were analyzed. GABARAP puncta per cell from five individual experiments were measured in parental (n = 513) and GABARAP KO (n = 460) cells by Fiji analysis tool in combination with an in-house developed macro for puncta analysis. Error bars represent mean ± SD. Significance was determined using unpaired one-tailed t-test with Welch's correction (***$p < 0.0001$).

human embryonic kidney 293 (HEK293) cells (Supplementary Fig. S5). This is consistent with the common view that LC3s and GABARAPs have concerted but also can exhibit distinct, non-overlapping intracellular localizations, which is accompanied with at least partial functional divergences[2,16,22,24,25].

Discussion

Antibodies rank amongst the most widespread tools in basic life science research. Concurrently, an extensive discourse regarding antibody performance is ongoing with the task to guard against misleading conclusions drawn from experiments that included insufficiently validated antibodies[19,26]. A validated antibody must show specificity, selectivity, and reproducibility in the context of its application. But antibody validation beyond the datasheet knowledge can be tedious, is frequently underestimated, and thus is widely ignored in project scheduling. By comparing antibody-based IF stains with their respective fluorescence protein (FP)-tagged antigen location, a recent report impressively demonstrates the high error rates of inadequately validated polyclonal antibodies during IF applications under high throughput conditions[27].

Autophagy as well as the characterization of mATG8 function, one of the key players in this process, is subject of intensive studies. Because autophagy is proven to take part in several human e.g. neurodegenerative diseases[28,29], deciphering the common and the unique features of individual ATG8 family members would contribute to our understanding of their underlying molecular mechanisms. Antibodies specific for each single mATG8 would improve the toolbox needed to elucidate the unique ATG8s' functions. GABARAP, -L1, and -L2 are closely related, short-sized proteins with 117 aa (or 116 aa post processing through ATG4) in length. They, *per se*, display a limited number of epitopes, and cross-reactivity with antibodies that originally had been raised against one of their relatives, have frequently been observed in the past[15]. However, some of the available anti-GABARAP, -L1, and -L2 antibodies exhibit a specific performance with denatured proteins, e.g. in western blotting (Supplementary Fig. S1). To our knowledge, no single antibody with proven specificity during IF has been described in the literature yet. The reason for this may be that the number of exposed linear epitopes, and thus the chance of targeting a unique epitope (as basis for antibody specificity), is generally higher under denaturating than under native or semi-native conditions. Conversely, discontinuous epitopes are destroyed by denaturation, but are exposed under native or semi-native conditions, e.g. as prevailing during dot blot, ELISA or after mild cross-linking used in bio-imaging.

In this study, we positively-screened almost 40 cell clones, which generate monoclonal antibodies against hGABARAP. Out of them, we established and characterized clone 8H5 in particular with the aim to validate its performance especially during IF. In sum, hybridoma supernatants containing anti-GABARAP (8H5) antibody showed high specificity for GABARAP without cross-reactivity for the other (recombinant and purified) ATG8 homologues GABARAPL1, -L2 or LC3A, -B, and -C both in dot blot (Fig. 1A) and in western blotting (Fig. 1C). In addition to its good selectivity anti-GABARAP (8H5) antibody was our best performer during ELISA regarding binding strengths (Fig. 1B). Notably, anti-GABARAP (8H5) antibody failed to detect endogenous, SDS-PAGE-separated GABARAP from mammalian cell lysates during subsequent IB in our hands. Possible reasons are the low abundance of GABARAP in cell lysates compared to the applied amount of purified recombinant protein samples in Fig. 1C and/or the denaturation of the epitope recognized by 8H5 during western blotting[30,31]. Interestingly, epitope mapping of anti-GABARAP (8H5) antibody revealed that it interacts with the

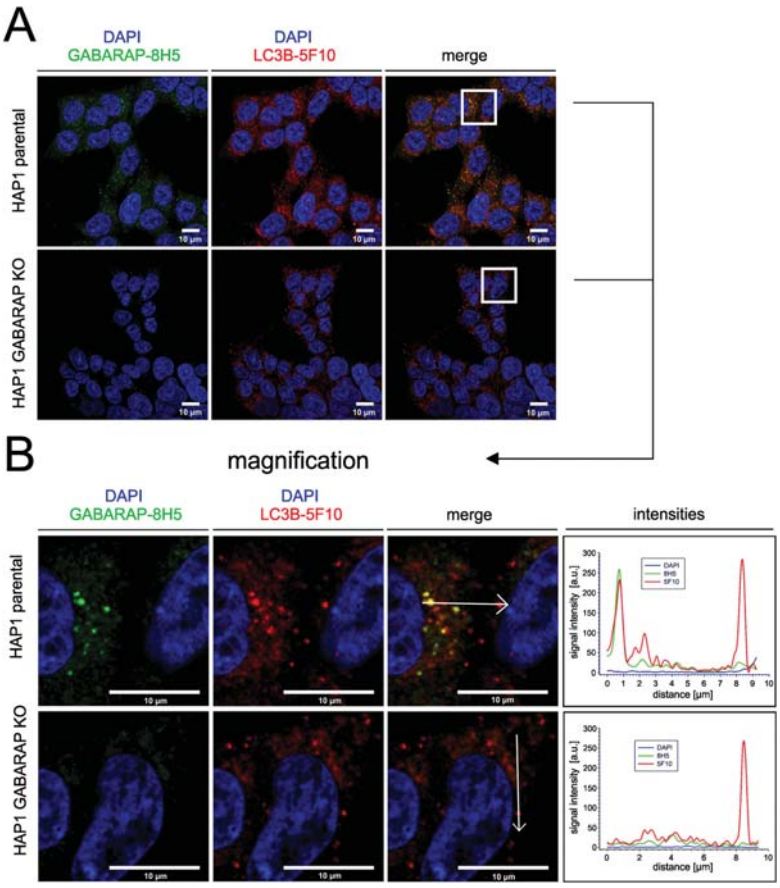

Figure 5. Anti-GABARAP (8H5) antibody detects endogenous GABARAP within some but not all LC3B$^+$ structures. (**A**) HAP1 parental and GABARAP KO cells were incubated for 3 h with 100 nM BafA1 in growth factor depleted medium. HAP1 cells were fixed with 4% PFA and immunolabeled with anti-GABARAP (8H5) and anti-LC3B (5F10) antibodies. Colocalization of LC3B (red) and GABARAP (green) is indicated by yellow puncta. Nuclei were counterstained with DAPI. (**B**) Intensity profiles of line segments (approx. 10 µm) drawn across the z-section shown for each channel. Overlap of anti-LC3B (5F10) (red) and anti-GABARAP (8H5) (green) antibodies' fluorescence intensity profiles (arbitrary units, a.u.) indicates colocalization of GABARAP with the autophagosomal marker LC3B.

α–helices 1 and 2 containing region (Fig. 2), suggesting that the existence of some α-helical secondary structure supports its efficient binding. According to the GABARAP structure a proper positioning of the non-conserved residues K13 and S16, which both are located within the binding epitope might be pivotal through acting as a GABARAP-unique platform for antibody binding. Because the complete GABARAP protein was applied as immunogen, it is likely, that under native conditions further parts of the GABARAP molecule contribute here by delivering the required scaffold for an optimal epitope presentation.

Following the latest recommendations for antibody validation[19], we next characterized the performance of anti-GABARAP (8H5) antibody during IF staining applications in-depth. We compared the anti-GABARAP (8H5) antibody-based staining with that of FP-tagged GABARAP, GABARAPL1, and GABARAPL2 ectopically expressed in HAP1 cells lacking endogenous GABARAP (Fig. 3A,B). Next, we compared the staining pattern of cells expressing all mATG8 family members at endogenous levels with that of cells lacking GABARAP, both under fed and growth-factor depleted/BafA1-treated conditions (Fig. 4). Furthermore, cells were simultaneously stained with anti-GABARAP (8H5) antibody and an antibody specifically recognizing LC3B, which is a common and independent marker for autophagosomes (Fig. 5).

Taken together, our results demonstrate that anti-GABARAP (8H5) antibody performs with high specificity in IF experiments. To our knowledge, we hereby provide the first staining results of endogenous GABARAP with an application- and target-specific in-depth validated antibody. In our opinion, this antibody can be very valuable for future studies that are aimed to resolve unique GABARAP functions in diverse cellular processes with already proven or assumed GABARAP-participation including autophagy, protein trafficking or unconventional secretion.

Recently, fluorescence protein-tagged, peptide-based sensors that can target mATG8s in a (semi)-specific manner have been published[32,33]. These sensors are based on peptides with LC3-interacting region (LIR) properties, showing selectivity, e.g. for GABARAP/GABARAPL1- or LC3B/LC3A-positive autophagosomes[32], or even for individual mATG8s[33]. Here, further engineering including the addition of domains for membrane recruitment or oligomerization, was necessary to achieve both selectivity and sufficient affinity of these sensors. While such sensors are very valuable for live-cell visualization of membrane-associated, lipidated mATG8 forms, and those ATG8 populations without tightly complexed intracellular LIR-containing binding partners, they likely fail to visualize both their soluble, unlipidated forms and their LIR-ligand complexed forms. We assume that anti-GABARAP (8H5) antibody can react with unlipidated GABARAP, and - because its epitope is largely separated from HP1 and HP2 - with such GABARAP molecules that are bound to an LIR-ligand. However, because its epitope includes with K13 one of the two ubiquitination sites (K13, K23) that recently have been identified for GABARAP[18], at least the K13-ubiquitinated GABARAP fraction will very likely not be stained by anti-GABARAP (8H5) antibody. Since its epitope overlaps with the microtubule-binding domain (amino acid residues 1–22) of GABARAP[34], further work is needed that has to clarify how anti-GABARAP (8H5) antibody performs with potentially microtubule-associated GABARAP molecules. Thus, anti-GABARAP (8H5) antibody not only discriminates GABARAP from its relatives but also opens avenues to distinguish between distinct cellular pools of GABARAP itself, a feature that can help to decipher distinct roles for the diverse variations of the same protein. Finally, because mammalian GABARAP sequences display 100% conservation, anti-GABARAP (8H5) antibody can be broadly used across mammalian species. Even within orthologous proteins from less related vertebrate, arthropode and nematode model organisms the anti-GABARAP (8H5) antibody epitope surrounding region is highly conserved (Supplementary Fig. S6). Thus, this antibody will likely be useful also in non-mammalian species. For improved results, the combination with anti-rat IgG2a subclass-specific secondary antibodies, especially for multiple labeling methods, is recommended.

Methods

Eukaryotic plasmids. Genes for GABARAP, GABARAPL1 and GABARAPL2 were subcloned from GST-fusion plasmids (Addgene IDs 73948, 73945 and 73518) by PCR amplification into the XhoI and BamHI sites of peYFP-C1 or peCFP-C1(Clontech), yielding peYFP-C1/GABARAP, peYFP-C1/GABARAPL1 and peCFP-C1/GABARAPL2.

Antibodies. The antibodies used throughout this study are listed in Supplementary Table S3.

Recombinant protein/antigen expression and purification. Cloning, expression and purification of human GABARAP (aa 1–117), GABARAPL1 (aa 1–117), GABARAPL2 (aa 1-117), MAP1-LC3A (aa 1–121), MAP1-LC3B (aa 1–125) and MAP1-LC3C (aa 1-147) was performed as previously described[35,36].

Antibody generation. Purified full length GABARAP protein N-terminally fused to glutathione-S-transferase (GST) was used as antigen for immunization. Approximately 50 µg of antigen dissolved in phosphate-buffered saline (PBS) was emulsified in an equal volume of incomplete Freund's adjuvant (Sigma-Aldrich, Germany) and 5 nmol CpG2006 (TIB MOLBIOL, Germany) and injected both intraperitoneally (ip) and subcutaneously (sc) into Lou/C rats. After 6 weeks, the animals received a booster injection (sc and ip) with 50 µg of antigen without Freund's adjuvant. Fusion of the myeloma cell line P3X63-Ag8.653[37] with immune spleen cells was performed according to the standard procedure described by Köhler and Milstein[38]. After fusion, the cells were cultured in 96-well cluster plates in standard medium supplemented with 20% fetal calf serum (FCS), 2% HCS (Capricorn Scientific, USA), and aminopterin (Life Technologies, Germany).

Hybridoma supernatants were tested in a solid-phase enzyme-linked immunoassay (ELISA). Plates were coated overnight with mouse-anti GST antibody (5 µg/ml) and after blocking with 2% FCS, GST-GABARAP fusion protein was added at 0.7 µg/ml for 60 min. Irrelevant GST-fusion protein served as negative control. Hybridoma supernatants (1:10 diluted) were added and GABARAP-bound antibodies were detected with a mixture of horseradish peroxidase (HRP)-coupled mouse monoclonal antibodies against rat IgG heavy chains. The secondary antibodies were visualized with 3,3′,5,5′-tetramethylbenzidine (TMB) substrate (Thermo Scientific, Germany) by measuring the absorbance at 650 nm with a microplate reader (Tecan, Switzerland). The IgG subclass was determined by ELISA with mouse anti-rat light chain antibodies as capture and HRP-coupled mouse anti-rat IgG subclass-specific antibodies for detection. The hybridoma cells of clone 8H5 (IgG2a/k) were stably subcloned twice by limiting dilution.

Dot blot analysis. Purified ATG8 family proteins (GABARAP, GABARAPL1, GABARAPL2, LC3A, LC3B and LC3C) were adjusted to a final concentration of 10 µM, respectively. 1 µl of each solution was transferred to a cellulose nitrate membrane considering an adequate spacing between all spots. After 5 min, membranes were blocked with tris-buffered saline-tween (TBS-T) (TBS, 0.1% Tween 20) including 5% nonfat-dried milk powder (AppliChem) for 30 min at room temperature (RT). The membrane was subsequently incubated with the primary antibody containing hybridoma supernatant (rat anti-GABARAP clone number 8H5) diluted in blocking buffer (1:1). Incubation was performed overnight at 4 °C. After three washing steps with TBS-T, HRP-coupled secondary antibody (mouse anti-rat-IgG2a-HRP; 1:1000) was applied for 1 h at RT. After three further washing steps with TBS-T, the membrane was incubated with the HRP substrate SuperSignal West Pico Chemiluminescent Substrate (Thermo Scientific, Germany) for 5 min at RT. Final quantification of immunosignal was performed using a chemiluminescence detection system (ChemiDoc, Bio-Rad, Hercules, CA, USA).

ELISA (for assessing binding specificity of selected hybridoma supernatants). 96 well Nunc-Immuno MicroWell Polysorp plates (Thermo Scientific, Germany) were coated with 700 ng of one GABARAP family protein per well and incubated for 1 h at RT. Wells were subsequently blocked for 30 min at RT

using TBS-T including 5% nonfat-dried milk powder (AppliChem, Germany). Hybridoma supernatant with primary antibody (rat anti-GABARAP clone 8H5) was diluted in blocking buffer (1:10) and was further transferred to 7 wells, respectively. Each of these wells contained a distinct protein of the GABARAP family. Incubation was performed for 1 h at RT. After three washing steps using TBS-T, a suitable HRP coupled secondary antibody (goat anti-rat IgG-HRP) was diluted (1:1000) and subsequently transferred to the wells. After 1 h of incubation at RT, each well was washed three times with TBS-T. The HRP substrate and TMB (Sigma-Aldrich, T5525, Germany) was finally applied to all wells according to manufacturer's instruction. Immunosignal was quantified at 450 nm (Fluostar Optima, BMG Labtechnologies GmbH, Germany).

Polyacrylamide gel electrophoresis and western blot analysis. Purified ATG8 family proteins (GABARAP, GABARAPL1, GABARAPL2, LC3A, LC3B and LC3C) were denatured at 95 °C for 5 min in SDS loading buffer (10% (v/v) glycerol, 2% (w/v) SDS, 2% (v/v) 2-mercaptoethanol, 50 mM Tris, pH 6.8, 0.75 g/l bromphenol blue). ATG8 family proteins (1 µg respectively) were then applied to a 12% SDS-PAGE and separated at 40 mA for 45 min. Gel staining was performed with coomassie staining solution (25% isopropanol, 10% acidic acid, 0.5 g/l coomassie brilliant blue R-250) and the destaining was done in hot water.

For western blot analysis, proteins were transferred to a PVDF membrane (pore size 0.2 µm) without preceding gel staining. Protein transfer was performed in a semi dry system at 25 V for 60 min. The membrane was subsequently washed in TBS-T and then blocked in TBS-T including 2.5% milk powder for 30 min. The blot was incubated with primary antibody containing hybridoma supernatant (rat anti-GABARAP (8H5) antibody) diluted in TBS-T (1:4) over night at 4 °C. After washing (3 times for 5 min, respectively) in TBS-T, the membrane was incubated with HRP-conjugated secondary antibody (goat anti-rat-HRP, Jackson 112–035–068, diluted 1:2000 in TBS-T) at RT for 1 h. The blot was washed (3 times for 5 min, respectively) in TBS-T and immunoreactivity was finally quantified as described for dot blot analysis.

Epitope mapping. Peptide scanning was performed using a cellulose membrane (Intavis AG, Germany) loaded with 12mer peptides representing the complete sequence of hGABARAP and overlapping by 10 amino acids, respectively. Every peptide was spotted on the membrane twice. Epitope mapping was done by washing the membrane with TBS-T, followed by a blocking step using TBS-T/5% nonfat-dried milk powder. After another washing step with TBS-T, primary antibody (rat anti-GABARAP (8H5) antibody hybridoma supernatant) was diluted with TBS-T (1:5) and applied over night at 4 °C. After 3 washing steps using TBS-T, HRP-coupled mouse anti-rat IgG2a antibody was diluted with TBS-T (1:2000) and applied for 2 h at RT. After another 3 washing steps with TBS-T, signal detection was performed by incubation with SuperSignal West Pico Chemiluminescent Substrate (Thermo Scientific, Germany) for 5 min at RT. Immunosignal was quantified using a chemiluminescence detection system (ChemiDoc, Bio-Rad, Hercules, CA, USA).

Cell culture and transfection. P3X63-Ag8.653 cells were cultured at 37 °C in a humidified 5% CO_2 incubator in standard medium RPMI 1640 (Sigma-Aldrich, Germany) supplemented with 1% glutamine, 1% non-essential amino acids, 1% sodium pyruvate, 1% penicillin/streptomycin (Sigma-Aldrich, Germany), and 2.5% FCS (Capricorn).

HAP1 cells are adherent human fibroblast-like cells with a near-haploid karyotype that have been derived from the male chronic myelogenous leukemia (CML) cell line KBM-7[39]. HAP1 parental (C631) and HAP1 GABARAP KO (HZGHC003054c004) cells were purchased from Horizon Discovery, UK. HAP1 cells were cultured at 37 °C in a humidified 5% CO_2 incubator in growth medium Iscove's Modified Dulbecco's Medium (IMDM – Gibco, Thermofisher Scientific, Germany) supplemented with 1% penicillin/streptomycin (Sigma-Aldrich, Germany), and 10% FCS (Sigma-Aldrich, Germany).

For transient transfection with peYFP-N1 empty vector (Clontech, USA), peYFP-GABARAP, peYFP-GABARAPL1, and peCFP-GABARAPL2 constructs, 1×10^5 HAP1 cells were seeded on a poly D-Lysine coated bottom dish (MatTek Corporation, MA, USA) and incubated in IMDM / 10% FCS, respectively. The next day transfection with 1.5 µg total DNA using Turbofectin 8.0 (OriGene, USA) was performed according to manufacturer's instructions.

Immunofluorescence. HAP1 cells (3×10^5) were seeded on a poly D-Lysine coated glass bottom dish (MatTek Corporation, MA, USA) and incubated in IMDM / 10% FCS. The next day, IMDM was removed and HAP1 cells were incubated for 3–4 h in IMDM medium with 10% FCS only or IMDM without 10% FCS including 100 nM Bafilomycin A1 (Sigma-Aldrich, Germany). Fixation with 4% (w/v) paraformaldehyde in PBS at RT for 10 min was followed by a washing step using PBS and addition of 0.2% TritonX-100 in PBS for 30 min at RT to permeabilize the cell membranes. After three washing steps with PBS, surfaces were blocked with 1% bovine serum albumin (BSA, Sigma-Aldrich, Germany) at RT for 60 min or overnight at 4–8 °C. Immunostaining was performed by addition of 1 mL undiluted hybridoma supernatant including anti-GABARAP (8H5) antibody and 1 µg/mL mouse monoclonal anti-LC3B (5F10) antibody and incubation for 60 min at RT under smooth shaking. Cells were washed three times for 5 min with PBS followed by incubation of an appropriate 1:250 diluted fluorescent labelled secondary antibody (goat anti-rat Alexa Fluor 488 for 8H5; goat anti-mouse Alexa Fluor 647 for mAb LC3B) for 60 min at RT in the dark, followed by two washing steps for 5 min with PBS. YFP, YFP-GABARAP, and YFP-GABARAPL1 transfected HAP1 cells were fixed 2 to 3 days after transfection. Fixing and staining procedure was done as described above, and a donkey anti-rat Cy5 secondary Ab (1:250) was used in combination with anti-GABARAP (8H5) antibody.

Image acquisition. Images were acquired using ZEN black 2009 on a LSM 710 confocal laser scanning system (Carl Zeiss MicroImaging Inc., Germany) with a Plan-Apochromat 63 × /1.40 Oil DIC M27 objective. The cell nuclei (DAPI) were measured in the 405 nm channel (MBS -405/760+). GABARAP puncta were detected

in the 488 nm channel (MBS 488/543/633) and LC3B puncta in the 633 nm channel (MBS 488/543/633), respectively. YFP was detected in channel 514 nm (MBS 458/514) and Cy5 in channel 633 nm (MBS 488/543/633).

Image evaluation. Image analysis was done using ImageJ / Fiji[40,41]. For quantitative and unbiased evaluation of anti-GABARAP (8H5) antibody a macro has been written and applied to images of parental and GABARAP KO cells. Within the macro a maximum intensity projection and a defined threshold (70/255) was used. After thresholding the images, a watershed algorithm was applied and puncta with a size >3 pixel were counted using the *Analyze Particles* tool of ImageJ. The puncta were analyzed in single cells using manually annotated regions of interest (ROIs) within the images. For better visibility in the print version, maximum intensity projections and an adjustment of brightness (20), contrast (40) and intensity (60) was applied equally for every figure using CorelDRAW 2017. For data analysis, GraphPad Prism Version 5.00 was used.

Data Availability Statement

No datasets were generated or analyzed during the current study.

References

1. Weiergräber, O. H., Schwarten, M., Strodel, B. & Willbold, D. Investigating Structure and Dynamics of Atg8 Family Proteins. *Methods in enzymology* **587**, 115–142, https://doi.org/10.1016/bs.mie.2016.09.056 (2017).
2. Le Grand, J. N. *et al*. GABARAPL1 (GEC1): original or copycat? *Autophagy* **7**, 1098–1107, https://doi.org/10.4161/auto.7.10.15904 (2011).
3. Schaaf, M. B., Keulers, T. G., Vooijs, M. A. & Rouschop, K. M. LC3/GABARAP family proteins: autophagy-(un)related functions. *FASEB journal: official publication of the Federation of American Societies for Experimental Biology* **30**, 3961–3978, https://doi.org/10.1096/fj.201600698R (2016).
4. Wang, H., Bedford, F. K., Brandon, N. J., Moss, S. J. & Olsen, R. W. GABA(A)-receptor-associated protein links GABA(A) receptors and the cytoskeleton. *Nature* **397**, 69–72, https://doi.org/10.1038/16264 (1999).
5. Green, F., O'Hare, T., Blackwell, A. & Enns, C. A. Association of human transferrin receptor with GABARAP. *FEBS Lett* **518**, 101–106 (2002).
6. Cook, J. L. *et al*. The trafficking protein GABARAP binds to and enhances plasma membrane expression and function of the angiotensin II type 1 receptor. *Circulation research* **102**, 1539–1547, https://doi.org/10.1161/CIRCRESAHA.108.176594 (2008).
7. Lainez, S. *et al*. GABAA receptor associated protein (GABARAP) modulates TRPV1 expression and channel function and desensitization. *FASEB journal: official publication of the Federation of American Societies for Experimental Biology* **24**, 1958–1970, https://doi.org/10.1096/fj.09-151472 (2010).
8. Ohsumi, Y. Historical landmarks of autophagy research. *Cell research* **24**, 9–23, https://doi.org/10.1038/cr.2013.169 (2014).
9. Ichimura, Y. *et al*. A ubiquitin-like system mediates protein lipidation. *Nature* **408**, 488–492, https://doi.org/10.1038/35044114 (2000).
10. Geng, J. & Klionsky, D. J. The Atg8 and Atg12 ubiquitin-like conjugation systems in macroautophagy. 'Protein modifications: beyond the usual suspects' review series. *EMBO reports* **9**, 859–864, https://doi.org/10.1038/embor.2008.163 (2008).
11. Tanida, I., Komatsu, M., Ueno, T. & Kominami, E. GATE-16 and GABARAP are authentic modifiers mediated by Apg7 and Apg3. *Biochem Biophys Res Commun* **300**, 637–644 (2003).
12. Kabeya, Y. *et al*. LC3, GABARAP and GATE16 localize to autophagosomal membrane depending on form-II formation. *Journal of cell science* **117**, 2805–2812, https://doi.org/10.1242/jcs.01131 (2004).
13. Chen, Z. W., Chang, C. S., Leil, T. A. & Olsen, R. W. C-terminal modification is required for GABARAP-mediated GABA(A) receptor trafficking. *J Neurosci* **27**, 6655–6663, https://doi.org/10.1523/JNEUROSCI.0919-07.2007 (2007).
14. Lee, Y. K. & Lee, J. A. Role of the mammalian ATG8/LC3 family in autophagy: differential and compensatory roles in the spatiotemporal regulation of autophagy. *BMB reports* **49**, 424–430 (2016).
15. Klionsky, D. J. *et al*. Guidelines for the use and interpretation of assays for monitoring autophagy (3rd edition). *Autophagy* **12**, 1–222, https://doi.org/10.1080/15548627.2015.1100356 (2016).
16. Nguyen, T. N. *et al*. Atg8 family LC3/GABARAP proteins are crucial for autophagosome-lysosome fusion but not autophagosome formation during PINK1/Parkin mitophagy and starvation. *The Journal of cell biology* **215**, 857–874, https://doi.org/10.1083/jcb.201607039 (2016).
17. Joachim, J. *et al*. Activation of ULK Kinase and Autophagy by GABARAP Trafficking from the Centrosome Is Regulated by WAC and GM130. *Mol Cell* **60**, 899–913, https://doi.org/10.1016/j.molcel.2015.11.018 (2015).
18. Joachim, J. *et al*. Centriolar Satellites Control GABARAP Ubiquitination and GABARAP-Mediated Autophagy. *Curr Biol* **27**, 2123–2136 e2127, https://doi.org/10.1016/j.cub.2017.06.021 (2017).
19. Uhlen, M. *et al*. A proposal for validation of antibodies. *Nature methods* **13**, 823–827, https://doi.org/10.1038/nmeth.3995 (2016).
20. Werner, G., Hagenmaier, H., Drautz, H., Baumgartner, A. & Zahner, H. Metabolic products of microorganisms. 224. Bafilomycins, a new group of macrolide antibiotics. Production, isolation, chemical structure and biological activity. *J Antibiot (Tokyo)* **37**, 110–117 (1984).
21. Drose, S. & Altendorf, K. Bafilomycins and concanamycins as inhibitors of V-ATPases and P-ATPases. *J Exp Biol* **200**, 1–8 (1997).
22. Koukourakis, M. I. *et al*. Autophagosome Proteins LC3A, LC3B and LC3C Have Distinct Subcellular Distribution Kinetics and Expression in Cancer Cell Lines. *PLoS One* **10**, e0137675, https://doi.org/10.1371/journal.pone.0137675 (2015).
23. Mizushima, N., Yoshimori, T. & Levine, B. Methods in mammalian autophagy research. *Cell* **140**, 313–326, https://doi.org/10.1016/j.cell.2010.01.028 (2010).
24. Joachim, J. & Tooze, S. A. Control of GABARAP-mediated autophagy by the Golgi complex, centrosome and centriolar satellites. *Biol Cell* **110**, 1–5, https://doi.org/10.1111/boc.201700046 (2018).
25. Hiyama, M. *et al*. Nutrient starvation affects expression of LC3 family at the feto-maternal interface during murine placentation. *J Vet Med Sci* **77**, 305–311, https://doi.org/10.1292/jvms.14-0490 (2015).
26. Meliopoulos, V. A. & Schultz-Cherry, S. Although it's painful: The importance of stringent antibody validation. *PLoS Pathog* **14**, e1006701, https://doi.org/10.1371/journal.ppat.1006701 (2018).
27. Skogs, M. *et al*. Antibody Validation in Bioimaging Applications Based on Endogenous Expression of Tagged Proteins. *Journal of proteome research* **16**, 147–155, https://doi.org/10.1021/acs.jproteome.6b00821 (2017).
28. Jiang, P. & Mizushima, N. Autophagy and human diseases. *Cell research* **24**, 69–79, https://doi.org/10.1038/cr.2013.161 (2014).
29. Kim, M., Ho, A. & Lee, J. H. Autophagy and Human Neurodegenerative Diseases-A Fly's Perspective. *Int J Mol Sci* **18**, https://doi.org/10.3390/ijms18071596 (2017).
30. Willingham, M. C. Conditional epitopes. is your antibody always specific? *J Histochem Cytochem* **47**, 1233–1236, https://doi.org/10.1177/002215549904701002 (1999).
31. Bordeaux, J. *et al*. Antibody validation. *Biotechniques* **48**, 197–209, https://doi.org/10.2144/000113382 (2010).

32. Lee, Y. K. *et al.* Development of LC3/GABARAP sensors containing a LIR and a hydrophobic domain to monitor autophagy. *The EMBO journal*. https://doi.org/10.15252/embj.201696315 (2017).
33. Stolz, A. *et al.* Fluorescence-based ATG8 sensors monitor localization and function of LC3/GABARAP proteins. *The EMBO journal* **36**, 549–564, https://doi.org/10.15252/embj.201695063 (2017).
34. Wang, H. & Olsen, R. W. Binding of the GABA(A) receptor-associated protein (GABARAP) to microtubules and microfilaments suggests involvement of the cytoskeleton in GABARAPGABA(A) receptor interaction. *Journal of neurochemistry* **75**, 644–655 (2000).
35. Ma, P. *et al.* Interaction of Bcl-2 with the autophagy-related GABAA receptor-associated protein (GABARAP): biophysical characterization and functional implications. *The Journal of biological chemistry* **288**, 37204–37215, https://doi.org/10.1074/jbc.M113.528067 (2013).
36. Krichel, C. *et al.* Sequence-specific 1H, 15N, and 13C resonance assignments of the autophagy-related protein LC3C. *Biomolecular NMR assignments* **10**, 41–43, https://doi.org/10.1007/s12104-015-9633-z (2016).
37. Kearney, J. F., Radbruch, A., Liesegang, B. & Rajewsky, K. A new mouse myeloma cell line that has lost immunoglobulin expression but permits the construction of antibody-secreting hybrid cell lines. *J Immunol* **123**, 1548–1550 (1979).
38. Kohler, G. & Milstein, C. Continuous cultures of fused cells secreting antibody of predefined specificity. *Nature* **256**, 495–497 (1975).
39. Carette, J. E. *et al.* Ebola virus entry requires the cholesterol transporter Niemann-Pick C1. *Nature* **477**, 340–343, https://doi.org/10.1038/nature10348 (2011).
40. Schindelin, J. *et al.* Fiji: an open-source platform for biological-image analysis. *Nature methods* **9**, 676–682, https://doi.org/10.1038/nmeth.2019 (2012).
41. Schneider, C. A., Rasband, W. S. & Eliceiri, K. W. NIH Image to ImageJ: 25 years of image analysis. *Nature methods* **9**, 671–675 (2012).
42. Sievers, F. *et al.* Fast, scalable generation of high-quality protein multiple sequence alignments using Clustal Omega. *Mol Syst Biol* **7**, 539, https://doi.org/10.1038/msb.2011.75 (2011).

Acknowledgements

We thank S. Weidtkamp-Peters for advice on image acquisition, M. Schwarten for help with PyMol, P. Ma for FP-fusion plasmid cloning, J. Post-Schulz for supporting IF staining of mouse brain slices and J. Fabig for valuable technical assistance. This study was funded by the Deutsche Forschungsgemeinschaft (DFG, German Research Foundation) – Projektnummer 190586431 – SFB 974, project B02 (D.W., I.M.S.), and project WE5343/1–1 (T.Z.), and by a grant from the Jürgen Manchot Foundation, Molecules of Infection Graduate School (MOI III) (D.W. and J.D.).

Author Contributions

D.W. and J.M. generated the original hypothesis. E.K., R.F. and J.M. generated and screened the antibody, J.M. purified the recombinantly expressed proteins, performed the dot blot assay and did the epitope mapping. I.M.S. conducted the cell culture experiments, IF-stainings, image acquisition and evaluation. T.Z. established the image analysis tool. I.M.S. and J.D. generated the HEK293 KO lines and performed the related IB experiments. D.W., J.M., S.H., provided intellectual contributions throughout and supervised the project. S.H., I.M.S. and J.M. took primary responsibility for writing the manuscript. All authors edited the manuscript.

Additional Information

Supplementary information accompanies this paper at https://doi.org/10.1038/s41598-018-36717-1.

Competing Interests: The authors declare no competing interests.

Publisher's note: Springer Nature remains neutral with regard to jurisdictional claims in published maps and institutional affiliations.

Supplementary Info

The highly GABARAP specific rat monoclonal antibody 8H5 visualizes GABARAP in immunofluorescence imaging at endogenous levels

Indra M. Simons[1], Jeannine Mohrlüder[2], Regina Feederle[3], Elisabeth Kremmer[4], Thomas Zobel[5], Jochen Dobner[1], Nicole Bleffert[1], Silke Hoffmann[2], Dieter Willbold[1,2]

[1]Institut für Physikalische Biologie, Heinrich-Heine-Universität, 40225 Düsseldorf, Germany

[2]Institute of Complex Systems, Structural Biochemistry (ICS-6), Forschungszentrum Jülich, 52425 Jülich, Germany

[3]Institute for Diabetes and Obesity, Monoclonal Antibody Core Facility [4]Institute for Molecular Immunology Helmholtz Center Munich, German Research Center for Environmental Health, 85764 Neuherberg, Germany

[5]Department of Biology, Center for Advanced Imaging (CAi), Heinrich-Heine-Universität, 40225 Düsseldorf, Germany

Supplementary Methods are related to Figure S1, S2, S4 and S5

Supplementary Figure 1 is related to all Figures dealing with HAP1 cells (Fig. 3, 4, 5)
Supplementary Figure 2 is related to Figure 4
Supplementary Figure 3 is related to Figures 1A, 1C, 2A, S1A and S1B
Supplementary Figure 4
Supplementary Figure 5 is related to Figure 5
Supplementary Figure 6
Supplementary Table 1 is related to Figure S1 B
Supplementary Table 2 is related to Figure Table S1 and Supplementary Figure S1 B
Supplementary Table 3 is related to all figures

Supplementary References are related to Figure S1

Supplementary Methods

Western blotting of mammalian cell lysates

For immunoblots depicted in figure S1, cells were washed once with warm PBS, dissociated with Trypsin-EDTA (Cytogen, Wetzlar, Germany) for 5 min, resuspended in medium and centrifuged for 3 min at 4 °C and 900 g. Afterwards, cell pellets were washed once with cold PBS and resuspended in lysis buffer (136 mM NaCl, 20 mM Tris-HCl, 10 % Glycerin, 2 mM EDTA, 50 mM β-Glycerophosphat, 20 mM Na-Pyrophosphat, 0.2 mM Pefablock, 5 µg/ml Aprotinin, 5 µg/ml Leupeptin, 4 mM Benzamidin, 1 mM Na_3VO_4 , 0.2 % SDS, pH 7.4) and frozen for 20 min at -20 °C. Subsequently, samples were thawed, sonicated thrice for 15 seconds at 100 % on ice and centrifuged for 15 min at 4 °C and 20 000 g to get rid of cell debris. Supernatants were transferred to fresh tubes and protein content measured with Bradford protein assay (Biorad, California, USA). 40 µg of whole cell protein lysates were then subjected to 12 % polyacrylamid SDS-PAGE. Proteins were then transferred onto a PVDF membrane via Semi-Dry Western Blot. Membranes were blocked with either 5 % milk in TBS-T or 5 % BSA in TBS-T for 1 h at room temperature (RT), followed by three times 20 min washing with TBS-T at RT incubation with primary antibody overnight at 4 °C and secondary HRP-coupled antibody for 1 h at RT. Blots were visualized by chemiluminescence (Western Lightning Plus-ECL, Perkin Elmer, Massachusetts, USA) and documented using the ChemiDoc system (Biorad, California, USA) or film (Amersham Hyperfilm ECL, GE, UK).

Generation of HEK293 knockout cell lines

HEK293 cells were nucleofected (Lonza, Basel, CH) with KO plasmids targeting *GABARAP* exon 1, -*L1* exon 2 and -*L2* exon 2 coexpressing either GFP, CFP or mCherry. KO plasmids are based on plasmid pSpCas9(BB)-2A-GFP (PX458), which was a gift from Feng Zhang (Addgene plasmid # 48138)[1]. Clonal lines were created by growth of single cell sorted FP positive cells via fluorescence activated cell sorting (FACS). Genomic mutations were validated via Sanger sequencing of PCR amplificates of the sgRNA target region +/- 200 bp (table S1) and analysed by TIDE and Crisp-ID[2,3], as listed in table S2.

Ethics statement

All animal experiments were performed in accordance with the German Law on the protection of animals (TierSchG §§ 7-9) and with permit from the local ethic committee (Landesamt für Natur, Umwelt und Verbraucherschutz Nordrhein-Westfalen (LANUV), North Rhine-Westphalia, Germany; AZ 84-02.04.2015.A106 and AZ 84-02.04.2014.A423).

Immunofluorescent analysis of mouse brain slices

Endogenous GABARAP in tissue sections was assessed by immunofluorescence analysis using 20 µm thick, sagittal sections of 20 weeks old mice divided by a cryostat (CM3050 S, Leica Biosystems Nussloch GmbH, Wetzlar, Germany). Formalin embedded brain sections were fixed for 10 min with 4 % PFA, three times washed for 5 min with (Tris-buffered saline) TBS and treated for 10 min with 70 % formic acid for antigen retrieval, followed by another three 5 min washing steps with TBS. After permeabilization with 1 % TBS-Triton-X (TBS-T) for 30 min, brain sections were blocked with 1 % BSA in TBS over night at 4 °C. Incubation with anti-GABARAP (8H5) antibody was performed with undiluted hybridoma supernatant for 2 h at RT. After three washing steps for 5 min with TBS, sections were incubated for 1 h with a goat anti-rat IgG+IgM (H&L) Alexa Fluor 488 secondary antibody (112-545-068, Dianova, 1:250 in 1 % BSA in TBS), followed by three 5 min washing steps with TBS. In addition, the secondary antibody was applied in the absence of primary antibody, to assess the specificity of the stain, and all residual staining was considered to be non-specific. Immunofluorescent sections were counterstained by DAPI (4,6-Diamidin-2-phenylindol) (Merck, Germany) and again washed as described. Brain sections were mounted with Aqua Poly/Mount (18606, Polysciences, Inc. Warrington, Pennsylvania, USA). Images were taken with a LSM 710 confocal laser scanning system (Carl Zeiss MicroImaging Inc., Germany) equipped with a EC Plan-Neofluar 20x/0.50 M27a or a Plan-Apochromat 63x/1.40 Oil DIC M27 objective.

Immunofluorescence

HEK293 cells (3 x 10^5) were seeded on a fibronectin (Sigma-Aldrich, Germany) coated glass bottom dish (ibidi, Germany) and incubated in DMEM supplemented with 10 % FCS for 24 hours. The next day, DMEM was removed and HEK293 cells were incubated for 3 h – 4 h in DMEM medium without 10 % FCS or Earle's Balanced Salts (EBSS, Sigma-Aldrich, Germany) including 100 nM Bafilomycin A1 (Sigma-Aldrich, Germany). Fixation with 4 % (w/v) paraformaldehyde (PFA) in PBS at RT for 10 min was followed by a washing step using PBS and addition of 0.2 % TritonX-100 in PBS for 30 min at RT to permeabilize the cell membranes. After three washing steps with PBS, surfaces were blocked with 1 % bovine serum albumin (BSA, Sigma-Aldrich, Germany) overnight at 4-8 °C. Immunostaining was performed by addition of 1 mL undiluted hybridoma supernatant including anti-GABARAP (8H5) and 1 µg/mL mouse monoclonal anti-LC3B (5F10) antibody and incubation for 60 min at RT under smooth shaking. Cells were washed three times for 5 min with PBS followed by incubation of an appropriate 1:250 diluted fluorescent labelled secondary antibody (goat anti-rat Alexa Fluor 488 for 8H5; goat anti-mouse Alexa Fluor 647 for mAb LC3B) for 60 min at RT in the dark, followed by two washing steps for 5 min with PBS.

HAP1 parental and GABARAP KO cells were cultured under growth factor deprivation with 100 nM BafA1 for 3 h. Cells were fixed with 4 % (w/v) PFA in PBS at RT or with 100 % methanol for 15 min at – 20 °C, both followed by washing twice for 5 min. Cells were immunolabeled with polyclonal

(pAb) GABARAP (Proteintech 1:200, abgent 1:25) or monoclonal GABARAP (Cell Signaling E1J4E, 1:200) antibodies followed by staining with Alexa Fluor 555 (pAb – 1 (Proteintech)) and with Alexa Fluor 488 (mAb (E1J4E) and pAb – 2 (abgent)).

Supplementary Figure S1

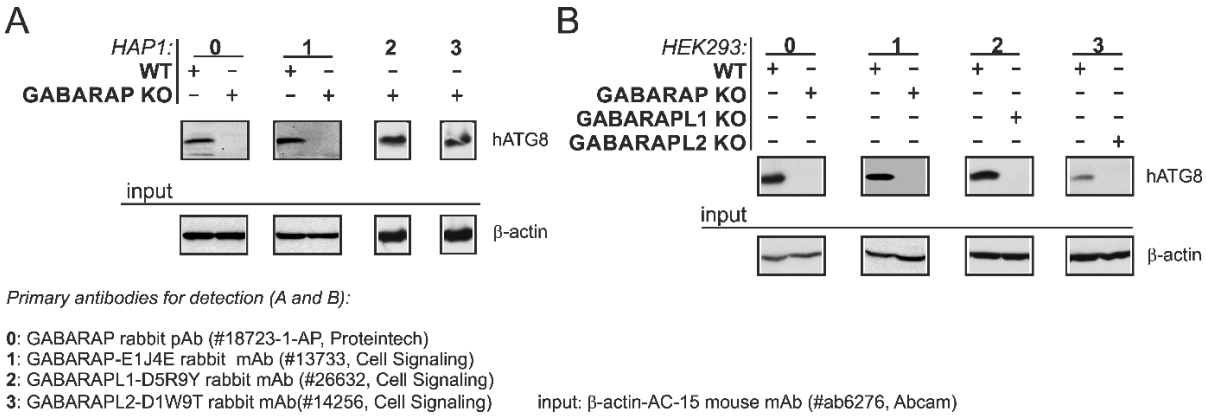

Primary antibodies for detection (A and B):

0: GABARAP rabbit pAb (#18723-1-AP, Proteintech)
1: GABARAP-E1J4E rabbit mAb (#13733, Cell Signaling)
2: GABARAPL1-D5R9Y rabbit mAb (#26632, Cell Signaling)
3: GABARAPL2-D1W9T rabbit mAb(#14256, Cell Signaling) input: β-actin-AC-15 mouse mAb (#ab6276, Abcam)

Supplementary Figure S1. Expression analysis of GABARAP, GABARAPL1, and GABARAPL2 in HAP1 (A) and HEK293 (B) cell lysates. (B) KO-validation of the primary antibodies used in (A) demonstrating their target specificity during immunoblotting applications. GABARAP TKO cells were created using the CRISPR/Cas9 system[1]. HEK293 KO cell lines in (B) were used to validate specificity of the antibodies used against GABARAP, GABARAP-L1 and GABARAP-L2 during immunoblotting. "hATG8" stands for the corresponding GABARAP-subfamily member, detected by the respective antibody. The corresponding full-length blots are given in Supplementary Fig. S3.

Supplementary Figure S2

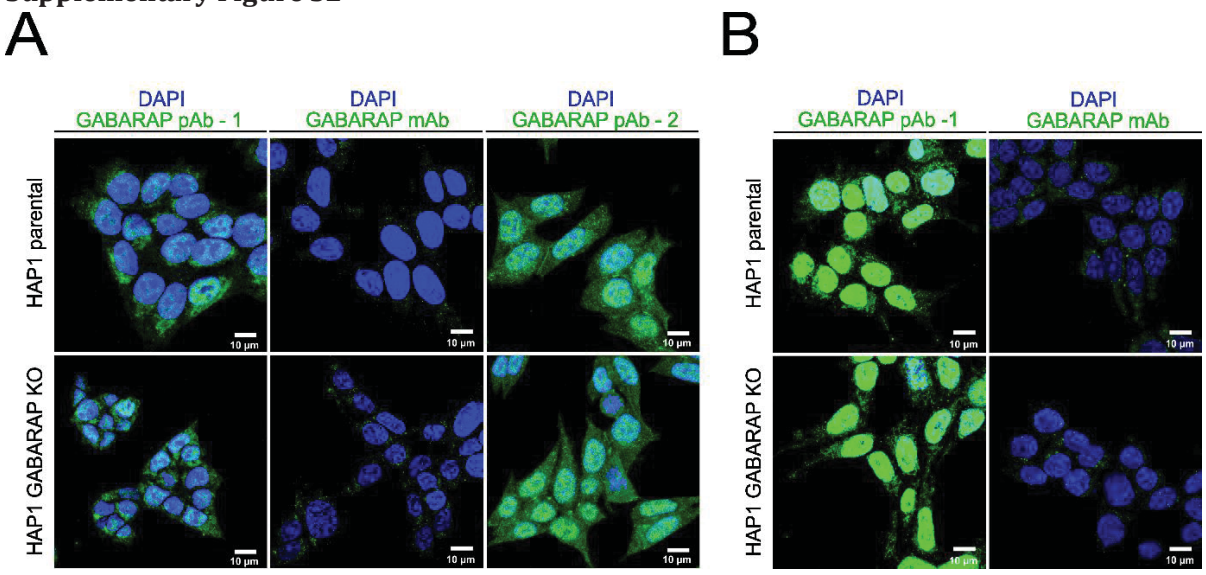

Supplementary Figure S2. Commercial antibodies fail to detect endogenous GABARAP in immunofluorescence in a specific manner. HAP1 parental and GABARAP KO cells were cultured under growth factor deprivation with 100 nM BafA1 for 3 h. Fixed cells were immunolabeled with polyclonal (pAb) GABARAP or monoclonal GABARAP antibodies. Under (A) a 4 % PFA fixation and a staining with Alexa555 (pAb – 1 (Proteintech)) and with Alexa488 (mAb (E1J4E) and pAb – 2 (abgent)) was applied. Under (B) a fixation with 4 % PFA and a staining with Alexa488 (pAb) and a methanol-based fixation protocol as recommended by the supplier for GABARAP mAb E1J4E with Alexa488 as secondary antibody was used, respectively. Nuclei were counterstained with DAPI.

Supplementary Figure S3

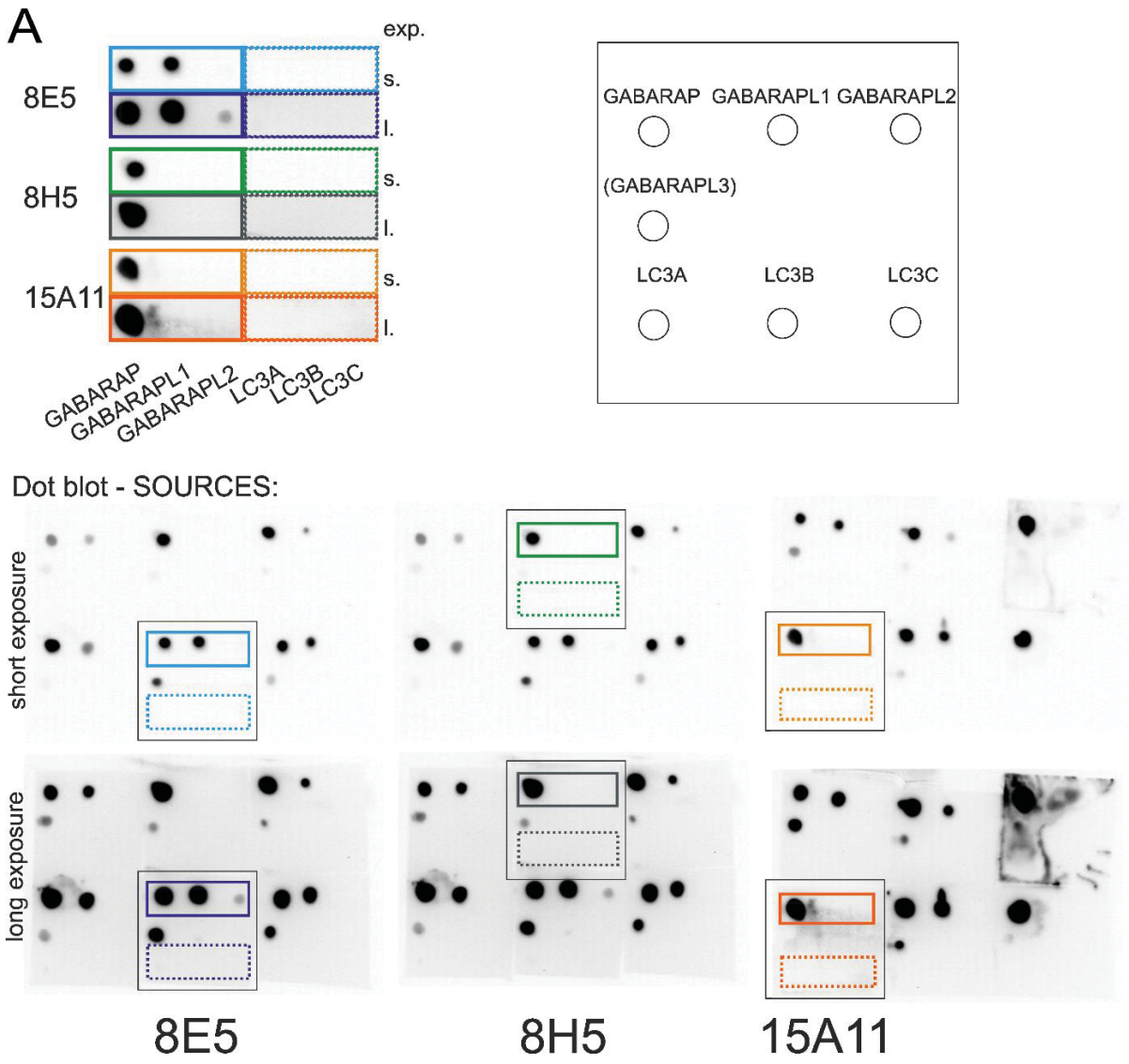

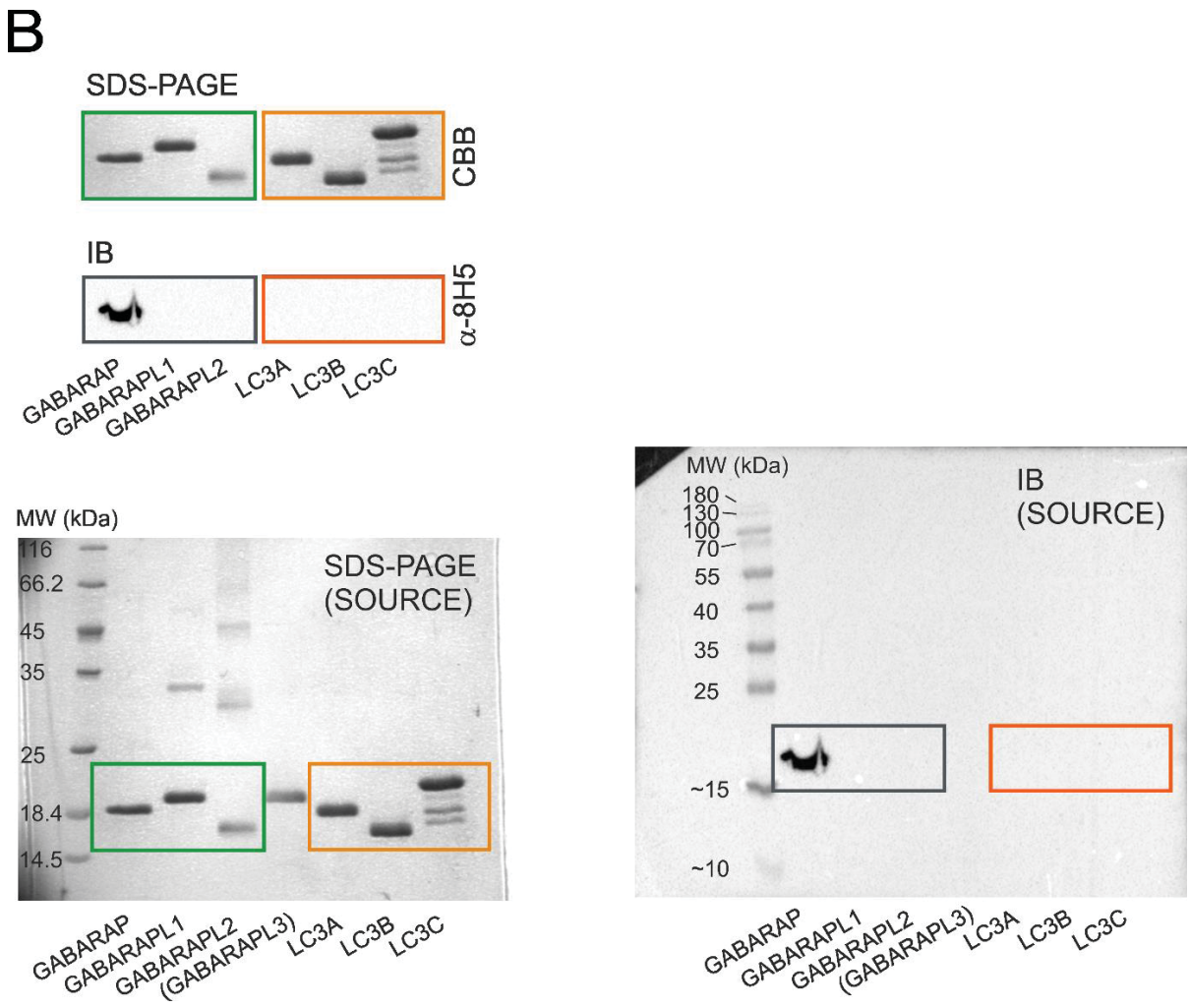

129

130

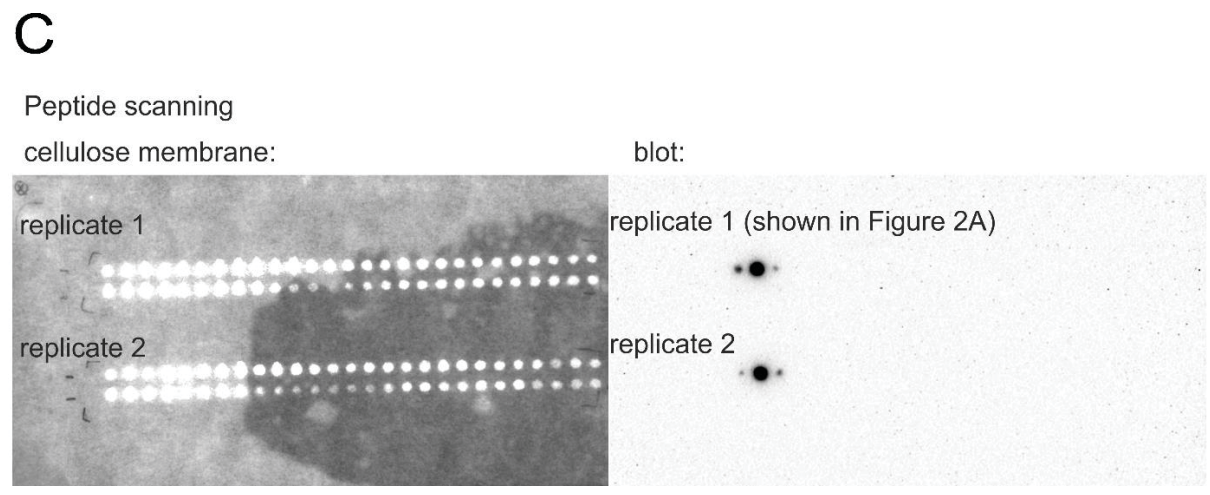

131

132

133

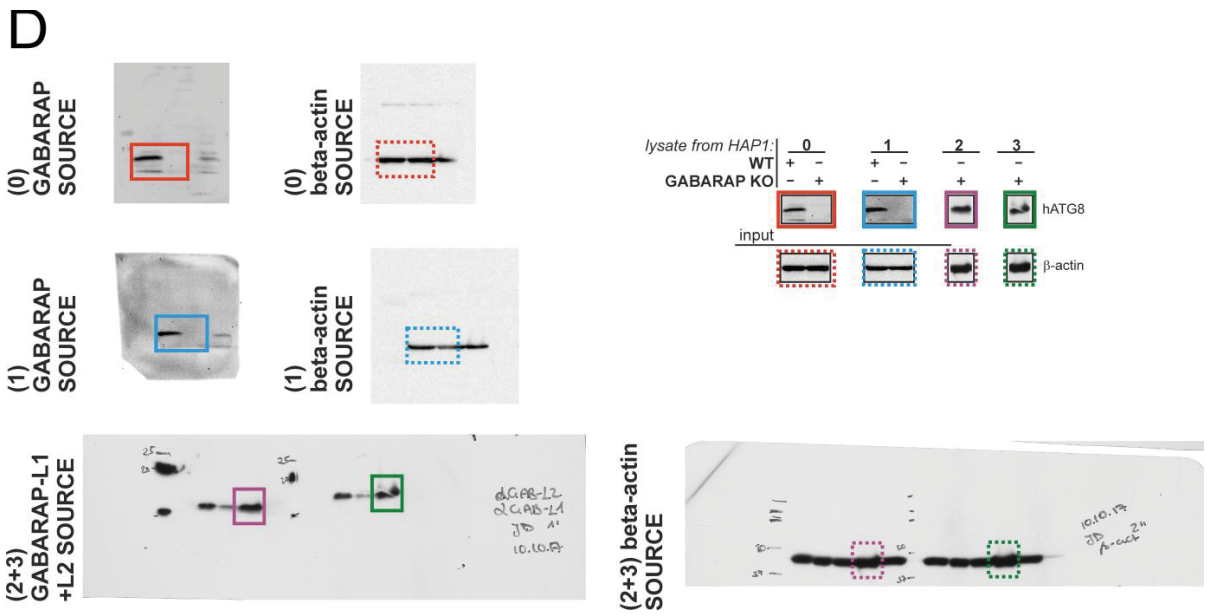

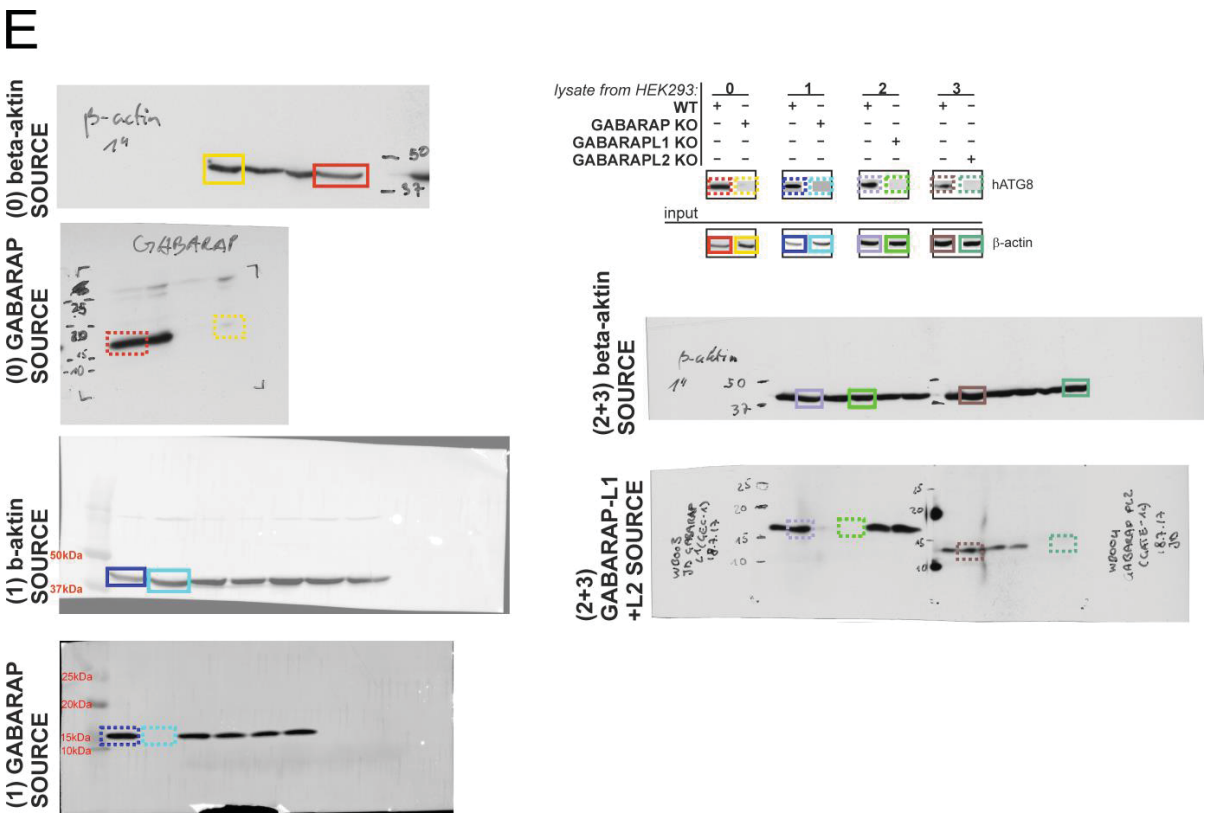

Supplementary Figure S3. Full-length-blots. (A) Uncropped dot blots related to Figure 1A. Note: Each individual exposure includes six blots incubated with one of six different hybridoma supernatants each. Only those incubated with GABARAP-8E5, -8H5 and -15A11 containing supernatants are highlighted. Beside purified GABARAP, -L1, -L2, LC3A, -B and –C the hybridoma supernatants were also tested for their reactivity with GABARAPL3. Because GABARAPL3 is assumed to be a "pseudogene", it was excluded during further analysis. (B) Uncropped SDS-PAGE and western blot membrane related to Figure 1C. (C) Uncropped cellulose membrane shown in Figure 2A used for epitope mapping of GABARAP-8H5. Transillumination and blot are given for both replicates. (D, E) Uncropped western blot membranes related to Supplementary Figure S1A, B.

Supplementary Figure S4

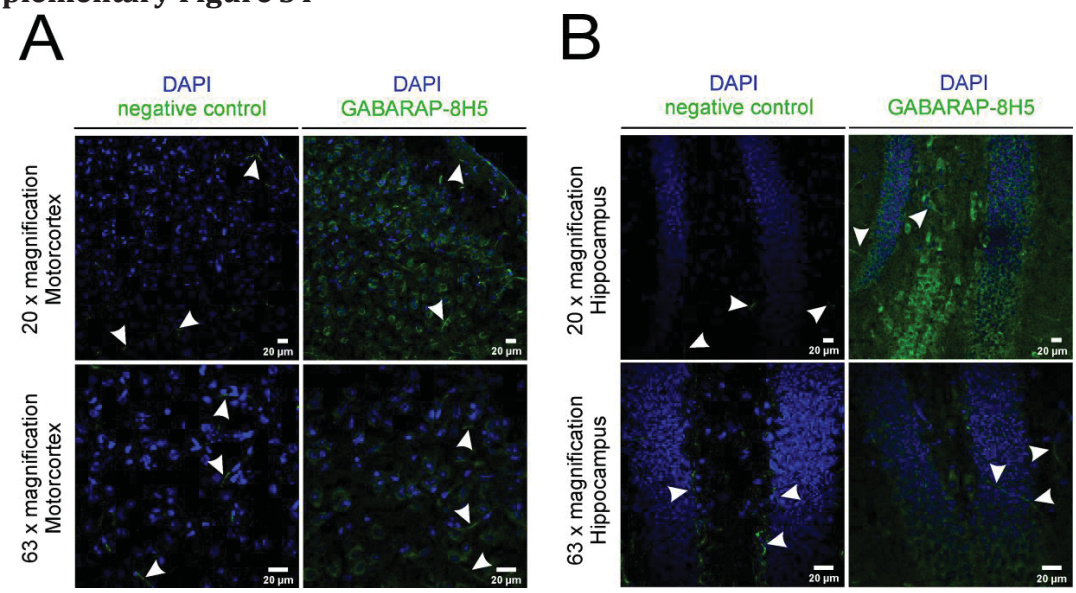

Supplementary Figure S4. Performance of anti-GABARAP (8H5) antibody during immunofluorescent analysis of mouse brain slices. Representative immunofluorescence images of motorcortex (A) or the hippocampal regions (B) of 20 weeks old mice stained with a goat anti-rat IgG+IgM (H&L) Alexa Fluor 488 secondary antibody in the absence (left panels) or presence of anti-GABARAP (8H5) primary antibody (right panels). All residual staining visible in the left panels is considered as non-specific, and likely represents blood vessels (white arrowheads). In the presence of anti-GABARAP (8H5) antibody a clear intra-cellular staining occurs (right panels). Interestingly, an antigen retrieval step as specified in the methods section was obligatory for positive staining results. Note that mouse and human GABARAP sequences display 100 % conservation. Counterstaining was performed with DAPI.

Supplementary Figure S5

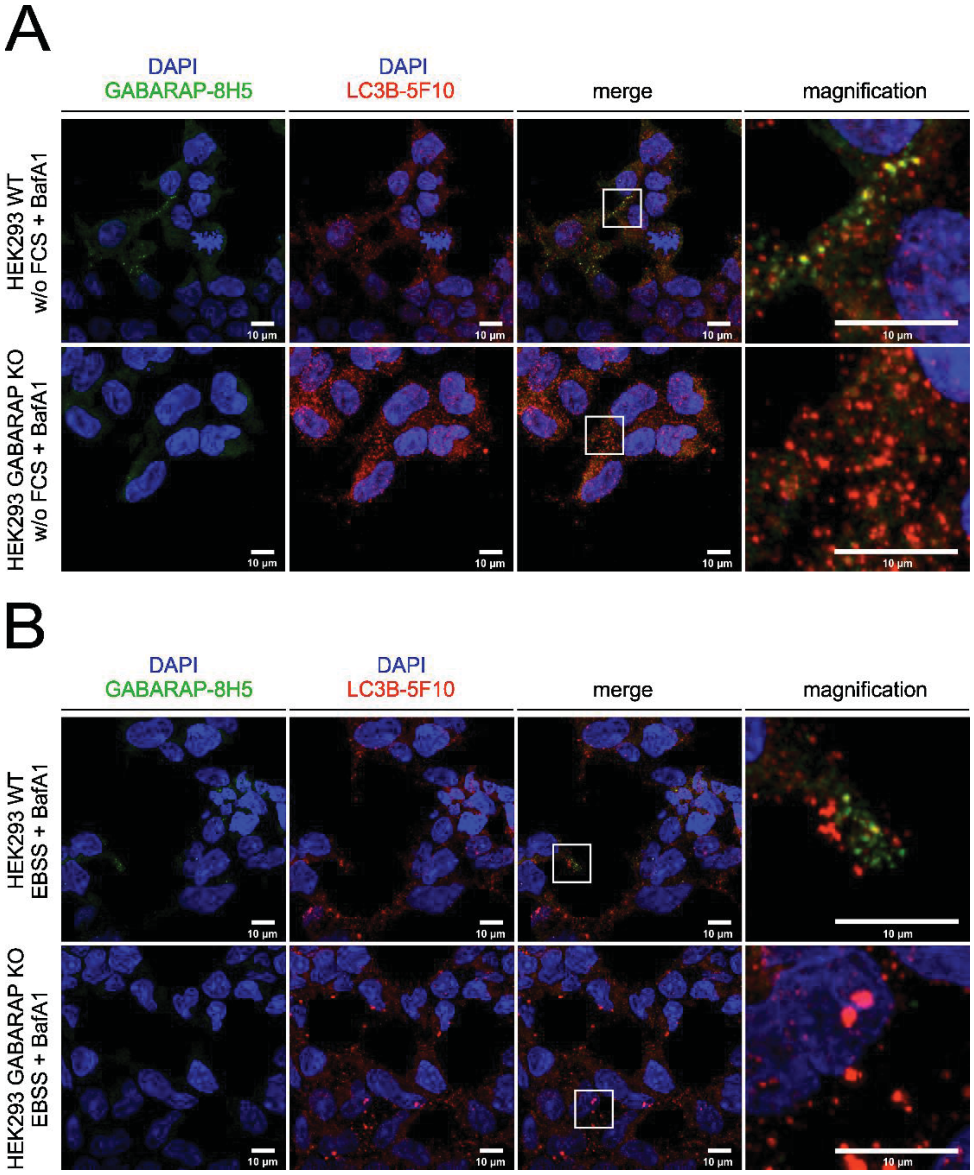

Supplementary Figure S5. Performance of anti-GABARAP (8H5) in HEK293 cells. HEK293 wildtype and GABARAP KO cells were incubated for 3 h in growth factor depleted medium (A) or in EBSS (B) both including 100 nM BafA1 each. Cells were fixed with 4 % PFA and immunolabeled with anti-GABARAP (8H5) and anti-LC3B (5F10) primary antibodies in combination with goat anti-rat IgG+IgM (H&L) Alexa Fluor 488 and anti-mouse IgG Alexa Fluor 647 secondary antibodies, respectively. Colocalization of LC3B (red) and GABARAP (green) is indicated by yellow puncta. Nuclei were counterstained with DAPI.

Supplementary Figure S6

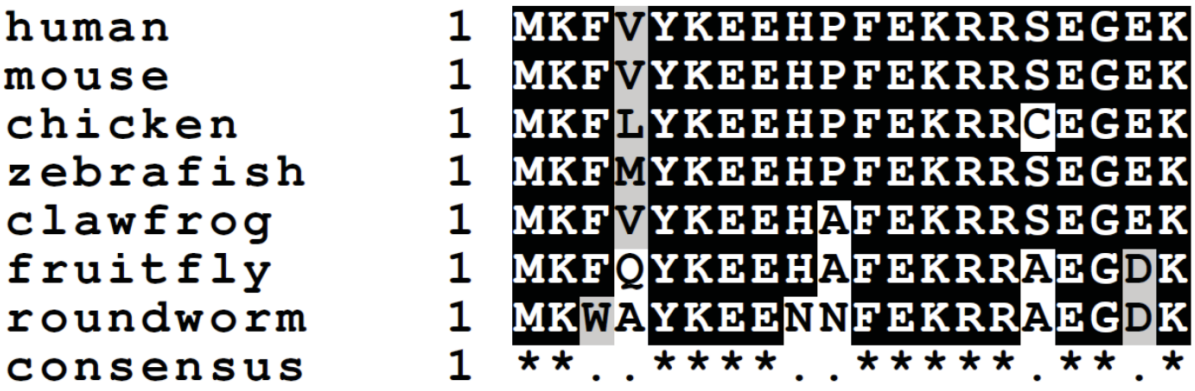

Supplementary Figure S6. The epitope for anti-GABARAP (8H5) antibody shows high conservation between GABARAP proteins from organisms of diverse phylogenetic classes. Aligned are the GABARAP residues 1 to 20 of human GABARAP with those of selected vertebrate, arthropode and nemathode orthologs using Boxshade 3.2.3. UniProtKB accession numbers of the entries used are: O95166 (Homo sapiens); Q9DCD6 (Mus musculus); A0A1L1RN80 (Gallus gallus); Q6PSS4 (Danio rerio); Q6NUG7 (Xenopus laevis); Q9W2S2 (Drosophila melanogaster; protein name: Atg8a); Q09490 (Caenorhabditis elegans; protein name: lgg-1).

Supplementary Table S1. Genotyping primers for sequencing analysis the HEK293 knockout cell lines.

Gene	Exon	Primer direction	Primer sequence (5' to 3')	PCR product (bp)
GABARAP	1	forward	GGGTTGGTGAATAGGGAAGTGG	392
GABARAP-L1	2	forward	TGCAGCTATAACCTCATGAAGCC	400
GABARAP-L2	2	forward	CTTGCTGGGAGCTAGTAGGG	402
GABARAP	1	reverse	CACTCCTTTCATCCTGGGTCC	392
GABARAP-L1	2	reverse	ACTCCAGAGCATCCCACTCA	400
GABARAP-L2	2	reverse	TGAGGCACCCTGAACAGCA	402

Supplementary Table S2. CRISPR sequence details and genotyping results of the knockout cell lines used.

Gene symbol	Uniprot	Gene ID/ location	Targeting strategy	CRISPR gRNA (PAM)	Main clone	unique alleles	Mutation	Protein impact
GABARAP	O95166	11337/NC_000017.11	first exon	GGATCTTCTCGCCCTCAGAGCGG	C2	1	c.[152_153insT]	p.[fs*0]
GABARAP-L1	Q9H0R8	23710/NC_000012.12	second exon	AGAGAAGGCTCCAAAAGCCAGGG	C10	2	c.[352_357del];[353_356]	p.[K38Tfs*10];[K38Nfs*3]
GABARAP-L2	P60520	11345/NC_000016.1	second exon	TCCCACAGAACACAGATGCGTGG	#8	1	c.[179_180insT]	p.[C15Lfs*27]

Formatting of indels detected in the knockout cell lines (Mutation column) and their resulting proteins (Protein impact column) is according to Human Genome Variation Society (http://varnomen.hgvs.org/). Mutation positions are determined in respect to the canonical isoform annotated in Uniprot, if more than one form exists. The numbers after the asterisks represent the number of amino acids present from the first amino acid changed to the next sequential stop codon. del, deletion; ins, insertion; c., coding DNA; p., protein; fs, frame shift; *, stop codon.

185 **Supplementary Table S1. Antibodies used throughout this study.**

Antibody	Company	Species	Catalog number (antigen used for antibody production)
primary Abs:			
anti-GABARAP clone 8H5	in-house	rat	(GST-hGABARAP_aa1-117)
anti-LC3B clone 5F10	Nanotools	mouse	0231-100 (synthetic peptide from N-terminus of hLC3B)
anti-GABARAP pAb	Proteintech	rabbit	18723-1-AP (GABARAP full-length protein)
anti-GABARAP clone E1J4E	Cell Signaling	rabbit	13733 (synthetic peptide surrounding R40 of hGABARAP)
anti-GABARAP pAb clone RB11846	Abgent/antibodies-online	rabbit	AP1821a/ABIN388564 (synthetic peptide between 1-31 aa from the N-terminal region of GABARAP)
anti-GABARAPL1 clone D5R9Y	Cell Signaling	rabbit	26632 (synthetic peptide corresponding to residues near the N-terminus of hGABARAPL1)
anti-GABARAPL2 clone D1W9T	Cell Signaling	rabbit	14256 (synthetic peptide corresponding to residues near the C-terminus of hGABARAPL2)
secondary Abs:			
anti-rat IgG2a-HRP	in-house	mouse	(rat IgG 2a)
anti-rat-IgG-HRP	Sigma	goat	A9037
anti-rat-IgG Alexa Fluor 488	Jackson ImmunoResearch	goat	112-545-068
anti-rat-IgG Cy5	Jackson ImmunoResearch	donkey	712-175-153
anti-mouse IgG Alexa Fluor 647	Abcam	goat	ab150115
anti-rabbit IgG Alexa Fluor 555	Abcam	donkey	ab150074
anti-rabbit IgG Alexa Fluor 647	Abcam	donkey	ab150075

186

187

188 **Additional References**
189

190 1. Ran, F.A., et al. Genome engineering using the CRISPR-Cas9 system. *Nat Protoc* **8**, 2281-308,
191 doi:10.1038/nprot.2013.143 (2013).
192 2. Dehairs, J., et al. CRISP-ID: decoding CRISPR mediated indels by Sanger sequencing. *Sci Rep* **6**,
193 28973, doi: 10.1038/srep28973 (2016).
194 3. Etard, C., et al. Tracking of Indels by DEcomposition is a Simple and Effective Method to Assess
195 Efficiency of Guide RNAs in Zebrafish. *Zebrafish* **14**, 586-588, doi: 10.1089/zeb.2017.1454
196 (2017).

3.2 Autophagy-Related Proteins GABARAP and LC3B Label Structures of Similar Size but Different Shape in Super-Resolution Imaging

Autoren:	Abdollahzadeh, I., Hendriks, J., Sanwald, J. L., Simons, I. M., Hoffmann, S., Weiergräber, O. H., Willbold, D., Gensch, T.
Journal:	*Molecules* **2019**, 24(9), 1833 veröffentlicht am 13.05.2019
DOI:	10.3390/molecules24091833
Impact Factor:	3,060 (2018), 5 Jahre: 3,380
Beitrag:	DNA-Präparation und Sequenzierung verwendeter Plasmide Zellkultivierung Hilfestellung bei Zellkulturexperimenten Korrektur des Manuskripts
Druckgenehmigung:	Dieser Abschnitt enthält eine vollständige Druckversion der Publikation publiziert in https://www.mdpi.com/journal/molecules

molecules

MDPI

Article

Autophagy-Related Proteins GABARAP and LC3B Label Structures of Similar Size but Different Shape in Super-Resolution Imaging

Iman Abdollahzadeh [1,2], Johnny Hendriks [1], Julia L. Sanwald [3], Indra M. Simons [3], Silke Hoffmann [2], Oliver H. Weiergräber [2,*], Dieter Willbold [2,3] and Thomas Gensch [1,*]

1 Institute of Complex Systems 4 (ICS-4, Cellular Biophysics), Forschungszentrum Jülich GmbH, Wilhelm-Johnen-Straße, 52428 Jülich, Germany; i.abdollahzadeh@fz-juelich.de (I.A.); jhendriks@upcmail.nl (J.H.)

2 Institute of Complex Systems 6 (ICS-6, Structural Biochemistry), Forschungszentrum Jülich GmbH, Wilhelm-Johnen-Straße, 52428 Jülich, Germany; si.hoffmann@fz-juelich.de (S.H.); d.willbold@fz-juelich.de (D.W.)

3 Institut für Physikalische Biologie, Heinrich-Heine-Universität Düsseldorf, Universitätsstraße 1, 40225 Düsseldorf, Germany; julia.sanwald@uni-duesseldorf.de (J.L.S.); indra.simons@uni-duesseldorf.de (I.M.S.)

* Correspondence: o.h.weiergraeber@fz-juelich.de (O.H.W.); t.gensch@fz-juelich.de (T.G.); Tel.: +49-2461-612028 (O.H.W.); +49-2461-618068 (T.G.)

Academic Editor: Jörg Fitter
Received: 20 March 2019; Accepted: 7 May 2019; Published: 13 May 2019

Abstract: Subcellular structures containing autophagy-related proteins of the Atg8 protein family have been investigated with conventional wide-field fluorescence and single molecule localisation microscopy. Fusion proteins of GABARAP and LC3B, respectively, with EYFP were overexpressed in HEK293 cells. While size distributions of structures labelled by the two proteins were found to be similar, shape distributions appeared quite disparate, with EYFP-GABARAP favouring circular structures and elliptical structures being dominant for EYFP-LC3B. The latter also featured a nearly doubled fraction of U-shape structures. The experimental results point towards highly differential localisation of the two proteins, which appear to label structures representing distinct stages or even specific channels of vesicular trafficking pathways. Our data also demonstrate that the application of super-resolution techniques expands the possibilities of fluorescence-based methods in autophagy studies and in some cases can rectify conclusions obtained from conventional fluorescence microscopy with diffraction-limited resolution.

Keywords: Atg8; autophagy; EYFP blinking; GABARAP; LC3B; shape distribution; single molecule localisation microscopy; SMLM; super-resolution

1. Introduction

Macroautophagy (hereafter autophagy) enables cells to replenish resources for energy metabolism and for anabolic reactions during periods of starvation, and to specifically dispose of large structures that are not amenable to proteasomal degradation. Correspondingly, autophagic cargo ranges from bulk cytosol to protein aggregates, damaged organelles, and even intracellular pathogens [1,2]. A hallmark of autophagy is the formation of double-membrane structures termed phagophores, which engulf cytoplasmic cargo and finally close to yield autophagosomes. The mature autophagosomes (several hundred nanometres in diameter) subsequently fuse with lysosomes, resulting in acidification and degradation of their contents by acid hydrolases. Genetic screening in yeast has led to the identification of more than 30 Atg genes, most of which are conserved in mammalian cells [3]. Among the corresponding

proteins, Atg8 homologs serve different functionalities in autophagosome biogenesis and cargo recruitment. While in yeast only a single Atg8 is expressed, in mammalian cells the family has expanded into a number of paralogs assigned to either the GABA type A receptor-associated protein (GABARAP) or the microtubule associated protein 1 light chain 3 (MAP1LC3, hereafter LC3) subfamily [4].

Numerous studies have shown that proteins of both subfamilies are crucial for mammalian autophagy, and that they exert individual as well as subfamily- and family-specific functions [5,6]. Many of these activities relate to covalent attachment of Atg8 proteins to membrane lipids via their C-termini, enabling them to attract other components to autophagic membranes. These interactions are usually mediated by short linear motifs termed LIRs (LC3 interacting regions) in the target proteins, which bind to conserved hydrophobic pockets on the Atg8 protein surface [7]. For instance, Atg8 family members are well-known to participate in the recruitment of cargo to the concave face of expanding phagophores, exhibiting different specificities for so-called cargo receptors or the cargo molecules themselves [8]. Moreover, data from knockdown experiments and interaction studies point to a mechanistic role of GABARAP-type proteins in both early and late stages of autophagosome formation, involving interactions with components of the autophagy-initiating ULK complex and of the lysosome fusion machinery, respectively [9–11]. Members of the LC3 subfamily, on the other hand, appear to mostly support expansion of phagophores [9], but the respective molecular interactions are poorly defined and may involve lipids rather than proteins. Indeed, similar to their yeast ortholog, mammalian Atg8 proteins have been implicated in the regulation of membrane curvature and in vesicle adhesion and (hemi)fusion [12,13]; the mechanisms underlying these activities and their biological relevance, however, are only beginning to be unravelled. It is worth noting that autophagosome biogenesis has recently been observed to occur even in the absence of Atg8 proteins, albeit with reduced efficiency [14]. While this finding indicates substantial redundancy in the autophagy pathway, supporting fall-back operation even after loss of important components, it does not compromise the utility of proteins belonging to the Atg8 family—to the extent they are expressed—as markers of autophagic structures. Indeed, they are among the first proteins to be found on emerging phagophores shortly after nucleation, and continue to be present on the outer (convex) face at least until autophagosome closure (possibly longer), while on the inner (concave) face they are delivered for degradation together with cargo material [15].

Given the limited size of autophagy-related membrane structures (≈50 nm–1.5 μm), the spatial distribution of associated proteins can only imperfectly be resolved by conventional fluorescence microscopy. This method is subject to the diffraction limit of optical microscopy, which is represented by the Abbe criterion as $d_{x,y} = \lambda/2NA$, where $d_{x,y}$ is the lateral resolution of the microscope, λ is the wavelength of the light, and NA is the numerical aperture of the optics. Hence, for a conventional microscope with NA ≈ 1, the Abbe limit for green light (λ ≈ 500 nm) is roughly 250 nm. The resolution improvement of fluorescence microscopy achieved with the development of super-resolution techniques enables the precise distribution of proteins of interest to be investigated [16]. One of the new methods is single-molecule localisation microscopy (SMLM), which relies on the accurate localisation ($d_{x,y}$ on the order of 10–30 nm) of single fluorescent proteins based on the point spread function of their emitted photons, requiring fluorescence events to be recorded individually [17].

In the current study, we have used SMLM to investigate the spatial distribution of Atg8 proteins in mammalian cells, under autophagy-inducing conditions, using GABARAP and LC3B as representatives of the two subfamilies. At the same time, we aimed to evaluate the impact of the improved lateral resolution in SMLM, compared to conventional fluorescence microscopy, on the results of morphometric analysis. The geometry of fluorophore distribution is of key importance for the interpretation of results in a biological context because it directly relates to the type and stage of the underlying membranous structures. As a first step, we therefore focussed on the development of categories appropriate for systematic investigation of geometrical parameters (such as shape and size) of Atg8-positive structures. Statistical data analysis of SMLM images acquired from cells expressing enhanced yellow fluorescent protein (EYFP) fusion proteins revealed striking differences in shape distribution between GABARAP and LC3B. Moreover, the SMLM-based shape classification is at variance with the one obtained from

conventional wide-field fluorescence microscopy, in particular if small- to medium-sized structures are considered.

2. Results

The shape and size distributions of EYFP-GABARAP and EYFP-LC3B containing structures, respectively, were investigated in fixed HEK293 cells, which were subjected to a standard protocol for enrichment of autophagic structures (starvation and block of autophagosome-lysosome fusion by application of bafilomycin A1) for 2 h right before fixation. For each overexpression, ten cells were selected for detailed evaluation. It was taken care that the selected cells were typical by not preferring cells with certain features, e.g., high (or low) number of fluorescent structures.

First, a fluorescence wide-field image (with diffraction-limited resolution) of the cell of interest was recorded using low excitation power. Subsequently, a pre-acquisition illumination (with 20- to 75-fold higher excitation power) of 20 to 120 s was performed, in which most of the EYFP molecules were photo-converted to metastable, non-fluorescent dark states. SMLM pictures of the EYFP-containing structures with super-resolution (i.e., resolution better than the diffraction limit) were obtained from a wide-field image series keeping the high excitation power mode and utilizing the enduring blinking behaviour of EYFP [18–21]. Measurement of this image series (typically 4000 frames with 50 ms observation time each) was started at the end of the pre-acquisition illumination period, when the remaining EYFP molecules in the fluorescent state were well separated and the maximum intensity in single frames equalled that known for our setup from other single molecule studies on EYFP. A computer program developed in our lab (SNSMIL; Shot Noise based Single Molecule Identification and Localisation [22]) was used to calculate a super-resolution SMLM picture from the image series.

Representative examples of fixed HEK293 cells (starved and bafilomycin A1-treated) expressing EYFP-GABARAP and EYFP-LC3B, respectively, are given in Figure 1. The super-resolved SMLM images (Figure 1B,D) reveal a much higher total number of EYFP-GABARAP containing structures (75 times more) and EYFP-LC3B containing structures (89 and 78 times more for the left and right cell, respectively), compared to the corresponding wide-field images. A similar increase is found for all cells expressing one or the other fluorescent Atg8 construct. The number of EYFP-LC3B containing structures per cell (2898 ± 844) is significantly larger compared to the number of EYFP-GABARAP containing structures (1777 ± 356).

Notably, the subcellular distributions of the two overexpressed Atg8 proteins fused to EYFP are quite different: While EYFP-GABARAP is found mainly in the cytoplasm, EYFP-LC3B shows a higher concentration in the nucleus than in the cytoplasm. The larger labelled structures, however, are exclusively found in the cytoplasm for both proteins. These findings are in good agreement with data reported in literature [1–6]. Indeed, LC3B is thought to reside in the cell nucleus in an inactive acetylated form, which serves as a reservoir to be mobilised upon autophagy stimulation [23]; a different LC3 fraction associated with nuclear insulin receptor substrate 1 (IRS-1) has been suggested to attenuate autophagy in certain tumour cells [24]. GABARAP reservoirs, by contrast, have been identified on the ER and in the pericentriolar matrix [25], but not in the nucleus. Since the entire process of autophagosome biogenesis, maturation and degradation is known to take place outside the nucleus, we decided to focus on the cytoplasmic fraction of the fluorescently labelled objects for further analysis. Re-examination of the SMLM images under this premise yields much more similar values of 1550 ± 286 cytoplasmic EYFP-GABARAP containing structures (CS-EYFP-GABARAP) and 1813 ± 233 cytoplasmic EYFP-LC3B containing structures (CS-EYFP-LC3B), respectively (see Table 1). Thus, the before determined larger number of fluorescently labelled structures in EYFP-LC3B expressing cells, compared to EYFP-GABARAP expressing cells, is caused to a large extent by the nuclear protein fraction in the former case. One last remark to Figure 1C,D, i.e., wide-field and SMLM fluorescence images of EYFP-LC3B expressing cells, needs to be made. The fluorescence intensity contrast between nucleus and cytoplasm in Figure 1C is considerably larger when compared to the difference in numbers of fluorescent structures in those two areas of the cell. This can be explained by properties of the two detection methods, e.g., the larger

focal depth of fluorescence wide-field imaging vs. single molecule detection or possible losses of single molecule detection when two many molecules emit in the same image.

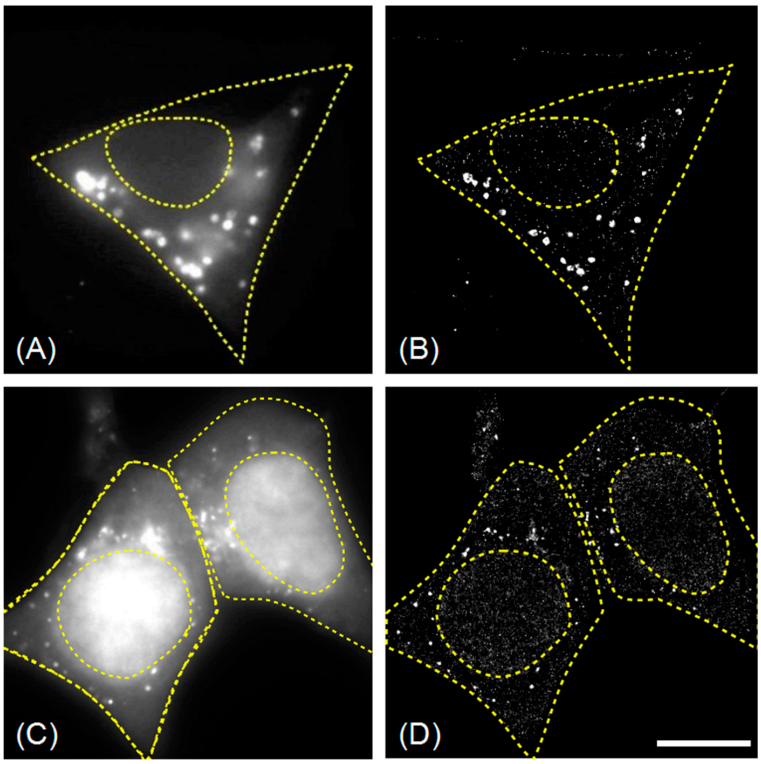

Figure 1. Wide-field (**A**,**C**) and SMLM (**B**,**D**) images of fixed HEK293 cells (starved and bafilomycin A1-treated) expressing EYFP-GABARAP (**A**,**B**), and EYFP-LC3B (**C**,**D**). In the wide-field fluorescence images only a few labelled structures are found (**A**: 22; **C**: 35 and 20 in the left and right cell, respectively), while in the corresponding super-resolution images (**B**,**D**) the numbers of EYFP-GABARAP containing structures (1640) and EYFP-LC3B containing structures (3100 and 1564) are almost two orders of magnitude larger. Scale bar (valid for **A**–**D**): 10 µm.

2.1. Size Distributions of Cytoplasmic EYFP-GABARAP and EYFP-LC3B Containing Structures

The size distributions of all CS-EYFP-GABARAP and CS-EYFP-LC3B are depicted in Figure 2. In general, they are very similar with mean and median slightly above and below 100 nm, respectively. The total number of CS-EYFP-LC3B per cell is only slightly larger than that of CS-EYFP-GABARAP. Notably, the vast majority of structures are smaller than the diffraction limit (ca. 200 nm for fluorescence imaging of EYFP).

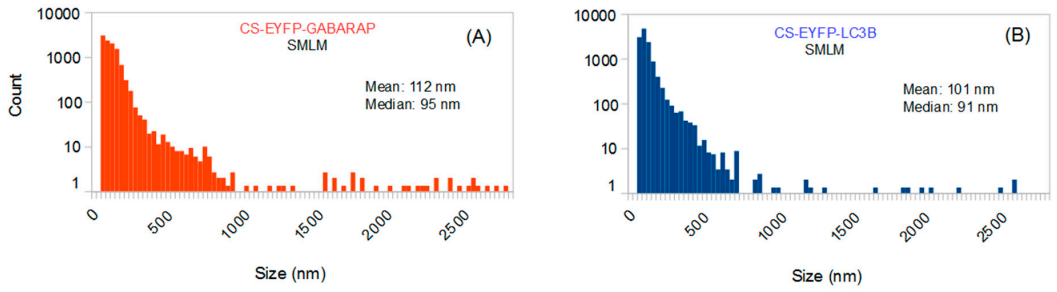

Figure 2. Size distributions (binning 32 nm) of all cytoplasmic, fluorescently labelled structures identified in the SMLM images of ten EYFP-GABARAP expressing (**A**) and ten EYFP-LC3B expressing HEK293 cells (**B**) under starvation and bafilomycin A1 treatment.

For a more appropriate and meaningful comparison of the shape distributions of CS-EYFP-GABARAP and CS-EYFP-LC3B (Section 2.2), we considered it useful to divide the fluorescently labelled structures into two groups with respect to their size, namely small and large structures, for two reasons. First, there might exist a bias towards identifying circular shapes for small fluorescently labelled structures because of limited resolution and pixel size (16 nm in SMLM images). Second, large and small fluorescently labelled structures might well have different origins or functions and, as a consequence, also different shape distributions. We applied two different splitting values, 100 nm and 300 nm. The portion of fluorescently labelled structures larger than 300 nm will contain basically all structures whose shapes could be also classified with conventional fluorescence microscopy techniques like laser-scanning confocal or wide-field fluorescence microscopy. On the other hand, 100 nm is the upper size limit for most common intracellular vesicles in endocytic and secretory pathways. Table 1 reveals that the value of 100 nm splits the CS-EYFP-GABARAP in almost equally large groups, while splitting at 300 nm sees only 2% of the CS-EYFP-GABARAP in the group of the large structures and 98% belong to the small structures. For CS-EYFP-LC3B we find almost the same behaviour with about 40% and 3% of the structures larger than 100 nm and 300 nm, respectively.

Application of single molecule fluorescence imaging techniques might lead to differences with respect to conventional fluorescence microscopy for two reasons: (1) the different resolution, affecting the apparent shapes of visible objects, and (2) the different detection probability for structures as a function of their size. For a meaningful comparison of the information provided by the two methods, we generated sets of CS-EYFP-GABARAP and CS-EYFP-LC3B identifiable on wide-field fluorescence images of the cells (see Table 1).

Table 1. Number of cytoplasmic structures containing EYFP-GABARAP and EYFP-LC3B identified in SMLM images. Counts are given for the entire size range considered (50 nm–2.8 μm) as well as for two sub-ranges (split alternatively at 100 nm or at 300 nm). For comparison, the numbers of cytoplasmic EYFP-GABARAP and EYFP-LC3B containing structures identified in the corresponding wide-field fluorescence images (named "conventional selection") are also given.

Overexpressed Protein	Size Category	Number of Structures	Fraction of Structures (%)
EYFP-GABARAP	50 nm–2.8 μm	15,501	100
	50 nm–100 nm	8009	51.66
	100 nm–2.8 μm	7492	48.33
	50 nm–300 nm	15,153	97.75
	300 nm–2.8 μm	348	2.25
	Conventional selection	348	
EYFP-LC3B	50 nm–2.8 μm	18,129	100
	50 nm–100 nm	11,579	63.87
	100 nm–2.8 μm	6550	36.13
	50 nm–300 nm	17,643	97.32
	300 nm–2.8 μm	486	2.68
	Conventional selection	486	

The size distributions of these "conventionally selected" CS-EYFP-GABARAP and CS-EYFP-LC3B are given in Figure 3. As expected, the results of SMLM-based size analysis differ from those obtained when all structures found in the SMLM images are considered (compare Figure 2A with Figures 3B and 2B with Figure 3D, respectively): No small structures (<300 nm) are found in the conventionally selected set, and mean and median are shifted towards higher values (between 455 and 533 nm). Interestingly, the size distributions of the conventionally selected CS-EYFP-GABARAP and CS-EYFP-LC3B, when determined in the conventional wide-field fluorescence images, were different from those using the respective super-resolution images (compare Figure 3A with Figures 3B and 3C with Figure 3D): There

is an increased number of structures smaller than 500 nm in the SMLM evaluation, although mean and median did not change dramatically.

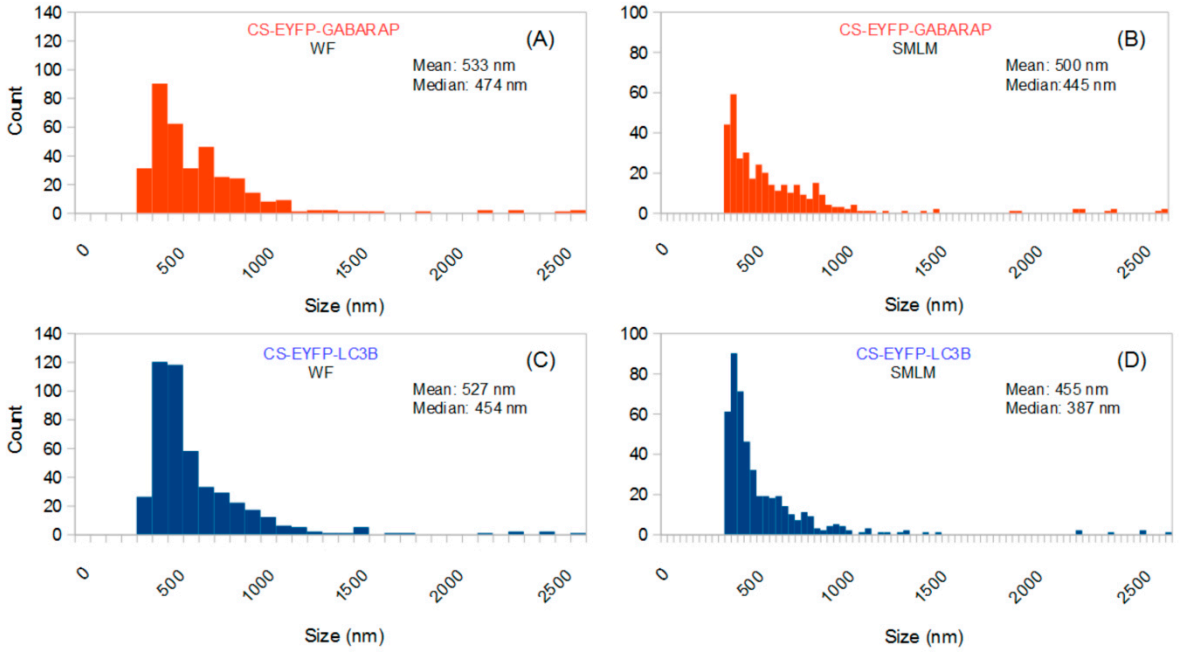

Figure 3. Size distributions of all conventionally selected fluorescently labelled structures (identified in wide-field images) of ten EYFP-GABARAP expressing (**A**,**B**) and ten EYFP-LC3B expressing fixed HEK293 cells (**C**,**D**) under starvation and bafilomycin A1 treatment, where size was determined in the wide-field fluorescence (**A**,**C**) and the SMLM images (**B**,**D**), respectively. Note the different binning used in **A**/**C** (80 nm) and **B**/**D** (32 nm), respectively, caused by the lower resolution in wide-field fluorescence compared to super-resolution microscopy.

2.2. *Shape Classification*

In the next step, we decided to group all fluorescently labelled cytoplasmic structures (within the size ranges defined above) according to their shapes. The shape classification used in this study has been limited to three geometrical categories, namely U-shape, circles and ellipses (abbreviated: u, c and e, respectively). This classification is based on the well-established mechanism of autophagosome formation (Figure 4G and [6,26,27]), where these three shape categories reflect all possible autophagic structures. In the beginning of autophagosome formation, a small double bilayer (i.e., a phagophore) grows around the cargo and may appear as a U-shape structure (when viewed from the side) or as a relatively small circular (when viewed along is longitudinal axis) or elliptical object (when viewed at intermediate angles) in the two-dimensional SMLM imaging mode. During the elongation phase, the phagophore geometry is approaching a half-moon or elliptical shape. Once the autophagosome is mature, its shape will be very similar to a sphere, i.e., a circle in our 2D-projection SMLM imaging mode, except for very large and asymmetrical cargo. In Figure 4, typical examples for the three categories of EYFP-GABARAP and EYFP-LC3B containing structures, respectively, from SMLM images of fixed HEK293 cells are depicted.

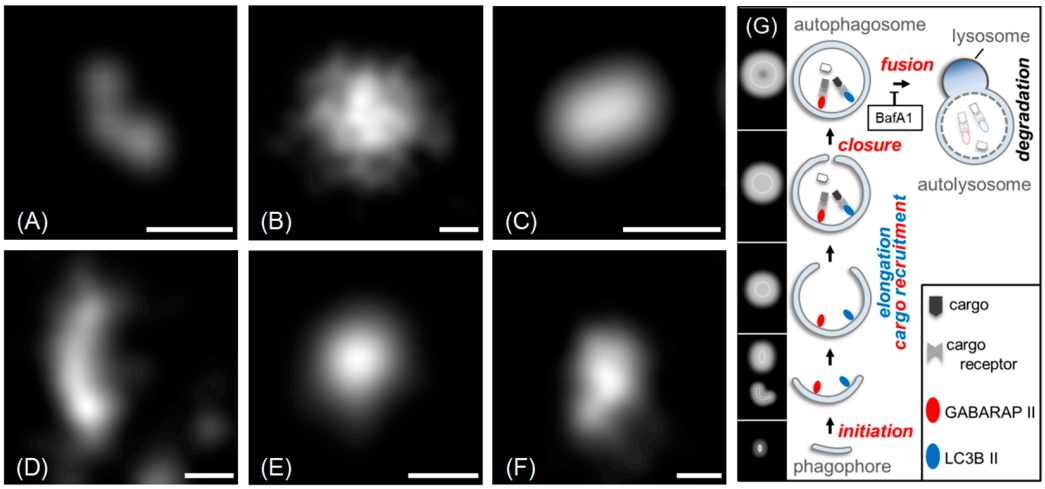

Figure 4. Examples for the three shape categories (**A**,**D**: U-shape; **B**,**E**: circle; **C**,**F**: ellipse). Structures in **A**, **B**, and **C** are from EYFP-GABARAP expressing cells, structures in **D**,**E**, and **F** are from EYFP-LC3B expressing cells (scale bars: 100 nm). In **G**, the presumed roles of GABARAP and LC3B at distinct stages of the autophagy pathway (phagophore initiation, elongation, closure, and fusion of the mature autophagosome with a lysosome to yield an autolysosome) are depicted. Steps that are assumed to require GABARAP and LC3B on the convex face of the isolation membrane (not drawn for clarity reasons) are highlighted in blue and red, respectively. As shown, GABARAP and LC3B can both link cargo materials to the concave face of the isolation membrane during selective autophagy in a cargo receptor-mediated manner. The various autophagic structures drawn as cross-sections are assigned to the respective 2D projections as anticipated in SMLM reconstructions (with a marked direction-dependence in the case of an early phagophore). Note, however, that SMLM cannot strictly distinguish between these membrane-bound autophagic organelles and other (vesicular or non-vesicular) structures populated by Atg8 proteins (see Discussion).

2.2.1. Shape Distributions of Cytoplasmic EYFP-GABARAP and EYFP-LC3B Containing Structures Selected in Super-Resolution Fluorescence Microscopy Images

Classification of all CS-EYFP-GABARAP in the SMLM images led to a unique shape distribution similarly found in all ten fixed HEK293 cells analysed (Figure 5). The number of CS-EYFP-GABARAP per cell varied between 350 and 2300 with a total number of 15501 in all ten cells (Table 1). To better compare the shape distributions of CS-EYFP-GABARAP, we considered it useful to divide the CS-EYFP-GABARAP in two groups, small and large structures, with two different splitting values, 100 and 300 nm, respectively (see paragraph 2.1). The shape distributions in the five size cases (all structures, and structures smaller/larger than 100 nm/300 nm) can be generally described as follows: The majority of CS-EYFP-GABARAP appear as circles, fewer structures as ellipses and a minor fraction shows U-shape (only for CS-EYFP-GABARAP larger than 300 nm, circles and ellipses have similar occurrence; Figure 5E). U-shape structures show the lowest percentage among CS-EYFP- GABARAP (only 9 to 23%) with the highest value in the group of the largest CS-EYFP-GABARAP (>300 nm).

Classification of all CS-EYFP-LC3B occurred in the same way as described above for CS-EYFP-GABARAP (applying again the separation values of 100 nm and 300 nm, respectively). The total number of CS-EYFP-LC3B in the ten analysed transfected HEK293 cells amounted to 18129 and was hence slightly (ca. 20%) larger compared to the experiments with CS-EYFP-GABARAP. Yet, comparison of the total number of labelled structures in an experiment based on overexpression of proteins is not useful, since a number of experimental parameters may vary in transient transfections (e.g., quality of DNA, efficiency of plasmid uptake, yield of chromophore maturation), preventing the reproducibility of absolute protein numbers. The shape distributions of structures labelled with Atg8-family proteins, on the other hand, will reflect specific properties and biological functions of GABARAP and LC3B, respectively, as long as expression levels are not too high.

Molecules **2019**, *24*, 1833

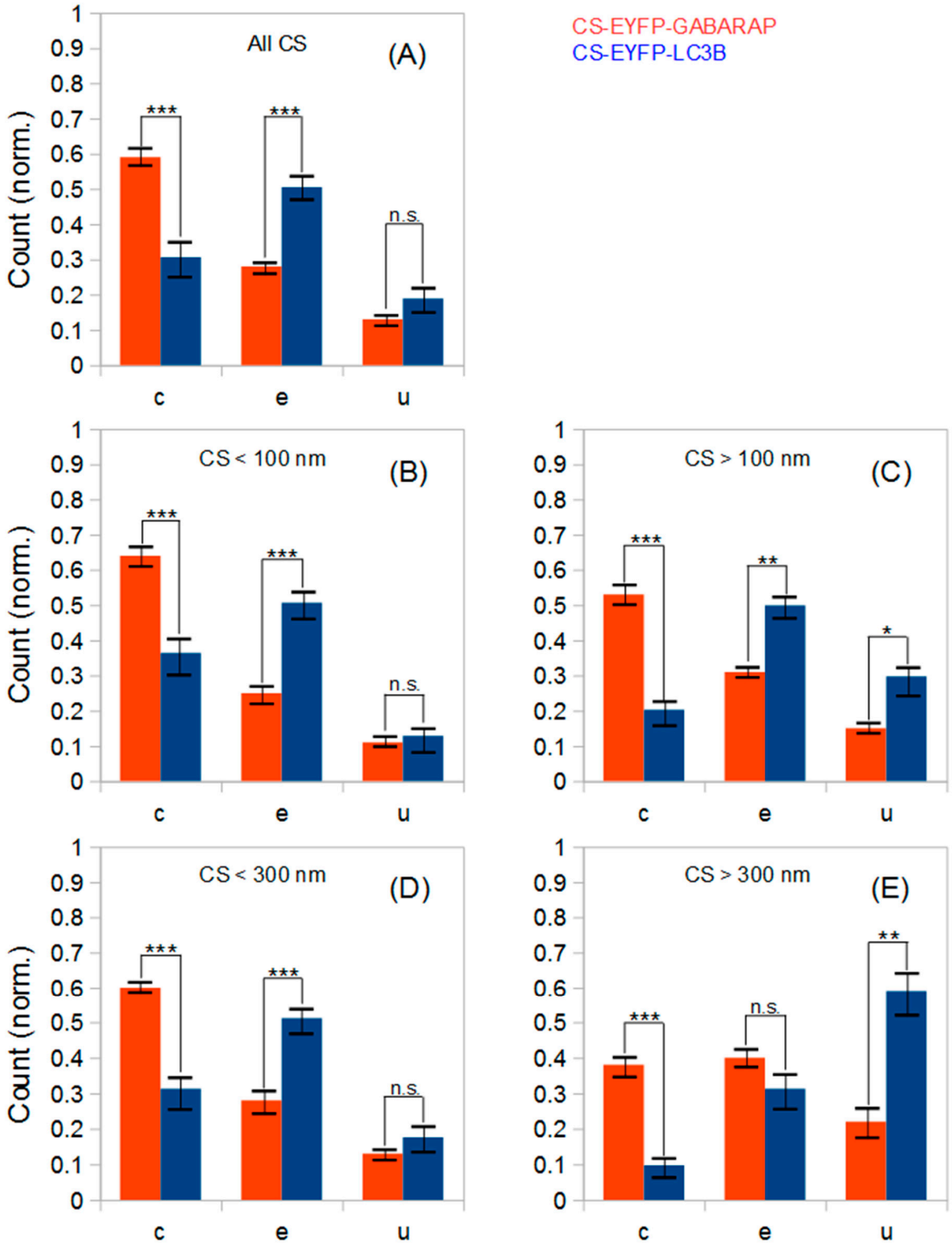

Figure 5. Shape analysis of all cytoplasmic fluorescent structures observed in SMLM images of ten HEK293 cells expressing either EYFP-GABARAP (red) or EYFP-LC3B (blue) under starvation and bafilomycin A1 treatment. (**A**) All CS-EYFP-GABARAP (15501) and CS-EYFP-LC3B (18129); (**B**) CS-EYFP-GABARAP (8009) and CS-EYFP-LC3B (11579) smaller than 100 nm; (**C**) CS-EYFP-GABARAP (7492) nd CS-EYFP-LC3B (6550) larger than 100 nm; (**D**) CS-EYFP-GABARAP (15153) and CS-EYFP-LC3B (17643) smaller than 300 nm; (**E**) CS-EYFP-GABARAP (348) and CS-EYFP-LC3B (486) larger than 300 nm. Error bars represent standard error of the mean. Statistical significance is represented as $P \leq 0.01$ (***); $P \leq 0.05$ (**), and $P \leq 0.1$ (*) from two-tailed t-tests (n.s., not significant). c, e and u stands for circles, ellipses and U-shapes.

The five shape distributions of CS-EYFP-LC3B are plotted in Figure 5 next to the corresponding ones of CS-EYFP-GABARAP, and direct comparison immediately reveals that populations of structures

labelled by EYFP-LC3B and EYFP-GABARAP differ from one another. For all five categories of CS-EYFP-LC3B, ellipses constitute the major fraction (31–51%), while circles—the major fraction for CS-EYFP-GABARAP—were only the second most prevalent for total and the small-size groups of CS-EYFP-LC3B (ca. 30%) and even the minor fraction for the large-size groups of CS-EYFP-LC3B (10–20%). U-shape objects among the CS-EYFP-LC3B were found to be present in higher relative amounts (13–59%) compared to CS-EYFP-GABARAP, being the most abundant shape for CS-EYFP-LC3B larger than 300 nm.

The total number of analysed structures is high and the shape distributions for CS-EYFP-GABARAP and CS-EYFP-LC3B, respectively, appear visually different, especially for the large-size structures. The number of cells analysed (10 for each protein), however, is only moderate. Nevertheless, we performed two-tailed t-tests to survey whether the differences in the relative abundances of circles, ellipses and U-shapes are statistically significant. The results are given in numbers in Table 2, and most of them are also shown graphically in Figure 5.

Table 2. P-values from two-tailed t-tests to assess the statistical significance of differences in the shape distributions (c, circles; e, ellipses; u, U-shapes) of (i) CS-EYFP-GABARAP vs. CS-EYFP-LC3B (various size classes), (ii) different size classes of CS-EYFP-GABARAP, (iii) different size classes of CS-EYFP-LC3B, and (iv) CS-EYFP-GABARAP or CS-EYFP-LC3B structures classified in wide-field vs. SMLM. P-values are indicated by shading and typeface (≤0.01, dark grey and bold face; ≤0.05, medium grey and bold face; ≤0.1, no shading and regular face) for ease of orientation.

	c	e	u
CS-EYFP-GABARAP vs. CS-EYFP-LC3B (50 nm–2.8 µm)	**0.0026**	**0.00050**	0.21
CS-EYFP-GABARAP vs. CS-EYFP-LC3B (< 100 nm)	**0.010**	**0.0053**	0.66
CS-EYFP-GABARAP vs. CS-EYFP-LC3B (> 100 nm)	**0.000026**	**0.019**	**0.10**
CS-EYFP-GABARAP vs. CS-EYFP-LC3B (< 300 nm)	**0.0024**	**0.00035**	0.29
CS-EYFP-GABARAP vs. CS-EYFP-LC3B (> 300 nm)	**0.000023**	0.49	**0.04**
CS-EYFP-GABARAP: CS < 100 nm vs. CS > 100 nm	0.29	0.54	0.20
CS-EYFP-GABARAP: CS < 300 nm vs. CS > 300 nm	**0.0042**	**0.02**	0.23
CS-EYFP-LC3B: CS < 100 nm vs. CS > 100 nm	**0.09**	0.71	**0.04**
CS-EYFP-LC3B: CS < 300 nm vs. CS > 300 nm	**0.03**	**0.08**	**0.02**
CS-EYFP-GABARAP: WF vs. SMLM	**0.000010**	0.50	**0.0018**
CS-EYFP-LC3B:WF vs. SMLM	**0.000010**	0.70	**0.01**

The five shape distributions of CS-EYFP-GABARAP are all statistically significantly different from the corresponding distributions of CS-EYFP-LC3B with at least one P-value smaller than 0.01 and a second one smaller than 0.05. The higher amount of U-shapes for larger cytoplasmic structures containing EYFP-LC3B compared to those containing EYFP-GABARAP is significant too–albeit at a weaker level. Thus, though the number of investigated cells is only moderately high (due to the time-consuming and elaborate size and shape analysis), the shape differences between the structures labelled by the two proteins are highly relevant.

2.2.2. Shape Distributions of Cytoplasmic EYFP-GABARAP and EYFP-LC3B Containing Structures Selected in Wide-Field Fluorescence Microscopy Images

Most fluorescence microscopy studies using Atg8-family proteins fused to fluorescent proteins until now have been carried out using fluorescence microscopy methods with diffraction-limited resolution. As pointed out in Section 2.1, we performed a "hybrid" analysis of our data set, where we carried out a conventional selection of CS-EYFP-GABARAP and CS-EYFP-LC3B and determined their size distribution via conventional as well as super-resolution imaging (Figure 3). As expected, the number of cytosolic fluorescently labelled structures detected by "conventional selection" was found largely reduced and is well below 50 per cell. The improved spatial resolution in the SMLM compared to wide-field fluorescence images, however, unearthed an even more serious observation. The result of

the shape classification for one and the same structure can be different in a wide-field fluorescence image and its corresponding SMLM image, respectively.

To demonstrate this issue, wide-field and super-resolution fluorescence images of five conventionally selected CS-EYFP-LC3B are depicted in Figure 6 (similar examples can be found for CS-EYFP-GABARAP). The structures in A and C are circles, while B, D and E fall into the ellipse category when judged by the wide-field fluorescence images. This simple picture changes when examining the fluorescent structures in the respective SMLM images. While the structures in A (circle) and B (ellipse) appears to have the same shape in super-resolution (compare with F and G, respectively), the other three structures have a different shape when imaged and analysed with higher spatial resolution. The ellipse in D turns into a U-shape in I, while the circle in C resolves into an inhomogeneous ellipse in H. The ellipse in E even appears to be clearly two objects in J, a U-shape and a circle.

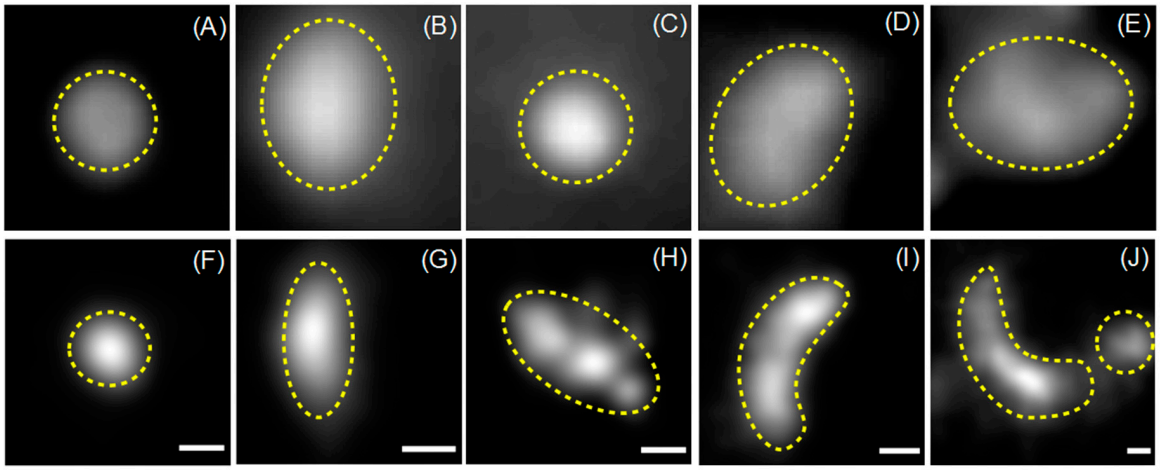

Figure 6. Wide-field fluorescence (**A**–**E**) and SMLM images (**F**–**J**) of five CS-EYFP-LC3B that were identified on the basis of the wide-field image (scale bars: 100 nm).

We analysed the shapes of the "conventionally selected" CS-EYFP-GABARAP and CS-EYFP-LC3B and made a striking observation. For both Atg8 proteins we find a significant difference of the shape distribution dependent on whether the shape was classified in wide-field or super-resolution fluorescence images (Figure 7). U-shapes are very rare (<3%) for CS-EYFP-GABARAP in wide-field fluorescence and grow to ca. 20% in super-resolution images. The relative amount of elliptical shape increases from below 15% to almost 40% on the expense of the circular shape, whose percentage drops from above 80% to 55% (Figure 7A). The change of shape distribution is even more pronounced for CS-EYFP-LC3B when comparing wide-field and super-resolution fluorescence imaging (Figure 7B). Here, circular shapes turn from the dominant fraction (75%) in wide-field fluorescence to the minor fraction (ca. 15%) in super-resolution fluorescence, while the percentage of elliptical shape more than doubles and U-shape grows from less than 5% to almost 40%. For both proteins, the relative abundances for circles and U-shapes are statistically highly significantly different as can be seen in Figure 7 and Table 2.

One more relevant observation of more general nature has to be stated, namely that the shape distributions of the structures containing the two Atg8 proteins appear very similar upon examination in conventional fluorescence microscopy with diffraction-limited resolution (none of the three shape categories has a statistically different relative abundance, see Table 2), but are rather different when shape is judged in super-resolution SMLM fluorescence microscopy. A direct comparison is depicted in Figure 7, since for both proteins the group of cytoplasmic fluorescent structures identified in wide-field images is identical to the group of cytoplasmic fluorescent structures larger than 300 nm identified in SMLM images (fractions of both circles and U-shapes are significantly different). Our data

point towards involvement of GABARAP and LC3B in different stages of autophagosome biogenesis or participation in further, non-autophagy related processes. But this difference would have been overlooked when using conventional fluorescence microscopy methods.

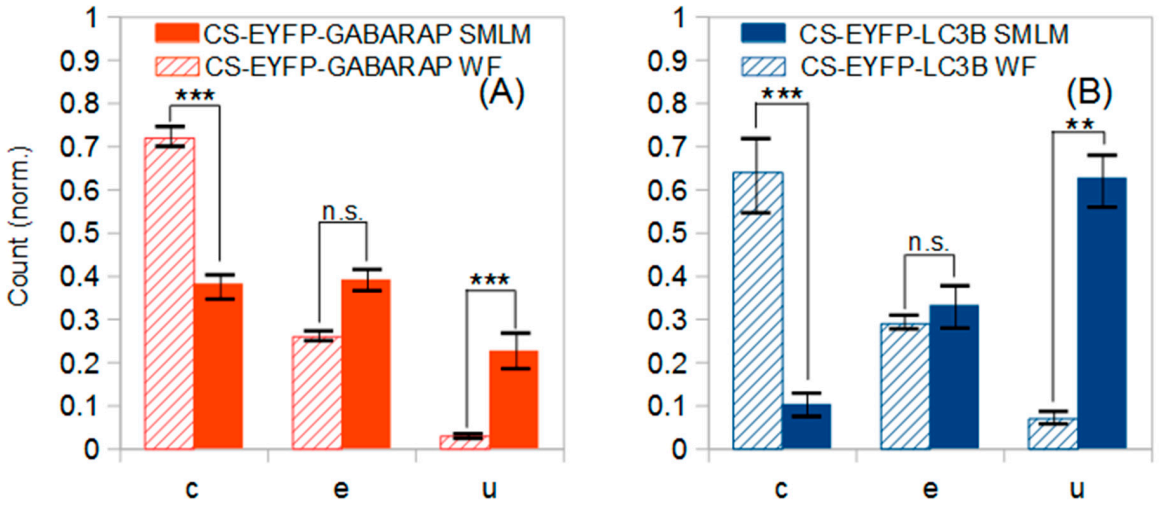

Figure 7. Shape distributions of fluorescently labelled cytoplasmic structures identified in the wide-field images of ten EYFP-GABARAP expressing and ten EYFP-LC3B expressing HEK293 cells, respectively, under starvation and bafilomycin A1 treatment. (**A**) Conventionally selected CS-EYFP-GABARAP (348) classified in wide-field fluorescence (hatched bars) and the same structures classified in the respective SMLM (full bars) images; (**B**) Conventionally selected CS-EYFP-LC3B (486) classified in wide-field fluorescence (hatched bars) and the same structures classified in the respective SMLM (full bars) images. Error bars represent standard error of the mean. Statistical significance is represented as $P \leq 0.01$ (***); $P \leq 0.05$ (**), and $P \leq 0.1$ (*) from two-tailed t-tests (n.s., not significant). c, e and u stands for circles, ellipses and U-shapes.

3. Discussion

The introduction of optical microscopes has marked a revolution in the biological sciences since it enabled the cellular structure of organisms to be directly viewed for the first time [28]. After several centuries, and notwithstanding numerous technical improvements, the basic principle of using lenses to generate magnified views of samples is still widely utilised and continues to provide valuable insight into biological matter. An important complement has been the development of fluorescent tags, which allowed structures of interest to be specifically labelled in both fixed and live cells and which integrated nicely with existing microscopic technology.

It therefore comes as no surprise that fluorescence-enhanced light microscopy has been a major visualisation tool in autophagy research [29]. Autophagic organelles are complex membrane structures undergoing shape transformations during their life cycle, and both morphogenesis and functionality of these membranes are thought to be controlled by associated proteins. Hence, specific microscopic detection of autophagy-related proteins may not only provide hints at their biological functions but can also help to visualise the underlying organelle as a whole, provided that the marker is indeed distributed throughout the structure of interest. Atg8 family proteins are thought to largely meet this requirement; while in-vitro experiments revealed a certain preference for curved membranes [12], enrichment at the edges of expanding phagophores, e.g., has not been demonstrated thus far. Over almost two decades, Atg8 imaging has contributed to a huge body of literature, the vast majority of which, however, has been compromised by the diffraction limit of conventional microscopy. Super-resolution techniques, which basically extract highly precise positional information from microscopic images which per se are diffraction-limited, help to alleviate this shortcoming and are starting to contribute new insight into the autophagy process.

In the current study, we have used SMLM to revisit several intriguing questions in the field: (1) the distribution of sizes and shapes of structures labelled by Atg8 family proteins, resulting from a non-synchronous evolution of numerous individual objects, and (2) the differential localisation of GABARAP and LC3B (representing the two Atg8 subfamilies), which is closely related to their functions on a molecular level.

Our data demonstrate that application of SMLM has the potential to provide superior results in comparison with conventional wide-field microscopy, in terms of both completeness of observations (Figures 1 and 2) and wealth of associated information (Figures 5 and 6). These criteria bear obvious relation with the nominal spatial resolution of the respective images. Observational completeness can be defined as the fraction of the items of interest that can be detected using the method in question. In our hands, SMLM captures about 50 times the number of EYFP-labelled structures found via wide-field microscopy; comprehensive analysis of the size distributions revealed this difference to be mainly due to a vast number of smaller structures (those with diameters < 300 nm) going unnoticed on the wide-field images (Table 1, Figure 3). This is a huge limitation given that a significant portion of autophagy-related structures should fall into this size range, including early isolation membranes and even smaller-sized mature autophagosomes. The advantages of super-resolution microscopy in terms of information content are supported by the observation that even a set of larger structures, which are readily visible on both wide-field and SMLM images, yields quite different data depending on the method used for analysis. In addition to a distortion of size distributions at lower resolution (Figure 3), we find large effects on the assignment of shapes (Figures 6 and 7). The latter illustrates what we consider the most significant corollary of the current study: While structures with dimensions on the order of (or slightly above) the diffraction limit may be readily detectable by conventional microscopy, the information extracted from such images should be treated with caution because sizes and shapes may be biased. Autophagy constitutes an instructive example of a process in which the morphology of organelles directly reflects their functional state, and misinterpretation of, e.g., a U-shape structure (commonly assigned to an early phagophore viewed from the side) as an elliptical object (usually assigned to a late phagophore or autophagosome) may affect biological conclusions drawn from experiments.

Besides these methodological aspects, our SMLM analysis using EYFP fusion proteins revealed important differences between the two Atg8 orthologs investigated. In particular, the shape distributions of the respective labelled structures are quite disparate, indicating differential (but possibly overlapping) localisation: GABARAP and LC3B may appear on phagophores at different stages of their evolution, but could also support distinct autophagic channels or participate in non-autophagy-related pathways. These considerations are well-supported by current evidence. For instance, experiments in which entire Atg8 subfamilies have been knocked down or knocked out in cultured cells suggested that LC3 proteins were mostly required for phagophore expansion, whereas GABARAP proteins acted at a later stage, such as maturation, closure, or autophagosome-lysosome fusion [9,14]. Such a division of tasks would seem consistent with the preponderance of circular and elliptical shapes in our SMLM images after overexpression of GABARAP and LC3B, respectively. It is interesting to note that this correlation can even be replicated in vitro: Vesicles coated with GABARAP tend to fuse into approximately spherical structures whereas LC3B coupling yields more elongated shapes [13]. Regarding their functions in cargo recruitment, members of the Atg8 family are well-established to differ in their affinities towards target structures, often with marked subfamily specificity [7], supporting the idea that the prevalence of different Atg8 orthologs on individual phagophores or autophagosomes may be modulated by the type of substrate. It is also worth noting that enrichment of Atg8 proteins in punctate objects does not necessarily signify phagophores or autophagosomes. The centrosomal pool of GABARAP, e.g., which is thought to play a critical role in autophagosome biogenesis, presumably consists of non-lipidated protein [25], and indeed, neither the centrosomal matrix nor the centriolar satellites shuttling GABARAP along microtubules contain membrane vesicles. Similarly, nuclear association of LC3 with IRS-1 leads to the formation of layered clusters not involving biological membranes [24].

Mammalian Atg8 proteins have also been found to associate with IRGM (immunity-related GTPase M) and the Q_a-SNARE syntaxin-17 (Stx17) in large protein complexes (so-called autophagosome recognition particles, ARPs) which deliver Stx17 to mature autophagosomes, thus enabling fusion with lysosomes. [30]. Again, these structures are assumed to be non-membranous, with IRGM shielding the transmembrane domain of Stx17. Finally, both GABARAP and LC3B participate in cellular processes that are unrelated to autophagy but do involve vesicular structures. Prominent examples include trafficking of vesicles carrying transmembrane receptors towards the plasma membrane, which is typically mediated by GABARAP subfamily proteins [5], and LC3-associated phagocytosis, which is usually engaged if membrane-wrapped extrinsic cargo is to be degraded [31]. A more general function in cellular signalling has emerged for GABARAP-type proteins, which are able to recruit a ubiquitin ligase targeting the RAC1-specific guanine nucleotide exchange factor TIAM1 (T-lymphoma invasion and metastasis-inducing protein 1). This process has been suggested to occur on nonautophagic membranes, although mechanistic connections to autophagy regulation may exist [32]. Based on these considerations, it seems very likely that a certain fraction of the objects labelled by EYFP-fused Atg8 proteins actually constitute non-membranous autophagic or membranous non-autophagic structures, and thus do not represent phagophores or autophagosomes. The abundance of fluorescently labelled particles in the sub-100 nm range, for instance, may be explained to a large part by non-vesicular structures like centriolar satellites or ARPs. While protein complexes of this size are clearly resolved in our SMLM images, they only contribute to a diffuse background in conventional diffraction-limited microscopy, preventing their differentiation from the cytosolic Atg8 pool. Despite the significant gain in spatial information provided by super-resolution fluorescence imaging, unambiguous assignment of structures to specific pathways or even intermediates thereof still requires secondary labelling for a plethora of markers, and will be the subject of future work.

In order to assess the localisation of GABARAP and LC3B, we have resorted to transient overexpression of fluorescent fusion proteins, which is part of the standard toolkit in cell biology research. In comparison to immunolabelling of endogenous protein, this strategy ensures decent signal strength and excellent specificity of detection, but comes with the downside of potentially non-specific localisation of overexpressed protein. The latter might accumulate at sites which are not significantly populated in parent cells, and even at physiological locations pathways may suffer from an overload of protein as well as the presence of the fusion partner. The strength of nuclear staining we observed with EYFP-LC3B even after autophagy stimulation may indicate such an effect of overexpression since it exceeds what has been described previously for endogenous LC3 detected by immunofluorescence. On the other hand, the numbers of cytoplasmic structures populated with EYFP-GABARAP and EYFP-LC3B are quite similar despite the fact that total cytoplasmic fluorescence (representing the abundance of the fusion protein) differs by a factor of five; this suggests that the overall activity of the respective pathways is at most moderately affected by Atg8 protein overexpression, thus supporting the validity of the approach. Development of cell lines stably expressing fluorescent fusion proteins under the control of endogenous promoters will be instrumental to avoid artefacts caused by protein overload while retaining the specificity of detection in both conventional and super-resolution imaging modes.

4. Materials and Methods

4.1. Eukaryotic Plasmids

The gene for GABARAP was subcloned from a GST-GABARAP-fusion plasmid (Addgene plasmid #73948 [33], Addgene, Watertown, MA, USA) by PCR amplification into the XhoI and BamHI sites of peYFP-C1 (Clontech, Mountain View, CA, USA), yielding peYFP-C1/GABARAP [34]. The fluorescent variant of LC3B was generated analogously, starting from a GST-fusion plasmid (Addgene plasmid #73949 [33], Addgene) and yielding peYFP-C1/LC3B.

4.2. Cell Culture and Transfection

Human embryonic kidney 293 (HEK293 [35]; Leibniz-Institute DSMZ–German Collection of Microorganisms and Cell Cultures, Braunschweig, Germany) cells were cultivated at 37 °C in a humidified incubator at 5% CO_2 in Dulbecco's Modified Eagle's Medium (DMEM, Cat. No. D5796, Sigma-Aldrich, Munich, Germany) supplemented with 1% penicillin/streptomycin (P/S, Sigma-Aldrich) and 10% Fetal Calf Serum (FCS, Sigma-Aldrich). For transient transfection with EYFP-GABARAP or EYFP-LC3B constructs, 6×10^5 HEK293 cells were seeded into a 6-well culture plate (Cat. No. 10062-892, VWR, Randor, PA, USA) containing DMEM with 10% FCS and 1% P/S. On the next day, transfection with 1.2 µg total DNA was performed using Polyfect (Cat. No. 301107, QIAGEN, Hilden, Germany) according to the manufacturer's instructions. The following day, $4–5 \times 10^4$ of the transfected cells were seeded into a fibronectin (Sigma-Aldrich) coated µ-dish (Cat. No. 81158, ibidi, Martinsried, Germany) containing DMEM with 10% FCS and 1% P/S and were cultivated for another day in the incubator.

4.3. Starvation

Transfected cells were starved with Hank's Balanced Salt Solution (HBSS, Cat. No. 14025050, Thermo Fisher Scientific, Waltham, MA, USA). For accumulation of autophagic structures in cells, 100 nM bafilomycin A1 (CAS No. 0088899552, Merck KGaA, Darmstadt, Germany) was used as an autophagosome-lysosome fusion blocking agent along with HBSS. Incubation took place at 37 °C and 5% CO_2 for 2 h.

4.4. Fixation

Since autophagic structures are supposed to be connected to cytoskeleton elements, a fixation procedure was used that minimises alterations to cytoskeleton components [36]. The cells were incubated in cytoskeleton buffer (phosphate-buffered saline (PBS, 137 mM NaCl, 2.7 mM KCl, 1.8 mM KH_2PO_4, 10 mM Na_2HPO_4, pH 7.4) containing 4 mM EGTA) for 5 min at 37 °C. Subsequently, cytoskeleton buffer was replaced with fixation solution (4% (*w/v*) paraformaldehyde in cytoskeleton buffer). Fixation took place at room temperature for 10–15 min. After that, cells were rinsed three times with 1 M glycine in PBS and two times with PBS.

4.5. Imaging

For visualisation of fluorescent structures with spatial resolution of the order of 20–30 nm, a home-built SMLM microscope was used [21,37,38]. For SMLM imaging of EYFP-GABARAP and EYFP-LC3B, cells were kept in PBS (pH 7.4). Cells, stored at 4 °C after fixation, were accommodated to room temperature for about 30 min before imaging, because otherwise the recorded image showed lateral and focal drift of the order of several hundreds of nanometres. EYFP was excited with the 514 nm line of an Ar+ laser (Innova 70C, Coherent, Santa Clara, CA, USA). In single-color SMLM experiments with either EYFP-GABARAP or EYFP-LC3B containing structures, the fluorescent protein was first bleached for 10–60 s with 75% laser power until single fluorescent EYFP molecules could be observed in the field of view. The acquired number of single molecule images amounted to 4000–8000. The camera exposure time was set to 50 ms. Image analysis and super-resolution reconstruction were performed with the SNSMIL software, which has been described elsewhere [22]. In this study, the SNSMIL quality parameter was set to 1 to ensure maximum single molecule identification efficiency. The uncertainties of x- and y-position of single EYFP-GABARAP and EYFP-LC3B molecules in the image plane were determined as 38 nm and 27 nm, respectively. With such experimental conditions, the practical resolution of structures in the SMLM images is well below 50 nm.

4.6. Shape and Size Analysis

Evaluation of shape and size of EYFP-GABARAP and EYFP-LC3B containing cytoplasmic structures was performed with the use of ImageJ [39] in a semi-automated approach. The reconstructed

super-resolved image was first converted to a binary image containing only values of 0 or 1. A lower size cut-off must be applied in order to discard very small structures originating from isolated EYFP emitters not linked to EYFP-GABARAP or EYFP-LC3B containing structures, autofluorescence, or noise. We chose 50 nm, well above the positional uncertainty for single molecule emitters in our setup. In the case of asymmetric objects, the longest dimension of the structure had to fall in this size range. Shape classification of CS-EYFP-GABARAP and CS-EYFP-LC3B was performed by visual inspection by the experimenter based on three different geometrical patterns, named circles (c), ellipses (e), and U-shapes (u; see paragraph 2.2 and Figure 4; compare also [40]). The statistical significance of differences in relative abundances of shapes was assessed with the two-tailed t-test function of LibreOffice Calc (Version 5.2; The Document Foundation, Berlin, Germany).

4.7. Selection of Cytoplasmic EYFP-GABARAP and EYFP-LC3B Containing Structures

In order to identify the part of cytoplasmic EYFP-GABARAP and EYFP-LC3B containing structures, a contour around the nucleus was drawn in the transmission (bright field) image of the cell. This contour was transferred to the corresponding SMLM image and the structures within the contour were registered as nucleus-related structures. The remainder of the detected fluorescent structures in the super-resolution image was considered cytoplasmic (yielding the subsets CS-EYFP-GABARAP and CS-EYFP-LC3B) and further analysed.

Author Contributions: Conceptualisation, T.G., S.H. and O.H.W.; methodology, T.G. and J.H.; software, T.G. and J.H.; validation, T.G.; formal analysis, I.A. and T.G.; investigation, I.A., T.G., S.H. and O.H.W.; resources, T.G., S.H., J.L.S., I.M.S.; data curation, I.A., T.G., S.H. and O.H.W.; writing—original draft preparation, I.A., T.G., O.H.W.; writing—review and editing, I.A.,T.G., J.H., S.H., J.L.S., I.M.S., O.H.W. and D.W.; visualisation, I.A., T.G., S.H.; supervision, T.G., S.H. and O.H.W.; project administration, T.G., S.H., O.H.W and D.W.; funding acquisition, T.G., O.H.W. and D.W.

Funding: I.A. was supported by funding of the Vorstandsdoktorandenprogramm of the Forschungszentrum Jülich to T.G., O.H.W., Christoph Fahlke (ICS-4) and D.W. This research was funded by the Deutsche Forschungsgemeinschaft (DFG, German Research Foundation)—Projektnummer 267205415—SFB 1208 (TP B02 to D.W.).

Acknowledgments: We thank Jochen Dobner for his valuable support.

Conflicts of Interest: The authors declare no conflict of interest. The funders had no role in the design of the study; in the collection, analyses, or interpretation of data; in the writing of the manuscript, or in the decision to publish the results.

References

1. He, C.; Klionsky, D.J. Regulation mechanisms and signaling pathways of autophagy. *Annu. Rev. Genet.* **2009**, *43*, 67–93. [CrossRef] [PubMed]
2. Ravikumar, B.; Sarkar, S.; Davies, J.E.; Futter, M.; Garcia-Arencibia, M.; Green-Thompson, Z.W.; Jimenez-Sanchez, M.; Korolchuk, V.I.; Lichtenberg, M.; Luo, S.; et al. Regulation of mammalian autophagy in physiology and pathophysiology. *Physiol. Rev.* **2010**, *90*, 1383–1435. [CrossRef] [PubMed]
3. Nakatogawa, H.; Suzuki, K.; Kamada, Y.; Ohsumi, Y. Dynamics and diversity in autophagy mechanisms: Lessons from yeast. *Nat. Rev. Mol. Cell Biol.* **2009**, *10*, 458–467. [CrossRef] [PubMed]
4. Weiergräber, O.H.; Mohrlüder, J.; Willbold, D. Atg8 family proteins—Autophagy and beyond. In *Autophagy—A Double-Edged Sword–Cell Survival or Death?* Bailly, Y., Ed.; InTech: Rijeka, Croatia, 2013; pp. 13–45. ISBN 978-953-51-1062-0.
5. Schaaf, M.B.; Keulers, T.G.; Vooijs, M.A.; Rouschop, K.M. LC3/GABARAP family proteins: Autophagy-(un)related functions. *FASEB J.* **2016**, *30*, 3961–3978. [CrossRef]
6. Abdollahzadeh, I.; Schwarten, M.; Gensch, T.; Willbold, D.; Weiergräber, O.H. The Atg8 family of proteins–modulating shape and functionality of autophagic membranes. *Front. Genet.* **2017**, *8*, 109. [CrossRef]
7. Birgisdottir, Å.B.; Lamark, T.; Johansen, T. The LIR motif-crucial for selective autophagy. *J. Cell Sci.* **2013**, *126*, 3237–3247. [CrossRef]
8. Zaffagnini, G.; Martens, S. Mechanisms of selective autophagy. *J. Mol. Biol.* **2016**, *428*, 1714–1724. [CrossRef]

9. Weidberg, H.; Shvets, E.; Shpilka, T.; Shimron, F.; Shinder, V.; Elazar, Z. LC3 and GATE-16/GABARAP subfamilies are both essential yet act differently in autophagosome biogenesis. *EMBO J.* **2010**, *29*, 1792–1802. [CrossRef]
10. Alemu, E.A.; Lamark, T.; Torgersen, K.M.; Birgisdottir, A.B.; Larsen, K.B.; Jain, A.; Olsvik, H.; Øvervatn, A.; Kirkin, V.; Johansen, T. ATG8 family proteins act as scaffolds for assembly of the ULK complex: Sequence requirements for LC3-interacting region (LIR) motifs. *J. Biol. Chem.* **2012**, *287*, 39275–39290. [CrossRef]
11. Kriegenburg, F.; Ungermann, C.; Reggiori, F. Coordination of autophagosome-lysosome fusion by Atg8 family members. *Curr. Biol.* **2018**, *28*, R512–R518. [CrossRef] [PubMed]
12. Knorr, R.L.; Nakatogawa, H.; Ohsumi, Y.; Lipowsky, R.; Baumgart, T.; Dimova, R. Membrane morphology is actively transformed by covalent binding of the protein Atg8 to PE-lipids. *PLoS ONE* **2014**, *9*, e115357. [CrossRef] [PubMed]
13. Landajuela, A.; Hervás, J.H.; Antón, Z.; Montes, L.R.; Gil, D.; Valle, M.; Rodriguez, J.F.; Goñi, F.M.; Alonso, A. Lipid geometry and bilayer curvature modulate LC3/GABARAP-mediated model autophagosomal elongation. *Biophys. J.* **2016**, *110*, 411–422. [CrossRef]
14. Nguyen, T.N.; Padman, B.S.; Usher, J.; Oorschot, V.; Ramm, G.; Lazarou, M. Atg8 family LC3/GABARAP proteins are crucial for autophagosome-lysosome fusion but not autophagosome formation during PINK1/Parkin mitophagy and starvation. *J. Cell Biol.* **2016**, *215*, 857–874. [CrossRef]
15. Yoshii, S.R.; Mizushima, N. Monitoring and measuring autophagy. *Int. J. Mol. Sci.* **2017**, *18*, 1865. [CrossRef]
16. Huang, B.; Bates, M.; Zhuang, X. Super-resolution fluorescence microscopy. *Annu. Rev. Biochem.* **2009**, *78*, 993–1016. [CrossRef] [PubMed]
17. Sauer, M.; Heilemann, M. Single-molecule localization microscopy in eukaryotes. *Chem. Rev.* **2017**, *117*, 7478–7509. [CrossRef]
18. Dickson, R.M.; Cubitt, A.B.; Tsien, R.Y.; Moerner, W.E. On/off blinking and switching behaviour of single molecules of green fluorescent protein. *Nature* **1997**, *388*, 355–358. [CrossRef] [PubMed]
19. Biteen, J.S.; Thompson, M.A.; Tselentis, N.K.; Bowman, G.R.; Shapiro, L.; Moerner, W.E. Super-resolution imaging in live Caulobacter crescentus cells using photoswitchable EYFP. *Nat. Methods* **2008**, *5*, 947–949. [CrossRef]
20. Lee, S.F.; Thompson, M.A.; Schwartz, M.A.; Shapiro, L.; Moerner, W.E. Super-Resolution Imaging of the Nucleoid-Associated Protein HU in Caulobacter crescentus. *Biophys. J.* **2011**, *100*, L31–L33. [CrossRef] [PubMed]
21. Stölting, G.; Campos de Oliveira, R.; Guzman, R.E.; Miranda-Laferte, E.; Conrad, R.; Jordan, N.; Schmidt, S.; Hendriks, J.; Gensch, T.; Hidalgo, P. Direct Interaction of CaVβ with Actin Up-regulates L-type Calcium Currents in HL-1 Cardiomyocytes. *J. Biol. Chem.* **2015**, *290*, 4561–4572. [CrossRef]
22. Tang, Y.; Dai, L.; Zhang, X.; Li, J.; Hendriks, J.; Fan, X.; Gruteser, N.; Meisenberg, A.; Baumann, A.; Katranidis, A.; et al. SNSMIL, a real-time single molecule identification and localization algorithm for super-resolution fluorescence microscopy. *Sci. Rep.* **2015**, *5*, 11073. [CrossRef]
23. Huang, R.; Xu, Y.; Wan, W.; Shou, X.; Qian, J.; You, Z.; Liu, B.; Chang, C.; Zhou, T.; Lippincott-Schwartz, J.; Liu, W. Deacetylation of nuclear LC3 drives autophagy initiation under starvation. *Mol. Cell* **2015**, *57*, 456–466. [CrossRef]
24. Lassak, A.; Dean, M.; Wyczechowska, D.; Wilk, A.; Marrero, L.; Trillo-Tinoco, J.; Boulares, A.H.; Sarkaria, J.N.; Del Valle, L.; Peruzzi, F.; Ochoa, A.; Reiss, K. Molecular and Structural Traits of Insulin Receptor Substrate 1/LC3 Nuclear Structures and Their Role in Autophagy Control and Tumor Cell Survival. *Mol. Cell Biol.* **2018**, *38*, e00608-17. [CrossRef] [PubMed]
25. Joachim, J.; Jefferies, H.B.; Razi, M.; Frith, D.; Snijders, A.P.; Chakravarty, P.; Judith, D.; Tooze, S.A. Activation of ULK Kinase and Autophagy by GABARAP Trafficking from the Centrosome Is Regulated by WAC and GM130. *Mol. Cell* **2015**, *60*, 899–913. [CrossRef]
26. Shibutani, S.T.; Yoshimori, T. A current perspective of autophagosome biogenesis. *Cell Res.* **2014**, *24*, 58–68. [CrossRef]
27. Carlsson, S.R.; Simonsen, A. Membrane dynamics in autophagosome biogenesis. *J. Cell Sci.* **2015**, *128*, 193–205. [CrossRef] [PubMed]
28. Wollman, A.J.; Nudd, R.; Hedlund, E.G.; Leake, M.C. From Animaculum to single molecules: 300 years of the light microscope. *Open Biol.* **2015**, *5*, 150019. [CrossRef] [PubMed]

29. Wang, Y.; Li, Y.; Wei, F.; Duan, Y. Optical Imaging Paves the Way for Autophagy Research. *Trends Biotechnol.* **2017**, *35*, 1181–1193. [CrossRef] [PubMed]
30. Kumar, S.; Jain, A.; Farzam, F.; Jia, J.; Gu, Y.; Choi, S.W.; Mudd, M.H.; Claude-Taupin, A.; Wester, M.J.; Lidke, K.A.; Rusten, T.E.; Deretic, V. Mechanism of Stx17 recruitment to autophagosomes via IRGM and mammalian Atg8 proteins. *J. Cell Biol.* **2018**, *217*, 997–1013. [CrossRef]
31. Fazeli, G.; Wehman, A.M. Safely removing cell debris with LC3-associated phagocytosis. *Biol. Cell* **2017**, *109*, 355–363. [CrossRef] [PubMed]
32. Genau, H.M.; Huber, J.; Baschieri, F.; Akutsu, M.; Dötsch, V.; Farhan, H.; Rogov, V.; Behrends, C. CUL3-KBTBD6/KBTBD7 ubiquitin ligase cooperates with GABARAP proteins to spatially restrict TIAM1-RAC1 signaling. *Mol. Cell* **2015**, *57*, 995–1010. [CrossRef] [PubMed]
33. Ma, P.; Schwarten, M.; Schneider, L.; Boeske, A.; Henke, N.; Lisak, D.; Weber, S.; Mohrlüder, J.; Stoldt, M.; Strodel, B.; et al. Interaction of Bcl-2 with the autophagy-related $GABA_A$ receptor-associated protein (GABARAP): Biophysical characterization and functional implications. *J. Biol. Chem.* **2013**, *288*, 37204–37215. [CrossRef] [PubMed]
34. Simons, I.M.; Mohrküder, J.; Feederle, R.; Kremmer, E.; Zobel, T.; Dobner, J.; Bleffert, N.; Hoffmann, Si.; Willbold, D. The highly GABARAP specific rat momoclonal antibody 8H5 visualizes GABARAP in immunofluorescence imaging at endogeneous levels. *Sci. Rep.* **2019**, *9*, 526. [CrossRef]
35. Graham, F.L.; Smiley, J.; Russell, W.C.; Nairn, R. Characteristics of a human cell line transformed by DNA from human adenovirus type 5. *J. Gen. Virol.* **1977**, *36*, 59–74. [CrossRef] [PubMed]
36. Allen, J.R.; Ross, S.T.; Davidson, M.W. Sample preparation for single molecule localization microscopy. *Phys. Chem. Chem. Phys.* **2013**, *15*, 18771–18783. [CrossRef]
37. Baumgart, M.; Huber, I.; Abdollahzadeh, I.; Gensch, T.; Frunzke, J. Heterologous expression of the Halothiobacillus neapolitanus carboxysomal gene cluster in Corynebacterium glutamicum. *J. Biotechnol.* **2017**, *258*, 126–135. [CrossRef] [PubMed]
38. Conrad, R.; Stölting, G.; Hendriks, J.; Ruello, G.; Kortzak, D.; Jordan, N.; Gensch, T.; Hidalgo, P. Rapid turnover of the cardiac L- type CaV1.2 calcium channel by endocytic recycling regulates its cell surface availability. *iScience* **2018**, *1*, 1–15. [CrossRef] [PubMed]
39. Schneider, C.A.; Rasband, W.S.; Eliceiri, K.W. NIH Image to ImageJ: 25 years of image analysis. *Nat. Meth.* **2012**, *9*, 671–675. [CrossRef]
40. Karanasios, E.; Walker, S.A.; Okkenhaug, H.; Manifava, M.; Hummel, E.; Zimmermann, H.; Ahmed, Q.; Domart, M.-C.; Collinson, L.; Ktistakis, N.T. Autophagy initiation by ULK complex assembly on ER tubulovesicular regions marked by ATG9 vesicles. *Nat. Commun.* **2016**, *7*, 12420. [CrossRef]

Sample Availability: Samples of the EYFP-GABARAP and EYFP-LC3B constructs for overexpression in mammalian cells are available from the authors.

3.3 Deficiency of GABARAP but not its Paralogs Causes Enhanced EGF-induced EGFR Degradation

Autoren: Dobner J., Simons, I. M., Rufinatscha K., Hänsch S., Abdollahzadeh, I., Gensch, T., Bode J. G., Hoffmann S., Willbold, D.

Journal: *Cells* **2020**, 9(5), 1296
veröffentlicht am 22.05.2020

DOI: 10.3390/cells9051296

Impact Factor: 4,829 (2018), 5,656 (2020)

Beitrag: Zellkultivierung, Vorbereitung der Proben und Durchführung aller Immunfluoreszenz-Versuche, deren Mikroskopie (LSM 710) und Auswertung

Lebendzell-Mikroskopie Aufnahmen mittels LSM710, Datennachbearbeitung und Zusammenstellung der Videos

Vorbereitung der Daten (einzelne Zellen per ROIs definieren) für die Auswertung der Rohdaten durch das *Center of Advanced Imaging* (CAi) (Imaris), Assistenz bei der Vesikelmodellierung mittels Imaris, weitere nachfolgende Auswertungen sowie graphische Darstellung der Immunfluoreszenz-Aufnahmen

Zellkultivierung, Vorbereitung der Proben und Versuchsdurchführung, Aufarbeitung der *spinning disk* Mikroskop (SDM)-Aufnahmen mit Hilfe eines eigens programmierten Makros und anschließende Auswertung der SDM Daten

Anfertigung von Abbildungen und Graphen

Korrektur des Manuskripts

Druckgenehmigung: Dieser Abschnitt enthält eine vollständige Druckversion der Publikation publiziert in https://www.mdpi.com/journal/cells

cells

MDPI

Article

Deficiency of GABARAP but Not Its Paralogs Causes Enhanced EGF-Induced EGFR Degradation

Jochen Dobner [1], Indra M. Simons [1,2], Kerstin Rufinatscha [3], Sebastian Hänsch [4], Melanie Schwarten [2], Oliver H. Weiergräber [2], Iman Abdollahzadeh [2,5], Thomas Gensch [5], Johannes G. Bode [3], Silke Hoffmann [2] and Dieter Willbold [1,2,*]

1 Institut für Physikalische Biologie, Heinrich-Heine-Universität Düsseldorf, 40225 Düsseldorf, Germany; j.dobner@fz-juelich.de (J.D.); i.simons@fz-juelich.de (I.M.S.)
2 Institute of Biological Information Processing: Structural Biochemistry (IBI-7), Forschungszentrum Jülich, 52425 Jülich, Germany; m.schwarten@fz-juelich.de (M.S.); o.h.weiergraeber@fz-juelich.de (O.H.W.); i.abdollahzadeh@fz-juelich.de (I.A.); si.hoffmann@fz-juelich.de (S.H.)
3 Department of Gastroenterology, Hepatology and Infectiology, University Hospital, Heinrich-Heine-Universität Düsseldorf, 40225 Düsseldorf, Germany; rufinats@hhu.de (K.R.); Johannes.Bode@med.uni-duesseldorf.de (J.G.B.)
4 Department of Biology, Center for Advanced Imaging (CAi), Heinrich-Heine-Universität Düsseldorf, 40225 Düsseldorf, Germany; Sebastian.Haensch@uni-duesseldorf.de
5 Institute of Biological Information Processing: Molecular and Cell Physiology (IBI-1), Forschungszentrum Jülich, 52425 Jülich, Germany; t.gensch@fz-juelich.de
* Correspondence: d.willbold@fz-juelich.de; Tel.: +49-2461-61-2100

Received: 27 February 2020; Accepted: 20 May 2020; Published: 22 May 2020

Abstract: The γ-aminobutyric acid type A receptor-associated protein (GABARAP) and its close paralogs GABARAPL1 and GABARAPL2 constitute a subfamily of the autophagy-related 8 (Atg8) protein family. Being associated with a variety of dynamic membranous structures of autophagic and non-autophagic origin, Atg8 proteins functionalize membranes by either serving as docking sites for other proteins or by acting as membrane tethers or adhesion factors. In this study, we describe that deficiency for GABARAP alone, but not for its close paralogs, is sufficient for accelerated EGF receptor (EGFR) degradation in response to EGF, which is accompanied by the downregulation of EGFR-mediated MAPK signaling, altered target gene expression, EGF uptake, and EGF vesicle composition over time. We further show that GABARAP and EGFR converge in the same distinct compartments at endogenous GABARAP expression levels in response to EGF stimulation. Furthermore, GABARAP associates with EGFR in living cells and binds to synthetic peptides that are derived from the EGFR cytoplasmic tail in vitro. Thus, our data strongly indicate a unique and novel role for GABARAP during EGFR trafficking.

Keywords: EGFR; GABARAP; receptor trafficking; degradation; Atg8; genome editing

1. Introduction

The epidermal growth factor receptor (EGFR/ErbB1) is a plasma membrane bound receptor tyrosine kinase (RTK) that is expressed in many different cell types and plays an important role in numerous processes, such as development, tissue homeostasis, and regeneration [1,2], by binding a variety of ligands, including transforming growth factor-α (TGF α) [3], amphiregulin [4], and the eponymous epidermal growth factor [5]. The binding of these ligands causes either homo- or heterodimerization with the other members of the erythroblastosis oncogene B (ErbB) superfamily ErbB2, ErbB3, and ErbB4 [6], leading to intrinsic kinase activation and autophosphorylation of distinct tyrosine residues in the C-terminal cytoplasmic region of the receptor [7,8]. The subsequent

recruitment and activation of various downstream signaling pathways causes a plethora of cellular effects, depending on which pathway is activated, including cell growth, proliferation, differentiation, and motility [9–11]. Dephosphorylation and/or degradation of the activated receptor are necessary to strictly control and regulate these signaling events, thus preventing the sustained activation and uncontrolled cell growth that are found in many types of cancer [12,13].

Ligand-associated EGFR undergoes rapid internalization [14,15], which can either be clathrin-dependent [16] or independent [17]. Whereas the former mainly occurs under low ligand concentrations, leading to sustained EGFR signaling and enhanced recycling back to the plasma membrane through a non-degradative sorting pathway, with the latter being accompanied by monoubiquitination at several sites and packaging of activated receptors in intraluminal vesicles (ILV) of multivesicular bodies (MVB), followed by maturation to late endosomes and ultimately fusion with the lysosome where the receptor is degraded by pH-dependent hydrolases [18].

Autophagy is an intracellular degradation pathway [19]. Upon stress conditions, such as nutrient starvation, but also in response to oxidative stress and pathogen infection [20], membrane cisternae in the cytosol of cells arise and engulf cargo either non-selectively or selectively. Their closure finally yields double-membrane vesicles, termed autophagosomes. Ultimately, their fusion with the lysosome leads to the degradation of autophagosomal content [21]. This enables cells to survive by repurposing amino acids and other resources, to get rid of damaged organelles [22], but also to eliminate pathogens [23]. The autophagic degradation of RET (receptor tyrosine kinase Proto-oncogene tyrosine-protein kinase receptor) and associated proto-oncogene tyrosine-protein kinase SRC via autophagy has also been reported [24,25]. Apart from degradation, components of the autophagic machinery are also implicated in the secretion processes by facilitating a form of unconventional protein secretion [26,27]. Proteins of the autophagy-related (Atg) protein family have first been identified in yeast and they are involved in every step of the autophagic process [28,29]. While, in yeast only a single *Atg8* gene exists [30], in mammalian cells the family has expanded into a number of paralogs [31]. The microtubule-associated proteins 1A/1B light chain 3 (LC3) proteins A, B, and C are grouped in the LC3 subfamily, whereas γ-aminobutyric acid type A receptor-associated protein (GABARAP) and its two paralogs GABARAPL1 and GABARAPL2 form the GABARAP subfamily, according to their degree of relation. Besides (canonical) autophagy, GABARAP subfamily members have been described to play pivotal roles in many cellular processes, such as immunity, receptor trafficking, unconventional secretion of leaderless proteins [32–34], and interaction with viral proteins [35–37]. However, because they share high sequence and structural similarity [38] within and between subfamilies, the elucidation of their exact and especially non-redundant functions requires the development of highly specific and sensitive readout systems. Progress towards this goal has been made in the field of autophagy, especially regarding their roles during autophagosome biogenesis (e.g., [39–41]) as well as selective cargo loading via cargo receptor interaction ([42–44]). Respective overviews can be found in several recent reviews (e.g., [32,34,45–48]). The direct binding of interaction partners to Atg8 proteins is mediated by a canonical interaction motif, generally known as LC3-interacting region (LIR) or GABARAP interaction motif (GIM) in the case of GABARAP subfamily ligands [49], which can reach various levels of specificity [50]. Very recently, an additional motif, related to the ubiquitin interacting motif (UIM), was described utilizing a binding region localized opposite to the LIR/GIM-docking site on the Atg8 protein surface [51].

Additionally, it has long been known that the proteins of the GABARAP subfamily are involved in the regulation of cell surface receptor trafficking. GABARAP was first described to be associated to the name-giving GABAA receptor [52] and implicated in its trafficking [53]. It was also described to be associated with the Transferrin receptor [54] and be important in the clustering of Transient receptor potential cation channel subfamily V member 1 (TRPV1) at the cell surface [55]. Furthermore, angiotensin II type 1 (AT1) receptor plasma membrane expression was described to be mediated by GABARAP [56], while sodium-dependent phosphate transport protein 2A (SLC34A1) levels were found to be increased in its absence [57]. Recently, GABARAPL2 was reported to be directly involved in

regulating the protein levels of Parkin associated endothelin like receptor (PAELR) [58]. GABARAPL1, in turn, has also been described to be implicated in trafficking of the GABAA receptor [59] and the κ-opioid receptor [60]. Importantly, GABARAPL1 has already been connected with increased EGFR surface expression under hypoxic conditions without altering the total EGFR levels [61]. However, in almost all above-mentioned autophagy-unrelated functions, systematic analysis revealing unique and non-redundant roles of the three human GABARAP subfamily members are largely lacking.

Therefore, the aim of this work was to analyze the role of the different members of the GABARAP subfamily of human Atg8 family proteins in trafficking, signaling, and degradation of the cell surface receptor EGFR as a model RTK.

2. Materials and Methods

2.1. Materials

A list of antibodies (Table A1) and RT-PCR primers (Table A2) used in this study can be found in Appendix A. Unless stated otherwise, antibodies were used at dilutions according to the manufacturer's instructions.

2.2. Cell Culture

Human hepatoma Huh7.5 cells [62] were maintained in Dulbecco's Modified Eagle Medium (DMEM) high glucose (F0445, Biochrom, Berlin, Germany) that was supplemented with 10% (*v*/*v*) heat-inactivated fetal bovine serum (FBS, 10270-106, ThermoFisher Scientific, Waltham, MA, USA), 2 mM L-glutamine (25040081, ThermoFisher Scientific), 1% penicillin/streptomycin (15140-122, ThermoFisher Scientific), 10 µL/mL non-essential amino acids (NEAA, 11140-035, ThermoFisher Scientific) at 37 °C and 5% CO_2. The use of the Huh7.5 cell line is covered by a material transfer agreement with Apath, L.L.C. (New York City, NY, USA). Human embryonic kidney 293 (HEK293) Flp-In T-Rex cells [63,64] were maintained in DMEM high glucose that was supplemented with 10% (*v*/*v*) heat-inactivated FBS at 37 °C and 5% CO_2. The cells were split regularly at 80% confluency and used for a maximum of 30 passages after thawing. Cells were routinely checked for mycoplasma contamination.

For treatment with EGF and inhibitors 0.14×10^6 cells were seeded two days prior treatment in wells of six-well plates. The cells were pretreated with either 10 µM lactacystin (L6785, Sigma–Aldrich, St. Louis, MO, USA) for 1 h, 100 µM chloroquine (14774, Cell Signaling Technologies, Danvers, MA, USA) for 2 h or left untreated, followed by treatment with 40 ng/mL EGF (11376454001, Roche, Basel, Switzerland) for up to 180 min.

2.3. CRISPR/Cas9 Mediated Knockout Generation

Knockout (KO) cell lines were generated, as described [65]. In brief, the cells were transfected with KO plasmids based on pSpCas9(BB)-2A-GFP (PX458) [66], single sorted for fluorescent protein (FP) positive signals via fluorescence-activated cell-sorting (FACS) in wells of 96-well plates, clonal lines recovered and occurrence of genome editing verified via the amplification of a 400 bp product flanking the target site and Sanger sequencing as well as on protein level with specific antibodies. Knock-in (KI) of an enhanced green fluorescent protein (EGFP) at the endogenous locus of GABARAP was achieved by transfecting a homology-directed repair (HDR-) plasmid containing homology arms 1 kbp up- and downstream of the CRISPR target site flanking the sequence for EGFP. The cells were serum starved 24 h prior transfection to enhance HDR, sorted by FACS as single cells in wells of 96-well plates, and recovered and analyzed as the KO cells. The resulting cell line was termed GFP-GABARAP. Sequences for primers used for Sanger sequencing can be found in Table S1.

2.4. Transient Transfection

Nucleofection was performed according to the manufacturer's instructions (Lonza, Basel, Switzerland) with 4D Nucleofector. In brief, HEK293 Flp-In T-REx cells were split 2–3 days prior to

nucleofection. On the day of nucleofection, 1×10^6 cells were nucleofected with 2 µg plasmid DNA and cell membranes recovered by adding warm RPMI (21875034, ThermoFisher Scientific) medium containing 10% FBS for 10 min. at 37 °C to each reaction. Afterwards, the cells were seeded into wells of 12-well plates and treated with 40 ng/mL EGF for up to 180 min. two days post nucleofection.

Lipofection with Lipofectamin2000 reagent was performed according to the manufacturer's instructions (11668019, Qiagen, Hilden, Germany). Briefly, one day prior transfection, 3×10^5 Huh7.5 cells were seeded in wells of 6-well plates in growth medium without antibiotics. On the day of transfection, 3 µg of each plasmid DNA and 10.5 µL Lipofectamin2000 reagent were diluted in 150 µL Opti MEM (1×) + GlutaMAX reduced serum medium (51985042, ThermoFisher Scientific), mixed and incubated for 5 min. at RT to form plasmid-lipid complexes. Afterwards, 250 µL of this solution were added dropwise to wells of the 6-well plates in order to reach a final plasmid amount of 2.5 µg per well and then incubated for two days at 37 °C until further experiments. EGFR-GFP was a gift from Alexander Sorkin (Addgene plasmid #32751).

2.5. Immunoblot

The cells were washed once with ice cold PBS and then harvested by scraping into cell lysis buffer (1% Triton, 20 mM Tris/HCl, pH 7.4, 13.6 mM NaCl, 2 mM EDTA, 50 mM β-glycerophosphate, 20 mM sodium pyrophosphate, 1 mM $Na3VO_4$, 4 mM benzamidine, 0.2 mM Pefabloc, 5 µg/mL aprotinin, 5 µg/mL leupeptin, 10% glycerol, and 0.2% SDS) on ice. Cell lysis was carried out by incubating samples on ice for 10 min. The supernatants were cleared by centrifugation at 20,000 g for 15 min. at 4 °C, transferred to fresh tubes, and protein concentration was determined by BCA assay. In general, 20–30 µg of whole cell protein lysate were supplemented with 4 × Lämmli buffer (250 mM Tris-HCl pH 6.8, 40% glycerol, 5% SDS, 0.005% bromophenol blue) supplemented with fresh 8% 2-mercaptoethanol, boiled for 7 min. at 95 °C and loaded on 10 or 12 %-PAA gels for SDS-PAGE. After SDS-PAGE, gels were imaged with BioRad Imager using the stain-free method in order to determine protein loading [67] and then transferred to 0.4 µm PVDF membrane via semidry blotting at 0.77 mA/cm^2 gel constant current for 1 h. The membranes were afterwards cut, washed for 5 min. with TBS containing 0.1% Tween20 (TBS-T) at RT, blocked with 5% BSA in TBS-T for 1 h at RT, and incubated with specific antibodies overnight at 4 °C. On the next day, blots were washed thrice with TBS-T at RT for 20 min. and incubated with fluorescently labeled secondary antibodies for 1 h at RT wrapped in aluminium foil. Afterward, membranes were washed thrice with TBS-T for 20 min. at RT. The protein levels were visualized either directly using BioRad Imager with detection settings specific for Alexa488 or Alexa647 in the case of fluorescent protein conjugated antibodies or after 2 min. incubation with Western Bright ECL spray (K-12049-D50, Advansta, San Jose, CA, USA) by chemiluminescence in case of HRP conjugated antibodies. The protein expression levels were normalized to total protein loading, as determined by stain-free analysis.

2.6. RT-PCR

The cells were washed once with PBS and harvested by scraping into cell lysis buffer RLT containing 0.01% 2-mercaptoethanol, followed by cell homogenization using Qiashredder spin columns (79656, Qiagen). The total RNA was extracted using RNeasy miniprep kit (74106, Qiagen). Concentration was determined by NanoDrop1000 and 1 µg total RNA was reverse transcribed into cDNA with Quantitect Reverse Transcription kit (205314, Qiagen) while using oligomeric (dT) primers and including a DNAse digestion step. The resulting cDNA was used in a 20 µL reaction mix containing 1 × SYBR green (A6002, Promega, Madison, WI, USA), 400 nM of each forward and reverse exon spanning specific primers, 1/250 diluted cDNA and RNAse free water. The mRNA levels were determined on Viia7 RT-PCR (ThermoFisher Scientific), normalized to *succinat dehydrogenase subunit a* (*SDHA*) as a reference gene, and expressed as fold-change compared to controls using the ΔΔCT method.

2.7. EGF Uptake Assay

For FACS-based EGF uptake assay, 0.07×10^6 cells were seeded in wells of 12-well plates two days prior experiment. On the day of experiment, the cells were stimulated for up to 180 min. with Alexa647 labelled EGF (E35351, ThermoFisher Scientific). Afterwards, the cells were harvested by trypsin-EDTA treatment for 4 min. at 37 °C, resuspended in ice cold FACS buffer (PBS containing 2 mM EGTA, 1% FBS), washed twice with fresh FACS buffer, and analyzed with FACS Aria III (BD Bioscience, Franklin Lakes, NJ, USA).

For pulse-based EGF uptake assay analyzed by immunofluorescence, Huh7.5 cells (2×10^5) were seeded on fibronectin (F1141, Sigma–Aldrich, St. Louis, MO, USA) coated glass bottom µ-dishes (81158, ibidi, Martinsried, Germany) one day before analysis. The next day, Huh7.5 cells were precooled on ice for 10 min. Afterwards, cells were incubated in cold medium supplemented with 40 ng/mL EGF-Alexa647 conjugate (E35351, ThermoFisher Scientific) for 1 h at 4 °C to enable prebinding to surface EGFR. The medium was then replaced by full medium without EGF-Alexa647 and cells were incubated in at 37 °C for 5, 10, 30, 60, 120, or 180 min. or directly washed once with high salt and low pH buffer (0.2 M sodium acetate and 0.5 M NaCl, pH 4.5) to remove unspecific binding, fixed for 10 min. with 4% PFA in PBS, and washed twice with PBS. After each incubation time point, corresponding cells were treated the same way.

For simultaneous immunofluorescence staining, fixed cells were permeabilized with 0.2% TritonX-100 in PBS for 30 min. at RT and then blocked with 1% bovine serum albumin (BSA, Sigma–Aldrich) at RT for 60 min. or overnight at 4–8 °C. Immunostaining was performed by incubation with primary antibodies for 60 min. at RT under gentle shaking. The cells were washed thrice for 5 min. with PBS followed by incubation with appropriate fluorescently labeled secondary antibody for 60 min. at RT in the dark, followed by two washing steps for 5 min. with PBS.

2.8. Confocal Laser Scanning Microscopy

Images were acquired using ZEN black 2009 software operating a LSM 710 confocal laser scanning system (Carl Zeiss MicroImaging Inc., Dunedin, FL, USA) with a Plan-Apochromat 63x/1.40 Oil DIC M27 objective. The cell nuclei were stained with DAPI and measured in the 405 nm channel (MBS -405/760+). GFP-GABARAP was detected in the 488 nm channel (MBS 488), Transferrin (Tf)-Alexa 555 conjugate (T35352, Thermo Fisher Scientific) in the 543 nm channel (MBS 458/543) and EGF-Alexa 647 conjugate in the 633 nm channel (MBS 488/543/633), respectively. HEK293 GFP-GABARAP KI cells (2×10^5) were seeded on fibronectin (F1141, Sigma–Aldrich) coated glass bottom µ-dishes (81158, ibidi), incubated overnight at 37 °C and 5% CO_2 in growth medium. Directly before measuring, medium was replaced by cold medium containing 40 ng/mL EGF-Alexa 647. Data were post-processed using ImageJ [68] (version: 2.0.0-rc-43/1.50e).

2.9. EGFR Surface Expression Analysis

Plasma membrane proteins exhibiting extracellular primary amines were isolated with Pierce Cell Surface Protein Isolation Kit (89881, Thermo Fisher Scientific) according to the manufacturer's instructions in order to analyze surface EGFR protein expression. In brief, two days prior labelling and isolation of plasma membrane proteins, 2×10^6 cells per flask for a total of four T75 flasks per cell line were seeded for each biological replicate. On the day of isolation, each flask was quickly washed twice with ice cold PBS on ice and then labeled with Sulfo-NHS-Biotin shaking for 30 min. at 4 °C. The labelling reaction was then quenched, cells were scraped into solution, centrifuged, and lysed with lysis buffer for 30 min. with additional vortexing (every 5 min.) and sonication (every 8 min.) steps. Lysates were cleared and biotinylated proteins bound to NeutrAvidin beads for 1 h at RT with end-over-end mixing. The proteins were eluted with elution buffer containing 50 mM DTT for 1 h at RT with end-over-end mixing. Protein concentrations of eluates were determined by BCA and equal amounts were processed and loaded on 10% PAA gels for immunoblot analysis.

2.10. Spinning Disc Confocal Fluorescence Microscopy

During measurement, the cells were maintained in a StageTop Incubator system (Okolab S.R.L., Pozzuoli, Italy) on the microscope stage at 37 °C, 85% humidity, and 5% CO_2. The spinning disk confocal fluorescence microscope (Acal BFI, Gröbenzell, Germany) is based on an inverted microscope (Eclipse Ti, Nikon Instruments Europe BV, Amsterdam, Netherlands) equipped with a multi-beam confocal scanner unit (CSU-W1, Yokogawa Deutschland GmbH, Ratingen, Germany) working according to the spinning disk confocal principle and two cw lasers for excitation at 488 nm (GFP-GABARAP) and 640 nm (EGF-Alexa647). The setup allows for fast (<50 ms) acquisition of confocal fluorescence images in three dimensions. Bright field images, as well as confocal fluorescence images with excitation at 488 and 640 nm, were recorded while using a 100 magnification oil immersion objective lens (CFI PLAN APOCHROMAT VC, NA = 1.40, Nikon) and appropriate multi-dichroic beamsplitter, an EMCCD camera (Ixon Ultra 897, Andor Technologies Ltd., Belfast, UK) as detector and an image splitting device (Optosplit II, Cairn Research, Faversham, UK) for the simultaneous observation of two spectral regions of the emitted light (EGFP: 540/75 nm (Omega Optics Filters, Brattleboro, VT, USA) and EGF-Alexa647: 675/67 nm Brightline HC (Semrock Optical Filters (IDEX Health & Science, Bristol, CT, USA), West Henrietta, NY, US), respectively). The software Andor IQ2 was used for image acquisition. The exposure time for single images was set between 300–500 ms, while the frame rate was set to the minimum. The laser power and number of focal planes (z-frames) were set for every measured cell individually between 1 and 3. Data were post-processed using ImageJ [68] (version: 2.0.0-rc-43/1.50e).

2.11. Image Analysis

The image analysis software "Imaris" (Bitplane, Zurich, Switzerland) was used for quantitative comparison of EGF-Alexa647 uptake over time. Z-Stacks of cells were acquired, as described before, applying the same microscopy hardware settings to ensure reproducibility between datasets and individual cells were extracted to single stacks manually. The EGF volumes were identified and rendered utilizing the "Imaris surface" feature. A surface smoothing factor of 0.05 µm was used as well as a volume thresholding based on absolute EGF signal intensity of 14. Touching objects were separated on a seed diameter of 1 µm. A set of minimum requirement feature filters were applied and repeatedly checked for quality by comparing it to non-rendered data to minimize background volumes. Final filter sets were set as following: Quality threshold of 1.89, Minimum number of Voxel of 1, Shortest axis of minimum 520 nm and minimum mean intensity of 21. The surface generation was applied in batch mode to all individual cells and mean intensity, surface volume, and surface number per cell were extracted for downstream analysis.

2.12. Bio-Layer Interferometry (BLI)

BLI was used to determine the binding affinity of GABARAP and EGFR derived peptides. Experiments were performed on an Octet Red 96 (FORTÉBIO, San Jose, CA, USA) while using solid-black 96-well plates at 25 °C and a shake speed of 1000 rpm. The BLI buffer contained 25 mM Tris-HCl, pH 7.5, 150 mM NaCl, 0.5 mM Tris(2-carboxyethyl)phosphin (TCEP), 0.1% Tween-20, 1 mg/mL bovine serum albumin (BSA). The EGFR peptides were synthesized and N-terminally biotinylated via an aminohexanoic acid linker as well as C-terminally amidated (CASLO, Lyngby, Denmark). GABARAP was expressed and purified, as described [69]. Peptides (50 µg/mL) or biotin (10 µg/mL) as reference were immobilized on High Precision Streptavidin (SAX) biosensors (FORTÉBIO, San Jose, CA, USA). The peptide immobilization levels were around 0.8 nm. GABARAP was used as analyte in increasing concentrations in 200 µL solution. Association of GABARAP was recorded for 300 s on ligand and reference biosensors, followed by a dissociation phase of 300 s. Steady-state evaluation was performed by plotting the respective response levels against the applied peptide concentrations.

The curves were fitted according to the following Langmuir's 1:1 binding model using OriginPro 2019 (OriginLab, Northampton, MA, USA):

$$\mathbf{y} = \frac{\mathbf{R_{max}x}}{\mathbf{K_D}+\mathbf{x}}, \quad (1)$$

with y corresponding to the binding signal (response), R_{max} the saturation binding signal, x the applied GABARAP concentration, and K_D the equilibrium dissociation constant.

2.13. Co-immunoprecipitation

For co-immunoprecipitation (Co-IP) analysis, the GFP-Trap technology employing high affinity VHH domain containing nanobodies for GFP binding (gtak-20, Chromotek, Islandia, NY, USA) was used according to the manufacturer's instructions. In brief, Huh7.5 GABARAP SKO cells were transfected via lipofection, as described and stimulated with 40 ng/mL EGF for 10 min. or left untreated. Afterwards, the cells were placed on ice, washed once with ice-cold PBS, and two 6-wells per condition scraped into 200 µL NP-40 lysis buffer (10 mM Tris/HCl pH 7.5, 150 mM NaCl, 0.5 mM EDTA, 0.5% Nonidet™ P40 Substitute, 0.09% sodium azide) containing protease and phosphatase inhibitors (78430, ThermoFisher Scientific). Cell lysis was carried out on ice for 30 min., with 10 s vortexing after every 10 min. Lysates were then cleared by centrifugation for 10 min. at 17 000 g at 4 °C and the supernatants containing proteins transferred to pre-cooled reaction tubes. The lysates were diluted with 300 µL ice-cold washing buffer (10 mM Tris/HCl pH 7.5, 150 mM NaCl, 0.5 mM EDTA.

0.018% sodium azide) containing protease and phosphatase inhibitors and 10% saved for input analysis. 25 µL of anti-GFP nanobody coupled agarose bead slurry was equilibrated with washing buffer, separated via a magnetic rack, and for Co-IP lysates were bound overnight at 4 °C with end-over-end mixing. Afterwards, 50 µL were saved for flow through analysis, beads were washed four times with ice-cold washing buffer, and finally eluted with 80 µL 2× Lämmli's SDS sample buffer (120 mM Tris/HCl pH 6.8, 20% glycerol, 4% SDS, 0.04% bromophenol blue, 8% 2-mercaptoethanol) by heating to 95 °C for 5 min. The samples were then analyzed by immunoblotting, as described.

2.14. Statistical Analysis

All of the statistical analyses were performed with the statistical analysis software package (SPSS, version 22; SPSS Inc., Chicago, IL, USA), unless stated otherwise. Descriptive data are expressed as means ± standard error of means (SEM). Normal distribution was assessed using the Shapiro–Wilk test, and data was transformed or bias-corrected accelerated bootstrapping performed prior to analysis where necessary. Statistical testing was performed, as described individually. In general, statistical significance was inferred at a two-tailed *p*-value of ≤ 0.05. To test the influence of each GABARAP family protein on total EGFR protein levels, dichotomous dummy-coded variables were used to express each genotype as either wildtype for a specific paralog (1) or as a knockout (0). Afterwards, bivariate correlation analysis (Spearman) was performed and two-tailed statistical significance was calculated.

3. Results

3.1. Deficiency for GABARAP, but Not GABARAPL1 or GABARAPL2 Is Associated with Increased Degradation of EGFR in Huh7.5 and HEK293 Cells

We generated HEK293 knockout (KO) cells deficient for each GABARAP subfamily member alone (SKO) or in double (DKO) and triple (TKO) combination using the CRISPR/Cas9 system to systematically investigate the role of GABARAP-subfamily proteins during EGFR degradation (Figure S1A, Table S1).

The cells were then stimulated with 40 ng/mL EGF, which is known to promote receptor degradation [70], for up to 180 min., and whole cell lysates were analyzed for total EGFR protein levels by immunoblot (Figure 1A). Figure 1B shows densitometric analyses of the genome-edited HEK293 cell lysates compared to their matching controls. Evidently, GABARAP SKO cells displayed significantly lower EGFR levels in whole cell lysates after 10 (1.24-fold, $p \leq 0.05$), 120 (1.84-fold, $p \leq 0.05$), and by

trend 180 min. (1.42-fold, $p = 0.07$) of EGF treatment as compared to the control levels. In contrast, neither single lack of GABARAPL1 nor GABARAPL2 led to significant differences in the total EGFR levels when compared to their respective controls, although GABARAPL1 deficiency resulted in a slight increase in EGFR at most time points, and a trend towards reduced EGFR levels could be observed for GABARAPL2 SKO cells after 180 min. of EGF treatment (1.19-fold, $p = 0.1$). Consistently, GABARAP/L1 DKO cells showed no differences in the EGFR levels as compared to the wildtype controls, neither unstimulated nor in response to EGF treatment, indicating that GABARAP and GABARAPL1 have opposite functions regarding EGFR degradation dynamics in this cell type. GABARAP/L2 DKO cells had significantly less EGFR after 10 (1.52-fold, $p \leq 0.05$) and by trend after 60 (1.69-fold, $p = 0.06$), 120 (1.73-fold, $p = 0.08$), and 180 min. (1.9-fold, $p = 0.1$) of EGF treatment, respectively, and thus performed like lacking solely GABARAP. A lack of both GABARAPL1 and GABARAPL2 resulted in EGFR levels as in the control samples, suggesting that GABARAP is the decisive factor for a correct EGFR degradation phenotype in HEK293 cells. Notably, TKO cells, lacking the whole GABARAP subfamily, showed slightly elevated unstimulated EGFR without reaching statistical significance. This phenotype might reflect the participation of the whole GABARAP subfamily in general cellular processes such as autophagy or lysosome biogenesis [71], which, due to functional redundancy emerges, most if none of the family members are present. We used dichotomous dummy-coded variables to indicate the genotypic status for each GABARAP-subfamily member in all applied HEK293 cell lines to analyze the correlation between the presence of each of the GABARAP subfamily proteins and EGFR levels after EGF stimulation (Figure 1C) (for details see Materials and Methods).

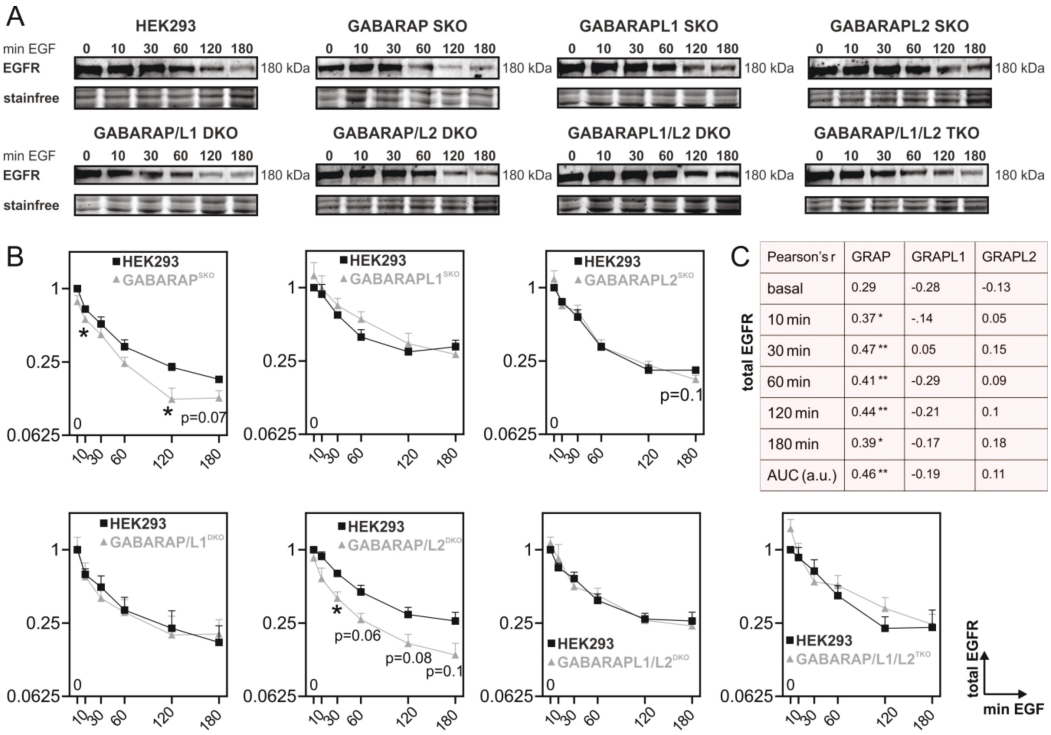

Figure 1. Epidermal growth factor (EGF)-induced EGF receptor (EGFR) degradation in HEK293 knockout (KO) cells. (**A**) Cells were treated with 40 ng/mL EGF for the indicated times. Afterwards, total EGFR protein levels in whole cell lysates were analyzed by immunoblot. Representative blots are shown for at least n = 3 independent experiments. (**B**) Densitometric analysis of at least n = 3 independent experiments. Controls are plotted for each experiment. Quantification of total EGFR protein levels was performed by normalization to stain-free loading control; levels are given relative to HEK293 control cells at unstimulated conditions (t = 0). Error bars represent standard error of means.

Asterisks mark significant differences versus the corresponding time point of control cells as calculated using independent t-test. $p \leq 0.05$ = *, $p \leq 0.01$ = **, $p \leq 0.001$ = ***. (**C**) Correlation of presence of each GABARAP with total EGFR levels in response to EGF treatment. Correlations were calculated taking every analyzed KO combination except GABARAP/L1/L2 TKO in HEK293 cells into account. Pearson correlation was used for calculation and two-tailed significances are denoted with asterisks: $p \leq 0.05$ = *, $p \leq 0.01$ = ** GRAP = GABARAP, GRAPL1 = GABARAPL1, GRAPL2 = GABARAPL2. Respective wildtype controls were run on the same PAGE for each KO cell line and can be found in Figure S6A which also shows the uncropped source blots.

As expected, the GABARAP availability was significantly and positively correlated with EGFR protein levels at each time point after EGF treatment (10 min., r = 0.37, $p \leq 0.05$; 30 min., r = 0.47, $p \leq 0.01$; 60 min., $r = 0.41$, $p \leq 0.01$; 120 min., $r = 0.44$, $p \leq 0.05$; 180 min., r = 0.39, $p \leq 0.05$) as well as with the corresponding integrated area under the curve (AUC, a.u.) of EGFR levels over time (r = 0.46, $p \leq 0.01$).

In addition to the above described experiments, we also applied the transient overexpression of GFP-fused EGFR to the same panel of genome-edited HEK293 cell lines and analyzed their respective EGFR-(GFP) levels upon EGF stimulation by immunoblot (Figure S2A). Densitometric analysis (Figure S2B) largely confirmed our results that were obtained for endogenous EGFR levels. Again, GABARAP deficiency alone or in combination with GABARAPL2 deficiency resulted in a significant reduction of EGFR levels. Interestingly, GABARAPL1/L2 DKO and GABARAP/L1/L2 TKO cells both showed significantly elevated EGFR levels under EGFR overexpression conditions, suggesting that some effects observed for overexpression are either dependent on receptor density or produced by the overexpression *per se*. In general, when comparing endogenous with overexpressed EGFR degradation dynamics, it is evident that EGFR overexpression strongly slows down degradation (Figure S2B, see EGFR-GFP vs. EGFR).

Overall, GABARAP deficiency appeared to accelerate EGFR degradation or, *vice versa*, GABARAP appeared to slow down EGFR degradation upon EGF stimulation in HEK293 cells.

We next used Huh7.5 cells for degradation analysis of endogenous EGFR to clarify whether the validity of the observed GABARAP-mediated effects on EGFR degradation can be extended to other cell lines and to rule out clonal effects of our genome-edited HEK293 cell lines. To that end, we first established Huh7.5 KO cells deficient for GABARAP, GABARAPL1, or GABARAPL2 alone or combinations of GABARAP/L2 and GABARAPL1/GABARAPL2 (Figure S1B, Table S1). Cells and lysates were treated, as described above, total EGFR was detected by immunoblotting (Figure 2A), and the respective densitometric analyses are summarized in Figure 2B. While the basal EGFR levels were unaltered in GABARAP SKO cells, the total EGFR levels were significantly reduced after 10 (1.3-fold, $p \leq 0.05$), 30 (2.14-fold, $p \leq 0.01$), 60 (2.7-fold, $p \leq 0.05$), 120 (3.56-fold, $p \leq 0.01$), and 180 min. (4.74-fold, $p \leq 0.001$) of treatment with EGF when compared to Huh7.5 control cells. GABARAPL1 and GABARAPL2 SKO cells were analyzed likewise with regards to EGFR protein levels in response to EGF treatment to analyze the role of the two other GABARAP subfamily members. Neither GABARAPL1 SKO nor GABARAPL2 SKO cells showed significantly reduced levels of EGFR in response to EGF stimulation when compared to Huh7.5 control cells. In fact, GABARAPL1 SKO cells displayed a slight trend towards higher EGFR total protein levels over time, while a slight but significant (1.32-fold, $p \leq 0.05$) increase in the basal total EGFR levels was observed for GABARAPL2 SKO cells. Strikingly, the only other analyzed Huh7.5 cell line showing the accelerated degradation of EGFR in response to EGF stimulation was the GABARAP/L2 DKO line after 10 (1.9-fold, $p \leq 0.05$), 30 (2.16-fold, $p \leq 0.05$), 60 (2-fold, $p \leq 0.05$), 120 (1.44-fold, $p \leq 0.01$), and 180 min. (3.29-fold, $p \leq 0.05$) of treatment with EGF, but not at basal levels as compared to Huh7.5 control cells. GABARAPL1/GABARAPL2 DKO cells displayed unaltered total EGFR levels when compared to Huh7.5 control cells, indicating that the lack of GABARAP alone was sufficient for driving accelerated EGFR degradation in these cells.

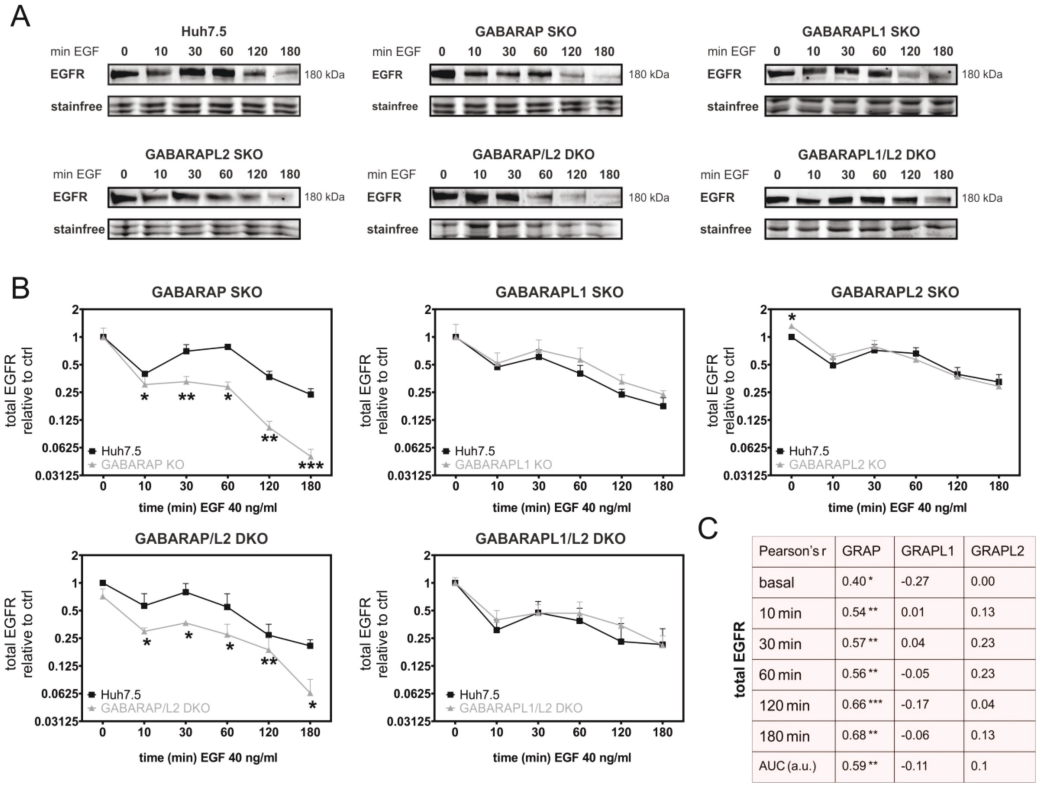

Pearson's r	GRAP	GRAPL1	GRAPL2
basal	0.40 *	-0.27	0.00
10 min	0.54 **	0.01	0.13
30 min	0.57 **	0.04	0.23
60 min	0.56 **	-0.05	0.23
120 min	0.66 ***	-0.17	0.04
180 min	0.68 **	-0.06	0.13
AUC (a.u.)	0.59 **	-0.11	0.1

Figure 2. EGF-induced EGFR degradation in Huh7.5 KO cells. (**A**) Cells were treated with 40 ng/mL EGF for the indicated times. Afterwards, total EGFR protein levels in whole cell lysates were analyzed by immunoblot. Representative blots are shown for n = 3 independent experiments. (**B**) Densitometric analysis of n = 3 independent experiments. Controls are directly plotted for each experiment. Quantification of EGFR protein levels was performed by normalization on stain-free loading control and calculated as percentage of Huh7.5 control cells at unstimulated conditions (t = 0). Representative blots are shown for a summary of n = 3 independent experiments. Error bars represent standard error of means. Asterisks mark significant differences versus the corresponding time point of control cells as calculated using independent t-test. $p < 0.05$ = *, $p < 0.01$ = **, $p < 0.001$ = ***. (**C**) Correlation of presence of each GABARAP with total EGFR levels in response to EGF treatment. Correlations were calculated taking every analyzed KO combination in Huh7.5 cells into account. Pearson correlation was used for calculation and two-tailed significances are denoted with asterisks: $p \leq 0.05$ = *, $p \leq 0.01$ = **. GRAP = GABARAP, GRAPL1 = GABARAPL1, GRAPL2 = GABARAPL2. Respective wildtype controls were run on the same PAGE for each KO cell line and can be found in Figure S6B which also shows the uncropped source blots.

The correlation analysis of EGFR degradation results from Huh7.5 cell derived lysates (Figure 2C) showed broad consistency with that based on the independent HEK293 cell lysates (Figure 1C): a strong and significant positive correlation of genotypes expressing GABARAP with total EGFR levels under basal conditions ($r = 0.4$, $p \leq 0.05$), as well as after 10 ($r = 0.54$, $p \leq 0.01$), 30 ($r = 0.57$, $p \leq 0.01$), 60 ($r = 0.56$, $p \leq 0.01$), 120 ($r = 0.66$, $p \leq 0.001$), and 180 ($r = 0.68$, $p \leq 0.01$) min. of EGF treatment, as well as with the integrated AUC of EGFR total protein levels ($r = 0.59$, $p \leq 0.01$) was revealed. No significant correlation for GABARAPL1 or GABARAPL2 with EGFR protein levels was found for any of the time points analyzed, although GABARAPL1 showed a trend towards negative correlation with EGFR levels at basal conditions ($r = -0.27$) and after 120 min. ($r = -0.17$) of EGF treatment. Clonal off-target effects as an explanation for the observed phenotype could be excluded with high confidence based on the close agreement of observations with two different cell lines.

In summary, the lack of GABARAP, either alone or in combination with GABARAPL2, was consistently and significantly associated with decreased total EGFR protein levels in response to EGF treatment in both Huh7.5 and HEK293 cells, whereas the presence of GABARAP in general was associated with higher EGFR total levels. Subsequently, we concentrated further efforts on the Huh7.5 GABARAP SKO cell line to analyze EGFR degradation dynamics and its implications in more detail.

3.2. GABARAP Deficiency Alters EGFR Signaling on Protein and Gene Expression Levels and Increases GABARAPL1 but Not GABARAPL2 Protein Expression

Next, we asked whether GABARAP deficiency is additionally accompanied by altered EGFR downstream signaling. Therefore, we analyzed the activation of EGFR itself as well as of EGFR-associated signaling, namely the phosphoinositide-3-kinase/proteinkinase B (PI3K/AKT) and mitogen-activated protein kinase/extracellular-signal regulated kinase (MAPK/ERK) signaling pathway, by immunoblot (Figure 3A). The phosphorylation of EGFR at Y1068 in GABARAP SKO cells was higher by trend after 10 min. of EGF treatment (1.36-fold, $p = 0.06$) as compared to Huh7.5 control cells, whereas it was not altered at later time points (Figure 3B). The activation of the PI3K/AKT pathway was analyzed by phosphorylation of AKT at S473 and it was not significantly influenced under the given circumstances (Figure 3C). Activating phosphorylation of ERK1/2 was reduced in GABARAP SKO cells at every time point analyzed with a significant reduction after 30 min. of EGF treatment (2.49-fold, $p \leq 0.05$, Figure 3D).

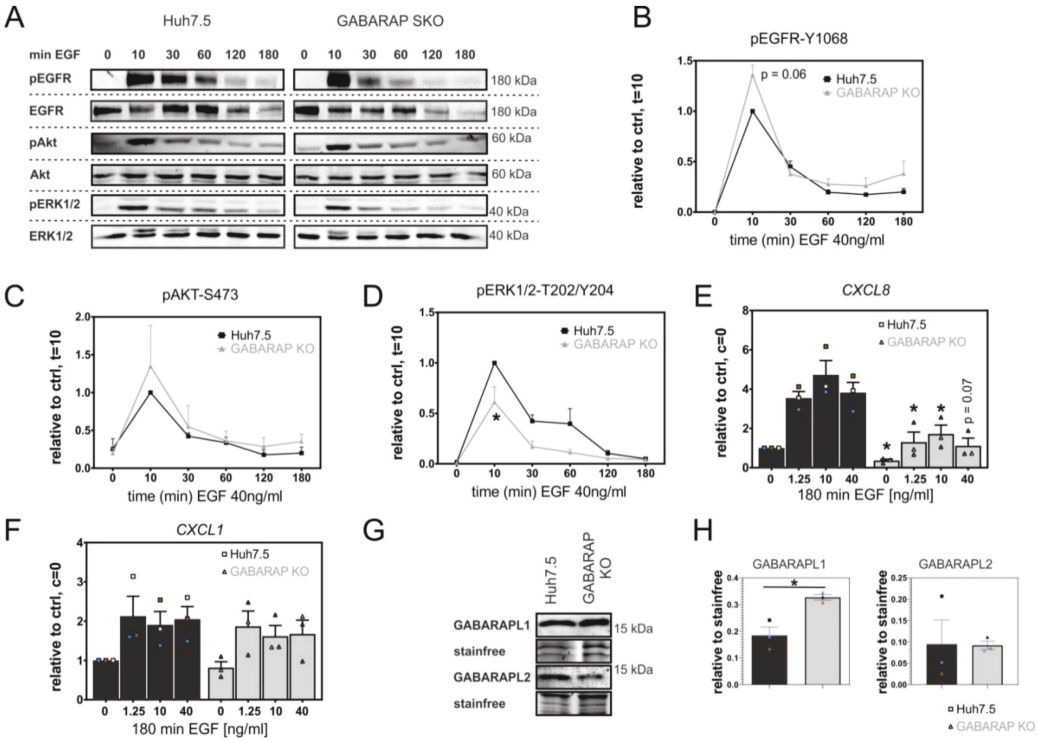

Figure 3. Analysis of EGF-induced EGFR phosphorylation, activation of downstream signaling and gene expression in GABARAP SKO and Huh7.5 control cells. (**A**) Huh7.5 and GABARAP SKO cells were treated with 40 ng/mL EGF for the indicated times. Afterwards, activating phosphorylations of the EGFR (**B**) and downstream PI3K/AKT (**C**) and MAPK/ERK (**D**) signaling pathways were analyzed by immunoblot. Quantification of phosphorylated proteins was performed by normalization to the corresponding total protein levels and calculated as percentage of Huh7.5 control cells after 10 min. of EGF treatment (t = 10). (**E** + **F**) Huh7.5 and GABARAP SKO cells were treated with the indicated concentrations of EGF for 180 min., followed by cell lysis, RNA extraction, reverse transcription and

quantitative real-time PCR (RT-PCR). Expression of target genes *CXCL8* (**E**) and *CXCL1* (**F**) was normalized to *succinate dehydrogenase* (*SDHA*) as reference gene and is expressed relative to unstimulated control cells. (**G**) Protein expression of GABARAP paralogs GABARAPL1 and GABARAPL2 was analyzed in Huh7.5 and GABARAP SKO cells and densitometric analysis performed to determine GABARAPL1 and GABARAPL2 protein levels in GABARAP SKO cells compared to Huh7.5 controls (**H**). Representative blots are shown for a summary of n = 3 independent experiments. Error bars represent standard errors of means. Asterisks mark significant differences versus the corresponding time point or concentration of control cells as calculated using independent t-test. $p \leq 0.05$ = *. (**E**,**F**,**H**) individual experiments are color-coded. Figure S6C shows uncropped source blots.

Next, the impact of GABARAP deficiency on EGFR target gene expression was analyzed. The mRNA levels of the C-X-C chemokine receptor 2 (CXCR2) ligand *CXCL8* alongside mRNA levels of another CXCR2 ligand, *CXCL1*, were analyzed after treatment with various concentrations of EGF because the gene expression of *CXCL8*was reported to be regulated by the EGFR/ERK signaling axis after HCV infection [72]. Strikingly, *CXCL8* transcripts were significantly reduced in GABARAP SKO cells at basal levels (2.75-fold, $p \leq 0.05$) and upon stimulation with 1.25 ng/mL (2.72-fold, $p \leq 0.05$), 10 ng/mL (2.75-fold, $p \leq 0.05$) and by trend 40 ng/mL EGF (3.42-fold, $p = 0.068$) for 180 min. compared to Huh7.5 control cells (Figure 3E). This was not the case for *CXCL1* (Figure 3F), suggesting different transcriptional regulation for these two chemokines through independent axes of EGFR transduced signaling.

In order to investigate the influence of GABARAP deficiency on protein levels of its paralogs GABARAPL1 and GABARAPL2, we analyzed their basal levels in Huh7.5 control and GABARAP SKO cells (Figure 3G). Interestingly, GABARAPL1 protein expression was significantly increased in GABARAP SKO cells (1.77-fold, $p \leq 0.05$), whereas the GABARAPL2 protein levels were not consistently influenced (Figure 3H) as compared to Huh7.5 control cells.

3.3. Basal EGFR Surface Expression Is Unaltered in GABARAP Deficient Cells, While EGF Uptake Capacity Is Impaired over Time

We isolated the surface proteins of Huh7.5 and GABARAP SKO cells via biotinylation (Figure 4A) and determined surface EGFR levels by immunoblot (Figure 4B) in order to check whether accelerated degradation of EGFR is simply caused by altered EGFR surface expression. Densitometric analysis revealed no alterations between GABARAP SKO and Huh7.5 control cells (Figure 4C), indicating that the trafficking of EGFR to the plasma membrane is not impaired in GABARAP SKO cells under basal levels of EGF. Consistent with unaltered EGFR total protein levels, the *EGFR* mRNA expression levels were not influenced by GABARAP deficiency (Figure 4D). We next asked whether the observed acceleration of EGFR degradation and alterations in downstream signaling events are caused by defects in EGF uptake or receptor endocytosis *per se*. Therefore, we carried out a FACS based assay. The cells were continuously treated with 40 ng/mL EGF that was conjugated to the fluorophore Alexa647 and the median fluorescence intensity (a.u.), reflecting the amount of intracellular EGF, was analyzed via FACS (Figure 4E). As EGFR is the only receptor for EGF, this directly reflects its internalization by endocytosis at early time points and accumulated intracellular EGF over time. However, Alexa647 is a pH-stable fluorophore and it is therefore not fully degraded by lysosomes similar to EGF quantum dots [73]. Hence, intracellular fluorescence at later time points might reflect free dye, at least to some extent. Nonetheless, this approach represented several cycles of EGFR internalization, which provides a measure of EGF uptake over time. Consistent with surface expression being unaltered, GABARAP SKO cells displayed unaltered median fluorescent intensity values after 10 min. of EGF-Alexa647 treatment, indicating that early internalization events are not impaired in GABARAP deficient cells. Over time, intracellular EGF-Alexa647 levels were lower in GABARAP SKO cells after 30, 60, and 120 min. by trend and significantly reduced after 180 min. (1.59-fold, $p \leq 0.01$) when compared to Huh7.5 control cells (Figure 4F). The obtained results with this continuous treatment conditions, which allow for several rounds of ligand binding and receptor cycling, indicate a shift from receptor recycling to

degradation in GABARAP SKO cells at later time points as compared to Huh7.5 control cells. This is in line with the immunoblot experiments and suggests that the reduction of EGF-Alexa647 levels is caused by a general reduction of EGFR protein levels over time in response to EGF treatment in GABARAP deficient cells.

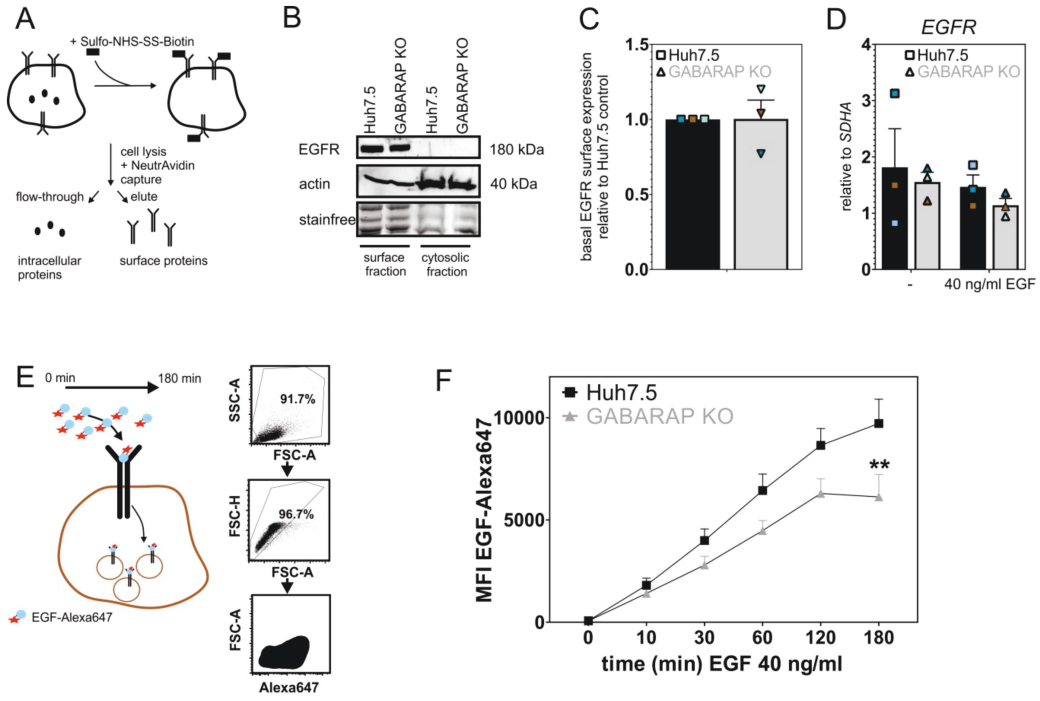

Figure 4. Analysis of EGFR surface expression by isolation of surface proteins and EGF-uptake in GABARAP SKO and Huh7.5 control cells by flow cytometry. (**A**) Primary amines of extracellular portions of plasma membrane proteins were conjugated to Sulfo-NHS-SS-Biotin. Afterwards, cells were lysed and biotinylated proteins captured via NeutrAvidin to separate surface from cytosolic proteins. (**B**) EGFR surface expression of Huh7.5 control and GABARAP SKO cells was determined by immunoblotting of the surface fraction lysate and (**C**) densitometric analysis performed to determine relative EGFR protein surface expression levels between Huh7.5 and GABARAP SKO cells (n = 3 independent experiments). (**D**) EGFR mRNA expression levels were analyzed at steady-state and after 180 min. of 40 ng/mL EGF treatment. Expression levels were normalized to *SDHA* expression and compared between Huh7.5 and GABARAP SKO cells. (**E**) Huh7.5 and GABARAP SKO cells were continuously treated with 40 ng/mL of Alexa647 labelled EGF over 180 min. Gates were set to get rid of debris and select for single cells. Intracellular EGF was determined by analyzing median fluorescence intensity (MFI) of EGF-Alexa647 positive cells (**F**). Line plot is a summary of n = 4 independent experiments. Error bars represent standard errors of mean. Asterisks mark significant differences to the corresponding time point of control cells as calculated using two-way analysis of variance with Bonferroni post-hoc testing with GraphPad Prism version 8.00 for Windows (GraphPad Software, La Jolla California US, www.graphpad.com). $p \leq 0.01$ = **. (**C** + **D**) Individual experiments are color-coded. Figure S6D shows uncropped source blots.

3.4. Tracking of Fluorescently-Labeled EGF Reveals Altered EGF Trafficking and Vesicular Composition in GABARAP Deficient Cells without Abrogation of General Endosomal Targeting

We used a pulse-based setup for confocal laser scanning microscopy imaging to address the question of whether GABARAP deficiency causes impaired intracellular trafficking of EGFR. The cells were pre-incubated with 40 ng/mL EGF-Alexa647 at 4 °C to saturate all EGFR binding sites at the plasma membrane, followed by acidic wash to remove unbound EGF and subsequent incubation at

37 °C to allow for internalization and trafficking of EGF pre-bound to EGFR (Figure 5A). As exemplarily shown for 5, 30 60, and 120 min. (Figure 5B), the cells were fixed at various time points after the EGF pulse and EGF accumulation was recorded as distinct dots, likely reflecting that EGFR accumulated in vesicles subsequent to ligand stimulation. EGF-Alexa647 containing vesicles were analyzed regarding the average number (Figure 5C), volume (Figure 5D) and intensity (Figure 5E) of individual vesicles per cell. Overall vesicular number per analyzed cell was significantly reduced after 60 (1.21-fold, $p \leq 0.05$) and 120 min. (1.29-fold, $p \leq 0.05$) of EGF-Alexa647 incubation. While the overall vesicular volume at 5 min. after the EGF-Alexa647 pulse was significantly increased in GABARAP SKO cells when compared to Huh7.5 control cells (1.15-fold, $p \leq 0.05$), it was found to be significantly lower after 30 min. (1.26-fold, $p \leq 0.001$) as compared to Huh7.5 control cells. Accordingly, the mean fluorescent intensity of analyzed vesicles after 5 min. of EGF-Alexa647 stimulation was significantly higher in GABARAP SKO cells when compared to Huh7.5 control cells (1.04-fold, $p \leq 0.05$), while it was found to be significantly decreased after 30 min. (1.07-fold, $p \leq 0.001$).

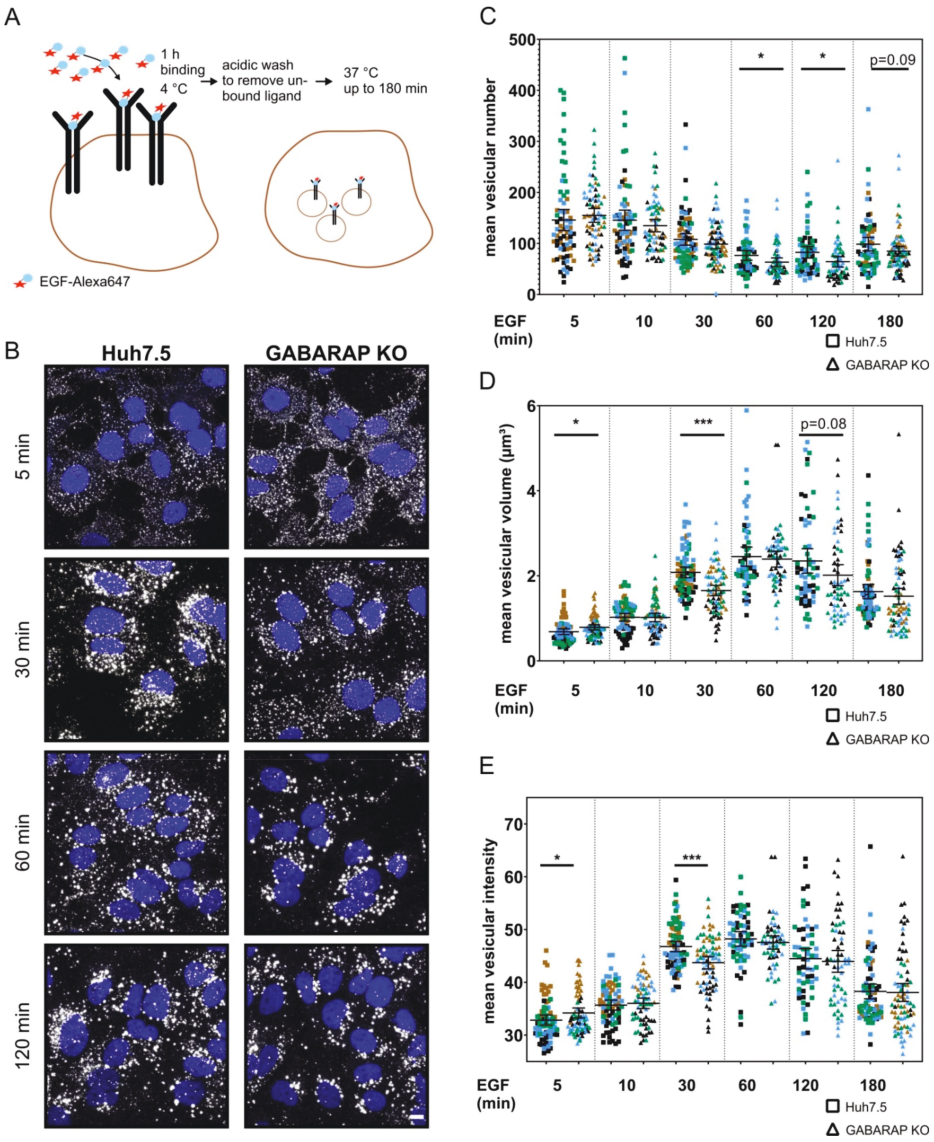

Figure 5. Analysis of EGF uptake in GABARAP SKO and Huh7.5 control cells via EGF-Alexa647 pulse by immunofluorescence imaging. (**A**) Huh7.5 and GABARAP SKO cells were treated with 40 ng/mL

Alexa647 labelled EGF at 4 °C to allow binding to EGFR. After rigorous washing, cells were placed at 37 °C and analyzed at distinct time points to assess EGF internalization. (**B**) Cells were fixed at basal levels and after 5, 10, 30, 60, 120, and 180 min. of EGF treatment. Nuclei were counterstained with DAPI and images of EGF positive puncta taken. Mean vesicular number (**C**), volume (**D**) and intensity (**E**) of imaged EGF-Alexa647 puncta were analyzed by Imaris. Single cells were cropped out of images, processed with ImageJ and Imaris (Bitplane, Zurich, Switzerland). Only vesicles with volumes > 0.1 μm^3) were taken into account. Fluorescent images are representative of at least n = 3 independent experiments. Individual experiments are color-coded; >50 cells per genotype and time point were analyzed. Error bars represent 95% confidence intervalls (CI) (**C**–**E**). Asterisks mark significant differences to the corresponding time point of control cells and were calculated using independent t-test. $p \leq 0.05$ = *, $p \leq 0.01$ = **, $p \leq 0.001$ = ***.

Next, we classified the obtained vesicle volumes and intensities into subgroups to visualize the more subtle differences that are not resolved by the global approach described above. The corresponding plots are shown in Supplementary Figure S3A,B. In summary, for vesicles of the smallest category (0.5–1 μm^3) similar numbers were found in GABARAP SKO and Huh7.5 control cells at all time points. Interestingly, for all other size categories and particularly at later stages starting at 30 min. post EGF-Alexa647 treatment, the numbers of observed vesicles were decreased in GABARAP deficient cells. Solely for the early 5 min. time point, increased numbers of vesicles of several categories were found for GABARAP SKO cells when compared to Huh7.5 control cells. Accordingly, vesicles of the lowest intensity (20–40) were not altered between GABARAP SKO and Huh7.5 cells, while vesicles of the remaining three intensity categories were significantly decreased, again especially starting at 30 min. post EGF-Alexa647 treatment. EGF-Alexa647 pulse-treated GABARAP SKO and Huh7.5 control cells were fixed and stained for early (RAB5), recycling (RAB11) or late (RAB7) endosomal marker proteins, to further analyze endosomal trafficking. Colocalization events of RAB5, RAB11, and RAB7 with EGF-Alexa647 (white arrows) were observed for GABARAP SKO and Huh7.5 control cells at every analyzed time point, indicating that the general ability of EGFR to reach the analyzed endosomal compartments is not abolished by GABARAP deficiency, as exemplarily shown for 10, 30, and 60 min. in Figure S3C. However, fixed cells and the analyzed set of time points might not be suitable to capture subtle and transient GABARAP-mediated interactions.

3.5. Accelerated EGFR Degradation in GABARAP Deficient Huh7.5 Cells Can Be Counteracted by Lysosomal and Proteasomal Inhibition

We then asked whether the acceleration in EGF-induced EGFR degradation in GABARAP deficient cells depends on the activity of the proteasomal or lysosomal machinery or whether degradation would occur through a different non-canonical mechanism. To this end, the inhibition of lysosomal or proteasomal activity was obtained by chloroquine or lactacystin treatment, respectively (Figure 6A), which are known to inhibit either lysosomal acidification (chloroquine) or proteasomal subunits (lactacystin) and cause delay in EGF-induced EGFR degradation [74–76]. The cells were treated with chloroquine and total EGFR levels as well as the activation of MAPK/ERK signaling in response to subsequent EGF stimulation was analyzed by immunoblot (Figure 6B). This led to a delay in EGF-induced EGFR degradation in Huh7.5 cells and could, at least partly, restore the declined EGFR levels observed in GABARAP SKO cells in response to EGF stimulation shown in Figure 2A, as the total EGFR levels were only significantly reduced after 60 min. (1.69-fold, $p \leq 0.05$), but not at any of the other time points compared to Huh7.5 control cells (Figure 6C). Interestingly, MAPK signaling assessed by activating phosphorylation of ERK1/2 was still found to be significantly reduced in GABARAP SKO cells after 30 (1.77-fold, $p \leq 0.01$), 120 (1.8-fold, $p \leq 0.05$), and 180 min. (1.82-fold, $p \leq 0.01$) of EGF treatment when compared to controls (Figure 6D). Next, lactacystin treatment was applied prior to EGF stimulation and immunoblot analysis (Figure 6E).

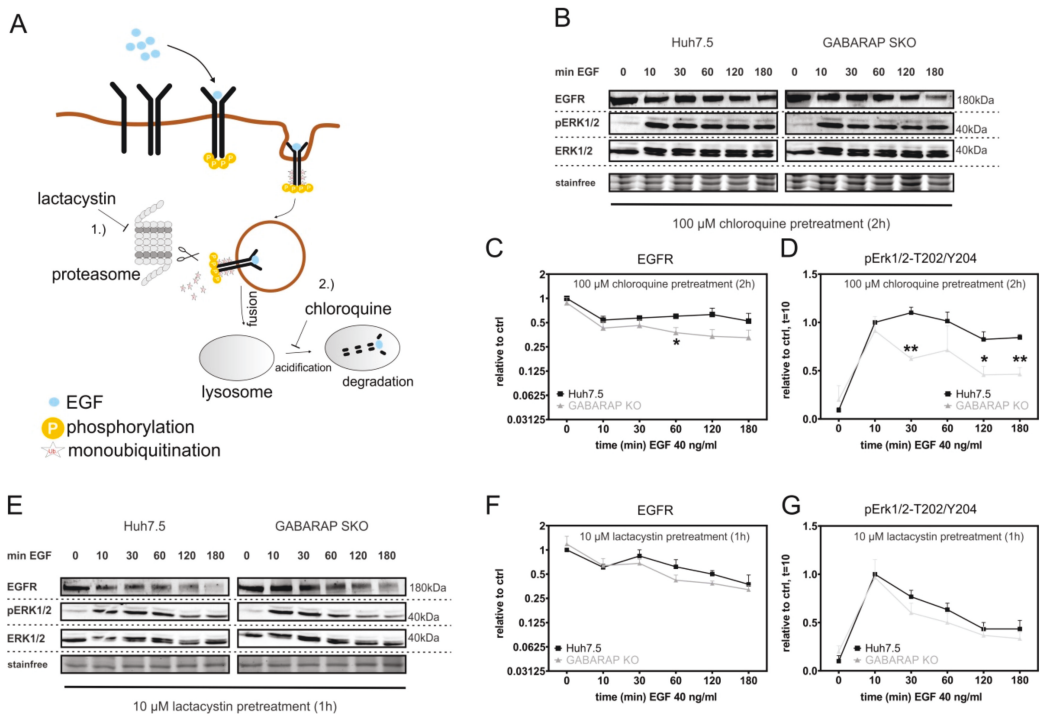

Figure 6. EGF-induced EGFR degradation after inhibition of lysosomal acidifcation and proteasomal inhibition in GABARAP SKO and Huh7.5 control cells. (**A**) Modes of action of the inhibitors used. Cells were pretreated with inhibitors of lysosomal acidifcation or proteasomal subunits and afterwards treated with 40 ng/mL EGF for the indicated times. (**B**–**D**) Cells were treated with lysosomal acidification inhibitor chloroquine. Total EGFR levels as well as activating phosphorylation of ERK1/2 at T202/Y204 were analyzed by immunoblotting and densitometry. (**D**–**G**) Cells were treated with proteasomal subunit inhibitor lactacystin. Total EGFR levels as well as activating phosphorylation of ERK1/2 at T202/Y204 were analyzed by immunoblotting and densitometry. Quantification of protein levels was performed by normalization to stain-free protein loading or the respective total levels of downstream signaling proteins and calculated as percentage of Huh7.5 control cells at unstimulated conditions (t = 0) for EGFR and peak activation levels (t = 10 min.) for ERK. Representative blots are shown for a summary of n ≥ 3 independent experiments. Error bars represent standard errors of means. Asterisk marks significant difference versus the corresponding time point of control cells as calculated using independent t-test. $p \leq 0.05$ = *. Figure S6E shows uncropped source blots.

Interestingly, this led to a delay in EGF-induced EGFR degradation in Huh7.5 control cells and abrogated the differences in EGFR protein between GABARAP SKO and Huh7.5 control cells after stimulation, as shown in Figure 2A, at any of the analyzed time points (Figure 6E). MAPK/ERK signaling was also found to be restored after lactacystin treatment in GABARAP SKO cells when compared to Huh7.5 control cells (Figure 6F). Taken together, these results indicated that GABARAP deficiency does not change the mechanism of EGFR degradation in general, but rather affects upstream events related to receptor trafficking. Impaired ERK signaling of GABARAP SKO cells under chloroquine treatment points to endosomal trafficking events when the cytoplasmic tail of the receptor is still able to contact the cytoplasm to activate downstream signaling molecules.

3.6. GABARAP and EGF Converge in Distinct Dynamic Vesicular Structures at Endogenous Expression Levels in HEK293 Cells

We asked whether both molecules localize to the same endosomal compartment after ligand stimulation to obtain an insight into the trafficking events underlying GABARAP-mediated regulation

of EGFR degradation. We generated a knock-in (KI) cell line expressing GFP-tagged GABARAP under control of the endogenous *GABARAP* promoter by CRISPR/Cas9 mediated genome editing to eliminate the impact of overexpression artifacts (Figure S1C, Table S1). The resulting GFP-GABARAP expression levels were sufficient for live cell microscopy, as demonstrated in Figure 7.

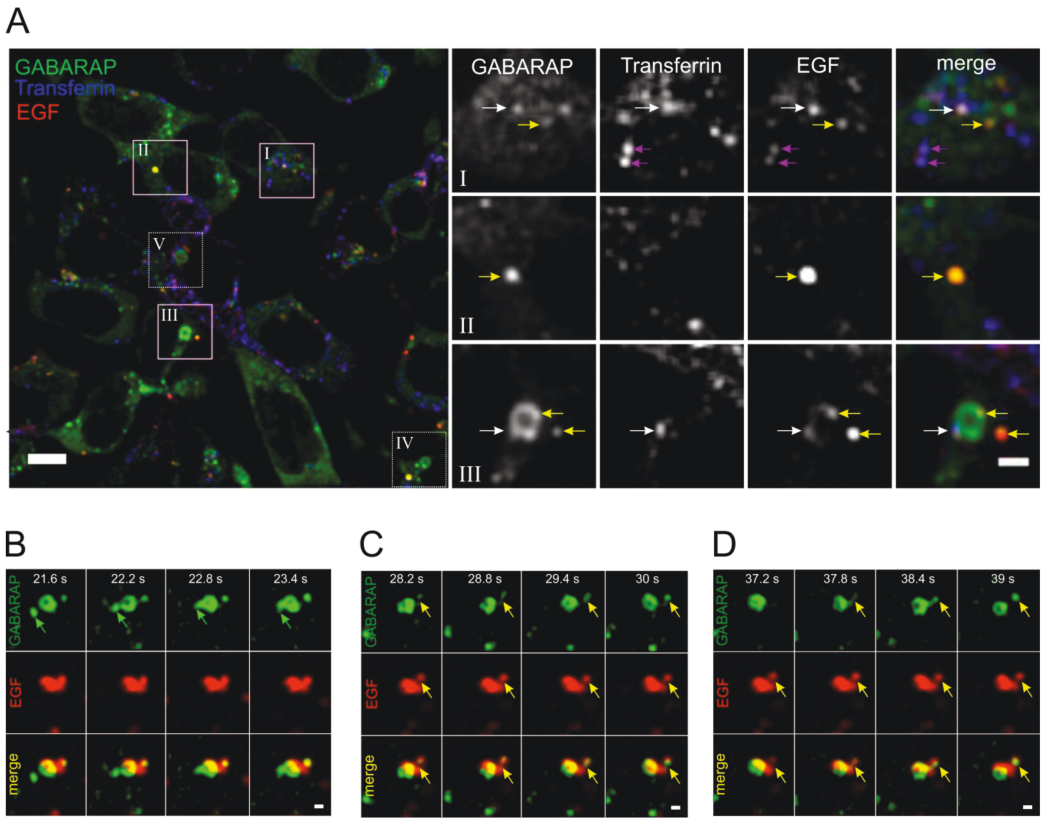

Figure 7. Live cell imaging of HEK293 knock-in cells expressing GFP-GABARAP under the endogenous *GABARAP* promoter after stimulation with EGF-Alexa647 and Tf-Alexa555. (**A**) HEK293 GFP-GABARAP knock-in (KI) cells were simultaneously treated with 40 ng/mL EGF-Alexa647 and 20 ng/mL Tf-Alexa555 for 60 min. and imaged under live-cell conditions by laser scanning confocal microscopy. White arrows highlight GABARAP/EGF/Tf triple-positive structures. Yellow arrows highlight GABARAP/EGF double-positive structures. Magenta arrowheads highlight EGF/Tf double-positive structures. In the merged images GABARAP fluorescence is depicted in green, EGF in red and Tf in blue. Snapshots are shown for selected time points of a 117 s time-lapse series consisting of 10 images with 13 s time intervals between images. In Figure S4, the complete time-lapse series of regions of interest I to V are shown, with a link to the corresponding movies. Scale bar in the overview = 10 µm, scale bar in close ups = 3 µm. (**B**–**D**) Spinning disk confocal fluorescence microscopy images of highly dynamic vesicles. GABARAP-only positive vesicles and large rings are highlighted by green arrows and GABARAP/EGF double-positive vesicles are highlighted by yellow arrows. In Figure S5 the complete time-lapse series is shown with a link to the corresponding movie. Scale bar = 3 µm.

GABARAP was found to be present in distinct structures in the cell's cytoplasm. These structures displayed different characteristics regarding their shape, size, and cargo, as determined by the simultaneous use of EGF-Alexa647 and Transferrin (Tf)-Alexa555 (Figure 7A, Figure S4 and Video S1). The latter was applied as a marker for endosomal compartments associated with recycling [77]. GABARAP and EGF frequently converged in punctate structures (yellow arrows), indicating that both

of the molecules are located within the same vesicle or at least adjacent vesicular structures. Some of these vesicles were additionally observed to be Tf-Alexa555 positive (white arrows), while others were found to be EGF and Tf double-positive (magenta arrows) without GABARAP localization. In contrast, we rarely observed GABARAP vesicles, which were additionally only Tf-positive. GABARAP and EGF also converged in Tf-negative ball-shaped structures (yellow arrows), indicating the accumulation of EGF and GABARAP within the same endosomal compartment, potentially associated with the degradative branch.

Strikingly, we frequently found large ring-like structures that were labeled with GABARAP (videos S1 III–V) of up to 3 µm in diameter. They were found at most once per cell and vesicles either double-positive for EGF and Tf or single-positive for EGF fused with the perimeters of these rings or budded off them. EGF accumulation was found in clusters resembling microdomains on these rings. Some, but not all, of these EGF clusters also contained Tf, suggesting that the respective parts of such rings might be associated with recycling. Altogether, these observations suggested that the large GABARAP-positive ring-like structures represent some sort of endosomal compartment, potentially a sorting endosome at the center of endosomal targeting either towards recycling or degradation.

We then subjected the GFP-GABARAP KI line to spinning disk confocal fluorescence microscopy to increase the temporal resolution (Figure 7B–D, Figure S5 and Video S2). After EGF-Alexa647 treatment, we could observe highly dynamic vesicular structures that were constantly fusing with and budding off the aforementioned GABARAP-positive rings. Figure 7B illustrates the fusion of a GABARAP single-positive vesicle with such a ring within a time frame as short as 1.2 s (green arrows). We also observed GABARAP vesicles that were EGF-Alexa647 positive (yellow arrows) and budded off the rings in a coordinated manner (Figure 7C). Frequently, these budding events were preceded by tubular protrusions (Figure 7D), which might represent molecules destined for recycling. Indeed, such cargo has been described to be sorted by tubular endosomal structures [78].

3.7. GABARAP Associates with EGFR during Co-Immunoprecipitation and Binds to Synthetic Peptides Derived from the EGFR Cytoplasmic Tail

We performed co-immunoprecipitation experiments, followed by *in vitro* interaction studies using purified GABARAP and synthetic peptides derived from the EGFR cytoplasmic tail, to investigate the nature of the transient co-migration observed during live cell imaging. As shown in Figure 8A, EGFR was co-immunoprecipitated by GFP-GABARAP but not by GFP from lysates of transiently transfected GABARAP SKO cells. This experiment confirmed an association between GABARAP and EGFR within cells. Interestingly, association was observed both under unstimulated conditions and after 10 min. of EGF treatment, supporting the idea of a GABARAP effect early in EGFR trafficking after ligand stimulation. The observed spatial overlap between GABARAP and EGFR during our live cell imaging studies, together with their observed co-immunoprecipitation, finally encouraged us to scan the EGFR sequence for canonical LIR/GIM motifs as putative direct GABARAP-binding sites. To address this, we used the iLIR tool [79]. Interestingly, EGFR indeed includes a putative extended LIR motif (xLIR) encompassing positions 1060 to 1065 (DTFLPV) within its cytoplasmic, regulatory tail (Figure 8B). Overall, this LIR motif contains four negatively charged and three phosphorylatable residues are located between P-8 and P-1, a further negatively charged residue at P + 5 and two phosphorylatable residues at P + 6 and P + 10. These features are in line with the established LIR-motifs of well-known GABARAP interactors, as demonstrated by alignment with the respective regions of ULK1, autophagy-related protein 13 (ATG13), Sequestosome-1 (SQSTM), pericentreolar material 1 (PCM1), and FIP200 [80].

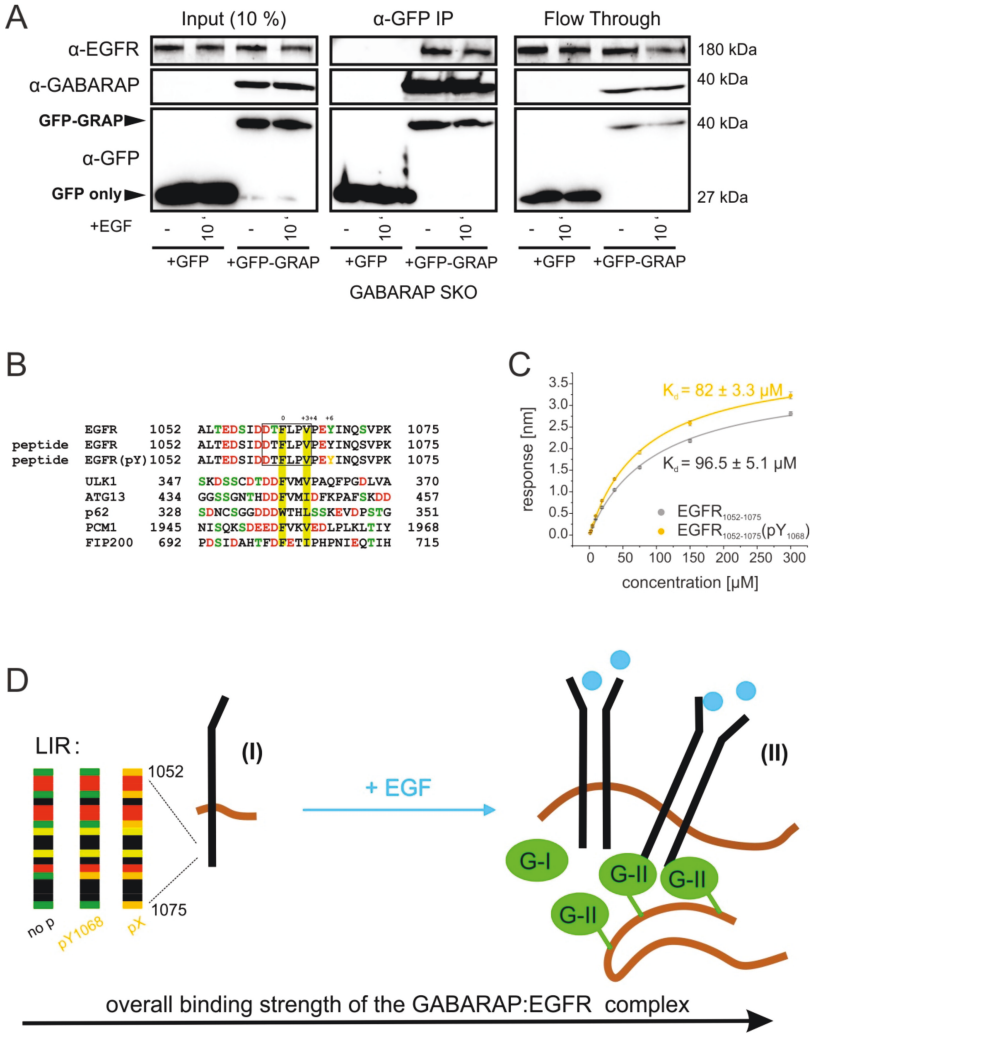

Figure 8. GABARAP associates with EGFR and binds to EGFR-derived peptides covering a putative LC3-interacting region (LIR) motif. (**A**) Co-Immunoprecipitation analysis between endogenous EGFR and transiently overexpressed GFP-GABARAP and GFP-only control in Huh7.5 GABARAP SKO cells. Figure S6F shows uncropped source blots. GRAP = GABARAP. (**B**) Sequence alignment of residues 1052 to 1075 of the cytoplasmic domain of EGFR with LIR-peptides from known GABARAP interaction partners. The core LIR motif is boxed and aromatic and hydrophobic residues in position 0 and +3 are depicted in yellow. Residues with negative charges are shown in red. Phosphorylatable residues are depicted in green. Both peptide sequences used for the BLI measurement shown in B are also depicted. Phosphorylated residue used in modified peptide is depicted in orange. Sequences were manually aligned according to the general core consensus (W/F/Y)-X-X-(L/I/V) where × may be any amino acid. (**C**) Ascending concentrations of recombinantly expressed and purified GABARAP were titrated to immobilized peptides and response measured by BLI. Measurements were performed in triplicates. Dissociation constants (Kd) of GABARAP were 96.5 ± 5.1 µM with the unmodified EGFR LIR peptide and 82 ± 3.3 µM with the phosphorylated peptide. (**D**) Model depicting modulation of binding affinity of GABARAP and EGFR. I: Phosphorylation of aa residues in the C-terminal tail of the receptor increases binding affinity through addition of negative charges. II: Increase of local concentration of EGFR due to ligand-induced dimerization and microclustering at the plasma membrane, as well as increase of local concentration of GABARAP due to lipidation, membrane association and possibly oligomerization increase avidity and, thus, overall binding strength of the GABARAP:EGFR complex. GABARAP is represented in green. G-I = unlipidated form of GABARAP, G-II = lipidated form of GABARAP.

Two aminoterminally biotinylated peptides covering the xLIR "DTFLPV" and additional eight positions up- and ten positions downstream, one of them phosphorylated at the regulatory Y1068, were subjected to biolayer interferometry (BLI) to analyze the binding affinity of GABARAP to this EGFR region. Figure 8C shows results of BLI measurements. The obtained dissociation constants were 96.5 µM (±5.1 µM) and 82 µM (±3.3 µM) for the unmodified and the modified peptide, respectively. These affinities appear relatively weak when compared to those of other known GABARAP protein interactors being in the low micromolar range [49]. Nonetheless, this interaction still might be of relevance e.g., in microdomains of locally clustered EGFR and GABARAP molecules (Figure 8D) by increasing overall avidity. Whether or not the xLIR motif is decisive for GABARAP binding to EGFR will be the subject of further investigation.

4. Discussion

In this study we identified a unique and novel role for GABARAP in EGF-induced trafficking and degradation of the EGFR, with implications for EGFR downstream signaling. Based on two independently generated HEK293 and Huh7.5 KO cell line panels, we could show that only cells lacking GABARAP, but not GABARAPL1 or GABARAPL2, displayed reduced total EGFR protein levels after EGF stimulation. We further showed that MAPK signaling downstream of EGFR was impaired in GABARAP deficient Huh7.5 cells, which translated into the reduction of EGFR target gene *CXCL8* expression. Consequently, we then explored the potential mechanistic role of GABARAP in the context of EGFR trafficking and degradation.

EGFR cycling can roughly be divided into five stages (Figure 9A): EGFR gene transcription and protein expression (1) are followed by post-translational modifications in the ER, trafficking through the Golgi-apparatus and surface targeting (2). Plasma membrane localized EGFR can then encounter extracellular stimuli, such as EGF. Ligand-bound EGFR is activated and internalized to strictly control signaling strength and duration (3). Subsequently, EGFR gets sorted within the endosomal system and is either recycled back to the plasma membrane (4) or targeted for degradation in the lysosome (5).

A

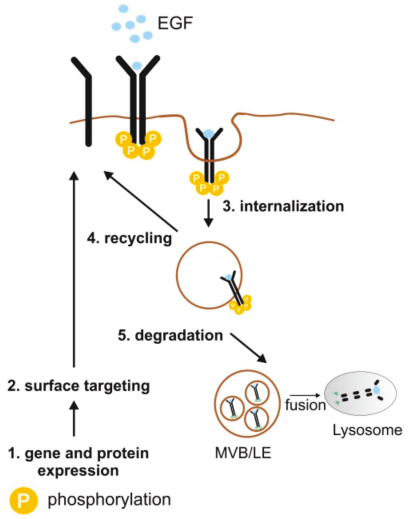

B

GABARAP protein interactions potentially influencing EGFR trafficking and degradation

level of interaction	affected process	interaction partner
direct	1 - 5	EGFR (figure 8)
indirect	3 [16, 70]	Clathrin [83]
	3 [84]	RTN3 [85]
	4 - 5 [88, 89]	NEDD4 [86]
	4 - 5 [88, 90]	CBL [25]
	5 [91]	CUL3 [92]
	4 [94]	TBC1D5/16 [95]
	5 [96]	RMC1 [41]
	3 + 4 [97]	OstIII [97]
	5 [101]	PLEKHM1 [49]

Figure 9. Scheme depicting EGFR internalization, trafficking and degradation including potential ways for GABARAP to take action. (**A**) 1. *EGFR* gene is expressed as mRNA and translated into protein followed by posttranslational modifications. 2. Trafficking through the Golgi apparatus regulates correct EGFR surface expression. 3. Upon extracellular ligand binding EGFR is internalized, sorted via the endosomal system and either targeted for recycling (4) or degradation (5). (**B**) List of processes that can be targeted by GABARAP either based on a direct interaction of GABARAP with EGFR as suggested in this study (grey) or indirectly by known or putative GABARAP interaction partners (light orange) with described activities in respective processes. MVB = multivesicular body, LE = late endosome.

An impact of GABARAP on basal protein levels of both total and cell surface localized EGFR seems unlikely, given our observations under unstimulated conditions. Additionally, steady state and EGF stimulated gene expression of the receptor was not influenced by GABARAP deficiency.

While we also did not observe an impact of GABARAP on the initial uptake of EGF-Alexa647, several hints strongly suggest that early internalization events might be slowed down by GABARAP. We found GABARAP deficiency associated with initially increased phosphorylation of EGFR Y1068, which is known to be associated with EGFR activation, growth factor receptor-bound protein 2 (GRB2), and E3 ubiquitin-protein ligase CBL binding, followed by internalization and subsequent degradation of the receptor [81]. We also observed higher volumes and intensities of EGF-containing vesicles as early as after 5 min. of EGF treatment in GABARAP deficient cells, indicating that GABARAP negatively influences the speed of early uptake events. Taken together, these observations suggest that GABARAP acts at an early stage of endosomal EGFR trafficking immediately downstream of ligand-induced receptor activation. In that way, increased EGFR degradation in GABARAP SKO cells would be a cumulative effect based on influencing early receptor dynamics.

Whether GABARAP influences EGFR activation through regulating the strength of dimer formation, as reported for different EGFR ligands [82], needs to be determined in further studies. As exemplarily shown in Figure 9B, a plethora of GABARAP interaction partners have already been reported to participate in endosomal sorting of the EGFR. The internalization of EGFR via clathrin-mediated endocytosis (CME) [16] might be modulated through direct interaction of GABARAP with the clathrin-heavy chain, which has already been described [83]. Interestingly, *CXCL8* expression was already reduced at low (i.e., 1.25 ng/mL) concentrations of EGF in the absence of GABARAP, indicating that CME, which is the major internalization route at low ligand concentrations [17], might be positively influenced by GABARAP. The high ligand concentrations that we mainly used in our study are known to activate clathrin-independent endocytosis (CIE), balancing the ratio of CME:CIE to about 1:1 [70]. CIE was reported to be mediated by ER/plasma membrane contact sites facilitated by reticulon 3 (RTN3) [84]. Intriguingly, RTN3 was recently described to interact with human Atg8 proteins through functional LIR motifs in the context of selective ER-phagy [85]. Thus, GABARAP could also sequester RTN3, hindering it from promoting CIE of EGFR. Thereby, GABARAP might shift the equilibrium towards enhanced CME and recycling.

Additionally, the E3 ubiquitin ligases NEDD4 and CBL have already been described to exhibit functional LIR motifs [25,86]. They take part in monoubiquitination of activated receptors, which is a signal for sorting into degradative compartments [87,88]. In particular, NEDD4 facilitates EGF-induced EGFR degradation by the ubiquitination of activated Cdc42-associated tyrosine kinase (ACK), leading to the degradation of both proteins [89]. Members of the E3 ubiquitin-protein ligase CBL family also target receptor tyrosine kinases for degradation by ubiquitination [90]. GABARAP might sequester these E3 ligases and, thus, prevent them from targeting receptors to degradation by monoubiquitination. With Cullin-3 (CUL3) another E3 ligase was reported to be positively involved in the maturation of late endosomes [91] and interact with GABARAP via KBTBD6/7 (Kelch repeat and BTB domain-containing protein 6/7) binding [92]. In this context, GABARAP might indirectly sequester CUL3 via KBTBD6/7, thereby inhibiting its positive effect on late endosome maturation and thus attenuate EGFR degradation.

Experimental evidence for GABARAP participating at the level of endosomal sorting comes from our EGF uptake results using confocal laser scanning microscopy, demonstrating that GABARAP SKO cells show altered vesicular size and EGF-Alexa647 loading, especially regarding larger vesicles with high fluorescence intensity at later time points upon stimulation.

The RAS-related in brain (RAB) protein family of small GTPases plays a major role in endocytic trafficking [93]. Several possibilities exist for GABARAP to influence RAB related processes. TBC1 domain family member 16 (TBC1D16) was described to be a negative regulator of RAB4A, thereby inhibiting the recycling of activated EGFR [94]. TBC1D16 was also reported to interact with Atg8 proteins in pulldown experiments, similar to other TBC domain containing proteins [95]. Whether

GABARAP directly interacts with TBC1D16 to counteract its negative effect on EGFR recycling or whether other TBC domain containing proteins are involved needs to be elucidated in future studies.

The association of the RAB proteins 5, 11, and 7 with EGF-Alexa647 was not found to be altered in GABARAP deficient cells during our experiments, implicating that GABARAP activity is not necessary for general endosomal targeting of EGFR. However, we cannot exclude that subtle or transient differences remained undetected under the experimental conditions used. Time-lapse live cell imaging while using KI cell lines expressing fluorescent protein tagged RABs can help to clarify this issue in more depth in the future.

KI cells expressing GFP-GABARAP under the endogenous *GABARAP* promoter enabled us to detect transient co-migration of GABARAP and EGF in the cytoplasm of cells under live conditions while using confocal laser scanning microscopy. Diverse punctate vesicular structures were frequently found along with GABARAP positive rings forming microdomain-like spots, which were either positive for EGF- or for the recycling compartment marker Transferrin, emphasizing the importance of GABARAP-related activity for EGFR trafficking. Using spinning disk confocal fluorescence microscopy we improved the temporal resolution up to 20-fold, enabling us to assess the dynamics of GABARAP- and EGF-containing vesicles. We observed highly dynamic GABARAP-, EGF- or GABARAP/EGF-containing vesicles fusing with or budding off such rings. These intracellular interactions strongly suggest that also later stages of endosomal trafficking that are not associated with Tf are affected by GABARAP, potentially correlating with a role in endosomal sorting and/or maturation.

A potential role of GABARAP in inhibiting endosome maturation is supported by the finding that the protein levels of the CCZ1/MON1 positive regulator RMC1 are elevated in cells deficient for the whole GABARAP subfamily [41]. CCZ1/MON1 acts as an activator of RAB7 [96]. The inhibition of late endosome maturation might be mediated by GABARAP preventing RMC1 from activating RAB7 through CCZ1/MON1. Another RAB regulator interacting with GABARAP is the RAC1 GEF Ost-III, which negatively regulates CME of receptors and it was found to be inhibited by ectopic GABARAP expression [97]. Two main degradative pathways play a role in EGF-induced EGFR degradation. First, proteasome-mediated deubiquitination of activated receptors is necessary for EGFR containing endosomes to mature into intraluminal vesicles (ILV) of multivesicular bodies (MVB) [98]. Second, processed receptors are targeted for degradation within the lysosomal compartment [99]. Proteasomal inhibition by lactacystin restored both EGFR protein levels and ERK1/2 phosphorylation to wildtype, indicating that GABARAP acts downstream or on the level of MVB maturation. In contrast, the inhibition of lysosomal acidification by chloroquine partly restored EGFR degradation towards wildtype levels. Notably, ERK1/2 phosphorylation was still impaired in GABARAP SKO cells. Chloroquine is known to inhibit EGFR degradation by preventing fusion of multivesicular bodies/late endosomes with the lysosome [100], indicating that GABARAP affects ERK1/2 activation earlier in the process. Thus, we hypothesize that GABARAP might act on the level of endosomal maturation and/or compartmentalization, e.g., by controlling maturation of EGFR containing vesicles into ILVs of MVBs upstream of lysosomal degradation.

Finally, Pleckstrin homology domain-containing family M member 1 (PLEKHM1) binding simultaneously to Atg8 family proteins and the homotypic fusion and protein sorting (HOPS) complex was reported to regulate ligand-induced EGFR degradation due to impaired lysosomal fusion [101]. Importantly, PLEKHM1 was found to contain a LIR displaying a much higher affinity to GABARAP subfamily proteins than LC3 subfamily proteins [49]. However, the binding of all GABARAP subfamily proteins was described to be in the low micromolar range, strongly suggesting that GABARAP function in this context might be redundant to GABARAPL1 and/or GABARAPL2.

GABARAP might also directly bind to EGFR under certain circumstances due to the existence of an xLIR motif, which we identified in the cytoplasmic domain of EGFR. The binding of EGFR LIR peptides to immobilized GABARAP was quite modest during our measurements as compared with most GABARAP interactions reported previously. Nevertheless, EGF stimulation is known to promote EGFR nanocluster formation [102,103] by receptor oligomerization and membrane bending [104] prior

to internalization [105]. GABARAP has also been described to form self-associated species [106]. Such clusters may increase the local EGFR and/or GABARAP concentration facilitating LIR-mediated binding. Indeed, we were able to show the co-immunoprecipitation of GFP-GABARAP and EGFR both with and without EGF treatment. These results and the observed comigration of GFP-GABARAP and EGF-Alexa647 strongly suggest an at least transient interaction between GABARAP and EGFR.

Such an interaction could either result in direct targeting of EGFR into autophagosomes or involve endosomal sorting. Direct autophagic targeting of proteins by GABARAP has recently been described for the nuclear receptor co-repressor 1 (NCOR1) [107]. On the other hand, EGFR activation actively suppresses autophagy by beclin 1 phosphorylation [108], and we did not use autophagy inducing conditions in our set up.

GABARAP might bind to EGFR-containing vesicles, presenting the xLIR motif on their outer face and thereby connect them to the microtubule network, which is known to associate with GABARAP [52]. In this case, EGFR vesicle transport would be mediated in a very direct manner.

Finally, several RTKs are associated with autophagy related processes. For example, protein turnover of TNFRSF12A (TNF receptor superfamily member 12 A) is regulated by mammalian Atg8 family proteins, with GABARAP and GABARAPL2 fulfilling different roles in this process [109]. Autophagy degraded the RTK ret proto-oncogene (RET) [24]. The former case supports the idea of non-redundant roles of GABARAP subfamily proteins, similar to what we observe for EGFR in Huh7.5 cells regarding GABARAP action.

5. Conclusions

Altogether, the presented data supports a unique and non-redundant role for GABARAP in the context of EGF-induced EGFR degradation. GABARAP may be able to influence EGFR trafficking on numerous levels, including, but very likely not limited to, a direct interaction with EGFR, as depicted in Figure 9. Therefore, further detailed studies will be necessary to determine the underlying molecular mechanism(s) of GABARAP interfering with EGFR trafficking and endosomal trafficking in general. It will also be of paramount importance to clarify the roles of the other two GABARAP subfamily proteins in that context. Lastly, we shall not forget the involvement of GABARAP subfamily proteins in important cellular processes, such as autophagy and lysosomal fusion, which cannot be ruled out to have an effect on most phenotypes in general. We have just started to uncover the mode of action of human Atg8 proteins and their contribution to cell surface receptor fate in general.

Supplementary Materials: The following are available online at http://www.mdpi.com/2073-4409/9/5/1296/s1, Figure S1: Verification of CRISPR/Cas9 knockout and knock-in cell lines on protein level, Table S1: CRISPR sequence details and genotyping results of the knockout cell lines used, Figure S2: Total EGFR levels in response to EGF treatment in HEK293 KO cells transiently overexpressing EGFR-GFP, Figure S3: Analysis of EGF-Alexa647 containing vesicles of GABARAP SKO and Huh7.5 cells by Imaris and analysis of endosomal markers RAB 5, RAB11 and RAB7 in response to EGF treatment in GABARAP SKO and Huh7.5 control cells, Figure S4: Montage of live cell imaging of HEK293 knock-in cells expressing GFP-GABARAP under the endogenous GABARAP promoter and stimulated with EGF-Alexa647 and Tf-Alexa555 by confocal laser scanning microscopy, Figure S5: Live cell imaging of HEK293 KI cells expressing GFP-GABARAP under the endogenous *GABARAP* promoter and stimulated with EGF-Alexa647 by spinning disk confocal fluorescence microscopy, Figure S6: Uncropped source blots of immunoblotting experiments, Movie S1: Live cell imaging of HEK293 knock-in cells expressing GFP-GABARAP under the endogenous GABARAP promoter and stimulated with EGF-Alexa647 and Tf-Alexa555 by confocal laser scanning microscopy and Movie S2: Live cell imaging of HEK293 KI cells expressing GFP-GABARAP under the endogenous GABARAP promoter and stimulated with EGF-Alexa647 by spinning disk confocal fluorescence microscopy.

Author Contributions: Conceptualization, J.D., O.H.W., J.G.B., S.H. and D.W.; Formal analysis, J.D., I.M.S., S.H. and M.S.; Funding acquisition, S.H. and D.W.; Investigation, J.D., I.M.S., K.R., M.S., I.A. and T.G.; Project administration, D.W.; Resources, S.H., T.G., J.G.B. and D.W.; Supervision, S.H. and D.W.; Validation, J.D. and I.M.S.; Visualization, J.D. and I.M.S.; Writing—original draft, J.D. and S.H.; Writing—review & editing, J.D., I.M.S., K.R., M.S., O.H.W., T.G., J.G.B., S.H. and D.W. All authors have read and agreed to the published version of the manuscript.

Funding: This work was supported by a grant from the Jürgen Manchot Foundation, Molecules of Infection Graduate School (MOI III) (J.D. and K.R.), funded by the Deutsche Forschungsgemeinschaft (DFG, German Research Foundation)–Project-ID 267205415–SFB 1208 (D.W.), funding for the Center for Advanced Imaging (WE5343/1-1) and by funding of the Vorstandsdoktorandenprogramm of the Forschungszentrum Jülich (I.A.). The authors declare that they have no conflicts of interest with the contents of this article.

Acknowledgments: We are grateful to Marianne Wammers for guidance with the FACS. We thank Claudia Hoppen for cloning of the original KO plasmids.

Conflicts of Interest: The authors declare no conflict of interest.

Appendix A

Table A1. Antibodies used in this study.

Antibody	Company	Species	Catalog Number/Dilution-Application (Antigen Used for Antibody Production)
primary Abs:			
anti-EGFR	Cell Signaling	rabbit	2232/1:1000-IB (synthetic peptide corresponding to residues surrounding Tyr1068 of human EGFR)
anti-EGFR	Cell Signaling	rabbit	4267/1:1000-IB (fusion protein containing the cytoplasmic domain of human EGFR)
anti-phospho-EGFR (Tyr1068)	Cell Signaling	rabbit	2234/1:1000–IB (synthetic peptide corresponding to residues surrounding Tyr1068 of human EGFR)
anti-Akt (pan)	Cell Signaling	mouse	2920/1:1000-IB (synthetic peptide at the carboxyterminal sequence of human Akt)
anti-phospho-Akt (Ser473)	Cell Signaling	rabbit	4060/1:1000-IB (synthetic phosphopeptide corresponding to residues around Ser473 of human Akt)
anti-p44/42 MAPK (Erk1/2)	Cell Signaling	rabbit	4695/1:1000-IB (synthetic peptide corresponding to residues near the C-terminus of rat p44 MAP kinase)
anti-phospho-p44/42 MAPK (Erk1/2) (Thr202/Tyr204)	Cell Signaling	mouse	9106/1:1000-IB (synthetic phospho-peptide (KLH-coupled) corresponding to residues surrounding Thr202/Tyr204 of human p44 MAP kinase)
anti-beta actin	Abcam	mouse	ab6276/1:15 000-IB (DDDIAALVIDNGSGK)
anti-GABARAP	Cell Signaling	rabbit	13733/1:1000-IB (synthetic peptide corresponding to residues surrounding Arg40 of human GABARAP)
anti-GABARAP	In-house	rat	In-house/undiluted-IF Institute for Diabetes and Obesity, Monoclonal Antibody Core Facility, GST-hGABARAP_aa1-117 [65]
anti-GABARAPL1	Cell Signaling	rabbit	26632/1:1000-IB (synthetic peptide corresponding to residues near the amino terminus of human GABARAPL1)
anti-GABARAPL2	Cell Signaling	rabbit	14256/1:1000-IB (synthetic peptide corresponding to residues near the carboxy terminus of human GABARAPL2)
anti-GFP (HRP-coupled)	Miltenyi Biotech	mouse	130-091-833/1:2000-IB (proprietary)
anti-RAB5	Cell Signaling	rabbit	3547S/1:100-IF (synthetic peptide corresponding to residues surrounding Gly190 of human Rab5A protein)
anti-RAB7	Cell Signaling	rabbit	9367S/1:100-IF (synthetic peptide corresponding to residues surrounding Glu188 of human Rab7 protein)

Table A1. *Cont.*

Antibody	Company	Species	Catalog Number/Dilution-Application (Antigen Used for Antibody Production)
anti-RAB11	Cell Signaling	rabbit	5589S/1:100-IF (synthetic peptide corresponding to residues near the amino terminus of human Rab11 protein.
secondary Abs:			
anti-Mouse IgG H&L (Alexa Fluor® 488)	Abcam	goat	150117/1:250–IF or 1:5000-IB (mouse IgG)
anti-Rabbit IgG H&L (Alexa Fluor® 647)	Abcam	goat	150083/1:250–IF or 1:5000-IB (rabbit IgG)
anti-rat IgG+IgM H&L (Alexa Fluor® 488)	Jackson ImmunoResearch	goat	112-545-068/1:250–IF (rat IgG + IgM)
anti-rabbit IgG H&L (Alexa Fluor® 555 preadsorbed)	Abcam	goat	150086/1:250–IF (rabbit IgG)

Table A2. Primers used in this study.

	Sequence (5′ → 3′)
qPCR	
CXCL8 forward	AGAAGTTTTTGAAGAGGGCTGAGA
CXCL8 reverse	CAGACCCACACAATACATGAAGTG
CXCL1 forward	CTGGCGGATCCAAGCAAAT
CXCL1 reverse	CATTCCCCTGCCTTCACAAT
SDHA forward	AGATGTGGTGTCTCGGTCGAT
SDHA reverse	CGTGATCTTTCTCAGGGCCA
EGFR forward	CATCCAGTGGCGGGACATAG
EGFR reverse	GGGACAGCTTGGATCACACT
Genotyping	
GABARAP forward	GGGTTGGTGAATAGGGAAGTGG
GABARAP reverse	CACTCCTTTCATCCTGGGTCC
GABARAPL1 forward	TGGGAACCTGATCCAAGACTC
GABARAPL1 reverse	GCCAGGAAGCTAGTCCAAAAC
GABARAPL2 forward	CTTGCTGGGAGCTAGTAGGG
GABARAPL2 reverse	TGAGGCACCCTGAACAGCA

References

1. Cohen, S.; Carpenter, G.; King, L. Epidermal growth factor-receptor-protein kinase interactions. Co-purification of receptor and epidermal growth factor-enhanced phosphorylation activity. *J. Biol. Chem.* **1980**, *255*, 4834–4842. [PubMed]
2. Chen, J.; Zeng, F.; Forrester, S.J.; Eguchi, S.; Zhang, M.-Z.; Harris, R.C. Expression and Function of the Epidermal Growth Factor Receptor in Physiology and Disease. *Physiol. Rev.* **2016**, *96*, 1025–1069. [CrossRef]
3. Roberts, A.B.; Lamb, L.C.; Newton, D.L.; Sporn, M.B.; De Larco, J.E.; Todaro, G.J. Transforming growth factors: Isolation of polypeptides from virally and chemically transformed cells by acid/ethanol extraction. *Proc. Natl. Acad. Sci. USA* **1980**, *77*, 3494–3498. [CrossRef] [PubMed]
4. Shoyab, M.; McDonald, V.L.; Bradley, J.G.; Todaro, G.J. Amphiregulin: A bifunctional growth-modulating glycoprotein produced by the phorbol 12-myristate 13-acetate-treated human breast adenocarcinoma cell line MCF-7. *Proc. Natl. Acad. Sci. USA* **2006**, *85*, 6528–6532. [CrossRef]
5. Cohen, S. Isolation of a mouse submaxillary gland protein accelerating incisor eruption and eyelid opening in the new-born animal. *J. Biol. Chem.* **1962**, *237*, 1555–1562.
6. Yarden, Y.; Sliwkowski, M.X. Untangling the ErbB signalling network. *Nat. Rev. Mol. Cell Biol.* **2001**, *2*, 127–137. [CrossRef]

7. Honegger, A.M.; Kris, R.M.; Ullrich, A.; Schlessinger, J. Evidence that autophosphorylation of solubilized receptors for epidermal growth factor is mediated by intermolecular cross-phosphorylation. *Proc. Natl. Acad. Sci. USA* **1989**, *86*, 925–929. [CrossRef]
8. Honegger, A.M.; Schmidt, A.; Ullrich, A.; Schlessinger, J. Evidence for epidermal growth factor (EGF)-induced intermolecular autophosphorylation of the EGF receptors in living cells. *Mol. Cell. Biol.* **1990**, *10*, 4035–4044. [CrossRef]
9. Xie, H.; Pallero, M.A.; Gupta, K.; Chang, P.; Ware, M.F.; Witke, W.; Kwiatkowski, D.J.; Lauffenburger, D.A.; Murphy-Ullrich, J.E.; Wells, A. EGF receptor regulation of cell motility: EGF induces disassembly of focal adhesions independently of the motility-associated PLCgamma signaling pathway. *J. Cell Sci.* **1998**, *111 Pt 5*, 615–624.
10. Wee, P.; Wang, Z. Epidermal growth factor receptor cell proliferation signaling pathways. *Cancers* **2017**, *9*, 52.
11. Uemura, T.; Kametaka, S.; Waguri, S. GGA2 interacts with EGFR cytoplasmic domain to stabilize the receptor expression and promote cell growth. *Sci. Rep.* **2018**, *8*, 1–14. [CrossRef] [PubMed]
12. Yarden, Y.; Pines, G. The ERBB network: At last, cancer therapy meets systems biology. *Nat. Rev. Cancer* **2012**, *12*, 553–563. [CrossRef] [PubMed]
13. Sigismund, S.; Avanzato, D.; Lanzetti, L. Emerging functions of the EGFR in cancer. *Mol. Oncol.* **2018**, *12*, 3–20. [CrossRef] [PubMed]
14. Carpenter, G.; Cohen, S. 125I-Labeled human epidermal growth factor: Binding, Internalization, and Degradation in Human Fibroblasts Antiserum to hEGF 1251-hEGF Binding Assay Iodination o f hEGF and Antiserum Autoradiography. *J. Cell Biol.* **1976**, *71*, 159–171. [CrossRef]
15. Haigler, H.T.; McKanna, J.A.; Cohen, S. Direct visualization of the binding and internalization of a ferritin conjugate of epidermal growth factor in human carcinoma cells A-431. *J. Cell Biol.* **1979**, *81*, 382–395. [CrossRef]
16. Hanover, J.A.; Willingham, M.C.; Pastan, I. Kinetics of transit of transferrin and epidermal growth factor through clathrin-coated membranes. *Cell* **1984**, *39*, 283–293. [CrossRef]
17. Sigismund, S.; Woelk, T.; Puri, C.; Maspero, E.; Tacchetti, C.; Transidico, P.; Di Fiore, P.P.; Polo, S. Clathrin-independent endocytosis of ubiquitinated cargos. *Proc. Natl. Acad. Sci. USA* **2005**, *102*, 2760–2765. [CrossRef]
18. Bakker, J.; Spits, M.; Neefjes, J.; Berlin, I. The EGFR odyssey—From activation to destruction in space and time. *J. Cell Sci.* **2017**, *130*, 4087–4096. [CrossRef]
19. Yu, L.; Chen, Y.; Tooze, S.A. Autophagy pathway: Cellular and molecular mechanisms. *Autophagy* **2018**, *14*, 207–215. [CrossRef]
20. Antonioli, M.; Di Rienzo, M.; Piacentini, M.; Fimia, G.M. Emerging Mechanisms in Initiating and Terminating Autophagy. *Trends Biochem. Sci.* **2017**, *42*, 28–41. [CrossRef]
21. Shibutani, S.T.; Yoshimori, T. A current perspective of autophagosome biogenesis. *Cell Res.* **2014**, *24*, 58–68. [CrossRef] [PubMed]
22. Anding, A.L.; Baehrecke, E.H. Cleaning House: Selective Autophagy of Organelles. *Dev. Cell* **2017**, *41*, 10–22. [CrossRef] [PubMed]
23. Mao, K.; Klionsky, D.J. Xenophagy: A battlefield between host and microbe, and a possible avenue for cancer treatment. *Autophagy* **2017**, *13*, 223–224. [CrossRef]
24. Sandilands, E.; Serrels, B.; Wilkinson, S.; Frame, M.C. Src-dependent autophagic degradation of Ret in FAK-signalling-defective cancer cells. *EMBO Rep.* **2012**, *13*, 733–740. [CrossRef] [PubMed]
25. Sandilands, E.; Serrels, B.; McEwan, D.G.; Morton, J.P.; MacAgno, J.P.; McLeod, K.; Stevens, C.; Brunton, V.G.; Langdon, W.Y.; Vidal, M.; et al. Autophagic targeting of Src promotes cancer cell survival following reduced FAK signalling. *Nat. Cell Biol.* **2012**, *14*, 51–60. [CrossRef]
26. Ponpuak, M.; Mandell, M.A.; Kimura, T.; Chauhan, S.; Cleyrat, C.; Deretic, V. Secretory autophagy. *Curr. Opin. Cell Biol.* **2015**, *35*, 106–116. [CrossRef]
27. Claude-Taupin, A.; Jia, J.; Mudd, M.; Deretic, V. Autophagy's secret life: Secretion instead of degradation. *Essays Biochem.* **2017**, *61*, 637–647.
28. Matsuura, A.; Tsukada, M.; Wada, Y.; Ohsumi, Y. Apg1p, a novel protein kinase required for the autophagic process in Saccharomyces cerevisiae. *Gene* **1997**, *192*, 245–250. [CrossRef]

29. Mizushima, N.; Yoshimori, T.; Ohsumi, Y. The Role of Atg Proteins in Autophagosome Formation. *Annu. Rev. Cell Dev. Biol.* **2011**, *27*, 107–132. [CrossRef]
30. Tsukada, M.; Ohsumi, Y. Isolation and characterization of autophagy-defective mutants of Saccharomyces cerevisiae. *FEBS Lett.* **1993**, *333*, 169–174. [CrossRef]
31. Shpilka, T.; Weidberg, H.; Pietrokovski, S.; Elazar, Z. Atg8: An autophagy-related ubiquitin-like protein family. *Genome Biol.* **2011**, *12*, 226. [CrossRef] [PubMed]
32. Weiergräber, O.; Mohrlüder, J.; Willbold, D. *Atg8 Family Proteins—Autophagy and Beyond. In Autophagy—A Double-Edged Sword—Cell Survival or Death?* InTech: Rijeka, Croatia, 2013; pp. 267–322.
33. Zhang, Z.; Xu, X.; Ma, J.; Wu, J.; Wang, Y.; Zhou, R.; Han, J. Gene Deletion of Gabarap Enhances Nlrp3 Inflammasome-Dependent Inflammatory Responses. *J. Immunol.* **2013**, *190*, 3517–3524. [CrossRef] [PubMed]
34. Keulers, T.G.; Schaaf, M.B.E.; Rouschop, K.M.A. Autophagy-dependent secretion: Contribution to tumor progression. *Front. Oncol.* **2016**, *6*, 251. [CrossRef] [PubMed]
35. Peng, G.; Yan, Y.; Zhu, C.; Wang, S.; Yan, X.; Lu, L.; Li, W.; Hu, J.; Wei, W.; Mu, Y.; et al. Borna Disease Virus P Protein Affects Neural Transmission through Interactions with Gamma-Aminobutyric Acid Receptor-Associated Protein. *J. Virol.* **2008**, *82*, 12487–12497. [CrossRef]
36. Chen, R.Y.; Shen, K.L.; Chen, Z.; Fan, W.W.; Xie, X.L.; Meng, C.; Chang, X.J.; Zheng, L.B.; Jeswin, J.; Li, C.H.; et al. White spot syndrome virus entry is dependent on multiple endocytic routes and strongly facilitated by Cq-GABARAP in a CME-dependent manner. *Sci. Rep.* **2016**, *6*. [CrossRef]
37. Boeske, A.; Schwarten, M.; Ma, P.; Tusche, M.; Mötter, J.; Möller, C.; Neudecker, P.; Hoffmann, S.; Willbold, D. Direct binding to GABARAP family members is essential for HIV-1 Nef plasma membrane localization. *Sci. Rep.* **2017**, *7*, 5797. [CrossRef]
38. Mohrlüder, J.; Schwarten, M.; Willbold, D. Structure and potential function of γ-aminobutyrate type A receptor-associated protein. *FEBS J.* **2009**, *276*, 4989–5005. [CrossRef]
39. Weidberg, H.; Shvets, E.; Shpilka, T.; Shimron, F.; Shinder, V.; Elazar, Z. LC3 and GATE-16/GABARAP subfamilies are both essential yet act differently in autophagosome biogenesis. *EMBO J.* **2010**, *29*, 1792–1802. [CrossRef]
40. Nguyen, T.N.; Padman, B.S.; Usher, J.; Oorschot, V.; Ramm, G.; Lazarou, M. Atg8 family LC3/GAB ARAP proteins are crucial for autophagosome-lysosome fusion but not autophagosome formation during PINK1/Parkin mitophagy and starvation. *J. Cell Biol.* **2016**, *215*, 857–874. [CrossRef]
41. Vaites, L.P.; Paulo, J.A.; Huttlin, E.L.; Harper, J.W. Systematic Analysis of Human Cells Lacking ATG8 Proteins Uncovers Roles for GABARAPs and the CCZ1/MON1 Regulator C18orf8/RMC1 in Macroautophagic and Selective Autophagic Flux. *Mol. Cell. Biol.* **2017**, *38*, e00392-17. [CrossRef]
42. Novak, I.; Kirkin, V.; McEwan, D.G.; Zhang, J.; Wild, P.; Rozenknop, A.; Rogov, V.; Löhr, F.; Popovic, D.; Occhipinti, A.; et al. Nix is a selective autophagy receptor for mitochondrial clearance. *EMBO Rep.* **2010**, *11*, 45–51. [CrossRef] [PubMed]
43. Rozenknop, A.; Rogov, V.V.; Rogova, N.Y.; Löhr, F.; Güntert, P.; Dikic, I.; Dötsch, V. Characterization of the interaction of GABARAPL-1 with the LIR motif of NBR1. *J. Mol. Biol.* **2011**, *410*, 477–487. [CrossRef] [PubMed]
44. Rogov, V.V.; Suzuki, H.; Fiskin, E.; Wild, P.; Kniss, A.; Rozenknop, A.; Kato, R.; Kawasaki, M.; McEwan, D.G.; Löhr, F.; et al. Structural basis for phosphorylation-triggered autophagic clearance of Salmonella. *Biochem. J.* **2013**, *454*, 459–466. [CrossRef] [PubMed]
45. Lee, Y.K.; Lee, J.A. Role of the mammalian ATG8/LC3 family in autophagy: Differential and compensatory roles in the spatiotemporal regulation of autophagy. *BMB Rep.* **2016**, *49*, 424–430. [CrossRef]
46. Zaffagnini, G.; Martens, S. Mechanisms of Selective Autophagy. *J. Mol. Biol.* **2016**, *428*, 1714–1724. [CrossRef]
47. Abdollahzadeh, I.; Schwarten, M.; Gensch, T.; Willbold, D.; Weiergräber, O.H. The Atg8 family of proteins-modulating shape and functionality of autophagic membranes. *Front. Genet.* **2017**, *8*, 109. [CrossRef]
48. Lystad. Simonsen Mechanisms and Pathophysiological Roles of the ATG8 Conjugation Machinery. *Cells* **2019**, *8*, 973. [CrossRef]
49. Rogov, V.V.; Stolz, A.; Ravichandran, A.C.; Rios-Szwed, D.O.; Suzuki, H.; Kniss, A.; Löhr, F.; Wakatsuki, S.; Dötsch, V.; Dikic, I.; et al. Structural and functional analysis of the GABARAP interaction motif (GIM). *EMBO Rep.* **2018**, *19*, e47268. [CrossRef]

50. Wirth, M.; Zhang, W.; Razi, M.; Nyoni, L.; Joshi, D.; O'Reilly, N.; Johansen, T.; Tooze, S.A.; Mouilleron, S. Molecular determinants regulating selective binding of autophagy adapters and receptors to ATG8 proteins. *Nat. Commun.* **2019**, *10*, 2055. [CrossRef]
51. Marshall, R.S.; Hua, Z.; Mali, S.; McLoughlin, F.; Vierstra, R.D. ATG8-Binding UIM Proteins Define a New Class of Autophagy Adaptors and Receptors. *Cell* **2019**, *177*, 766–781. [CrossRef]
52. Wang, H.; Bedford, F.K.; Brandon, N.J.; Moss, S.J.; Olsen, R.W. GABA(A)-receptor-associated protein links GABA(A) receptors and the cytoskeleton. *Nature* **1999**, *397*, 69–72. [CrossRef] [PubMed]
53. Chen, L.; Wang, H.; Vicini, S.; Olsen, R.W. The gamma -aminobutyric acid type A (GABAA) receptor-associated protein (GABARAP) promotes GABAA receptor clustering and modulates the channel kinetics. *Proc. Natl. Acad. Sci. USA* **2000**, *97*, 11557–11562. [CrossRef] [PubMed]
54. Green, F.; O'Hare, T.; Blackwell, A.; Enns, C.A. Association of human transferrin receptor with GABARAP. *FEBS Lett.* **2002**, *518*, 101–106. [CrossRef]
55. Laínez, S.; Valente, P.; Ontoria-Oviedo, I.; Estévez-Herrera, J.; Camprubí-Robles, M.; Ferrer-Montiel, A.; Planells-Cases, R. GABAA receptor associated protein (GABARAP) modulates TRPV1 expression and channel function and desensitization. *FASEB J.* **2010**, *24*, 1958–1970. [CrossRef] [PubMed]
56. Cook, J.L.; Re, R.N.; DeHaro, D.L.; Abadie, J.M.; Peters, M.; Alam, J. The trafficking protein GABARAP binds to and enhances plasma membrane expression and function of the angiotensin II type 1 receptor. *Circ. Res.* **2008**, *102*, 1539–1547. [CrossRef] [PubMed]
57. Reining, S.C.; Liesegang, A.; Betz, H.; Biber, J.; Murer, H.; Hernando, N. Expression of renal and intestinal Na/Pi cotransporters in the absence of GABARAP. *Pflug. Arch. Eur. J. Physiol.* **2010**, *460*, 207–217. [CrossRef]
58. Dutta, P.; Dargahi, L.; O'Connell, K.E.; Bolia, A.; Ozkan, B.; Sailer, A.W.; Dev, K.K. A novel modelling mechanism of PAEL receptor and GABARAPL2 interaction involved in Parkinson's disease. *Neurosci. Lett.* **2018**, *673*, 12–18. [CrossRef]
59. Mansuy, V.; Boireau, W.; Fraichard, A.; Schlick, J.L.; Jouvenot, M.; Delage-Mourroux, R. GEC1, a protein related to GABARAP, interacts with tubulin and GABA A receptor. *Biochem. Biophys. Res. Commun.* **2004**, *325*, 639–648. [CrossRef]
60. Chen, C.; Li, J.G.; Chen, Y.; Huang, P.; Wang, Y.; Liu-Chen, L.Y. GEC1 interacts with the κ opioid receptor and enhances expression of the receptor. *J. Biol. Chem.* **2006**, *281*, 7983–7993. [CrossRef]
61. Keulers, T.G.; Schaaf, M.B.E.; Peeters, H.J.M.; Savelkouls, K.G.M.; Vooijs, M.A.; Bussink, J.; Jutten, B.; Rouschop, K.M.A. GABARAPL1 is required for increased EGFR membrane expression during hypoxia. *Radiother. Oncol.* **2015**, *116*, 417–422. [CrossRef]
62. Blight, K.J.; McKeating, J.A.; Rice, C.M. Highly Permissive Cell Lines for Subgenomic and Genomic Hepatitis C Virus RNA Replication. *J. Virol.* **2002**, *76*, 13001–13014. [CrossRef] [PubMed]
63. O'Gorman, S.; Fox, D.T.; Wahl, G.M. Recombinase-mediated gene activation and site-specific integration in mammalian cells. *Science* **1991**, *251*, 1351–1355. [CrossRef] [PubMed]
64. Russell, W.C.; Graham, F.L.; Smiley, J.; Nairn, R. Characteristics of a Human Cell Line Transformed by DNA from Human Adenovirus Type 5. *J. Gen. Virol.* **1977**, *36*, 59–72.
65. Simons, I.M.; Mohrlüder, J.; Feederle, R.; Kremmer, E.; Zobel, T.; Dobner, J.; Bleffert, N.; Hoffmann, S.; Willbold, D. The highly GABARAP specific rat monoclonal antibody 8H5 visualizes GABARAP in immunofluorescence imaging at endogenous levels. *Sci. Rep.* **2019**, *9*, 526. [CrossRef]
66. Ran, F.A.; Hsu, P.D.; Wright, J.; Agarwala, V.; Scott, D.A.; Zhang, F. Genome engineering using the CRISPR-Cas9 system. *Nat. Protoc.* **2013**, *8*, 2281–2308. [CrossRef] [PubMed]
67. Rivero-Gutiérrez, B.; Anzola, A.; Martínez-Augustin, O.; De Medina, F.S. Stain-free detection as loading control alternative to Ponceau and housekeeping protein immunodetection in Western blotting. *Anal. Biochem.* **2014**, *467*, 1–3. [CrossRef]
68. Schindelin, J.; Arganda-Carreras, I.; Frise, E.; Kaynig, V.; Longair, M.; Pietzsch, T.; Preibisch, S.; Rueden, C.; Saalfeld, S.; Schmid, B.; et al. Fiji: An open-source platform for biological-image analysis. *Nat. Methods* **2012**, *9*, 676–682. [CrossRef]
69. Möckel, C.; Kubiak, J.; Schillinger, O.; Kühnemuth, R.; Della Corte, D.; Schröder, G.F.; Willbold, D.; Strodel, B.; Seidel, C.A.M.; Neudecker, P. Integrated NMR, Fluorescence, and Molecular Dynamics Benchmark Study of Protein Mechanics and Hydrodynamics. *J. Phys. Chem. B* **2019**, *123*, 1453–1480. [CrossRef]

70. Sigismund, S.; Argenzio, E.; Tosoni, D.; Cavallaro, E.; Polo, S.; Di Fiore, P.P. Clathrin-Mediated Internalization Is Essential for Sustained EGFR Signaling but Dispensable for Degradation. *Dev. Cell* **2008**, *15*, 209–219. [CrossRef]
71. Gu, Y.; Princely Abudu, Y.; Kumar, S.; Bissa, B.; Choi, S.W.; Jia, J.; Lazarou, M.; Eskelinen, E.; Johansen, T.; Deretic, V. Mammalian Atg8 Proteins Regulate Lysosome and Autolysosome Biogenesis Through SNAREs. *EMBO J.* **2019**, *38*, e101994. [CrossRef]
72. Groepper, C.; Rufinatscha, K.; Schröder, N.; Stindt, S.; Ehlting, C.; Albrecht, U.; Bock, H.H.; Bartenschlager, R.; Häussinger, D.; Bode, J.G. HCV modifies EGF signalling and upregulates production of CXCR2 ligands: Role in inflammation and antiviral immune response. *J. Hepatol.* **2018**, *69*, 594–602. [CrossRef] [PubMed]
73. Salova, A.V.; Belyaeva, T.N.; Leontieva, E.A.; Kornilova, E.S. EGF receptor lysosomal degradation is delayed in the cells stimulated with EGF-Quantum dot bioconjugate but earlier key events of endocytic degradative pathway are similar to that of native EGF. *Oncotarget* **2017**, *8*, 44335–44350. [CrossRef] [PubMed]
74. Sorkin, A.; Carter, R. Endocytosis of Functional Epidermal Growth Factor Receptor-Green Fluorescent Protein Chimera. *J. Biol. Chem.* **1998**, *273*, 35000–35007.
75. Ettenberg, S.A.; Magnifico, A.; Cuello, M.; Nau, M.M.; Rubinstein, Y.R.; Yarden, Y.; Weissman, A.M.; Lipkowitz, S. Cbl-b-dependent Coordinated Degradation of the Epidermal Growth Factor Receptor Signaling Complex. *J. Biol. Chem.* **2001**, *276*, 27677–27684. [CrossRef] [PubMed]
76. Alwan, H.A.J.; Van Zoelen, E.J.J.; Van Leeuwen, J.E.M. Ligand-induced lysosomal epidermal growth factor receptor (EGFR) degradation is preceded by proteasome-dependent EGFR de-ubiquitination. *J. Biol. Chem.* **2003**, *278*, 35781–35790. [CrossRef]
77. Mayle, K.M.; Le, A.M.; Kamei, D.T. The intracellular trafficking pathway of transferrin. *Biochim. Biophys. Acta (BBA)-Gen. Subj.* **2012**, *1820*, 264–281. [CrossRef] [PubMed]
78. Mesaki, K.; Tanabe, K.; Obayashi, M.; Oe, N.; Takei, K. Fission of tubular endosomes triggers endosomal acidification and movement. *PLoS ONE* **2011**, *6*, e19764. [CrossRef]
79. Jacomin, A.C.; Samavedam, S.; Promponas, V.; Nezis, I.P. iLIR database: A web resource for LIR motif-containing proteins in eukaryotes. *Autophagy* **2016**, *12*, 1945–1953. [CrossRef]
80. Kirkin, V.; Rogov, V.V. A Diversity of Selective Autophagy Receptors Determines the Specificity of the Autophagy Pathway. *Mol. Cell* **2019**, *76*, 268–285. [CrossRef]
81. Capuani, F.; Conte, A.; Argenzio, E.; Marchetti, L.; Priami, C.; Polo, S.; Di Fiore, P.P.; Sigismund, S.; Ciliberto, A. Quantitative analysis reveals how EGFR activation and downregulation are coupled in normal but not in cancer cells. *Nat. Commun.* **2015**, *6*, 7999. [CrossRef]
82. Freed, D.M.; Bessman, N.J.; Kiyatkin, A.; Salazar-Cavazos, E.; Byrne, P.O.; Moore, J.O.; Valley, C.C.; Ferguson, K.M.; Leahy, D.J.; Lidke, D.S.; et al. EGFR Ligands Differentially Stabilize Receptor Dimers to Specify Signaling Kinetics. *Cell* **2017**, *171*, 683–695. [CrossRef] [PubMed]
83. Mohrlüder, J.; Hoffmann, Y.; Stangler, T.; Hänel, K.; Willbold, D. Identification of clathrin heavy chain as a direct interaction partner for the γ-aminobutyric acid type A receptor associated protein. *Biochemistry* **2007**, *46*, 14537–14543. [CrossRef] [PubMed]
84. Caldieri, G.; Barbieri, E.; Nappo, G.; Raimondi, A.; Bonora, M.; Conte, A.; Verhoef, L.G.G.C.; Confalonieri, S.; Malabarba, M.G.; Bianchi, F.; et al. Reticulon 3-Dependent ER-PM contact sites control EGFR nonclathrin endocytosis. *Science* **2017**, *356*, 617–624. [CrossRef] [PubMed]
85. Grumati, P.; Morozzi, G.; Hölper, S.; Mari, M.; Harwardt, M.L.I.E.; Yan, R.; Müller, S.; Reggiori, F.; Heilemann, M.; Dikic, I. Full length RTN3 regulates turnover of tubular endoplasmic reticulum via selective autophagy. *Elife* **2017**, *6*, e25555. [CrossRef]
86. Sun, A.; Wei, J.; Childress, C.; Shaw, J.H.; Peng, K.; Shao, G.; Yang, W.; Lin, Q. The E3 ubiquitin ligase NEDD4 is an LC3-interactive protein and regulates autophagy. *Autophagy* **2017**, *13*, 522–537. [CrossRef]
87. Haglund, K.; Sigismund, S.; Polo, S.; Szymkiewicz, I.; Di Fiore, P.P.; Dikic, I. Multiple monoubiquitination of RTKs is sufficient for their endocytosis and degradation. *Nat. Cell Biol.* **2003**, *5*, 461–466. [CrossRef]
88. Critchley, W.; Pellet-Many, C.; Ringham-Terry, B.; Harrison, M.; Zachary, I.; Ponnambalam, S. Receptor Tyrosine Kinase Ubiquitination and De-Ubiquitination in Signal Transduction and Receptor Trafficking. *Cells* **2018**, *7*, 22. [CrossRef]
89. Lin, Q.; Wang, J.; Childress, C.; Sudol, M.; Carey, D.J.; Yang, W. HECT E3 Ubiquitin Ligase Nedd4-1 Ubiquitinates ACK and Regulates Epidermal Growth Factor (EGF)-Induced Degradation of EGF Receptor and ACK. *Mol. Cell. Biol.* **2010**, *30*, 1541–1554. [CrossRef]

90. Mohapatra, B.; Ahmad, G.; Nadeau, S.; Zutshi, N.; An, W.; Scheffe, S.; Dong, L.; Feng, D.; Goetz, B.; Arya, P.; et al. Protein tyrosine kinase regulation by ubiquitination: Critical roles of Cbl-family ubiquitin ligases. *Biochim. Biophys. Acta (BBA)-Mol. Cell Res.* **2013**, *1833*, 122–139. [CrossRef]
91. Huotari, J.; Meyer-Schaller, N.; Hubner, M.; Stauffer, S.; Katheder, N.; Horvath, P.; Mancini, R.; Helenius, A.; Peter, M. Cullin-3 regulates late endosome maturation. *Proc. Natl. Acad. Sci. USA* **2012**, *109*, 823–828. [CrossRef]
92. Genau, H.M.; Huber, J.; Baschieri, F.; Akutsu, M.; Dötsch, V.; Farhan, H.; Rogov, V.; Behrends, C. CUL3-KBTBD6/KBTBD7Ubiquitin Ligase Cooperates with GABARAP Proteins to Spatially Restrict TIAM1-RAC1 Signaling. *Mol. Cell* **2015**, *57*, 995–1010. [CrossRef] [PubMed]
93. Wandinger-Ness, A.; Zerial, M. Rab proteins and the compartmentalization of the endosomal system. *Cold Spring Harb. Perspect. Biol.* **2014**, *6*, a022616. [CrossRef] [PubMed]
94. Goueli, B.S.; Powell, M.; Finger, E.C.; Pfeffer, S.R. TBC1D16 is a Rab4A GTPase activating protein that regulates receptor recycling and EGF receptor signaling. *Proc. Natl. Acad. Sci. USA* **2012**, *109*, 15787–15792. [CrossRef] [PubMed]
95. Popovic, D.; Akutsu, M.; Novak, I.; Harper, J.W.; Behrends, C.; Dikic, I. Rab GTPase-Activating Proteins in Autophagy: Regulation of Endocytic and Autophagy Pathways by Direct Binding to Human ATG8 Modifiers. *Mol. Cell. Biol.* **2012**, *32*, 1733–1744. [CrossRef]
96. Nordmann, M.; Cabrera, M.; Perz, A.; Bröcker, C.; Ostrowicz, C.; Engelbrecht-Vandré, S.; Ungermann, C. The Mon1-Ccz1 complex is the GEF of the late endosomal Rab7 homolog Ypt7. *Curr. Biol.* **2010**, *20*, 1654–1659. [CrossRef]
97. Ieguchi, K.; Ueda, S.; Kataoka, T.; Satoh, T. Role of the guanine nucleotide exchange factor Ost in negative regulation of receptor endocytosis by the small GTPase Rac. *J. Biol. Chem.* **2007**, *282*, 23296–23305. [CrossRef]
98. Longva, K.E.; Blystad, F.D.; Stang, E.; Larsen, A.M.; Johannessen, L.E.; Madshus, I.H. Ubiquitination and proteasomal activity is required for transport of the EGF receptor to inner membranes of multivesicular bodies. *J. Cell Biol.* **2002**, *156*, 843–854. [CrossRef]
99. Luzio, J.P.; Pryor, P.R.; Bright, N.A. Lysosomes: Fusion and function. *Nat. Rev. Mol. Cell Biol.* **2007**, *8*, 622–632. [CrossRef]
100. Oksvold, M.P.; Skarpen, E.; Wierød, L.; Paulsen, R.E.; Huitfeldt, H.S. Re-localization of activated EGF receptor and its signal transducers to multivesicular compartments downstream of early endosomes in response to EGF. *Eur. J. Cell Biol.* **2001**, *80*, 285–294. [CrossRef]
101. McEwan, D.G.; Popovic, D.; Gubas, A.; Terawaki, S.; Suzuki, H.; Stadel, D.; Coxon, F.P.; MirandadeStegmann, D.; Bhogaraju, S.; Maddi, K.; et al. PLEKHM1 regulates autophagosome-lysosome fusion through HOPS complex and LC3/GABARAP proteins. *Mol. Cell* **2015**, *57*, 39–54. [CrossRef]
102. Ariotti, N.; Liang, H.; Xu, Y.; Zhang, Y.; Yonekubo, Y.; Inder, K.; Du, G.; Parton, R.G.; Hancock, J.F.; Plowman, S.J. Epidermal Growth Factor Receptor Activation Remodels the Plasma Membrane Lipid Environment To Induce Nanocluster Formation. *Mol. Cell. Biol.* **2010**, *30*, 3795–3804. [CrossRef] [PubMed]
103. Liang, S.I.; van Lengerich, B.; Eichel, K.; Cha, M.; Patterson, D.M.; Yoon, T.Y.; von Zastrow, M.; Jura, N.; Gartner, Z.J. Phosphorylated EGFR Dimers Are Not Sufficient to Activate Ras. *Cell Rep.* **2018**, *22*, 2593–2600. [CrossRef] [PubMed]
104. Needham, S.R.; Roberts, S.K.; Arkhipov, A.; Mysore, V.P.; Tynan, C.J.; Zanetti-Domingues, L.C.; Kim, E.T.; Losasso, V.; Korovesis, D.; Hirsch, M.; et al. EGFR oligomerization organizes kinase-active dimers into competent signalling platforms. *Nat. Commun.* **2016**, *7*, 13307. [CrossRef] [PubMed]
105. Heukers, R.; Vermeulen, J.F.; Fereidouni, F.; Bader, A.N.; Voortman, J.; Roovers, R.C.; Gerritsen, H.C.; Van Bergen En Henegouwen, P.M.P. Endocytosis of EGFR requires its kinase activity and N-terminal transmembrane dimerization motif. *J. Cell Sci.* **2013**, *126*, 4900–4912. [CrossRef] [PubMed]
106. Pacheco, V.; Ma, P.; Thielmann, Y.; Hartmann, R.; Weiergräber, O.H.; Mohrlüder, J.; Willbold, D. Assessment of GABARAP self-association by its diffusion properties. *J. Biomol. NMR* **2010**, *48*, 49–58. [CrossRef] [PubMed]
107. Saito, T.; Kuma, A.; Sugiura, Y.; Ichimura, Y.; Obata, M.; Kitamura, H.; Okuda, S.; Lee, H.C.; Ikeda, K.; Kanegae, Y.; et al. Autophagy regulates lipid metabolism through selective turnover of NCoR1. *Nat. Commun.* **2019**, *10*, 1567. [CrossRef]

108. Wei, Y.; Zou, Z.; Becker, N.; Anderson, M.; Sumpter, R.; Xiao, G.; Kinch, L.; Koduru, P.; Christudass, C.S.; Veltri, R.W.; et al. EGFR-Mediated Beclin 1 Phosphorylation in Autophagy Suppression, Tumor Progression, and Tumor Chemoresistance. *Cell* **2013**, *154*, 1269–1284. [CrossRef]
109. Winer, H.; Fraiberg, M.; Abada, A.; Dadosh, T.; Tamim-Yecheskel, B.C.; Elazar, Z. Autophagy differentially regulates TNF receptor Fn14 by distinct mammalian Atg8 proteins. *Nat. Commun.* **2018**, *9*, 3744. [CrossRef]

Supplemental Figures

Deficiency of GABARAP but not its paralogs causes enhanced EGF-induced EGFR degradation

Jochen Dobner[1], Indra M. Simons[1, 2], Kerstin Rufinatscha[3], Sebastian Hänsch [4], Melanie Schwarten[2], Oliver H. Weiergräber[2], Iman Abdollahzadeh[2, 5], Thomas Gensch[5], Johannes G. Bode[3], Silke Hoffmann[2], Dieter Willbold[1, 2]*

[1] Institut für Physikalische Biologie, Heinrich-Heine-Universität Düsseldorf, Universitätsstraße 1, 40225 Düsseldorf, Germany
[2] Institute of Biological Information Processing: Structural Biochemistry (IBI-7), Forschungszentrum Jülich, 52425 Jülich, Germany
[3] Department of Gastroenterology, Hepatology and Infectiology, University Hospital, Heinrich-Heine-Universität Düsseldorf, Moorenstraße 5, 40225 Düsseldorf, Germany
[4] Department of Biology, Center for Advanced Imaging (CAi), Heinrich-Heine-Universität Düsseldorf, Universitätsstraße 1, 40225 Düsseldorf, Germany
[5] Institute of Biological Information Processing – Molecular and Cell Physiology (IBI-1), Forschungszentrum Jülich, 52425 Jülich, Germany

Supplementary Figure S1 is related to Figures 1-8
Supplementary Figure S2 is related to Figure 1
Supplementary Figure S3 is related to Figure 5
Supplementary Figure S4 is related to Figure 7 and Movie S1
Supplementary Figure S5 is related to Figure 7 and Movie S2
Supplementary Figure S6 is related to Figures 1-4, 6, 8 and Figure S2
Supplementary Table S1 is related to Figures 1-8
Movie S1 is related to Figures 7 and S4
Movie S2 is related to Figures 7 and S5

Supplemental Figures S1 - 6, Table S1, Movies S1 - 2

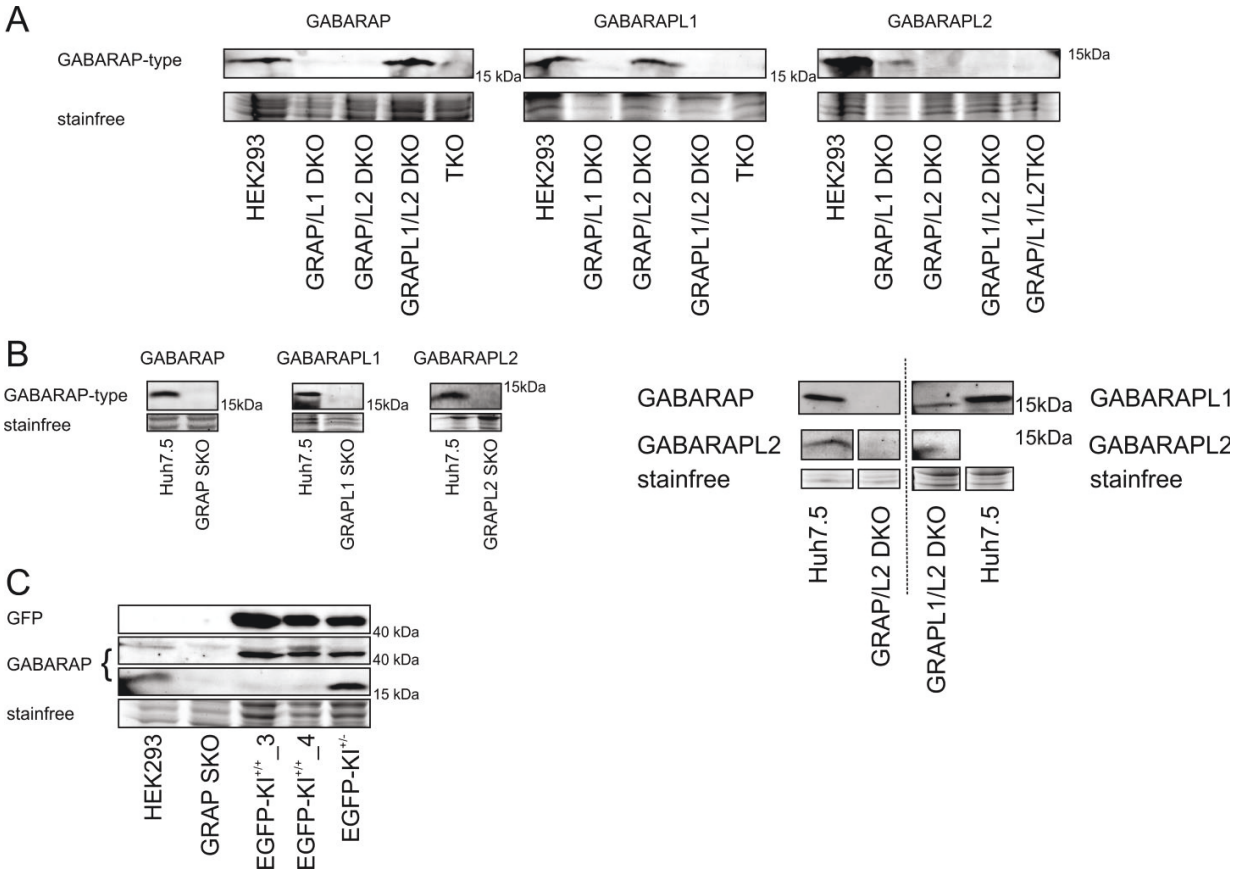

Figure S1: Verification of CRISPR/Cas9 knockout and knock-in cell lines on protein level.
Whole cell protein lysates were isolated and analyzed for presence of the indicated GABARAP subfamily member. (A) HEK293 based clonal KO cell lines. (B) Huh7.5 based clonal KO cell lines. (C) HEK293 based KI clonal lines. GRAP = GABARAP, GRAPL1 = GABARAPL1, GRAPL2 = GABARAPL2, TKO = GABARAP/L1/L2 TKO. SKO = single knockout, DKO = double knockout, TKO = triple knockout. Figure S7 G shows uncropped source blots

Table S1: CRISPR sequence details and genotyping results of the knockout cell lines used.

HEK293 GABARAP, GABARAPL1 and GABARAPL2 SKOs have already been published (Simons *et al.*, 2019).

Gene Symbol	Uniprot	GeneID/ Location	Targeting strategy	CRISPR gRNA (PAM)	Main clone	Unique Alleles	Mutation	Protein Impact
Huh7.5								
GABARAP	O95166	11337/NC_000017.11	first exon	GGATCTTCTCGCCCTCAGAG CGG	3	1	c.[152_153insT]	p.[fs*0]
GABARAPL1	Q9H0R8	23710/NC_000012.12	second exon	AGAGAAGGCTCCAAAAGCC AGGG	G5	3	c.[352_358_del];[353_356del];[154_355del]	p.[K38Gfs*9];[K38Gfs*11];[K38Sfs*3]
GABARAPL2	P60520	11345/NC_000016.1	second exon	TCCCACAGAACACAGATGCG TGG	F6	1	c.[179_180insT]	p.[C15Lfs*27]
GABARAP/L2 DKO	O95166	11337/NC_000017.11	first exon	GGATCTTCTCGCCCTCAGAG CGG	G8	2	c.[152_153insTT];[152_154insGG]	p.[E17Lfs*36];[E17Gfs*14]
	P60520	11345/NC_000016.1	second exon	TCCCACAGAACACAGATGCG TGG		2	c.[179_180insT];[179_180insTG]	p.[C15Lfs*27];[V16Afs*15]
GABARAPL1/L2 DKO	Q9H0R8	23710/NC_000012.12	second exon	AGAGAAGGCTCCAAAAGCC AGGG	F5	2	c.[354_355del];[355del]	p.[K38Nfs*3];[A39Pfs*10]
	P60520	11345/NC_000016.1	second exon	TCCCACAGAACACAGATGCG TGG		1	c.[179_180insT]	p.[C15Lfs*27]
HEK293								
GABARAP	O95166	11337/NC_000017.11	first exon	GGATCTTCTCGCCCTCAGAG CGG	C2	1	c.[152_153insT]	p.[fs*0]
GABARAPL1	Q9H0R8	23710/NC_000012.12	second exon	AGAGAAGGCTCCAAAAGCC AGGG	C10	2	c.[352_357del];[353_356]	p.[K38Tfs*10];[K38Nfs*3]

GABARAPL2	P60520	11345/NC_000016.1	second exon	TCCCACAGAACACAGATGCG<u>TGG</u>	#8	1	c.[179_180insT]	p.[C15Lfs*27]
GABARAP/L1 DKO	O95166	11337/NC_000017.11	first exon	GGATCTTCTCGCCCTCAGAG<u>CGG</u>	A11 (based on C10)	2	c.[152_153insT];[148_151del]	p.[fs*0];[K23Nfs*6]
GABARAP/L2 DKO	P60520	11345/NC_000016.1	second exon	TCCCACAGAACACAGATGCG<u>TGG</u>	#8 (based on C2)	1	c.[179_180insT]	p.[C15Lfs*27]
GABARAPL1/L2 DKO	P60520	11345/NC_000016.1	second exon	TCCCACAGAACACAGATGCG<u>TGG</u>	B3 (based on C10)	1	c.[179_180insT]	p.[C15Lfs*27]
GABARAP/L1/L2 TKO	O95166 P60520	11337/NC_000017.11 11345/NC_000016.1	first exon second exon	GGATCTTCTCGCCCTCAGAG<u>CGG</u> TCCCACAGAACACAGATGCG<u>TGG</u>	#3 (based on C10)	1 1	c.[152_153insT] c.[179_180insT]	p.[fs*0] p.[C15Lfs*27]
GABARAP	O95166	11337/NC_000017.11	first exon +linearized HDR plasmid	TACACGAACTTCATCCTCCC<u>GGG</u>	3	1	c.[ins717+21bpEGFP+linker]	p.[ins239+7aaEGFP+linker]

Formatting of indels detected in the knockout cell lines (Mutation column) and their resulting proteins (Protein impact column) is according to Human Genome Variation Society (http://varnomen.hgvs.org/). Mutation positions are determined in respect to the canonical isoform annotated in Uniprot, if more than one form exists. The numbers after the asterisks represent the number of amino acids present from the first amino acid changed to the next sequential stop codon. del, deletion; ins, insertion; c., coding DNA; p., protein; fs, frame shift; *, stop codon.

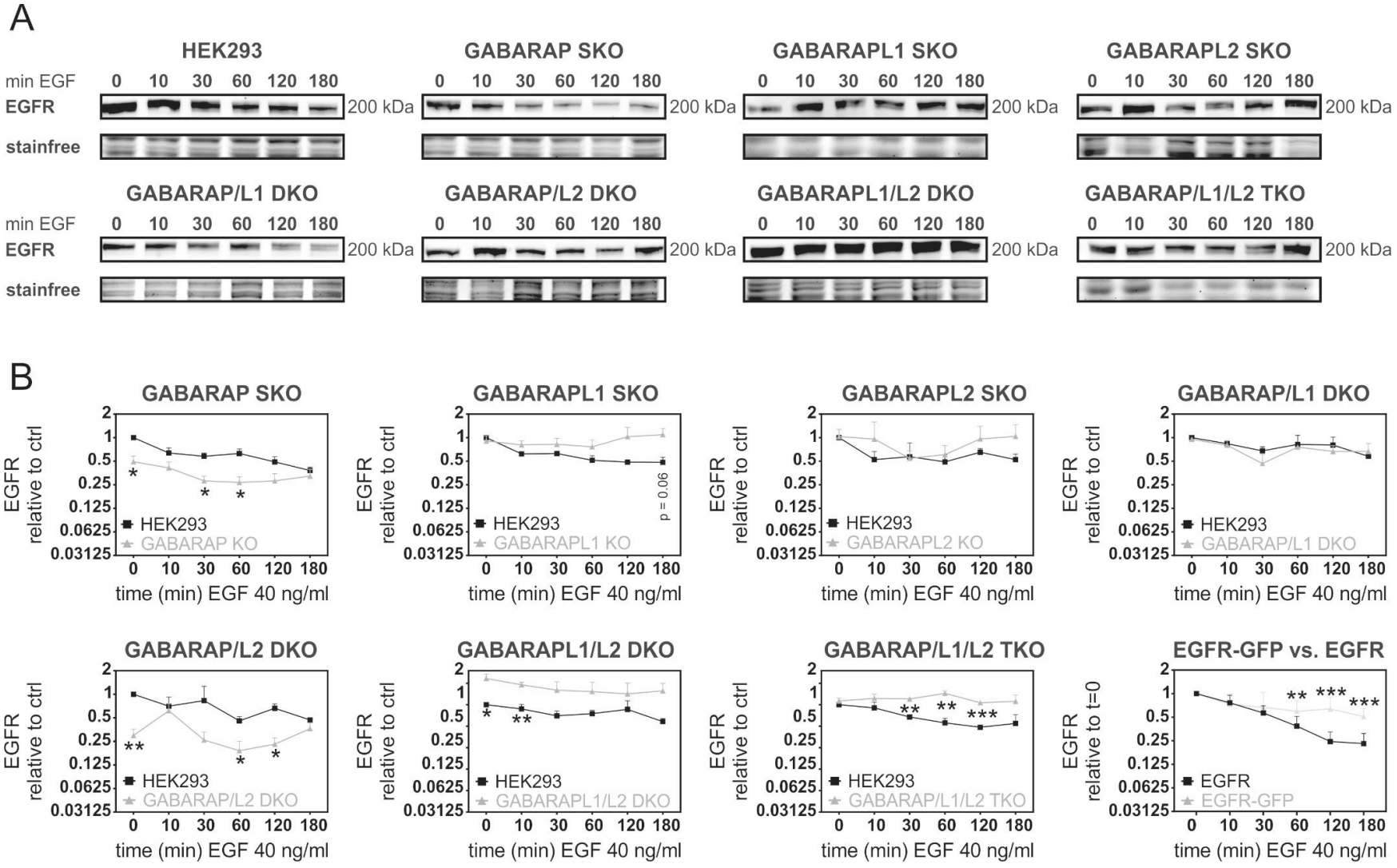

Figure S2: Total EGFR levels in response to EGF treatment in HEK293 KO cells transiently overexpressing EGFR-GFP.
(A) Cells were transfected with 2 µg EGFR-GFP expression plasmid and two days post transfection treated with 40 ng/ml EGF for the indicated time points. Afterwards, total EGFR protein levels in whole cell lysates were analyzed by immunoblot. Representative blots are shown for at least n = 3 independent experiments. (B) Densitometric analysis of at least n = 3 independent experiments. Controls are directly associated to each experiment. Kinetics of EGF-induced EGFR-GFP degradation in EGFR-GFP transfected HEK293 compared to endogenous EGFR degradation is shown (EGFR-GFP n = ≥ 23, EGFR n = 20). Quantification of EGFR(-GFP) protein levels was performed by normalization on stain-free loading control and calculated as percentage of HEK293 control cells at unstimulated conditions (t = 0). For comparison between EGFR-GFP overexpression and endogenous EGFR, kinetics of each level of EGFR expression (overexpression or endogenous) is displayed (t = 0 for each condition individually). Error bars represent standard error of means. Asterisks mark significant differences versus the corresponding time point of control cells and were calculated using independent t-test. $p \leq 0.05$ = *, $p \leq 0.01$ = **, $p \leq 0.001$ = ***. Respective wildtype controls were run on the same PAGE for each KO cell line and can be found in figure S7 H which also shows the uncropped source blots.

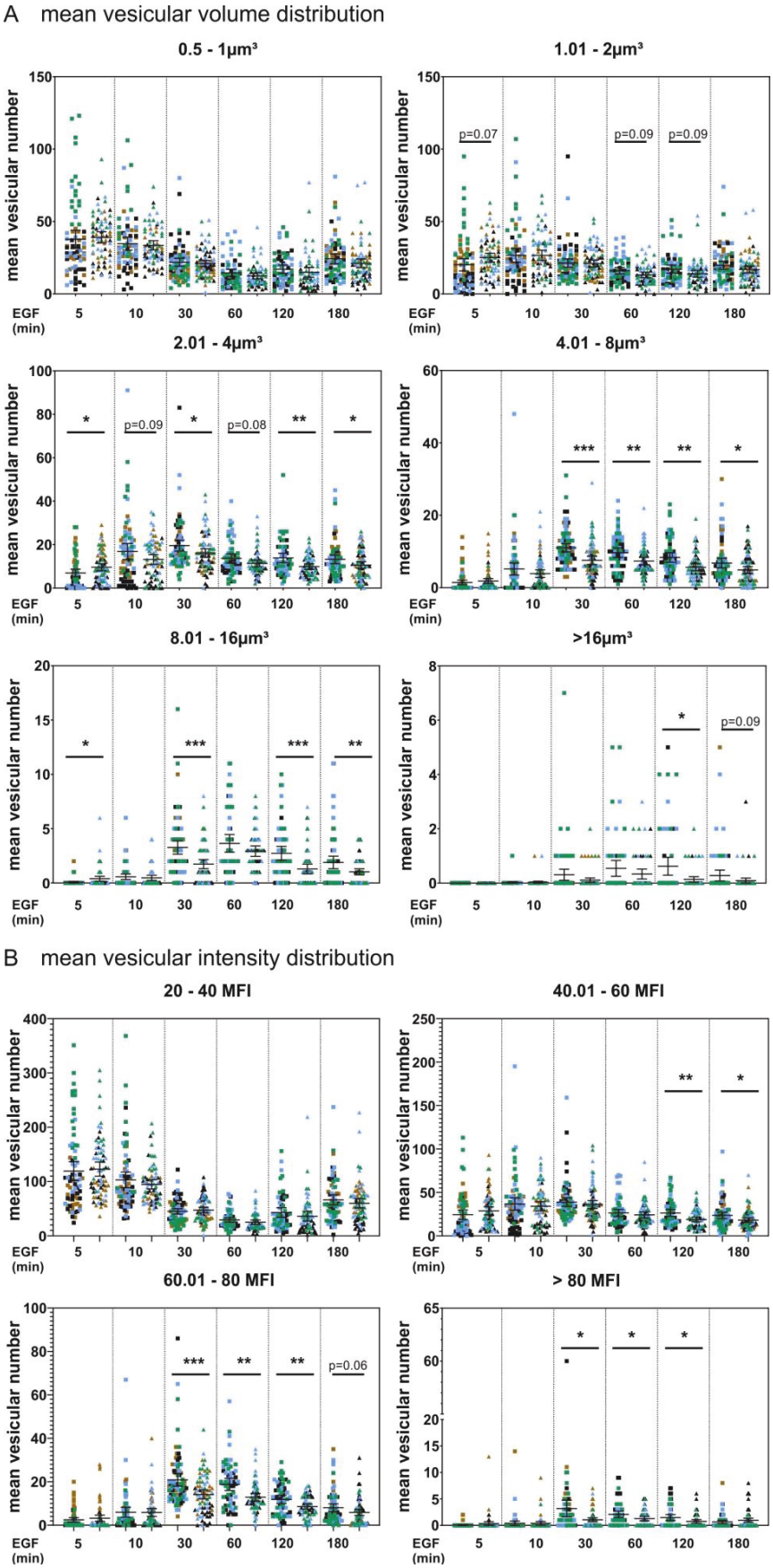
A mean vesicular volume distribution
0.5 - 1µm³
1.01 - 2µm³
2.01 - 4µm³
4.01 - 8µm³
8.01 - 16µm³
>16µm³
mean vesicular number
EGF (min)
5
10
30
60
120
180
p=0.07
p=0.09
p=0.08
p=0.06
B mean vesicular intensity distribution
20 - 40 MFI
40.01 - 60 MFI
60.01 - 80 MFI
> 80 MFI

C

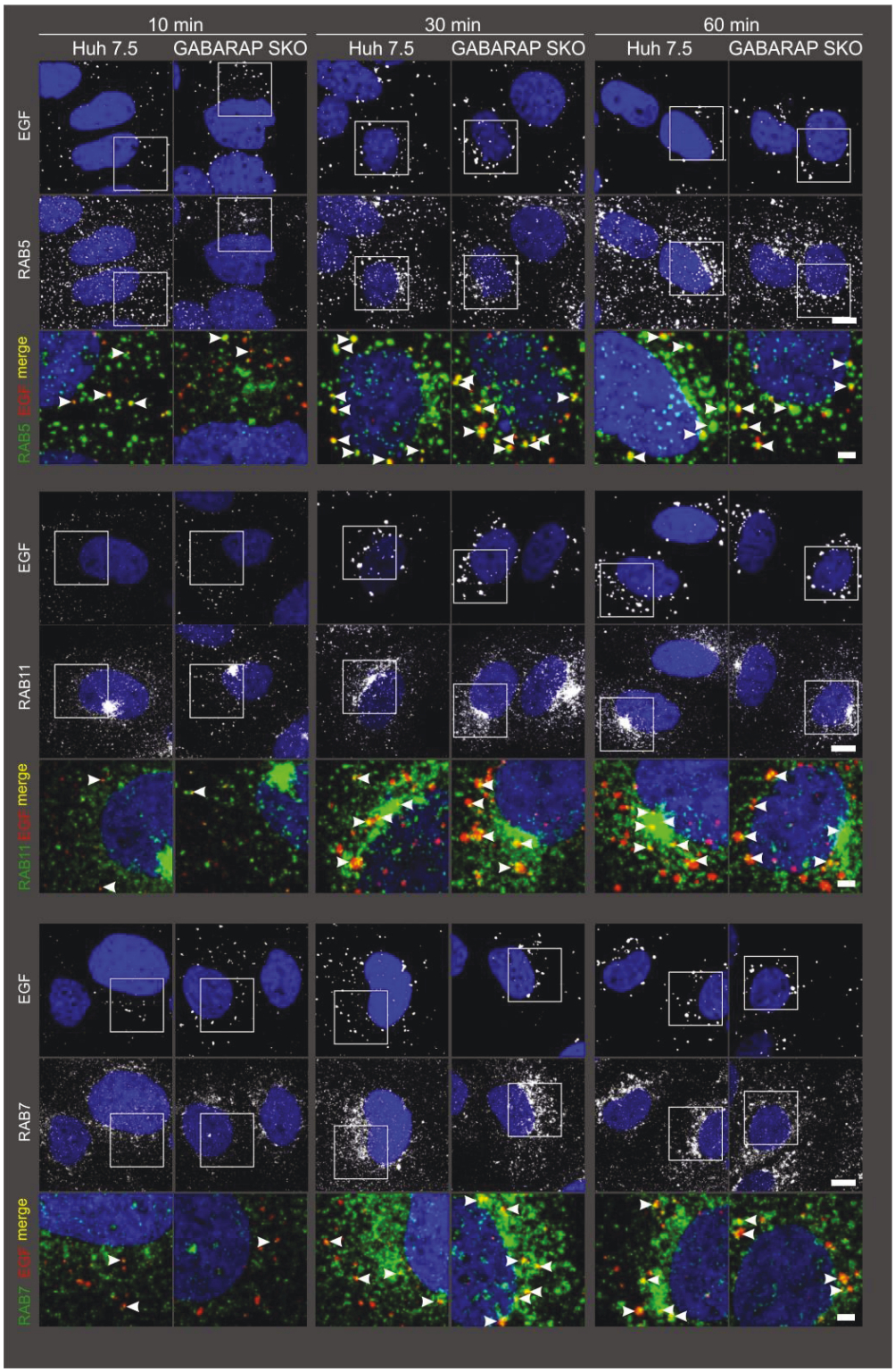

Figure S3: Analysis of EGF-Alexa647 containing vesicles of GABARAP SKO and Huh7.5 cells by Imaris and analysis of endosomal markers RAB 5, RAB11 and RAB7 in response to EGF treatment in GABARAP SKO and Huh7.5 control cells.

Vesicles of GABARAP SKO and Huh7.5 control cells which were treated with 40 ng/ml EGF-Alexa647 were modelled with Imaris imaging analysis software (described in detail in figure 5 and materials and methods section). (A) Mean vesicular volumes were largely unaffected by GABARAP-deficiency in GABARAP SKO cells although tendency for less vesicles with a diameter of 16 – 32 μm^3 was observable for GABARAP SKO cells after 30 min of treatment. Asterisks mark significant differences at indicated time points versus control cells as calculated using independent t-test. $p \leq 0.01$ = **. (B) Mean fluorescence intensities of EGF-Alexa647 positive vesicles classified into four arbitrary groups for GABARAP SKO and Huh7.5 control cells revealed significantly less vesicles with highest mean fluorescence intensities > 80 for GABARAP SKO cells compared to Huh7.5 control cells after 30 min of treatment. (B+C) Individual experiments are color-coded; > 50 cells per genotype and time point were analyzed. Error bars represent 95 % CI (C-E). Asterisks mark significant differences to the corresponding time point of control cells and were calculated using independent t-test. $p \leq 0.05$ = *, $p \leq 0.01$ = **, $p \leq 0.001$ = ***. (C) Huh7.5 and GABARAP SKO cells were pulse-treated with 40 ng/ml EGF-Alexa647 at 4 °C to allow binding to EGFR. After rigorous washing, cells were placed at 37 °C, fixed at distinct time points and stained for early (RAB5), recycling (RAB11) or late (RAB7) endosomes. All analyzed RAB proteins strongly accumulated within the first 30 min after EGF-Alexa647 pulse. Colocalization analysis of RAB proteins with EGF-Alexa647 (white arrowheads) revealed no alterations between GABARAP SKO and Huh7.5 control cells. MFI = mean fluorescence intensity Scale bar = 10 μm, scale bar zoom = 3 μm.

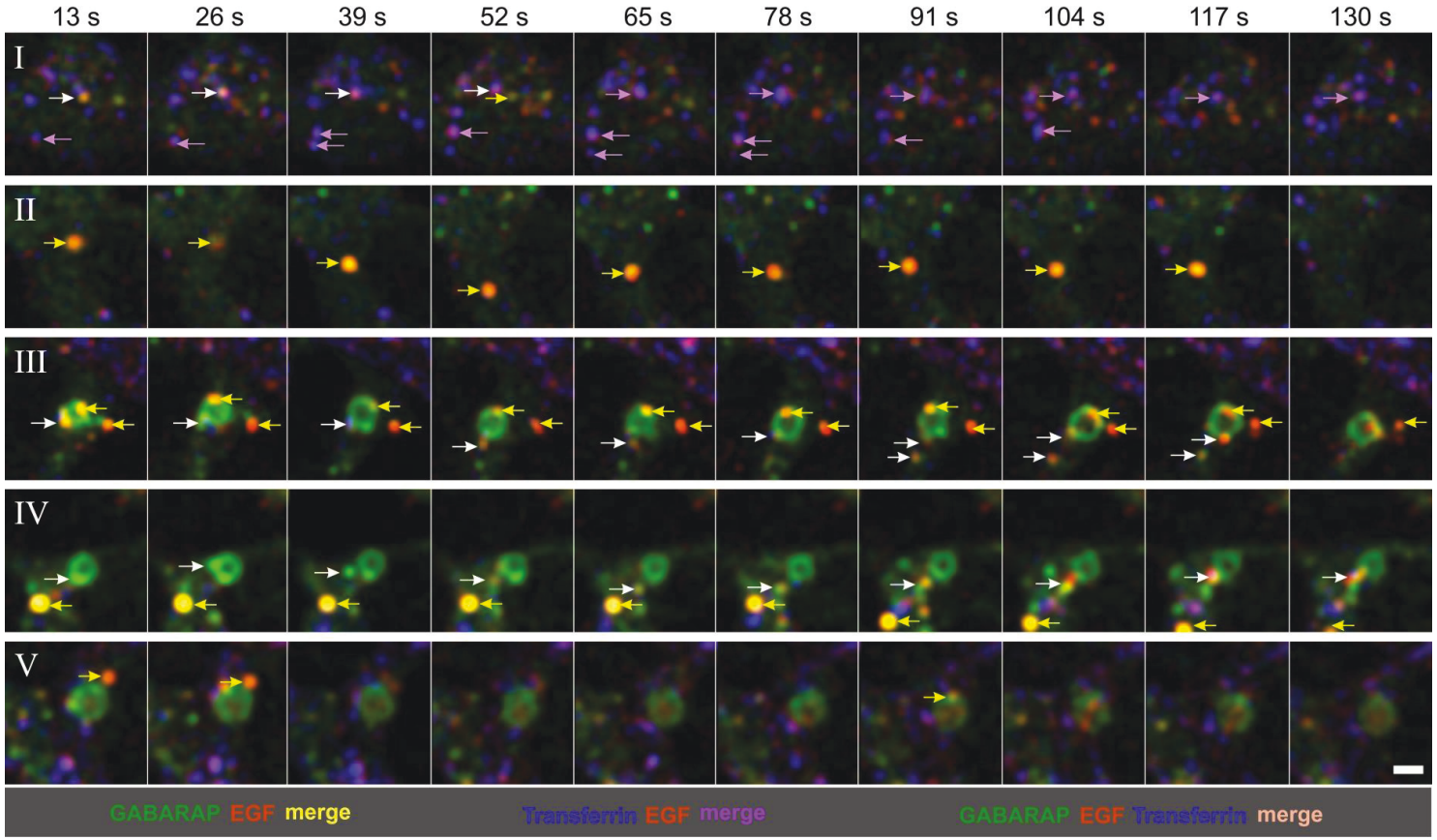

Figure S4: Montage of live cell imaging of HEK293 knock-in cells expressing GFP-GABARAP under the endogenous *GABARAP* promoter and stimulated with EGF-Alexa647 and Tf-Alexa555 by confocal laser scanning microscopy.

HEK293 GFP-GABARAP KI cells were simultaneously treated with 40 ng/ml EGF-Alexa647 and 20 ng/ml Tf-Alexa555 for 60 min and imaged under live-cell conditions by laser scanning microscopy. The montage shows snapshots of regions of interest I to V indicated in figure 7 A, covering a 117 s time frame. Images were taken at intervals of 13 s. Selected GABARAP/EGF positive signals are marked with yellow arrows, GABARAP/EGF/Tf positive structures with white arrows and EGF/Tf positive vesicles with magenta arrows. Video can be found under movie S1. Scale bar = 3 μm.

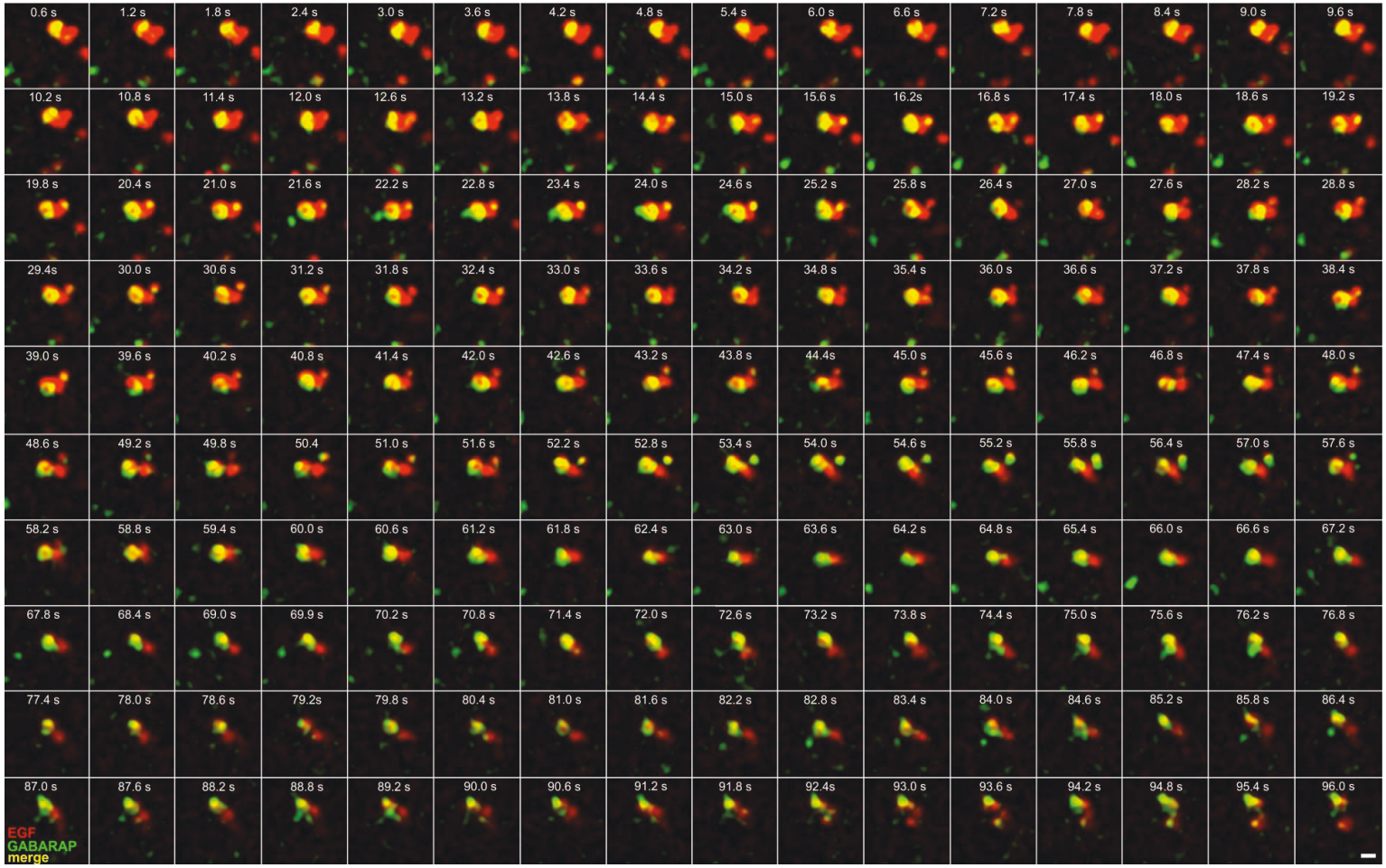

Figure S5: Live cell imaging of HEK293 KI cells expressing GFP-GABARAP under the endogenous *GABARAP* promoter and stimulated with EGF-Alexa647 by spinning disk confocal fluorescence microscopy.

HEK293 GFP-GABARAP KI cells were treated with 40 ng/ml EGF-Alexa647 for 60 min and imaged under live-cell conditions by spinning disk confocal fluorescence microscopy. The montage features selected time points for areas shown in figures 7 B to D. Dynamic vesicles which are GABARAP positive (green structures), EGF positive (red structures) or GABARAP/EGF double positive (yellow structures) are shown over a time course of 95.4 s with intervals of 0.6 s between images. GABARAP is shown in green and EGF in red. Video can be found under movie S2. Scale bar = 3μm.

A Source blots corresponding to figure 1

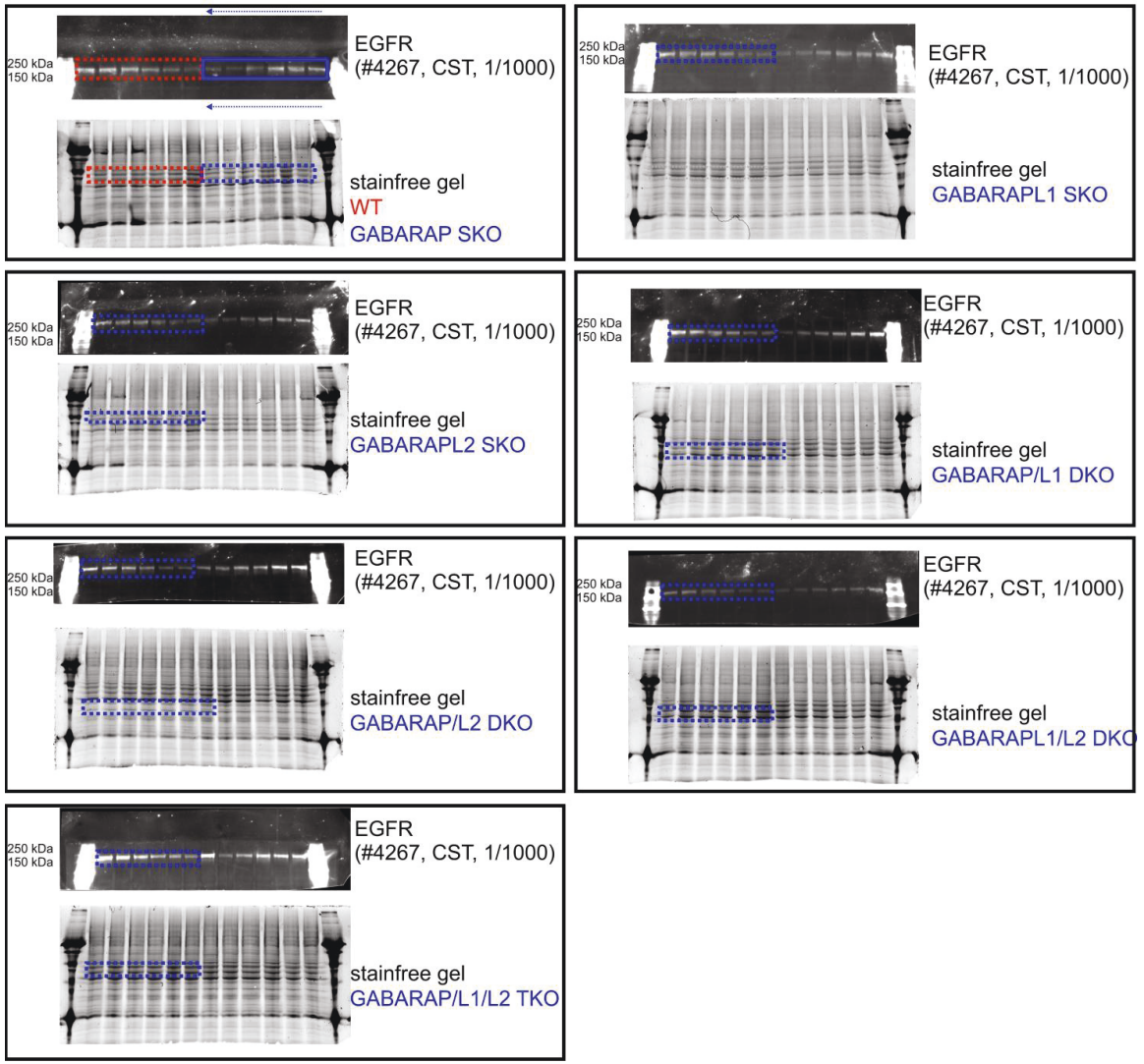

105

B Source blots corresponding to figure 2

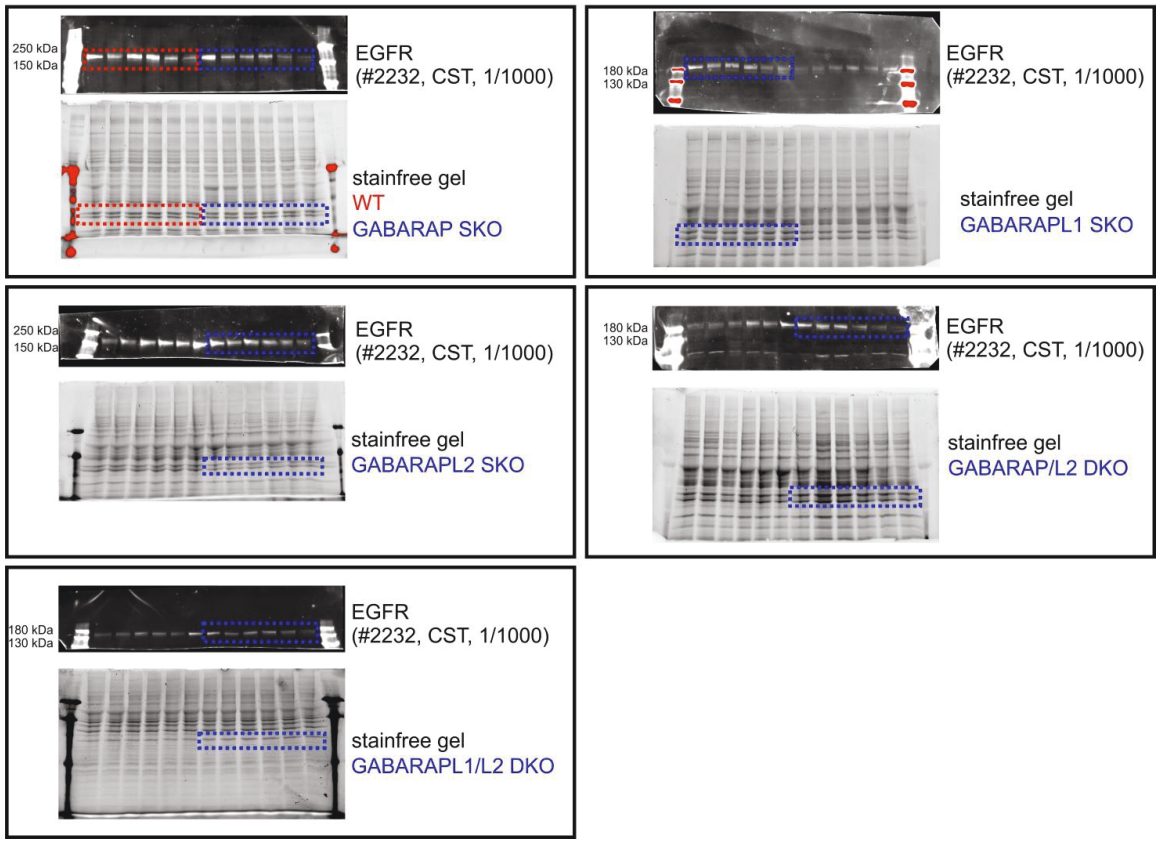

106

122

C Source blots corresponding to figure 3

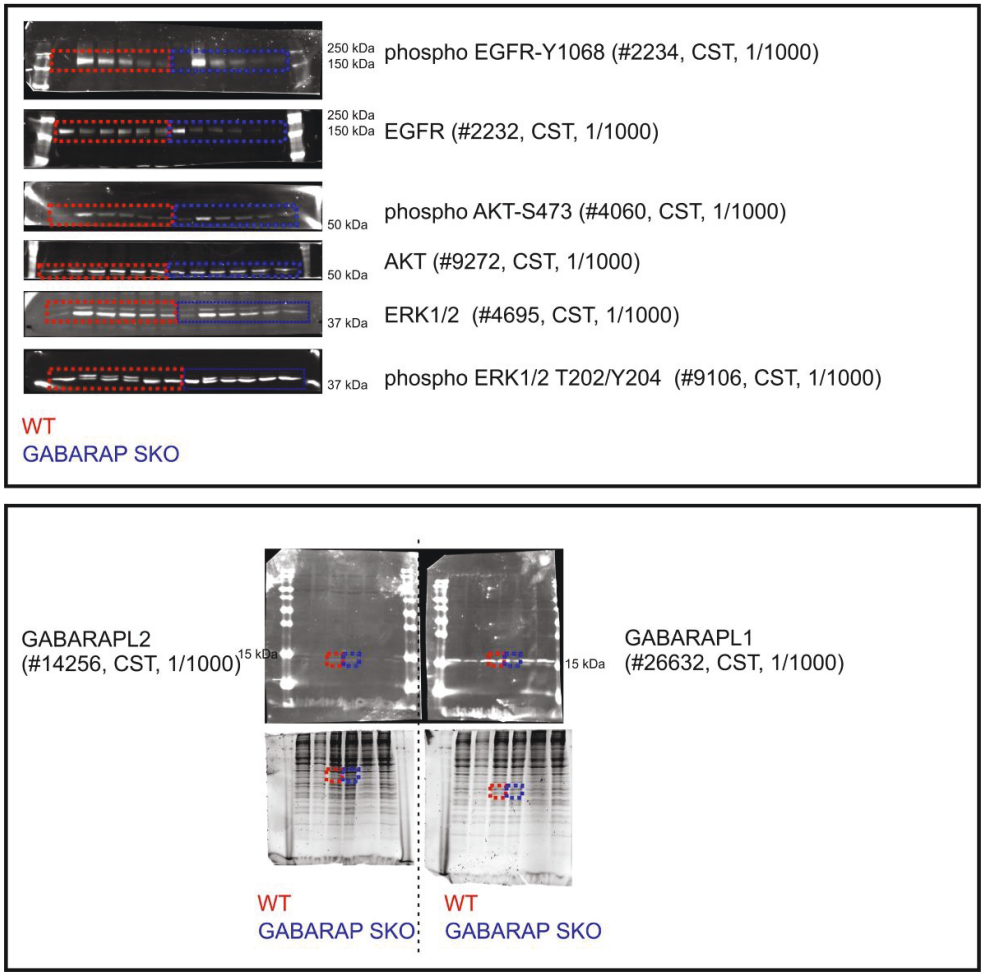

107

D Source blots corresponding to figure 4

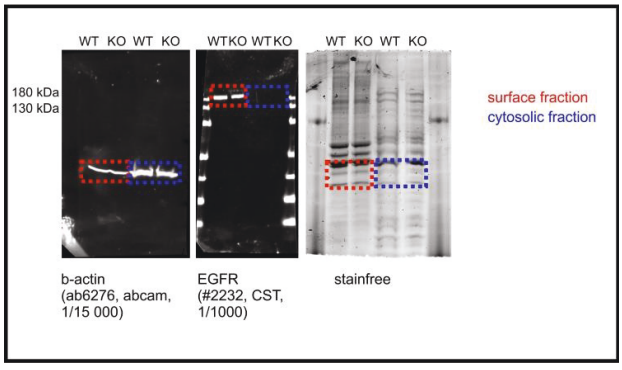

108

E Source blots corresponding to figure 6

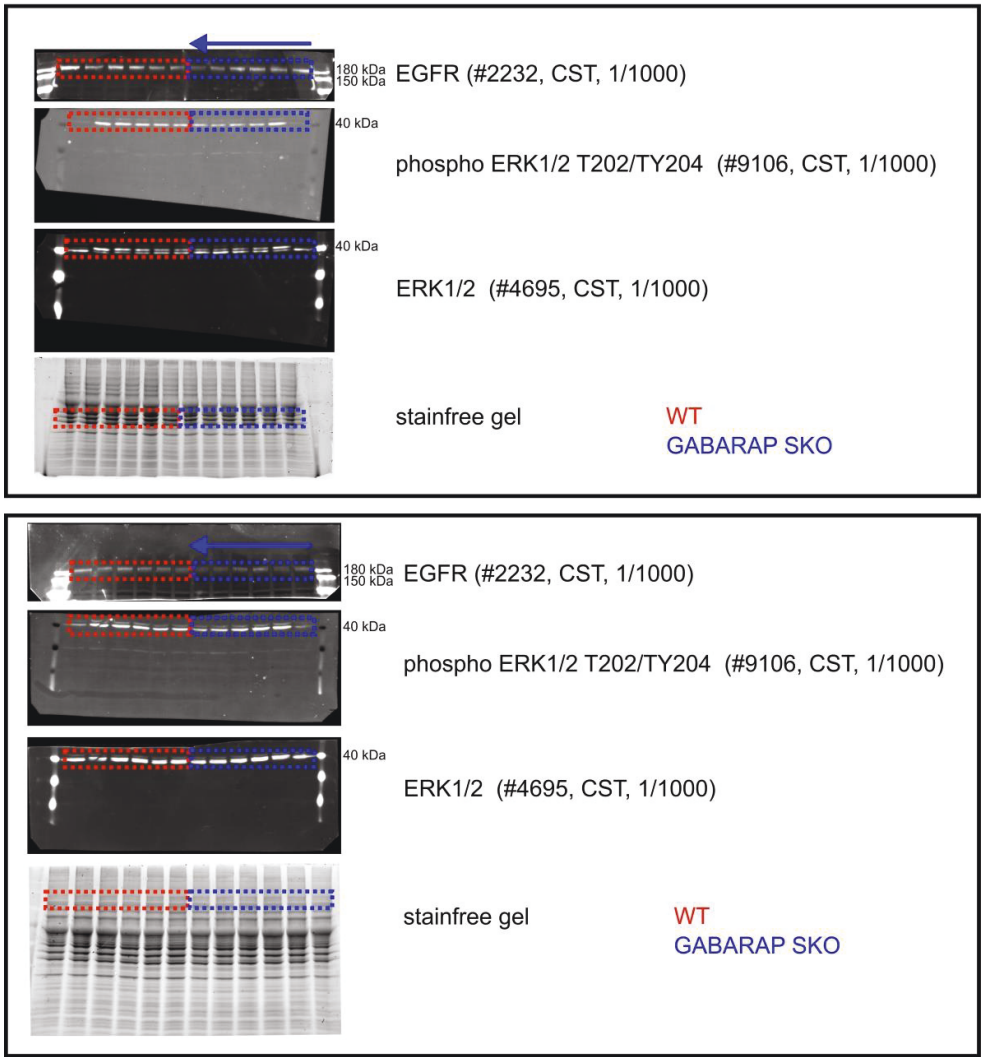

F Source blots corresponding to figure 8

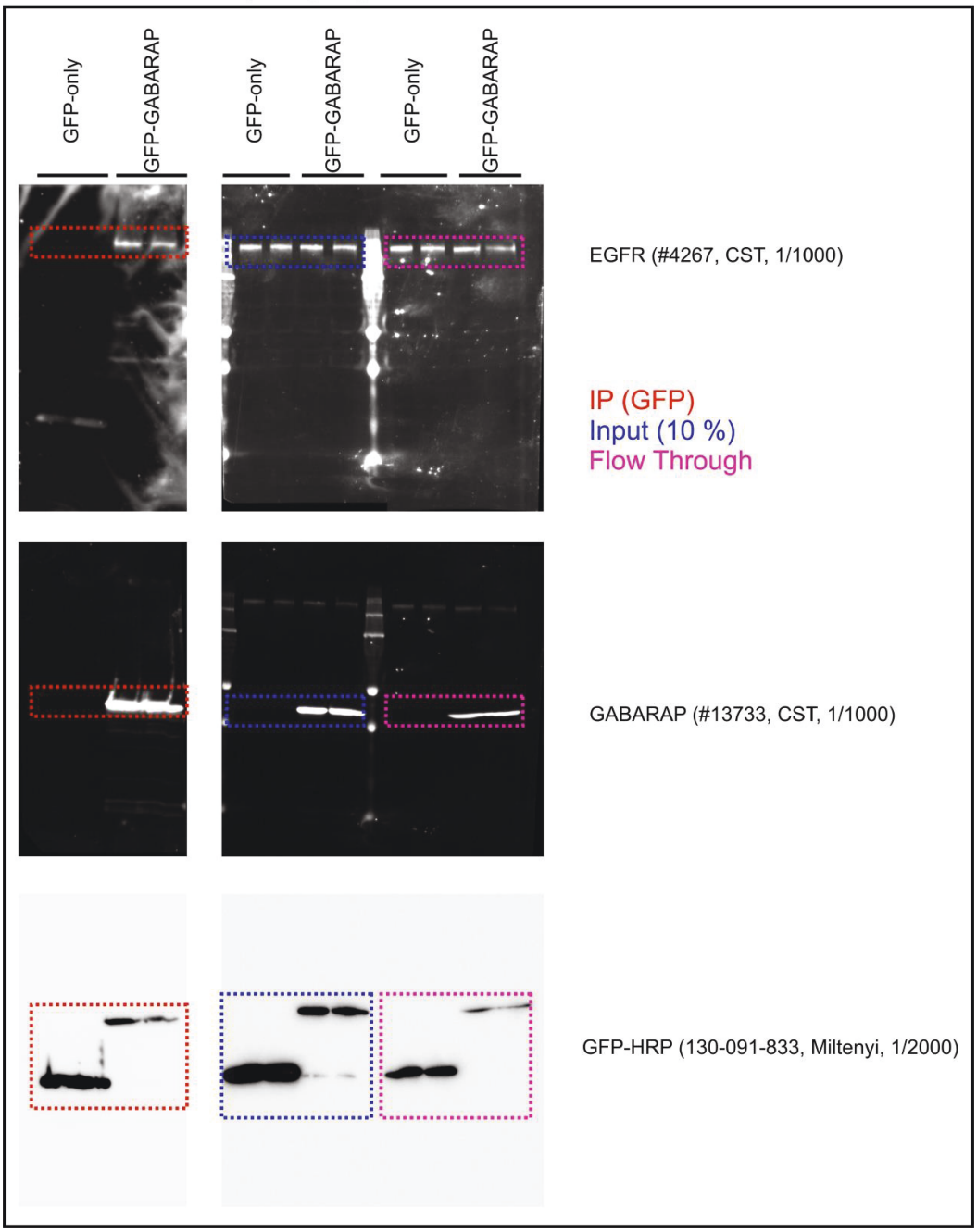

111

G Source blots corresponding to figure S1

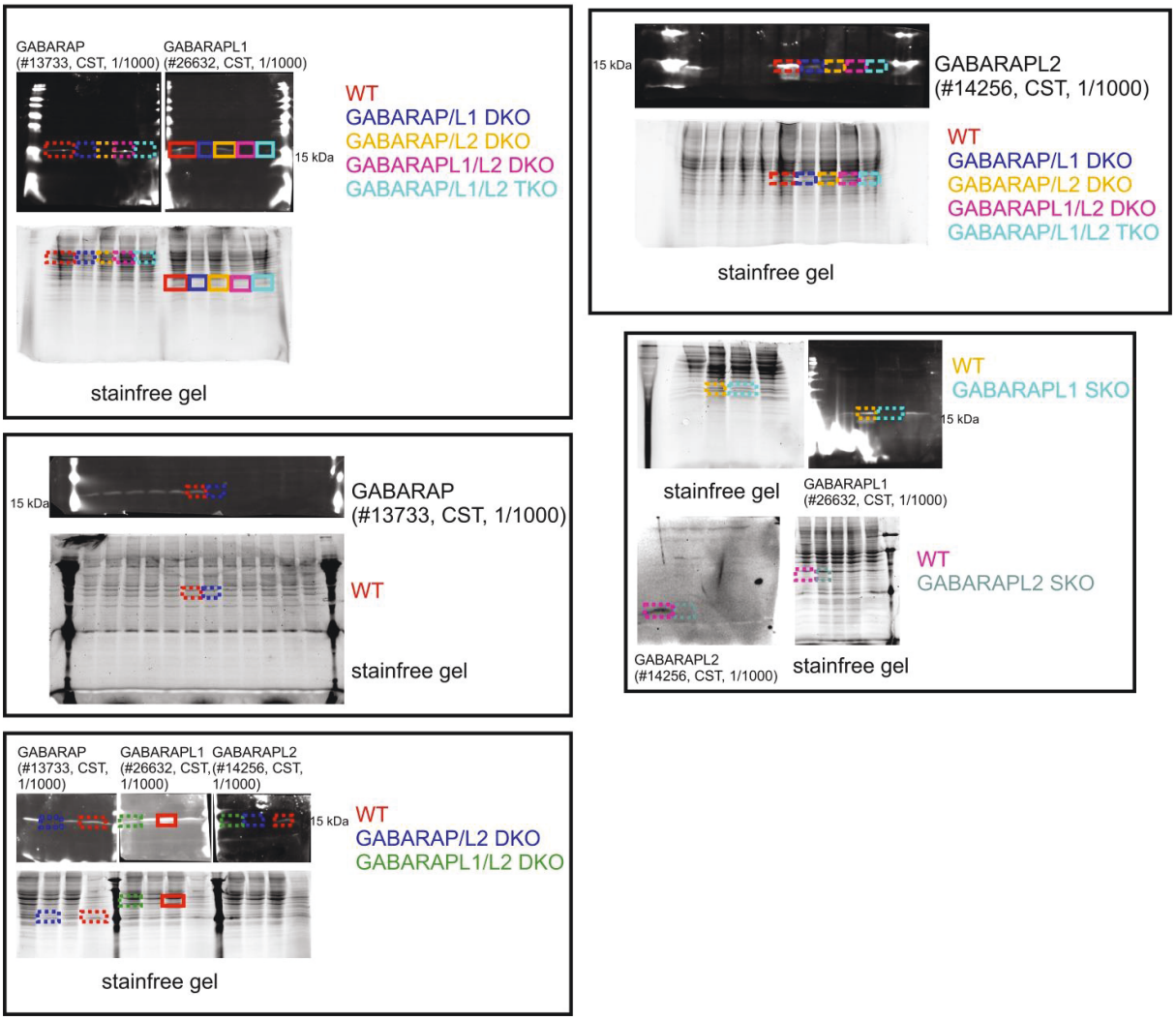

112

H Source blots corresponding to figure S2

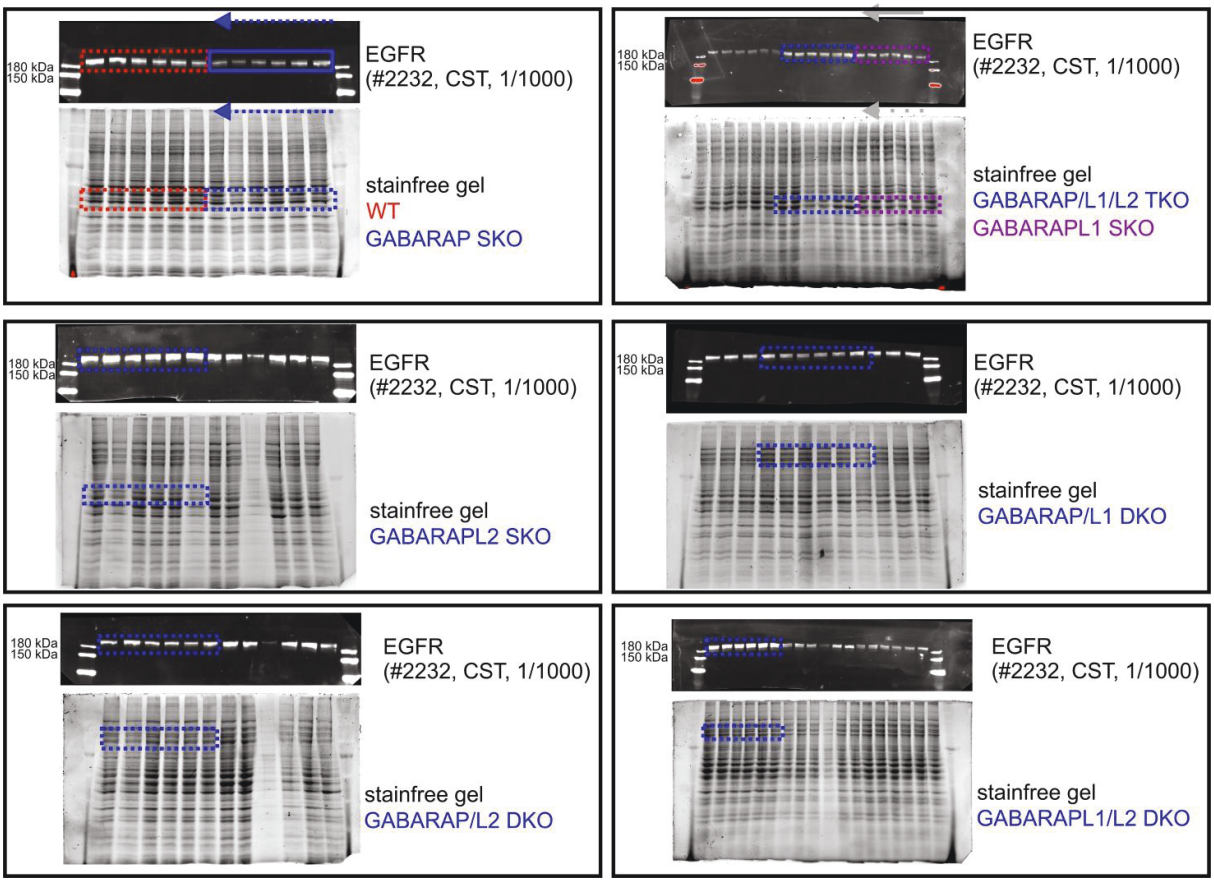

Figure S6: Uncropped source blots of immunoblotting experiments.

This figure contains the source blots corresponding to respective immunoblotting experiments as indicated. (A) Uncropped source blots corresponding to figure 1. (B) Uncropped source blots corresponding to figure 2. (C) Uncropped source blots corresponding to figure 3. (D) Uncropped source blots corresponding to figure 4. (E) Uncropped source blots corresponding to figure 6. (F) Uncropped source blots corresponding to figure 8. (G) Uncropped source blots corresponding to figure S1. (H) Uncropped source blots corresponding to figure S2. Used antibodies are indicated for each blot.

4 Weitere Ergebnisse

4.1 Klonierung von *Multicolor*-FACS CRISPR/Cas9-Vektoren zur Generierung von Einfach-, Doppel- und Dreifach-GABARAPs KO-Zelllinien

Um eine effiziente Genomeditierung unterschiedlicher Zelllinien und bestenfalls eine Ausschaltung von bis zu drei Genloci parallel zu erlangen, wurde in dieser Arbeit ein *multi-color fluorescence-activated cell sorting* (FACS)-taugliches Plasmidset von GABARAP-, GABARAPL1- und GABARAPL2-KO-Plasmiden etabliert (siehe 8.4). Dabei diente das *green fluorescent protein* (GFP)-GABARAP KO-Plasmid (mit *small guide ribonucleic acid* (sgRNA) gegen Exon 1, 2, 3) (siehe 9.1.1) als Ausgangsvektor für die in dieser Arbeit klonierten *cyan fluorescent protein* (CFP)-GABARAPL1- (mit sgRNA gegen Exon 2 und 3B) (siehe 8.4.3) und mCherry-GABARAPL2- (mit sgRNA gegen Exon 2A, 2B und 3) (siehe 8.4.4) Plasmidkonstrukte.

Durch Verwendung dreier in ihren Extinktions- und Emissionseigenschaften unterschiedlicher Proteine, wie EGFP ($488_{ex}/507_{em}$) [273; 274], ECFP ($434_{ex}/477_{em}$) [275-277] und mCherry ($587_{ex}/610_{em}$) [278] sollten Zellen, die erfolgreich mit entweder ein, zwei oder drei der KO-Plasmide transfiziert worden sind, mittels Fluoreszenz-basierter Sortierung (FACS) separiert werden können. Deswegen wurde in dieser Arbeit zunächst das in den KO-Plasmiden standardmäßig vorhandene EGFP im Falle der GABARAPL1-KO-Plasmide gegen ECFP (siehe 8.4.3) und im Falle der GABARAPL2-KO-Plasmide gegen mCherry substituiert (siehe 8.4.4).

Um das im PX458-Vektor (siehe 8.4) vorhandene EGFP gegen ECFP- bzw. mCherry-Fluoreszenzproteine austauschen zu können, wurde zunächst mittels *QuikChange*-PCR eine EGFP-flankierende XhoI-Schnittstelle eingebracht. Anschließend wurde ein synthetisches EGFP-Gen mit einer EGFP-flankierenden HindIII-Restriktionsschnittstelle designt und erfolgreich in das PX458-Vektorplasmid (siehe 8.4) kloniert.

Eine effiziente Klonierung der gewünschten ECFP-GABARAPL1- und mCherry-GABARAPL2-Plasmidkonstrukte gelang dadurch, dass die zuvor von Claudia Hoppen in das GFP-PX458-Grundgerüst eingebrachten sgRNAs (sgRNA gegen Exons aus den jeweiligen Plasmiden) durch Restriktionsverdau mit XbaI und NotI gewonnen und in die neu klonierten ECFP- bzw. mCherry-Plasmide eingebracht wurden. Letztendlich konnten die ECFP-

GABARAPL1- (mit sgRNA gegen Exon 2 und 3B) und mCherry-GABARAPL2- (mit sgRNA gegen Exon 2A, 2B und 3) Plasmidkonstrukte erfolgreich generiert wurden.

Aufgrund der verschiedenen Fluoreszenzen sollten Zellen, die z.B. positiv für alle drei Farben sind, und demnach Kandidaten für einen direkt erzeugten TKO für GABARAP, GABARAPL1 und GABARAPL2 darstellen, mittels FACS sortiert werden können (siehe Abbildung 4.1).

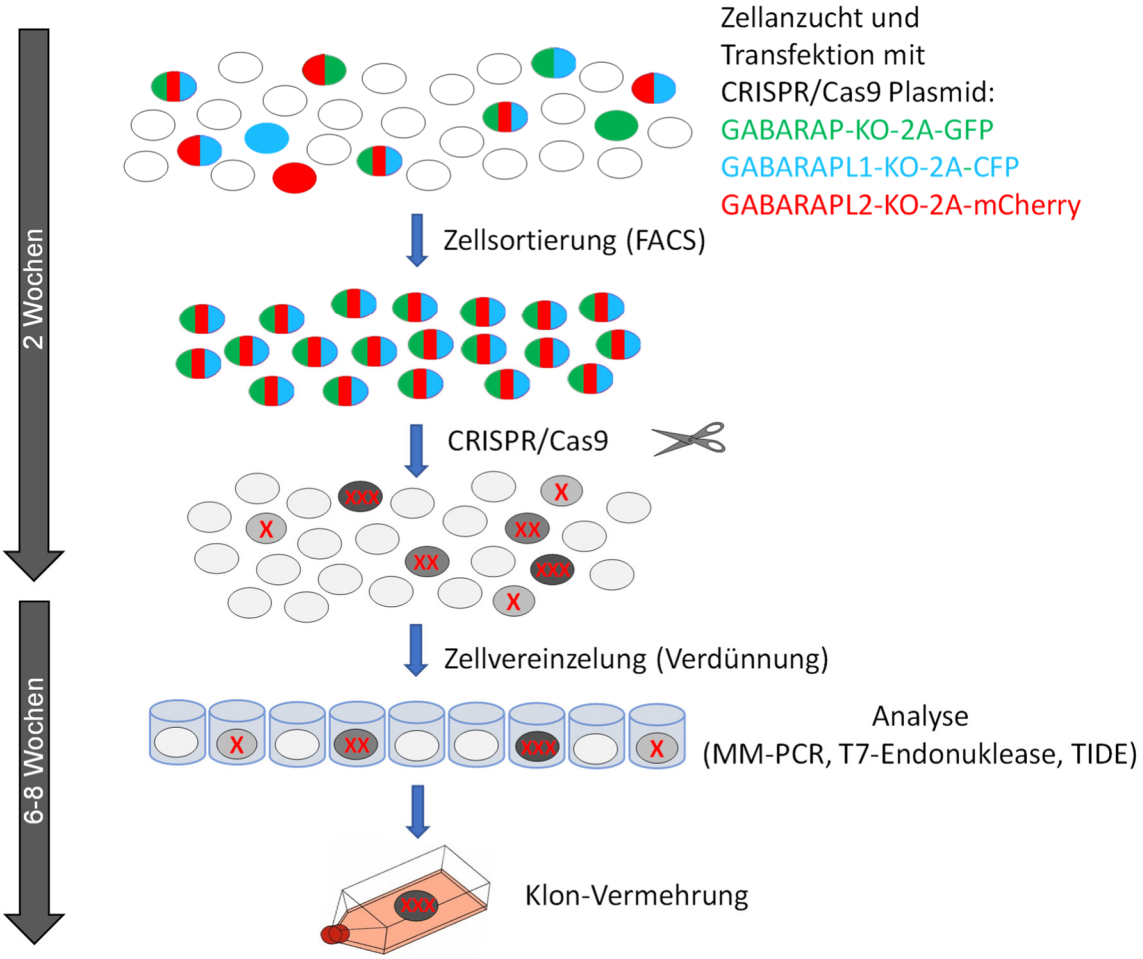

Abbildung 4.1: Schema der KO-Generierung mittels *Multicolor*-FACS
Bei der Transfektion mit drei verschiedenen Plasmiden, die jeweils ein anderes Fluoreszenzprotein exprimieren, kam es in den Zellen zu einer Mischkultur unterschiedlich transfizierter Zellen. Mit Hilfe der durchflusszytometrischen fluoreszenzbasierten Sortierung erfolgte eine Selektion und Vereinzelung der Zellen, die für alle drei Fluoreszenzfarbstoffe (GFP, CFP, mCherry) gleichzeitig positiv sind. Nach Regeneration und Vermehrung der vereinzelten Zellen wurden diese hinsichtlich einer erfolgten Genomeditierung mittels *mismatch*-PCR bzw. T7-Endonuklease Spaltungs-*Assay* analysiert und die Anzahl eingebrachter Insertionen und Deletionen (InDels) nach erfolgter Sequenzierung durch eine Software namens TIDE ermittelt.

Dies sollte eine erhebliche Zeitersparnis zur konventionellen TKO-Generierung erbringen, da hier jeder KO-Event sukzessiv erfolgt und somit dreimal eine klonale Linie propagiert werden muss (siehe Abbildung 1.7). Zu bedenken bleibt, dass farblich dreifach-positive Zellen nicht automatisch einen erfolgten Dreifach-KO anzeigen, da die

Genomeditierung trotz erfolgter Transfektion nur mit einer bestimmten Erfolgsrate und nicht zwingend gleichzeitig für alle drei Genloci und auf allen relevanten Chromosomen stattfindet. Eine Multi-Fluoreszenz-basierte Zellsortierung und -Vereinzelung würde jedoch erlauben nach farblich dreifach-positiven Zellen vorzuselektieren und so die Wahrscheinlichkeit erhöhen im anschließenden *Screening* Zellen mit den gewünschten Mehrfach-KOs identifizieren zu können.

Die Selektion der Zellen mittels FACS und weitere Generierung der KO-Zelllinien wurde anschließend von Jochen Dobner durchgeführt und validiert.

Die Zellen (z.B. HEK293 Flp-In T-REx) wurden mit jeweils einem EGFP-GABARAP, ECFP-GABARAPL1 und mCherry-GABARAPL2 CRISPR/Cas9 KO-Plasmid, das jeweils eine sgRNA-Sequenz gegen ein Exon enthielt, transfiziert (siehe Abbildung 4.1). Zuvor wurden die jeweiligen sgRNA-Sequenz-Effizienzen ermittelt und die sgRNA-Sequenz mit der höchsten Effizienz zur Transfektion verwendet.

Nach FACS-Sortierung der mit den drei Plasmiden (EGFP-GABARAP, ECFP-GABARAPL1 und mCherry-GABARAPL2) transfizierten Zellen konnte nach persönlicher Mitteilung eine Transfektionseffizienz von ca. 1,6 % erzielt werden, es zeigten also 1,6 % der Zellen eine Dreifachfärbung. Nach Transfektion der EGFP-GABARAP und mCherry-GABARAPL2 KO-Plasmide und anschließender FACS-basierten Sortierung konnte eine deutlich höhere Transfektionseffizienz von 11 % erreicht werden. Die Kombination von ECFP-GABARAPL1 und mCherry-GABARAPL2 KO-Plasmiden wie auch die alleinige Transfektion des ECFP-GABARAPL1 KO-Plasmids wiesen eine Transfektionseffizienz von unter 1 % auf.

4.2 Validierung von anti-GABARAP/-L1/-L2 Antikörpern

Zusätzlich zur erfolgreichen Validierung des anti-GABARAP (8H5) Antikörpers für IF [267] wurden parallel anti-GABARAPL1 (1C2) und anti-GABARAPL2 (1E5) Antikörper (siehe 1.2.2.1) aus Hybridomaüberständen für eine IF-Anwendung in parentalen HAP1-Zellen und HAP1 GABARAPL1 KO- bzw. GABARAPL2 KO-Zellen getestet. In allen untersuchten Zellen zeigte sich sowohl bei den parentalen als auch bei den jeweiligen HAP1 KO-Zellen eine deutliche Fluoreszenz-Färbung (Abbildung 4.2). Die Antikörper gegen GABARAPL1 und GABARAPL2 konnten somit nicht für IF-Färbungen genutzt werden, da für GABARAPL1 bzw. GABARAPL2 keine spezifische Färbung erzielt werden konnte.

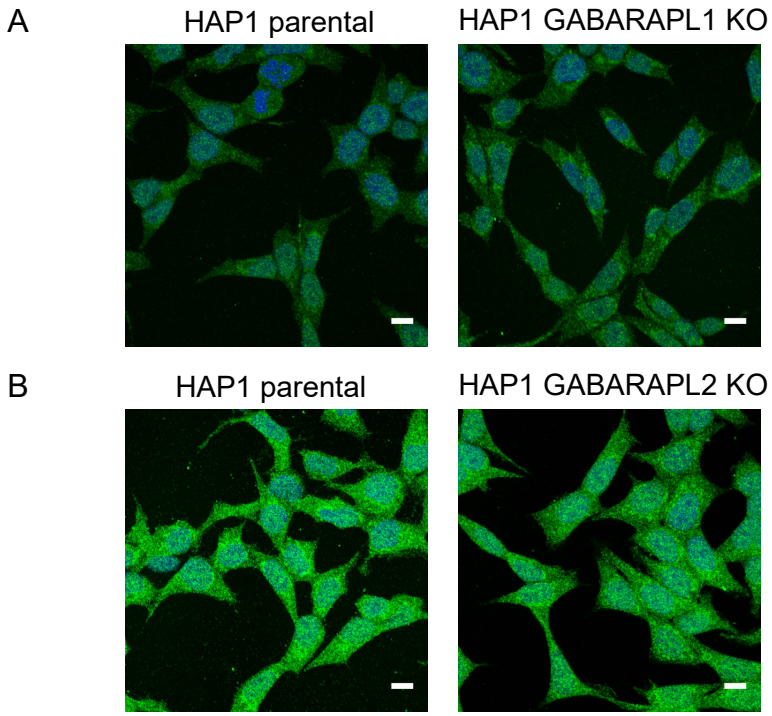

Abbildung 4.2: Testung der anti-GABARAPL1/-L2 Antikörper für IF-Färbungen.
HAP1 Zellen wurden mit 4 % Paraformaldehyd (PFA) fixiert, permeabilisiert, mit anti-GABARAPL1 (A) oder anti-GABARAPL2 Antikörper-haltigen Hybridomaüberständen 1 h bei Raumtemperatur inkubiert und anschließend 1 h mit einem anti-Ratte bzw. anti-Maus Alexa488 Sekundärantikörper inkubiert. Die Zellkerne wurden mit 4′,6-Diamidin-2-phenylindol (DAPI) gegengefärbt. Der *scale bar* entspricht 10 µm.

4.3 Kolokalisationsanalysen von endogenem GABARAP mit EGF(R) und den Endosomen-Markerproteinen Rab5, Rab7 und Rab11

Neben der Analyse eines putativ abweichenden Endozytose-Transportweges des EGFRs in GABARAP defizienten Zellen [145] wurde zudem die Kolokalisation von GABARAP mit Rab-Proteinen und EGF-gebundenen EGFR untersucht (Abbildung 4.3). Nach einem *pulse-chase* Experiment mit anschließender Fixierung und Färbung von Huh7.5 Zellen waren wenige GABARAP *puncta*, die mit Rab-Proteinen und/oder EGF-gebundenen EGFR kolokalisierten, erkennbar. Eine Kolokalisation des EGF(R)s mit Rab-Proteinen konnte hingegen oft beobachtet werden. Mit Hilfe der Software Imaris (Bitplan) wurde eine objektbasierte Kolokalisationsauswertung angestrebt, die jedoch nur für Rab5- und nicht für Rab7- und Rab11-gefärbte Zellen umsetzbar war. Da die meisten Kolokalisationen nach 30 und 60 Minuten beobachtet werden konnten, wurden diese Zeitpunkte für die Auswertung herangezogen.

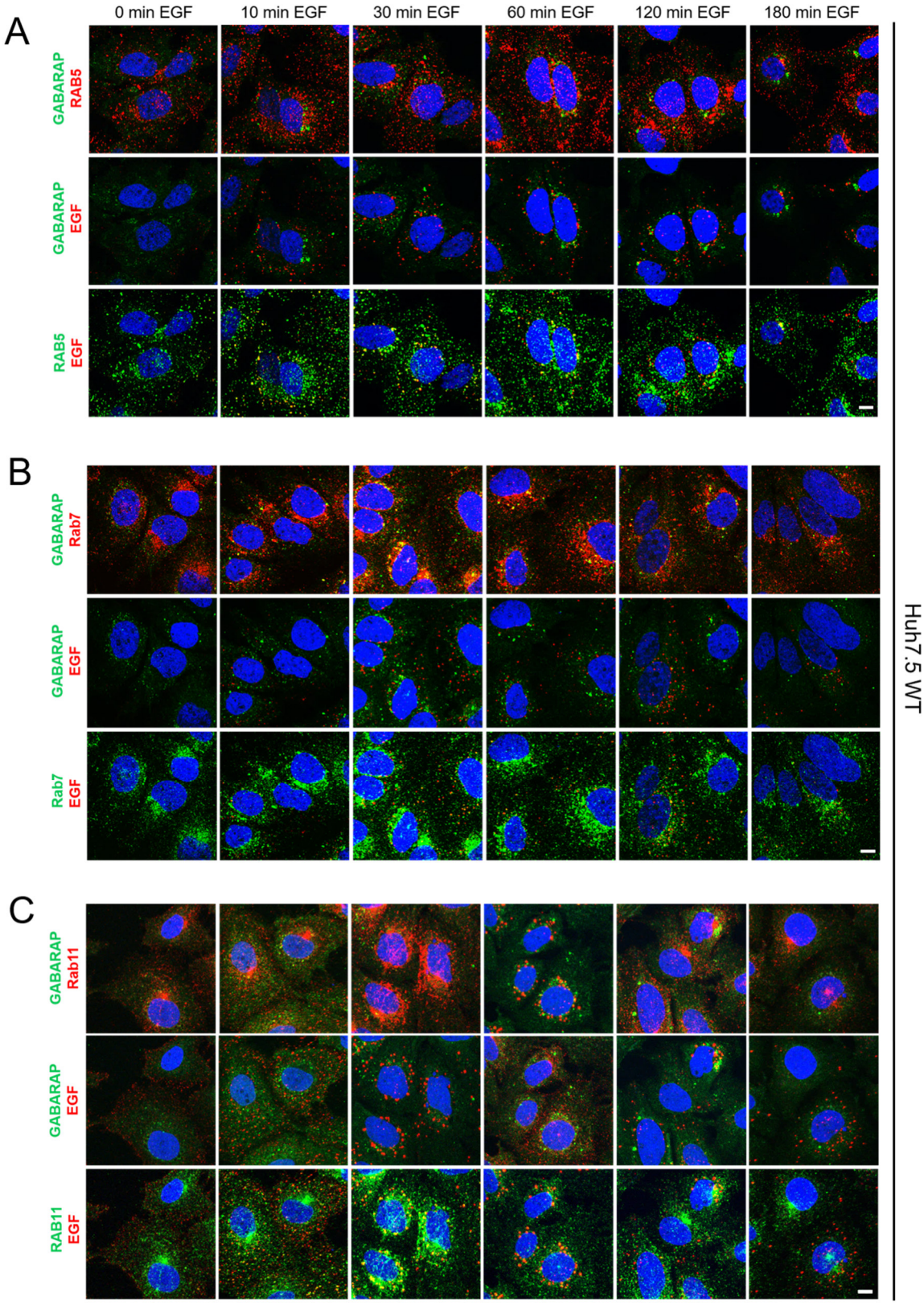

Abbildung 4.3: Kolokalisationsanalysen von GABARAP, EGF und Rab-Proteinen.
Huh7.5 Zellen wurden zunächst 10 Minuten auf Eis gestellt und anschließend eine Stunde bei 4 °C mit EGF-Alexa Fluor 647 vorinkubiert. Danach wurden die Zellen gewaschen und direkt mit 4 % PFA fixiert oder mit Vollmedium ohne EGF-Alexa Fluor 647 für 10, 30, 60, 120 oder 180 Minuten bei 37 °C inkubiert und entsprechend der jeweiligen Zeitpunkte fixiert und permeabilisiert. Die IF-Färbung erfolgte mit anti-GABARAP (8H5) und Rab5 (A), Rab7 (B) oder Rab11 (C) Antikörpern. Die Zellkerne wurden mit DAPI gegengefärbt. Der *scale bar* entspricht 10 µm.

Die Auswertung der Kolokalisationen von EGF mit Rab5 (EGF/Rab5) durch die objektbasierte Methode mittels Imaris zeigte 30 Minuten nach begonnener Rezeptorinternalisierung bei Betrachtung dreier Datensätze signifikant weniger EGF/Rab5 Kolokalisationen bei den GABARAP KO-Zellen (Abbildung 4.4 A).

Zusätzlich wurden andere Kolokalisationsauswertungsmethoden wie der *Pearson`s Correlation Coefficient* (PCC) und der *Mander`s Correlation Coefficient* (MCC) (M1, M2) zur Datenanalyse verwendet. Bei den Auswertungsmethoden PCC und MCC bedeutet ein Wert von 0 keine Korrelation und ein Wert von 1 eine vollständige Korrelation.

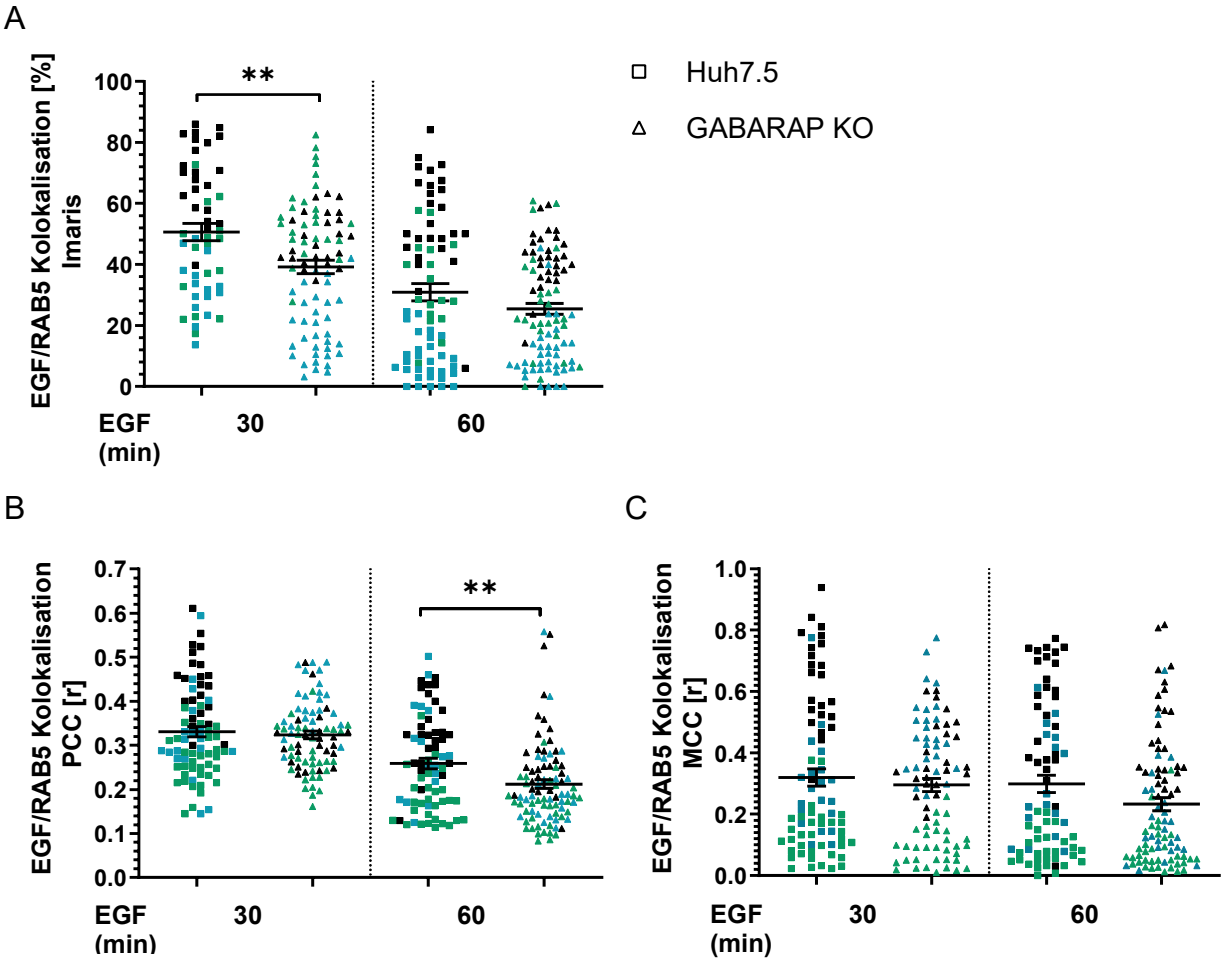

Abbildung 4.4: Diverse Auswertungsmethoden der EGF/Rab5-Kolokalisationen
Die Auswertung der EGF/Rab5-Kolokalisationen wurde mit drei verschiedenen Methoden durchgeführt: mit **(A)** einer objektbasierten Methode (Imaris), **(B)** dem *Pearson`s Correlation Coefficient* (PCC) und **(C)** dem *Mander`s Correlation Coefficient* M1+M2 (MCC). Gezeigt sind Mittelwerte ± *standard error of means* (SEM) von drei unabhängigen Experimenten, die jeweils farbcodiert sind. Es wurden > 15 Zellen pro Genotyp und Zeitpunkt analysiert. Die statistische Auswertung wurde mit einem *unpaired two-tailed* t-Test mit *Welch correction* durchgeführt (** $p \leq 0.01$).

Insgesamt lagen die Kolokalisationen bei der Auswertung mittels Imaris im Bereich von 30 bis 50 % bzw. nach Auswertung durch PCC (Abbildung 4.4 B) und MCC (Abbildung 4.4

C) bei einem Korrelationskoeffizienten zwischen 0,2 und 0,3, was einer partiellen Kolokalisation entspricht. Nach Auswertung mittels PCC konnte keine signifikante Reduktion der EGF/Rab5-Kolokalisationen in GABARAP-defizienten Zellen nachgewiesen werden. Bei der Auswertung der Datensätze durch PCC konnte bei den GABARAP KO-Zellen eine signifikante Reduktion der EGF/Rab5-Kolokalisationen bei einem Zeitpunkt von 60 Minuten beobachtet werden, wohingegen bei den Auswertungen mit Imaris und dem MCC eine tendentiell, jedoch nicht signifikant verminderte EGF/Rab5-Kolokalisation bei den GABARAP KO-Zellen nach 60 Minuten gezeigt werden konnte.

4.4 Material und Methoden

4.4.1 Klonierung von *Multicolor*-FACS CRISPR/Cas9-Vektoren zur Generierung von Einfach-, Doppel- und Dreifach-GABARAPs KO-Zelllinien

Das CRISPR/Cas9 KO-Plasmid pSpCas9(BB)-2A-GFP (PX458) (siehe 8.4) stammt aus dem Feng Zhang Labor [243]. Das sgRNA-Design der 20 Nukleotid (nt)-langen *target*-Sequenzen (siehe 8.2) zum gezielten Einbringen von Doppelstrangbrüchen unter Berücksichtigung der *on*- und *off-target*-Effekte und Einbringen der jeweiligen sgRNA-Sequenzen in das PX458-Plasmid erfolgte durch Claudia Hoppen mit Hilfe des *gUIDEbook gRNA Design for CRISPR genome editing* (Horizon Discovery Group, Cambridge, UK) Programms [259].

In dieser Arbeit wurde die EGFP-flankierende XhoI-Schnittstelle durch einen Basenaustausch (A6320C) mit einer *QuikChange*-PCR (siehe 8.1) unter Verwendung des Agilent *QuikChange* II XL Kit (Agilent, Santa Clara, USA) nach Herstellerangaben in das pSpCas9(BB)-2A-GFP (PX458)-Plasmid eingebracht. Die HindIII-Schnittstelle wurde neu in das Plasmid eingefügt. Dazu wurde ein 829 Basenpaar großes synthetische Gen mit der gegenläufigen EGFP-flankierenden HindIII-Restriktionsschnittstelle bei der Firma ThermoFisher Scientific/Invitrogen GeneArt (Waltham, MA, USA) synthetisiert (siehe Anhang 8.2). Das synthetische Gen wurde über die FseI- und XhoI-Restriktionsschnittstelle in das PX458-Vektorplasmid eingebracht.

Die Gensequenz für mCherry wurde mittels PCR aus dem pTRE3G-BI-mCherry Vektor (Clontech/TaKaRa, Catalog No. 631333, Kusatsu, Japan) mit einer HindIII (*forward*)- und XhoI (*reverse*)-Schnittstelle (siehe 8.1) synthetisiert.

Die Gensequenz für ECFP wurde aus dem pECFP-C1-Vektorplasmid (Clontech/TaKaRa, Catalog No. 6076-1, Kusatsu, Japan) ebenfalls mit den entsprechenden flankierenden HindIII- und XhoI-Schnittstellen mittels PCR synthetisiert.

Die Sequenzen für ECFP (siehe 8.4.3) und mCherry (siehe 8.4.4) wurden nach Ausschneiden der vorhandenen EGFP-Sequenz (XhoI/HindIII) an die Position des EGFPs über die XhoI- und HindIII-Schnittstellen in den PX458-Vektor eingebracht.

4.4.2 IF-Färbungen mittels anti-GABARAPL1/-L2 Antikörpern

Für die Immunfluoreszenz (IF)-Färbung wurden die zuvor mit 4 % Paraformaldehyd (PFA) fixierten Zellen für 30 min mit 0,2 % Triton X-100/ *phosphate-buffered saline* (PBS)-Lösung bei Raumtemperatur (RT) unter Schwenken inkubiert. Danach wurden die Zellen für 1 h mit 1 % bovinem Serumalbumin (BSA, Sigma-Aldrich, St. Louis, USA) bei RT unter Schwenken oder über Nacht bei 4-8 °C inkubiert. Die IF erfolgte durch Zugabe von 1 mL unverdünntem Ratte-anti-GABARAPL1 (1C2) bzw. Maus-anti-GABARAPL2 (1E5) Antikörper haltigem Hybridoma-Überstand. Die Zellen wurden für 1 h unter Schwenken bei RT mit dem jeweiligen Antikörper inkubiert. Anschließend wurden die Zellen dreimal 5 min mit 1 x PBS gewaschen und danach für 1 h abgedunkelt bei RT unter Schwenken mit dem jeweiligen 1:250-verdünnten fluoreszenzmarkierten anti-Ratte Alexa Fluor 488 (Jackson ImmunoResearch, 112-545-068, West Grove, USA) bzw. anti-Maus Alexa Fluor 488 (abcam, ab150117, Cambridge, UK) Antikörper inkubiert. Danach wurden die Zellen zweimal 5 min mit 1 x PBS unter Schwenken gewaschen, 10 min mit 4′,6-Diamidin-2-phenylindol (DAPI, Sigma-Aldrich, St. Louis, USA) bei RT inkubiert und zweimal 5 min mit 1 x PBS gewaschen. Die Zellen wurden anschließend mikroskopiert oder in PBS mit 0,05 % Natriumazid gelagert.

4.4.3 EGF *pulse-chase assay* und IF-Färbungen

Für den Pulsmarkierungsversuch (*pulse-chase assay*) zur Verfolgung der Aufnahme von fluoreszenzmarkiertem EGF wurden 2 x 10^5 Huh7.5 Zellen auf einem mit Fibronektin (F1141, Sigma-Aldrich, St. Louis, USA) beschichteten Glasboden einer µ-Schale (81158, ibidi, Martinsried, Germany) in *Dulbecco's Modified Eagle's Medium* (DMEM - D5796, Sigma-Aldrich, St. Louis, USA), supplementiert mit 10 % *fetal calf serum* (FCS) (F9665, Sigma-Aldrich, St. Louis, USA) und 1 % *Minimum Essential Medium with non-essential amino acids* (MEM NEAA, 11140-035, Gibco, ThermoFisher Scientific, Waltham, MA, USA), ausgesät. Am nächsten Tag wurden die Huh7.5 für 10 min auf Eis vorgekühlt. Anschließend wurde das Medium durch kaltes DMEM (Vollmedium: 10 % FCS/1 % MEM NEAA) mit dem Zusatz von 40 ng/mL biotinyliertem EGF, welches an Alexa Fluor 647-Streptavidin komplexiert ist (E35351, ThermoFisher Scientific, Waltham, MA, USA), ersetzt. Nach einer Stunde Vorinkubation der Zellen mit EGF-Alexa Fluor 647 bei 4-8 °C wurden die Zellen entweder direkt mit kaltem Wasch-Puffer mit einem hohen Salzgehalt und niedrigem pH-Wert (0,2 M Natriumacetat und 0,5 M NaCl bei pH 4,5) vorsichtig gewaschen (0 min-Wert) oder es wurde

frisches DMEM-Vollmedium hinzugegeben und die Zellen wurden für 5 min, 10 min, 30 min, 60 min, 120 min oder 180 min bei 37 °C und 5 % CO_2 inkubiert. Nach jedem Inkubations-Endzeitpunkt wurden die Zellen mit dem bereits erwähnten kalten Wasch-Puffer gewaschen, für 10 min mit 4 % PFA bei RT unter Schwenken fixiert und anschließend zweimal für 5 min mit verdünnter, phosphatgepufferter Kochsalzlösung (1 x PBS) gewaschen.

Für die IF-Färbung wurden die zuvor fixierten Zellen für 30 min mit 0,2 % Triton X-100/PBS-Lösung bei RT unter Schwenken inkubiert. Danach wurden die Zellen für 1 h mit 1 % bovinen Serumalbumin (BSA, Sigma-Aldrich, St. Louis, USA) bei RT unter Schwenken oder über Nacht bei 4-8 °C inkubiert.

Die IF erfolgte durch Zugabe von 1 mL unverdünntem anti-GABARAP (8H5) Antikörper-haltigen Hybridoma-Überstand [267] zusammen mit monoklonalem Kaninchen anti-Rab5 (Klon C8B1, 3547S, Cell Signaling Technologies, Danvers, MA, USA), anti-Rab7 (Klon D95F2, 9367S, Cell Signaling Technologies, Danvers, MA, USA) oder anti-Rab11 (Klon D4F5, 5589S, Cell Signaling Technologies, Danvers, MA, USA) Antikörper. Die Zellen wurden für 1 h unter Schwenken mit dem jeweiligen Antikörper bei RT inkubiert. Anschließend wurden die Zellen dreimal 5 min mit 1 x PBS gewaschen und danach für 1 h abgedunkelt bei RT unter Schwenken mit dem jeweiligen 1:250-verdünnten fluoreszenzmarkierten Sekundärantikörper Ziege anti-Ratte Alexa Fluor 488 (112-545-068, Jackson ImmunoResearch, West Grove, PA, USA) für anti-GABARAP (8H5) und Ziege-anti-Kaninchen Alexa Fluor 555 (ab150086, abcam, Cambridge, UK) inkubiert. Danach wurden die Zellen zweimal 5 min mit 1 x PBS unter Schwenken gewaschen, 10 min mit DAPI (Sigma-Aldrich, St. Louis, USA) bei RT inkubiert und zweimal 5 min mit 1 x PBS gewaschen. Die Zellen wurden anschließend mikroskopiert oder in PBS mit 0,05 % Natriumazid gelagert.

4.4.4 *Laser scanning* Mikroskopie (LSM) – Aufnahmebedingungen

Die mikroskopischen Bildaufnahmen wurden mit Hilfe der ZEN black 2009 Software an einem konfokalen LSM 710 System (Carl Zeiss MicroImaging Inc., Oberkochen, Deutschland) mit einem Plan-Apochromat 63x/1.40 Oil DIC M27 Objektiv aufgenommen. Die mit DAPI gefärbten Zellkerne wurden im 405 nm-Kanal (MBS -405/760+), GABARAP puncta im 488 nm-Kanal (MBS 488), Alexa Fluor 555 konjugierte Rab-Proteine im 543 nm-Kanal (MBS 458/543) und Alexa Fluor 647-markiertem EGF im 633 nm-Kanal (MBS 488/543/633) aufgenommen.

4.4.5 Kolokalisationsanalysen

Zur objektbasierten Analyse der EGFR-, GABARAP- und Rab5-Kolokalisationen diente zunächst das *„imaris spots" feature* der Software „Imaris" (Bitplane, Zürich, Schweiz). Dabei wurde eine initiale Vesikelgröße von 0,6 µm (xy-Achse) und 1,2 µm (z-Achse) festgelegt. Zur Reduzierung der Hintergrundfärbung wurde ein qualitativer Schwellenwert von 8 (EGFR), 13 (GABARAP) und 15 (Rab5) angewandt. Eine Größenzunahme der Vesikelgrößen, basierend auf der absoluten Signalintensität, wurde bei einem Signalrand-Durchmesser mit Schwellenwerten von 55 (EGFR), 120 (GABARAP) und 55 (Rab5) zugelassen. Im zweiten Schritt wurde die paarweise Assoziation von EGFR-, GABARAP- und Rab5-Vesikeln mit einem maximalen 3D-Mittelpunktabstand von 500 nm mittels "*Imaris Xtension: spots colocalization"* durchgeführt. Die Vesikelgenerierung und objektbasierende Assoziation wurden durch ein *batch*-Verfahren durchgeführt. Die nachfolgende weitere Datenanalyse erfolgte manuell.

Die Analyse der Datensätze mittels *Pearson's Correlation Coefficient* und *Mander's Correlation Coefficient* (M1+M2) wurde mit Fiji (Fiji Is Just Image J) version: 2.0.0-rc-43/1.50e ; Java 1.6.0_24 [64-bit] [279] durchgeführt und erfolgte mit Hilfe des *Just Another Colocalization Plugin* (JACoP) Plugins und der programmierten Makros, die unter Kapitel 8.5.2 und 8.5.3 aufgeführt sind. GraphPad Prism Version 8 für Windows (GraphPad Software, La Jolla California US) wurde zur Datenanalyse und CorelDRAW 2017 (Corel Corporation, Ottawa, Kanada) sowie Microsoft Office (Microsoft, Redmond, USA) wurden zur Bildbearbeitung und Dokumentation verwendet.

5 Diskussion

5.1 Werkzeuge zur differentiellen Untersuchung der ATG8-Paraloge

Die vornehmlich durch Autophagie bekannte ATG8-Proteinfamilie, welche auch Autophagie-unabhängige Funktionen ausübt, ist häufig nur mit Hilfe von fluoreszenzmarkierten ATG8-Reportern, Überexpressionskonstrukten oder für IF-Anwendungen unzureichend validierten Antikörpern untersucht worden (z.B. [72; 92; 280; 236]). Auch wenn ein Antikörper in einem Immunoblot (*Western Blot*) auf Proteinebene spezifisch bindet, so kann es sein, dass der gleiche Antikörper bei IF-Färbungen, wo das Protein meist in nativer, nicht denaturierter Form vorliegt, kreuzreagiert und somit zu falsch-positiven Ergebnissen führt [240; 242]. Es ist daher unumgänglich, Antikörper Applikations-spezifisch zu validieren [281]. Viele der bislang veröffentlichten Forschungsergebnisse zur Aufklärung ATG8-abhängiger Funktionen sind mit Hilfe einer Herabregulation durch z.B. siRNA-vermittelten *knockdown* (KD), und nicht durch vollständiges Ausschalten des Gens (KO), wie es inzwischen mit Hilfe von CRISPR/Cas9 möglich ist, entstanden [72]. Es kann davon ausgegangen werden, dass manche Ergebnisse, die auf Antikörper-basierten IF-Färbungen beruhen, nicht alleinig auf z.B. GABARAP, sondern auch auf die nahen Verwandten GABARAPL1 oder GABARAPL2 zutreffen. Auch Ergebnisse, die auf Verwendung von Zellen mit Gen-KD beruhen, können von den gewonnenen Ergebnissen, die auf einem vollständigen Gen-KO basieren, abweichen. Je nachdem, was untersucht werden soll, ist der Einsatz von KDs sinnvoller als das Gen durch KO gänzlich auszuschalten. Ein vollständiger KO eines Gens kann unter Umständen zur Letalität des Organismus führen, wie es für z.B. ATG5 in Mäusen beschrieben wurde [282; 283]. In diesen Fällen könnte das Gen mit Hilfe von z.B. *small hairpin* (sh)RNA herabreguliert werden [283]. Ein KO kann auch dazu führen, dass andere Proteine anders handeln oder hochreguliert werden [284]. Der Verlust eines ausgeschalteten Gens bzw. Proteins kann vor allem bei homologen Proteinen teilweise kompensiert werden, wie es beispielsweise für ATG4 KO-Zellen beschrieben werden konnte [284; 285].

Insgesamt können mit Hilfe von diversen KO-Zelllinien oder auch durch KDs wichtige Funktionen einzelner Proteine innerhalb eines Organismus aufgeklärt werden.

Innerhalb dieser Doktorarbeit sollten Werkzeuge, wie z.B. CRISPR/Cas9 KO-Plasmide bzw. daraus resultierende ATG8 KO-Zelllinien, die eine genaue Untersuchung der

einzelnen Mitglieder der ATG8-Proteinfamilie, insbesondere der GABARAP-Unterfamilie ermöglichen, etabliert werden, um diese in Zukunft zur differenzierten Erforschung neuer Funktionen und Interaktionspartner der GABARAP-Proteine anwenden zu können.

5.1.1 Effiziente Erzeugung diverser Doppel- und Dreifach-KO-Zelllinien durch *Multicolor*-FACS CRISPR/Cas9-Vektoren

Zu Beginn der Arbeit wurde mit der Klonierung von CRISPR/Cas9 KO-Plasmiden (siehe 8.4) der Grundstein zur effizienten Generierung von DKO- und TKO-Zelllinien gelegt. So konnten im Laufe dieser Arbeit in unserer Arbeitsgruppe eine Reihe von ATG8 KO-Zelllinien etabliert und für weitere Untersuchungen verwendet werden.

Mit Hilfe der verschiedenen Fluoreszenzen (EGFP, ECFP, mCherry) sollte eine gleichzeitige Sortierung der erfolgreich transfizierten Zellen mittels FACS ermöglicht werden (siehe 4.1). Dadurch sollten DKO- und TKO-Zelllinien schneller generiert werden, indem nicht jedes KO-Plasmid einzeln nacheinander eingebracht werden müsste, sondern die verschiedenen KO-Plasmide gleichzeitig eingebracht werden könnten. Zudem müssten auf diese Weise nicht nach jedem einzelnen KO-Plasmid-Schritt *off-target*-Effekte ausgelesen werden, sondern nur von der entstandenen finalen Zelllinie, was wiederum Zeit und Kosten spart.

Die Selektion der Zellen mittels FACS wurde in Kooperation mit Jochen Dobner durchgeführt. Mit dem verwendeten FACS Aria III-Gerät war eine genaue Abgrenzung von ECFP und EGFP aufgrund der dort vorhandenen Laser und Filter nicht vollständig möglich. Die Anregungswellenlängen der verwendeten FACS Aria III-Laser liegen bei 375 nm für z.B. DAPI und 488 nm für z.B. EGFP, so dass eine Anregung von ECFP ($435_{ex}/474_{em}$) [286] mit dem in diesem FACS-Gerät verbauten 375 nm-Laser nicht ausreichend möglich war. Die ECFP Fluoreszenz war sehr schwach und deshalb für eine FACS-basierte Sortierung nur bedingt nutzbar (siehe Kapitel 4.1). Mit einem FACS-Gerät, das einen 405 nm-Laser und einen 488 nm-Laser mit entsprechenden Filtern besitzt, wäre eine adäquatere Anregung des ECFPs sowie eine genauere Trennung des CFP-Kanals vom GFP-Kanal möglich. In Zukunft könnte daher z.B. anstatt ECFP ein Fluoreszenzprotein im Ultraviolett-Bereich, wie z.B. *enhanced blue fluorescence protein* (EBFP, $380_{ex}/440_{em}$) [287], ausgewählt werden, da EBFP mit einer Wellenlänge von 375 nm angeregt wird. Zudem käme es bei Verwendung von EBFP zu weniger Interferenz mit dem Spektralbereich von EGFP ($488_{ex}/507_{em}$) [273; 274]. Die Kombination von EBFP, EGFP oder mCherry (587/610) [278] und z.B. miRFP

($674_{ex}/703_{em}$), das im nahen Infrarotbereich Bereich liegt [288], sollte aufgrund der weit auseinanderliegenden Spektren eine jeweils geeignete Anregung sowie Abgrenzung der einzelnen Kanäle ermöglichen.

Alternativ zu dem hier verwendeten PX458-Plasmid gibt es z.B. das hSpCas9-2A-Puro V2.0 (PX459)-Plasmid, welches ebenfalls von Ran *et al.* entwickelt wurde. Es enthält kein Fluoreszenzprotein als Selektionsmarker, sondern das Antibiotikum Puromycin [243]. Erfolgreich transfizierte Zellen, die eine Puromycin-Resistenz über das Plasmid erworben haben, könnten in Puromycin-haltigem Medium überleben, wohingegen untransfizierte Zellen sterben würden. Eine gleichzeitige Selektion verschiedener Plasmide zur Erzeugung eines TKOs wäre mit dieser Methode jedoch nur möglich, wenn die transfizierten Plasmide unterschiedliche Antibiotika-Resistenzen besäßen. Zur Selektion von Zellen, die alle drei Plasmide aufgenommen haben, müssten dem Selektionsmedium drei verschiedene Antibiotika zugesetzt werden, was im Vergleich zur Selektion über verschiedene Fluoreszenzproteine eine deutlich höhere Belastung für die Zellen ergäbe, weshalb die gleichzeitige Anwendung der *Multicolor*-Fluoreszenzplasmide in dieser Arbeit bevorzugt wurde.

Um die Wahrscheinlichkeit von *off-target*-Effekten zu minimieren, könnte das ebenfalls von Ran *et al.* entwickelte *dual-nickase high-fidelity* Cas9-System verwendet werden [289]. Dabei wird die Position je eines in räumlicher Nähe zueinander liegenden Einzelstrangbruchs mit Hilfe von zwei verschiedenen sgRNAs festgelegt. Beide sgRNAs sind dabei komplementär zu den auf den gegenüberliegenden Strängen befindlichen Zielsequenzen. Die mutierte Cas9 D10A Nickase (Cas9n) schneidet anschließend die DNA-Einzelstränge, die von den beiden sgRNAs flankiert werden. Es kommt also zu einem versetzenden Schnitt der Einzelstränge und nicht wie bei der Cas9 Nickase zu einem direkten Doppelstrangbruch der DNA. Die Zielspezifität wird durch die Verwendung eines *dual-nickase high fidelity* Cas9-Systems deutlich erhöht, da es unwahrscheinlich ist, dass zwei Einzelstrangbrüche außerhalb der Zielsequenz in ausreichender Nähe zueinander generiert werden, um einen Doppelstrangbruch zu verursachen. [289]

5.1.1.1 Erhöhung der Transfektionseffizienz und Zellviabilität durch Nukleofektion

Das CRISPR/Cas9-System ist eine inzwischen weit verbreitete Genomeditierungsmethode, um Gene gezielt auszuschalten. Es ist jedoch nicht immer problemlos in jeder Zelllinie anwendbar. Insbesondere bei primären Zellen können oft nur geringe Transfektionsraten erzielt werden. Bei dem in dieser Arbeit angewandten Typ-II CRISPR/Cas9-System, bei dem alle Komponenten zusammen auf einem Plasmid liegen (siehe 8.4), ist es oftmals problematisch, das Plasmid aufgrund seiner Größe (> 9 kB) über chemische Transfektion (z.B. Polyfektion/Lipofektion) in die Zelle einzubringen. Die DNA könnte effizienter mittels viraler Transduktion, die mit Hilfe von z.B. Lentiviralen-Vektoren durchgeführt wird, eingebracht werden. Die virale Transduktion birgt jedoch einige Sicherheitsrisiken und darf deshalb nur in einem S2-Labor durchgeführt werden [290].

In Kooperation mit Jochen Dobner wurde in dieser Arbeit die unter S1-Bedingungen anwendbare effiziente nicht virale Elektroporationsmethode (Nukleofektion) genutzt, mit der die CRISPR/Cas9 PX458 KO-Plasmid-DNA in die Zelle eingebracht werden konnte [291]. Bei dieser Methode wird der Transport der DNA direkt in den Zellkern ermöglicht [291]. Im Vergleich zu chemischen Transfektionsmethoden ist die toxizitätsbedingte Zellsterblichkeit bei der Nukleofektion geringer, weshalb diese Vorgehensweise bevorzugt wurde [290].

5.1.2 Applikationsabhängiger Einfluss der Immunogenauswahl auf die anti-GABARAP Antikörper-Spezifität

Wie bereits zuvor erwähnt, binden viele Antikörper unspezifisch und/oder haben eine hohe Kreuzreaktivität mit Proteinen, die eine hohe Sequenz- und Strukturähnlichkeit zum Zielprotein aufweisen (Kapitel 1.2). Bei IF-Färbungen spielen Kreuzreaktionen der eingesetzten Antikörper eine große Rolle, da es dadurch zu falsch positiven Signalen oder hohen Hintergrundsignalen kommen kann. Diese Signale können durch Interaktion des Antikörpers mit zum Zielprotein nahe verwandten Proteinen oder anderen Proteinen mit ähnlichem Epitop hervorgerufen werden und führen zu Fehlinterpretationen der mit solchen Antikörpern erhaltenen Färbungen [240; 281].

Die Proteine der GABARAP-Unterfamilie weisen eine sehr hohe Struktur- und Sequenzhomologie auf (siehe Kapitel 1.1.2) und die meisten erwerblichen Antikörper sind für den Käufer unzureichend und intransparent validiert [292; 293]. Eine entsprechende

Validierung des Antikörpers durch den Endverbraucher selbst ist daher meist unerlässlich, jedoch sehr zeitintensiv [293; 237].

Innerhalb dieser Arbeit wurden daher kommerziell erworbene und die in Kooperation generierten monoklonalen Antikörper gegen GABARAPs, anti-GABARAP (8H5), anti-GABARAPL1 (1C2) und anti-GABARAPL2 (1E5) (siehe 4.2), unter Beachtung diverser Richtlinien zur Antikörper-Validierung [294], zu denen unter anderem genetische (GABARAP KO-Zelllinien) und orthogonale (Autophagosomen-Quantifizierung unter nährstoffarmen Bedingungen) Verfahren zählen, auf ihre Spezifität bei IF-Färbungen getestet [267]. Bei allen von uns getesteten kommerziell erwerblichen anti-GABARAP Antikörpern (polyklonale und monoklonale) konnte trotz spezifischer Banden im *Western Blot* eine Kreuzreaktion mit insbesondere GABARAPL1 bei IF-Färbungen nicht ausgeschlossen werden [267].

Außerdem wurden Fluoreszenz-markierte Proteine (EYFP-GABARAPL1, ECFP-GABARAPL2) transient exprimiert und der anti-GABARAP (8H5) Antikörper dadurch auf Kreuzreaktivität mit GABARAPL1/-L2 getestet [267]. Ein unabhängig validierter LC3B Antikörper [295] kolokalisierte mit anti-GABARAP (8H5) Antikörper gefärbten Strukturen und zeigte dadurch, dass es sich bei den GABARAP positiven Strukturen um Autophagosomen handelte [267], da LC3B in der Literatur als ein weit verbreiteter Autophagosomen-Marker beschrieben wird [9].

Die hier durchgeführten Experimente haben gezeigt, dass von den getesteten Hybridoma-Überständen der anti-GABARAP (8H5) Antikörper die höchste Spezifität für GABARAP hatte und keine Kreuzreaktionen mit GABARAPL1 und/oder GABARAPL2 aufwies. In den GABARAP KO-Zellen war lediglich eine leichte Hintergrundfärbung vorhanden, die eventuell auf die Verwendung eines nicht Subklassen-spezifischen Sekundär-Antikörpers oder eine GABARAP-unabhängige unspezifische Färbung eines Proteins mit ähnlichem Epitop zurückzuführen ist. In den Wildtyp-Zellen waren hingegen deutliche GABARAP-positive *puncta* zu erkennen, die teilweise mit LC3B kolokalisierten [267]. Die anderen in dieser Arbeit getesteten Hybridoma-Überstände der anti-GABARAPL1 (1C2) und anti-GABARAPL2 (1E5) Antikörper zeigten neben Färbungen der Wildtypzellen in den entsprechenden KO-Zelllinien ebenfalls deutliche Färbungen (siehe Kapitel 4.2) und mussten somit als untauglich für diese Anwendung klassifiziert werden.

Die fehlende Spezifität von anti-GABARAPL1 (1C2) und anti-GABARAPL2 (1E5) in IF-Färbungen, könnte darauf zurückzuführen sein, dass die Tiere für die Generierung dieser Antikörper mit kurzen GABARAPL1/-L2-Peptidfragmenten und nicht, wie im Falle des anti-

GABARAP (8H5) Antikörpers, mit den jeweiligen rekombinanten Volllänge-Proteinen immunisiert worden waren.

Die meisten kommerziellen Antikörper werden als Antigene gegen kurze Peptide, die aus Regionen mit möglichst geringer Homologie abgeleitet werden gewonnen [296; 297], da Peptide leicht zu synthetisieren und oftmals kostengünstiger als Volllängen-Protein Antigene sind [296; 297].

Ein auf dem Zielprotein liegendes Antikörper-Epitop kann in verschiedenen Konformationen exisitieren [296]. So kann das Epitop bei vollständig denaturierten Proteinen linear vorliegen, wohingegen es bei gefalteten Proteinen oft aus mehreren diskontinuierlichen Regionen bestehen und dadurch sehr komplex sein kann [298; 296]. Werden für die Immunisierung Peptide verwendet, so bestehen diese in der Regel aus 12-20 Aminosäuren, umfassen selten mehr als ein Epitop und liegen meist linear und ungefaltet vor, es wird also keine Sekundär- oder Tertiärstruktur ausgebildet [296]. Dadurch sind die gegen Peptidfragmente gebildeten Antikörper oftmals nicht in der Lage, Epitope nativ gefalteter Proteine zu erkennen [296]. Zur Immunisierung eingesetzte Antigene aus Volllängen-Proteinen bilden eher native Strukturen aus, beinhalten Oberflächenregionen und besitzen gegebenenfalls mehrere immunogene Epitope [296]. Die Antikörper haben dementsprechend auch eher die Möglichkeit, Epitope auf nativ vorliegenden Proteinen zu detektieren und zu binden. Bei IF-Färbungen liegt das Protein meist in seiner nativen Form vor, da die Probe nicht durch z.B. Aufkochen, was meist bei Proben für einen *Western Blot* der Fall ist, denaturiert wird, sondern lediglich fixiert wird.

Wie bereits erwähnt, wurde der anti-GABARAP (8H5) Antikörper mit Hilfe von rekombinantem Volllängen-GABARAP erzeugt und ist deshalb eher in der Lage, das Epitop eines nativ vorliegenden Proteins zu binden.

Alternativ zur Volllängen-Immunisierung könnte auch eine sogenannte DNA-Immunisierung verwendet werden. Dabei werden Tiere mit einem Expressionsplasmid, welches für das gewünschte Antigen codiert, immunisiert [296]. Das native Antigen mit posttranskriptionellen Modifikationen wird nachfolgend direkt im Tier (*in vivo*) exprimiert und die Antikörperproduktion angeregt [299]. Das Plasmid kann auch in Säugerzellen transfiziert werden, die anschließend das Antigen produzieren. Mit dem Antigen können dann wiederum Tiere immunisiert werden, die daraufhin Antikörper produzieren [299].

5.2 Detaillierte Untersuchung der ATG8s mittels *single-molecule localization* Mikroskopie (SMLM)

Der anti-GABARAP (8H5) Antikörper wurde auch für eine Anwendung innerhalb der *Superresolution*-Mikroskopie in Kooperation mit dem IBI-1 (Molekular- und Zellphysiologie, ehemals ICS-4) experimentell getestet. Nach persönlicher Mitteilung war eine Abgrenzung GABARAP-positiver Strukturen von der Hintergrundfärbung bzw. von einer unspezifischen Färbung anderer zellulärer Strukturen sowie eine differenzierte Auswertung in dieser hohen Auflösung nicht exakt möglich (Daten nicht gezeigt). Da es sich bei dem anti-GABARAP Antikörper um einen relativ großen IgG-Antikörper handelt, an welchen ein fluoreszenzgekoppelter Sekundärantikörper bindet, könnte es sein, dass es aufgrund der Antikörpergröße zu einem sogenannten Verknüpfungsfehler (*linkage error*) von ca. 10 nm gekommen ist [300; 301]. Der *linkage error* ist vor allem bei größeren Proteinen, wie einem Antikörper (ca. 150 kDa), bei SMLM ein gängiges Problem und beschreibt den Verknüpfungsabstand zwischen dem Fluoreszenzfarbstoff und dem Zielprotein, was zu Ungenauigkeiten bei der Proteinpositionsbestimmung führen kann [302]. Außerdem kann die Signalamplifikation zwischen Primär- und Sekundärantikörper die Quantifizierung von Zielepitopen verhindern [302].

Zu Beginn der parallellaufenden Doktorarbeit von Iman Abdollahzadeh lag der validierte anti-GABARAP (8H5) Antikörper noch nicht vor. Die Untersuchungen der ATG8s mittels Einzelmolekül-Lokalisations-Mikroskopie (SMLM) fanden mit transient ATG8-transfizierten Zelllinien statt [63]. Es konnte mit Hilfe von transient exprimierten YFP-GABARAP und YFP-LC3B HEK293-Zellen gezeigt werden, dass LC3B vermehrt in elliptischen und U-förmigen Strukturen vorkommt, was die Beteiligung von LC3B an der frühen Phagophoren-Ausbildung widerspiegelt [63]. GABARAP konnte hingegen vermehrt in kreisförmigen Strukturen detektiert werden [63], was dafürspricht, dass GABARAP vermehrt an der Autophagosomen-Schließung [72] und Autophagosomen-Lysosomen Fusion [74; 48] beteiligt ist.

Für hochauflösende SMLM-Aufnahmen der ATG8s auf endogenem Niveau konnte die neu generierte EGFP-KI GABARAP HEK293-Zelllinie bislang nicht verwendet werden, da das endogen exprimierte GFP weder photoaktivierbar noch photoschaltbar ist und infolgedessen nicht durch Licht bestimmter Wellenlänge und Intensität gezielt aktiviert oder deaktiviert werden kann [303]. Für SMLM-Aufnahmen ist es jedoch notwendig, dass das Fluoreszenzprotein photoaktivierbar und photoschaltbar ist [303; 304]. Zukünftig könnte zum

einen statt des herkömmlichen GFPs ein spezielles *photoactivatable* (PA)-Fluoreszenzprotein, wie z.B. PA-GFP [305] oder ein anderes photoaktivierbares Fluoreszenzprotein wie Dendra2 [306] verwendet werden. Zum anderen könnten sogenannte *Nanobody anti-GFP booster* Antikörper, welche mit einem photoaktivierbaren Fluoreszenzfarbstoff (z.B. Alexa Fluor 647) gekoppelt sind, die Detektion der endogen exprimierenden EGFP-KI GABARAP HEK293-Zellen mittels SMLM verbessern [300]. Bei Nano-Antikörpern, auch Einzeldomänenantikörper genannt, handelt es sich um Antikörper, die aus nur einer Aminosäurenkette bestehen und dadurch einfach rekombinant exprimiert werden können [303]. Wie der Name schon sagt, sind Nano-Antikörper sehr klein (ca. 10-15 kDa), was darauf zurückzuführen ist, dass sie aus einer einzelnen, monomeren variablen Domäne eines Schweren-Ketten-Antikörpers, der bei z.B. Kamelen (*Camelus dromedarius*) [307] natürlich vorkommt, bestehen. Durch den Einsatz von Nano-Antikörpern kann der Abstand zwischen Fluorophor und Zielprotein verringert werden, was zu einem geringeren *linkage error* führen kann [302].

5.3 Partielle Kolokalisationen von endogenem GABARAP mit EGF(R) und Rab-Markerproteinen

Der neu entwickelte, spezifische anti-GABARAP (8H5) Antikörper diente unter anderem der Untersuchung des endosomalen Transportweges von GABARAP und dem EGFR auf endogenem Expressionslevel in Huh7.5-Leberzellen. Dazu wurden innerhalb dieser Arbeit Kolokalisationsuntersuchungen von GABARAP mit den endosomalen Markerproteinen Rab5 (frühe Endosomen), Rab7 (späte Endosomen) und Rab11 (Recycling-Endosomen) nach Stimulation mit fluoreszenzmarkiertem EGF durchgeführt (siehe Kapitel 4.3).

5.3.1 Anwendungsspezifische Auswahl der Kolokalisationsauswertung

Eine zuverlässige Auswertung der Kolokalisationen in Kooperation mit dem *Center of Advanced Imaging* (CAi) mit einer objektbasierten Methode durch die Software „Imaris“ war nur für Rab5 möglich (Kapitel 4.3), da das Programm eine Vesikelanalyse, die auf kreisrunden Strukturen basiert, durchführt. Die gefärbten Rab7- und Rab11-Proteinstrukturen wiesen jedoch keine kreisförmigen Vesikel auf, sondern eher eine schlauchförmige Gestalt, für welche keine automatisierte Auswertungsmethode zur Verfügung stand. Außerdem zeigte sich bei der in dieser Arbeit durchgeführten Kolokalisationsauswertung mit anderen

Methoden, wie dem Pearson's *Correlation Coefficient* (PCC) oder Mander's *Correlation Coefficient* Koeffizienten M1+M2 (MCC), dass die an verschiedenen Tagen erhaltenen technischen Datensätze sehr inhomogen waren und sehr stark untereinander variierten (beispielhaft für Rab5 gezeigt in Kapitel 4.3). Die Fluktuationen zwischen den an verschiedenen Versuchstagen erzeugten Replikaten könnten aus der Verwendung abweichender bzw. höherer Passagen der Zellen resultieren oder eventuell daran liegen, dass sich die Zellen z.B. in einem anderen Zellzyklus befunden haben.

Der PCC ist eine Methode, die mittels linearer Regression die Korrelation zwischen zwei Bildintensitäten einschätzt [308], wohingegen der MCC angibt, in welchem Maß sich die jeweiligen Intensitäten der untersuchten Bildkanäle überlagern. Aufgrund der hohen Sensitivität gegenüber Hintergrundfärbungen wird bei der Auswertung mittels MCC durch den Anwender selbst ein Schwellenwert (*threshold*) definiert, wodurch die Hintergrundfärbung minimiert wird [308; 309]. Der MCC scheint im Vergleich zum PCC für die Analyse endosomaler Kompartimente, wie Dunn *et al.* es anhand einer Kolokalisationsanalyse von GFP-Rab7 mit *low density lipoprotein* (LDL) zeigen konnten, geeigneter zu sein, da bei diesen Färbungen die Pixelintensitäten der beiden analysierten Proben nicht durch einen einfachen, linearen Zusammenhang beschrieben werden [309]. Auch wenn die Fluoreszenzintensitäten der analysierten Proben stark voneinander abweichen, sollte man eher der Analyse mittels MCC vertrauen [310].

Die Kolokalisationsanalyse sollte deshalb immer für jede Auswertung individuell je nach Färbung und Bildqualität erfolgen und anhand der vorliegenden Gegebenheiten sollte eine geeignete Kolokalisationsauswertungsmethode ausgewählt werden.

Insgesamt ist eine eindeutige Aussage nach Analyse der gewonnen Daten derzeit nicht sicher möglich, da die mit Hilfe der verschiedenen Auswertungsmethoden erhaltenen Daten voneinander abweichen und auch aufgrund variierender Zellgrößen innerhalb einer Stichprobe sehr inhomogen sind.

Alles in allem erscheint jedoch eine Assoziation von GABARAP sowohl mit dem EGFR also auch mit den jeweiligen untersuchten Rab-Proteinen möglich, da diese eventuell nur transient auftreten und deshalb bei fixierten Zellen nicht in einem hohen Maß identifiziert werden können.

5.3.1.1 Reproduzierbarkeit mikroskopischer Daten: Wenn keine Zelle der anderen gleicht

Die Reproduzierbarkeit von Mikroskopiedaten ist oftmals aufgrund von z.B. Zellpassagen-bedingtem unterschiedlichen Zellwachstum und Zellviabilität herausfordernd. Aber auch die mikroskopischen Aufnahmebedingungen, wie z.B. die Auswahl des passenden Objektivs und entsprechender Anregungsstärke müssen adäquat gewählt werden [311]. So sollten bei einem Vergleich von WT- mit KO-Zellen die gleichen Aufnahmeeinstellungen verwendet werden [312]. Die mikroskopischen Aufnahmen sollten zudem ohne *bias* an verschiedenen Regionen in einem *well* aufgenommen werden und die Daten bestenfalls automatisiert mit Hilfe von z.B. Makros ausgewertet werden [312].

Häufig ist es auch problematisch, Antikörper-basierte Ergebnisse zu reproduzieren, da es zu Unterschieden zwischen den jeweiligen Chargen kommen kann [241]. Um diesem Problem entgegen zu wirken, könnten direkt größere Mengen des benötigten Antikörpers mit derselben LOT-Nummer bestellt werden oder man greift auf monoklonale Antikörper, die in Hybridomzellen vermehrt werden (siehe dazu Kapitel 1.2.2.1), zurück welche von einem Zellklon abstammen. Jedoch ist auch dabei zu beachten, dass es bei Hybridomaüberständen ebenfalls zu Zellpassagen-bedingten Abweichungen je Charge kommen kann.

5.4 Lebendzellmikroskopie unter endogenen Bedingungen mit Hilfe der EGFP-KI GABARAP HEK293-Zellen

Für IF-Färbungen werden die Zellen meist fixiert und permeabilisiert, damit die Antikörper in die Zellen gelangen können. Da Mikroskop-Aufnahmen von fixierten Zellen lediglich eine Momentaufnahme der Transportprozesse in der Zelle widerspiegeln, wurden neben fixierten Zellen ebenfalls mikroskopische Aufnahmen mit Hilfe einer durch Jochen Dobner generierten EGFP-KI GABARAP HEK293-Zelllinie, die mit EGFP-fusioniertes endogenes GABARAP exprimiert, gemacht. Die EGFP-KI GABARAP HEK293-Zelllinie ermöglichte in dieser Arbeit Lebendzell-Aufnahmen von endogenem GABARAP zusammen mit dem EGFR, der indirekt durch Alexa Fluor 647-markierten EGF, der als Ligand an den EGFR bindet, dargestellt wurde.

Die EGFP-KI GABARAP HEK293-Zelllinie bietet den Vorteil transiente Kontakte, Dynamiken und Transportwege von Proteinen *live* mikroskopisch verfolgen zu können. Die Auswahl der für *Multicolor*-Aufnahmen geeigneten Fluoreszenzproteine bzw.

Fluoreszenzfarbstoffe ist dabei zu bedenken, da es bei der Verwendung mehrerer Fluoreszenzen bei Aufnahmen von Multi-Kanal-Bildern zu einem *crosstalk* bzw. *bleedthrough* kommen kann, was es gerade bei der Untersuchung von Kolokalisationen zu vermeiden gilt [313]. Diese Effekte können durch die Verwendung von Fluoreszenzfarbstoffen in gleichen Konzentrationen mit weit voneinander entfernt liegenden Extinktions- und Emissionsspektren und durch sogenanntes *multitracking* bei den Mikroskopaufnahmen, also einer sequenziellen, nacheinander erfolgenden Bildaufnahme (Bild für Bild) und nicht einer simultanen Bildaufnahme, weitestgehend vermieden werden [314; 315].

Überexprimierte Fluoreszenzproteine sollten u.a. aufgrund der abweichenden Expressionslevel und damit zusammenhängenden höheren Fluoreszenzintensitäten nicht für Versuche zusammen mit endogen markierten Fluoreszenzproteinen verwendet werden. Stattdessen sollte mit endogenen Markern, wie z.B. Lysotracker oder weiteren eingebrachten Fluoreszenzprotein-KIs (z.B. von Rab-Proteinen), gearbeitet werden. Zudem führt eine Überexpression gegebenenfalls zu Zellstress und einer einhergehenden erhöhten Autophagie-Rate, die wiederum Einfluss auf die GABARAP-Lokalisation haben kann [93]. Beim Gebrauch von Proteinen, die das Fluoreszenzprotein auf endogenem Level exprimieren, sollte ebenfalls bedacht werden, dass das Fluoreszenzprotein auch dort zu sterischen Hinderungen führen kann. Nguyen *et al*. konnten zeigen, dass die Funktionalität von GFP-markierten LC3s und GABARAPs während der Mitophagie beeinträchtigt sein kann [74]. Eine Möglichkeit dem entgegenzuwirken, ist die Benutzung von heterozygoten KI-Zelllinien, d.h. einer Zelllinie in der sowohl das FP-markierte als auch das unmarkierte Protein gleichzeitig vorliegen.

Auch das Ausbleichen (*photo-bleaching*) der Fluoreszenzfarbstoffe kann vor allem bei längeren Lebendzellaufnahmen eine Schwierigkeit darstellen [313]. Daher sollten z.B. Fluoreszenzfarbstoffe mit hoher Helligkeit bzw. Fluoreszenzintensität verwendet werden, damit die Laserstärke dementsprechend niedrig gewählt werden kann, was einen *photo-bleaching* Effekt minimiert [315].

Bei den Lebendzellaufnahmen der EGFP-KI GABARAP HEK293-Zelllinie konnten nach Zugabe der EGFR- und TrfR-Liganden EGF bzw. Trf partielle Kolokalisationen von GABARAP sowohl mit dem EGF-Alexa Fluor 647 gebundenen EGFR als auch mit dem Trf-Alexa Fluor 555 gebundenen TrfR oder beiden zusammen beobachtet werden [145]. GABARAP konnte dabei in verschiedenen Strukturen, z.B. als kreisrunde vesikuläre, schlauchförmige oder aneinanderhängende „perlschnurartige“ Strukturen innerhalb der Zelle

gefunden werden [145]. Besonders auffallend waren dabei ca. 3 µm-große, ringartige GABARAP-haltige Strukturen, die bei den Lebendzell-Aufnahmen mittels *laser scanning* Mikroskopie (LSM), aber auch durch *spinning disk* Mikroskopie (SDM) (in Kooperation mit dem IBI-1) identifiziert werden konnten [145].

Vor kurzem haben Leidal *et al.* beschrieben, dass die LC3-Konjugationsmaschinerie für die Verpackung von RNA-bindenden Proteinen (RBP) und die Sekretion extrazellulärer Vesikel (EV) benötigt wird [113]. Endogenes lipidiertes LC3 konnte dort im Lumen von MVBs innerhalb von ILVs detektiert werden. Bei der von uns beobachteten ringartigen GABARAP-haltigen Struktur konnte GABARAP primär in der Membran, also vermutlich in lipidierter GABARAP-II Form, beobachtet werden. GABARAP könnte analog zu LC3 auch innerhalb von Vesikeln, also auf der zum Vesikellumen zugewandten Membranseite bzw. in ILVs, die sich wiederum innerhalb von MVBs befinden, vorliegen. Dort vorhandenes GABARAP könnte jedoch aufgrund der in den KI-Zellen eingesetzten pH-sensitiven EGFP-Fluoreszenz, die ab einem pH-Wert unter 7 signifikant abnimmt [305; 316], mikroskopisch nicht hinreichend sichtbar sein.

Außerdem konnten Leidal *et al.* zeigen, dass lipidiertes LC3 mit zwei der untersuchten RBPs interagiert und zusammen mit den RBPs in EVs angereichert wird [113]. Aus unserem Arbeitskreis konnte Julia Sanwald GABARAP in EVs nachweisen, was darauf hindeutet, dass GABARAP selbst sekretiert wird und eine Rolle bei der Sekretion spielen könnte [317].

Des Weiteren könnte GABARAP eventuell bei der Sortierung von Proteinen wie dem EGFR über ein endosomales Sortierungskompartiment in z.B. MVBs oder EVs von Bedeutung sein. Bei den beobachteten vesikulären Strukturen könnte es sich eventuell um eine Komponente des endosomalen Sortiersystems, ein sogenanntes Sortier-Endosom (*sorting endosome*) handeln, dessen pH-Wert bei ~ 6 liegt [318], was zu einer EGFP-Fluoreszenzabnahme im Lumen des Vesikels führen könnte. Für den TrfR wurde bereits beschrieben, dass er nach Clathrin-abhängiger Internalisierung zunächst zu Sortier-Endosomen, die neben dem *endocytic recycling compartment* (ERC) zu den frühen Endosomen zählen, transportiert wird [319; 320]. Durch den leicht sauren pH-Wert innerhalb des Sortier-Endosoms trennen sich gegebenenfalls die Liganden vom Rezeptor [318; 319]. Vom Sortier-Endosom aus wird der Cargo dann entweder in ein Recycling-Endosom oder ein spätes Endosom sortiert [318]. Nach fünf bis zehn Minuten Verweildauer wandert das Sortier-Endosom entlang der Mikrotubuli und es kommt zur sogenannten Maturation [320]. In dieser Zeit fusionieren keine weiteren endosomalen Vesikel mehr mit dem Sortier-Endosom. Der pH-Wert wird aufgrund der Anreicherung saurer Hydrolasen immer niedriger (pH ~ 5,0-6,0)

und das Sortier-Endosom geht in das späte Endosom über, das letztendlich mit einem Lysosom (pH ~ 4,5-5,5) verschmilzt, wodurch der Inhalt degradiert wird [320; 321]. Analog zum TrfR, der in dieser Arbeit neben dem EGFR ebenfalls an den Membranen GABARAP-haltiger vesikulärer Strukturen identifiziert werden konnte [145], kann der EGF-gebundene EGFR nach Clathrin-abhängiger Internalisierung ebenfalls zunächst in ein solches Sortier-Endosom transportiert werden [322], was unsere Vermutung, dass es sich bei der mikroskopisch sichtbaren vesikulären Struktur um ein Sortier-Endosom handeln könnte, bestärkt.

Eine weitere Möglichkeit, die Funktionen der ATG8s und auch das putativ GABARAP-abhängige EGFR-*trafficking* hochauflösend in der Zelle unter Lebendzellbedingungen detailliert zu untersuchen, wäre es, Lebendzell-Mikroskopieaufnahmen mittels *live cell stimulated emission depletion* (STED) durchzuführen. Diese Aufnahmen wären beispielsweise mit Hilfe von SiR-SNAP, SiR-CLIP [323; 324] oder SiR-Halo [325] *tags* möglich [326]. So könnte in Zukunft die EGFR- und GABARAP- Interaktion mit Hilfe von zweifarbiger Lebendzell-STED-Mikroskopie beispielsweise durch Verwendung eines EGFR-$SNAP_f$-Chromeo 494 in Kombination mit einem GABARAP-$CLIP_f$-ATTO 647N-*tags* untersucht werden [324].

Insgesamt konnte bereits mit Hilfe der konfokalen LSM und SDM eine transiente Interaktion von GABARAP mit dem EGFR und dessen Dynamik unter Lebendzellbedingungen beobachtet werden [145], welche es in Zukunft genauer zu untersuchen gilt.

6 Fazit und Ausblick

In den letzten Jahren wird die weitreichende Bedeutung der GABARAP-Proteinfamilie für eine Vielzahl zellulärer Prozesse, welche Autophagie, Proteintransport und -sekretion, aber auch die Strukturierung ganzer Kompartimente wie dem Golgi-Apparat umfassen, immer eminenter. Verbunden damit steigt die Dringlichkeit, GABARAP, GABARAPL1 und GABARAPL2 spezifisch im Experiment adressieren zu können. Mangels geeigneter Systeme fand und findet immer noch die funktionelle Charakterisierung GABARAP-artiger Proteine meist unter deren Überexpression statt. Anderenfalls können, retrospektiv betrachtet, in Experimenten beobachtete Effekte unter endogenen Bedingungen einem spezifischen Paralog oft nicht zweifelsfrei zugeordnet werden.

Mit der Entwicklung eines GABARAP-spezifischen anti-GABARAP Antikörpers, der in der Immunfluoreszenz-Anwendung nicht mit GABARAPL1 und GABARAPL2 kreuzreagiert, konnte eine wichtige Lücke geschlossen werden. Mit dem anti-GABARAP (8H5) Antikörper lässt sich nun endogenes GABARAP spezifisch, z.B. in fixierten Zellen, aber auch in Gewebeschnitten lokalisieren und so bestimmten Zellkompartimenten oder Gewebsregionen zuordnen. So wurde eine Option geschaffen, um Funktionen, die alleinig auf GABARAP und nicht auf seine nahen verwandten Proteine zurückgehen, zu untersuchen [267].

Durch neu generierte GABARAP KO-Zelllinien (HEK293 und Huh7.5), die neben den kommerziell erwerblichen HAP1 GABARAP KO-Zellen ebenfalls zur Validierung des Antikörpers herangezogen wurden, konnte der Antikörper positiv hinsichtlich seiner hohen GABARAP-Spezifität getestet und für IF-Färbungen verwendet werden [267]. Eine wichtige Erkenntnis bei der Evaluierung aller Hybridoma-Überstände war, dass nur mit Volllänge-Protein immunisierte Tiere einen spezifischen Antikörper hervorbrachten, was mit Beobachtungen anderer übereinstimmt [296].

Hierauf aufbauend könnten zukünftig in ähnlicher Weise spezifische Antikörper gegen GABARAPL1 und GABARAPL2 erzeugt werden, für welche bislang unter Einsatz von Peptidantigenen die Identifizierung von Antikörper-Kandidaten für Paralog-spezifische IF-Färbungen nicht gelang (siehe Kapitel 4.2).

Ein anderer Ansatz, um die intrazelluläre Lokalisation von GABARAP im Vergleich zu LC3B zu untersuchen, ergab sich in Kooperation mit dem IBI-1 (ehemals ICS-4, Forschungszentrum Jülich). Der Fokus wurde hierbei auf die mikroskopische Untersuchung

mittels SMLM gelegt. Dabei wurden GABARAP- und LC3B-positive Strukturen in Bezug auf Größe und Form mit Hilfe von EYFP-GABARAP und EYFP-LC3B exprimierenden HEK293-Zelllinien analysiert [63]. Ein interessanter Aspekt aus dieser Arbeit war, dass EYFP-GABARAP bevorzugt zirkuläre Strukturen und EYFP-LC3B vornehmlich elliptische Strukturen ausgebildet hat [63]. Es bleibt abzuwarten, ob solche Strukturen auch unter endogenen Bedingungen in dieser Form auftreten. Eine mögliche Herangehensweise GABARAP auf endogenem Level zu untersuchen, wäre SMLM Aufnahmen z.B. mit Hilfe einer neu erzeugten GABARAP Dendra-KI-Zelllinie durchzuführen und zu analysieren.

Die Beteiligung von GABARAP an Transportprozessen diverser Rezeptoren ist in der Literatur seit langem beschrieben (z.B. [97; 327; 112]), aber hinsichtlich der zugehörigen GABARAP-Funktionen nur ansatzweise verstanden.

Unsere Arbeitsgruppe konnte kürzlich zeigen, dass GABARAP an der Regulation der EGF-Rezeptordegradation beteiligt ist. Bei einer GABARAP-Defizienz kam es zu einem schnelleren EGFR-Abbau, was auf Proteinebene und auch durch Fluoreszenzfärbungen festgestellt werden konnte. Eine Frage, die wir uns stellten, war, ob eine GABARAP-Defizienz womöglich grundlegend die Reifung des am EGFR-Transport beteiligten endosomalen Systems beeinflusst. Zur Klärung dieser Fragestellung wurden innerhalb dieser Arbeit IF-Färbungen der Markerproteine Rab5 (frühe Endosomen), Rab11 (Recycling-Endosomen) und Rab7 (späte Endosomen) durchgeführt und mögliche Unterschiede des EGFR-Transportweges zwischen Wildtyp- und GABARAP KO-Zellen untersucht. Dabei waren keine signifikanten Unterschiede in Bezug auf die Kolokalisationen der jeweiligen Rab-Proteine mit dem EGF-gebundenen EGFR ersichtlich. Demnach kann der EGFR sowohl in Wildtyp als auch in GABARAP KO-Zellen alle untersuchten endosomalen Kompartimente erreichen [145].

Durch LSM und SDM Lebendzellmikroskopie einer homo- und heterozygoten HEK293 EGFP-KI GABARAP HEK293-Zelllinie konnte eine putative Interaktion des EGF-Alexa Fluor 647 gebundenen EGFRs mit GABARAP beobachtet werden. Es konnten sowohl anterograde und retrograde vesikuläre Komigrationen als auch eine ca. 3 µm-große dynamische vesikuläre Struktur, an deren GABARAP-haltigen Membranen Fusionsprozesse EGF-gebundener EGFRs und Trf-gebundener TrfR stattfanden, beobachtet werden [145]. Diese äußerst dynamischen vesikulären Strukturen gilt es in weiteren Experimenten genauer zu erörtern. Dies könnte mit Hilfe von Endosomen-Markern wie den Rab-Proteinen (siehe dazu Kapitel 1.1.3.2) geschehen. In Zukunft könnte dies beispielsweise mit einer

kombinierten endogen exprimierenden Fluoreszenzprotein (FP)-KI GABARAP und FP-KI Rab Zelllinie möglich sein.

Neben einer bereits ausgemachten putativen direkten Interaktion von GABARAP mit einem *extended* LIR (xLIR)-Motiv an Position 1060 bis 1065 (DTFLPV) innerhalb des zytoplasmatischen, regulatorischen Teils des EGFRs [145], könnten weitere LIR Motive innerhalb des EGFRs auf eine Interaktion mit GABARAP untersucht werden, die bereits mit Hilfe von iLIR [146] in der extrazellulären und der zytoplasmatischen Domäne des EGFRs identifiziert werden konnten. Ebenso wären verschiedenste indirekte Interaktionsmöglichkeiten denkbar. Eine mögliche Interaktion von GABARAP, mit z.B. dem Rab4A GTPase-aktivierenden Protein TBC1D16 (Abbildung 6.1), stünde in Einklang mit Studien, in denen bereits Interaktionen mit LC3/ATG8-Proteinen und Rab-GAPs TBC1D5 [227; 328; 329] bzw. TBC1D25 / *Ornithine Aminotransferase-Like 1* (OATL1) [330] beschrieben werden konnten.

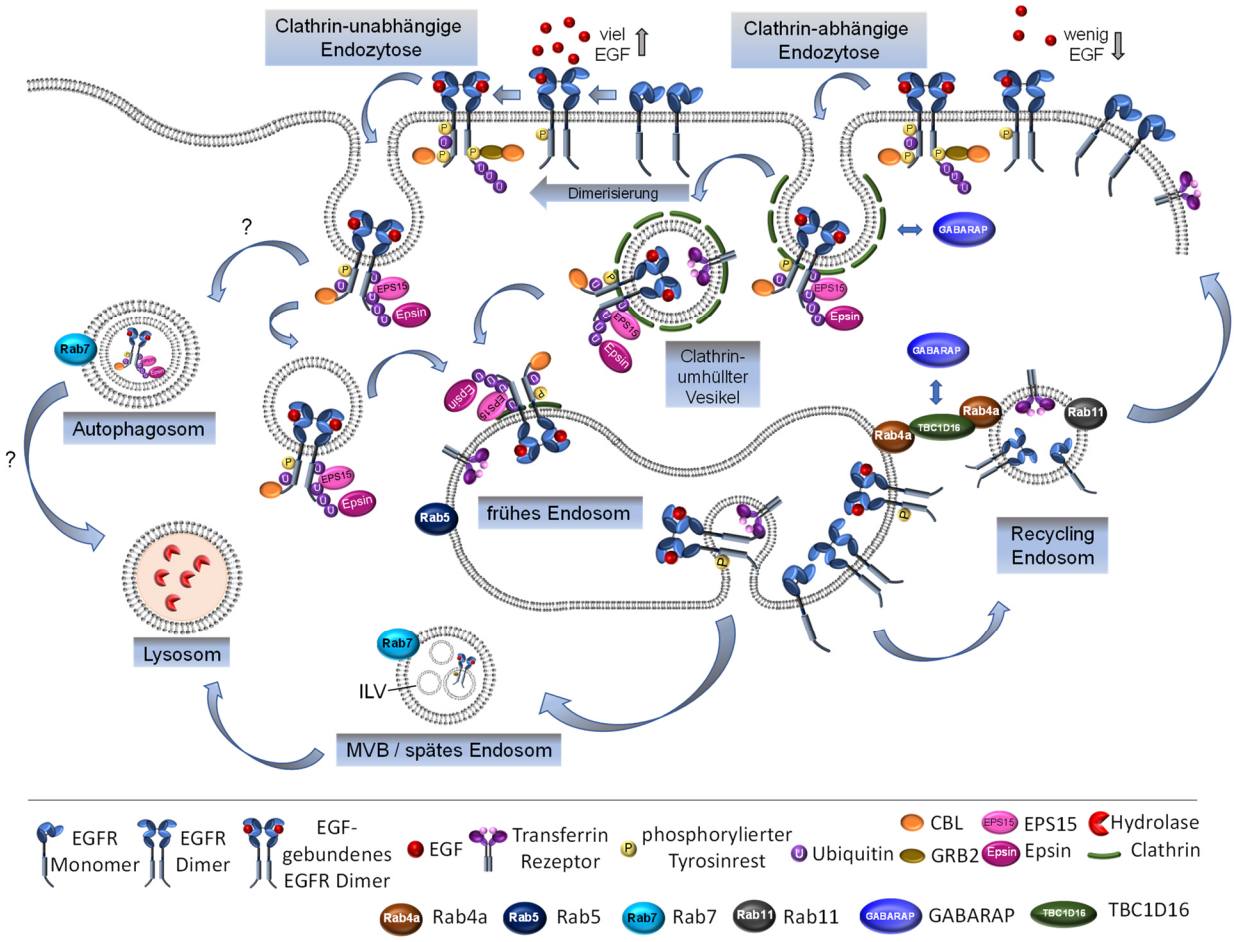

Abbildung 6.1: Putativ GABARAP-vermittelter Einfluss auf die EGF-Rezeptorinternalisierung
Neben der bereits in Abbildung 1.5 beschriebenen Rezeptor-Internalisierung sind putative direkte und indirekte GABARAP-Interaktionen dargestellt. Wie bereits bekannt ist, kommt es *in vitro* zu einer direkten Interaktion von GABARAP mit den schweren Ketten des Clathrins. Eine noch nicht beschriebene Interaktion könnte mit dem Protein TBC1D16 auf direktem oder indirektem Wege stattfinden, wodurch es zu einer Beeinflussung des Rab4A vermittelten Rezeptor-Recyclings kommen kann. (Modifiziert nach [202])

Rab4A befindet sich in frühen Endosomen und Recycling-Endosomen und wird für ein schnelles Recycling von z.B. Transferrin-Rezeptoren von frühen Endosomen zur Zelloberfläche benötigt [331]. Über TBC1D16 wird Rab4A negativ beeinflusst [332]. So könnte GABARAP direkt oder indirekt mit TBC1D16 interagieren und dadurch die Rab4A-Aktivierung und das damit einhergehende Rezeptor-Recycling beeinflussen (siehe Abbildung 6.1). Diesen Aspekt gilt es ebenfalls in nachfolgenden Experimenten genauer zu untersuchen. Dazu könnten, wie bereits oben erwähnt, beispielsweise weitere KI-Zelllinien für Rab- oder andere Markerproteine mit SMLM-tauglichen Fluoreszenzproteinen, wie z.B. Dendra2 generiert werden.

Nicht unerwähnt bleiben sollte die bereits innerhalb unseres Instituts beschriebene direkte Interaktion von GABARAP mit den schweren Ketten des Clathrins *in vitro* (Abbildung 6.1) [123], wodurch es zu einer GABARAP-vermittelten Beeinflussung der Clathrin-abhängigen Rezeptor-Endozytose kommen könnte. Um einen möglichen Zusammenhang genauer zu erörtern, könnten EGF-*pulse chase* Experimente mit anschließender IF-Färbung von Clathrin und GABARAP durchführt werden.

Lohnend erscheint auch eine Untersuchung des Zusammenspiels von GABARAP und dem EGFR unter Autophagie-induzierten Bedingungen, da es in der Literatur bereits Hinweise auf einen *cross-talk* zwischen Autophagie und den EGFR-vermittelten Signalwegen gibt [147; 151].

In einem parallel zu dieser Arbeit durchgeführten Dissertationsprojekt innerhalb unserer Arbeitsgruppe konnten bereits durch eine APEX2-GABARAP Proxitom-Analyse weitere putative GABARAP-Interaktionspartner ausgemacht werden [317].

Für die Zukunft ist demnach zu erwarten, dass sich unser Wissen zur Biologie der GABARAP-artigen Proteine, u.a. mit Hilfe der GABARAP KO-Zelllinien, spezifischen GABARAP Antikörpern und weiteren endogen markierten GABARAP/-L1/-L2-Fluoreszenzprotein gekoppelten KI-Zelllinien noch um eine ganze Reihe neuer und interessanter Aspekte erweitern wird.

7 Literaturverzeichnis

[1] Yorimitsu, T. and Klionsky, D. J. (2005). 'Autophagy: molecular machinery for self-eating', *Cell Death Differ*, 12 Suppl 2: 1542-52.

[2] Parzych, K. R. and Klionsky, D. J. (2014). 'An overview of autophagy: morphology, mechanism, and regulation', *Antioxid Redox Signal*, 20(3): 460-73.

[3] Gatica, D., Lahiri, V. and Klionsky, D. J. (2018). 'Cargo recognition and degradation by selective autophagy', *Nat Cell Biol*, 20(3): 233-42.

[4] Ke, P. Y. (2017). 'Horning cell self-digestion: Autophagy wins the 2016 Nobel Prize in Physiology or Medicine', *Biomed J*, 40(1): 5-8.

[5] Deter, R. L. and De Duve, C. (1967). 'Influence of glucagon, an inducer of cellular autophagy, on some physical properties of rat liver lysosomes', *J Cell Biol*, 33(2): 437-49.

[6] Takeshige, K., Baba, M., Tsuboi, S., Noda, T. and Ohsumi, Y. (1992). 'Autophagy in yeast demonstrated with proteinase-deficient mutants and conditions for its induction', *J Cell Biol*, 119(2): 301-11.

[7] Tsukada, M. and Ohsumi, Y. (1993). 'Isolation and characterization of autophagy-defective mutants of Saccharomyces cerevisiae', *FEBS Lett*, 333(1-2): 169-74.

[8] Reggiori, F. and Klionsky, D. J. (2013). 'Autophagic processes in yeast: mechanism, machinery and regulation', *Genetics*, 194(2): 341-61.

[9] Klionsky, D. J., Abdelmohsen, K., Abe, A., Abedin, M. J., Abeliovich, H., Acevedo Arozena, A., Adachi, H., Adams, C. M., Adams, P. D., Adeli, K., Adhihetty, P. J., Adler, S. G.*, et al.* (2016). 'Guidelines for the use and interpretation of assays for monitoring autophagy (3rd edition)', *Autophagy*, 12(1): 1-222.

[10] Wesselborg, S. and Stork, B. (2015). 'Autophagy signal transduction by ATG proteins: from hierarchies to networks', *Cell Mol Life Sci*, 72(24): 4721-57.

[11] De Duve, C. and Wattiaux, R. (1966). 'Functions of lysosomes', *Annu Rev Physiol*, 28: 435-92.

[12] Yang, Z. and Klionsky, D. J. (2010). 'Eaten alive: a history of macroautophagy', *Nat Cell Biol*, 12(9): 814-22.

[13] Oku, M. and Sakai, Y. (2018). 'Three distinct types of microautophagy based on membrane dynamics and molecular machineries', *Bioessays*, 40(6): e1800008.

[14] Chiang, H. L., Terlecky, S. R., Plant, C. P. and Dice, J. F. (1989). 'A role for a 70-kilodalton heat shock protein in lysosomal degradation of intracellular proteins', *Science*, 246(4928): 382-5.

[15] Kaushik, S. and Cuervo, A. M. (2012). 'Chaperone-mediated autophagy: a unique way to enter the lysosome world', *Trends Cell Biol*, 22(8): 407-17.

[16] Ji, C. H. and Kwon, Y. T. (2017). 'Crosstalk and interplay between the ubiquitin-proteasome system and autophagy', *Mol Cells*, 40(7): 441-49.

[17] Kirkin, V. and Rogov, V. V. (2019). 'A diversity of selective autophagy receptors determines the specificity of the autophagy pathway', *Mol Cell*, 76(2): 268-85.

[18] Johansen, T. and Lamark, T. (2020). 'Selective autophagy: ATG8 family proteins, LIR motifs and cargo receptors', *J Mol Biol*, 432(1): 80-103.

[19] Harding, T. M., Hefner-Gravink, A., Thumm, M. and Klionsky, D. J. (1996). 'Genetic and phenotypic overlap between autophagy and the cytoplasm to vacuole protein targeting pathway', *J Biol Chem*, 271(30): 17621-4.

[20] Scott, S. V., Hefner-Gravink, A., Morano, K. A., Noda, T., Ohsumi, Y. and Klionsky, D. J. (1996). 'Cytoplasm-to-vacuole targeting and autophagy employ the same machinery to deliver proteins to the yeast vacuole', *Proc Natl Acad Sci U S A*, 93(22): 12304-8.

[21] Bernales, S., Schuck, S. and Walter, P. (2007). 'ER-phagy: selective autophagy of the endoplasmic reticulum', *Autophagy*, 3(3): 285-7.

[22] Lewis, Margaret Reed and Lewis, Warren Harmon (1915). 'Mitochondria (and other cytoplasmic structures) in tissue cultures', *American Journal of Anatomy*, 17(3): 339-401.

[23] Kim, I., Rodriguez-Enriquez, S. and Lemasters, J. J. (2007). 'Selective degradation of mitochondria by mitophagy', *Arch Biochem Biophys*, 462(2): 245-53.

[24] Wang, K. and Klionsky, D. J. (2011). 'Mitochondria removal by autophagy', *Autophagy*, 7(3): 297-300.

[25] Youle, R. J. and Narendra, D. P. (2011). 'Mechanisms of mitophagy', *Nat Rev Mol Cell Biol*, 12(1): 9-14.

[26] Samson, E. (1981). 'Xenophagy', *Br Dent J*, 150(5): 136.

[27] Tuttle, D. L., Lewin, A. S. and Dunn, W. A., Jr. (1993). 'Selective autophagy of peroxisomes in methylotrophic yeasts', *Eur J Cell Biol*, 60(2): 283-90.

[28] Hutchins, M. U., Veenhuis, M. and Klionsky, D. J. (1999). 'Peroxisome degradation in Saccharomyces cerevisiae is dependent on machinery of macroautophagy and the Cvt pathway', *J Cell Sci*, 112 (Pt 22): 4079-87.

[29] Dunn, W. A., Jr., Cregg, J. M., Kiel, J. A., van der Klei, I. J., Oku, M., Sakai, Y., Sibirny, A. A., Stasyk, O. V. and Veenhuis, M. (2005). 'Pexophagy: the selective autophagy of peroxisomes', *Autophagy*, 1(2): 75-83.

[30] Overbye, A., Fengsrud, M. and Seglen, P. O. (2007). 'Proteomic analysis of membrane-associated proteins from rat liver autophagosomes', *Autophagy*, 3(4): 300-22.

[31] Tasdemir, E., Maiuri, M. C., Tajeddine, N., Vitale, I., Criollo, A., Vicencio, J. M., Hickman, J. A., Geneste, O. and Kroemer, G. (2007). 'Cell cycle-dependent induction of autophagy, mitophagy and reticulophagy', *Cell Cycle*, 6(18): 2263-7.

[32] Kraft, C., Deplazes, A., Sohrmann, M. and Peter, M. (2008). 'Mature ribosomes are selectively degraded upon starvation by an autophagy pathway requiring the Ubp3p/Bre5p ubiquitin protease', *Nat Cell Biol*, 10(5): 602-10.

[33] Klionsky, D. J. and Emr, S. D. (2000). 'Autophagy as a regulated pathway of cellular degradation', *Science*, 290(5497): 1717-21.

[34] Eskelinen, E. L. and Saftig, P. (2009). 'Autophagy: a lysosomal degradation pathway with a central role in health and disease', *Biochim Biophys Acta*, 1793(4): 664-73.

[35] Hyttinen, J. M., Niittykoski, M., Salminen, A. and Kaarniranta, K. (2013). 'Maturation of autophagosomes and endosomes: a key role for Rab7', *Biochim Biophys Acta*, 1833(3): 503-10.

[36] Mizushima, N. and Komatsu, M. (2011). 'Autophagy: renovation of cells and tissues', *Cell*, 147(4): 728-41.

[37] Levine, B. and Kroemer, G. (2019). 'Biological functions of autophagy genes: a disease perspective', *Cell*, 176(1-2): 11-42.

[38] Hansen, M., Rubinsztein, D. C. and Walker, D. W. (2018). 'Autophagy as a promoter of longevity: insights from model organisms', *Nat Rev Mol Cell Biol*, 19(9): 579-93.

[39] Kaur, J. and Debnath, J. (2015). 'Autophagy at the crossroads of catabolism and anabolism', *Nat Rev Mol Cell Biol*, 16(8): 461-72.

[40] Viret, C. and Faure, M. (2019). 'Regulation of syntaxin 17 during autophagosome maturation', *Trends Cell Biol*, 29(1): 1-3.

[41] Ebner, P., Poetsch, I., Deszcz, L., Hoffmann, T., Zuber, J. and Ikeda, F. (2018). 'The IAP family member BRUCE regulates autophagosome-lysosome fusion', *Nat Commun*, 9(1): 599.

[42] Nakamura, S. and Yoshimori, T. (2017). 'New insights into autophagosome-lysosome fusion', *J Cell Sci*, 130(7): 1209-16.

[43] Wirawan, E., Vanden Berghe, T., Lippens, S., Agostinis, P. and Vandenabeele, P. (2012). 'Autophagy: for better or for worse', *Cell Res*, 22(1): 43-61.

[44] Kim, J., Kundu, M., Viollet, B. and Guan, K. L. (2011). 'AMPK and mTOR regulate autophagy through direct phosphorylation of Ulk1', *Nat Cell Biol*, 13(2): 132-41.

[45] Meijer, A. J., Lorin, S., Blommaart, E. F. and Codogno, P. (2015). 'Regulation of autophagy by amino acids and MTOR-dependent signal transduction', *Amino Acids*, 47(10): 2037-63.

[46] Alers, S., Loffler, A. S., Wesselborg, S. and Stork, B. (2012). 'Role of AMPK-mTOR-Ulk1/2 in the regulation of autophagy: cross talk, shortcuts, and feedbacks', *Mol Cell Biol*, 32(1): 2-11.

[47] Grunwald, D. S., Otto, N. M., Park, J. M., Song, D. and Kim, D. H. (2019). 'GABARAPs and LC3s have opposite roles in regulating ULK1 for autophagy induction', *Autophagy*: 1-15.

[48] Kriegenburg, F., Ungermann, C. and Reggiori, F. (2018). 'Coordination of autophagosome-lysosome fusion by Atg8 family members', *Curr Biol*, 28(8): R512-R18.

[49] Stork, B. and Dengjel, J. (2017). 'Study of ULK1 catalytic activity and its regulation', *Methods Enzymol*, 587: 391-404.

[50] Nakatogawa, H., Suzuki, K., Kamada, Y. and Ohsumi, Y. (2009). 'Dynamics and diversity in autophagy mechanisms: lessons from yeast', *Nat Rev Mol Cell Biol*, 10(7): 458-67.

[51] Polson, H. E., de Lartigue, J., Rigden, D. J., Reedijk, M., Urbe, S., Clague, M. J. and Tooze, S. A. (2010). 'Mammalian Atg18 (WIPI2) localizes to omegasome-anchored phagophores and positively regulates LC3 lipidation', *Autophagy*, 6(4): 506-22.

[52] Wallot-Hieke, N., Verma, N., Schlutermann, D., Berleth, N., Deitersen, J., Bohler, P., Stuhldreier, F., Wu, W., Seggewiss, S., Peter, C., Gohlke, H., Mizushima, N.*, et al.* (2018). 'Systematic analysis of ATG13 domain requirements for autophagy induction', *Autophagy*, 14(5): 743-63.

[53] Okazaki, N., Yan, J., Yuasa, S., Ueno, T., Kominami, E., Masuho, Y., Koga, H. and Muramatsu, M. (2000). 'Interaction of the Unc-51-like kinase and microtubule-associated protein light chain 3 related proteins in the brain: possible role of vesicular transport in axonal elongation', *Brain Res Mol Brain Res*, 85(1-2): 1-12.

[54] Le Grand, J. N., Chakrama, F. Z., Seguin-Py, S., Fraichard, A., Delage-Mourroux, R., Jouvenot, M. and Boyer-Guittaut, M. (2011). 'GABARAPL1 (GEC1): original or copycat?', *Autophagy*, 7(10): 1098-107.

[55] Hurley, J. H. and Young, L. N. (2017). 'Mechanisms of Autophagy Initiation', *Annu Rev Biochem*, 86: 225-44.

[56] Chowdhury, S., Otomo, C., Leitner, A., Ohashi, K., Aebersold, R., Lander, G. C. and Otomo, T. (2018). 'Insights into autophagosome biogenesis from structural and biochemical analyses of the ATG2A-WIPI4 complex', *Proc Natl Acad Sci U S A*, 115(42): E9792-E801.

[57] Gómez-Sánchez, R., Rose, J., Guimarães, R., Mari, M., Papinski, D., Rieter, E., Geerts, W. J., Hardenberg, R., Kraft, C., Ungermann, C. and Reggiori, F. (2018). 'Atg9 establishes Atg2-dependent contact sites between the endoplasmic reticulum and phagophores', *The Journal of Cell Biology*, 217(8): 2743-63.

[58] Nascimbeni, A. C., Giordano, F., Dupont, N., Grasso, D., Vaccaro, M. I., Codogno, P. and Morel, E. (2017). 'ER-plasma membrane contact sites contribute to autophagosome biogenesis by regulation of local PI3P synthesis', *EMBO J*, 36(14): 2018-33.

[59] Axe, E. L., Walker, S. A., Manifava, M., Chandra, P., Roderick, H. L., Habermann, A., Griffiths, G. and Ktistakis, N. T. (2008). 'Autophagosome formation from membrane compartments enriched in phosphatidylinositol 3-phosphate and dynamically connected to the endoplasmic reticulum', *J Cell Biol*, 182(4): 685-701.

[60] Tooze, S. A. and Yoshimori, T. (2010). 'The origin of the autophagosomal membrane', *Nat Cell Biol*, 12(9): 831-5.

[61] Abdollahzadeh, I., Schwarten, M., Gensch, T., Willbold, D. and Weiergräber, O. H. (2017). 'The Atg8 family of proteins-modulating shape and functionality of autophagic membranes', *Front Genet*, 8: 109.

[62] Yoshii, S. R. and Mizushima, N. (2017). 'Monitoring and measuring autophagy', *Int J Mol Sci*, 18(9): 1865.

[63] Abdollahzadeh, I., Hendriks, J., Sanwald, J. L., Simons, I. M., Hoffmann, S., Weiergräber, O. H., Willbold, D. and Gensch, T. (2019). 'Autophagy-related proteins GABARAP and LC3B label structures of similar size but different shape in super-resolution imaging', *Molecules*, 24(9): 1833.

[64] Mizushima, N., Yamamoto, A., Hatano, M., Kobayashi, Y., Kabeya, Y., Suzuki, K., Tokuhisa, T., Ohsumi, Y. and Yoshimori, T. (2001). 'Dissection of autophagosome formation using Apg5-deficient mouse embryonic stem cells', *J Cell Biol*, 152(4): 657-68.

[65] Ichimura, Y., Kirisako, T., Takao, T., Satomi, Y., Shimonishi, Y., Ishihara, N., Mizushima, N., Tanida, I., Kominami, E., Ohsumi, M., Noda, T. and Ohsumi, Y. (2000). 'A ubiquitin-like system mediates protein lipidation', *Nature*, 408(6811): 488-92.

[66] Tanida, I., Komatsu, M., Ueno, T. and Kominami, E. (2003). 'GATE-16 and GABARAP are authentic modifiers mediated by Apg7 and Apg3', *Biochem Biophys Res Commun*, 300(3): 637-44.

[67] Nakatogawa, H. (2013). 'Two ubiquitin-like conjugation systems that mediate membrane formation during autophagy', *Essays Biochem*, 55: 39-50.

[68] Grimmel, M., Backhaus, C. and Proikas-Cezanne, T. (2015). 'WIPI-mediated autophagy and longevity', *Cells*, 4(2): 202-17.

[69] He, C. and Klionsky, D. J. (2009). 'Regulation mechanisms and signaling pathways of autophagy', *Annu Rev Genet*, 43: 67-93.

[70] Schwarten, M., Mohrlüder, J., Ma, P., Stoldt, M., Thielmann, Y., Stangler, T., Hersch, N., Hoffmann, B., Merkel, R. and Willbold, D. (2009). 'Nix directly binds to GABARAP: a possible crosstalk between apoptosis and autophagy', *Autophagy*, 5(5): 690-8.

[71] Novak, I., Kirkin, V., McEwan, D. G., Zhang, J., Wild, P., Rozenknop, A., Rogov, V., Lohr, F., Popovic, D., Occhipinti, A., Reichert, A. S., Terzic, J.*, et al.* (2010). 'Nix is a selective autophagy receptor for mitochondrial clearance', *EMBO Rep*, 11(1): 45-51.

[72] Weidberg, H., Shvets, E., Shpilka, T., Shimron, F., Shinder, V. and Elazar, Z. (2010). 'LC3 and GATE-16/GABARAP subfamilies are both essential yet act differently in autophagosome biogenesis', *EMBO J*, 29(11): 1792-802.

[73] Alemu, E. A., Lamark, T., Torgersen, K. M., Birgisdottir, A. B., Larsen, K. B., Jain, A., Olsvik, H., Overvatn, A., Kirkin, V. and Johansen, T. (2012). 'ATG8 family proteins act as scaffolds for assembly of the ULK complex: sequence requirements for LC3-interacting region (LIR) motifs', *J Biol Chem*, 287(47): 39275-90.

[74] Nguyen, T. N., Padman, B. S., Usher, J., Oorschot, V., Ramm, G. and Lazarou, M. (2016). 'Atg8 family LC3/GABARAP proteins are crucial for autophagosome-lysosome fusion but not autophagosome formation during PINK1/Parkin mitophagy and starvation', *J Cell Biol*, 215(6): 857-74.

[75] Bozic, M., van den Bekerom, L., Milne, B. A., Goodman, N., Roberston, L., Prescott, A. R., Macartney, T. J., Dawe, N. and McEwan, D. G. (2020). 'A conserved ATG2-GABARAP family interaction is critical for phagophore formation', *EMBO Rep*, 21(3): e48412.

[76] Liang, C., Feng, P., Ku, B., Dotan, I., Canaani, D., Oh, B. H. and Jung, J. U. (2006). 'Autophagic and tumour suppressor activity of a novel Beclin1-binding protein UVRAG', *Nat Cell Biol*, 8(7): 688-99.

[77] Jiang, P., Nishimura, T., Sakamaki, Y., Itakura, E., Hatta, T., Natsume, T. and Mizushima, N. (2014). 'The HOPS complex mediates autophagosome-lysosome fusion through interaction with syntaxin 17', *Mol Biol Cell*, 25(8): 1327-37.

[78] Sun, Q., Westphal, W., Wong, K. N., Tan, I. and Zhong, Q. (2010). 'Rubicon controls endosome maturation as a Rab7 effector', *Proc Natl Acad Sci U S A*, 107(45): 19338-43.

[79] Wang, C. W., Stromhaug, P. E., Shima, J. and Klionsky, D. J. (2002). 'The Ccz1-Mon1 protein complex is required for the late step of multiple vacuole delivery pathways', *J Biol Chem*, 277(49): 47917-27.

[80] Nordmann, M., Cabrera, M., Perz, A., Brocker, C., Ostrowicz, C., Engelbrecht-Vandre, S. and Ungermann, C. (2010). 'The Mon1-Ccz1 complex is the GEF of the late endosomal Rab7 homolog Ypt7', *Curr Biol*, 20(18): 1654-9.

[81] McEwan, D. G., Popovic, D., Gubas, A., Terawaki, S., Suzuki, H., Stadel, D., Coxon, F. P., Miranda de Stegmann, D., Bhogaraju, S., Maddi, K., Kirchof, A., Gatti, E.*, et al.* (2015).

'PLEKHM1 regulates autophagosome-lysosome fusion through HOPS complex and LC3/GABARAP proteins', *Mol Cell*, 57(1): 39-54.

[82] Birgisdottir, A. B., Lamark, T. and Johansen, T. (2013). 'The LIR motif - crucial for selective autophagy', *J Cell Sci*, 126(Pt 15): 3237-47.

[83] Itakura, E., Kishi-Itakura, C. and Mizushima, N. (2012). 'The hairpin-type tail-anchored SNARE syntaxin 17 targets to autophagosomes for fusion with endosomes/lysosomes', *Cell*, 151(6): 1256-69.

[84] Wang, Z., Miao, G., Xue, X., Guo, X., Yuan, C., Wang, Z., Zhang, G., Chen, Y., Feng, D., Hu, J. and Zhang, H. (2016). 'The vici syndrome protein EPG5 is a Rab7 effector that determines the fusion specificity of autophagosomes with late endosomes/lysosomes', *Mol Cell*, 63(5): 781-95.

[85] Diao, J., Liu, R., Rong, Y., Zhao, M., Zhang, J., Lai, Y., Zhou, Q., Wilz, L. M., Li, J., Vivona, S., Pfuetzner, R. A., Brunger, A. T.*, et al.* (2015). 'ATG14 promotes membrane tethering and fusion of autophagosomes to endolysosomes', *Nature*, 520(7548): 563-6.

[86] Bainton, D. F. (1981). 'The discovery of lysosomes', *J Cell Biol*, 91(3 Pt 2): 66-76.

[87] Gordon, G. B., Miller, L. R. and Bensch, K. G. (1965). 'Studies on the intracellular digestive process in mammalian tissue culture cells', *J Cell Biol*, 25(2): 41-55.

[88] Werner, G., Hagenmaier, H., Drautz, H., Baumgartner, A. and Zahner, H. (1984). 'Metabolic products of microorganisms. 224. Bafilomycins, a new group of macrolide antibiotics. Production, isolation, chemical structure and biological activity', *J Antibiot (Tokyo)*, 37(2): 110-7.

[89] Drose, S. and Altendorf, K. (1997). 'Bafilomycins and concanamycins as inhibitors of V-ATPases and P-ATPases', *J Exp Biol*, 200(Pt 1): 1-8.

[90] Vaites, L. P., Paulo, J. A., Huttlin, E. L. and Harper, J. W. (2018). 'Systematic Analysis of Human Cells Lacking ATG8 Proteins Uncovers Roles for GABARAPs and the CCZ1/MON1 Regulator C18orf8/RMC1 in Macroautophagic and Selective Autophagic Flux', *Mol Cell Biol*, 38(1).

[91] Padman, B. S., Nguyen, T. N. and Lazarou, M. (2017). 'Autophagosome formation and cargo sequestration in the absence of LC3/GABARAPs', *Autophagy*, 13(4): 772-74.

[92] Joachim, J., Jefferies, H. B., Razi, M., Frith, D., Snijders, A. P., Chakravarty, P., Judith, D. and Tooze, S. A. (2015). 'Activation of ULK kinase and autophagy by GABARAP trafficking from the centrosome is regulated by WAC and GM130', *Mol Cell*, 60(6): 899-913.

[93] Joachim, J., Razi, M., Judith, D., Wirth, M., Calamita, E., Encheva, V., Dynlacht, B. D., Snijders, A. P., O'Reilly, N., Jefferies, H. B. J. and Tooze, S. A. (2017). 'Centriolar satellites control GABARAP ubiquitination and GABARAP-mediated autophagy', *Curr Biol*, 27(14): 2123-36.

[94] Huang, R., Xu, Y., Wan, W., Shou, X., Qian, J., You, Z., Liu, B., Chang, C., Zhou, T., Lippincott-Schwartz, J. and Liu, W. (2015). 'Deacetylation of nuclear LC3 drives autophagy initiation under starvation', *Mol Cell*, 57(3): 456-66.

[95] Wu, F., Watanabe, Y., Guo, X. Y., Qi, X., Wang, P., Zhao, H. Y., Wang, Z., Fujioka, Y., Zhang, H., Ren, J. Q., Fang, T. C., Shen, Y. X.*, et al.* (2015). 'Structural basis of the differential function of the two C. elegans Atg8 homologs, LGG-1 and LGG-2, in autophagy', *Mol Cell*, 60(6): 914-29.

[96] Schaaf, M. B., Keulers, T. G., Vooijs, M. A. and Rouschop, K. M. (2016). 'LC3/GABARAP family proteins: autophagy-(un)related functions', *FASEB J*, 30(12): 3961-78.

[97] Wang, H., Bedford, F. K., Brandon, N. J., Moss, S. J. and Olsen, R. W. (1999). 'GABA(A)-receptor-associated protein links GABA(A) receptors and the cytoskeleton', *Nature*, 397(6714): 69-72.

[98] Vernier-Magnin, S., Muller, S., Sallot, M., Radom, J., Musard, J. F., Adami, P., Dulieu, P., Remy-Martin, J. P., Jouvenot, M. and Fraichard, A. (2001). 'A novel early estrogen-regulated gene gec1 encodes a protein related to GABARAP', *Biochem Biophys Res Commun*, 284(1): 118-25.

[99] Legesse-Miller, A., Sagiv, Y., Porat, A. and Elazar, Z. (1998). 'Isolation and characterization of a novel low molecular weight protein involved in intra-Golgi traffic', *J Biol Chem*, 273(5): 3105-9.

[100] Sagiv, Y., Legesse-Miller, A., Porat, A. and Elazar, Z. (2000). 'GATE-16, a membrane transport modulator, interacts with NSF and the Golgi v-SNARE GOS-28', *EMBO J*, 19(7): 1494-504.

[101] Wang, H. and Olsen, R. W. (2000). 'Binding of the GABA(A) receptor-associated protein (GABARAP) to microtubules and microfilaments suggests involvement of the cytoskeleton in GABARAPGABA(A) receptor interaction', *J Neurochem*, 75(2): 644-55.

[102] Mansuy, V., Boireau, W., Fraichard, A., Schlick, J. L., Jouvenot, M. and Delage-Mourroux, R. (2004). 'GEC1, a protein related to GABARAP, interacts with tubulin and GABA(A) receptor', *Biochem Biophys Res Commun*, 325(2): 639-48.

[103] Chen, C., Li, J. G., Chen, Y., Huang, P., Wang, Y. and Liu-Chen, L. Y. (2006). 'GEC1 interacts with the kappa opioid receptor and enhances expression of the receptor', *J Biol Chem*, 281(12): 7983-93.

[104] Sievers, F., Wilm, A., Dineen, D., Gibson, T. J., Karplus, K., Li, W., Lopez, R., McWilliam, H., Remmert, M., Soding, J., Thompson, J. D. and Higgins, D. G. (2011). 'Fast, scalable generation of high-quality protein multiple sequence alignments using Clustal Omega', *Mol Syst Biol*, 7: 539.

[105] Weiergräber, O. H., Mohrlüder, J. and Willbold, D. (2013). 'Atg8 Family Proteins - Autophagy and Beyond.' in *Autophagy - A Double-Edged Sword - Cell Survival or Death?* (Yannick Bailly, IntechOpen)

[106] Thielmann, Y., Weiergräber, O. H., Ma, P., Schwarten, M., Mohrlüder, J. and Willbold, D. (2009). 'Comparative modeling of human NSF reveals a possible binding mode of GABARAP and GATE-16', *Proteins*, 77(3): 637-46.

[107] Duran, J. M., Anjard, C., Stefan, C., Loomis, W. F. and Malhotra, V. (2010). 'Unconventional secretion of Acb1 is mediated by autophagosomes', *J Cell Biol*, 188(4): 527-36.

[108] Manjithaya, R. and Subramani, S. (2011). 'Autophagy: a broad role in unconventional protein secretion?', *Trends Cell Biol*, 21(2): 67-73.

[109] Münz, C. (2017). 'The Autophagic Machinery in Viral Exocytosis', *Front Microbiol*, 8: 269.

[110] Peng, G., Yan, Y., Zhu, C., Wang, S., Yan, X., Lu, L., Li, W., Hu, J., Wei, W., Mu, Y., Chen, Y., Feng, Y.*, et al.* (2008). 'Borna disease virus P protein affects neural transmission through interactions with gamma-aminobutyric acid receptor-associated protein', *J Virol*, 82(24): 12487-97.

[111] Mann, S. S. and Hammarback, J. A. (1994). 'Molecular characterization of light chain 3. A microtubule binding subunit of MAP1A and MAP1B', *J Biol Chem*, 269(15): 11492-7.

[112] Green, F., O'Hare, T., Blackwell, A. and Enns, C. A. (2002). 'Association of human transferrin receptor with GABARAP', *FEBS Lett*, 518(1-3): 101-6.

[113] Leidal, A. M., Huang, H. H., Marsh, T., Solvik, T., Zhang, D., Ye, J., Kai, F., Goldsmith, J., Liu, J. Y., Huang, Y. H., Monkkonen, T., Vlahakis, A.*, et al.* (2020). 'The LC3-conjugation machinery specifies the loading of RNA-binding proteins into extracellular vesicles', *Nat Cell Biol*, 22(2): 187-99.

[114] Coyle, J. E., Qamar, S., Rajashankar, K. R. and Nikolov, D. B. (2002). 'Structure of GABARAP in two conformations: implications for GABA(A) receptor localization and tubulin binding', *Neuron*, 33(1): 63-74.

[115] Lee, Y. K. and Lee, J. A. (2016). 'Role of the mammalian ATG8/LC3 family in autophagy: differential and compensatory roles in the spatiotemporal regulation of autophagy', *BMB Rep*, 49(8): 424-30.

[116] Matteoni, R. and Kreis, T. E. (1987). 'Translocation and clustering of endosomes and lysosomes depends on microtubules', *J Cell Biol*, 105(3): 1253-65.

[117] Jahreiss, L., Menzies, F. M. and Rubinsztein, D. C. (2008). 'The itinerary of autophagosomes: from peripheral formation to kiss-and-run fusion with lysosomes', *Traffic*, 9(4): 574-87.

[118] Lainez, S., Valente, P., Ontoria-Oviedo, I., Estevez-Herrera, J., Camprubi-Robles, M., Ferrer-Montiel, A. and Planells-Cases, R. (2010). 'GABAA receptor associated protein (GABARAP) modulates TRPV1 expression and channel function and desensitization', *FASEB J*, 24(6): 1958-70.

[119] Cook, J. L., Re, R. N., deHaro, D. L., Abadie, J. M., Peters, M. and Alam, J. (2008). 'The trafficking protein GABARAP binds to and enhances plasma membrane expression and function of the angiotensin II type 1 receptor', *Circ Res*, 102(12): 1539-47.

[120] Chen, C., Wang, Y., Huang, P. and Liu-Chen, L. Y. (2011). 'Effects of C-terminal modifications of GEC1 protein and gamma-aminobutyric acid type A (GABA(A)) receptor-associated protein (GABARAP), two microtubule-associated proteins, on kappa opioid receptor expression', *J Biol Chem*, 286(17): 15106-15.

[121] Kittler, J. T., Delmas, P., Jovanovic, J. N., Brown, D. A., Smart, T. G. and Moss, S. J. (2000). 'Constitutive endocytosis of GABAA receptors by an association with the adaptin AP2 complex modulates inhibitory synaptic currents in hippocampal neurons', *J Neurosci*, 20(21): 7972-7.

[122] Hanover, J. A., Willingham, M. C. and Pastan, I. (1984). 'Kinetics of transit of transferrin and epidermal growth factor through clathrin-coated membranes', *Cell*, 39(2 Pt 1): 283-93.

[123] Mohrlüder, J., Hoffmann, Y., Stangler, T., Hänel, K. and Willbold, D. (2007). 'Identification of clathrin heavy chain as a direct interaction partner for the gamma-aminobutyric acid type A receptor associated protein', *Biochemistry*, 46(50): 14537-43.

[124] Chen, Y., Sun, H. Q., Eichorst, J. P., Albanesi, J. P., Yin, H. and Mueller, J. D. (2018). 'Comobility of GABARAP and phosphatidylinositol 4-Kinase 2A on cytoplasmic vesicles', *Biochemistry*, 57(26): 3556-59.

[125] Albanesi, J., Wang, H., Sun, H. Q., Levine, B. and Yin, H. (2015). 'GABARAP-mediated targeting of PI4K2A/PI4KIIalpha to autophagosomes regulates PtdIns4P-dependent autophagosome-lysosome fusion', *Autophagy*, 11(11): 2127-29.

[126] Nakamura, T., Hayashi, T., Nasu-Nishimura, Y., Sakaue, F., Morishita, Y., Okabe, T., Ohwada, S., Matsuura, K. and Akiyama, T. (2008). 'PX-RICS mediates ER-to-Golgi transport of the N-cadherin/beta-catenin complex', *Genes Dev*, 22(9): 1244-56.

[127] Stangler, T., Mayr, L. M. and Willbold, D. (2002). 'Solution structure of human GABA(A) receptor-associated protein GABARAP: implications for biolgoical function and its regulation', *J Biol Chem*, 277(16): 13363-6.

[128] Mohrlüder, J., Schwarten, M. and Willbold, D. (2009). 'Structure and potential function of gamma-aminobutyrate type A receptor-associated protein', *FEBS J*, 276(18): 4989-5005.

[129] Rogov, V. V., Stolz, A., Ravichandran, A. C., Rios-Szwed, D. O., Suzuki, H., Kniss, A., Lohr, F., Wakatsuki, S., Dotsch, V., Dikic, I., Dobson, R. C. and McEwan, D. G. (2017). 'Structural and functional analysis of the GABARAP interaction motif (GIM)', *EMBO Rep*, 18(8): 1382-96.

[130] Park, I., Chung, J., Walsh, C. T., Yun, Y., Strominger, J. L. and Shin, J. (1995). 'Phosphotyrosine-independent binding of a 62-kDa protein to the src homology 2 (SH2) domain of p56lck and its regulation by phosphorylation of Ser-59 in the lck unique N-terminal region', *Proc Natl Acad Sci U S A*, 92(26): 12338-42.

[131] Pankiv, S., Clausen, T. H., Lamark, T., Brech, A., Bruun, J. A., Outzen, H., Overvatn, A., Bjorkoy, G. and Johansen, T. (2007). 'p62/SQSTM1 binds directly to Atg8/LC3 to facilitate degradation of ubiquitinated protein aggregates by autophagy', *J Biol Chem*, 282(33): 24131-45.

[132] Johansen, T. and Lamark, T. (2011). 'Selective autophagy mediated by autophagic adapter proteins', *Autophagy*, 7(3): 279-96.

[133] Bjorkoy, G., Lamark, T., Brech, A., Outzen, H., Perander, M., Overvatn, A., Stenmark, H. and Johansen, T. (2005). 'p62/SQSTM1 forms protein aggregates degraded by autophagy and has a protective effect on huntingtin-induced cell death', *J Cell Biol*, 171(4): 603-14.

[134] Kim, P. K., Hailey, D. W., Mullen, R. T. and Lippincott-Schwartz, J. (2008). 'Ubiquitin signals autophagic degradation of cytosolic proteins and peroxisomes', *Proc Natl Acad Sci U S A*, 105(52): 20567-74.

[135] Khaminets, A., Heinrich, T., Mari, M., Grumati, P., Huebner, A. K., Akutsu, M., Liebmann, L., Stolz, A., Nietzsche, S., Koch, N., Mauthe, M., Katona, I.*, et al.* (2015). 'Regulation of endoplasmic reticulum turnover by selective autophagy', *Nature*, 522(7556): 354-8.

[136] Wirth, M., Zhang, W., Razi, M., Nyoni, L., Joshi, D., O'Reilly, N., Johansen, T., Tooze, S. A. and Mouilleron, S. (2019). 'Molecular determinants regulating selective binding of autophagy adapters and receptors to ATG8 proteins', *Nat Commun*, 10(1): 2055.

[137] Li, J., Zhu, R., Chen, K., Zheng, H., Zhao, H., Yuan, C., Zhang, H., Wang, C. and Zhang, M. (2018). 'Potent and specific Atg8-targeting autophagy inhibitory peptides from giant ankyrins', *Nat Chem Biol*, 14(8): 778-87.

[138] Pankiv, S., Alemu, E. A., Brech, A., Bruun, J. A., Lamark, T., Overvatn, A., Bjorkoy, G. and Johansen, T. (2010). 'FYCO1 is a Rab7 effector that binds to LC3 and PI3P to mediate microtubule plus end-directed vesicle transport', *J Cell Biol*, 188(2): 253-69.

[139] Olsvik, H. L., Lamark, T., Takagi, K., Larsen, K. B., Evjen, G., Overvatn, A., Mizushima, T. and Johansen, T. (2015). 'FYCO1 contains a C-terminally extended, LC3A/B-preferring LC3-interacting region (LIR) motif required for efficient maturation of autophagosomes during basal autophagy', *J Biol Chem*, 290(49): 29361-74.

[140] Huber, J., Obata, M., Gruber, J., Akutsu, M., Lohr, F., Rogova, N., Guntert, P., Dikic, I., Kirkin, V., Komatsu, M., Dotsch, V. and Rogov, V. V. (2019). 'An atypical LIR motif within UBA5

(ubiquitin like modifier activating enzyme 5) interacts with GABARAP proteins and mediates membrane localization of UBA5', *Autophagy*: 1-15.

[141] Young, P., Deveraux, Q., Beal, R. E., Pickart, C. M. and Rechsteiner, M. (1998). 'Characterization of two polyubiquitin binding sites in the 26 S protease subunit 5a', *J Biol Chem*, 273(10): 5461-7.

[142] Hofmann, K. and Falquet, L. (2001). 'A ubiquitin-interacting motif conserved in components of the proteasomal and lysosomal protein degradation systems', *Trends Biochem Sci*, 26(6): 347-50.

[143] Marshall, R. S., Hua, Z., Mali, S., McLoughlin, F. and Vierstra, R. D. (2019). 'ATG8-binding UIM proteins define a new class of autophagy adaptors and receptors', *Cell*, 177(3): 766-81 e24.

[144] Herzog, L. K., Kevei, E., Marchante, R., Bottcher, C., Bindesboll, C., Lystad, A. H., Pfeiffer, A., Gierisch, M. E., Salomons, F. A., Simonsen, A., Hoppe, T. and Dantuma, N. P. (2019). 'The Machado-Joseph disease deubiquitylase ataxin-3 interacts with LC3C/GABARAP and promotes autophagy', *Aging Cell*, 19: e13051.

[145] Dobner, J., Simons, I.M., Rufinatscha K., Hänsch, S., Schwarten, M., Weiergräber, O. H., Abdollahzadeh, I., Gensch, T., Bode, J. G., Hoffmann, S., Willbold, D. (2020). 'Deficiency of GABARAP but not its paralogs causes enhanced EGF-induced EGFR degradation', *Cells*, 9(5): 1296.

[146] Jacomin, A. C., Samavedam, S., Promponas, V. and Nezis, I. P. (2016). 'iLIR database: A web resource for LIR motif-containing proteins in eukaryotes', *Autophagy*, 12(10): 1945-53.

[147] Fraser, J., Cabodevilla, A. G., Simpson, J. and Gammoh, N. (2017). 'Interplay of autophagy, receptor tyrosine kinase signalling and endocytic trafficking', *Essays Biochem*, 61(6): 597-607.

[148] Li, H., You, L., Xie, J., Pan, H. and Han, W. (2017). 'The roles of subcellularly located EGFR in autophagy', *Cell Signal*, 35: 223-30.

[149] Fraser, J., Simpson, J., Fontana, R., Kishi-Itakura, C., Ktistakis, N. T. and Gammoh, N. (2019). 'Targeting of early endosomes by autophagy facilitates EGFR recycling and signalling', *EMBO Rep*, 20(10): e47734.

[150] De Iuliis, V., Marino, A., Caruso, M., Capodifoglio, S., Flati, V., Marynuk, A., Marricareda, V., Ursi, S., Lanuti, P., Talora, C., Conti, P., Martinotti, S.*, et al.* (2018). 'Autophagy processes are dependent on EGF receptor signaling', *Oncotarget*, 9(54): 30289-303.

[151] Papandreou, M. E. and Tavernarakis, N. (2020). 'Crosstalk between endo/exocytosis and autophagy in health and disease', *Biotechnol J*: e1900267.

[152] Cohen, S., Carpenter, G. and King, L., Jr. (1980). 'Epidermal growth factor-receptor-protein kinase interactions. Co-purification of receptor and epidermal growth factor-enhanced phosphorylation activity', *J Biol Chem*, 255(10): 4834-42.

[153] Real, F. X., Rettig, W. J., Chesa, P. G., Melamed, M. R., Old, L. J. and Mendelsohn, J. (1986). 'Expression of epidermal growth factor receptor in human cultured cells and tissues: relationship to cell lineage and stage of differentiation', *Cancer Res*, 46(9): 4726-31.

[154] Chen, Jianchun, Zeng, Fenghua, Forrester, Steven J., Eguchi, Satoru, Zhang, Ming-Zhi and Harris, Raymond C. (2016). 'Expression and function of the epidermal growth factor receptor in physiology and disease', *Physiological Reviews*, 96(3): 1025-69.

[155] Bublil, E. M. and Yarden, Y. (2007). 'The EGF receptor family: spearheading a merger of signaling and therapeutics', *Curr Opin Cell Biol*, 19(2): 124-34.

[156] Sassen, A., Rochon, J., Wild, P., Hartmann, A., Hofstaedter, F., Schwarz, S. and Brockhoff, G. (2008). 'Cytogenetic analysis of HER1/EGFR, HER2, HER3 and HER4 in 278 breast cancer patients', *Breast Cancer Res*, 10(1): R2.

[157] Ullrich, A., Coussens, L., Hayflick, J. S., Dull, T. J., Gray, A., Tam, A. W., Lee, J., Yarden, Y., Libermann, T. A., Schlessinger, J., *et al.* (1984). 'Human epidermal growth factor receptor cDNA sequence and aberrant expression of the amplified gene in A431 epidermoid carcinoma cells', *Nature*, 309(5967): 418-25.

[158] Wee, P. and Wang, Z. (2017). 'Epidermal growth factor receptor cell proliferation signaling pathways', *Cancers (Basel)*, 9(5): 52.

[159] Ogiso, H., Ishitani, R., Nureki, O., Fukai, S., Yamanaka, M., Kim, J. H., Saito, K., Sakamoto, A., Inoue, M., Shirouzu, M. and Yokoyama, S. (2002). 'Crystal structure of the complex of human epidermal growth factor and receptor extracellular domains', *Cell*, 110(6): 775-87.

[160] Zhang, X., Gureasko, J., Shen, K., Cole, P. A. and Kuriyan, J. (2006). 'An allosteric mechanism for activation of the kinase domain of epidermal growth factor receptor', *Cell*, 125(6): 1137-49.

[161] Ferguson, K. M. (2008). 'Structure-based view of epidermal growth factor receptor regulation', *Annu Rev Biophys*, 37: 353-73.

[162] Kwon, Y., Kim, M., Jung, H. S., Kim, Y. and Jeoung, D. (2019). 'Targeting autophagy for overcoming resistance to anti-EGFR treatments', *Cancers (Basel)*, 11(9): 1374.

[163] Zanetti-Domingues, L. C., Korovesis, D., Needham, S. R., Tynan, C. J., Sagawa, S., Roberts, S. K., Kuzmanic, A., Ortiz-Zapater, E., Jain, P., Roovers, R. C., Lajevardipour, A., van Bergen En Henegouwen, P. M. P.*, et al.* (2018). 'The architecture of EGFR's basal complexes reveals autoinhibition mechanisms in dimers and oligomers', *Nat Commun*, 9(1): 4325.

[164] Jorissen, R. N., Walker, F., Pouliot, N., Garrett, T. P., Ward, C. W. and Burgess, A. W. (2003). 'Epidermal growth factor receptor: mechanisms of activation and signalling', *Exp Cell Res*, 284(1): 31-53.

[165] Schlessinger, J. (2000). 'Cell signaling by receptor tyrosine kinases', *Cell*, 103(2): 211-25.

[166] Freed, D. M., Bessman, N. J., Kiyatkin, A., Salazar-Cavazos, E., Byrne, P. O., Moore, J. O., Valley, C. C., Ferguson, K. M., Leahy, D. J., Lidke, D. S. and Lemmon, M. A. (2017). 'EGFR ligands differentially stabilize receptor dimers to specify signaling kinetics', *Cell*, 171(3): 683-95 e18.

[167] Ferguson, K. M., Darling, P. J., Mohan, M. J., Macatee, T. L. and Lemmon, M. A. (2000). 'Extracellular domains drive homo- but not hetero-dimerization of erbB receptors', *EMBO J*, 19(17): 4632-43.

[168] Schlessinger, J. (1988). 'Signal transduction by allosteric receptor oligomerization', *Trends Biochem Sci*, 13(11): 443-7.

[169] Roberts, A. B., Lamb, L. C., Newton, D. L., Sporn, M. B., De Larco, J. E. and Todaro, G. J. (1980). 'Transforming growth factors: isolation of polypeptides from virally and chemically transformed cells by acid/ethanol extraction', *Proc Natl Acad Sci U S A*, 77(6): 3494-8.

[170] Shoyab, M., Plowman, G. D., McDonald, V. L., Bradley, J. G. and Todaro, G. J. (1989). 'Structure and function of human amphiregulin: a member of the epidermal growth factor family', *Science*, 243(4894 Pt 1): 1074-6.

[171] Cohen, S. (1962). 'Isolation of a mouse submaxillary gland protein accelerating incisor eruption and eyelid opening in the new-born animal', *J Biol Chem*, 237: 1555-62.

[172] Honegger, A. M., Kris, R. M., Ullrich, A. and Schlessinger, J. (1989). 'Evidence that autophosphorylation of solubilized receptors for epidermal growth factor is mediated by intermolecular cross-phosphorylation', *Proc Natl Acad Sci U S A*, 86(3): 925-9.

[173] Lemmon, M. A., Schlessinger, J. and Ferguson, K. M. (2014). 'The EGFR family: not so prototypical receptor tyrosine kinases', *Cold Spring Harb Perspect Biol*, 6(4): a020768.

[174] Sierke, S. L., Longo, G. M. and Koland, J. G. (1993). 'Structural basis of interactions between epidermal growth factor receptor and SH2 domain proteins', *Biochem Biophys Res Commun*, 191(1): 45-54.

[175] Wagner, M. J., Stacey, M. M., Liu, B. A. and Pawson, T. (2013). 'Molecular mechanisms of SH2- and PTB-domain-containing proteins in receptor tyrosine kinase signaling', *Cold Spring Harb Perspect Biol*, 5(12): a008987.

[176] Yarden, Y. and Sliwkowski, M. X. (2001). 'Untangling the ErbB signalling network', *Nat Rev Mol Cell Biol*, 2(2): 127-37.

[177] Bjorge, J. D., Chan, T. O., Antczak, M., Kung, H. J. and Fujita, D. J. (1990). 'Activated type I phosphatidylinositol kinase is associated with the epidermal growth factor (EGF) receptor following EGF stimulation', *Proc Natl Acad Sci U S A*, 87(10): 3816-20.

[178] Freudlsperger, C., Burnett, J. R., Friedman, J. A., Kannabiran, V. R., Chen, Z. and Van Waes, C. (2011). 'EGFR-PI3K-AKT-mTOR signaling in head and neck squamous cell carcinomas: attractive targets for molecular-oriented therapy', *Expert Opin Ther Targets*, 15(1): 63-74.

[179] Anderson, N. G., Maller, J. L., Tonks, N. K. and Sturgill, T. W. (1990). 'Requirement for integration of signals from two distinct phosphorylation pathways for activation of MAP kinase', *Nature*, 343(6259): 651-3.

[180] Darnell, J. E., Jr., Kerr, I. M. and Stark, G. R. (1994). 'Jak-STAT pathways and transcriptional activation in response to IFNs and other extracellular signaling proteins', *Science*, 264(5164): 1415-21.

[181] Quesnelle, K. M., Boehm, A. L. and Grandis, J. R. (2007). 'STAT-mediated EGFR signaling in cancer', *J Cell Biochem*, 102(2): 311-9.

[182] Lemmon, M. A. and Schlessinger, J. (2010). 'Cell signaling by receptor tyrosine kinases', *Cell*, 141(7): 1117-34.

[183] Viegas, A., Yin, D. M., Borggräfe, J., Viennet, T., Falke, M., Schmitz, A., Famulok, M. and Etzkorn, M. (2020). 'Molecular architecture of a network of potential intracellular EGFR modulators: ARNO, CaM, phospholipids, and the juxtamembrane segment', *Structure*, 28(1): 54-62 e5.

[184] Li, X., Huang, Y., Jiang, J. and Frank, S. J. (2008). 'ERK-dependent threonine phosphorylation of EGF receptor modulates receptor downregulation and signaling', *Cell Signal*, 20(11): 2145-55.

[185] McLaughlin, S., Smith, S. O., Hayman, M. J. and Murray, D. (2005). 'An electrostatic engine model for autoinhibition and activation of the epidermal growth factor receptor (EGFR/ErbB) family', *J Gen Physiol*, 126(1): 41-53.

[186] Maeda, R., Sato, T., Okamoto, K., Yanagawa, M. and Sako, Y. (2018). 'Lipid-protein interplay in dimerization of juxtamembrane domains of epidermal growth factor receptor', *Biophys J*, 114(4): 893-903.

[187] Rayego-Mateos, S., Rodrigues-Diez, R., Morgado-Pascual, J. L., Valentijn, F., Valdivielso, J. M., Goldschmeding, R. and Ruiz-Ortega, M. (2018). 'Role of epidermal growth factor receptor (EGFR) and its ligands in kidney inflammation and damage', *Mediators Inflamm*, 2018: 8739473.

[188] Burke, P., Schooler, K. and Wiley, H. S. (2001). 'Regulation of epidermal growth factor receptor signaling by endocytosis and intracellular trafficking', *Mol Biol Cell*, 12(6): 1897-910.

[189] Avraham, R. and Yarden, Y. (2011). 'Feedback regulation of EGFR signalling: decision making by early and delayed loops', *Nat Rev Mol Cell Biol*, 12(2): 104-17.

[190] Sigismund, S., Woelk, T., Puri, C., Maspero, E., Tacchetti, C., Transidico, P., Di Fiore, P. P. and Polo, S. (2005). 'Clathrin-independent endocytosis of ubiquitinated cargos', *Proc Natl Acad Sci U S A*, 102(8): 2760-5.

[191] Sigismund, S., Argenzio, E., Tosoni, D., Cavallaro, E., Polo, S. and Di Fiore, P. P. (2008). 'Clathrin-mediated internalization is essential for sustained EGFR signaling but dispensable for degradation', *Dev Cell*, 15(2): 209-19.

[192] de Melker, A. A., van der Horst, G., Calafat, J., Jansen, H. and Borst, J. (2001). 'c-Cbl ubiquitinates the EGF receptor at the plasma membrane and remains receptor associated throughout the endocytic route', *J Cell Sci*, 114(Pt 11): 2167-78.

[193] Levkowitz, G., Klapper, L. N., Tzahar, E., Freywald, A., Sela, M. and Yarden, Y. (1996). 'Coupling of the c-Cbl protooncogene product to ErbB-1/EGF-receptor but not to other ErbB proteins', *Oncogene*, 12(5): 1117-25.

[194] Levkowitz, G., Waterman, H., Zamir, E., Kam, Z., Oved, S., Langdon, W. Y., Beguinot, L., Geiger, B. and Yarden, Y. (1998). 'c-Cbl/Sli-1 regulates endocytic sorting and ubiquitination of the epidermal growth factor receptor', *Genes Dev*, 12(23): 3663-74.

[195] de Melker, A. A., van der Horst, G. and Borst, J. (2004). 'c-Cbl directs EGF receptors into an endocytic pathway that involves the ubiquitin-interacting motif of Eps15', *J Cell Sci*, 117(Pt 21): 5001-12.

[196] Jiang, X., Huang, F., Marusyk, A. and Sorkin, A. (2003). 'Grb2 regulates internalization of EGF receptors through clathrin-coated pits', *Mol Biol Cell*, 14(3): 858-70.

[197] Benmerah, A., Lamaze, C., Begue, B., Schmid, S. L., Dautry-Varsat, A. and Cerf-Bensussan, N. (1998). 'AP-2/Eps15 interaction is required for receptor-mediated endocytosis', *J Cell Biol*, 140(5): 1055-62.

[198] Chen, H., Fre, S., Slepnev, V. I., Capua, M. R., Takei, K., Butler, M. H., Di Fiore, P. P. and De Camilli, P. (1998). 'Epsin is an EH-domain-binding protein implicated in clathrin-mediated endocytosis', *Nature*, 394(6695): 793-7.

[199] Katzmann, D. J., Babst, M. and Emr, S. D. (2001). 'Ubiquitin-dependent sorting into the multivesicular body pathway requires the function of a conserved endosomal protein sorting complex, ESCRT-I', *Cell*, 106(2): 145-55.

[200] Reggiori, F. and Pelham, H. R. (2001). 'Sorting of proteins into multivesicular bodies: ubiquitin-dependent and -independent targeting', *EMBO J*, 20(18): 5176-86.

[201] Urbanowski, J. L. and Piper, R. C. (2001). 'Ubiquitin sorts proteins into the intralumenal degradative compartment of the late-endosome/vacuole', *Traffic*, 2(9): 622-30.

[202] Haglund, K. and Dikic, I. (2012). 'The role of ubiquitylation in receptor endocytosis and endosomal sorting', *J Cell Sci*, 125(Pt 2): 265-75.

[203] Futter, C. E., Pearse, A., Hewlett, L. J. and Hopkins, C. R. (1996). 'Multivesicular endosomes containing internalized EGF-EGF receptor complexes mature and then fuse directly with lysosomes', *J Cell Biol*, 132(6): 1011-23.

[204] Longva, K. E., Blystad, F. D., Stang, E., Larsen, A. M., Johannessen, L. E. and Madshus, I. H. (2002). 'Ubiquitination and proteasomal activity is required for transport of the EGF receptor to inner membranes of multivesicular bodies', *J Cell Biol*, 156(5): 843-54.

[205] Xu, S. W., Law, B. Y., Mok, S. W., Leung, E. L., Fan, X. X., Coghi, P. S., Zeng, W., Leung, C. H., Ma, D. L., Liu, L. and Wong, V. K. (2016). 'Autophagic degradation of epidermal growth factor receptor in gefitinib-resistant lung cancer by celastrol', *Int J Oncol*, 49(4): 1576-88.

[206] Eden, E. R., Huang, F., Sorkin, A. and Futter, C. E. (2012). 'The role of EGF receptor ubiquitination in regulating its intracellular traffic', *Traffic*, 13(2): 329-37.

[207] Waterman, H. and Yarden, Y. (2001). 'Molecular mechanisms underlying endocytosis and sorting of ErbB receptor tyrosine kinases', *FEBS Lett*, 490(3): 142-52.

[208] Schade, A. L. and Caroline, L. (1946). 'An iron-binding component in human blood plasma', *Science*, 104(2702): 340-1.

[209] Schade, A. L., Reinhart, R. W. and Levy, H. (1949). 'Carbon dioxide and oxygen in complex formation with iron and siderophilin, the iron-binding component of human plasma', *Arch Biochem*, 20(1): 170-2.

[210] Jandl, J. H. and Katz, J. H. (1963). 'The plasma-to-cell cycle of transferrin', *J Clin Invest*, 42: 314-26.

[211] Karin, M. and Mintz, B. (1981). 'Receptor-mediated endocytosis of transferrin in developmentally totipotent mouse teratocarcinoma stem cells', *J Biol Chem*, 256(7): 3245-52.

[212] Dautry-Varsat, A., Ciechanover, A. and Lodish, H. F. (1983). 'pH and the recycling of transferrin during receptor-mediated endocytosis', *Proc Natl Acad Sci U S A*, 80(8): 2258-62.

[213] Willingham, M. C., Hanover, J. A., Dickson, R. B. and Pastan, I. (1984). 'Morphologic characterization of the pathway of transferrin endocytosis and recycling in human KB cells', *Proc Natl Acad Sci U S A*, 81(1): 175-9.

[214] Touchot, N., Chardin, P. and Tavitian, A. (1987). 'Four additional members of the ras gene superfamily isolated by an oligonucleotide strategy: molecular cloning of YPT-related cDNAs from a rat brain library', *Proc Natl Acad Sci U S A*, 84(23): 8210-4.

[215] Salminen, A. and Novick, P. J. (1987). 'A ras-like protein is required for a post-Golgi event in yeast secretion', *Cell*, 49(4): 527-38.

[216] Pfeffer, S. R. (2013). 'Rab GTPase regulation of membrane identity', *Curr Opin Cell Biol*, 25(4): 414-9.

[217] Guadagno, N. A. and Progida, C. (2019). 'Rab GTPases: switching to human diseases', *Cells*, 8(8): 909.

[218] Pfeffer, S. R. (1992). 'GTP-binding proteins in intracellular transport', *Trends Cell Biol*, 2(2): 41-6.

[219] Pfeffer, S. R. (1994). 'Rab GTPases: master regulators of membrane trafficking', *Curr Opin Cell Biol*, 6(4): 522-6.

[220] Pylypenko, O., Hammich, H., Yu, I. M. and Houdusse, A. (2018). 'Rab GTPases and their interacting protein partners: Structural insights into Rab functional diversity', *Small GTPases*, 9(1-2): 22-48.

[221] Stenmark, H. and Olkkonen, V. M. (2001). 'The Rab GTPase family', *Genome Biol*, 2(5): reviews3007.1–07.7.

[222] Stenmark, H., Parton, R. G., Steele-Mortimer, O., Lutcke, A., Gruenberg, J. and Zerial, M. (1994). 'Inhibition of rab5 GTPase activity stimulates membrane fusion in endocytosis', *EMBO J*, 13(6): 1287-96.

[223] Andres, D. A., Seabra, M. C., Brown, M. S., Armstrong, S. A., Smeland, T. E., Cremers, F. P. and Goldstein, J. L. (1993). 'cDNA cloning of component A of Rab geranylgeranyl transferase and demonstration of its role as a Rab escort protein', *Cell*, 73(6): 1091-9.

[224] Magee, T. and Newman, C. (1992). 'The role of lipid anchors for small G proteins in membrane trafficking', *Trends Cell Biol*, 2(11): 318-23.

[225] Pfeffer, S. R., Dirac-Svejstrup, A. B. and Soldati, T. (1995). 'Rab GDP dissociation inhibitor: putting rab GTPases in the right place', *J Biol Chem*, 270(29): 17057-9.

[226] Itzen, A. and Goody, R. S. (2011). 'GTPases involved in vesicular trafficking: structures and mechanisms', *Semin Cell Dev Biol*, 22(1): 48-56.

[227] Popovic, D., Akutsu, M., Novak, I., Harper, J. W., Behrends, C. and Dikic, I. (2012). 'Rab GTPase-activating proteins in autophagy: regulation of endocytic and autophagy pathways by direct binding to human ATG8 modifiers', *Mol Cell Biol*, 32(9): 1733-44.

[228] Chavrier, P., Parton, R. G., Hauri, H. P., Simons, K. and Zerial, M. (1990). 'Localization of low molecular weight GTP binding proteins to exocytic and endocytic compartments', *Cell*, 62(2): 317-29.

[229] Ullrich, O., Reinsch, S., Urbe, S., Zerial, M. and Parton, R. G. (1996). 'Rab11 regulates recycling through the pericentriolar recycling endosome', *J Cell Biol*, 135(4): 913-24.

[230] Hutagalung, A. H. and Novick, P. J. (2011). 'Role of Rab GTPases in membrane traffic and cell physiology', *Physiol Rev*, 91(1): 119-49.

[231] Puri, C., Vicinanza, M. and Rubinsztein, D. C. (2018). 'Phagophores evolve from recycling endosomes', *Autophagy*, 14(8): 1475-77.

[232] Puri, C., Vicinanza, M., Ashkenazi, A., Gratian, M. J., Zhang, Q., Bento, C. F., Renna, M., Menzies, F. M. and Rubinsztein, D. C. (2018). 'The RAB11A-positive compartment is a primary platform for autophagosome assembly mediated by WIPI2 recognition of PI3P-RAB11A', *Dev Cell*, 45(1): 114-31 e8.

[233] Wei, Y., Zou, Z., Becker, N., Anderson, M., Sumpter, R., Xiao, G., Kinch, L., Koduru, P., Christudass, C. S., Veltri, R. W., Grishin, N. V., Peyton, M.*, et al.* (2013). 'EGFR-mediated Beclin 1 phosphorylation in autophagy suppression, tumor progression, and tumor chemoresistance', *Cell*, 154(6): 1269-84.

[234] Moriya, H. (2015). 'Quantitative nature of overexpression experiments', *Mol Biol Cell*, 26(22): 3932-9.

[235] Lamark, T. and Johansen, T. (2012). 'Aggrephagy: selective disposal of protein aggregates by macroautophagy', *Int J Cell Biol*, 2012: 736905.

[236] Mareninova, O. A., Jia, W., Gretler, S. R., Holthaus, C. L., Thomas, D. D. H., Pimienta, M., Dillon, D. L., Gukovskaya, A. S., Gukovsky, I. and Groblewski, G. E. (2020). 'Transgenic expression of GFP-LC3 perturbs autophagy in exocrine pancreas and acute pancreatitis responses in mice', *Autophagy*: 1-14.

[237] Meliopoulos, V. A. and Schultz-Cherry, S. (2018). 'Although it's painful: The importance of stringent antibody validation', *PLoS Pathog*, 14(1): e1006701.

[238] Rink, L., Kruse, A. and Haase, H. (2012). 'Immunologie für Einsteiger.', 5. Auflage, (Spektrum Akademischer Verlag: Heidelberg): 89-97; 115-118

[239] Alberts, B., Johnson, A., Lewis, J., Raff, M., Roberts, K., Walter, P. and Jaenicke, L. (2004). 'Molekularbiologie der Zelle.', 4. Auflage (Wiley-VCH Verlag GmbH & Co. KGaA: Weinheim): 551-553; 1607-1618

[240] Willingham, M. C. (1999). 'Conditional epitopes. Is your antibody always specific?', *J Histochem Cytochem*, 47(10): 1233-6.

[241] Baker, M. (2015). 'Reproducibility crisis: Blame it on the antibodies', *Nature*, 521(7552): 274-6.

[242] Lund-Johansen, F. and Browning, M. D. (2017). 'Should we ignore western blots when selecting antibodies for other applications?', *Nat Methods*, 14(3): 215.

[243] Ran, F. A., Hsu, P. D., Wright, J., Agarwala, V., Scott, D. A. and Zhang, F. (2013). 'Genome engineering using the CRISPR-Cas9 system', *Nat Protoc*, 8(11): 2281-308.

[244] Doudna, J. A. and Sontheimer, E. J. (2014). 'Methods in Enzymology. The use of CRISPR/Cas9, ZFNs, and TALENs in generating site-specific genome alterations. Preface', *Methods Enzymol*, 546: xix-xx.

[245] Klermund, J. and Cathomen, T. (2019). 'Grundlagen und klinische Anwendung der Genomeditierung', *Monatsschrift Kinderheilkunde*, 168(1): 39-46.

[246] Gaj, T., Gersbach, C. A. and Barbas, C. F., 3rd (2013). 'ZFN, TALEN, and CRISPR/Cas-based methods for genome engineering', *Trends Biotechnol*, 31(7): 397-405.

[247] Rodgers, K. and McVey, M. (2016). 'Error-prone repair of DNA double-strand breaks', *J Cell Physiol*, 231(1): 15-24.

[248] Doudna, J. A. (2020). 'The promise and challenge of therapeutic genome editing', *Nature*, 578(7794): 229-36.

[249] Jinek, M., Chylinski, K., Fonfara, I., Hauer, M., Doudna, J. A. and Charpentier, E. (2012). 'A programmable dual-RNA-guided DNA endonuclease in adaptive bacterial immunity', *Science*, 337(6096): 816-21.

[250] Kim, Y. G., Cha, J. and Chandrasegaran, S. (1996). 'Hybrid restriction enzymes: zinc finger fusions to Fok I cleavage domain', *Proc Natl Acad Sci U S A*, 93(3): 1156-60.

[251] Stepanenko, A. A. and Dmitrenko, V. V. (2015). 'HEK293 in cell biology and cancer research: phenotype, karyotype, tumorigenicity, and stress-induced genome-phenotype evolution', *Gene*, 569(2): 182-90.

[252] Essletzbichler, P., Konopka, T., Santoro, F., Chen, D., Gapp, B. V., Kralovics, R., Brummelkamp, T. R., Nijman, S. M. and Burckstummer, T. (2014). 'Megabase-scale deletion using CRISPR/Cas9 to generate a fully haploid human cell line', *Genome Res*, 24(12): 2059-65.

[253] Vouillot, L., Thelie, A. and Pollet, N. (2015). 'Comparison of T7E1 and surveyor mismatch cleavage assays to detect mutations triggered by engineered nucleases', *G3 (Bethesda)*, 5(3): 407-15.

[254] Parkinson, M. J. and Lilley, D. M. (1997). 'The junction-resolving enzyme T7 endonuclease I: quaternary structure and interaction with DNA', *J Mol Biol*, 270(2): 169-78.

[255] White, M. F., Giraud-Panis, M. J., Pohler, J. R. and Lilley, D. M. (1997). 'Recognition and manipulation of branched DNA structure by junction-resolving enzymes', *J Mol Biol*, 269(5): 647-64.

[256] Guschin, D. Y., Waite, A. J., Katibah, G. E., Miller, J. C., Holmes, M. C. and Rebar, E. J. (2010). 'A rapid and general assay for monitoring endogenous gene modification', *Methods Mol Biol*, 649: 247-56.

[257] Brinkman, E. K., Chen, T., Amendola, M. and van Steensel, B. (2014). 'Easy quantitative assessment of genome editing by sequence trace decomposition', *Nucleic Acids Res*, 42(22): e168.

[258] Brogna, S. and Wen, J. (2009). 'Nonsense-mediated mRNA decay (NMD) mechanisms', *Nat Struct Mol Biol*, 16(2): 107-13.

[259] Hoppen, C. (2015). 'Ausschalten humaner Atg8 Paraloge durch CRISPR/Cas9 vermittelter Genom-Editierung', *Heinrich-Heine-Universität Düsseldorf*.

[260] Lipman, N. S., Jackson, L. R., Trudel, L. J. and Weis-Garcia, F. (2005). 'Monoclonal versus polyclonal antibodies: distinguishing characteristics, applications, and information resources', *ILAR J*, 46(3): 258-68.

[261] Köhler, G. and Milstein, C. (1975). 'Continuous cultures of fused cells secreting antibody of predefined specificity', *Nature*, 256(5517): 495-7.

[262] Greenfield, E. A. (2018). 'Polyethylene Glycol Fusion for Hybridoma Production', *Cold Spring Harb Protoc*, 2018(3).

[263] Kennett, R. G. (1979). 'Monoclonal antibodies. Hybrid myelomas - a revolution in serology and immunogenetics', *Am J Hum Genet*, 31(5): 539-47.

[264] Steinitz, M. (2009). 'Three decades of human monoclonal antibodies: past, present and future developments', *Hum Antibodies*, 18(1-2): 1-10.

[265] Michnick, S. W. and Sidhu, S. S. (2008). 'Submitting antibodies to binding arbitration', *Nat Chem Biol*, 4(6): 326-9.

[266] Grunow, R., D'Apuzzo, M., Wyss-Coray, T., Frutig, K. and Pichler, W. J. (1994). 'A cell surface ELISA for the screening of monoclonal antibodies to antigens on viable cells in suspension', *J Immunol Methods*, 171(1): 93-102.

[267] Simons, I. M., Mohrlüder, J., Feederle, R., Kremmer, E., Zobel, T., Dobner, J., Bleffert, N., Hoffmann, S. and Willbold, D. (2019). 'The highly GABARAP specific rat monoclonal antibody 8H5 visualizes GABARAP in immunofluorescence imaging at endogenous levels', *Sci Rep*, 9(1): 526.

[268] Vidarsson, G., Dekkers, G. and Rispens, T. (2014). 'IgG subclasses and allotypes: from structure to effector functions', *Front Immunol*, 5: 520.

[269] Murphy, K.M. (2011). 'Janeway's Immunobiology.', 8. Edition (Taylor & Francis Group: New York, USA; Abingdon, UK): 134-153; 173-179

[270] Hudson, P. J. and Souriau, C. (2003). 'Engineered antibodies', *Nat Med*, 9(1): 129-34.

[271] Holliger, P. and Hudson, P. J. (2005). 'Engineered antibody fragments and the rise of single domains', *Nat Biotechnol*, 23(9): 1126-36.

[272] Flanagan, Robert J. and Jones, Alison L. (2004). 'Fab antibody fragments', *Drug Safety*, 27(14): 1115-33.

[273] Cormack, B. P., Valdivia, R. H. and Falkow, S. (1996). 'FACS-optimized mutants of the green fluorescent protein (GFP)', *Gene*, 173(1 Spec No): 33-8.

[274] Zhang, G., Gurtu, V. and Kain, S. R. (1996). 'An enhanced green fluorescent protein allows sensitive detection of gene transfer in mammalian cells', *Biochem Biophys Res Commun*, 227(3): 707-11.

[275] Heim, R. and Tsien, R. Y. (1996). 'Engineering green fluorescent protein for improved brightness, longer wavelengths and fluorescence resonance energy transfer', *Curr Biol*, 6(2): 178-82.

[276] Heim, R., Prasher, D. C. and Tsien, R. Y. (1994). 'Wavelength mutations and posttranslational autoxidation of green fluorescent protein', *Proc Natl Acad Sci U S A*, 91(26): 12501-4.

[277] Tsien, R. Y. (1998). 'The green fluorescent protein', *Annu Rev Biochem*, 67: 509-44.

[278] Shaner, N. C., Campbell, R. E., Steinbach, P. A., Giepmans, B. N., Palmer, A. E. and Tsien, R. Y. (2004). 'Improved monomeric red, orange and yellow fluorescent proteins derived from Discosoma sp. red fluorescent protein', *Nat Biotechnol*, 22(12): 1567-72.

[279] Schindelin, J., Arganda-Carreras, I., Frise, E., Kaynig, V., Longair, M., Pietzsch, T., Preibisch, S., Rueden, C., Saalfeld, S., Schmid, B., Tinevez, J. Y., White, D. J.*, et al.* (2012). 'Fiji: an open-source platform for biological-image analysis', *Nat Methods*, 9(7): 676-82.

[280] Wang, H., Sun, H. Q., Zhu, X., Zhang, L., Albanesi, J., Levine, B. and Yin, H. (2015). 'GABARAPs regulate PI4P-dependent autophagosome:lysosome fusion', *Proc Natl Acad Sci U S A*, 112(22): 7015-20.

[281] Skogs, M., Stadler, C., Schutten, R., Hjelmare, M., Gnann, C., Bjork, L., Poser, I., Hyman, A., Uhlen, M. and Lundberg, E. (2017). 'Antibody validation in bioimaging applications based on endogenous expression of tagged proteins', *J Proteome Res*, 16(1): 147-55.

[282] Mizushima, N. and Levine, B. (2010). 'Autophagy in mammalian development and differentiation', *Nat Cell Biol*, 12(9): 823-30.

[283] Cassidy, L. D., Young, A. R., Perez-Mancera, P. A., Nimmervoll, B., Jaulim, A., Chen, H. C., McIntyre, D. J. O., Brais, R., Ricketts, T., Pacey, S., De La Roche, M., Gilbertson, R. J.*, et al.*

(2018). 'A novel Atg5-shRNA mouse model enables temporal control of Autophagy in vivo', *Autophagy*, 14(7): 1256-66.

[284] El-Brolosy, M. A. and Stainier, D. Y. R. (2017). 'Genetic compensation: A phenomenon in search of mechanisms', *PLoS Genet*, 13(7): e1006780.

[285] Kauffman, K. J., Yu, S., Jin, J., Mugo, B., Nguyen, N., O'Brien, A., Nag, S., Lystad, A. H. and Melia, T. J. (2018). 'Delipidation of mammalian Atg8-family proteins by each of the four ATG4 proteases', *Autophagy*, 14(6): 992-1010.

[286] Lelimousin, M., Noirclerc-Savoye, M., Lazareno-Saez, C., Paetzold, B., Le Vot, S., Chazal, R., Macheboeuf, P., Field, M. J., Bourgeois, D. and Royant, A. (2009). 'Intrinsic dynamics in ECFP and Cerulean control fluorescence quantum yield', *Biochemistry*, 48(42): 10038-46.

[287] Yang, T. T., Sinai, P., Green, G., Kitts, P. A., Chen, Y. T., Lybarger, L., Chervenak, R., Patterson, G. H., Piston, D. W. and Kain, S. R. (1998). 'Improved fluorescence and dual color detection with enhanced blue and green variants of the green fluorescent protein', *J Biol Chem*, 273(14): 8212-6.

[288] Piatkevich, K. D., Jung, E. E., Straub, C., Linghu, C., Park, D., Suk, H. J., Hochbaum, D. R., Goodwin, D., Pnevmatikakis, E., Pak, N., Kawashima, T., Yang, C. T.*, et al.* (2018). 'A robotic multidimensional directed evolution approach applied to fluorescent voltage reporters', *Nat Chem Biol*, 14(4): 352-60.

[289] Ran, F. A., Hsu, P. D., Lin, C. Y., Gootenberg, J. S., Konermann, S., Trevino, A. E., Scott, D. A., Inoue, A., Matoba, S., Zhang, Y. and Zhang, F. (2013). 'Double nicking by RNA-guided CRISPR Cas9 for enhanced genome editing specificity', *Cell*, 154(6): 1380-9.

[290] Aluigi, M., Fogli, M., Curti, A., Isidori, A., Gruppioni, E., Chiodoni, C., Colombo, M. P., Versura, P., D'Errico-Grigioni, A., Ferri, E., Baccarani, M. and Lemoli, R. M. (2006). 'Nucleofection is an efficient nonviral transfection technique for human bone marrow-derived mesenchymal stem cells', *Stem Cells*, 24(2): 454-61.

[291] Siemen, H., Nix, M., Endl, E., Koch, P., Itskovitz-Eldor, J. and Brustle, O. (2005). 'Nucleofection of human embryonic stem cells', *Stem Cells Dev*, 14(4): 378-83.

[292] Couchman, J. R. (2009). 'Commercial antibodies: the good, bad, and really ugly', *J Histochem Cytochem*, 57(1): 7-8.

[293] Bordeaux, J., Welsh, A., Agarwal, S., Killiam, E., Baquero, M., Hanna, J., Anagnostou, V. and Rimm, D. (2010). 'Antibody validation', *Biotechniques*, 48(3): 197-209.

[294] Uhlen, M., Bandrowski, A., Carr, S., Edwards, A., Ellenberg, J., Lundberg, E., Rimm, D. L., Rodriguez, H., Hiltke, T., Snyder, M. and Yamamoto, T. (2016). 'A proposal for validation of antibodies', *Nat Methods*, 13(10): 823-7.

[295] Koukourakis, M. I., Kalamida, D., Giatromanolaki, A., Zois, C. E., Sivridis, E., Pouliliou, S., Mitrakas, A., Gatter, K. C. and Harris, A. L. (2015). 'Autophagosome proteins LC3A, LC3B and LC3C have distinct subcellular distribution kinetics and expression in cancer cell lines', *PLoS One*, 10(9): e0137675.

[296] Brown, M. C., Joaquim, T. R., Chambers, R., Onisk, D. V., Yin, F., Moriango, J. M., Xu, Y., Fancy, D. A., Crowgey, E. L., He, Y., Stave, J. W. and Lindpaintner, K. (2011). 'Impact of immunization technology and assay application on antibody performance - a systematic comparative evaluation', *PLoS One*, 6(12): e28718.

[297] Lee, B. S., Huang, J. S., Jayathilaka, L. P., Lee, J. and Gupta, S. (2016). 'Antibody Production with Synthetic Peptides', *Methods Mol Biol*, 1474: 25-47.

[298] Laver, W. G., Air, G. M., Webster, R. G. and Smith-Gill, S. J. (1990). 'Epitopes on protein antigens: misconceptions and realities', *Cell*, 61(4): 553-6.

[299] Bates, M. K., Zhang, G., Sebestyen, M. G., Neal, Z. C., Wolff, J. A. and Herweijer, H. (2006). 'Genetic immunization for antibody generation in research animals by intravenous delivery of plasmid DNA', *Biotechniques*, 40(2): 199-208.

[300] Ries, J., Kaplan, C., Platonova, E., Eghlidi, H. and Ewers, H. (2012). 'A simple, versatile method for GFP-based super-resolution microscopy via nanobodies', *Nat Methods*, 9(6): 582-4.

[301] Virant, D., Traenkle, B., Maier, J., Kaiser, P. D., Bodenhofer, M., Schmees, C., Vojnovic, I., Pisak-Lukats, B., Endesfelder, U. and Rothbauer, U. (2018). 'A peptide tag-specific nanobody enables high-quality labeling for dSTORM imaging', *Nat Commun*, 9(1): 930.

[302] Moore, R. P. and Legant, W. R. (2018). 'Improving probes for super-resolution', *Nat Methods*, 15(9): 659-60.

[303] Platonova, E., Winterflood, C. M., Junemann, A., Albrecht, D., Faix, J. and Ewers, H. (2015). 'Single-molecule microscopy of molecules tagged with GFP or RFP derivatives in mammalian cells using nanobody binders', *Methods*, 88: 89-97.

[304] Betzig, E., Patterson, G. H., Sougrat, R., Lindwasser, O. W., Olenych, S., Bonifacino, J. S., Davidson, M. W., Lippincott-Schwartz, J. and Hess, H. F. (2006). 'Imaging intracellular fluorescent proteins at nanometer resolution', *Science*, 313(5793): 1642-5.

[305] Patterson, G. H. and Lippincott-Schwartz, J. (2002). 'A photoactivatable GFP for selective photolabeling of proteins and cells', *Science*, 297(5588): 1873-7.

[306] Gurskaya, N. G., Verkhusha, V. V., Shcheglov, A. S., Staroverov, D. B., Chepurnykh, T. V., Fradkov, A. F., Lukyanov, S. and Lukyanov, K. A. (2006). 'Engineering of a monomeric green-to-red photoactivatable fluorescent protein induced by blue light', *Nat Biotechnol*, 24(4): 461-5.

[307] Hamers-Casterman, C., Atarhouch, T., Muyldermans, S., Robinson, G., Hamers, C., Songa, E. B., Bendahman, N. and Hamers, R. (1993). 'Naturally occurring antibodies devoid of light chains', *Nature*, 363(6428): 446-8.

[308] Bolte, S. and Cordelieres, F. P. (2006). 'A guided tour into subcellular colocalization analysis in light microscopy', *J Microsc*, 224(Pt 3): 213-32.

[309] Dunn, K. W., Kamocka, M. M. and McDonald, J. H. (2011). 'A practical guide to evaluating colocalization in biological microscopy', *Am J Physiol Cell Physiol*, 300(4): C723-42.

[310] Zinchuk, V., Zinchuk, O. and Okada, T. (2007). 'Quantitative colocalization analysis of multicolor confocal immunofluorescence microscopy images: pushing pixels to explore biological phenomena', *Acta Histochem Cytochem*, 40(4): 101-11.

[311] Waters, J. C. (2009). 'Accuracy and precision in quantitative fluorescence microscopy', *J Cell Biol*, 185(7): 1135-48.

[312] Lee, Jen-Yi, Kitaoka, Maiko and Drubin, David G. (2018). 'A beginner's guide to rigor and reproducibility in fluorescence imaging experiments', *Molecular Biology of the Cell*, 29(13): 1519-25.

[313] Arppe, R., Carro-Temboury, M. R., Hempel, C., Vosch, T. and Just Sorensen, T. (2017). 'Investigating dye performance and crosstalk in fluorescence enabled bioimaging using a model system', *PLoS One*, 12(11): e0188359.

[314] Marriott, G.; Parker, I. (2003). 'Biophotonics Part A. Methods in Enzymology.', 360 (Academic Press: San Diego, CA)

[315] Frigault, M. M., Lacoste, J., Swift, J. L. and Brown, C. M. (2009). 'Live-cell microscopy - tips and tools', *J Cell Sci*, 122(Pt 6): 753-67.

[316] Kneen, M., Farinas, J., Li, Y. and Verkman, A. S. (1998). 'Green fluorescent protein as a noninvasive intracellular pH indicator', *Biophys J*, 74(3): 1591-9.

[317] Sanwald, J. L., Poschmann, G., Stühler, K., Behrends, C., Hoffmann, S. and Willbold, D. (2020). 'The GABARAP co-secretome identified by APEX2-GABARAP proximity labelling of extracellular vesicles', *Cells*, 9(6): 1468.

[318] Dunn, K. W. and Maxfield, F. R. (1992). 'Delivery of ligands from sorting endosomes to late endosomes occurs by maturation of sorting endosomes', *J Cell Biol*, 117(2): 301-10.

[319] Johnson, L. S., Dunn, K. W., Pytowski, B. and McGraw, T. E. (1993). 'Endosome acidification and receptor trafficking: bafilomycin A1 slows receptor externalization by a mechanism involving the receptor's internalization motif', *Mol Biol Cell*, 4(12): 1251-66.

[320] Maxfield, F. R. and McGraw, T. E. (2004). 'Endocytic recycling', *Nat Rev Mol Cell Biol*, 5(2): 121-32.

[321] Presley, J. F., Mayor, S., McGraw, T. E., Dunn, K. W. and Maxfield, F. R. (1997). 'Bafilomycin A1 treatment retards transferrin receptor recycling more than bulk membrane recycling', *J Biol Chem*, 272(21): 13929-36.

[322] Madshus, I. H. and Stang, E. (2009). 'Internalization and intracellular sorting of the EGF receptor: a model for understanding the mechanisms of receptor trafficking', *J Cell Sci*, 122(Pt 19): 3433-9.

[323] Gautier, A., Juillerat, A., Heinis, C., Correa, I. R., Jr., Kindermann, M., Beaufils, F. and Johnsson, K. (2008). 'An engineered protein tag for multiprotein labeling in living cells', *Chem Biol*, 15(2): 128-36.

[324] Pellett, P. A., Sun, X., Gould, T. J., Rothman, J. E., Xu, M. Q., Correa, I. R., Jr. and Bewersdorf, J. (2011). 'Two-color STED microscopy in living cells', *Biomed Opt Express*, 2(8): 2364-71.

[325] Los, G. V., Encell, L. P., McDougall, M. G., Hartzell, D. D., Karassina, N., Zimprich, C., Wood, M. G., Learish, R., Ohana, R. F., Urh, M., Simpson, D., Mendez, J.*, et al.* (2008). 'HaloTag: a novel protein labeling technology for cell imaging and protein analysis', *ACS Chem Biol*, 3(6): 373-82.

[326] Lukinavicius, G., Umezawa, K., Olivier, N., Honigmann, A., Yang, G., Plass, T., Mueller, V., Reymond, L., Correa, I. R., Jr., Luo, Z. G., Schultz, C., Lemke, E. A.*, et al.* (2013). 'A near-infrared fluorophore for live-cell super-resolution microscopy of cellular proteins', *Nat Chem*, 5(2): 132-9.

[327] Kittler, J. T., Rostaing, P., Schiavo, G., Fritschy, J. M., Olsen, R., Triller, A. and Moss, S. J. (2001). 'The subcellular distribution of GABARAP and its ability to interact with NSF suggest a role for this protein in the intracellular transport of GABA(A) receptors', *Mol Cell Neurosci*, 18(1): 13-25.

[328] Popovic, D. and Dikic, I. (2014). 'TBC1D5 and the AP2 complex regulate ATG9 trafficking and initiation of autophagy', *EMBO Rep*, 15(4): 392-401.

[329] Kern, A., Dikic, I. and Behl, C. (2015). 'The integration of autophagy and cellular trafficking pathways via RAB GAPs', *Autophagy*, 11(12): 2393-7.

[330] Itoh, T., Kanno, E., Uemura, T., Waguri, S. and Fukuda, M. (2011). 'OATL1, a novel autophagosome-resident Rab33B-GAP, regulates autophagosomal maturation', *J Cell Biol*, 192(5): 839-53.

[331] van der Sluijs, P., Hull, M., Webster, P., Male, P., Goud, B. and Mellman, I. (1992). 'The small GTP-binding protein rab4 controls an early sorting event on the endocytic pathway', *Cell*, 70(5): 729-40.

[332] Goueli, B. S., Powell, M. B., Finger, E. C. and Pfeffer, S. R. (2012). 'TBC1D16 is a Rab4A GTPase activating protein that regulates receptor recycling and EGF receptor signaling', *Proc Natl Acad Sci U S A*, 109(39): 15787-92.

8 Anhang

8.1 Primer-Sequenzen

Tabelle 8.1: Liste der für die PCR-Ansätze verwendeten Primer
Die jeweiligen Enzymschnittstellen sind farblich markiert (XhoI: gelb, HindIII: türkis). Die Primer wurden von der Firma BioTeZ Berlin-Buch GmbH (Berlin, Deutschland) bezogen.

Bezeichnung des Primers	Sequenz (5‘ → 3‘)
XhoI Schnittstelle	tgatcagcgag*ctcgag*ttagaattccttgtacagc gctgtacaaggaattctaa*ctcgag*ctcgctgatca
mCherry_forward (HindIII)	ggagga*aagctta*atggtgagcaagggcgaggaggataac
mCherry_reverse (XhoI)	ggagga*ctcgag*ctacttgtacagctcgtccatg
ECFP_forward (HindIII)	ggagga*aagctt*aatggtgagcaagggcgaggagctgttcaccg
ECFP_reverse (XhoI)	ggagga*ctcgag*ttacttgtacagctcgtccatgccgagagtg

8.2 sgRNA-Sequenzen in den PX458-Plasmidkonstrukten

Tabelle 8.2: 20nt sgRNA-Sequenzen
Die sgRNA-Sequenzen wurden von der Firma BioTeZ Berlin-Buch GmbH (Berlin, Deutschland) bezogen.

Bezeichnung der sgRNA	Sequenz (5‘ → 3‘)
GABARAP_Exon1(-)	GGATCTTCTCGCCCTCAGAG
GABARAP_Exon2	TTATCAGGTGATAGTAGAAA
GABARAP_Exon3	GCGAATTCATCTCCGAGCTG
GEC1_Exon2	AGAGAAGGCTCCAAAAGCCA
GEC1_Exon3B(-)	TACCTCATACAGTTGGCCCA
GATE16_Exon2A	TCCCACAGAACACAGATGCG
GATE16_Exon2B(-)	ATATTTCGCTCGAATCTTCG
GATE16_Exon3	GGTTCCATCTGATATCACTG

8.3 Synthetisches Gen mit HindIII-Schnittstelle zur Einbringung von GFP

Das 829 bp große synthetische Gen (Lot No.: 1953110, 16ACCBOP in einem pMA-T GeneArt *Cloning Vector* mit Ampicillin-Resistenz) wurde von der Firma ThermoFisher Scientific / Invitrogen GeneArt (Waltham, MA, USA) synthetisiert. Das synthetische Gen mit gewünschter HindIII-Restriktionsschnittstelle (cyan markiert) wurde über die FseI- (grau markiert) und XhoI- (gelb markiert) Schnittstellen in das PX458-Plasmidrückgrat eingebracht.

```
      FseI
     ------+-
   1 ggccggccag gcaaaaaaga aaaaggaatt cggcagtgga gagggcagag gaagtctgct
     ccggccggtc cgttttttct ttttccttaa gccgtcacct ctcccgtctc cttcagacga

                                        HindIII
                                        -+----
  61 aacatgcggt gacgtcgagg agaatcctgg cccaagcttg gtgagcaagg gcgaggagct
     ttgtacgcca ctgcagctcc tcttaggacc gggttcgaac cactcgttcc cgctcctcga

 121 gttcaccggg gtggtgccca tcctggtcga gctggacggc gacgtaaacg gccacaagtt
     caagtggccc caccacgggt aggaccagct cgacctgccg ctgcatttgc cggtgttcaa

 181 cagcgtgtcc ggcgagggcg agggcgatgc cacctacggc aagctgaccc tgaagttcat
     gtcgcacagg ccgctcccgc tcccgctacg gtggatgccg ttcgactggg acttcaagta

 241 ctgcaccacc ggcaagctgc ccgtgccctg gcccaccctc gtgaccaccc tgacctacgg
     gacgtggtgg ccgttcgacg ggcacgggac cgggtgggag cactggtggg actggatgcc

 301 cgtgcagtgc ttcagccgct accccgacca catgaagcag cacgacttct tcaagtccgc
     gcacgtcacg aagtcggcga tggggctggt gtacttcgtc gtgctgaaga agttcaggcg

 361 catgcccgaa ggctacgtcc aggagcgcac catcttcttc aaggacgacg gcaactacaa
     gtacgggctt ccgatgcagg tcctcgcgtg gtagaagaag ttcctgctgc cgttgatgtt

 421 gacccgcgcc gaggtgaagt tcgagggcga caccctggtg aaccgcatcg agctgaaggg
     ctgggcgcgg ctccacttca agctcccgct gtgggaccac ttggcgtagc tcgacttccc

 481 catcgacttc aaggaggacg gcaacatcct ggggcacaag ctggagtaca actacaacag
     gtagctgaag ttcctcctgc cgttgtagga ccccgtgttc gacctcatgt tgatgttgtc

 541 ccacaacgtc tatatcatgg ccgacaagca gaagaacggc atcaaggtga acttcaagat
     ggtgttgcag atatagtacc ggctgttcgt cttcttgccg tagttccact tgaagttcta

 601 ccgccacaac atcgaggacg gcagcgtgca gctcgccgac cactaccagc agaacacccc
     ggcggtgttg tagctcctgc cgtcgcacgt cgagcggctg gtgatggtcg tcttgtgggg

 661 catcggcgac ggccccgtgc tgctgcccga caaccactac ctgagcaccc agtccgccct
     gtagccgctg ccggggcacg acgacgggct gttggtgatg gactcgtggg tcaggcggga

 721 gagcaaagac cccaacgaga agcgcgatca catggtcctg ctggagttcg tgaccgccgc
     ctcgtttctg gggttgctct tcgcgctagt gtaccaggac gacctcaagc actggcggcg

                                                  XhoI
                                                 -+----
 781 cgggatcact ctcggcatgg acgagctgta caaggaattc taactcgag
     gccctagtga gagccgtacc tgctcgacat gttccttaag attgagctc
```

8.4 Aufbau der in dieser Arbeit verwendeten Plasmide

Die DNA-Sequenzierungen erfolgten durch die Firma Microsynth Seqlab GmbH (Göttingen, Deutschland). Die gezeigten Sequenzen und Plasmide wurden, wenn nicht anders gekennzeichnet, mittels Clone Manager 9 (Scientific & Educational Software, Cary, USA) erstellt.

8.4.1 Aufbau des pSpCas9(BB)-2A-GFP (PX458) Vektors

Eine schematische Darstellung des Plasmids #48138 (addgene) [243] ist in Abbildung 8.1 gezeigt.

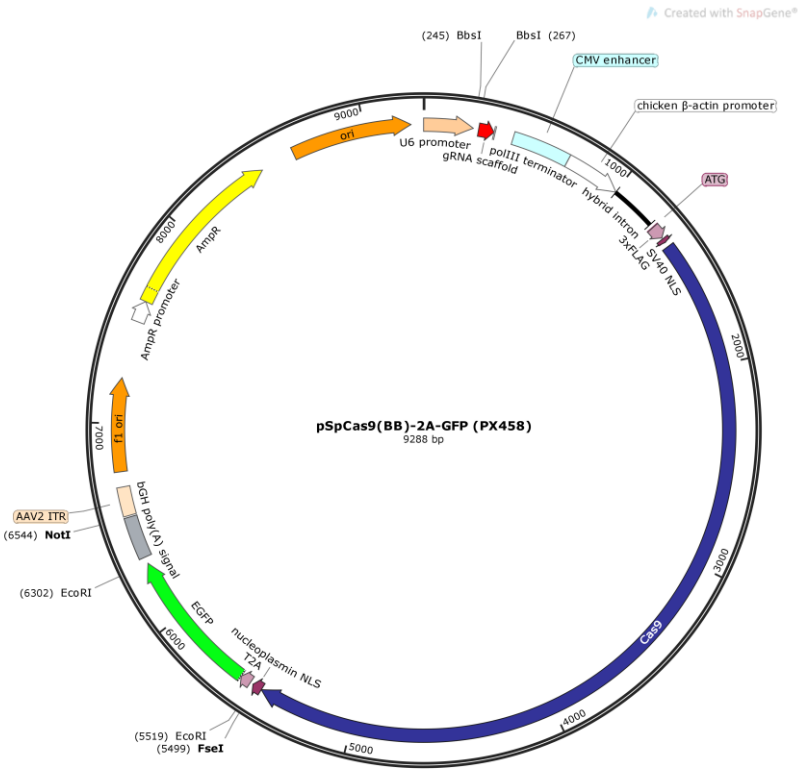

Abbildung 8.1: Aufbau des Plasmids pSpCas9(BB)-2A-GFP (PX458)
In das 9288 bp große Plasmid wurde die sgRNA-Gensequenz gegen GABARAP bzw. GABARAPL1 bzw. GABARAPL2 eingebracht. Es besitzt unter anderem diverse Schnittstellen für Restriktionsenzyme, einen Replikationsursprung (f1 ori) und eine Ampicillin-Resistenz (AmpR) in *E. coli* sowie einen weiteren Replikationsursprung (ori) und U6 Promotor für die Expression in Säugerzellen. Die *gRNA scaffold* Sequenz beinhaltet die Restriktionsschnittstellen für BbsI/BpiI, über die die gewünschte sgRNA in das Plasmid eingebracht werden kann. Anschließend folgt die Cas9-Sequenz aus *S. pyogenes* und eine Sequenz für das Fluoreszenzprotein EGFP, die unter einem humanen Cytomegalovirus (CMV) *enhancer* und *chicken β-actin* Promotor exprimiert werden. Am Insert befindet sich N-terminal eine 3 x FLAG-Sequenz und C-terminal die EGFP-Sequenz, die durch eine *nucleoplasmin nuclear localization signal* (NLS)- und 2A-Sequenz von Cas9 abgegrenzt wird. https://www.addgene.org/48138, 01.07.2020, 16:00, generiert mit SnapGene (GSL Biotech, San Diego, USA, erhältlich unter snapgene.com), [243]

8.4.2 DNA-Sequenz des pSpCas9(BB)-2A-GFP (PX458)-Vektors mit XhoI- und HindIII-Restriktionsschnittstellen

```
   1  gagggcctat ttcccatgat tccttcatat ttgcatatac gatacaaggc tgttagagag
      ctcccggata aagggtacta aggaagtata aacgtatatg ctatgttccg acaatctctc

  61  ataattggaa ttaatttgac tgtaaacaca aagatattag tacaaaatac gtgacgtaga
      tattaacctt aattaaactg acatttgtgt ttctataatc atgttttatg cactgcatct

 121  aagtaataat ttcttgggta gtttgcagtt ttaaaattat gttttaaaat ggactatcat
      ttcattatta aagaacccat caaacgtcaa aattttaata caaaatttta cctgatagta

 181  atgcttaccg taacttgaaa gtatttcgat ttcttggctt tatatatctt gtggaaagga
      tacgaatggc attgaacttt cataaagcta aagaaccgaa atatatagaa caccttcct

                  BbsI      BbsI
                 ------   -------
 241  cgaaacaccg ggtcttcgag aagacctgtt ttagagctag aaatagcaag ttaaaataag
      gctttgtggc ccagaagctc ttctggacaa aatctcgatc tttatcgttc aattttattc

 301  gctagtccgt tatcaacttg aaaaagtggc accgagtcgg tgctttttg ttttagagct
      cgatcaggca atagttgaac tttttcaccg tggctcagcc acgaaaaaac aaaatctcga

 361  agaaatagca agttaaaata aggctagtcc gtttttagcg cgtgcgccaa ttctgcagac
      tctttatcgt tcaattttat tccgatcagg caaaaatcgc gcacgcggtt aagacgtctg

                     KpnI
                    -----+
                   Acc65I
                   -+----
             XbaI
           -+-----
 421  aaatggctct agaggtaccc gttacataac ttacggtaaa tggcccgcct ggctgaccgc
      tttaccgaga tctccatggg caatgtattg aatgccattt accgggcgga ccgactggcg

 481  ccaacgaccc ccgcccattg acgtcaatag taacgccaat agggactttc cattgacgtc
      ggttgctggg ggcgggtaac tgcagttatc attgcggtta tccctgaaag gtaactgcag

 541  aatgggtgga gtatttacgg taaactgccc acttggcagt acatcaagtg tatcatatgc
      ttacccacct cataaatgcc atttgacggg tgaaccgtca tgtagttcac atagtatacg

 601  caagtacgcc ccctattgac gtcaatgacg gtaaatggcc cgcctggcat tgtgcccagt
      gttcatgcgg gggataactg cagttactgc catttaccgg gcggaccgta acacgggtca

                                              SnaBI
                                             ----+--
 661  acatgacctt atgggacttt cctacttggc agtacatcta cgtattagtc atcgctatta
      tgtactggaa taccctgaaa ggatgaaccg tcatgtagat gcataatcag tagcgataat

 721  ccatggtcga ggtgagcccc acgttctgct tcactctccc catctccccc ccctccccac
      ggtaccagct ccactcgggg tgcaagacga agtgagaggg gtagaggggg gggaggggtg

 781  ccccaatttt gtatttattt atttttaat tattttgtgc agcgatgggg gcgggggggg
      ggggttaaaa cataaataaa taaaaaatta ataaaacacg tcgctacccc cgccccccc

 841  gggggggggcg cgcgccaggc ggggcggggc ggggcgaggg gcggggcggg gcgaggcgga
```

```
      ccccccccgc gcgcggtccg ccccgccccg ccccgctccc cgccccgccc cgctccgcct
       >>.........................Cas9 1.........................>
         g  g  a   r  a  r   r  g  g   a  g  r  g   a  g  r   g  e  a

 901  gaggtgcggc ggcagccaat cagagcggcg cgctccgaaa gtttccтttt atggcgaggc
      ctccacgccg ccgtcggtta gtctcgccgc gcgaggcttt caaaggaaaa taccgctccg
      >.........................Cas9 1.........................>
      e  r  c  g   g  s  q   s  e  r   r  a  p  k   v  s  f   y  g  e

 961  ggcggcggcg gcggccctat aaaaagcgaa gcgcgcggcg ggcgggagtc gctgcgacgc
      ccgccgccgc cgccgggata tttttcgctt cgcgcgccgc ccgccctcag cgacgctgcg
      >.........................Cas9 1.........................>
      a  a  a  a   a  a  l   -  k  a   k  r  a  a   g  g  s   r  c  d

1021  tgccttcgcc ccgtgccccg ctccgccgcc gcctcgcgcc gcccgccccg gctctgactg
      acggaagcgg ggcacggggc gaggcggcgg cggagcgcgg cgggcggggc cgagactgac
      >............Cas9 1............>>
      a  a  f  a   p  c  p   a  p  p   p
                                  >>..........Cas9............>
                                    p  r  a   a  r  p   g  s  d

1081  accgcgttac tcccacaggt gagcgggcgg gacggccctt ctcctccggg ctgtaattag
      tggcgcaatg agggtgtcca ctcgcccgcc ctgccgggaa gaggaggccc gacattaatc
      >.........................Cas9.........................>
      -  p  r  y   s  h  r   -  a  g   g  t  a  l   l  l  r   a  v  i

1141  ctgagcaaga ggtaagggtt taagggatgg ttggttggtg gggtattaat gtttaattac
      gactcgttct ccattcccaa attccctacc aaccaaccac cccataatta caaattaatg
      >.........................Cas9.........................>
      s  -  a  r   g  k  g   l  r  d   g  w  l  v   g  y  -   c  l  i

             AarI                              AgeI
           --------                          -+-----
1201  ctggagcacc tgcctgaaat cacttttttt caggttggac cggtgccacc atggactata
      gacctcgtgg acggacttta gtgaaaaaaa gtccaacctg gccacggtgg tacctgatat
      >.........................Cas9.........................>
      t  w  s  t   c  l  k   s  l  f   f  r  l  d   r  c  h   h  g  l


1261  aggaccacga cggagactac aaggatcatg atattgatta caaagacgat gacgataaga
      tcctggtgct gcctctgatg ttcctagtac tataactaat gtttctgcta ctgctattct
      >.........................Cas9.........................>
      -  g  p  r   r  r  l   q  g  s   -  y  -  l   q  r  r   -  r  -


1321  tggccccaaa gaagaagcgg aaggtcggta tccacggagt cccagcagcc gacaagaagt
      accggggttt cttcttcgcc ttccagccat aggtgcctca gggtcgtcgg ctgttcttca
      >.........................Cas9.........................>
      d  g  p  k   e  e  a   e  g  r   y  p  r  s   p  s  s   r  q  e


1381  acagcatcgg cctggacatc ggcaccaact ctgtgggctg ggccgtgatc accgacgagt
      tgtcgtagcc ggacctgtag ccgtggttga gacacccgac ccggcactag tggctgctca
      >.........................Cas9.........................>
      v  q  h  r   p  g  h   r  h  q   l  c  g  l   g  r  d   h  r  r


1441  acaaggtgcc cagcaagaaa ttcaaggtgc tgggcaacac cgaccggcac agcatcaaga
      tgttccacgg gtcgttcttt aagttccacg acccgttgtg gctggccgtg tcgtagttct
      >.........................Cas9.........................>
      v  q  g  a   q  q  e   i  q  g   a  g  q  h   r  p  a   q  h  q
```

```
1501  agaacctgat cggagccctg ctgttcgaca gcggcgaaac agccgaggcc acccggctga
      tcttggacta gcctcgggac gacaagctgt cgccgctttg tcggctccgg tgggccgact
      >..............................Cas9..............................>
      e  e  p  d   r  s  p   a  v  r   q  r  r  n   s  r  g   h  p  a

                                                                  BglII
                                                                 -+----
1561  agagaaccgc cagaagaaga tacaccagac ggaagaaccg gatctgctat ctgcaagaga
      tctcttggcg gtcttcttct atgtggtctg ccttcttggc ctagacgata gacgttctct
      >..............................Cas9..............................>
      e  e  n  r   q  k  k   i  h  q   t  e  e  p   d  l  l   s  a  r

1621  tcttcagcaa cgagatggcc aaggtggacg acagcttctt ccacagactg gaagagtcct
      agaagtcgtt gctctaccgg ttccacctgc tgtcgaagaa ggtgtctgac cttctcagga
      >..............................Cas9..........................>>
      d  l  q  q   r  d  g   q  g  g   r  q  l  l   p  q  t   g  r

1681  tcctggtgga agaggataag aagcacgagc ggcaccccat cttcggcaac atcgtggacg
      aggaccacct tctcctattc ttcgtgctcg ccgtggggta gaagccgttg tagcacctgc

1741  aggtggccta ccacgagaag taccccacca tctaccacct gagaaagaaa ctggtggaca
      tccaccggat ggtgctcttc atggggtggt agatggtgga ctctttcttt gaccacctgt

1801  gcaccgacaa ggccgacctg cggctgatct atctggccct ggcccacatg atcaagttcc
      cgtggctgtt ccggctggac gccgactaga tagaccggga ccgggtgtac tagttcaagg

1861  ggggccactt cctgatcgag ggcgacctga accccgacaa cagcgacgtg gacaagctgt
      ccccggtgaa ggactagctc ccgctggact tggggctgtt gtcgctgcac ctgttcgaca

1921  tcatccagct ggtgcagacc tacaaccagc tgttcgagga aaaccccatc aacgccagcg
      agtaggtcga ccacgtctgg atgttggtcg acaagctcct tttggggtag ttgcggtcgc

1981  gcgtggacgc caaggccatc ctgtctgcca gactgagcaa gagcagacgg ctggaaaatc
      cgcacctgcg gttccggtag gacagacggt ctgactcgtt ctcgtctgcc gacctttag

2041  tgatcgccca gctgcccggc gagaagaaga atggcctgtt cggaaacctg attgccctga
      actagcgggt cgacgggccg ctcttcttct taccggacaa gcctttggac taacgggact

2101  gcctgggcct gacccccaac ttcaagagca acttcgacct ggccgaggat gccaaactgc
      cggacccgga ctgggggttg aagttctcgt tgaagctgga ccggctccta cggtttgacg

2161  agctgagcaa ggacacctac gacgacgacc tggacaacct gctggcccag atcggcgacc
      tcgactcgtt cctgtggatg ctgctgctgg acctgttgga cgaccgggtc tagccgctgg

2221  agtacgccga cctgtttctg gccgccaaga acctgtccga cgccatcctg ctgagcgaca
      tcatgcggct ggacaaagac cggcggttct tggacaggct gcggtaggac gactcgctgt
```

```
2281  tcctgagagt gaacaccgag atcaccaagg ccccccctgag cgcctctatg atcaagagat
      aggactctca cttgtggctc tagtggttcc ggggggactc gcggagatac tagttctcta

2341  acgacgagca ccaccaggac ctgaccctgc tgaaagctct cgtgcggcag cagctgcctg
      tgctgctcgt ggtggtcctg gactgggacg actttcgaga gcacgccgtc gtcgacggac

2401  agaagtacaa agagattttc ttcgaccaga gcaagaacgg ctacgccggc tacattgacg
      tcttcatgtt tctctaaaag aagctggtct cgttcttgcc gatgcggccg atgtaactgc

2461  gcggagccag ccaggaagag ttctacaagt tcatcaagcc catcctggaa aagatggacg
      cgcctcggtc ggtccttctc aagatgttca agtagttcgg gtaggacctt ttctacctgc

2521  gcaccgagga actgctcgtg aagctgaaca gagaggacct gctgcggaag cagcggacct
      cgtggctcct tgacgagcac ttcgacttgt ctctcctgga cgacgccttc gtcgcctgga
                                ORF Cas9

2581  tcgacaacgg cagcatcccc caccagatcc acctgggaga gctgcacgcc attctgcggc
      agctgttgcc gtcgtagggg gtggtctagg tggaccctct cgacgtgcgg taagacgccg

2641  ggcaggaaga tttttaccca ttcctgaagg acaaccggga aaagatcgag aagatcctga
      ccgtccttct aaaaatgggt aaggacttcc tgttggccct tttctagctc ttctaggact

                                 ApaI
                                -----+
                                PspOMI
                                -+----
2701  ccttccgcat cccctactac gtgggccctc tggccagggg aaacagcaga ttcgcctgga
      ggaaggcgta ggggatgatg cacccgggag accggtcccc tttgtcgtct aagcggacct

2761  tgaccagaaa gagcgaggaa accatcaccc cctggaactt cgaggaagtg gtggacaagg
      actggtcttt ctcgctcctt tggtagtggg ggaccttgaa gctccttcac cacctgttcc

2821  gcgcttccgc ccagagcttc atcgagcgga tgaccaactt cgataagaac ctgcccaacg
      cgcgaaggcg ggtctcgaag tagctcgcct actggttgaa gctattcttg gacgggttgc

2881  agaaggtgct gcccaagcac agcctgctgt acgagtactt caccgtgtat aacgagctga
      tcttccacga cgggttcgtg tcggacgaca tgctcatgaa gtggcacata ttgctcgact

2941  ccaaagtgaa atacgtgacc gagggaatga gaaagcccgc cttcctgagc ggcgagcaga
      ggtttcactt tatgcactgg ctcccttact ctttcgggcg gaaggactcg ccgctcgtct

3001  aaaaggccat cgtggacctg ctgttcaaga ccaaccggaa agtgaccgtg aagcagctga
      ttttccggta gcacctggac gacaagttct ggttggcctt tcactggcac ttcgtcgact
                           >>..............dCas9-R2.................>
                             l  f  k   t  n  r   k  v  t  v   k  q  l

3061  aagaggacta cttcaagaaa atcgagtgct tcgactccgt ggaaatctcc ggcgtggaag
      ttctcctgat gaagttcttt tagctcacga agctgaggca cctttagagg ccgcaccttc
```

```
      >.........................dCas9-R2.........................>
       k  e  d   y  f  k  k   i  e  c   f  d  s   v  e  i  s   g  v  e

                        PasI
                      --+-----
3121  atcggttcaa cgcctccctg ggcacatacc acgatctgct gaaaattatc aaggacaagg
      tagccaagtt gcggagggac ccgtgtatgg tgctagacga cttttaatag ttcctgttcc
      >.........................dCas9-R2.........................>
       d  r  f   n  a  s  l   g  t  y   h  d  l   l  k  i  i   k  d  k

                                                EcoRV
                                               ----+--
3181  acttcctgga caatgaggaa aacgaggaca ttctggaaga tatcgtgctg accctgacac
      tgaaggacct gttactcctt ttgctcctgt aagaccttct atagcacgac tgggactgtg
      >.........................dCas9-R2.........................>
       d  f  l   d  n  e  e   n  e  d   i  l  e   d  i  v  l   t  l  t

3241  tgtttgagga cagagagatg atcgaggaac ggctgaaaac ctatgcccac ctgttcgacg
      acaaactcct gtctctctac tagctccttg ccgacttttg gatacgggtg gacaagctgc
      >.........................dCas9-R2.........................>
       l  f  e   d  r  e  m   i  e  e   r  l  k   t  y  a  h   l  f  d

3301  acaaagtgat gaagcagctg aagcggcgga gatacaccgg ctggggcagg ctgagccgga
      tgtttcacta cttcgtcgac ttcgccgcct ctatgtggcc gaccccgtcc gactcggcct
      >.........................dCas9-R2.........................>
       d  k  v   m  k  q  l   k  r  r   r  y  t   g  w  g  r   l  s  r

3361  agctgatcaa cggcatccgg gacaagcagt ccggcaagac aatcctggat ttcctgaagt
      tcgactagtt gccgtaggcc ctgttcgtca ggccgttctg ttaggaccta aaggacttca
      >.........................dCas9-R2.........................>
       k  l  i   n  g  i  r   d  k  q   s  g  k   t  i  l  d   f  l  k

3421  ccgacggctt cgccaacaga aacttcatgc agctgatcca cgacgacagc ctgaccttta
      ggctgccgaa gcggttgtct ttgaagtacg tcgactaggt gctgctgtcg gactggaaat
      >.........................dCas9-R2.........................>
       s  d  g   f  a  n  r   n  f  m   q  l  i   h  d  d  s   l  t  f

3481  aagaggacat ccagaaagcc caggtgtccg gccagggcga tagcctgcac gagcacattg
      ttctcctgta ggtctttcgg gtccacaggc cggtcccgct atcggacgtg ctcgtgtaac
      >.........................dCas9-R2.........................>
       k  e  d   i  q  k  a   q  v  s   g  q  g   d  s  l  h   e  h  i

3541  ccaatctggc cggcagcccc gccattaaga agggcatcct gcagacagtg aaggtggtgg
      ggttagaccg gccgtcgggg cggtaattct tcccgtagga cgtctgtcac ttccaccacc
      >.........................dCas9-R2.........................>
       a  n  l   a  g  s  p   a  i  k   k  g  i   l  q  t  v   k  v  v

3601  acgagctcgt gaaagtgatg ggccggcaca agcccgagaa catcgtgatc gaaatggcca
      tgctcgagca ctttcactac ccggccgtgt tcgggctctt gtagcactag ctttaccggt
      >.........................dCas9-R2.........................>
       d  e  l   v  k  v  m   g  r  h   k  p  e   n  i  v  i   e  m  a
```

```
3661  gagagaacca gaccacccag aagggacaga agaacagccg cgagagaatg aagcggatcg
      ctctcttggt ctggtgggtc ttccctgtct tcttgtcggc gctctcttac ttcgcctagc
      >.........................dCas9-R2.........................>
       r  e  n   q  t  t  q   k  g  q   k  n  s   r  e  r  m   k  r  i

3721  aagagggcat caaagagctg ggcagccaga tcctgaaaga acaccccgtg gaaaacaccc
      ttctcccgta gtttctcgac ccgtcggtct aggactttct tgtggggcac cttttgtggg
      >.........................dCas9-R2.........................>
       e  e  g   i  k  e  l   g  s  q   i  l  k   e  h  p  v   e  n  t

3781  agctgcagaa cgagaagctg tacctgtact acctgcagaa tgggcgggat atgtacgtgg
      tcgacgtctt gctcttcgac atggacatga tggacgtctt acccgcccta tacatgcacc
      >.........................dCas9-R2.........................>
       q  l  q   n  e  k  l   y  l  y   y  l  q   n  g  r  d   m  y  v

3841  accaggaact ggacatcaac cggctgtccg actacgatgt ggaccatatc gtgcctcaga
      tggtccttga cctgtagttg gccgacaggc tgatgctaca cctggtatag cacggagtct
      >.........................dCas9-R2.........................>
       d  q  e   l  d  i  n   r  l  s   d  y  d   v  d  h  i   v  p  q

3901  gctttctgaa ggacgactcc atcgacaaca aggtgctgac cagaagcgac aagaaccggg
      cgaaagactt cctgctgagg tagctgttgt tccacgactg gtcttcgctg ttcttggccc
      >.........................dCas9-R2.........................>
       s  f  l   k  d  d  s   i  d  n   k  v  l   t  r  s  d   k  n  r

3961  gcaagagcga caacgtgccc tccgaagagg tcgtgaagaa gatgaagaac tactggcggc
      cgttctcgct gttgcacggg aggcttctcc agcacttctt ctacttcttg atgaccgccg
      >.........................dCas9-R2.........................>
       g  k  s   d  n  v  p   s  e  e   v  v  k   k  m  k  n   y  w  r

4021  agctgctgaa cgccaagctg attacccaga gaaagttcga caatctgacc aaggccgaga
      tcgacgactt gcggttcgac taatgggtct ctttcaagct gttagactgg ttccggctct
      >.........................dCas9-R2.........................>
       q  l  l   n  a  k  l   i  t  q   r  k  f   d  n  l  t   k  a  e

4081  gaggcggcct gagcgaactg gataaggccg gcttcatcaa gagacagctg gtggaaaccc
      ctccgccgga ctcgcttgac ctattccggc cgaagtagtt ctctgtcgac caccttgggg
      >.........dCas9-R2.........>>
       r  g  g   l  s  e  l   d  k

                    PmlI
                   ---+--
4141  ggcagatcac aaagcacgtg gcacagatcc tggactcccg gatgaacact aagtacgacg
      ccgtctagtg tttcgtgcac cgtgtctagg acctgagggc ctacttgtga ttcatgctgc

4201  agaatgacaa gctgatccgg gaagtgaaag tgatcaccct gaagtccaag ctggtgtccg
      tcttactgtt cgactaggcc cttcactttc actagtggga cttcaggttc gaccacaggc

4261  atttccggaa ggatttccag ttttacaaag tgcgcgagat caacaactac caccacgccc
      taaaggcctt cctaaaggtc aaaatgtttc acgcgctcta gttgttgatg gtggtgcggg

4321  acgacgccta cctgaacgcc gtcgtgggaa ccgccctgat caaaaagtac cctaagctgg
      tgctgcggat ggacttgcgg cagcaccctt ggcgggacta gtttttcatg ggattcgacc

4381  aaagcgagtt cgtgtacggc gactacaagg tgtacgacgt gcggaagatg atcgccaaga
      tttcgctcaa gcacatgccg ctgatgttcc acatgctgca cgccttctac tagcggttct
```

```
4441  gcgagcagga aatcggcaag gctaccgcca agtacttctt ctacagcaac atcatgaact
      cgctcgtcct ttagccgttc cgatggcggt tcatgaagaa gatgtcgttg tagtacttga

4501  ttttcaagac cgagattacc ctggccaacg gcgagatccg gaagcggcct ctgatcgaga
      aaaagttctg gctctaatgg gaccggttgc cgctctaggc cttcgccgga gactagctct

4561  caaacggcga aaccggggag atcgtgtggg ataagggccg ggattttgcc accgtgcgga
      gtttgccgct ttggcccctc tagcacaccc tattcccggc cctaaaacgg tggcacgcct

4621  aagtgctgag catgccccaa gtgaatatcg tgaaaaagac cgaggtgcag acaggcggct
      ttcacgactc gtacggggtt cacttatagc acttttctg gctccacgtc tgtccgccga

4681  tcagcaaaga gtctatcctg cccaagagga acagcgataa gctgatcgcc agaaagaagg
      agtcgtttct cagataggac gggttctcct tgtcgctatt cgactagcgg tctttcttcc

          KflI
        --+----
4741  actgggaccc taagaagtac ggcggcttcg acagccccac cgtggcctat tctgtgctgg
      tgaccctggg attcttcatg ccgccgaagc tgtcggggtg gcaccggata agacacgacc

4801  tggtggccaa agtggaaaag ggcaagtcca agaaactgaa gagtgtgaaa gagctgctgg
      accaccggtt tcacctttc ccgttcaggt tctttgactt ctcacacttt ctcgacgacc

         BsaBI
       -----+-----
4861  ggatcaccat catggaaaga agcagcttcg agaagaatcc catcgacttt ctggaagcca
      cctagtggta gtacctttct tcgtcgaagc tcttcttagg gtagctgaaa gaccttcggt

4921  agggctacaa agaagtgaaa aaggacctga tcatcaagct gcctaagtac tccctgttcg
      tcccgatgtt tcttcacttt ttcctggact agtagttcga cggattcatg agggacaagc

                            BsmI
                           ------
4981  agctggaaaa cggccggaag agaatgctgg cctctgccgg cgaactgcag aagggaaacg
      tcgacctttt gccggccttc tcttacgacc ggagacggcc gcttgacgtc ttcccttgc

5041  aactggccct gccctccaaa tatgtgaact tcctgtacct ggccagccac tatgagaagc
      ttgaccggga cgggaggttt atacacttga aggacatgga ccggtcggtg atactcttcg

5101  tgaagggctc ccccgaggat aatgagcaga aacagctgtt tgtggaacag cacaagcact
      acttcccgag ggggctccta ttactcgtct ttgtcgacaa acaccttgtc gtgttcgtga

5161  acctggacga gatcatcgag cagatcagcg agttctccaa gagagtgatc ctggccgacg
      tggacctgct ctagtagctc gtctagtcgc tcaagaggtt ctctcactag gaccggctgc

5221  ctaatctgga caaagtgctg tccgcctaca acaagcaccg ggataagccc atcagagagc
      gattagacct gtttcacgac aggcggatgt tgttcgtggc cctattcggg tagtctctcg

5281  aggccgagaa tatcatccac ctgtttaccc tgaccaatct gggagcccct gccgccttca
      tccggctctt atagtaggtg gacaaatggg actggttaga ccctcgggga cggcggaagt

5341  agtactttga caccaccatc gaccggaaga ggtacaccag caccaaagag gtgctggacg
      tcatgaaact gtggtggtag ctggccttct ccatgtggtc gtggtttctc cacgacctgc

5401  ccaccctgat ccaccagagc atcaccggcc tgtacgagac acggatcgac ctgtctcagc
      ggtgggacta ggtggtctcg tagtggccgg acatgctctg tgcctagctg gacagagtcg
                          FseI upstream Primer 1

                                          FseI
                                        ------+--
```

```
5461  tgggaggcga caaaaggccg gcggccacga aaaaggccgg ccaggcaaaa aagaaaaagg
      accctccgct gttttccggc cgccggtgct ttttccggcc ggtccgtttt ttcttttttcc

5521  aattcggcag tggagagggc agaggaagtc tgctaacatg cggtgacgtc gaggagaatc
      ttaagccgtc acctctcccg tctccttcag acgattgtac gccactgcag ctcctcttag
           >>...................2 A viral protein.....................>
             g   s   g   e   g   r   g   s   l   l   t   c   g   d   v   e   e   n

             HindIII
             -+-----
5581  ctggcccaag cttggtgagc aagggcgagg agctgttcac cggggtggtg cccatcctgg
      gaccgggttc gaaccactcg ttcccgctcc tcgacaagtg gccccaccac gggtaggacc
      HindIII Schnittstelle
      >.....>> 2 A viral protein
       p   g   p
                     >>.....................EGFP.....................>
                       v   s   k   g   e   e   l   f   t   g   v   v   p   i   l

5641  tcgagctgga cggcgacgta aacggccaca agttcagcgt gtccggcgag ggcgagggcg
      agctcgacct gccgctgcat ttgccggtgt tcaagtcgca caggccgctc ccgctcccgc
      >..............................EGFP..............................>
       v   e   l   d   g   d   v   n   g   h   k   f   s   v   s   g   e   g   e   g

5701  atgccaccta cggcaagctg accctgaagt tcatctgcac caccggcaag ctgcccgtgc
      tacggtggat gccgttcgac tgggacttca agtagacgtg gtggccgttc gacgggcacg
      >..............................EGFP..............................>
       d   a   t   y   g   k   l   t   l   k   f   i   c   t   t   g   k   l   p   v

5761  cctggcccac cctcgtgacc accctgacct acggcgtgca gtgcttcagc cgctaccccg
      ggaccgggtg ggagcactgg tgggactgga tgccgcacgt cacgaagtcg gcgatggggc
      >..............................EGFP..............................>
       p   w   p   t   l   v   t   t   l   t   y   g   v   q   c   f   s   r   y   p

5821  accacatgaa gcagcacgac ttcttcaagt ccgccatgcc cgaaggctac gtccaggagc
      tggtgtactt cgtcgtgctg aagaagttca ggcggtacgg gcttccgatg caggtcctcg
      >..............................EGFP..............................>
       d   h   m   k   q   h   d   f   f   k   s   a   m   p   e   g   y   v   q   e

5881  gcaccatctt cttcaaggac gacggcaact acaagacccg cgccgaggtg aagttcgagg
      cgtggtagaa gaagttcctg ctgccgttga tgttctgggc gcggctccac ttcaagctcc
      >..............................EGFP..............................>
       r   t   i   f   f   k   d   d   g   n   y   k   t   r   a   e   v   k   f   e

5941  gcgacaccct ggtgaaccgc atcgagctga agggcatcga cttcaaggag gacggcaaca
      cgctgtggga ccacttggcg tagctcgact tcccgtagct gaagttcctc ctgccgttgt
      >..............................EGFP..............................>
       g   d   t   l   v   n   r   i   e   l   k   g   i   d   f   k   e   d   g   n

6001  tcctggggca caagctggag tacaactaca acagccacaa cgtctatatc atggccgaca
      aggaccccgt gttcgacctc atgttgatgt tgtcggtgtt gcagatatag taccggctgt
      >..............................EGFP..............................>
       i   l   g   h   k   l   e   y   n   y   n   s   h   n   v   y   i   m   a   d

6061  agcagaagaa cggcatcaag gtgaacttca agatccgcca caacatcgag gacggcagcg
      tcgtcttctt gccgtagttc cacttgaagt tctaggcggt gttgtagctc ctgccgtcgc
      >..............................EGFP..............................>
       k   q   k   n   g   i   k   v   n   f   k   i   r   h   n   i   e   d   g   s

6121  tgcagctcgc cgaccactac cagcagaaca cccccatcgg cgacggcccc gtgctgctgc
      acgtcgagcg gctggtgatg gtcgtcttgt gggggtagcc gctgccgggg cacgacgacg
      >..............................EGFP..............................>
```

```
       v  q  l   a  d  h  y   q  q  n   t  p  i   g  d  g  p   v  l  l

6181   ccgacaacca ctacctgagc acccagtccg ccctgagcaa agaccccaac gagaagcgcg
       ggctgttggt gatggactcg tgggtcaggc gggactcgtt tctggggttg ctcttcgcgc
       >.............................EGFP.............................>
        p  d  n   h  y  l  s   t  q  s   a  l  s   k  d  p  n   e  k  r

6241   atcacatggt cctgctggag ttcgtgaccg ccgccgggat cactctcggc atggacgagc
       tagtgtacca ggacgacctc aagcactggc ggcggcccta gtgagagccg tacctgctcg
       >.............................EGFP.............................>
        d  h  m   v  l  l  e   f  v  t   a  a  g   i  t  l  g   m  d  e


        BsrGI              XhoI
       -+----             -+-----
6301   tgtacaagga attctaactc gagctcgctg atcagcctcg actgtgcctt ctagttgcca
       acatgttcct taagattgag ctcgagcgac tagtcggagc tgacacggaa gatcaacggt
        QuikChangePrimer XhoI CTCGAG XhoI
       >.EGFP>>
        l  y  k

6361   gccatctgtt gtttgcccct cccccgtgcc ttccttgacc ctggaaggtg ccactcccac
       cggtagacaa caaacgggga gggggcacgg aaggaactgg gaccttccac ggtgagggtg

6421   tgtcctttcc taataaaatg aggaaattgc atcgcattgt ctgagtaggt gtcattctat
       acaggaaagg attattttac tcctttaacg tagcgtaaca gactcatcca cagtaagata

6481   tctggggggt ggggtggggc aggacagcaa gggggaggat tgggaagaga atagcaggca
       agacccccca ccccaccccg tcctgtcgtt ccccctccta acccttctct tatcgtccgt

                 NotI
              ---+-----
6541   tgctggggag cggccgcagg aacccctagt gatggagttg gccactccct ctctgcgcgc
       acgacccctc gccggcgtcc ttggggatca ctacctcaac cggtgaggga gagacgcgcg

6601   tcgctcgctc actgaggccg ggcgaccaaa ggtcgcccga cgcccgggct ttgcccgggc
       agcgagcgag tgactccggc ccgctggttt ccagcgggct gcgggcccga aacgggcccg

                                                 BbeI
                                               ------+
                                                 SfoI
                                               ----+--
                                                 NarI
                                               ---+---
                                                 KasI
                                               -+-----
                                          SbfI
                                        ------+-
6661   ggcctcagtg agcgagcgag cgcgcagctg cctgcagggg cgcctgatgc ggtatttttct
       ccggagtcac tcgctcgctc gcgcgtcgac ggacgtcccc gcggactacg ccataaaaga


6721   ccttacgcat ctgtgcggta tttcacaccg catacgtcaa agcaaccata gtacgcgccc
       ggaatgcgta gacacgccat aaagtgtggc gtatgcagtt tcgttggtat catgcgcggg
       NotI downstream Primer

6781   tgtagcggcg cattaagcgc ggcgggtgtg gtggttacgc gcagcgtgac cgctacactt
       acatcgccgc gtaattcgcg ccgcccacac caccaatgcg cgtcgcactg gcgatgtgaa

6841   gccagcgccc tagcgcccgc tcctttcgct ttcttccctt cctttctcgc cacgttcgcc
       cggtcgcggg atcgcgggcg aggaaagcga aagaagggaa ggaaagagcg gtgcaagcgg
```

```
6901  ggctttcccc gtcaagctct aaatcggggg ctccctttag ggttccgatt tagtgcttta
      ccgaaagggg cagttcgaga tttagccccc gagggaaatc ccaaggctaa atcacgaaat

6961  cggcacctcg accccaaaaa acttgatttg ggtgatggtt cacgtagtgg gccatcgccc
      gccgtggagc tggggttttt tgaactaaac ccactaccaa gtgcatcacc cggtagcggg

7021  tgatagacgg tttttcgccc tttgacgttg gagtccacgt tctttaatag tggactcttg
      actatctgcc aaaaagcggg aaactgcaac ctcaggtgca agaaattatc acctgagaac

                                                              PsiI
                                                            ----+--
7081  ttccaaactg gaacaacact caaccctatc tcgggctatt cttttgattt ataagggatt
      aaggtttgac cttgttgtga gttgggatag agcccgataa gaaaactaaa tattccctaa

7141  ttgccgattt cggcctattg gttaaaaaat gagctgattt aacaaaaatt taacgcgaat
      aacggctaaa gccggataac caatttttta ctcgactaaa ttgtttttaa attgcgctta

7201  tttaacaaaa tattaacgtt tacaatttta tggtgcactc tcagtacaat ctgctctgat
      aaattgtttt ataattgcaa atgttaaaat accacgtgag agtcatgtta gacgagacta

7261  gccgcatagt taagccagcc ccgacacccg ccaacacccg ctgacgcgcc ctgacgggct
      cggcgtatca attcggtcgg ggctgtgggc ggttgtgggc gactgcgcgg gactgcccga

7321  tgtctgctcc cggcatccgc ttacagacaa gctgtgaccg tctccgggag ctgcatgtgt
      acagacgagg gccgtaggcg aatgtctgtt cgacactggc agaggccctc gacgtacaca

7381  cagaggtttt caccgtcatc accgaaacgc gcgagacgaa agggcctcgt gatacgccta
      gtctccaaaa gtggcagtag tggctttgcg cgctctgctt tcccggagca ctatgcggat

7441  tttttatagg ttaatgtcat gataataatg gtttcttaga cgtcaggtgg cacttttcgg
      aaaaatatcc aattacagta ctattattac caaagaatct gcagtccacc gtgaaaagcc

7501  ggaaatgtgc gcggaacccc tatttgttta tttttctaaa tacattcaaa tatgtatccg
      cctttacacg cgccttgggg ataaacaaat aaaaagattt atgtaagttt atacataggc

7561  ctcatgagac aataaccctg ataaatgctt caataatatt gaaaaaggaa gagtatgagt
      gagtactctg ttattgggac tatttacgaa gttattataa ctttttcctt ctcatactca

7621  attcaacatt tccgtgtcgc ccttattccc ttttttgcgg cattttgcct tcctgttttt
      taagttgtaa aggcacagcg ggaataaggg aaaaaacgcc gtaaaacgga aggacaaaaa

7681  gctcacccag aaacgctggt gaaagtaaaa gatgctgaag atcagttggg tgcacgagtg
      cgagtgggtc tttgcgacca ctttcatttt ctacgacttc tagtcaaccc acgtgctcac

7741  ggttacatcg aactggatct caacagcggt aagatccttg agagttttcg ccccgaagaa
      ccaatgtagc ttgacctaga gttgtcgcca ttctaggaac tctcaaaagc ggggcttctt

7801  cgttttccaa tgatgagcac ttttaaagtt ctgctatgtg gcgcggtatt atcccgtatt
      gcaaaaggtt actactcgtg aaaatttcaa gacgatacac cgcgccataa tagggcataa

7861  gacgccgggc aagagcaact cggtcgccgc atacactatt ctcagaatga cttggttgag
      ctgcggcccg ttctcgttga gccagcggcg tatgtgataa gagtcttact gaaccaactc

7921  tactcaccag tcacagaaaa gcatcttacg gatggcatga cagtaagaga attatgcagt
      atgagtggtc agtgtctttt cgtagaatgc ctaccgtact gtcattctct taatacgtca

                                                            PvuI
                                                          -----+-
7981  gctgccataa ccatgagtga taacactgcg gccaacttac ttctgacaac gatcggagga
      cgacggtatt ggtactcact attgtgacgc cggttgaatg aagactgttg ctagcctcct
```

```
8041  ccgaaggagc taaccgcttt tttgcacaac atgggggatc atgtaactcg ccttgatcgt
      ggcttcctcg attggcgaaa aaacgtgttg taccccctag tacattgagc ggaactagca

8101  tgggaaccgg agctgaatga agccatacca aacgacgagc gtgacaccac gatgcctgta
      acccttggcc tcgacttact tcggtatggt ttgctgctcg cactgtggtg ctacggacat

                        FspI
                       ---+---
8161  gcaatggcaa caacgttgcg caaactatta actggcgaac tacttactct agcttcccgg
      cgttaccgtt gttgcaacgc gtttgataat tgaccgcttg atgaatgaga tcgaagggcc

8221  caacaattaa tagactggat ggaggcggat aaagttgcag gaccacttct gcgctcggcc
      gttgttaatt atctgaccta cctccgccta tttcaacgtc ctggtgaaga cgcgagccgg

                                                                SacII
                                                               ----+-
8281  cttccggctg gctggtttat tgctgataaa tctggagccg gtgagcgtgg aagccgcggt
      gaaggccgac cgaccaaata acgactattt agacctcggc cactcgcacc ttcggcgcca

8341  atcattgcag cactggggcc agatggtaag ccctcccgta tcgtagttat ctacacgacg
      tagtaacgtc gtgaccccgg tctaccattc gggagggcat agcatcaata gatgtgctgc

8401  gggagtcagg caactatgga tgaacgaaat agacagatcg ctgagatagg tgcctcactg
      ccctcagtcc gttgatacct acttgcttta tctgtctagc gactctatcc acggagtgac

8461  attaagcatt ggtaactgtc agaccaagtt tactcatata tactttagat tgatttaaaa
      taattcgtaa ccattgacag tctggttcaa atgagtatat atgaaatcta actaaatttt

8521  cttcattttt aatttaaaag gatctaggtg aagatccttt ttgataatct catgaccaaa
      gaagtaaaaa ttaaattttc ctagatccac ttctaggaaa aactattaga gtactggttt

8581  atcccttaac gtgagttttc gttccactga gcgtcagacc ccgtagaaaa gatcaaagga
      tagggaattg cactcaaaag caaggtgact cgcagtctgg ggcatctttt ctagtttcct

8641  tcttcttgag atcctttttt tctgcgcgta atctgctgct tgcaaacaaa aaaaccaccg
      agaagaactc taggaaaaaa agacgcgcat tagacgacga acgtttgttt ttttggtggc

8701  ctaccagcgg tggtttgttt gccggatcaa gagctaccaa ctctttttcc gaaggtaact
      gatggtcgcc accaaacaaa cggcctagtt ctcgatggtt gagaaaaagg cttccattga

8761  ggcttcagca gagcgcagat accaaatact gtccttctag tgtagccgta gttaggccac
      ccgaagtcgt ctcgcgtcta tggtttatga caggaagatc acatcggcat caatccggtg

8821  cacttcaaga actctgtagc accgcctaca tacctcgctc tgctaatcct gttaccagtg
      gtgaagttct tgagacatcg tggcggatgt atggagcgag acgattagga caatggtcac

8881  gctgctgcca gtggcgataa gtcgtgtctt accgggttgg actcaagacg atagttaccg
      cgacgacggt caccgctatt cagcacagaa tggcccaacc tgagttctgc tatcaatggc

8941  gataaggcgc agcggtcggg ctgaacgggg ggttcgtgca cacagcccag cttggagcga
      ctattccgcg tcgccagccc gacttgcccc ccaagcacgt gtgtcgggtc gaacctcgct

9001  acgacctaca ccgaactgag atacctacag cgtgagctat gagaaagcgc cacgcttccc
      tgctggatgt ggcttgactc tatggatgtc gcactcgata ctctttcgcg gtgcgaaggg

9061  gaagggagaa aggcggacag gtatccggta agcggcaggg tcggaacagg agagcgcacg
      cttccctctt tccgcctgtc cataggccat tcgccgtccc agccttgtcc tctcgcgtgc

9121  agggagcttc caggggggaaa cgcctggtat ctttatagtc ctgtcgggtt tcgccacctc
      tccctcgaag gtccccctttt gcggaccata gaaatatcag gacagcccaa agcggtggag
```

```
9181  tgacttgagc gtcgattttt gtgatgctcg tcaggggggc ggagcctatg gaaaaacgcc
      actgaactcg cagctaaaaa cactacgagc agtccccccg cctcggatac ctttttgcgg

                                                                AflIII
                                                               --+----
                                                                 PciI
                                                               --+----
9241  agcaacgcgg cctttttacg gttcctggcc ttttgctggc cttttgctca catgt
      tcgttgcgcc ggaaaaatgc caaggaccgg aaaacgaccg gaaaacgagt gtaca
```

8.4.2.1 Plasmidkarte von pSpCas9(BB)-2A-GFP (PX458) mit XhoI- und HindIII-Restriktionsschnittstellen

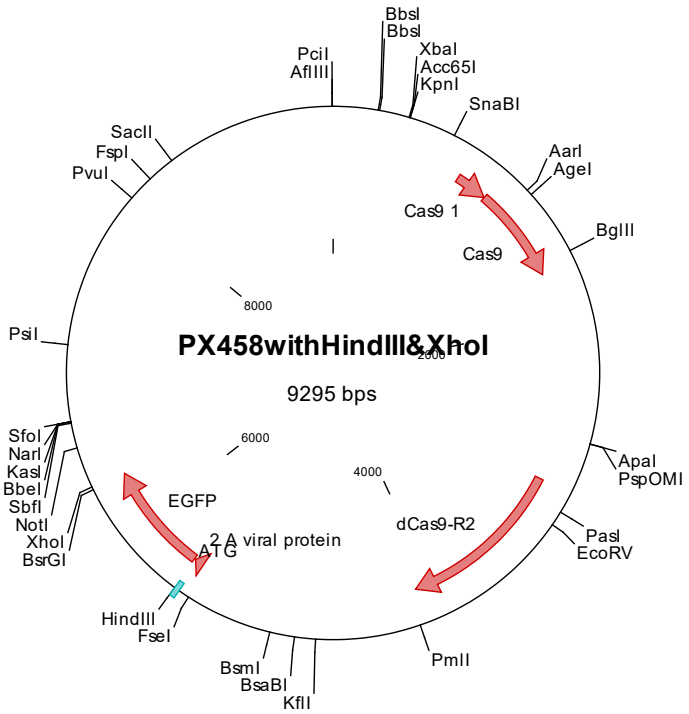

Abbildung 8.2: Aufbau des Plasmids pSpCas9(BB)-2A-GFP (PX458) mit XhoI- und HindIII-Restriktionsschnittstellen
In das 9295 bp große Plasmid wurde die sgRNA-Gensequenz gegen GABARAP (Exon 1/2/3) eingebracht. Neben den vorhandenen Schnittstellen für Restriktionsenzyme wurde eine zusätzliche für XhoI und HindIII eingebracht, einen Replikationsursprung (f1 ori) und eine Ampicillin-Resistenz (AmpR) in *E. coli* sowie einen weiteren Replikationsursprung (ori) und U6 Promotor für die Expression in Säugerzellen. Die *gRNA scaffold* Sequenz beinhaltet die Restriktionsschnittstellen für BbsI/BpiI, über die die gewünschte sgRNA in das Plasmid eingebracht werden kann. Anschließend folgt die Cas9-Sequenz aus *S. pyogenes* und eine Sequenz für das Fluoreszenzprotein EGFP, die unter einem humanen Cytomegalovirus (CMV) *enhancer* und *chicken β-actin* Promotor exprimiert werden. Am Insert befindet sich N-terminal eine 3 x FLAG-Sequenz und C-terminal die EGFP-Sequenz, die durch eine *nucleoplasmin nuclear localization signal* (NLS)- und 2A-Sequenz von Cas9 abgegrenzt wird.

8.4.3 DNA-Sequenz des pSpCas9(BB)-2A-ECFP (PX458)-Vektors mit XhoI- und HindIII-Restriktionsschnittstellen

```
   1  gagggcctat ttcccatgat tccttcatat ttgcatatac gatacaaggc tgttagagag
      ctcccggata aagggtacta aggaagtata aacgtatatg ctatgttccg acaatctctc
       -  G  P   I  S  H  D   S  F  I   F  A  Y   T  I  Q  G   C  -  R

  61  ataattggaa ttaatttgac tgtaaacaca aagatattag tacaaaatac gtgacgtaga
      tattaacctt aattaaactg acatttgtgt ttctataatc atgttttatg cactgcatct
       D  N  W   N  -  F  D   C  K  H   K  D  I   S  T  K  Y   V  T  -

 121  aagtaataat ttcttgggta gtttgcagtt ttaaaattat gttttaaaat ggactatcat
      ttcattatta aagaacccat caaacgtcaa aattttaata caaaatttta cctgatagta
       K  V  I   I  S  W  V   V  C  S   F  K  I   M  F  -  N   G  L  S

 181  atgcttaccg taacttgaaa gtatttcgat ttcttggctt tatatatctt gtggaaagga
      tacgaatggc attgaacttt cataaagcta aagaaccgaa atatatagaa caccttcct
       Y  A  Y   R  N  L  K   V  F  R   F  L  G   F  I  Y  L   V  E  R

                 BbsI      BbsI
                 ------   -------
 241  cgaaacaccg ggtcttcgag aagacctgtt ttagagctag aaatagcaag ttaaaataag
      gctttgtggc ccagaagctc ttctggacaa aatctcgatc tttatcgttc aattttattc
       T  K  H   R  V  F  E   K  T  C   F  R  A   R  N  S  K   L  K  -

 301  gctagtccgt tatcaacttg aaaaagtggc accgagtcgg tgctttttg ttttagagct
      cgatcaggca atagttgaac tttttcaccg tggctcagcc acgaaaaaac aaaatctcga
       G  -  S   V  I  N  L   K  K  W   H  R  V   G  A  F  L   F  -  S

 361  agaaatagca agttaaaata aggctagtcc gttttagcg cgtgcgccaa ttctgcagac
      tctttatcgt tcaattttat tccgatcagg caaaaatcgc gcacgcggtt aagacgtctg
       -  K  -   Q  V  K  I   R  L  V   R  F  -   R  V  R  Q   F  C  R

                    KpnI
                   -----+
                   Acc65I
                   -+----
            XbaI
          -+-----
 421  aaatggctct agaggtaccc gttacataac ttacggtaaa tggcccgcct ggctgaccgc
      tttaccgaga tctccatggg caatgtattg aatgccattt accgggcgga ccgactggcg
       Q  M  A   L  E  V  P   V  T  -   L  T  V   N  G  P  P   G  -  P

 481  ccaacgaccc ccgcccattg acgtcaatag taacgccaat agggactttc cattgacgtc
      ggttgctggg ggcgggtaac tgcagttatc attgcggtta tccctgaaag gtaactgcag
       P  N  D   P  R  P  L   T  S  I   V  T  P   I  G  T  F   H  -  R

 541  aatgggtgga gtatttacgg taaactgccc acttggcagt acatcaagtg tatcatatgc
      ttacccacct cataaatgcc atttgacggg tgaaccgtca tgtagttcac atagtatacg
       Q  W  V   E  Y  L  R   -  T  A   H  L  A   V  H  Q  V   Y  H  M

 601  caagtacgcc ccctattgac gtcaatgacg gtaaatggcc cgcctggcat tgtgcccagt
      gttcatgcgg gggataactg cagttactgc catttaccgg gcggaccgta acacgggtca
       P  S  T   P  P  I  D   V  N  D   G  K  W   P  A  W  H   C  A  Q

                                                  SnaBI
                                                 ----+--
 661  acatgacctt atgggacttt cctacttggc agtacatcta cgtattagtc atcgctatta
```

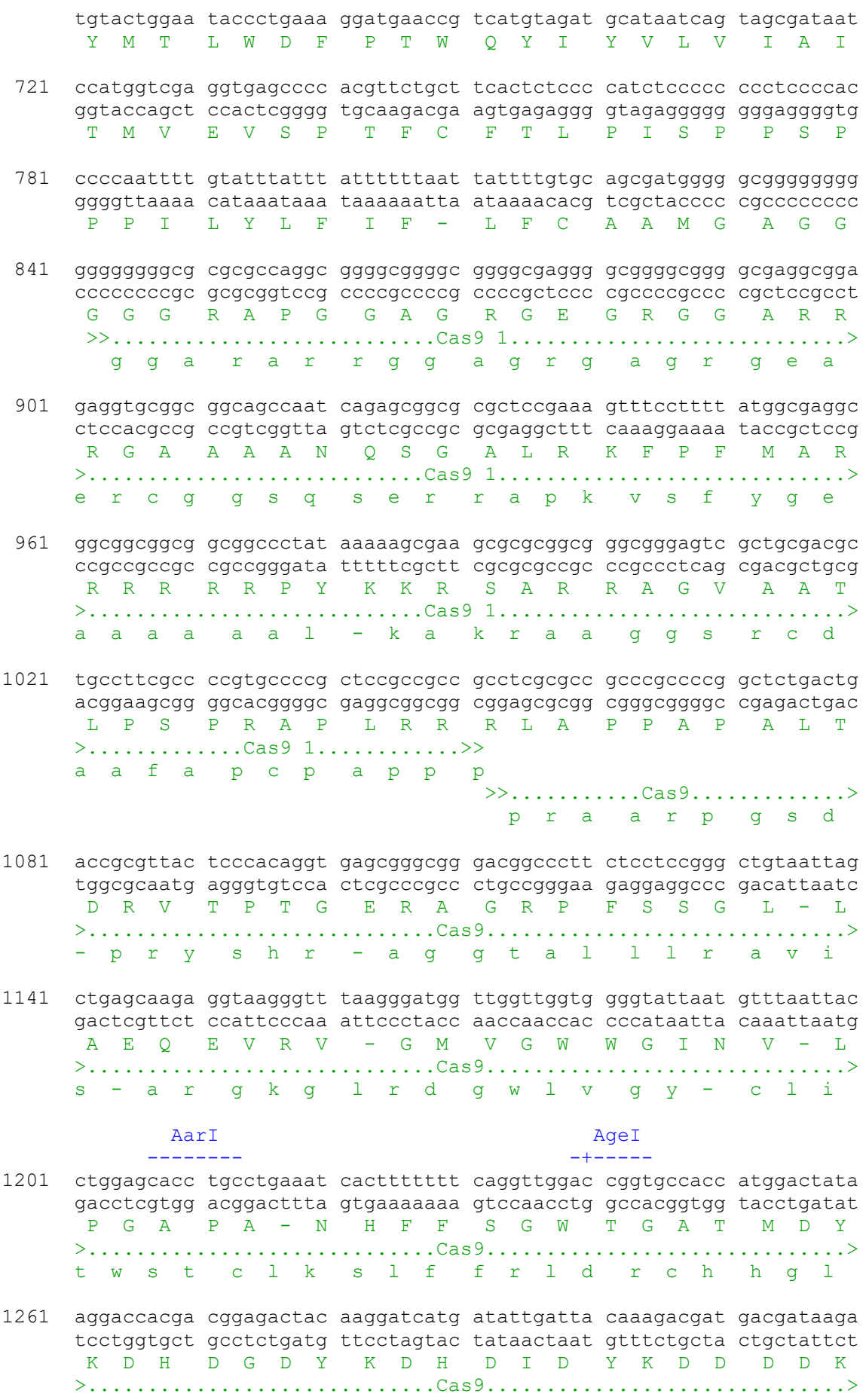
AarI
AgeI
Cas9 1
Cas9

```
      -  g  p  r   r  r  l   q  g  s   -  y  -  l   q  r  r   -  r  -

1321  tggccccaaa gaagaagcgg aaggtcggta tccacggagt cccagcagcc gacaagaagt
      accggggttt cttcttcgcc ttccagccat aggtgcctca gggtcgtcgg ctgttcttca
       M  A  P   K  K  K  R   K  V  G   I  H  G   V  P  A  A   D  K  K
      >.............................Cas9.............................>
      d  g  p  k   e  e  a   e  g  r   y  p  r  s   p  s  s   r  q  e

1381  acagcatcgg cctggacatc ggcaccaact ctgtgggctg ggccgtgatc accgacgagt
      tgtcgtagcc ggacctgtag ccgtggttga gacacccgac ccggcactag tggctgctca
       Y  S  I   G  L  D  I   G  T  N   S  V  G   W  A  V  I   T  D  E
      >.............................Cas9.............................>
      v  q  h  r   p  g  h   r  h  q   l  c  g  l   g  r  d   h  r  r

1441  acaaggtgcc cagcaagaaa ttcaaggtgc tgggcaacac cgaccggcac agcatcaaga
      tgttccacgg gtcgttcttt aagttccacg acccgttgtg gctggccgtg tcgtagttct
       Y  K  V   P  S  K  K   F  K  V   L  G  N   T  D  R  H   S  I  K
      >.............................Cas9.............................>
      v  q  g  a   q  q  e   i  q  g   a  g  q  h   r  p  a   q  h  q

1501  agaacctgat cggagccctg ctgttcgaca gcggcgaaac agccgaggcc acccggctga
      tcttggacta gcctcgggac gacaagctgt cgccgctttg tcggctccgg tgggccgact
       K  N  L   I  G  A  L   L  F  D   S  G  E   T  A  E  A   T  R  L
      >.............................Cas9.............................>
      e  e  p  d   r  s  p   a  v  r   q  r  r  n   s  r  g   h  p  a

                                                                  BglII
                                                                 -+----
1561  agagaaccgc cagaagaaga tacaccagac ggaagaaccg gatctgctat ctgcaagaga
      tctcttggcg gtcttcttct atgtggtctg ccttcttggc ctagacgata gacgttctct
       K  R  T   A  R  R  R   Y  T  R   R  K  N   R  I  C  Y   L  Q  E
      >.............................Cas9.............................>
      e  e  n  r   q  k  k   i  h  q   t  e  e  p   d  l  l   s  a  r

1621  tcttcagcaa cgagatggcc aaggtggacg acagcttctt ccacagactg gaagagtcct
      agaagtcgtt gctctaccgg ttccacctgc tgtcgaagaa ggtgtctgac cttctcagga
       I  F  S   N  E  M  A   K  V  D   D  S  F   F  H  R  L   E  E  S
      >............................Cas9...........................>>
      d  l  q  q   r  d  g   q  g  g   r  q  l  l   p  q  t   g  r

1681  tcctggtgga agaggataag aagcacgagc ggcaccccat cttcggcaac atcgtggacg
      aggaccacct tctcctattc ttcgtgctcg ccgtggggta gaagccgttg tagcacctgc
       F  L  V   E  E  D  K   K  H  E   R  H  P   I  F  G  N   I  V  D

1741  aggtggccta ccacgagaag taccccacca tctaccacct gagaaagaaa ctggtggaca
      tccaccggat ggtgctcttc atggggtggt agatggtgga ctctttcttt gaccacctgt
       E  V  A   Y  H  E  K   Y  P  T   I  Y  H   L  R  K  K   L  V  D

1801  gcaccgacaa ggccgacctg cggctgatct atctggccct ggcccacatg atcaagttcc
      cgtggctgtt ccggctggac gccgactaga tagaccggga ccgggtgtac tagttcaagg
       S  T  D   K  A  D  L   R  L  I   Y  L  A   L  A  H  M   I  K  F

1861  ggggccactt cctgatcgag ggcgacctga accccgacaa cagcgacgtg gacaagctgt
      ccccggtgaa ggactagctc ccgctggact tggggctgtt gtcgctgcac ctgttcgaca
       R  G  H   F  L  I  E   G  D  L   N  P  D   N  S  D  V   D  K  L

1921  tcatccagct ggtgcagacc tacaaccagc tgttcgagga aaaccccatc aacgccagcg
      agtaggtcga ccacgtctgg atgttggtcg acaagctcct tttggggtag ttgcggtcgc
       F  I  Q   L  V  Q  T   Y  N  Q   L  F  E   E  N  P  I   N  A  S

1981  gcgtggacgc caaggccatc ctgtctgcca gactgagcaa gagcagacgg ctggaaaatc
```

```
      cgcacctgcg gttccggtag gacagacggt ctgactcgtt ctcgtctgcc gacctttag
       G  V  D   A  K  A  I   L  S  A   R  L  S   K  S  R  R   L  E  N

2041  tgatcgccca gctgcccggc gagaagaaga atggcctgtt cggaaacctg attgccctga
      actagcgggt cgacgggccg ctcttcttct taccggacaa gcctttggac taacgggact
       L  I  A   Q  L  P  G   E  K  K   N  G  L   F  G  N  L   I  A  L

2101  gcctgggcct gacccccaac ttcaagagca acttcgacct ggccgaggat gccaaactgc
      cggacccgga ctgggggttg aagttctcgt tgaagctgga ccggctccta cggtttgacg
       S  L  G   L  T  P  N   F  K  S   N  F  D   L  A  E  D   A  K  L

2161  agctgagcaa ggacacctac gacgacgacc tggacaacct gctggcccag atcggcgacc
      tcgactcgtt cctgtggatg ctgctgctgg acctgttgga cgaccgggtc tagccgctgg
       Q  L  S   K  D  T  Y   D  D  D   L  D  N   L  L  A  Q   I  G  D

2221  agtacgccga cctgtttctg gccgccaaga acctgtccga cgccatcctg ctgagcgaca
      tcatgcggct ggacaaagac cggcggttct tggacaggct gcggtaggac gactcgctgt
       Q  Y  A   D  L  F  L   A  A  K   N  L  S   D  A  I  L   L  S  D

2281  tcctgagagt gaacaccgag atcaccaagg ccccccctgag cgcctctatg atcaagagat
      aggactctca cttgtggctc tagtggttcc gggggggactc gcggagatac tagttctcta
       I  L  R   V  N  T  E   I  T  K   A  P  L   S  A  S  M   I  K  R

2341  acgacgagca ccaccaggac ctgaccctgc tgaaagctct cgtgcggcag cagctgcctg
      tgctgctcgt ggtggtcctg gactgggacg actttcgaga gcacgccgtc gtcgacggac
       Y  D  E   H  H  Q  D   L  T  L   L  K  A   L  V  R  Q   Q  L  P

2401  agaagtacaa agagattttc ttcgaccaga gcaagaacgg ctacgccggc tacattgacg
      tcttcatgtt tctctaaaag aagctggtct cgttcttgcc gatgcggccg atgtaactgc
       E  K  Y   K  E  I  F   F  D  Q   S  K  N   G  Y  A  G   Y  I  D

2461  gcggagccag ccaggaagag ttctacaagt tcatcaagcc catcctggaa aagatggacg
      cgcctcggtc ggtccttctc aagatgttca agtagttcgg gtaggacctt ttctacctgc
       G  G  A   S  Q  E  E   F  Y  K   F  I  K   P  I  L  E   K  M  D

2521  gcaccgagga actgctcgtg aagctgaaca gagaggacct gctgcggaag cagcggacct
      cgtggctcct tgacgagcac ttcgacttgt ctctcctgga cgacgccttc gtcgcctgga
       G  T  E   E  L  L  V   K  L  N   R  E  D   L  L  R  K   Q  R  T

2581  tcgacaacgg cagcatcccc caccagatcc acctgggaga gctgcacgcc attctgcggc
      agctgttgcc gtcgtagggg gtggtctagg tggaccctct cgacgtgcgg taagacgccg
       F  D  N   G  S  I  P   H  Q  I   H  L  G   E  L  H  A   I  L  R

2641  ggcaggaaga tttttaccca ttcctgaagg acaaccggga aaagatcgag aagatcctga
      ccgtccttct aaaaatgggt aaggacttcc tgttggccct tttctagctc ttctaggact
       R  Q  E   D  F  Y  P   F  L  K   D  N  R   E  K  I  E   K  I  L

                              ApaI
                             -----+
                             PspOMI
                             -+----
2701  ccttccgcat cccctactac gtgggccctc tggccagggg aaacagcaga ttcgcctgga
      ggaaggcgta ggggatgatg cacccgggag accggtcccc tttgtcgtct aagcggacct
       T  F  R   I  P  Y  Y   V  G  P   L  A  R   G  N  S  R   F  A  W

2761  tgaccagaaa gagcgaggaa accatcaccc cctggaactt cgaggaagtg gtggacaagg
      actggtcttt ctcgctcctt tggtagtggg ggaccttgaa gctccttcac cacctgttcc
       M  T  R   K  S  E  E   T  I  T   P  W  N   F  E  E  V   V  D  K

2821  gcgcttccgc ccagagcttc atcgagcgga tgaccaactt cgataagaac ctgcccaacg
      cgcgaaggcg ggtctcgaag tagctcgcct actggttgaa gctattcttg gacgggttgc
```

```
       G  A  S   A  Q  S  F   I  E  R   M  T  N   F  D  K  N   L  P  N

2881   agaaggtgct gcccaagcac agcctgctgt acgagtactt caccgtgtat aacgagctga
       tcttccacga cgggttcgtg tcggacgaca tgctcatgaa gtggcacata ttgctcgact
        E  K  V   L  P  K  H   S  L  L   Y  E  Y   F  T  V  Y   N  E  L

2941   ccaaagtgaa atacgtgacc gagggaatga gaaagcccgc cttcctgagc ggcgagcaga
       ggtttcactt tatgcactgg ctcccttact ctttcgggcg gaaggactcg ccgctcgtct
        T  K  V   K  Y  V  T   E  G  M   R  K  P   A  F  L  S   G  E  Q

3001   aaaaggccat cgtggacctg ctgttcaaga ccaaccggaa agtgaccgtg aagcagctga
       ttttccggta gcacctggac gacaagttct ggttggcctt tcactggcac ttcgtcgact
        K  K  A   I  V  D  L   L  F  K   T  N  R   K  V  T  V   K  Q  L
                              >>..............dCas9-R2.................>

3061   aagaggacta cttcaagaaa atcgagtgct tcgactccgt ggaaatctcc ggcgtggaag
       ttctcctgat gaagttcttt tagctcacga agctgaggca cctttagagg ccgcaccttc
        K  E  D   Y  F  K  K   I  E  C   F  D  S   V  E  I  S   G  V  E
       >............................dCas9-R2............................>

                        PasI
                      --+-----
3121   atcggttcaa cgcctccctg ggcacatacc acgatctgct gaaaattatc aaggacaagg
       tagccaagtt gcggagggac ccgtgtatgg tgctagacga cttttaatag ttcctgttcc
        D  R  F   N  A  S  L   G  T  Y   H  D  L   L  K  I  I   K  D  K
       >............................dCas9-R2............................>

                                                 EcoRV
                                                ----+--
3181   acttcctgga caatgaggaa aacgaggaca ttctggaaga tatcgtgctg accctgacac
       tgaaggacct gttactcctt ttgctcctgt aagaccttct atagcacgac tgggactgtg
        D  F  L   D  N  E  E   N  E  D   I  L  E   D  I  V  L   T  L  T
       >............................dCas9-R2............................>

3241   tgtttgagga cagagagatg atcgaggaac ggctgaaaac ctatgcccac ctgttcgacg
       acaaactcct gtctctctac tagctccttg ccgacttttg gatacgggtg gacaagctgc
        L  F  E   D  R  E  M   I  E  E   R  L  K   T  Y  A  H   L  F  D
       >............................dCas9-R2............................>

3301   acaaagtgat gaagcagctg aagcggcgga gatacaccgg ctggggcagg ctgagccgga
       tgtttcacta cttcgtcgac ttcgccgcct ctatgtggcc gaccccgtcc gactcggcct
        D  K  V   M  K  Q  L   K  R  R   R  Y  T   G  W  G  R   L  S  R
       >............................dCas9-R2............................>

3361   agctgatcaa cggcatccgg gacaagcagt ccggcaagac aatcctggat ttcctgaagt
       tcgactagtt gccgtaggcc ctgttcgtca ggccgttctg ttaggaccta aaggacttca
        K  L  I   N  G  I  R   D  K  Q   S  G  K   T  I  L  D   F  L  K
       >............................dCas9-R2............................>

3421   ccgacggctt cgccaacaga aacttcatgc agctgatcca cgacgacagc ctgaccttta
       ggctgccgaa gcggttgtct ttgaagtacg tcgactaggt gctgctgtcg gactggaaat
        S  D  G   F  A  N  R   N  F  M   Q  L  I   H  D  D  S   L  T  F
       >............................dCas9-R2............................>

3481   aagaggacat ccagaaagcc caggtgtccg gccagggcga tagcctgcac gagcacattg
       ttctcctgta ggtctttcgg gtccacaggc cggtcccgct atcggacgtg ctcgtgtaac
        K  E  D   I  Q  K  A   Q  V  S   G  Q  G   D  S  L  H   E  H  I
       >............................dCas9-R2............................>

3541   ccaatctggc cggcagcccc gccattaaga agggcatcct gcagacagtg aaggtggtgg
       ggttagaccg gccgtcgggg cggtaattct tcccgtagga cgtctgtcac ttccaccacc
```

```
        A  N  L   A  G  S  P   A  I  K   K  G  I   L  Q  T  V   K  V  V
       >.........................dCas9-R2.........................>

 3601  acgagctcgt gaaagtgatg ggccggcaca agcccgagaa catcgtgatc gaaatggcca
       tgctcgagca ctttcactac ccggccgtgt tcgggctctt gtagcactag ctttaccggt
        D  E  L   V  K  V  M   G  R  H   K  P  E   N  I  V  I   E  M  A
       >.........................dCas9-R2.........................>

 3661  gagagaacca gaccacccag aagggacaga agaacagccg cgagagaatg aagcggatcg
       ctctcttggt ctggtgggtc ttccctgtct tcttgtcggc gctctcttac ttcgcctagc
        R  E  N   Q  T  T  Q   K  G  Q   K  N  S   R  E  R  M   K  R  I
       >.........................dCas9-R2.........................>

 3721  aagagggcat caaagagctg ggcagccaga tcctgaaaga acaccccgtg gaaaacaccc
       ttctcccgta gtttctcgac ccgtcggtct aggactttct tgtggggcac cttttgtggg
        E  E  G   I  K  E  L   G  S  Q   I  L  K   E  H  P  V   E  N  T
       >.........................dCas9-R2.........................>

3781  agctgcagaa cgagaagctg tacctgtact acctgcagaa tgggcgggat atgtacgtgg
       tcgacgtctt gctcttcgac atggacatga tggacgtctt acccgcccta tacatgcacc
        Q  L  Q   N  E  K  L   Y  L  Y   Y  L  Q   N  G  R  D   M  Y  V
       >.........................dCas9-R2.........................>

 3841  accaggaact ggacatcaac cggctgtccg actacgatgt ggaccatatc gtgcctcaga
       tggtccttga cctgtagttg gccgacaggc tgatgctaca cctggtatag cacggagtct
        D  Q  E   L  D  I  N   R  L  S   D  Y  D   V  D  H  I   V  P  Q
       >.........................dCas9-R2.........................>


 3901  gctttctgaa ggacgactcc atcgacaaca aggtgctgac cagaagcgac aagaaccggg
       cgaaagactt cctgctgagg tagctgttgt tccacgactg gtcttcgctg ttcttggccc
        S  F  L   K  D  D  S   I  D  N   K  V  L   T  R  S  D   K  N  R
       >.........................dCas9-R2.........................>

 3961  gcaagagcga caacgtgccc tccgaagagg tcgtgaagaa gatgaagaac tactggcggc
       cgttctcgct gttgcacggg aggcttctcc agcacttctt ctacttcttg atgaccgccg
        G  K  S   D  N  V  P   S  E  E   V  V  K   K  M  K  N   Y  W  R
       >.........................dCas9-R2.........................>

 4021  agctgctgaa cgccaagctg attacccaga gaaagttcga caatctgacc aaggccgaga
       tcgacgactt gcggttcgac taatgggtct ctttcaagct gttagactgg ttccggctct
        Q  L  L   N  A  K  L   I  T  Q   R  K  F   D  N  L  T   K  A  E
       >.........................dCas9-R2.........................>

 4081  gaggcggcct gagcgaactg gataaggccg gcttcatcaa gagacagctg gtggaaaccc
       ctccgccgga ctcgcttgac ctattccggc cgaagtagtt ctctgtcgac caccttgggg
        R  G  G   L  S  E  L   D  K  A   G  F  I   K  R  Q  L   V  E  T
       >..........dCas9-R2.........>>
                       PmlI
                      ---+--
 4141  ggcagatcac aaagcacgtg gcacagatcc tggactcccg gatgaacact aagtacgacg
       ccgtctagtg tttcgtgcac cgtgtctagg acctgagggc ctacttgtga ttcatgctgc
        R  Q  I   T  K  H  V   A  Q  I   L  D  S   R  M  N  T   K  Y  D

 4201  agaatgacaa gctgatccgg gaagtgaaag tgatcaccct gaagtccaag ctggtgtccg
       tcttactgtt cgactaggcc cttcactttc actagtggga cttcaggttc gaccacaggc
        E  N  D   K  L  I  R   E  V  K   V  I  T   L  K  S  K   L  V  S

 4261  atttccggaa ggatttccag ttttacaaag tgcgcgagat caacaactac caccacgccc
       taaaggcctt cctaaaggtc aaaatgtttc acgcgctcta gttgttgatg gtggtgcggg
        D  F  R   K  D  F  Q   F  Y  K   V  R  E   I  N  N  Y   H  H  A
```

```
4321  acgacgccta cctgaacgcc gtcgtgggaa ccgccctgat caaaaagtac cctaagctgg
      tgctgcggat ggacttgcgg cagcaccctt ggcgggacta gtttttcatg ggattcgacc
       H  D  A   Y  L  N  A   V  V  G   T  A  L   I  K  K  Y   P  K  L

4381  aaagcgagtt cgtgtacggc gactacaagg tgtacgacgt gcggaagatg atcgccaaga
      tttcgctcaa gcacatgccg ctgatgttcc acatgctgca cgccttctac tagcggttct
       E  S  E   F  V  Y  G   D  Y  K   V  Y  D   V  R  K  M   I  A  K

4441  gcgagcagga aatcggcaag gctaccgcca agtacttctt ctacagcaac atcatgaact
      cgctcgtcct ttagccgttc cgatggcggt tcatgaagaa gatgtcgttg tagtacttga
       S  E  Q   E  I  G  K   A  T  A   K  Y  F   F  Y  S  N   I  M  N

4501  ttttcaagac cgagattacc ctggccaacg gcgagatccg gaagcggcct ctgatcgaga
      aaaagttctg gctctaatgg gaccggttgc cgctctaggc cttcgccgga gactagctct
       F  F  K   T  E  I  T   L  A  N   G  E  I   R  K  R  P   L  I  E

4561  caaacggcga aaccggggag atcgtgtggg ataagggccg ggattttgcc accgtgcgga
      gtttgccgct ttggcccctc tagcacaccc tattcccggc cctaaaacgg tggcacgcct
       T  N  G   E  T  G  E   I  V  W   D  K  G   R  D  F  A   T  V  R

4621  aagtgctgag catgccccaa gtgaatatcg tgaaaaagac cgaggtgcag acaggcggct
      ttcacgactc gtacggggtt cacttatagc acttttctg gctccacgtc tgtccgccga
       K  V  L   S  M  P  Q   V  N  I   V  K  K   T  E  V  Q   T  G  G

4681  tcagcaaaga gtctatcctg cccaagagga acagcgataa gctgatcgcc agaaagaagg
      agtcgtttct cagataggac gggttctcct tgtcgctatt cgactagcgg tctttcttcc
       F  S  K   E  S  I  L   P  K  R   N  S  D   K  L  I  A   R  K  K

          KflI
        --+----
4741  actgggaccc taagaagtac ggcggcttcg acagccccac cgtggcctat tctgtgctgg
      tgaccctggg attcttcatg ccgccgaagc tgtcggggtg gcaccggata agacacgacc
       D  W  D   P  K  K  Y   G  G  F   D  S  P   T  V  A  Y   S  V  L

4801  tggtggccaa agtggaaaag ggcaagtcca agaaactgaa gagtgtgaaa gagctgctgg
      accaccggtt tcacctttc ccgttcaggt tctttgactt ctcacacttt ctcgacgacc
       V  V  A   K  V  E  K   G  K  S   K  K  L   K  S  V  K   E  L  L

        BsaBI
      -----+-----
4861  ggatcaccat catggaaaga agcagcttcg agaagaatcc catcgacttt ctggaagcca
      cctagtggta gtaccttttct tcgtcgaagc tcttcttagg gtagctgaaa gaccttcggt
       G  I  T   I  M  E  R   S  S  F   E  K  N   P  I  D  F   L  E  A

4921  agggctacaa agaagtgaaa aaggacctga tcatcaagct gcctaagtac tccctgttcg
      tcccgatgtt tcttcacttt ttcctggact agtagttcga cggattcatg agggacaagc
       K  G  Y   K  E  V  K   K  D  L   I  I  K   L  P  K  Y   S  L  F

                            BsmI
                           ------
4981  agctggaaaa cggccggaag agaatgctgg cctctgccgg cgaactgcag aagggaaacg
      tcgacctttt gccggccttc tcttacgacc ggagacggcc gcttgacgtc ttcccttgc
       E  L  E   N  G  R  K   R  M  L   A  S  A   G  E  L  Q   K  G  N

5041  aactggccct gccctccaaa tatgtgaact tcctgtacct ggccagccac tatgagaagc
      ttgaccggga cgggaggttt atacacttga aggacatgga ccggtcggtg atactcttcg
       E  L  A   L  P  S  K   Y  V  N   F  L  Y   L  A  S  H   Y  E  K

5101  tgaagggctc ccccgaggat aatgagcaga aacagctgtt tgtggaacag cacaagcact
      acttcccgag ggggctccta ttactcgtct ttgtcgacaa acaccttgtc gtgttcgtga
```

```
       L  K  G   S  P  E  D   N  E  Q   K  Q  L   F  V  E  Q   H  K  H

5161   acctggacga gatcatcgag cagatcagcg agttctccaa gagagtgatc ctggccgacg
       tggacctgct ctagtagctc gtctagtcgc tcaagaggtt ctctcactag gaccggctgc
        Y  L  D   E  I  I  E   Q  I  S   E  F  S   K  R  V  I   L  A  D

5221   ctaatctgga caaagtgctg tccgcctaca acaagcaccg ggataagccc atcagagagc
       gattagacct gtttcacgac aggcggatgt tgttcgtggc cctattcggg tagtctctcg
        A  N  L   D  K  V  L   S  A  Y   N  K  H   R  D  K  P   I  R  E

5281   aggccgagaa tatcatccac ctgtttaccc tgaccaatct gggagcccct gccgccttca
       tccggctctt atagtaggtg gacaaatggg actggttaga ccctcgggga cggcggaagt
        Q  A  E   N  I  I  H   L  F  T   L  T  N   L  G  A  P   A  A  F

5341   agtactttga caccaccatc gaccggaaga ggtacaccag caccaaagag gtgctggacg
       tcatgaaact gtggtggtag ctggccttct ccatgtggtc gtggtttctc cacgacctgc
        K  Y  F   D  T  T  I   D  R  K   R  Y  T   S  T  K  E   V  L  D

5401   ccaccctgat ccaccagagc atcaccggcc tgtacgagac acggatcgac ctgtctcagc
       ggtgggacta ggtggtctcg tagtggccgg acatgctctg tgcctagctg gacagagtcg
        A  T  L   I  H  Q  S   I  T  G   L  Y  E   T  R  I  D   L  S  Q

                                                FseI
                                              ------+--
5461   tgggaggcga caaaaggccg gcggccacga aaaaggccgg ccaggcaaaa aagaaaaagg
       accctccgct gttttccggc cgccggtgct ttttccggcc ggtccgtttt ttctttttcc
        L  G  G   D  K  R  P   A  A  T   K  K  A   G  Q  A  K   K  K  K

5521   aattcggcag tggagagggc agaggaagtc tgctaacatg cggtgacgtc gaggagaatc
       ttaagccgtc acctctcccg tctccttcag acgattgtac gccactgcag ctcctcttag
        E  F  G   S  G  E  G   R  G  S   L  L  T   C  G  D  V   E  E  N
           >>...................2 A viral protein.....................>
```

```
          HindIII
          -+-----
5581   ctggcccaag cttaatggtg agcaagggcg aggagctgtt caccggggtg gtgcccatcc
       gaccgggttc gaattaccac tcgttcccgc tcctcgacaa gtggccccac cacgggtagg
        P  G  P   S  L  M  V   S  K  G   E  E  L   F  T  G  V   V  P  I
       >.....>> 2 A viral protein
                     >>.....................eCFP.....................>

5641   tggtcgagct ggacggcgac gtaaacggcc acaagttcag cgtgtccggc gagggcgagg
       accagctcga cctgccgctg catttgccgg tgttcaagtc gcacaggccg ctcccgctcc
        L  V  E   L  D  G  D   V  N  G   H  K  F   S  V  S  G   E  G  E
       >.............................eCFP.............................>

5701   gcgatgccac ctacggcaag ctgaccctga agttcatctg caccaccggc aagctgcccg
       cgctacggtg gatgccgttc gactgggact tcaagtagac gtggtggccg ttcgacgggc
        G  D  A   T  Y  G  K   L  T  L   K  F  I   C  T  T  G   K  L  P
       >.............................eCFP.............................>

5761   tgccctggcc caccctcgtg accaccctga cctggggcgt gcagtgcttc agccgctacc
       acgggaccgg gtgggagcac tggtgggact ggaccccgca cgtcacgaag tcggcgatgg
        V  P  W   P  T  L  V   T  T  L   T  W  G   V  Q  C  F   S  R  Y
       >.............................eCFP.............................>
```

```
5821  ccgaccacat gaagcagcac gacttcttca agtccgccat gcccgaaggc tacgtccagg
      ggctggtgta cttcgtcgtg ctgaagaagt tcaggcggta cgggcttccg atgcaggtcc
       P  D  H   M  K  Q  H   D  F  F   K  S  A   M  P  E  G   Y  V  Q
      >.............................eCFP.............................>

5881  agcgcaccat cttcttcaag gacgacggca actacaagac ccgcgccgag gtgaagttcg
      tcgcgtggta gaagaagttc ctgctgccgt tgatgttctg ggcgcggctc cacttcaagc
       E  R  T   I  F  F  K   D  D  G   N  Y  K   T  R  A  E   V  K  F
      >.............................eCFP.............................>

5941  agggcgacac cctggtgaac cgcatcgagc tgaagggcat cgacttcaag gaggacggca
      tcccgctgtg ggaccacttg gcgtagctcg acttcccgta gctgaagttc ctcctgccgt
       E  G  D   T  L  V  N   R  I  E   L  K  G   I  D  F  K   E  D  G
      >.............................eCFP.............................>

6001  acatcctggg gcacaagctg gagtacaact acatcagcca caacgtctat atcaccgccg
      tgtaggaccc cgtgttcgac ctcatgttga tgtagtcggt gttgcagata tagtggcggc
       N  I  L   G  H  K  L   E  Y  N   Y  I  S   H  N  V  Y   I  T  A
      >.............................eCFP.............................>

6061  acaagcagaa gaacggcatc aaggccaact tcaagatccg ccacaacatc gaggacggca
      tgttcgtctt cttgccgtag ttccggttga agttctaggc ggtgttgtag ctcctgccgt
       D  K  Q   K  N  G  I   K  A  N   F  K  I   R  H  N  I   E  D  G
      >.............................eCFP.............................>

6121  gcgtgcagct cgccgaccac taccagcaga acacccccat cggcgacggc cccgtgctgc
      cgcacgtcga gcggctggtg atggtcgtct tgtggggtga gccgctgccg gggcacgacg
       S  V  Q   L  A  D  H   Y  Q  Q   N  T  P   I  G  D  G   P  V  L
      >.............................eCFP.............................>

6181  tgcccgacaa ccactacctg agcacccagt ccgccctgag caaagacccc aacgagaagc
      acgggctgtt ggtgatggac tcgtgggtca ggcgggactc gtttctgggg ttgctcttcg
       L  P  D   N  H  Y  L   S  T  Q   S  A  L   S  K  D  P   N  E  K
      >.............................eCFP.............................>

6241  gcgatcacat ggtcctgctg gagttcgtga ccgccgccgg gatcactctc ggcatggacg
      cgctagtgta ccaggacgac ctcaagcact ggcggcggcc ctagtgagag ccgtacctgc
       R  D  H   M  V  L  L   E  F  V   T  A  A   G  I  T  L   G  M  D
      >.............................eCFP.............................>

          BsrGI         XhoI
         -+----        -+----
6301  agctgtacaa gtaactcgag ctcgctgatc agcctcgact gtgccttcta gttgccagcc
      tcgacatgtt cattgagctc gagcgactag tcggagctga cacggaagat caacggtcgg
       E  L  Y   K  -  L  E   L  A  D   Q  P  R   L  C  L  L   V  A  S
      >...eCFP..>>

6361  atctgttgtt tgcccctccc ccgtgccttc cttgaccctg gaaggtgcca ctcccactgt
      tagacaacaa acggggaggg ggcacggaag gaactgggac cttccacggt gagggtgaca
       H  L  L   F  A  P  P   P  C  L   P  -  P   W  K  V  P   L  P  L

6421  cctttcctaa taaaatgagg aaattgcatc gcattgtctg agtaggtgtc attctattct
      ggaaaggatt attttactcc tttaacgtag cgtaacagac tcatccacag taagataaga
       S  F  P   N  K  M  R   K  L  H   R  I  V   -  V  G  V   I  L  F

6481  ggggggtggg gtggggcagg acagcaaggg ggaggattgg gaagagaata gcaggcatgc
      cccccaccc caccccgtcc tgtcgttccc cctcctaacc cttctcttat cgtccgtacg
       W  G  V   G  W  G  R   T  A  R   G  R  I   G  K  R  I   A  G  M

            NotI
         --+------
```

```
6541  tggggagcgg ccgcaggaac ccctagtgat ggagttggcc actccctctc tgcgcgctcg
      acccctcgcc ggcgtccttg gggatcacta cctcaaccgg tgagggagag acgcgcgagc
       L  G  S   G  R  R  N   P  -  -   W  S  W   P  L  P  L   C  A  L

6601  ctcgctcact gaggccgggc gaccaaaggt cgcccgacgc ccgggctttg cccgggcggc
      gagcgagtga ctccggcccg ctggtttcca gcgggctgcg ggcccgaaac gggcccgccg
       A  R  S   L  R  P  G   D  Q  R   S  P  D   A  R  A  L   P  G  R

                                                 BbeI
                                               -----+-
                                                 SfoI
                                               ---+---
                                                 NarI
                                               --+----
                                                 KasI
                                               -+-----
                                          SbfI
                                        -------+-
6661  ctcagtgagc gagcgagcgc gcagctgcct gcaggggcgc ctgatgcggt attttctcct
      gagtcactcg ctcgctcgcg cgtcgacgga cgtccccgcg gactacgcca taaaagagga
       P  Q  -   A  S  E  R   A  A  A   C  R  G   A  -  C  G   I  F  S

6721  tacgcatctg tgcggtattt cacaccgcat acgtcaaagc aaccatagta cgcgccctgt
      atgcgtagac acgccataaa gtgtggcgta tgcagtttcg ttggtatcat gcgcgggaca
       L  R  I   C  A  V  F   H  T  A   Y  V  K   A  T  I  V   R  A  L

6781  agcggcgcat taagcgcggc gggtgtggtg gttacgcgca gcgtgaccgc tacacttgcc
      tcgccgcgta attcgcgccg cccacaccac caatgcgcgt cgcactggcg atgtgaacgg
       -  R  R   I  K  R  G   G  C  G   G  Y  A   Q  R  D  R   Y  T  C

6841  agcgccctag cgcccgctcc tttcgctttc ttcccttcct ttctcgccac gttcgccggc
      tcgcgggatc gcgggcgagg aaagcgaaag aagggaagga aagagcggtg caagcggccg
       Q  R  P   S  A  R  S   F  R  F   L  P  F   L  S  R  H   V  R  R

6901  tttccccgtc aagctctaaa tcgggggctc cctttagggt tccgatttag tgctttacgg
      aaaggggcag ttcgagattt agcccccgag ggaaatccca aggctaaatc acgaaatgcc
       L  S  P   S  S  S  K   S  G  A   P  F  R   V  P  I  -   C  F  T

6961  cacctcgacc ccaaaaaact tgatttgggt gatggttcac gtagtgggcc atcgccctga
      gtggagctgg ggtttttga actaaaccca ctaccaagtg catcacccgg tagcgggact
       A  P  R   P  Q  K  T   -  F  G   -  W  F   T  -  W  A   I  A  L

7021  tagacggttt ttcgcccttt gacgttggag tccacgttct ttaatagtgg actcttgttc
      atctgccaaa aagcgggaaa ctgcaacctc aggtgcaaga aattatcacc tgagaacaag
       I  D  G   F  S  P  F   D  V  G   V  H  V   L  -  -  W   T  L  V

                                                                PsiI
                                                              ---+---
7081  caaactggaa caacactcaa ccctatctcg ggctattctt ttgatttata agggattttg
      gtttgacctt gttgtgagtt gggatagagc ccgataagaa aactaaatat tccctaaaac
       P  N  W   N  N  T  Q   P  Y  L   G  L  F   F  -  F  I   R  D  F

7141  ccgatttcgg cctattggtt aaaaaatgag ctgatttaac aaaaatttaa cgcgaatttt
      ggctaaagcc ggataaccaa ttttttactc gactaaattg tttttaaatt gcgcttaaaa
       A  D  F   G  L  L  V   K  K  -   A  D  L   T  K  I  -   R  E  F

7201  aacaaaatat taacgtttac aattttatgg tgcactctca gtacaatctg ctctgatgcc
      ttgttttata attgcaaatg ttaaaatacc acgtgagagt catgttagac gagactacgg
       -  Q  N   I  N  V  Y   N  F  M   V  H  S   Q  Y  N  L   L  -  C

7261  gcatagttaa gccagccccg acacccgcca acacccgctg acgcgccctg acgggcttgt
```

```
      cgtatcaatt cggtcggggc tgtgggcggt tgtgggcgac tgcgcgggac tgcccgaaca
       R  I  V   K  P  A  P   T  P  A   N  T  R   -  R  A  L   T  G  L

7321  ctgctcccgg catccgctta cagacaagct gtgaccgtct ccgggagctg catgtgtcag
      gacgagggcc gtaggcgaat gtctgttcga cactggcaga ggccctcgac gtacacagtc
       S  A  P   G  I  R  L   Q  T  S   C  D  R   L  R  E  L   H  V  S

7381  aggttttcac cgtcatcacc gaaacgcgcg agacgaaagg gcctcgtgat acgcctattt
      tccaaaagtg gcagtagtgg ctttgcgcgc tctgctttcc cggagcacta tgcggataaa
       E  V  F   T  V  I  T   E  T  R   E  T  K   G  P  R  D   T  P  I

7441  ttataggtta atgtcatgat aataatggtt tcttagacgt caggtggcac ttttcgggga
      aatatccaat tacagtacta ttattaccaa agaatctgca gtccaccgtg aaaagccccc
       F  I  G   -  C  H  D   N  N  G   F  L  D   V  R  W  H   F  S  G

7501  aatgtgcgcg gaacccctat ttgtttattt ttctaaatac attcaaatat gtatccgctc
      ttacacgcgc cttggggata aacaaataaa aagatttatg taagtttata cataggcgag
       K  C  A   R  N  P  Y   L  F  I   F  L  N   T  F  K  Y   V  S  A

7561  atgagacaat aaccctgata aatgcttcaa taatattgaa aaaggaagag tatgagtatt
      tactctgtta ttgggactat ttacgaagtt attataactt tttccttctc atactcataa
       H  E  T   I  T  L  I   N  A  S   I  I  L   K  K  E  E   Y  E  Y

7621  caacatttcc gtgtcgccct tattcccttt tttgcggcat tttgccttcc tgtttttgct
      gttgtaaagg cacagcggga ataagggaaa aaacgccgta aaacggaagg acaaaaacga
       S  T  F   P  C  R  P   Y  S  L   F  C  G   I  L  P  S   C  F  C

7681  cacccagaaa cgctggtgaa agtaaaagat gctgaagatc agttgggtgc acgagtgggt
      gtgggtcttt gcgaccactt tcattttcta cgacttctag tcaacccacg tgctcaccca
       S  P  R   N  A  G  E   S  K  R   C  -  R   S  V  G  C   T  S  G

7741  tacatcgaac tggatctcaa cagcggtaag atccttgaga gttttcgccc cgaagaacgt
      atgtagcttg acctagagtt gtcgccattc taggaactct caaaagcggg gcttcttgca
       L  H  R   T  G  S  Q   Q  R  -   D  P  -   E  F  S  P   R  R  T

7801  tttccaatga tgagcacttt taaagttctg ctatgtggcg cggtattatc ccgtattgac
      aaaggttact actcgtgaaa atttcaagac gatacaccgc gccataatag ggcataactg
       F  S  N   D  E  H  F   -  S  S   A  M  W   R  G  I  I   P  Y  -

7861  gccgggcaag agcaactcgg tcgccgcata cactattctc agaatgactt ggttgagtac
      cggcccgttc tcgttgagcc agcggcgtat gtgataagag tcttactgaa ccaactcatg
       R  R  A   R  A  T  R   S  P  H   T  L  F   S  E  -  L   G  -  V

7921  tcaccagtca cagaaaagca tcttacggat ggcatgacag taagagaatt atgcagtgct
      agtggtcagt gtcttttcgt agaatgccta ccgtactgtc attctcttaa tacgtcacga
       L  T  S   H  R  K  A   S  Y  G   W  H  D   S  K  R  I   M  Q  C

                                                          PvuI
                                                         ----+--
7981  gccataacca tgagtgataa cactgcggcc aacttacttc tgacaacgat cggaggaccg
      cggtattggt actcactatt gtgacgccgg ttgaatgaag actgttgcta gcctcctggc
       C  H  N   H  E  -  -   H  C  G   Q  L  T   S  D  N  D   R  R  T

8041  aaggagctaa ccgctttttt gcacaacatg ggggatcatg taactcgcct tgatcgttgg
      ttcctcgatt ggcgaaaaaa cgtgttgtac cccctagtac attgagcgga actagcaacc
       E  G  A   N  R  F  F   A  Q  H   G  G  S   C  N  S  P   -  S  L

8101  gaaccggagc tgaatgaagc cataccaaac gacgagcgtg acaccacgat gcctgtagca
      cttggcctcg acttacttcg gtatggtttg ctgctcgcac tgtggtgcta cggacatcgt
       G  T  G   A  E  -  S   H  T  K   R  R  A   -  H  H  D   A  C  S
```

```
                  FspI
                  ---+--
8161  atggcaacaa cgttgcgcaa actattaact ggcgaactac ttactctagc ttcccggcaa
      taccgttgtt gcaacgcgtt tgataattga ccgcttgatg aatgagatcg aagggccgtt
       N  G  N   N  V  A  Q   T  I  N   W  R  T   T  Y  S  S   F  P  A

8221  caattaatag actggatgga ggcggataaa gttgcaggac cacttctgcg ctcggccctt
      gttaattatc tgacctacct ccgcctattt caacgtcctg gtgaagacgc gagccgggaa
       T  I  N   R  L  D  G   G  G  -   S  C  R   T  T  S  A   L  G  P

                                                              SacII
                                                              ----+-
8281  ccggctggct ggtttattgc tgataaatct ggagccggtg agcgtggaag ccgcggtatc
      ggccgaccga ccaaataacg actatttaga cctcggccac tcgcaccttc ggcgccatag
       S  G  W   L  V  Y  C   -  -  I   W  S  R   -  A  W  K   P  R  Y

8341  attgcagcac tggggccaga tggtaagccc tcccgtatcg tagttatcta cacgacgggg
      taacgtcgtg accccggtct accattcggg agggcatagc atcaatagat gtgctgcccc
       H  C  S   T  G  A  R   W  -  A   L  P  Y   R  S  Y  L   H  D  G

8401  agtcaggcaa ctatggatga acgaaataga cagatcgctg agataggtgc ctcactgatt
      tcagtccgtt gatacctact tgctttatct gtctagcgac tctatccacg gagtgactaa
       E  S  G   N  Y  G  -   T  K  -   T  D  R   -  D  R  C   L  T  D

8461  aagcattggt aactgtcaga ccaagtttac tcatatatac tttagattga tttaaaactt
      ttcgtaacca ttgacagtct ggttcaaatg agtatatatg aaatctaact aaattttgaa
       -  A  L   V  T  V  R   P  S  L   L  I  Y   T  L  D  -   F  K  T

8521  catttttaat ttaaaaggat ctaggtgaag atccttttg ataatctcat gaccaaaatc
      gtaaaaatta aattttccta gatccacttc taggaaaaac tattagagta ctggttttag
       S  F  L   I  -  K  D   L  G  E   D  P  F   -  -  S  H   D  Q  N

8581  ccttaacgtg agttttcgtt ccactgagcg tcagaccccg tagaaaagat caaaggatct
      ggaattgcac tcaaaagcaa ggtgactcgc agtctggggc atcttttcta gtttcctaga
       P  L  T   -  V  F  V   P  L  S   V  R  P   R  R  K  D   Q  R  I

8641  tcttgagatc ctttttttct gcgcgtaatc tgctgcttgc aaacaaaaaa accaccgcta
      agaactctag gaaaaaaaga cgcgcattag acgacgaacg tttgtttttt tggtggcgat
       F  L  R   S  F  F  S   A  R  N   L  L  L   A  N  K  K   T  T  A

8701  ccagcggtgg tttgtttgcc ggatcaagag ctaccaactc tttttccgaa ggtaactggc
      ggtcgccacc aaacaaacgg cctagttctc gatggttgag aaaaaggctt ccattgaccg
       T  S  G   G  L  F  A   G  S  R   A  T  N   S  F  S  E   G  N  W

8761  ttcagcagag cgcagatacc aaatactgtc cttctagtgt agccgtagtt aggccaccac
      aagtcgtctc gcgtctatgg tttatgacag gaagatcaca tcggcatcaa tccggtggtg
       L  Q  Q   S  A  D  T   K  Y  C   P  S  S   V  A  V  V   R  P  P

8821  ttcaagaact ctgtagcacc gcctacatac ctcgctctgc taatcctgtt accagtggct
      aagttcttga gacatcgtgg cggatgtatg gagcgagacg attaggacaa tggtcaccga
       L  Q  E   L  C  S  T   A  Y  I   P  R  S   A  N  P  V   T  S  G

8881  gctgccagtg gcgataagtc gtgtcttacc gggttggact caagacgata gttaccggat
      cgacggtcac cgctattcag cacagaatgg cccaacctga gttctgctat caatggccta
       C  C  Q   W  R  -  V   V  S  Y   R  V  G   L  K  T  I   V  T  G

8941  aaggcgcagc ggtcgggctg aacgggggt tcgtgcacac agcccagctt ggagcgaacg
      ttccgcgtcg ccagcccgac ttgccccca agcacgtgtg tcgggtcgaa cctcgcttgc
       -  G  A   A  V  G  L   N  G  G   F  V  H   T  A  Q  L   G  A  N

9001  acctacaccg aactgagata cctacagcgt gagctatgag aaagcgccac gcttcccgaa
```

```
      tggatgtggc ttgactctat ggatgtcgca ctcgatactc tttcgcggtg cgaagggctt
       D  L  H   R  T  E  I   P  T  A   -  A  M   R  K  R  H   A  S  R

9061  gggagaaagg cggacaggta tccggtaagc ggcagggtcg gaacaggaga gcgcacgagg
      ccctctttcc gcctgtccat aggccattcg ccgtcccagc cttgtcctct cgcgtgctcc
       R  E  K   G  G  Q  V   S  G  K   R  Q  G   R  N  R  R   A  H  E

9121  gagcttccag ggggaaacgc ctggtatctt tatagtcctg tcgggtttcg ccacctctga
      ctcgaaggtc ccccttgcg  gaccatagaa atatcaggac agcccaaagc ggtggagact
       G  A  S   R  G  K  R   L  V  S   L  -  S   C  R  V  S   P  P  L

9181  cttgagcgtc gatttttgtg atgctcgtca gggggggcgga gcctatggaa aaacgccagc
      gaactcgcag ctaaaaacac tacgagcagt ccccccgcct cggatacctt tttgcggtcg
       T  -  A   S  I  F  V   M  L  V   R  G  A   E  P  M  E   K  R  Q

                                                          AflIII
                                                         -+-----
                                                           PciI
                                                         -+-----
9241  aacgcggcct ttttacggtt cctggccttt tgctggcctt ttgctcacat gt
      ttgcgccgga aaaatgccaa ggaccggaaa acgaccggaa aacgagtgta ca
       Q  R  G   L  F  T  V   P  G  L   L  L  A   F  C  S  H
```

8.4.3.1 Plasmidkarte von pSpCas9(BB)-2A-ECFP (PX458) mit XhoI- und HindIII-Restriktionsschnittstellen

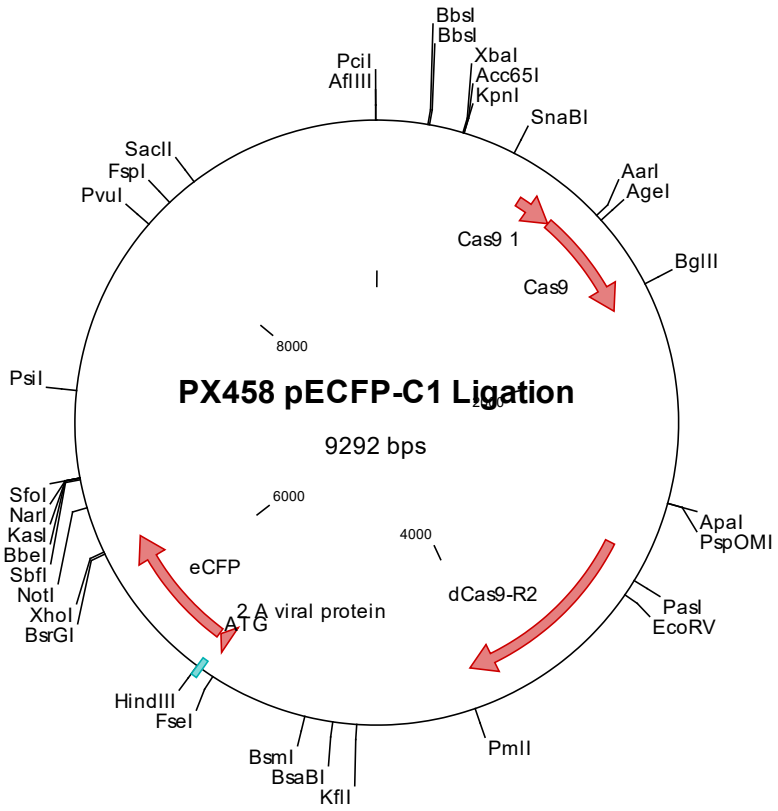

Abbildung 8.3: Aufbau des Plasmids pSpCas9(BB)-2A-ECFP (PX458) mit XhoI- und HindIII-Restriktionsschnittstellen
In das 9288 bp große Plasmid wurde die sgRNA-Gensequenz gegen GABARAPL1 (Exon 2/3B) eingebracht. Neben den vorhandenen Schnittstellen für Restriktionsenzyme wurde eine zusätzliche für XhoI und HindIII eingebracht, einen Replikationsursprung (f1 ori) und eine Ampicillin-Resistenz (AmpR) in *E. coli* sowie einen weiteren Replikationsursprung (ori) und U6-Promotor für die Expression in Säugerzellen. Die *gRNA scaffold* Sequenz beinhaltet die Restriktionsschnittstellen für BbsI/BpiI, über die die gewünschte sgRNA in das Plasmid eingebracht werden kann. Anschließend folgt die Cas9-Sequenz aus *S. pyogenes* und eine Sequenz für das Fluoreszenzprotein EGFP, die unter einem humanen Cytomegalovirus (CMV) *enhancer* und *chicken β-actin* Promotor exprimiert werden. Am Insert befindet sich N-terminal eine 3 x FLAG-Sequenz und C-terminal die ECFP-Sequenz, die durch eine *nucleoplasmin nuclear localization signal* (NLS)- und 2A-Sequenz von Cas9 abgegrenzt wird.

8.4.4 DNA-Sequenz des pSpCas9(BB)-2A-mCherry (PX458) Vektors mit XhoI- und HindIII-Restriktionsschnittstellen

```
   1  gagggcctat ttcccatgat tccttcatat ttgcatatac gatacaaggc tgttagagag
      ctcccggata aagggtacta aggaagtata aacgtatatg ctatgttccg acaatctctc
       -  G  P   I  S  H  D   S  F  I   F  A  Y   T  I  Q  G   C  -  R

                                                    TatI     BsaAI
                                                  --+-----   ----+--
  61  ataattggaa ttaatttgac tgtaaacaca aagatattag tacaaaatac gtgacgtaga
      tattaacctt aattaaactg acatttgtgt ttctataatc atgttttatg cactgcatct
       D  N  W   N  -  F  D   C  K  H   K  D  I   S  T  K  Y   V  T  -

 121  aagtaataat ttcttgggta gtttgcagtt ttaaaattat gttttaaaat ggactatcat
      ttcattatta aagaacccat caaacgtcaa aattttaata caaaatttta cctgatagta
       K  V  I   I  S  W  V   V  C  S   F  K  I   M  F  -  N   G  L  S

 181  atgcttaccg taacttgaaa gtatttcgat ttcttggctt tatatatctt gtggaaagga
      tacgaatggc attgaacttt cataaagcta aagaaccgaa atatatagaa caccttcct
       Y  A  Y   R  N  L  K   V  F  R   F  L  G   F  I  Y  L   V  E  R

                  BbsI     BbsI
                 ------  -------
 241  cgaaacaccg ggtcttcgag aagacctgtt ttagagctag aaatagcaag ttaaaataag
      gctttgtggc ccagaagctc ttctggacaa aatctcgatc tttatcgttc aattttattc
       T  K  H   R  V  F  E   K  T  C   F  R  A   R  N  S  K   L  K  -

 301  gctagtccgt tatcaacttg aaaaagtggc accgagtcgg tgctttttg ttttagagct
      cgatcaggca atagttgaac tttttcaccg tggctcagcc acgaaaaaac aaaatctcga
       G  -  S   V  I  N  L   K  K  W   H  R  V   G  A  F  L   F  -  S

                                                                PstI
                                                               -----+
                                                                SfcI
                                                               -+----
 361  agaaatagca agttaaaata aggctagtcc gtttttagcg cgtgcgccaa ttctgcagac
      tctttatcgt tcaatttat tccgatcagg caaaaatcgc gcacgcggtt aagacgtctg
       -  K  -   Q  V  K  I   R  L  V   R  F  -   R  V  R  Q   F  C  R

                     KpnI
                    -----+
                    Acc65I
                    -+----
              XbaI
             -+-----
 421  aaatggctct agaggtaccc gttacataac ttacggtaaa tggcccgcct ggctgaccgc
      tttaccgaga tctccatggg caatgtattg aatgccattt accgggcgga ccgactggcg
       Q  M  A   L  E  V  P   V  T  -   L  T  V   N  G  P  P   G  -  P

 481  ccaacgaccc ccgcccattg acgtcaatag taacgccaat agggactttc cattgacgtc
      ggttgctggg ggcgggtaac tgcagttatc attgcggtta tccctgaaag gtaactgcag
       P  N  D   P  R  P  L   T  S  I   V  T  P   I  G  T  F   H  -  R

        TaqII                                     TatI
       ------                                   -+-----
 541  aatgggtgga gtatttacgg taaactgccc acttggcagt acatcaagtg tatcatatgc
      ttacccacct cataaatgcc atttgacggg tgaaccgtca tgtagttcac atagtatacg
```

```
      Q  W  V   E  Y  L  R   -  T  A   H  L  A   V  H  Q  V   Y  H  M

                                                                 TatI
                                                               -+----
601   caagtacgcc ccctattgac gtcaatgacg gtaaatggcc cgcctggcat tgtgcccagt
      gttcatgcgg gggataactg cagttactgc catttaccgg gcggaccgta acacgggtca
       P  S  T   P  P  I  D   V  N  D   G  K  W   P  A  W  H   C  A  Q

                                          BsaAI
                                         ----+--
                                   TatI   SnaBI
                                  -+----  ----+--
661   acatgacctt atgggacttt cctacttggc agtacatcta cgtattagtc atcgctatta
      tgtactggaa taccctgaaa ggatgaaccg tcatgtagat gcataatcag tagcgataat
       Y  M  T   L  W  D  F   P  T  W   Q  Y  I   Y  V  L  V   I  A  I

      BtgI
     -+----
      NcoI          BanII
     -+----        -----+
721   ccatggtcga ggtgagcccc acgttctgct tcactctccc catctccccc ccctccccac
      ggtaccagct ccactcgggg tgcaagacga agtgagaggg gtagaggggg gggaggggtg
       T  M  V   E  V  S  P   T  F  C   F  T  L   P  I  S  P   P  S  P

                                         BsgI
                                        -------
781   ccccaatttt gtatttattt atttttaat tattttgtgc agcgatgggg gcgggggggg
      ggggttaaaa cataaataaa taaaaaatta ataaaacacg tcgctacccc cgccccccc
       P  P  I   L  Y  L  F   I  F  -   L  F  C   A  A  M  G   A  G  G

841   gggggggcg cgcgccaggc ggggcggggc ggggcgaggg gcggggcggg gcgaggcgga
      ccccccccgc gcgcggtccg ccccgccccg ccccgctccc cgccccgccc cgctccgcct
       G  G  G   R  A  P  G   G  A  G   R  G  E   G  R  G  G   A  R  R
       >>.............................Cas9 1.............................>

                              BsrBI
                             ---+--
901   gaggtgcggc ggcagccaat cagagcggcg cgctccgaaa gtttcctttt atggcgaggc
      ctccacgccg ccgtcggtta gtctcgccgc gcgaggcttt caaaggaaaa taccgctccg
       R  G  A   A  A  A  N   Q  S  G   A  L  R   K  F  P  F   M  A  R
      >.............................Cas9 1.............................>

961   ggcggcggcg gcggccctat aaaaagcgaa gcgcgcggcg ggcgggagtc gctgcgacgc
      ccgccgccgc cgccgggata tttttcgctt cgcgcgccgc ccgccctcag cgacgctgcg
       R  R  R   R  R  P  Y   K  K  R   S  A  R   R  A  G  V   A  A  T
      >.............................Cas9 1.............................>

                        BsrBI
                       ----+--
1021  tgccttcgcc ccgtgccccg ctccgccgcc gcctcgcgcc gcccgccccg gctctgactg
      acggaagcgg ggcacggggc gaggcggcgg cggagcgcgg cgggcggggc cgagactgac
       L  P  S   P  R  A  P   L  R  R   R  L  A   P  P  A  P   A  L  T
      >.............Cas9 1.............>>

                                        >>...........Cas9.............>

                             BsrBI
                            ---+--
1081  accgcgttac tcccacaggt gagcgggcgg gacggccctt ctcctccggg ctgtaattag
      tggcgcaatg agggtgtcca ctcgcccgcc ctgccgggaa gaggaggccc gacattaatc
       D  R  V   T  P  T  G   E  R  A   G  R  P   F  S  S  G   L  -  L
```

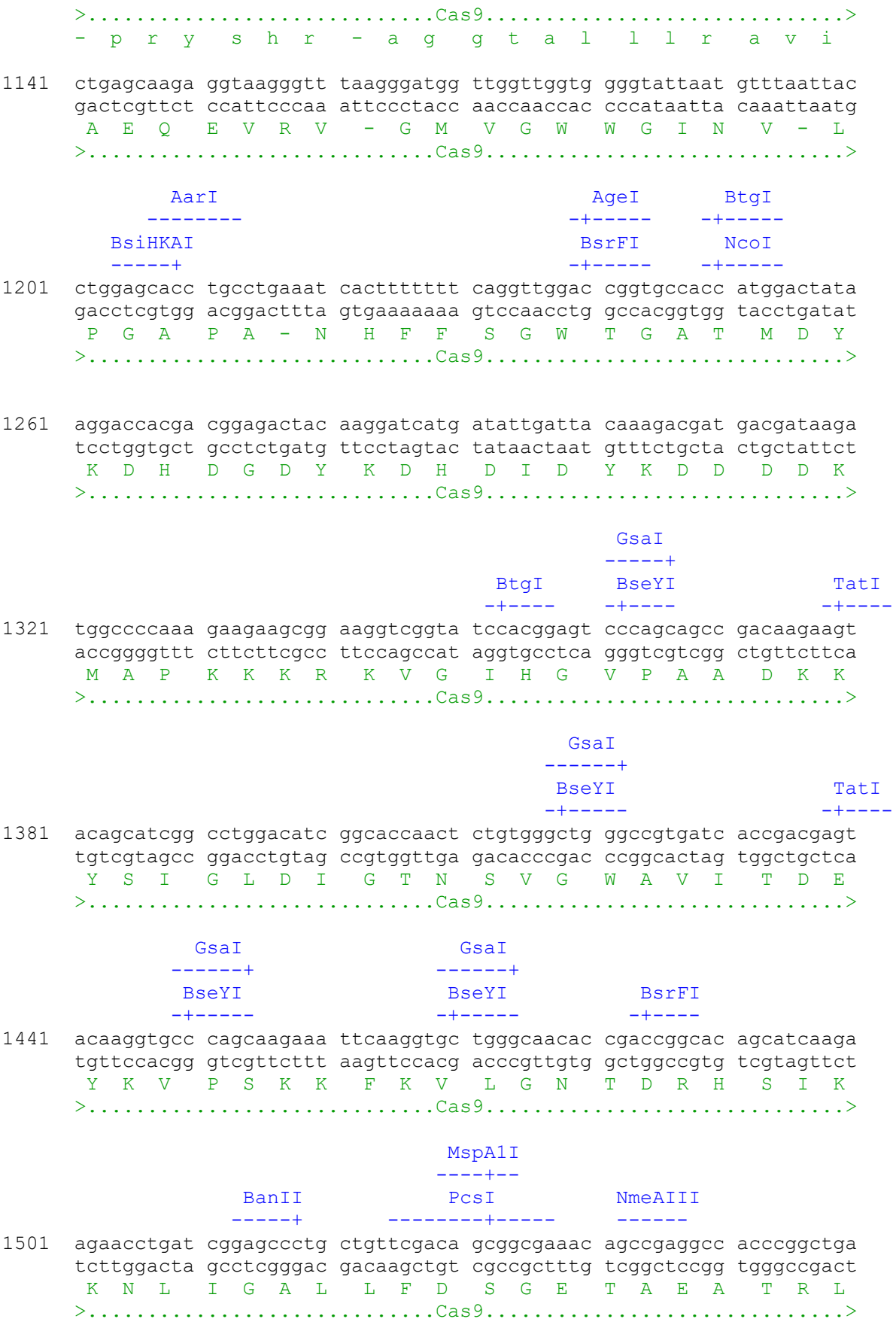
>.....Cas9.....>
- p r y s h r - a g g t a l l l r a v i
1141 ctgagcaaga ggtaagggtt taagggatgg ttggttggtg gggtattaat gtttaattac
gactcgttct ccattcccaa attccctacc aaccaaccac cccataatta caaattaatg
A E Q E V R V - G M V G W W G I N V - L
>.....Cas9.....>
AarI
BsiHKAI
AgeI
BsrFI
BtgI
NcoI
1201 ctggagcacc tgcctgaaat cactttttt caggttggac cggtgccacc atggactata
gacctcgtgg acggacttta gtgaaaaaa gtccaacctg gccacggtgg tacctgatat
P G A P A - N H F F S G W T G A T M D Y
>.....Cas9.....>
1261 aggaccacga cggagactac aaggatcatg atattgatta caaagacgat gacgataaga
tcctggtgct gcctctgatg ttcctagtac tataactaat gtttctgcta ctgctattct
K D H D G D Y K D H D I D Y K D D D D K
>.....Cas9.....>
GsaI
BtgI
BseYI
TatI
1321 tggccccaaa gaagaagcgg aaggtcggta tccacggagt cccagcagcc gacaagaagt
accggggttt cttcttcgcc ttccagccat aggtgcctca gggtcgtcgg ctgttcttca
M A P K K K R K V G I H G V P A A D K K
>.....Cas9.....>
GsaI
BseYI
TatI
1381 acagcatcgg cctggacatc ggcaccaact ctgtgggctg ggccgtgatc accgacgagt
tgtcgtagcc ggacctgtag ccgtggttga gacacccgac ccggcactag tggctgctca
Y S I G L D I G T N S V G W A V I T D E
>.....Cas9.....>
GsaI
BseYI
GsaI
BseYI
BsrFI
1441 acaaggtgcc cagcaagaaa ttcaaggtgc tgggcaacac cgaccggcac agcatcaaga
tgttccacgg gtcgttcttt aagttccacg acccgttgtg gctggccgtg tcgtagttct
Y K V P S K K F K V L G N T D R H S I K
>.....Cas9.....>
MspA1I
BanII
PcsI
NmeAIII
1501 agaacctgat cggagccctg ctgttcgaca gcggcgaaac agccgaggcc acccggctga
tcttggacta gcctcgggac gacaagctgt cgccgctttg tcggctccgg tgggccgact
K N L I G A L L F D S G E T A E A T R L
>.....Cas9.....>

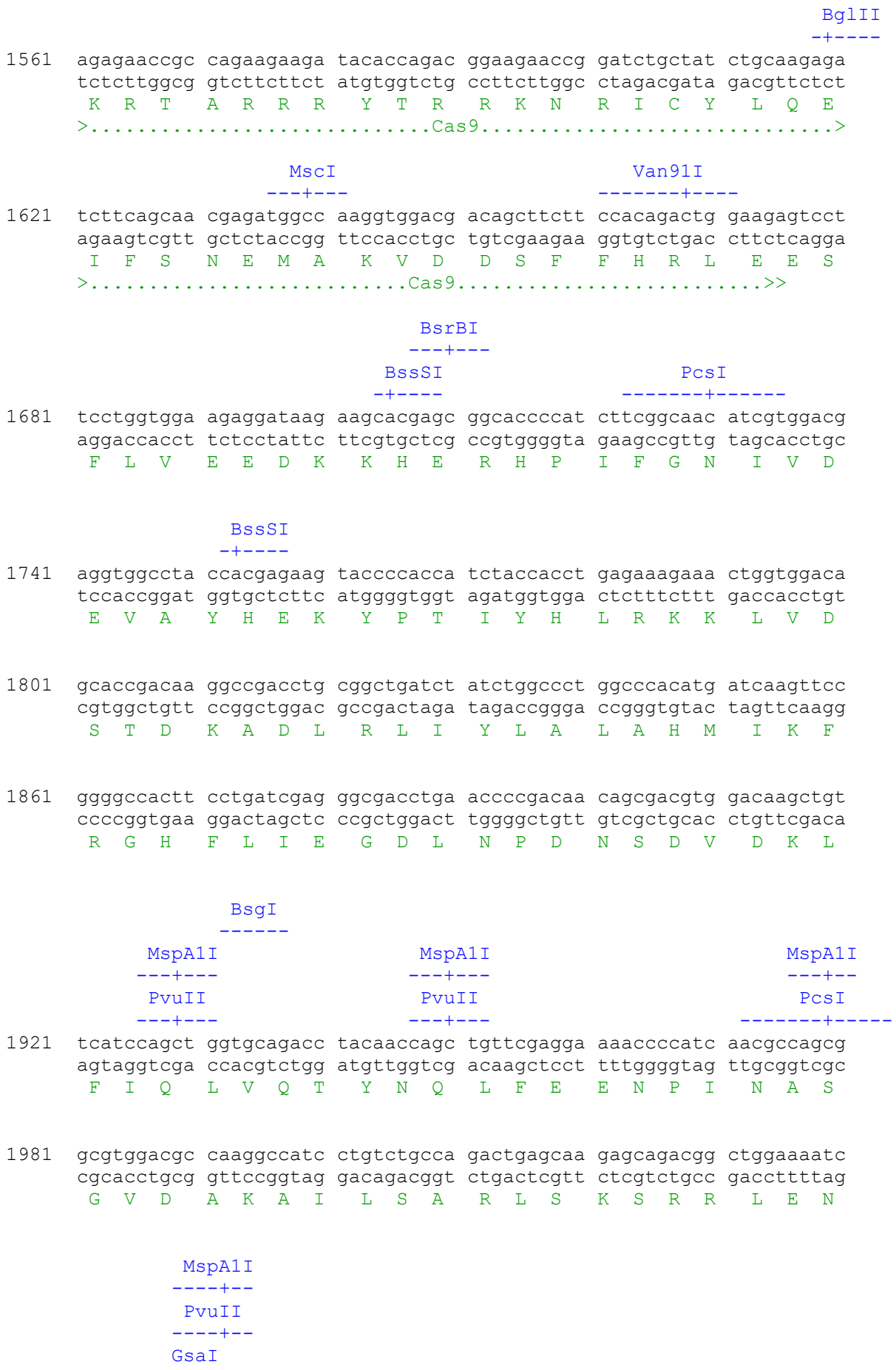
BglII
1561 agagaaccgc cagaagaaga tacaccagac ggaagaaccg gatctgctat ctgcaagaga
tctcttggcg gtcttcttct atgtggtctg ccttcttggc ctagacgata gacgttctct
K R T A R R R Y T R R K N R I C Y L Q E
>.....Cas9.....>
MscI
Van91I
1621 tcttcagcaa cgagatggcc aaggtggacg acagcttctt ccacagactg gaagagtcct
agaagtcgtt gctctaccgg ttccacctgc tgtcgaagaa ggtgtctgac cttctcagga
I F S N E M A K V D D S F F H R L E E S
>.....Cas9.....>>
BsrBI
BssSI
PcsI
1681 tcctggtgga agaggataag aagcacgagc ggcaccccat cttcggcaac atcgtggacg
aggaccacct tctcctattc ttcgtgctcg ccgtggggta gaagccgttg tagcacctgc
F L V E E D K K H E R H P I F G N I V D
BssSI
1741 aggtggccta ccacgagaag taccccacca tctaccacct gagaaagaaa ctggtggaca
tccaccggat ggtgctcttc atggggtggt agatggtgga ctctttcttt gaccacctgt
E V A Y H E K Y P T I Y H L R K K L V D
1801 gcaccgacaa ggccgacctg cggctgatct atctggccct ggcccacatg atcaagttcc
cgtggctgtt ccggctggac gccgactaga tagaccggga ccgggtgtac tagttcaagg
S T D K A D L R L I Y L A L A H M I K F
1861 ggggccactt cctgatcgag ggcgacctga accccgacaa cagcgacgtg gacaagctgt
ccccggtgaa ggactagctc ccgctggact tggggctgtt gtcgctgcac ctgttcgaca
R G H F L I E G D L N P D N S D V D K L
BsgI
MspA1I
PvuII
MspA1I
PvuII
MspA1I
PcsI
1921 tcatccagct ggtgcagacc tacaaccagc tgttcgagga aaaccccatc aacgccagcg
agtaggtcga ccacgtctgg atgttggtcg acaagctcct tttggggtag ttgcggtcgc
F I Q L V Q T Y N Q L F E E N P I N A S
1981 gcgtggacgc caaggccatc ctgtctgcca gactgagcaa gagcagacgg ctggaaaatc
cgcacctgcg gttccggtag gacagacggt ctgactcgtt ctcgtctgcc gacctttag
G V D A K A I L S A R L S K S R R L E N
MspA1I
PvuII
GsaI

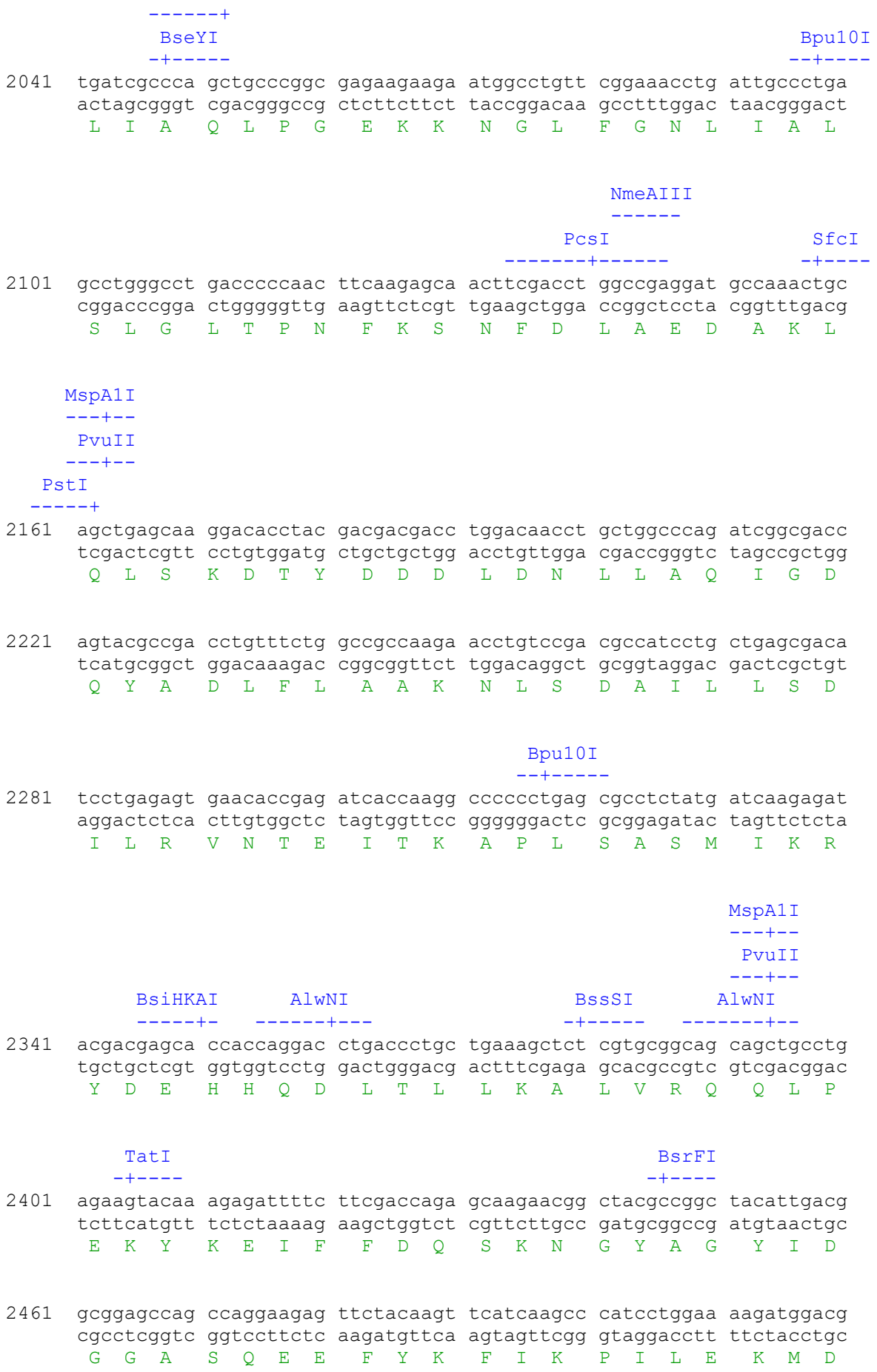
BseYI
Bpu10I
2041 tgatcgccca gctgcccggc gagaagaaga atggcctgtt cggaaacctg attgccctga
actagcgggt cgacgggccg ctcttcttct taccggacaa gcctttggac taacgggact
L I A Q L P G E K K N G L F G N L I A L
NmeAIII
PcsI
SfcI
2101 gcctgggcct gacccccaac ttcaagagca acttcgacct ggccgaggat gccaaactgc
cggacccgga ctgggggttg aagttctcgt tgaagctgga ccggctccta cggtttgacg
S L G L T P N F K S N F D L A E D A K L
MspA1I
PvuII
PstI
2161 agctgagcaa ggacacctac gacgacgacc tggacaacct gctggcccag atcggcgacc
tcgactcgtt cctgtggatg ctgctgctgg acctgttgga cgaccgggtc tagccgctgg
Q L S K D T Y D D D L D N L L A Q I G D
2221 agtacgccga cctgtttctg gccgccaaga acctgtccga cgccatcctg ctgagcgaca
tcatgcggct ggacaaagac cggcggttct tggacaggct gcggtaggac gactcgctgt
Q Y A D L F L A A K N L S D A I L L S D
Bpu10I
2281 tcctgagagt gaacaccgag atcaccaagg ccccctgag cgcctctatg atcaagagat
aggactctca cttgtggctc tagtggttcc ggggggactc gcggagatac tagttctcta
I L R V N T E I T K A P L S A S M I K R
MspA1I
PvuII
BsiHKAI
AlwNI
BssSI
AlwNI
2341 acgacgagca ccaccaggac ctgaccctgc tgaaagctct cgtgcggcag cagctgcctg
tgctgctcgt ggtggtcctg gactgggacg actttcgaga gcacgccgtc gtcgacggac
Y D E H H Q D L T L L K A L V R Q Q L P
TatI
BsrFI
2401 agaagtacaa agagattttc ttcgaccaga gcaagaacgg ctacgccggc tacattgacg
tcttcatgtt tctctaaaag aagctggtct cgttcttgcc gatgcggccg atgtaactgc
E K Y K E I F F D Q S K N G Y A G Y I D
2461 gcggagccag ccaggaagag ttctacaagt tcatcaagcc catcctggaa aagatggacg
cgcctcggtc ggtccttctc aagatgttca agtagttcgg gtaggacctt ttctacctgc
G G A S Q E E F Y K F I K P I L E K M D

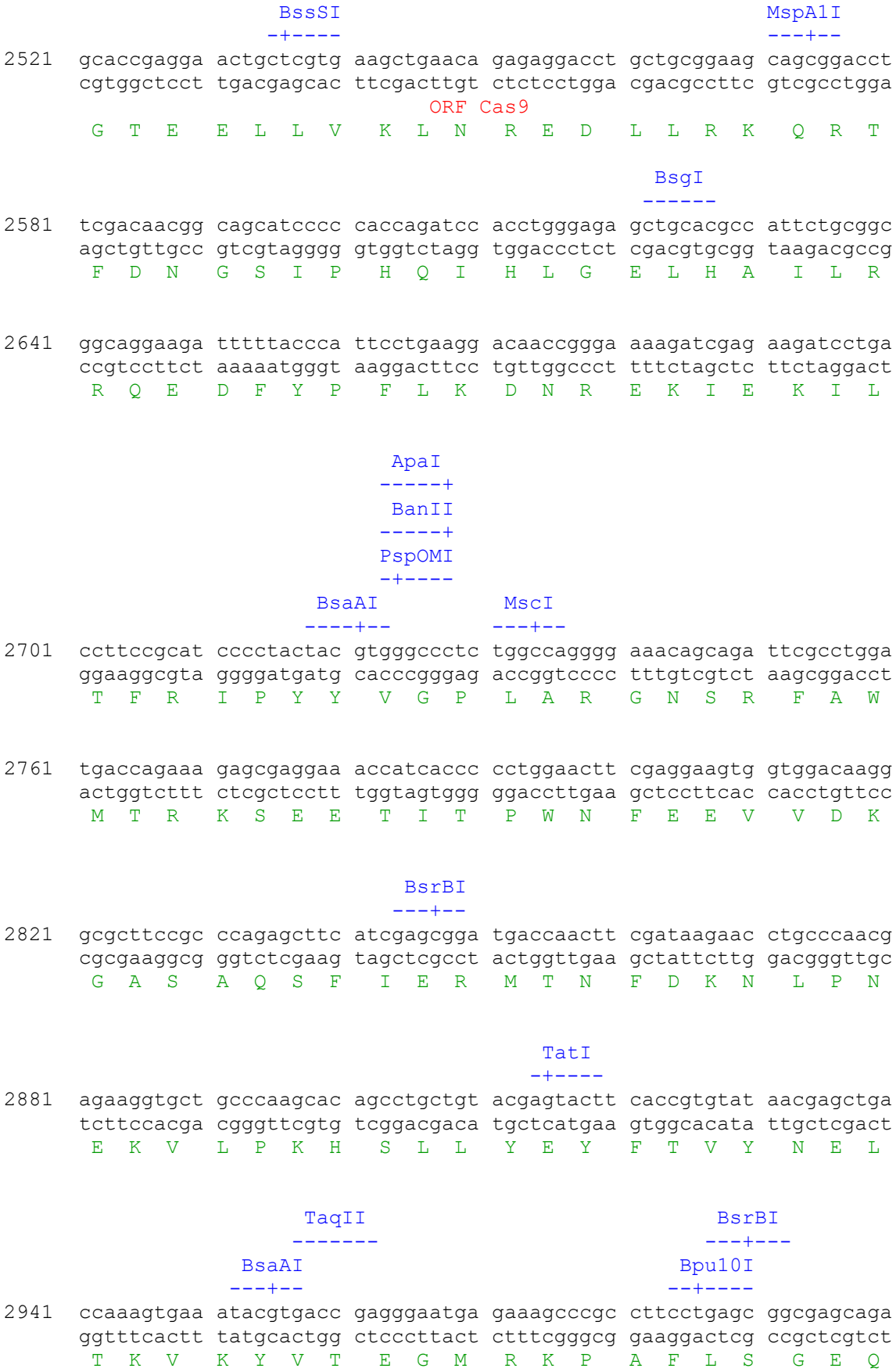
BssSI
MspA1I
ORF Cas9
BsgI
ApaI
BanII
PspOMI
BsaAI
MscI
BsrBI
TatI
TaqII
BsrBI
BsaAI
Bpu10I

```
                                                                    MspA1I
                                                                    ---+--
                                                                     PvuII
                                                                    ---+--
3001  aaaaggccat cgtggacctg ctgttcaaga ccaaccggaa agtgaccgtg aagcagctga
      ttttccggta gcacctggac gacaagttct ggttggcctt tcactggcac ttcgtcgact
       K  K  A   I  V  D  L   L  F  K   T  N  R   K  V  T  V   K  Q  L
                          >>.............dCas9-R2.................>

                                  PcsI         BtgI
                           -------+------  -+-----
3061  aagaggacta cttcaagaaa atcgagtgct tcgactccgt ggaaatctcc ggcgtggaag
      ttctcctgat gaagttcttt tagctcacga agctgaggca cctttagagg ccgcaccttc
       K  E  D   Y  F  K  K   I  E  C   F  D  S   V  E  I  S   G  V  E
      >............................dCas9-R2............................>

                        PasI
                      --+-----
3121  atcggttcaa cgcctccctg ggcacatacc acgatctgct gaaaattatc aaggacaagg
      tagccaagtt gcggagggac ccgtgtatgg tgctagacga cttttaatag ttcctgttcc
       D  R  F   N  A  S  L   G  T  Y   H  D  L   L  K  I  I   K  D  K
      >............................dCas9-R2............................>

                                              EcoRV
                                             ----+--
3181  acttcctgga caatgaggaa aacgaggaca ttctggaaga tatcgtgctg accctgacac
      tgaaggacct gttactcctt ttgctcctgt aagaccttct atagcacgac tgggactgtg
       D  F  L   D  N  E  E   N  E  D   I  L  E   D  I  V  L   T  L  T
      >............................dCas9-R2............................>

3241  tgtttgagga cagagagatg atcgaggaac ggctgaaaac ctatgcccac ctgttcgacg
      acaaactcct gtctctctac tagctccttg ccgacttttg gatacgggtg gacaagctgc
       L  F  E   D  R  E  M   I  E  E   R  L  K   T  Y  A  H   L  F  D
      >............................dCas9-R2............................>

                                                GsaI
                                               ------+
                        MspA1I                  BseYI
                        ---+--                  --+----
                         PvuII                BsrFI
                        ---+--               -+-----
3301  acaaagtgat gaagcagctg aagcggcgga gatacaccgg ctggggcagg ctgagccgga
      tgtttcacta cttcgtcgac ttcgccgcct ctatgtggcc gaccccgtcc gactcggcct
       D  K  V   M  K  Q  L   K  R  R   R  Y  T   G  W  G  R   L  S  R
      >............................dCas9-R2............................>

                               AhdI
                              ------+-----
3361  agctgatcaa cggcatccgg gacaagcagt ccggcaagac aatcctggat ttcctgaagt
      tcgactagtt gccgtaggcc ctgttcgtca ggccgttctg ttaggaccta aaggacttca
       K  L  I   N  G  I  R   D  K  Q   S  G  K   T  I  L  D   F  L  K
      >............................dCas9-R2............................>

                                     MspA1I
                                    ----+--
                                     PvuII
                                    ----+--
3421  ccgacggctt cgccaacaga aacttcatgc agctgatcca cgacgacagc ctgaccttta
      ggctgccgaa gcggttgtct ttgaagtacg tcgactaggt gctgctgtcg gactggaaat
       S  D  G   F  A  N  R   N  F  M   Q  L  I   H  D  D  S   L  T  F
```

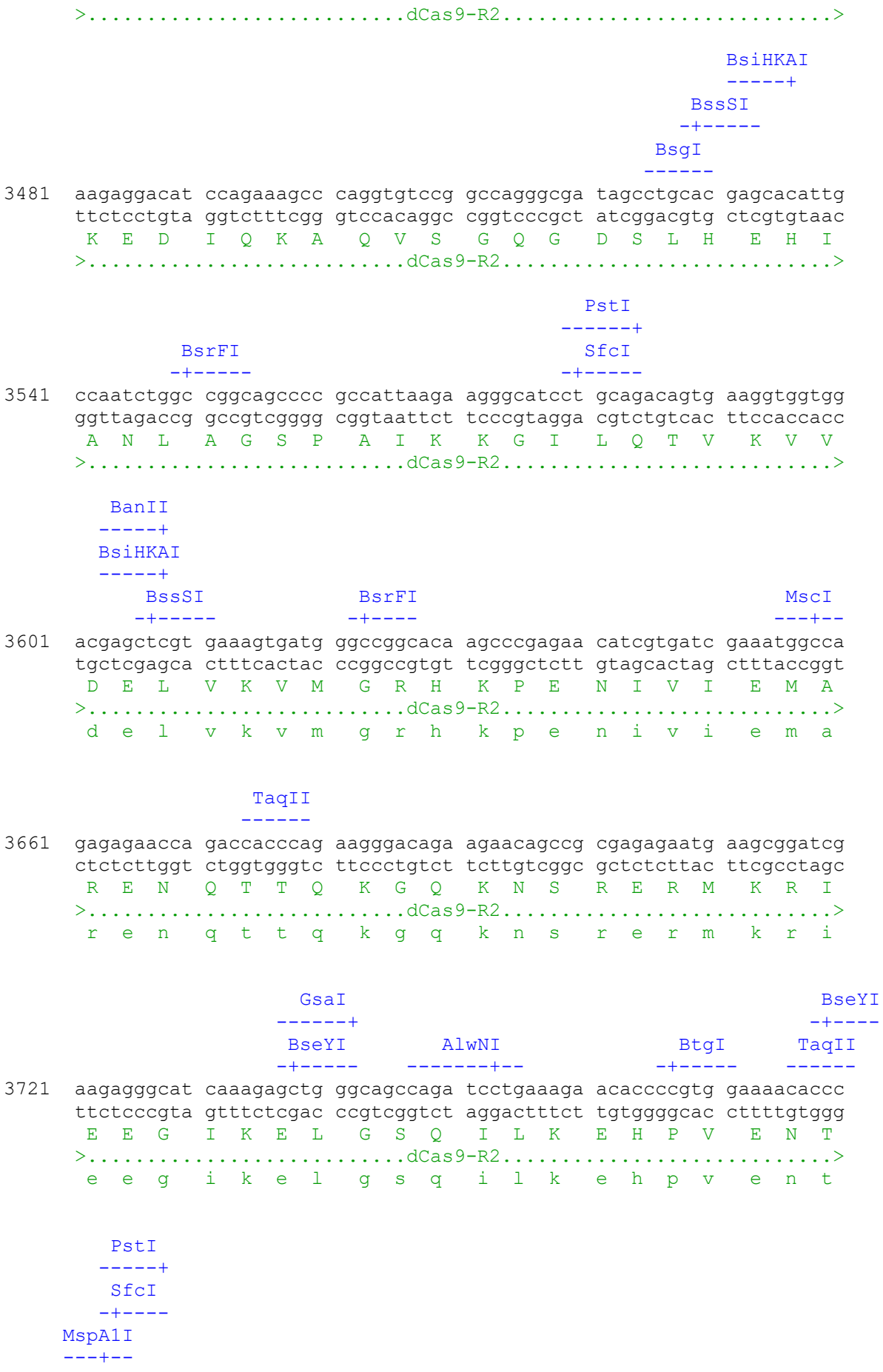
>.....dCas9-R2.....>
BsiHKAI
BssSI
BsgI
3481 aagaggacat ccagaaagcc caggtgtccg gccagggcga tagcctgcac gagcacattg
ttctcctgta ggtctttcgg gtccacaggc cggtcccgct atcggacgtg ctcgtgtaac
K E D I Q K A Q V S G Q G D S L H E H I
PstI
BsrFI
SfcI
3541 ccaatctggc cggcagcccc gccattaaga agggcatcct gcagacagtg aaggtggtgg
ggttagaccg gccgtcgggg cggtaattct tcccgtagga cgtctgtcac ttccaccacc
A N L A G S P A I K K G I L Q T V K V V
BanII
BsiHKAI
BssSI
BsrFI
MscI
3601 acgagctcgt gaaagtgatg ggccggcaca agcccgagaa catcgtgatc gaaatggcca
tgctcgagca ctttcactac ccggccgtgt tcgggctctt gtagcactag ctttaccggt
D E L V K V M G R H K P E N I V I E M A
d e l v k v m g r h k p e n i v i e m a
TaqII
3661 gagagaacca gaccacccag aagggacaga agaacagccg cgagagaatg aagcggatcg
ctctcttggt ctggtgggtc ttccctgtct tcttgtcggc gctctcttac ttcgcctagc
R E N Q T T Q K G Q K N S R E R M K R I
r e n q t t q k g q k n s r e r m k r i
GsaI
BseYI
BseYI
AlwNI
BtgI
TaqII
3721 aagagggcat caaagagctg ggcagccaga tcctgaaaga acaccccgtg gaaaacaccc
ttctcccgta gtttctcgac ccgtcggtct aggactttct tgtggggcac cttttgtggg
E E G I K E L G S Q I L K E H P V E N T
e e g i k e l g s q i l k e h p v e n t
PstI
SfcI
MspA1I

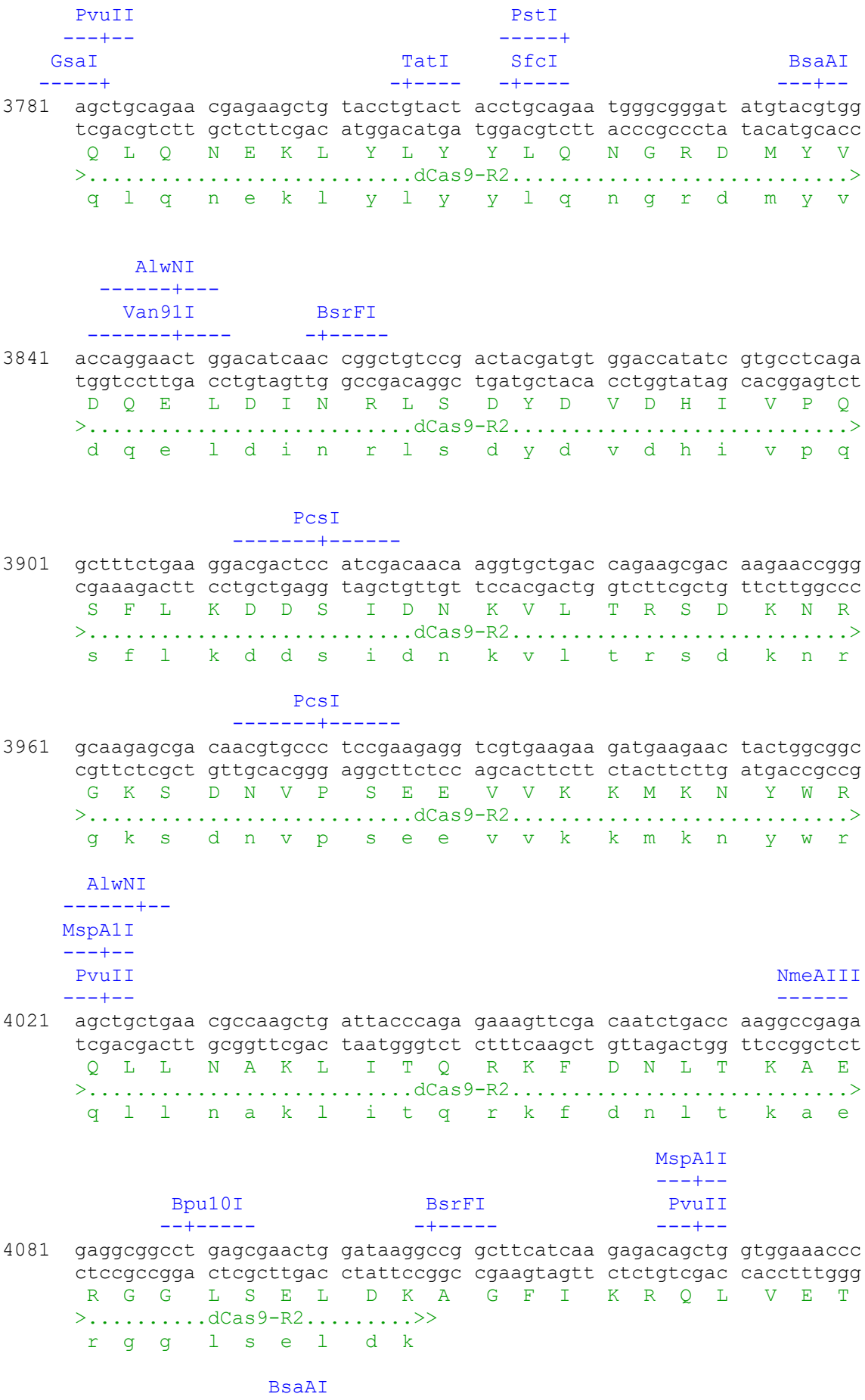
PvuII
PstI
GsaI
TatI
SfcI
BsaAI
3781 agctgcagaa cgagaagctg tacctgtact acctgcagaa tgggcgggat atgtacgtgg
tcgacgtctt gctcttcgac atggacatga tggacgtctt acccgcccta tacatgcacc
Q L Q N E K L Y L Y Y L Q N G R D M Y V
>.....dCas9-R2.....>
q l q n e k l y l y y l q n g r d m y v
AlwNI
Van91I
BsrFI
3841 accaggaact ggacatcaac cggctgtccg actacgatgt ggaccatatc gtgcctcaga
tggtccttga cctgtagttg gccgacaggc tgatgctaca cctggtatag cacggagtct
D Q E L D I N R L S D Y D V D H I V P Q
>.....dCas9-R2.....>
d q e l d i n r l s d y d v d h i v p q
PcsI
3901 gctttctgaa ggacgactcc atcgacaaca aggtgctgac cagaagcgac aagaaccggg
cgaaagactt cctgctgagg tagctgttgt tccacgactg gtcttcgctg ttcttggccc
S F L K D D S I D N K V L T R S D K N R
>.....dCas9-R2.....>
s f l k d d s i d n k v l t r s d k n r
PcsI
3961 gcaagagcga caacgtgccc tccgaagagg tcgtgaagaa gatgaagaac tactggcggc
cgttctcgct gttgcacggg aggcttctcc agcacttctt ctacttcttg atgaccgccg
G K S D N V P S E E V V K K M K N Y W R
>.....dCas9-R2.....>
g k s d n v p s e e v v k k m k n y w r
AlwNI
MspA1I
PvuII
NmeAIII
4021 agctgctgaa cgccaagctg attacccaga gaaagttcga caatctgacc aaggccgaga
tcgacgactt gcggttcgac taatgggtct ctttcaagct gttagactgg ttccggctct
Q L L N A K L I T Q R K F D N L T K A E
>.....dCas9-R2.....>
q l l n a k l i t q r k f d n l t k a e
MspA1I
Bpu10I
BsrFI
PvuII
4081 gaggcggcct gagcgaactg gataaggccg gcttcatcaa gagacagctg gtggaaaccc
ctccgccgga ctcgcttgac ctattccggc cgaagtagtt ctctgtcgac caccttgggg
R G G L S E L D K A G F I K R Q L V E T
>.....dCas9-R2.....>>
r g g l s e l d k
BsaAI


PmlI
AlwNI
4141 ggcagatcac aaagcacgtg gcacagatcc tggactcccg gatgaacact aagtacgacg
ccgtctagtg tttcgtgcac cgtgtctagg acctgagggc ctacttgtga ttcatgctgc
R Q I T K H V A Q I L D S R M N T K Y D
4201 agaatgacaa gctgatccgg gaagtgaaag tgatcaccct gaagtccaag ctggtgtccg
tcttactgtt cgactaggcc cttcactttc actagtggga cttcaggttc gaccacaggc
E N D K L I R E V K V I T L K S K L V S
4261 atttccggaa ggatttccag ttttacaaag tgcgcgagat caacaactac caccacgccc
taaaggcctt cctaaaggtc aaaatgtttc acgcgctcta gttgttgatg gtggtgcggg
D F R K D F Q F Y K V R E I N N Y H H A
Bpu10I
4321 acgacgccta cctgaacgcc gtcgtgggaa ccgccctgat caaaaagtac cctaagctgg
tgctgcggat ggacttgcgg cagcaccctt ggcgggacta gtttttcatg ggattcgacc
H D A Y L N A V V G T A L I K K Y P K L
PcsI
PcsI
4381 aaagcgagtt cgtgtacggc gactacaagg tgtacgacgt gcggaagatg atcgccaaga
tttcgctcaa gcacatgccg ctgatgttcc acatgctgca cgccttctac tagcggttct
E S E F V Y G D Y K V Y D V R K M I A K
TatI
SfcI
4441 gcgagcagga aatcggcaag gctaccgcca agtacttctt ctacagcaac atcatgaact
cgctcgtcct ttagccgttc cgatggcggt tcatgaagaa gatgtcgttg tagtacttga
S E Q E I G K A T A K Y F F Y S N I M N
TaqII
MscI
4501 ttttcaagac cgagattacc ctggccaacg gcgagatccg gaagcggcct ctgatcgaga
aaaagttctg gctctaatgg gaccggttgc cgctctaggc cttcgccgga gactagctct
F F K T E I T L A N G E I R K R P L I E
4561 caaacggcga aaccggggag atcgtgtggg ataagggccg ggattttgcc accgtgcgga
gtttgccgct ttggcccctc tagcacaccc tattcccggc cctaaaacgg tggcacgcct
T N G E T G E I V W D K G R D F A T V R
BsgI
TaqII
4621 aagtgctgag catgccccaa gtgaatatcg tgaaaaagac cgaggtgcag acaggcggct
ttcacgactc gtacgggggtt cacttatagc acttttttctg gctccacgtc tgtccgccga
K V L S M P Q V N I V K K T E V Q T G G
4681 tcagcaaaga gtctatcctg cccaagagga acagcgataa gctgatcgcc agaaagaagg
agtcgtttct cagataggac gggttctcct tgtcgctatt cgactagcgg tctttcttcc
F S K E S I L P K R N S D K L I A R K K
KflI
PcsI
BtgI
4741 actgggaccc taagaagtac ggcggcttcg acagccccac cgtggcctat tctgtgctgg
tgaccctggg attcttcatg ccgccgaagc tgtcggggtg gcaccggata agacacgacc
D W D P K K Y G G F D S P T V A Y S V L

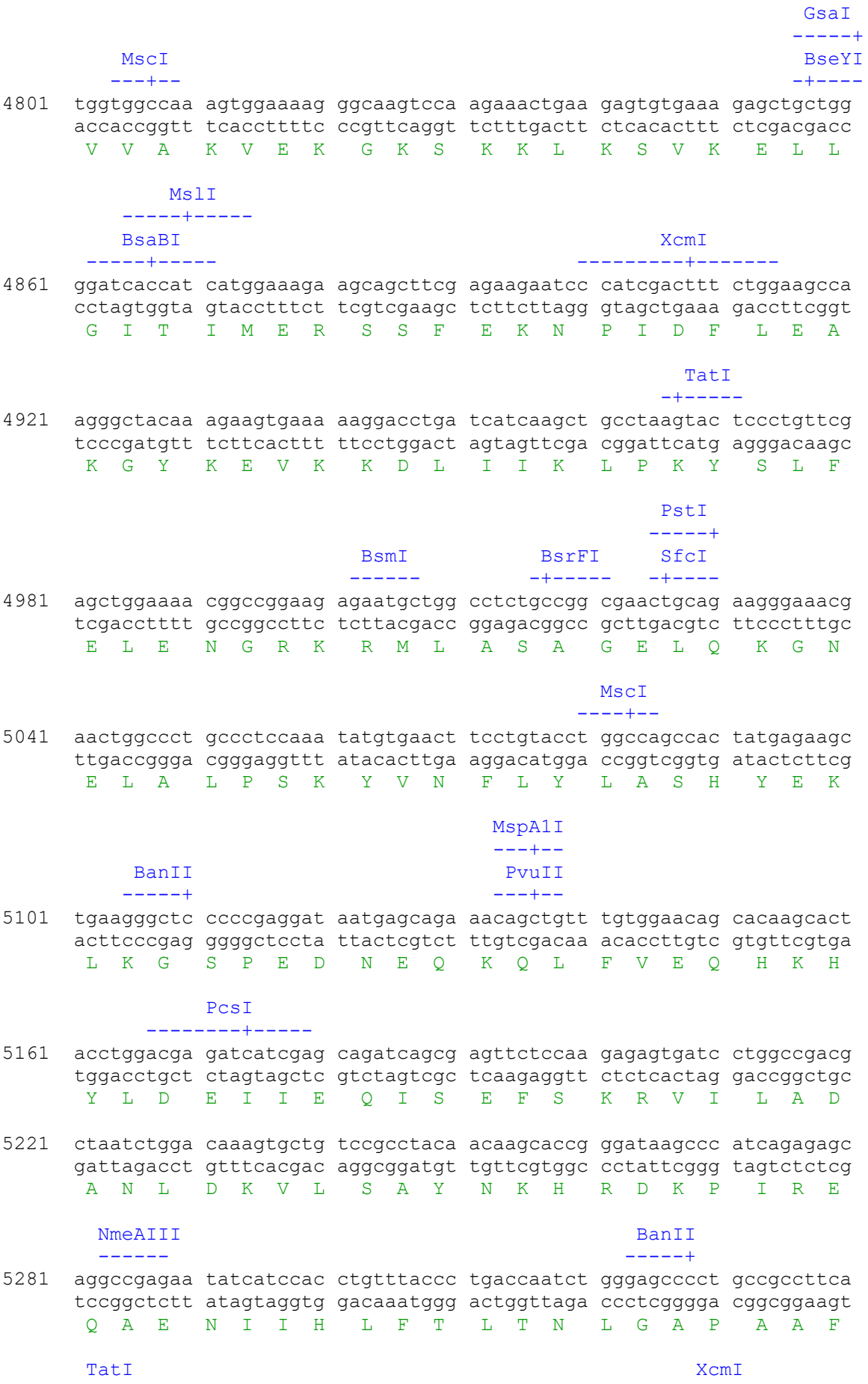
GsaI
MscI
BseYI
MslI
BsaBI
XcmI
TatI
PstI
BsmI
BsrFI
SfcI
MscI
MspA1I
BanII
PvuII
PcsI
NmeAIII
BanII
TatI
XcmI

```
      -+----                                          --------+-------
5341  agtactttga caccaccatc gaccggaaga ggtacaccag caccaaagag gtgctggacg
      tcatgaaact gtggtggtag ctggccttct ccatgtggtc gtggtttctc cacgacctgc
       K  Y  F   D  T  T  I   D  R  K   R  Y  T   S  T  K  E   V  L  D

                                                                   BseYI
                                                                  -+----
                                                                MspA1I
                                                                ---+--
                                    BsrFI                        PvuII
                                   -+----                       ---+--
5401  ccaccctgat ccaccagagc atcaccggcc tgtacgagac acggatcgac ctgtctcagc
      ggtgggacta ggtggtctcg tagtggccgg acatgctctg tgcctagctg gacagagtcg
                           FseI upstream Primer 1
       A  T  L   I  H  Q  S   I  T  G   L  Y  E   T  R  I  D   L  S  Q

                                              FseI
                                            ------+--
     GsaI              BsrFI                  BsrFI
    -----+            -+-----                -+-----
5461  tgggaggcga caaaaggccg gcggccacga aaaaggccgg ccaggcaaaa aagaaaaagg
      accctccgct gttttccggc cgccggtgct ttttccggcc ggtccgtttt ttctttttcc
       L  G  G   D  K  R  P   A  A  T   K  K  A   G  Q  A  K   K  K  K

5521  aattcggcag tggagagggc agaggaagtc tgctaacatg cggtgacgtc gaggagaatc
      ttaagccgtc acctctcccg tctccttcag acgattgtac gccactgcag ctcctcttag
       E  F  G   S  G  E  G   R  G  S   L  L  T   C  G  D  V   E  E  N
           >>...................2 A viral protein.....................>

            HindIII                                    MscI
            -+-----                                   ---+--
5581  ctggcccaag cttaatggtg agcaagggcg aggaggataa catggccatc atcaaggagt
      gaccgggttc gaattaccac tcgttcccgc tcctcctatt gtaccggtag tagttcctca
      HindIII Schnittstelle''HindIII mCherry Primer
       P  G  P   S  L  M  V   S  K  G   E  E  D   N  M  A  I   I  K  E
      >.....>> 2 A viral protein
                    >>...................mCherry.....................>

                    BsiHKAI
                    -----+
                     ApaLI       BanII            BssSI
                    -+----      -----+-          -+----
5641  tcatgcgctt caaggtgcac atggagggct ccgtgaacgg ccacgagttc gagatcgagg
      agtacgcgaa gttccacgtg tacctcccga ggcacttgcc ggtgctcaag ctctagctcc
       F  M  R   F  K  V  H   M  E  G   S  V  N   G  H  E  F   E  I  E
      >.............................mCherry.............................>

                                  TaqII
                                 -------
5701  gcgagggcga gggccgcccc tacgagggca cccagaccgc caagctgaag gtgaccaagg
      cgctcccgct cccggcgggg atgctcccgt gggtctggcg gttcgacttc cactggttcc
       G  E  G   E  G  R  P   Y  E  G   T  Q  T   A  K  L  K   V  T  K
      >.............................mCherry.............................>

                                AhdI
                               ------+-----
5761  gtggcccccc gcccttcgcc tgggacatcc tgtcccctca gttcatgtac ggctccaagg
      caccgggggа cgggaagcgg accctgtagg acaggggagt caagtacatg ccgaggttcc
       G  G  P   L  P  F  A   W  D  I   L  S  P   Q  F  M  Y   G  S  K
      >.............................mCherry.............................>
```

```
        BsaAI
       ---+--
5821   cctacgtgaa gcaccccgcc gacatccccg actacttgaa gctgtccttc cccgagggct
       ggatgcactt cgtggggcgg ctgtaggggc tgatgaactt cgacaggaag gggctcccga
        A  Y  V   K  H  P  A   D  I  P   D  Y  L   K  L  S  F   P  E  G
       >.............................mCherry.............................>

5881   tcaagtggga gcgcgtgatg aacttcgagg acggcggcgt ggtgaccgtg acccaggact
       agttcaccct cgcgcactac ttgaagctcc tgccgccgca ccactggcac tgggtcctga
        F  K  W   E  R  V  M   N  F  E   D  G  G   V  V  T  V   T  Q  D
       >.............................mCherry.............................>

             PstI
           -----+-
             SbfI
          ------+--
             SfcI
           -+-----
5941   cctccctgca ggacggcgag ttcatctaca aggtgaagct gcgcggcacc aacttccccc
       ggagggacgt cctgccgctc aagtagatgt tccacttcga cgcgccgtgg ttgaagggga
        S  S  L   Q  D  G  E   F  I  Y   K  V  K   L  R  G  T   N  F  P
       >.............................mCherry.............................>

                                          GsaI
                                         -----+
                                          BseYI
                                         -+----
                                     Van91I
                                   --------+---
                                     BtgI
                                   -+-----
                                     NcoI                      BsrBI
                                   -+-----                    ---+--
6001   ccgacggccc cgtaatgcag aagaaaacca tgggctggga ggcctcctcc gagcggatgt
       ggctgccggg gcattacgtc ttcttttggt acccgaccct ccggaggagg ctcgcctaca
              QuikChangePrimer BbsI destroy
        S  D  G   P  V  M  Q   K  K  T   M  G  W   E  A  S  S   E  R  M
       >.............................mCherry.............................>

                  BbeI
                 -----+
                  SfoI
                 ---+--
                  NarI
                 --+---
                  KasI                        AlwNI
                 -+----                     -------+--
6061   accccgagga cggcgccctg aagggcgaga tcaagcagag gctgaagctg aaggacggcg
       tggggctcct gccgcgggac ttcccgctct agttcgtctc cgacttcgac ttcctgccgc
        Y  P  E   D  G  A  L   K  G  E   I  K  Q   R  L  K  L   K  D  G
       >.............................mCherry.............................>

                  DrdI                                      MspA1I
               --------+----                                ---+--
                  BbvCI                                     PvuII
                 --+----                                    ---+--
                  Bpu10I                                 BsgI
                 --+----                                -------
6121   gccactacga cgctgaggtc aagaccacct acaaggccaa gaagcccgtg cagctgcccg
       cggtgatgct gcgactccag ttctggtgga tgttccggtt cttcgggcac gtcgacgggc
```

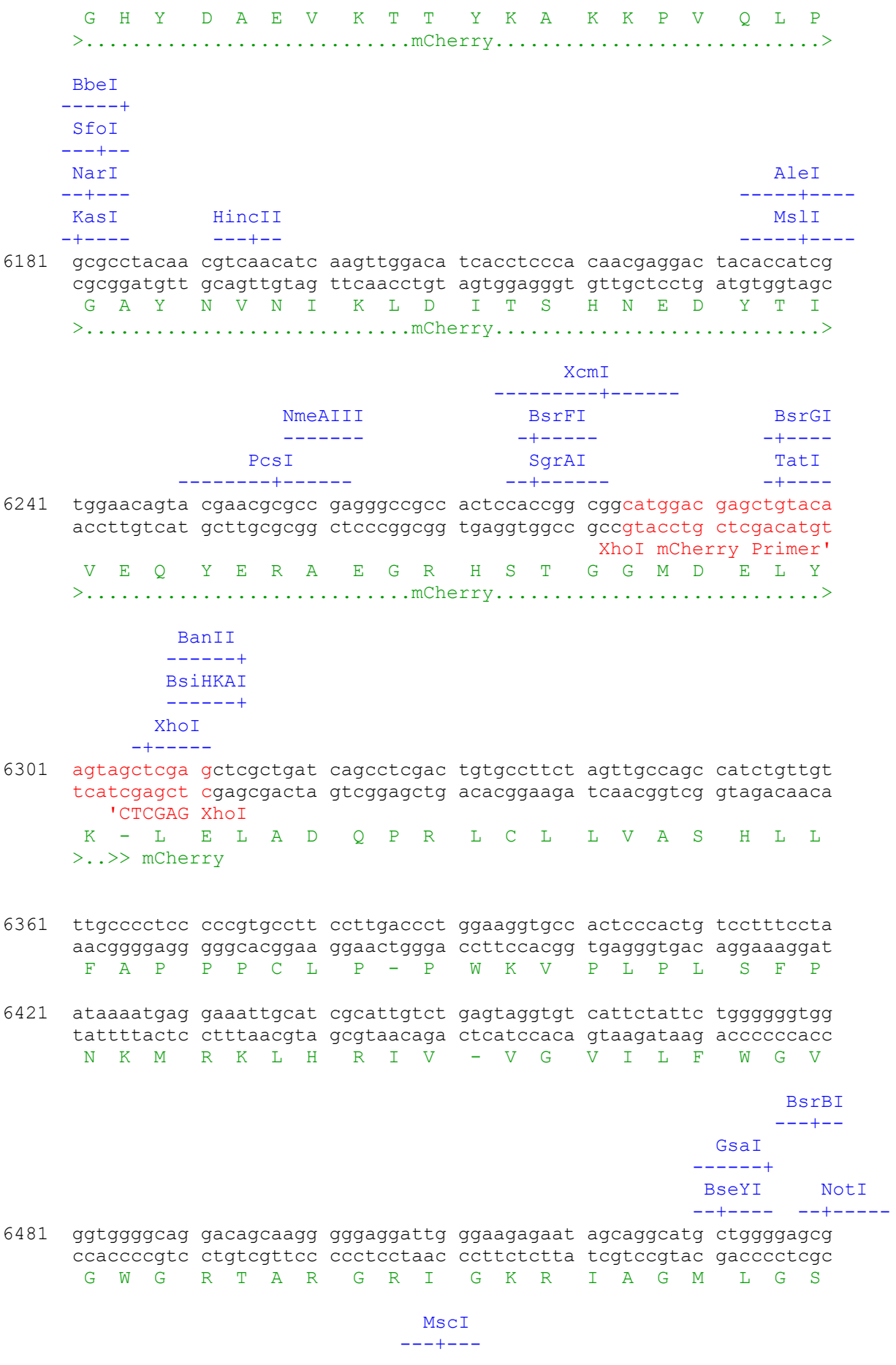
G H Y D A E V K T T Y K A K K P V Q L P
>.....mCherry.....>
BbeI
SfoI
NarI
AleI
KasI
HincII
MslI
6181 gcgcctacaa cgtcaacatc aagttggaca tcacctccca caacgaggac tacaccatcg
cgcggatgtt gcagttgtag ttcaacctgt agtggagggt gttgctcctg atgtggtagc
G A Y N V N I K L D I T S H N E D Y T I
>.....mCherry.....>
XcmI
NmeAIII
BsrFI
BsrGI
PcsI
SgrAI
TatI
6241 tggaacagta cgaacgcgcc gagggccgcc actccaccgg cggcatggac gagctgtaca
accttgtcat gcttgcgcgg ctcccggcgg tgaggtggcc gccgtacctg ctcgacatgt
XhoI mCherry Primer'
V E Q Y E R A E G R H S T G G M D E L Y
>.....mCherry.....>
BanII
BsiHKAI
XhoI
6301 agtagctcga gctcgctgat cagcctcgac tgtgccttct agttgccagc catctgttgt
tcatcgagct cgagcgacta gtcggagctg acacggaaga tcaacggtcg gtagacaaca
'CTCGAG XhoI
K - L E L A D Q P R L C L L V A S H L L
>..>> mCherry
6361 ttgcccctcc cccgtgcctt ccttgaccct ggaaggtgcc actcccactg tcctttccta
aacggggagg gggcacggaa ggaactggga ccttccacgg tgagggtgac aggaaaggat
F A P P P C L P - P W K V P L P L S F P
6421 ataaaatgag gaaattgcat cgcattgtct gagtaggtgt cattctattc tgggggggtgg
tattttactc ctttaacgta gcgtaacaga ctcatccaca gtaagataag acccccccacc
N K M R K L H R I V - V G V I L F W G V
BsrBI
GsaI
BseYI
NotI
6481 ggtggggcag gacagcaagg gggaggattg ggaagagaat agcaggcatg ctggggagcg
ccaccccgtc ctgtcgttcc ccctcctaac ccttctctta tcgtccgtac gacccctcgc
G W G R T A R G R I G K R I A G M L G S
MscI

```
6541  gccgcaggaa cccctagtga tggagttggc cactccctct ctgcgcgctc gctcgctcac
      cggcgtcctt ggggatcact acctcaaccg gtgagggaga gacgcgcgag cgagcgagtg
       G  R  R   N  P  -  -   W  S  W   P  L  P   L  C  A  L   A  R  S

                    AhdI
                  ------+-----
6601  tgaggccggg cgaccaaagg tcgcccgacg cccgggcttt gcccgggcgg cctcagtgag
      actccggccc gctggtttcc agcgggctgc gggcccgaaa cgggcccgcc ggagtcactc
       L  R  P   G  D  Q  R   S  P  D   A  R  A   L  P  G  R   P  Q  -

                                  BbeI
                                ------+
                                  SfoI
                                ---+---
                             PstI
                           ------+
                             SbfI
                          -------+-
                             SfcI
                           --+----
                    MspA1I          NarI
                    ---+--        --+----
                     PvuII          KasI
                    ---+--        -+-----
6661  cgagcgagcg cgcagctgcc tgcaggggcg cctgatgcgg tattttctcc ttacgcatct
      gctcgctcgc gcgtcgacgg acgtccccgc ggactacgcc ataaaagagg aatgcgtaga
                                                 NotI downstream Primer
       A  S  E   R  A  A  A   C  R  G   A  -  C   G  I  F  S   L  R  I

                                                       SfcI
                                                     -+-----
6721  gtgcggtatt tcacaccgca tacgtcaaag caaccatagt acgcgccctg tagcggcgca
      cacgccataa agtgtggcgt atgcagtttc gttggtatca tgcgcgggac atcgccgcgt
       C  A  V   F  H  T  A   Y  V  K   A  T  I   V  R  A  L   -  R  R


6781  ttaagcgcgg cgggtgtggt ggttacgcgc agcgtgaccg ctacacttgc cagcgcccta
      aattcgcgcc gcccacacca ccaatgcgcg tcgcactggc gatgtgaacg gtcgcgggat
       I  K  R   G  G  C  G   G  Y  A   Q  R  D   R  Y  T  C   Q  R  P

          BsrBI                                          BsrFI
         ---+--                                        -+-----
6841  gcgcccgctc ctttcgcttt cttcccttcc tttctcgcca cgttcgccgg ctttccccgt
      cgcgggcgag gaaagcgaaa gaagggaagg aaagagcggt gcaagcggcc gaaaggggca
       S  A  R   S  F  R  F   L  P  F   L  S  R   H  V  R  R   L  S  P

                      BanII
                     -----+-
6901  caagctctaa atcgggggct ccctttaggg ttccgattta gtgctttacg gcacctcgac
      gttcgagatt tagcccccga gggaaatccc aaggctaaat cacgaaatgc cgtggagctg
       S  S  S   K  S  G  A   P  F  R   V  P  I   -  C  F  T   A  P  R

                      TaqII         BsaAI
                     -------       ----+--
6961  cccaaaaaac ttgatttggg tgatggttca cgtagtgggc catcgccctg atagacggtt
      gggtttttttg aactaaaccc actaccaagt gcatcacccg gtagcgggac tatctgccaa
       P  Q  K   T  -  F  G   -  W  F   T  -  W   A  I  A  L   I  D  G

                    DrdI
                  -------+-----
7021  tttcgccctt tgacgttgga gtccacgttc tttaatagtg gactcttgtt ccaaactgga
```

```
      aaagcgggaa actgcaacct caggtgcaag aaattatcac ctgagaacaa ggtttgacct
       F  S  P   F  D  V  G   V  H  V   L  -  -   W  T  L  V   P  N  W

                                              PsiI
                                            ---+---
7081  acaacactca accctatctc gggctattct tttgatttat aagggatttt gccgatttcg
      tgttgtgagt tgggatagag cccgataaga aaactaaata ttccctaaaa cggctaaagc
       N  N  T   Q  P  Y  L   G  L  F   F  -  F   I  R  D  F   A  D  F

7141  gcctattggt taaaaaatga gctgatttaa caaaaattta acgcgaattt taacaaaata
      cggataacca atttttttact cgactaaatt gtttttaaat tgcgcttaaa attgttttat
       G  L  L   V  K  K  -   A  D  L   T  K  I   -  R  E  F   -  Q  N

                           BsiHKAI
                           -----+
                            ApaLI      TatI
                           -+----     -+----
7201  ttaacgttta caattttatg gtgcactctc agtacaatct gctctgatgc cgcatagtta
      aattgcaaat gttaaaatac cacgtgagag tcatgttaga cgagactacg gcgtatcaat
       I  N  V   Y  N  F  M   V  H  S   Q  Y  N   L  L  -  C   R  I  V

                                  MspA1I              DrdI
                                 ---+---          -------+-----
7261  agccagcccc gacacccgcc aacacccgct gacgcgccct gacgggcttg tctgctcccg
      tcggtcgggg ctgtgggcgg ttgtgggcga ctgcgcggga ctgcccgaac agacgagggc
       K  P  A   P  T  P  A   N  T  R   -  R  A   L  T  G  L   S  A  P

7321  gcatccgctt acagacaagc tgtgaccgtc tccgggagct gcatgtgtca gaggttttca
      cgtaggcgaa tgtctgttcg acactggcag aggccctcga cgtacacagt ctccaaaagt
       G  I  R   L  Q  T  S   C  D  R   L  R  E   L  H  V  S   E  V  F

                           PcsI                BssSI
                       --------+-----        -+----
7381  ccgtcatcac cgaaacgcgc gagacgaaag ggcctcgtga tacgcctatt tttataggtt
      ggcagtagtg gctttgcgcg ctctgctttc ccggagcact atgcggataa aaatatccaa
       T  V  I   T  E  T  R   E  T  K   G  P  R   D  T  P  I   F  I  G

7441  aatgtcatga taataatggt ttcttagacg tcaggtggca cttttcgggg aaatgtgcgc
      ttacagtact attattacca aagaatctgc agtccaccgt gaaaagcccc tttacacgcg
       -  C  H   D  N  N  G   F  L  D   V  R  W   H  F  S  G   K  C  A

                                                    BsrBI
                                                   ---+---
7501  ggaaccccta tttgtttatt tttctaaata cattcaaata tgtatccgct catgagacaa
      ccttggggat aaacaaataa aaagatttat gtaagtttat acataggcga gtactctgtt
       R  N  P   Y  L  F  I   F  L  N   T  F  K   Y  V  S  A   H  E  T

                                                                 MslI
                                                               -----+----
7561  taaccctgat aaatgcttca ataatattga aaaaggaaga gtatgagtat tcaacatttc
      attgggacta tttacgaagt tattataact ttttccttct catactcata agttgtaaag
       I  T  L   I  N  A  S   I  I  L   K  K  E   E  Y  E  Y   S  T  F

                                                              TaqII
                                                             ------
7621  cgtgtcgccc ttattccctt ttttgcggca ttttgccttc ctgtttttgc tcacccagaa
      gcacagcggg aataagggaa aaaacgccgt aaaacggaag gacaaaaacg agtgggtctt
       P  C  R   P  Y  S  L   F  C  G   I  L  P   S  C  F  C   S  P  R

                                          BsiHKAI
                                          ------+
```

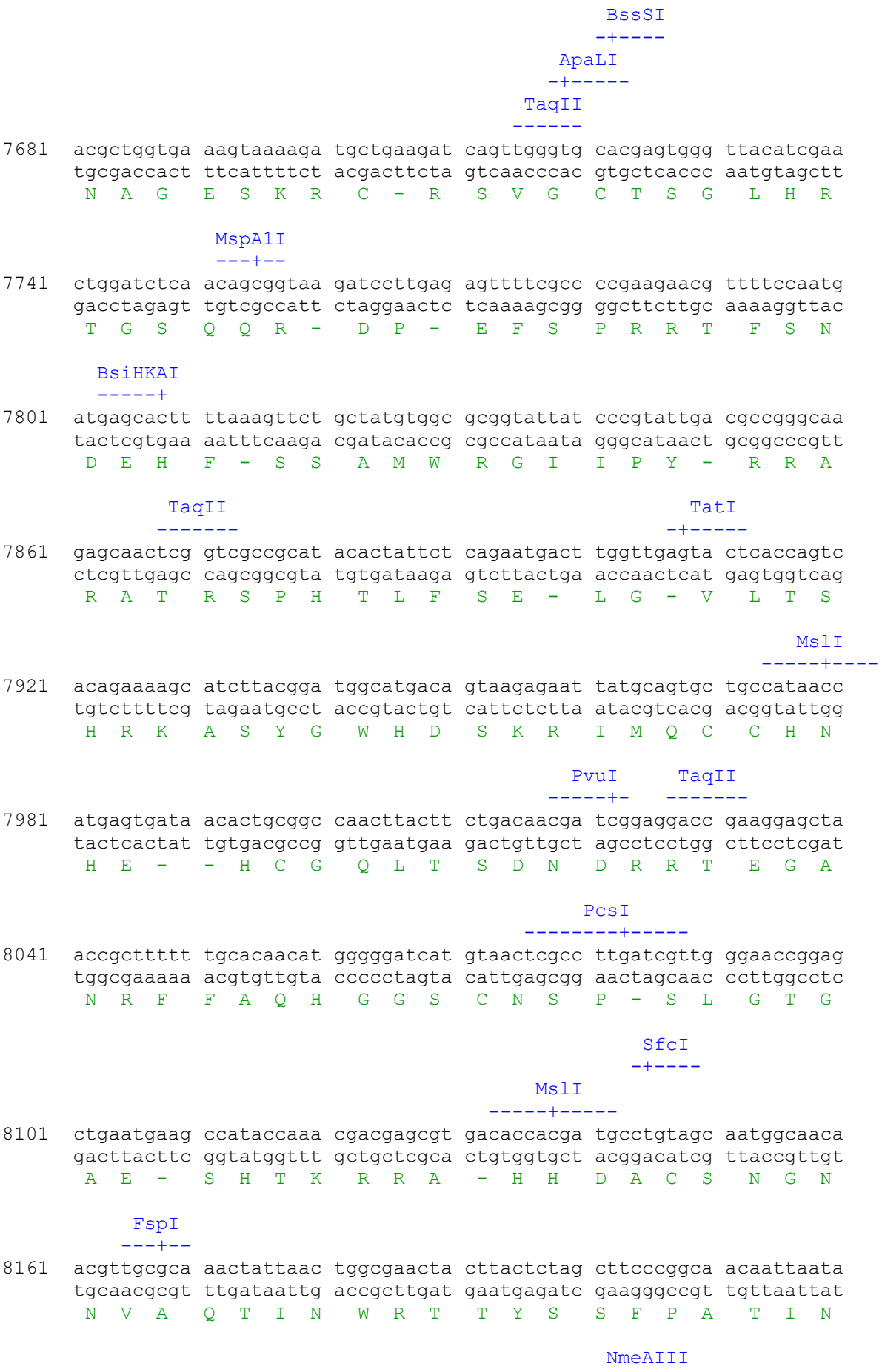
BssSI
ApaLI
TaqII
7681 acgctggtga aagtaaaaga tgctgaagat cagttgggtg cacgagtggg ttacatcgaa
tgcgaccact ttcatttttct acgacttcta gtcaacccac gtgctcaccc aatgtagctt
N A G E S K R C - R S V G C T S G L H R
MspA1I
7741 ctggatctca acagcggtaa gatccttgag agttttcgcc ccgaagaacg ttttccaatg
gacctagagt tgtcgccatt ctaggaactc tcaaaagcgg ggcttcttgc aaaaggttac
T G S Q Q R - D P - E F S P R R T F S N
BsiHKAI
7801 atgagcactt ttaaagttct gctatgtggc gcggtattat cccgtattga cgccgggcaa
tactcgtgaa aatttcaaga cgatacaccg cgccataata gggcataact gcggcccgtt
D E H F - S S A M W R G I I P Y - R R A
TaqII
TatI
7861 gagcaactcg gtcgccgcat acactattct cagaatgact tggttgagta ctcaccagtc
ctcgttgagc cagcggcgta tgtgataaga gtcttactga accaactcat gagtggtcag
R A T R S P H T L F S E - L G - V L T S
MslI
7921 acagaaaagc atcttacgga tggcatgaca gtaagagaat tatgcagtgc tgccataacc
tgtcttttcg tagaatgcct accgtactgt cattctctta atacgtcacg acggtattgg
H R K A S Y G W H D S K R I M Q C C H N
PvuI
TaqII
7981 atgagtgata acactgcggc caacttactt ctgacaacga tcggaggacc gaaggagcta
tactcactat tgtgacgccg gttgaatgaa gactgttgct agcctcctgg cttcctcgat
H E - - H C G Q L T S D N D R R T E G A
PcsI
8041 accgcttttt tgcacaacat gggggatcat gtaactcgcc ttgatcgttg ggaaccggag
tggcgaaaaa acgtgttgta ccccctagta cattgagcgg aactagcaac ccttggcctc
N R F F A Q H G G S C N S P - S L G T G
SfcI
MslI
8101 ctgaatgaag ccataccaaa cgacgagcgt gacaccacga tgcctgtagc aatggcaaca
gacttacttc ggtatggttt gctgctcgca ctgtggtgct acggacatcg ttaccgttgt
A E - S H T K R R A - H H D A C S N G N
FspI
8161 acgttgcgca aactattaac tggcgaacta cttactctag cttcccggca acaattaata
tgcaacgcgt ttgataattg accgcttgat gaatgagatc gaagggccgt tgttaattat
N V A Q T I N W R T T Y S S F P A T I N
NmeAIII

```
                                                      ------
8221  gactggatgg aggcggataa agttgcagga ccacttctgc gctcggccct tccggctggc
      ctgacctacc tccgcctatt tcaacgtcct ggtgaagacg cgagccggga aggccgaccg
       R  L  D   G  G  G  -   S  C  R   T  T  S   A  L  G  P   S  G  W

                                                     MspA1I
                                                     ---+--
                                                      SacII
                                                     ----+-
                                    BsrFI             BtgI
                                   -+----            -+----
8281  tggtttattg ctgataaatc tggagccggt gagcgtggaa gccgcggtat cattgcagca
      accaaataac gactatttag acctcggcca ctcgcacctt cggcgccata gtaacgtcgt
       L  V  Y   C  -  -  I   W  S  R   -  A  W   K  P  R  Y   H  C  S

                                                           AhdI
                                                     ------+-----
8341  ctggggccag atggtaagcc ctcccgtatc gtagttatct acacgacggg gagtcaggca
      gaccccggtc taccattcgg gagggcatag catcaataga tgtgctgccc ctcagtccgt
       T  G  A   R  W  -  A   L  P  Y   R  S  Y   L  H  D  G   E  S  G

8401  actatggatg aacgaaatag acagatcgct gagataggtg cctcactgat taagcattgg
      tgatacctac ttgctttatc tgtctagcga ctctatccac ggagtgacta attcgtaacc
       N  Y  G   -  T  K  -   T  D  R   -  D  R   C  L  T  D   -  A  L

8461  taactgtcag accaagttta ctcatatata ctttagattg atttaaaact tcatttttaa
      attgacagtc tggttcaaat gagtatatat gaaatctaac taaattttga agtaaaaatt
       V  T  V   R  P  S  L   L  I  Y   T  L  D   -  F  K  T   S  F  L

8521  tttaaaagga tctaggtgaa gatccttttt gataatctca tgaccaaaat cccttaacgt
      aaattttcct agatccactt ctaggaaaaa ctattagagt actggtttta gggaattgca
       I  -  K   D  L  G  E   D  P  F   -  -  S   H  D  Q  N   P  L  T

8581  gagttttcgt tccactgagc gtcagacccc gtagaaaaga tcaaaggatc ttcttgagat
      ctcaaaagca aggtgactcg cagtctgggg catcttttct agtttcctag aagaactcta
       -  V  F   V  P  L  S   V  R  P   R  R  K   D  Q  R  I   F  L  R

                                                                MspA1I
                                                                ---+--
8641  cctttttttc tgcgcgtaat ctgctgcttg caaacaaaaa aaccaccgct accagcggtg
      ggaaaaaaag acgcgcatta gacgacgaac gtttgttttt ttggtggcga tggtcgccac
       S  F  F   S  A  R  N   L  L  L   A  N  K   K  T  T  A   T  S  G

8701  gtttgtttgc cggatcaaga gctaccaact ctttttccga aggtaactgg cttcagcaga
      caaacaaacg gcctagttct cgatggttga gaaaaaggct tccattgacc gaagtcgtct
       G  L  F   A  G  S  R   A  T  N   S  F  S   E  G  N  W   L  Q  Q

8761  gcgcagatac caaatactgt ccttctagtg tagccgtagt taggccacca cttcaagaac
      cgcgtctatg gtttatgaca ggaagatcac atcggcatca atccggtggt gaagttcttg
       S  A  D   T  K  Y  C   P  S  S   V  A  V   V  R  P  P   L  Q  E

        SfcI                                              AlwNI
       -+----                                            ------+---
8821  tctgtagcac cgcctacata cctcgctctg ctaatcctgt taccagtggc tgctgccagt
      agacatcgtg gcggatgtat ggagcgagac gattaggaca atggtcaccg acgacggtca
       L  C  S   T  A  Y  I   P  R  S   A  N  P   V  T  S  G   C  C  Q

8881  ggcgataagt cgtgtcttac cgggttggac tcaagacgat agttaccgga taaggcgcag
      ccgctattca gcacagaatg gcccaacctg agttctgcta tcaatggcct attccgcgtc
       W  R  -   V  V  S  Y   R  V  G   L  K  T   I  V  T  G   -  G  A
```

```
                                BsiHKAI
                                -----+
                                 ApaLI      GsaI
                                -+----     -----+
   MspA1I                 PcsI              BseYI
   ---+--          -------+------          -+----
8941  cggtcgggct gaacgggggg ttcgtgcaca cagcccagct tggagcgaac gacctacacc
      gccagcccga cttgcccccc aagcacgtgt gtcgggtcga acctcgcttg ctggatgtgg
       A  V  G   L  N  G  G   F  V  H   T  A  Q   L  G  A  N   D  L  H

                  SfcI
                 -+----
9001  gaactgagat acctacagcg tgagctatga gaaagcgcca cgcttcccga agggagaaag
      cttgactcta tggatgtcgc actcgatact ctttcgcggt gcgaagggct tccctctttc
       R  T  E   I  P  T  A   -  A  M   R  K  R   H  A  S  R   R  E  K

                                                       BssSI
                                                      -+----
9061  gcggacaggt atccggtaag cggcagggtc ggaacaggag agcgcacgag ggagcttcca
      cgcctgtcca taggccattc gccgtcccag ccttgtcctc tcgcgtgctc cctcgaaggt
       G  G  Q   V  S  G  K   R  Q  G   R  N  R   R  A  H  E   G  A  S

                                                            DrdI
                                                   --------+----
9121  gggggaaacg cctggtatct ttatagtcct gtcgggtttc gccacctctg acttgagcgt
      ccccctttgc ggaccataga aatatcagga cagcccaaag cggtggagac tgaactcgca
       R  G  K   R  L  V  S   L  -  S   C  R  V   S  P  P  L   T  -  A

9181  cgatttttgt gatgctcgtc agggggggcgg agcctatgga aaaacgccag caacgcggcc
      gctaaaaaca ctacgagcag tccccccgcc tcggatacct ttttgcggtc gttgcgccgg
       S  I  F   V  M  L  V   R  G  A   E  P  M   E  K  R  Q   Q  R  G

                                              AflIII
                                             -+-----
                                               PciI
                                             -+-----
9241  tttttacggt tcctggcctt ttgctggcct tttgctcaca tgt
      aaaaatgcca aggaccggaa aacgaccgga aaacgagtgt aca
       L  F  T   V  P  G  L   L  L  A   F  C  S   H
```

8.4.4.1 Plasmidkarte von pSpCas9(BB)-2A-mCherry (PX458) mit XhoI- und HindIII-Restriktionsschnittstellen

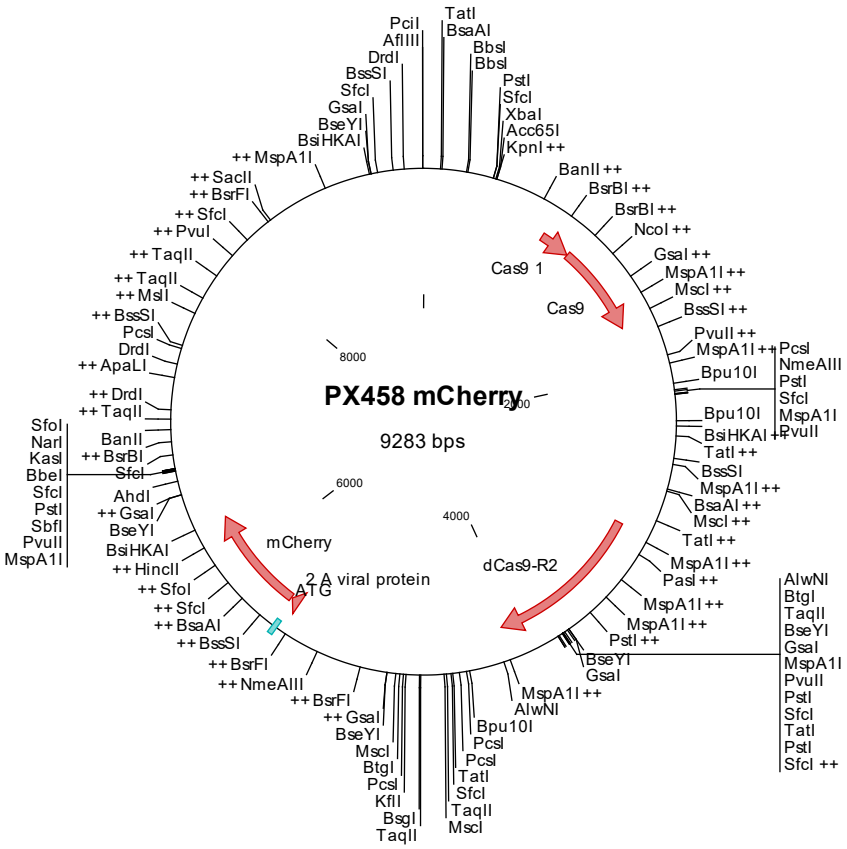

Abbildung 8.4: Aufbau des Plasmids pSpCas9(BB)-2A-mCherry (PX458) mit XhoI- und HindIII-Restriktionsschnittstellen
In das 9283 bp große Plasmid wurde die sgRNA-Gensequenz gegen GABARAPL2 (Exon 2A/2B/3) eingebracht. Neben den vorhandenen Schnittstellen für Restriktionsenzyme wurde eine zusätzliche für XhoI und HindIII eingebracht, einen Replikationsursprung (f1 ori) und eine Ampicillin-Resistenz (AmpR) in *E. coli* sowie einen weiteren Replikationsursprung (ori) und U6 Promotor für die Expression in Säugerzellen. Die *gRNA scaffold* Sequenz beinhaltet die Restriktionsschnittstellen für BbsI/BpiI, über die die gewünschte sgRNA in das Plasmid eingebracht werden kann. Anschließend folgt die Cas9-Sequenz aus *S. pyogenes* und eine Sequenz für das Fluoreszenzprotein EGFP, die unter einem humanen Cytomegalovirus (CMV) *enhancer* und *chicken β-actin* Promotor exprimiert werden. Am Insert befindet sich N-terminal eine 3 x FLAG-Sequenz und C-terminal die mCherry-Sequenz, die durch eine *nucleoplasmin nuclear localization signal* (NLS)- und 2A-Sequenz von Cas9 abgegrenzt wird.

8.5 Makros

Die in dieser Arbeit verwendeten Makros wurden in Zusammenarbeit mit Alexander Schomburg und Sebastian Hänsch (CAi, HHU Düsseldorf) programmiert.

8.5.1 *Spinning Disk* Mikroskopie: Video-Generierung

```
dir = getDirectory("Choose a Directory ");
setBatchMode(true);
print("\\Clear");

// asking for offset information
xOffset = getNumber("Offset for X?", -4);
yOffset = getNumber("Offset for Y?", -3);

findTif(dir, xOffset, yOffset);
exit();

function findTif(dir, xOffset, yOffset) {
    list = getFileList(dir);
    convertedFiles = 0;

    for (i = 0; i < list.length; i++) {
        if (endsWith(list[i], "/")) {
                        findTif("" + dir + list[i], xOffset, yOffset);
         } else if (!matches(list[i], "(?i).*_(merged|647|488)_.*\\.tiff?") &&
         matches(list[i], "(?i).*tiff?")) {
            convert_image(list[i], dir, xOffset, yOffset);
            showProgress(i, list.length);
            convertedFiles++;
        }
    }
        print("Directory: " + dir);
        print("Finished converting " + convertedFiles + " files.");
}

function append(arr, value) {
        arr2 = newArray(arr.length+1);
        for (i=0; i<arr.length; i++) arr2[i] = arr[i];
        arr2[arr.length] = value;
        return arr2;
}

function convert_image(file_tif, dir_tif, xOffset, yOffset) {
    inFile = dir_tif + file_tif;
        outDir = dir_tif;
    outFile = substring(file_tif, 0, indexOf(file_tif, "."));
    frameRate = 3;
        IJ.redirectErrorMessages();
        zStacks647 = newArray(0);
        zStacks488 = newArray(0);

        print("File: " + inFile);

        // getting snapshot informations
        repeatNumber = 0;
        zStacksNumber = 0;
        txtFile = outDir + outFile + ".txt";
        if (File.exists(txtFile)) {
                print("TXT information found!");
                txtContent = File.openAsString(txtFile);
                txtLines = split(txtContent, "\n");
```

```
            for (n=0; n < txtLines.length; n++) {
                    if (matches(txtLines[n], ".*Repeat T - .* times.*")) {
                            repeatString = split(txtLines[n], "-");
                            repeatNumber = split(repeatString[1], " ");
                            repeatNumber = parseInt(repeatNumber[0]);
            } else if (matches(txtLines[n], ".*Repeat Z - .* in .* planes.*")) {
                            zStacksString = split(txtLines[n], "in");
                            zStacksNumber = split(zStacksString[1], " ");
                            zStacksNumber = parseInt(zStacksNumber[0]);
                    }
            }
            // in case there were no z stacks at all
            if (repeatNumber > 0 && zStacksNumber == 0) {
                    zStacksNumber = 1;
            }
    }
    if (repeatNumber == 0) {
            repeatNumber = getNumber("Number of repetitions?", 40);
    }
    if (zStacksNumber == 0) {
            zStacksNumber = getNumber("Number of zStacks?", 10);
    }
    print("xOffset: " + xOffset);
    print("yOffset: " + yOffset);
    print("Repeats: " + repeatNumber);
    print("zStacks: " + zStacksNumber);

// 647 laser image
open(inFile);
    run("Specify...", "width=512 height=256 x=0 y=0 slice=1");
    run("Crop");
    nSlices647 = nSlices;
    run("Make Substack...", "  slices=2-" + nSlices647 + "-2");
    for (i = 1; i <= zStacksNumber; i++) {
        print("Creating zStack " + i + " image (647) of " + file_tif + "...");
            selectWindow("Substack (2-" + nSlices647 + "-2)");
            run("Make Substack...", "  slices=" + i + "-" + nSlices + "-" + zStacksNumber);
            run("Red");
            run("Enhance Contrast", "saturated=0.35");

    run("Translate...", "x=" + xOffset + " y=" + yOffset + " interpolation=None stack");
            saveAs("TIFF", outDir + outFile + "_647_" + i);
            zStacks647 = append(zStacks647, outFile + "_647_" + i + ".tif");
    }

    // close all windows
wait(60);
while (nImages>0) {
            selectImage(nImages);
            close();
    }

    // 488 laser image
open(inFile);
    run("Specify...", "width=512 height=256 x=0 y=256 slice=1");
    run("Crop");
    nSlices488 = nSlices;
    run("Make Substack...", "  slices=1-" + nSlices488 + "-2");
    for (i = 1; i <= zStacksNumber; i++) {
            print("Creating zStack " + i + " image (488) of " + file_tif + "...");
            selectWindow("Substack (1-" + nSlices488 + "-2)");
            run("Make Substack...", "  slices=" + i + "-" + nSlices + "-" + zStacksNumber);
            run("Green");
            run("Enhance Contrast", "saturated=0.35");
            saveAs("TIFF", outDir + outFile + "_488_" + i);
            zStacks488 = append(zStacks488, outFile + "_488_" + i + ".tif");
    }
```

```
        // close all windows
    wait(60);
    while (nImages>0) {
              selectImage(nImages);
              close();
        }

        if(zStacks647.length == zStacks488.length) {
              for (i=0; i < zStacks647.length; i++) {
                    j = i + 1;
                    print("Merging zStack " + j + " of " + file_tif + "...");
                    open(outDir + zStacks647[i]);
                    open(outDir + zStacks488[i]);
                    run("Merge Channels...", "c1=" + zStacks647[i] + " c2=" + zStacks488[i]
+ " create");
                    run("Subtract Background...", "rolling=50");
                  run("Smooth");
                  run("Label...", "format=00:00:00 starting=0.0 interval=0.6 x=5 y=20 font=18
text=[] range=1-320 use");
                    run("AVI... ", "compression=None frame=3" + frameRate + " save=[" +
outDir + outFile + "_merged_" + j + ".avi]");
                    saveAs("Tiff", outDir + outFile + "_merged_" + j + ".tif");
                    selectWindow(outFile + "_merged_" + j + ".tif");
                    close();
              }
        } else {
              print("Error: Number of zStacks differ for 647 and 488!");
        }
        print("Completed.");
        print("\\Clear");
}
```

8.5.2 Pearsons Korrelationskoeffizient-Auswertung der einzelnen Zellen nach z-Projektion

```
dir = getDirectory("Choose Source Directory");
setBatchMode(true);
print("\\Clear");
findTif(dir);
exit();

function findTif(dir) {
    list = getFileList(dir);
    colocatedImages = 0;

    for (i = 0; i < list.length; i++) {
        if (endsWith(list[i], "/")) {
                    findTif("" + dir + list[i]);
        } else if (matches(list[i], "(?i).*.lsm")) {
            colocate_image(list[i], dir);
            showProgress(i, list.length);
            colocatedImages++;
        }
    }
        print("Directory: " + dir);
        print("Finished colocating " + colocatedImages + " images.");
}

function colocate_image(file_lsm, dir_lsm) {
        //Prepare opening dimension-swapped images from ome.tif format in batch routine
```

```
        run("Bio-Formats Importer", "open=["+dir_lsm+file_lsm+"] color_mode=Default
rois_import=[ROI manager] view=Hyperstack stack_order=XYCZT swap_dimensions z_1=10 c_1=5
t_1=1");
        name = getInfo("image.filename");
        ImageTitle = getTitle();
        EndPosition = lastIndexOf(ImageTitle,".lsm");
        PureName = substring(ImageTitle,0,EndPosition);

        //Make Maximum Intensity Projection
        run("Z Project...", "projection=[Max Intensity]");
        selectWindow(name);
        close();
        rename(name);

        //Kill the other channels
        run("Arrange Channels...", "new=45");

        ///Give correct coloring
        Stack.setChannel(1);
        run("Blue");
        Stack.setChannel(2);
        run("Red");

        //Split channels and rename
        run("Split Channels");
        selectWindow("C1-"+name);
        rename("Blue");
        selectWindow("C2-"+name);
        rename("Red");
        selectWindow("Red");
        rename("1");
        selectWindow("Blue");
        rename("2");

        //Create colocalization
        selectWindow("1");
        selectWindow("2");
        run("JACoP ", "imga=1 imgb=2 pearson");

        //Close the windows
        selectWindow("1");
        close();
        selectWindow("2");
        close();

        //Saving the log
        selectWindow("Log");
        saveAs("Text", dir_lsm+"\\Analyzed_EGF_Rab-"+PureName+".txt");
        print("\\Clear");
}
```

8.5.3 Mander`s Koeffizient (M1+M2)-Auswertung der einzelnen Zellen nach z-Projektion

```
dir = getDirectory("Choose Source Directory");
setBatchMode(true);
print("\\Clear");
findTif(dir);
exit();

function findTif(dir) {
    list = getFileList(dir);
    colocatedImages = 0;

    for (i = 0; i < list.length; i++) {
        if (endsWith(list[i], "/")) {
                        findTif("" + dir + list[i]);
        } else if (matches(list[i], "(?i).*.lsm")) {
            colocate_image(list[i], dir);
            showProgress(i, list.length);
            colocatedImages++;
        }
    }
       print("Directory: " + dir);
       print("Finished colocating " + colocatedImages + " images.");
}

function colocate_image(file_lsm, dir_lsm) {
       //Prepare opening dimension-swapped images from ome.tif format in batch routine
       run("Bio-Formats     Importer",     "open=["+dir_lsm+file_lsm+"]     color_mode=Default
rois_import=[ROI  manager]  view=Hyperstack  stack_order=XYCZT  swap_dimensions  z_1=10  c_1=5
t_1=1");
       name = getInfo("image.filename");
       ImageTitle = getTitle();
       EndPosition = lastIndexOf(ImageTitle,".lsm");
       PureName = substring(ImageTitle,0,EndPosition);

//Make Maximum Intensity Projection
       run("Z Project...", "projection=[Max Intensity]");
       selectWindow(name);
       close();
       rename(name);

       //Kill the other channels
       run("Arrange Channels...", "new=45");

       ///Give correct coloring
       Stack.setChannel(1);
       run("Blue");
       Stack.setChannel(2);
       run("Red");

       //Split channels and rename
       run("Split Channels");
       selectWindow("C1-"+name);
       rename("Blue");
       selectWindow("C2-"+name);
       rename("Red");
       selectWindow("Red");
       rename("1");
       selectWindow("Blue");
       rename("2");

       //Create colocalization
       selectWindow("1");
```

```
        selectWindow("2");
        run("JACoP ", "imga=2 imgb=1 thra=75 thrb=25 mm");

        //Close the windows
        selectWindow("1");
        close();
        selectWindow("2");
        close();

        //Saving the log
        selectWindow("Log");
        saveAs("Text", dir_lsm+"\\Analyzed_EGF_Rab-"+PureName+".txt");
        print("\\Clear");
}
```

9 Liste der Publikationen

I. I. M. Simons, J. Mohrlüder, R. Feederle, E. Kremmer, T. Zobel, J. Dobner, N. Bleffert, S. Hoffmann, und D. Willbold (2019). 'The highly GABARAP specific rat monoclonal antibody 8H5 visualizes GABARAP in immunofluorescence imaging at endogenous levels', *Sci Rep*, 9: 526.

II. I. Abdollahzadeh, J. Hendriks, J. L. Sanwald, I. M. Simons, S. Hoffmann, O. H. Weiergräber, D. Willbold, und T. Gensch (2019). 'Autophagy-Related Proteins GABARAP and LC3B Label Structures of Similar Size but Different Shape in Super-Resolution Imaging', *Molecules*, 24(9): 1833.

III. J. Dobner, I. M. Simons, K. Rufinatscha, S. Hänsch, I. Abdollahzadeh, T. Gensch, J.G. Bode, S. Hoffmann, D. Willbold (2020). Deficiency of GABARAP but not its paralogs causes enhanced EGF-induced EGFR degradation. *Cells*, 9 (5):1296

10 Liste der Posterpräsentationen

Indra M. Simons, Jeannine Mohrlüder, Regina Feederle, Elisabeth Kremmer, Thomas Zobel, Jochen Dobner, Nicole Bleffert, Silke Hoffmann, Dieter Willbold
"A rat monoclonal antibody which specifically detects mammalian GABARAP in confocal immunofluorescence imaging", Keystone Symposia on Molecular and Cellular Biology, Selective Autophagy (Z2), Kyoto, Japan, 2018

Indra M. Simons, Jeannine Mohrlüder, Regina Feederle, Elisabeth Kremmer, Thomas Zobel, Jochen Dobner, Nicole Bleffert, Silke Hoffmann, Dieter Willbold
"A rat monoclonal antibody which specifically detects mammalian GABARAP in confocal immunofluorescence imaging", Tracking Life Symposium, RWTH Aachen, Deutschland, 2018

Indra M. Simons, Jochen Dobner, Jeannine Mohrlüder, Iman Abdollahzadeh, Sebastian Hänsch, Thomas Gensch, Silke Hoffmann, Dieter Willbold
"Monitoring GABARAP without cross-reactivity of its close paralogs by microscopy under endogenous conditions: GABARAP meets EGFR", GMB/DGZ Fall Conference 2019, Age-Related Human Diseases, Special Focus: Autophagy, Tübingen, Deutschland, 2019

11 Danksagung

An dieser Stelle möchte ich mich bei allen bedanken, die zum Erfolg meines Studiums und dieser Arbeit beigetragen haben.

Mein besonderer Dank geht an Herrn Prof. Dr. Dieter Willbold für den interessanten Themenvorschlag und die Möglichkeit, meine Doktorarbeit am *Institute of Complex Systems 6* (ICS-6), jetzt Institut für Biologische Informationsprozesse (IBI-7: Strukturbiochemie) bzw. am Institut für Physikalische Biologie durchführen zu können.

Herrn Prof. Dr. Björn Stork danke ich für die nicht selbstverständliche Übernahme des Zweitgutachtens.

Ein herzliches Dankeschön geht zudem an Frau Dr. Silke Hoffmann für die sehr gute Betreuung sowie umfassende Unterstützung bei meiner Doktorarbeit.

Zudem bedanke ich mich bei allen vom SFB1208, insbesondere bei meinem Mentor Prof. Dr. Thomas Klein und bei Prof. Dr. Stefanie Weidtkamp-Peters, Dr. Thomas Zobel und Dr. Sebastian Hänsch vom CAi für die nette Kooperation.

Auch bei Dr. Thomas Gensch, Dr. Iman Abdollahzadeh, Dr. Oliver Weiergräber und Dr. Melanie Schwarten möchte ich mich für die gute Zusammenarbeit und Tipps bedanken.

Bei Jochen Dobner bedanke ich mich herzlich für die sehr gute Zusammenarbeit und Generierung der *Knockout*- und *Knock-In*-Zelllinien.

Des Weiteren möchte ich mich bei Julia Post-Schulz, Dr. Marianne Schulte, Karoline Santur, Serife Akgül, Irina Apanasenko und Lena Mangels für die netten Gespräche und Unterstützung bedanken.

Ganz besonders möchte ich mich bei meiner Kollegin Julia Sanwald für ihre Hilfe in jeglicher Hinsicht bedanken.

Julia Post-Schulz, Dr. Sarah Schemmert und Dominik Honold danke ich besonders für die Hilfe bei den Hirnschnitt-Färbungen.

Bei Markus Tusche, Dominik Honold und Julia Sanwald möchte ich mich für das Verständnis bedanken, wenn ich mal wieder den ganzen Tag die Zellkultur beschlagnahmt habe.

Für die gewissenhafte Überprüfung meiner Doktorarbeit auf Unstimmigkeiten sprachlicher Art möchte ich mich an dieser Stelle bei meiner Mutter bedanken.

Für die aufmunternden Worte und die Unterstützung, vor allem bei der Programmierung der Makros bedanke ich mich ganz besonders bei meinem Freund Alexander.

Zum Schluss möchte ich mich bei meinen Eltern, die mein Biologiestudium ermöglicht haben und mich während dieser Zeit immer unterstützt haben, bedanken.